Daniel José da Costa Barbosa

Ecstasy's neurotoxicity: *in vitro* findings from mitochondria to the cell

Tese do 3º Ciclo de Estudos Conducentes ao Grau de Doutoramento em Ciências Farmacêuticas na Especialidade de Toxicologia

PhD thesis of the 3rd Cycle of Studies in Pharmaceutical Sciences on the Specialty of Toxicology

Trabalho realizado sob a orientação de
Elaborated under supervision of

Professor Doutor Félix Dias Carvalho

Professor Doutor João Paulo Soares Capela

Professor Doutor Jorge Miguel de Ascensão Oliveira

Outubro de 2013

É AUTORIZADA A REPRODUÇÃO PARCIAL DESTA TESE, APENAS PARA EFEITOS DE INVESTIGAÇÃO, MEDIANTE DECLARAÇÃO ESCRITA DO INTERESSADO, QUE A TAL SE COMPROMETE.

PARA SER GRANDE, *sê inteiro: nada*
Teu exagera ou exclui.
Sê todo em cada coisa. Põe quanto és
No mínimo que fazes.
Assim em cada lago a lua toda
Brilha, porque alta vive.

Ricardo Reis

Aos meus Pais, Laurentino e Maria do Céu,

Por tudo.

À Renata e à Vânia,

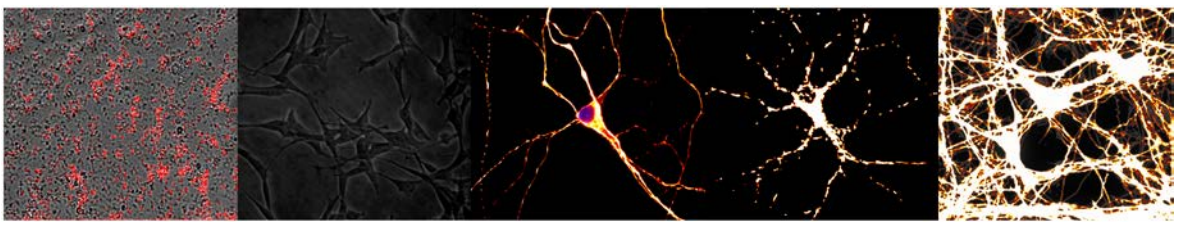
Para sempre.

Observa cada caminho de perto
E deliberadamente. Experimenta-o
Tantas vezes quantas julgares necessário.
Depois pergunta a ti próprio:
Este caminho tem coração?
Se tiver, é um bom caminho;
Se não tiver, não serve para nada.

Carlos Castaneda

À pessoa cujo caminho o coração ditou,
mas que porventura estou destinado a esquecer.
Tu sabes quem és … e Eu gostava de saber.

Publications



Publications

The following published or submitted manuscripts, as well as a manuscript under preparation, were designed in the scope of this thesis:

► Barbosa DJ, Capela JP, Oliveira, JMA, Silva R, Ferreira LM, Siopa F, Branco PS, Fernandes E, Duarte JA, Bastos ML, Carvalho F (2012). Pro-oxidant effects of "Ecstasy" and its metabolites in mouse brain synaptosomes. Br J Pharmacol 165:1017-1033.

► Barbosa DJ, Capela JP, Ferreira LM, Branco PS, Fernandes E, Bastos ML and Carvalho F. MDMA metabolites and monoamine neurotransmittters stimulate the Na^+/K^+ ATPase activity in mouse brain synaptosomes. *Manuscript under preparation*.

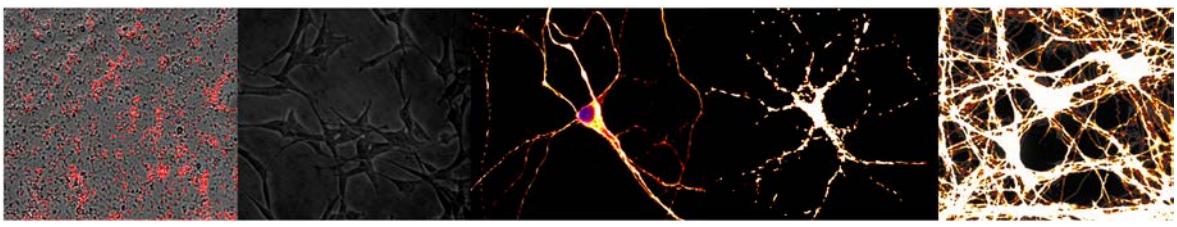
► Barbosa DJ, Capela JP, Silva R, Ferreira LM, Branco PS, Fernandes E, Bastos ML, Carvalho F (2013). "Ecstasy"-induced toxicity in SH-SY5Y differentiated cells: role of hyperthermia and metabolites. Arch Toxicol. DOI 10.1007/s00204-013-1147-9.

► Barbosa DJ, Capela JP, Silva R, Vilas-Boas V, Ferreira LM, Branco PS, Fernandes E, Bastos ML, Carvalho F (2013). The mixture of "ecstasy" and its metabolites is toxic to human SH-SY5Y differentiated cells, at *in vivo* relevant concentrations. Arch Toxicol. [Epub ahead of print].

► Barbosa DJ, Serrat R, Mirra S, Quevedo M, Barreda EG, Àvila J, Fernandes E, Bastos ML, Capela JP, Carvalho F, Soriano E. MDMA impairs mitochondrial neuronal trafficking in a Tau- and Mitofusin 2/Drp1-dependent manner. *Manuscript submitted for publication*.

► Barbosa DJ, Serrat R, Mirra S, Quevedo M, Barreda EG, Àvila J, Fernandes E, Bastos ML, Capela JP, Carvalho F, Soriano E. The mixture of "ecstasy" and its metabolites, at *in vivo* relevant concentrations, impairs mitochondrial trafficking and increases organelle's fragmentation in hippocampal neurons. *Manuscript under submission*.

Acnowledgements



Acknowledgements

► First and foremost, I would like to thank my supervisor, Professor Félix Dias Carvalho, for accepting to supervise my PhD with this interesting project. I must thank to the great and bright scientist always open to discuss new ideas, for having been able to focus me, define the framework of this thesis, and find a logic in it. For his modesty, his solidarity, his infinite kindness, and for the good person he is, who gives hope in humanity. His amazing energy, creativity and uprightness definitively make him an example for me, as a scientist and as a person.

► I would like to deeply thank my co-supervisors, Professor João Paulo Capela and Professor Jorge M. A. Oliveira, for the guidance over these four years. I must thank for the encouragement and for all the techniques and experiences that certainly will be useful in my professional and personal life.

► I am very grateful to Professor Eduardo Soriano and Dr. Romàn Serrat for the given opportunity to work in their group at Institute for Research in Biomedicine, in Barcelona. I must thank for sharing scientific knowledge and expertise in the mitochondria world. Since the beginning I never felt as a stranger. I was received with extreme professionalism, kindness, sympathy and, above all, affection, which says everything about your kind personality. I greatly benefited from this collaboration and I hope to work together with you in the future. Your contribution was essencial to convert this thesis into an exceptional work.

► I am very thankful to Professor Maria de Lourdes Bastos for all the useful comments and suggestions that certainly improved this thesis. I would like to express my deep admiration for you.

► I would like to thank Professor Fernando Remião and Professor Helena Carmo for all the friendship, comments and suggestions, which contributed to the development of new ideas. Many thanks for your presence and your support. And, yes, the lab was my second house, sometimes the first.

► I am also thankful to the non-teaching staff of the Toxicology Laboratory, namely Dra. Paula Pinho, Dra. Sónia Fraga, Dra. Vera Costa and Dra. Márcia Carvalho, for their support along the years. In particular, I would like to thank Eng. Maria Elisa Soares for the friendship, the affection, the empathy, the “good morning” of all the days, the sweets. She was as a mother for me. Thank you very much.

► I am very grateful to Professor Eduarda Fernandes for all the support, suggestions and friendship and for providing the MDMA. To Professor Luísa Ferreira and Professor Paula Sério Branco, at FCT-UNL, I would like to thank all the support and for providing the MDMA metabolites.

► I must express my thankfulness to all my lab fellows in the Toxicology Laboratory, at FFUP, with whom I had the opportunity to learn and spend very nice times. I must mention Teresa Baltazar, Ana Oliveira, Márcia Monteiro, Juliana Garcia, Luciana Rossato, Marcelo Arbo, Diana Silva, Filipa Ponte, Maria João Valente, Tiago Nogueira, Rita Feio, Mariline Gameiro, Ana Margarida Araújo, José Luís Sousa and all the new MSc students (they are so many). I am very grateful for the learning, help and friendship. I am also grateful to Cátia Faria and Mrs. Júlia for their help and comprehension along this time.

► I also want to thank everyone in the “Development and Regeneration Lab”, at IRB Barcelona, for the support and hospitality. I apologize not mentioning them all because they are so many. I must, however, thank to Serena Mirra and Martí Quevedo, the other members of the “Mitochondria Group”, for the learning, experimental help and friendship. In particular, I would like to thank Oriol Ros for the help on the preparation of neuronal cultures and for all the scientific discussions, which were very important during my stay at Barcelona. I also thank to the staff of the advanced digital microscopy core facility at IRB for their help with the microscopy systems.

► Agradeço à Professora Narcisa Pinto por tudo quanto me ensinou e pelos valores que me incutiu, bem como pela sua presença ao longo dos anos. Sem qualquer dúvida que a forma como me marcou diz muito acercada da pessoa que hoje sou. O meu muito obrigado.

► Expresso o meu mais profundo agradecimento a toda a minha família, desde os meus avós, aos meus tios e primos pela força e ânimo que tantas vezes necessitei, pelo seu acreditar que tanta força me deu ao longo deste período e, acima de tudo, pela incessante disponibilidade que sempre manifestaram.

► Em particular, e de um modo muito especial, queria agradecer ao meu avô José Gomes de Azevedo, que muito embora não tivesse o privilégio de acompanhar presencialmente o meu crescimento desde os 13 anos, jamais esteve ou estará ausente na minha vida. Admiro a sua inquestionável coragem e determinação, o seu saber, a sua compreensão, bem como tudo quanto me ensinou. Ensinaste-me a ser perseverante, a correr atrás daquilo em que acredito. Esta tese … é a nossa tese!

► Declaro o meu mais marcado agradecimento aos meus pais, Laurentino e Maria do Céu, pelo incondicional apoio, pela imensurável paciência, pela determinação e por tudo quanto abdicaram em detrimento de mim. Sem a vossa presença nada teria sido igual, nada teria sido especial. Peço-lhes desculpa pelas angústias e preocupações que lhes causei. Peço-lhes igualmente desculpa pela minha, por vezes incompreensível, forma mais distante de lidar convosco, bem como pela minha reserva em expor o que vai dentro de mim, mas que sempre aceitaram e compreenderam. Estou-lhes profundamente grato por tudo, para todo o sempre.

► A ti, Vânia, agradeço-te teres feito parte desta fase da minha vida. É difícil expressar em palavras aquilo que sinto … típico! É tão-somente impossível como querer manter vivo um ser humano sem coração. Não há forma de o exteriorizar. A ajuda que sempre me prestaste, as palavras de incentivo, as manifestações de carinho e amizade, o acreditar, o compreender da minha forma de ser, o respeitar as minhas ideias e opiniões, o assentires fazer parte da minha vida mesmo sabendo que talvez não te pudesse retribuir, o respeitar as minhas diferenças. Vives para dar alegrias às pessoas que te rodeiam. Felizmente sou uma dessas pessoas! Estou-te profundamente grato e espero puder retribuir-te tudo quanto fizeste por mim.

► A ti, Renata … é impossível descrever o quanto te estou grato. Este é o momento em que as lágrimas correm sem que as consiga conter, em que a razão se perde, em que tudo jamais será igual. Agradeço-te a incessante disponibilidade que sempre manifestaste, as palavras de incitamento, as vezes que me fizeste sorrir, a amizade, as manifestações de carinho, o assentires fazer parte da minha vida, o respeitares a minhas diferenças, os momentos de alegria que fizeste questão de dividir comigo. Peço-te desculpa pelas vezes em que te magoei, pela forma menos correta com que lidei com determinadas situações, pelas merecidas retribuições que fui incapaz de te prestar em determinadas alturas. Tudo quanto se possa imaginar ela fê-lo por mim, do mais simples ao mais complexo, do início ao … só espero que não exista um fim. Estou-te eternamente grato por tudo. Se pudesse escolher aqueles que estariam ao meu lado a partir de agora, não teria dúvidas!

► Finally, I acknowledge to the following institutions for the support of this thesis:

- "Fundação para a Ciência e a Tecnologia", Portugal, for the indispensable financial support under the grant SFRH/BD/64939/2009 and under the project PTDC/SAU-FCF/102958/2008, "Programa Operacional Temático Fatores de Competitividade

(COMPTE) do Quadro Comunitário de Apoio III" and "Fundo Comunitário Europeu (FEDER) (FCOMP-01-0124-FEDER-011079)".

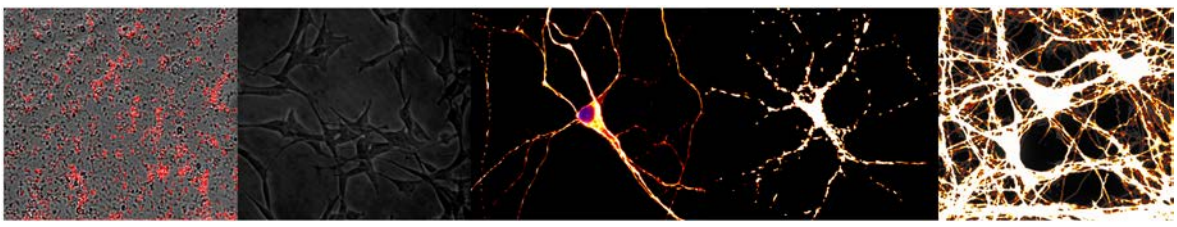
- "Ministerio de Ciencia e Innovacion", Spain, for the finantial support under the grant BFU2008-3980.

- REQUI*M*TE, associated laboratories.

- Toxicology Laboratory, Department of Biological Sciences, Faculty of Pharmacy, University of Porto.

- "Development and Regeneration Lab", Institute for Research in Biomedicine.

Abstracts



Ecstasy's neurotoxicity: *in vitro* findings from mitochondria to the cell

Abstract

3,4-Methylenedioxymethamphetamine (MDMA; "ecstasy"), a psychoactive substance with hallucinogenic properties, is a worldwide major recreational drug of abuse with well-known acute- and long-lasting neurotoxic effects, which have been disclosed both in laboratory animal models and humans. Despite the large amount of data concerning MDMA's neurotoxicity, acquired by many different research groups along several years, the mechanisms involved in MDMA-induced neurotoxicity are still not completely revealed. The studies presented in this thesis aimed to contribute to a better understanding of the mechanistic basis underlying MDMA's neurotoxicity, at molecular and cellular level. Thus, through the use of different approaches and *in vitro* neuronal models, the role of metabolism, monoamine neurotransmitters and hyperthermia was investigated, with special focus on mitochondrial-dependent trails.

In mouse brain synaptosomes, MDMA metabolites and monoamine neurotransmitters induced a concentration- and time-dependent hydrogen peroxide (H_2O_2) formation, which was independent on mitochondrial polarization status and partially rescued by antioxidants. Monoamine oxidase-mediated metabolism also contributed to the H_2O_2 production induced by the neurotransmitters serotonin and dopamine. The toxic effect involved oxidative modifications, such as lipid peroxidation, protein carbonylation and formation of quinoproteins. Additionally, MDMA metabolites and monoamine neurotransmitters stimulated the Na^+- and K^+-activated adenosine 5'-triphosphatase (Na^+/K^+ ATPase) activity, in a concentration-dependent manner, an effect also partially attenuated by the antioxidant *N*-acetylcysteine (NAC).

In SH-SY5Y differentiated cells, MDMA metabolites induced mitochondrial dysfunction and cell death in a concentration-dependent manner, which was differently affected by time and temperature of exposure. The catechol precursors α-methyldopamine and *N*-methyl-α-methyldopamine revealed to be less toxic than their corresponding monoconjugates with reduced glutathione (GSH) or NAC. As observed in the synaptosome model, MDMA, at the range of concentrations tested, did not reveal apparent toxicity. The MDMA metabolites were poorly accumulated in the intracellular compartment and their concentration in cell culture medium decreased over time, an effect potentiated by hyperthermia. In the same experimental model, the mixture of MDMA and its metabolites, at a range of concentrations with remarkable relevance to the *in vivo* scenario, triggered toxicity in a time- and temperature-dependent manner, which was fully protected by the antioxidant NAC and accompanied by caspase 3 activation. Notably, as a

mixture, MDMA and its metabolites presented a different toxicity profile, compared to each compound alone, even at equimolar concentrations. Intracellular Ca^{2+} raises, increased formation of reactive oxygen species and *de novo* synthesis of GSH were also associated with the toxic effects triggered by this mixture in SH-SY5Y differentiated cells.

The neuronal integrity and functionality are dependent upon the proper maintenance of a healthy mitochondrial population, through fusion/fission events, and efficient distribution of functional mitochondria. Therefore, the effects of MDMA on mitochondrial dynamics were also investigated. MDMA, at a non-cytotoxic concentration, dramatically impaired axonal transport of mitochondria in hippocampal neurons, in a time-dependent manner, which was acompanied by an increase in intracellular Ca^{2+} levels, both in the cell body and neuronal extensions. MDMA's mitochondrial trafficking phenotype relied on Miro1-independent mechanisms, but was mainly dependent on Tau protein phosphorylation by glycogen synthase 3β. Notably, impaired mitochondrial movement was also observed for the non-cytotoxic mixture of MDMA and its metabolites. The mitochondrial trafficking deficits triggered either by MDMA or by the mixture of MDMA and its metabolites were linked to increased mitochondrial fragmentation, and largely depended on mitofusin 2 and dynamin-related protein 1 functions, thus supporting a role for fusion/fission events in the mitochondrial trafficking phenotype regulated by MDMA.

In conclusion, the studies included in this thesis allowed to increase the understanding about the cellular and molecular targets of MDMA and its metabolites at neuronal level, with remarkable focus on mitochondrial-dependent pathways, providing, therefore, an important headway in the MDMA's neurotoxicity field.

Keywords

3,4-Methylenedioxymethamphetamine (MDMA; "ecstasy"); MDMA metabolites; Mitochondrial trafficking; Oxidative stress; Neurotoxicity.

Ecstasy's neurotoxicity: *in vitro* findings from mitochondria to the cell

Resumo

A 3,4-metilenodioximetanfetamina (MDMA; "ecstasy"), uma substância psicoativa com propriedades alucinogénias, é uma das principais drogas de abuso a nível mundial com efeitos neurotóxicos de curta e longa duração bem documentados, os quais têm sido observados em modelos animais de laboratório e em humanos Apesar da elevada quantidade de estudos realizados por diversos grupos de investigação diferentes, ao longo de vários anos, os mecanismos subjacentes à neurotoxicidade induzida pela MDMA ainda não estão completamente elucidados. Os estudos apresentados nesta tese têm como objetivo contribuir para uma melhor compreensão das bases mecanísticas a nível molecular e celular subjacentes à neurotoxicidade da MDMA. Assim, através do uso de diferentes abordagens e diferentes modelos neuronais *in vitro*, o papel do metabolismo, dos neurotransmissores monoaminérgicos e da hipertermia foi estudado, com especial destaque para vias dependentes da mitocôndria.

Em sinaptossomas de cérebro de murganho, os metabolitos da MDMA e os neurotransmissores monoaminérgicos induziram a formação de peróxido de hidrogénio (H_2O_2) de uma forma dependente do tempo e da concentração, a qual foi independente do estado de polarização mitocondrial e parcialmente atenuada por antioxidantes. O metabolismo mediado pela monoamina oxídase também contribuiu para a produção de H_2O_2 induzida pelos neurotransmissores serotonina e dopamina. O efeito tóxico envolveu modificações oxidativas, tais como peroxidação lipídica, carbonilação proteica e formação de quinoproteínas. Adicionalmente, os metabolitos da MDMA e os neurotransmissores monoaminados estimularam a actividade da adenosina 5'-trifosfatase activada pelo Na^+ e pelo K^+ (Na^+/K^+ ATPase), de uma maneira dependente da concentração, um efeito também parcialmente atenuado pelo antioxidante *N*-acetilcisteína (NAC).

Em células SH-SY5Y diferenciadas, os metabolitos da MDMA induziram disfunção mitocondrial e morte celular de uma maneira dependente da concentração, a qual foi diferentemente afetada pelo tempo e pela temperatura de exposição. Os percursores catecólicos α-metildopamina e *N*-metil-α-metildopamina revelaram ser menos tóxicos que os seus correspondentes monoconjugados com a glutationa reduzida (GSH) ou com a NAC. Como observado no modelo sinaptossoma, a MDMA, na gama de concentrações testada, não revelou toxicidade significativa. Os metabolitos da MDMA não atingiram elevadas concentrações no compartimento intracelular e a sua concentração no meio de cultura diminuiu ao longo do tempo, um efeito potenciado pela hiperthermia. No mesmo modelo experimental, a mistura de MDMA e seus metabolitos, numa gama de

concentrações com notável relevância para o cenário *in vivo*, induziu toxicidade de uma forma dependente do tempo e da temperatura de exposição, a qual foi totalmente prevenida pelo antioxidante NAC e acompanhada pela ativação da caspase 3. Notavelmente, como uma mistura, a MDMA e os seus metabolitos apresentaram um diferente perfil de toxicidade, comparativamente à toxicidade observada para cada composto isoladamente, em concentrações equimolares. Um aumento nos níveis intracelulares de Ca^{2+}, formação aumentada de espécies reativas de oxigénio e síntese *de novo* de GSH foram também associados com os efeitos tóxicos induzidos por esta mistura em células SH-SY5Y diferenciadas.

A integridade e funcionalidade neuronais estão dependentes da manutenção de uma população de mitocôndrias saudáveis, através de eventos de fusão/fissão, e de uma eficiente distribuição das mitocôndrias funcionais. Por esse motivo, os efeitos da MDMA na dinâmica mitocondrial foram também estudados. A MDMA, numa concentração não citotóxica, comprometeu significativamente o transporte axonal de mitocôndrias em neurónios do hipocampo, de uma forma dependente do tempo, o qual foi acompanhado por um aumento dos níveis intracelulares de Ca^{2+}, tanto no corpo celular como nas extensões neuronais. O fenótipo de tráfego mitocondrial induzido pela MDMA envolveu mecanismos independentes da proteína Miro1, dependendo, no entanto, da fosforilação da proteína Tau pela sintetase 3β do glicogénio. Notavelmente, uma diminuição da mobilidade mitocondrial foi também observada para a mistura não citotóxica de MDMA e seus metabolitos. Os défices de tráfego mitocondrial provocados quer pela MDMA, quer pela mistura de MDMA e seus metabolitos, foram associados a uma aumentada fragmentação mitocondrial, e dependeram largamente das funções da mitofusina 2 e da proteína 1 relacionada com a dinamina, sustentando, assim, um papel para os eventos de fusão/fissão no fenótipo de tráfego mitocondrial regulado pela MDMA.

Em conclusão, os estudos incluídos nesta dissertação permitiram aumentar a compreensão sobre os alvos moleculares e celulares da MDMA e dos seus metabolitos a nível neuronal, com especial destaque para vias dependentes da mitocôndria, proporcionando assim progressos importantes no âmbito da neurotoxicidade da MDMA.

Palavras-chave

3,4-Metilenodioximetanfetamina (MDMA; “ecstasy”), Metabolitos da MDMA; Tráfego mitocondrial; Stresse oxidativo; Neurotoxicidade.

Index

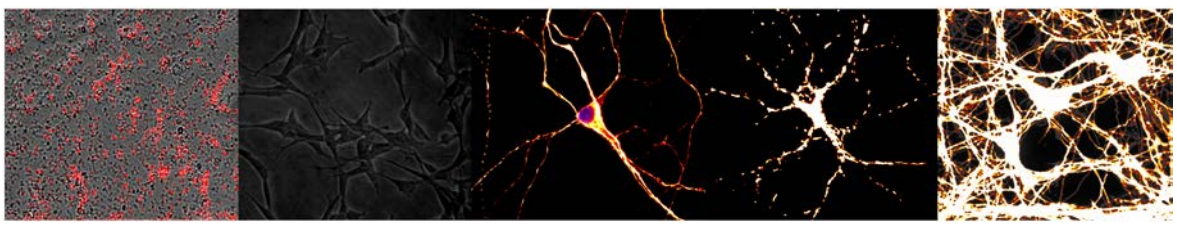


Table of Contents

Publications ..... **xv**

Acknowledgements ..... **xix**

Abstract ..... **xxv**

Keywords ..... **xxvi**

Resumo ..... **xxvii**

Palavras-chave ..... **xxviii**

Table of Contents ..... **xxxi**

Index of Figures ..... **xxxv**

Index of Tables ..... **xxxvii**

Abbreviations List ..... **xli**

Outline of the Thesis ..... **xlvii**

Chapter I **1**

I.1 General Introduction 5

I.1.1 Neurotoxicity 7

I.1.1.1 MDMA's neurotoxicity 9

I.1.1.1.1 MDMA and the monoaminergic system: implications on drug´s neurotoxicity 12

I.1.1.1.2 The role of metabolism on MDMA's neurotoxicity 16

I.1.1.1.3 The role of hyperthermia on MDMA's neurotoxicity 20

I.1.2 Neurotoxicity assessment 26

I.1.2.1 Use of *in vitro* systems in evaluating neurotoxicity 27

I.1.2.1.1 Advantages and limitations in using *in vitro* systems for neurotoxicity assessment 28

I.1.2.1.1.1 Acess to the cellular environment 30

I.1.2.1.1.2 Toxicokinetics 30

I.1.2.1.1.3 Exposure time 33

I.1.2.1.1.4 Lack of cellular homeostatic mechanisms 34

I.1.2.1.1.5 Multiple interspecies comparisons 35

I.1.2.1.1.6 Heterogeneity of the nervous system 35

I.1.2.1.2 Use of *in vitro* systems for mechanistic studies 37

I.1.2.1.3 Use of *in vitro* systems for neurotoxicity screening 38

I.1.2.2 Types of *in vitro* systems for neurotoxicity assessment 42
I.1.2.2.1 Uses and limitations of *in vitro* models 43
I.1.2.2.2 Subcellular systems 44
I.1.2.2.2.1 Synaptosomes 44
I.1.2.2.3 Cellular systems 47
I.1.2.2.3.1 Immortalized cell lines 48
I.1.2.2.3.1.1 Cell lines of neuronal origin 50
I.1.2.2.3.1.1.1 Neuroblastoma cell lines 50
I.1.2.2.3.1.1.1.1 SY-SY5Y cells: a human neuroblastoma cell line 51
I.1.2.2.3.2 Primary cultures 55
I.1.2.2.3.2.1 Dissociated primary cultures 55
I.1.2.2.3.2.1.1 Neuronal primary cultures 57
I.1.2.2.3.2.1.1.1 Hippocampal primary cultures 59
I.1.3 The pivotal role of mitochondria in neurons 62
I.1.4 Mitochondrial transport in neurons 64
I.1.4.1 Motor proteins 66
I.1.4.1.1 Kinesin motors 66
I.1.4.1.1.1 Adaptor proteins for kinesin motors 67
I.1.4.1.2 Dynein motors 69
I.1.4.1.3 Myosin motors 70
I.1.4.2 Regulation of mitochondrial transport 71
I.1.4.2.1 Regulation of mitochondrial transport by cytosolic Ca^{2+} 72
I.1.4.2.2 Regulation of mitochondrial transport by microtubule-associated proteins… 74
I.1.4.2.3 Regulation of mitochondrial transport by phosphatase and tensin homolog-induced putative kinase 1/Parkin 76
I.1.4.2.4 Other regulators of mitochondrial transport 76
I.1.4.2.4.1 Mitochondrial Ca^{2+} 77
I.1.4.2.4.2 Mitofusin 2 77
I.1.4.2.4.3 Serotonin and Dopamine 78
I.1.4.2.4.4 Histone deacetylases 78
I.1.4.2.4.5 Adenosine 5’-diphosphate/adenosine 5’-triphosphate 79
I.1.4.2.4.6 Nitric oxide 80
I.1.4.2.4.7 Nerve growth factor 80
I.1.4.2.4.8 Proteins of the Armcx family 80
I.1.4.2.4.9 Hypoxia up-regulated mitochondrial movement regulator and β *O*-linked *N*-acetylglucosamine transferase 81

I.1.4.2.4.10 RhoA/lysophosphatidic acid 81
I.1.5 Mitochondrial fusion/fission 83
I.1.5.1 Mitochondrial fusion 83
I.1.5.2 Mitochondrial fission 84
I.1.6 Interplay between mitochondrial fusion/fission and transport 88
I.2 Main Goals of the Thesis 93

Chapter II 95
II.1 Manuscript 1 97
II.2 Manuscript 2 117
II.3 Manuscript 3 139
II.4 Manuscript 4 173
II.5 Manuscript 5 195
II.6 Manuscript 6 219

Chapter III 247
III.1 Integrated Discussion 251
III.1.1 Studies in mouse brain synaptosomes 251
III.1.2 Studies in SH-SY5Y differentiated cells 255
III.1.3 Studies in cultured hippocampal neurons 262
III.2 Main Conclusions 273

Chapter IV 275
IV.1 References 279

Index of Figures

Figure 1. Pharmacological mechanism of action of MDMA at the neuronal serotonergic terminal and synapse. 13

Figure 2. Major pathways of MDMA metabolism. 17

Figure 3. Representative images of synaptosomes with their mitochondria labeled with tetramethylrhodamine methyl ester (TMRM). 44

Figure 4. Brightfield images of SH-SY5Y cells in their undifferentiated state or after differentiation with RA/TPA (3 days with 10 µM RA followed by additional 3 days with 80 nM TPA). 53

Figure 5. Hippocampal primary cells isolated from mouse embryos at embryonic day (E) 16. 60

Figure 6. Mitochondrial transport in neurons. 65

Figure 7. Primary structure of Miro protein. 67

Figure 8. Models of Miro as a Ca^{2+} sensor in regulating mitochondrial motility. 73

Figure 9. Mitochondrial fusion. 84

Figure 10. Mitochondrial fission. 85

Figure 11. Cellular and physiological roles of mitochondrial fusion/fission. 89

Figure 12. Mitochondrial fusion, fission and transport in neurons. 263

Figure 13. Postulated mechanisms for the mitochondrial trafficking impairment induced by MDMA in hippocampal neurons. 268

Index of Tables

Table 1. Advantages and limitations in using *in vitro* neuronal systems for neurotoxicological studies. 29

Table 2. Characteristics of synaptosomes. 45

Table 3. Advantages and limitations in using synaptosomes as *in vitro* model for neurotoxicological studies. 46

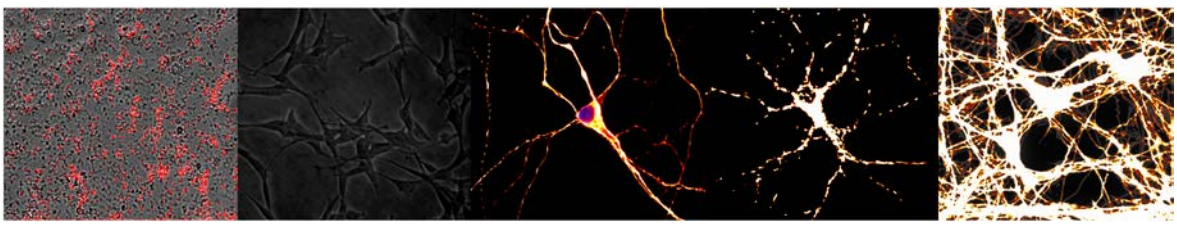
Table 4. Advantages and limitations in using immortalized cell lines as *in vitro* models for neurotoxicological studies. 49

Table 5. Characteristics of the SH-SY5Y cell line. 52

Table 6. Advantages and limitations in using dissociated primary cultures as *in vitro* models for neurotoxicological studies. 57

Table 7. Characteristics of hippocampal primary cultures. 61

Abbreviations List



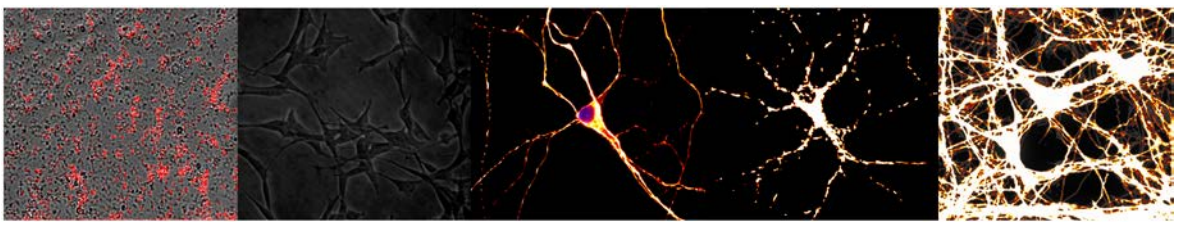
Abbreviations List

2,5-(GSH)-α-MeDA	2,5-bis(glutathion-*S*-yl)-α-methyldopamine
5-(GSH)-α-MeDA	5-(glutathion-*S*-yl)-α-methyldopamine
5-(GSH)-N-Me-α-MeDA	5-(glutathion-*S*-yl)-*N*-methyl-α-methyldopamine
5-HIAA	5-hydroxyindoleacetic acid
5-HT	serotonin, 5-hydroxytryptamine
5-HT$_{2A}$	serotonin 2A receptor
5-HTT	serotonin transporter
5-(NAC)-α-MeDA	5-(*N*-acetylcysteine-*S*-yl)-α-methyldopamine
5-(NAC)-N-Me-α-MeDA	5-(*N*-acetylcysteine-*S*-yl)-*N*-methyl-α-methyldopamine
ACh	acetylcholine
ADP	adenosine 5'-diphosphate
Akt	protein kinase B
AMPT	α-methyl-*p*-tyrosine
ATP	adenosine 5'-triphosphate
ATPase	adenosine 5'-triphosphatase
BBB	blood-brain barrier
BDNF	brain-derived neurotrophic factor
CMT2A	Charcot-Marie-Tooth neuropathy 2A
CNS	central nervous system
CSF	cerebrospinal fluid
CTX	cortex
CYP450	cytochrome P450
DAT	dopamine transporter
DNA	deoxyribonucleic acid
Drp1	dynamin-related protein 1
E	embryonic day
ETC	electron transport chain
FEZ1	fasciculation and elongation protein-ζ1
Fis1	mitochondrial fission protein 1
GABA	gamma-aminobutyric acid
GLU	glutamate
GSK3β	glycogen synthase 3β
γ-GT	γ-glutamyltransferase
GTP	guanosine 5'-triphosphate
GTPase	guanosine 5'-triphosphatase

H_2O_2	hydrogen peroxide
HDAC	histone deacetylase
HIP	hippocampus
i.c.v.	intracerebroventricular
i.p.	intraperitoneal
L-Dopa	*L*-3,4-dihydroxyphenylalanine
$\Delta\Psi_m$	mitochondrial membrane potential
MAO	monoamine oxidase
MAP	microtubule-associated protein
MDA	3,4-methylenedioxyamphetamine
MDMA	3,4-methylenedioxymethamphetamine; “ecstasy”
α-MeDA	α-methyldopamine
Mff	mitochondrial fission factor
Mfn	mitofusin
MIEF1	mitochondrial elongation factor 1
MK-801	dizocilpine
MPP^+	*N*-methyl-4-phenylpyridinium ion
MPTP	1-methyl-4-phenyl-1,2,3,6-tetrahydropyridine
MRP	multidrug resistance protein
mtDNA	mitochondrial deoxyribonucleic acid
MTT	3-[4,5-dimethylthiazol-2-yl]-2,5-diphenyltetrazolium
NA	noradrenaline
Na^+/K^+ ATPase	Na^+- and K^+-activated adenosine 5’-triphosphatase
NAC	*N*-acetylcysteine
NAT	noradrenaline transporter
NFs	neurofilaments or intermediate filaments
NGF	nerve growth factor
NMDA	*N*-methyl-*D*-aspartate
N-Me-α-MeDA	*N*-methyl-α-methyldopamine
NO	nitric oxide
NPY	neuropeptide Y
NSE	neuron-specific enolase
OGT	β *O*-linked *N*-acetylglucosamine transferase
OPA1	optic atrophy 1
PINK1	phosphatase and tensin homolog-induced putative kinase 1
RA	retinoic acid
RanBP2	RAN-binding protein 2

RNA	ribonucleic acid
ROS	reactive oxygen species
s.c.	subcutaneous
TH	tyrosine hydroxylase
TMRM	tetramethylrhodamine methyl ester
TPA	12-*O*-tetradecanoylphorbol-13-acetate
VMAT	vesicular monoamine transporter

Outline of the Thesis



Outline of the Thesis

This thesis was divided into four main chapters:

► **Chapter I - General Introduction and Main Goals of the Thesis**

In chapter I, a review of the existing literature about (1) “ecstasy”-induced neurotoxicity, (2) *in vitro* neurotoxicity testing and (3) mitochondrial fusion/fission and transport in neurons are presented, to provide a good basis to a better understanding of the obtained results in the scope of this thesis. Finally, the end of this chapter includes the main goals of the thesis.

► **Chapter II - Experimental Section, Results and Partial Discussions**

This chapter includes the manuscripts published or submitted for publication, as well as a manuscript under preparation, designed in the scope of this thesis.

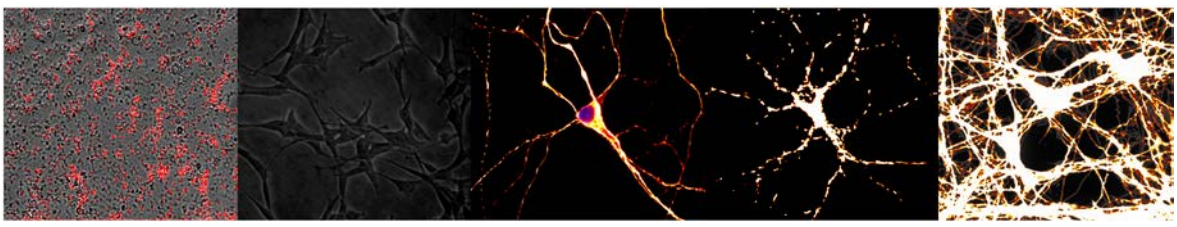
► **Chapter III - Integrated Discussion and Main Conclusions**

The third chapter integrates all the results obtained, as well as their relevance on “ecstasy”’s neurotoxicity. In the end, a list of the main conclusions that can be taken from the studies included in this thesis are summarized.

► **Chapter IV - References**

The last chapter lists all the references of the literature used in the general introduction and integrated discussion.

Chapter I



General Introduction

I.1 General Introduction

The recreational use of stimulant, entactogenic or psychoactive drugs, such as amphetamine-like compounds, namely 3,4-methylenedioxymethamphetamine (MDMA; “ecstasy”), is an important health risk factor (Kalant, 2001; Capela *et al.*, 2009; Hill and Thomas, 2011; Carvalho *et al.*, 2012). MDMA is a powerful hallucinogenic drug, which has raised concern worldwide because of its high abuse liability. Moreover, a plethora of studies have demonstrated that MDMA has the potential to induce neurotoxicity, both in laboratory animals (Stone *et al.*, 1987; O'Hearn *et al.*, 1988; Hatzidimitriou *et al.*, 1999; Bai *et al.*, 2001; Cadet *et al.*, 2001; Granado *et al.*, 2008; Granado *et al.*, 2011) and humans (McCann *et al.*, 1994; Quednow *et al.*, 2006; Roberts *et al.*, 2009; Adamaszek *et al.*, 2010; Tai *et al.*, 2011; Parrott, 2012), as documented by several studies conducted in human MDMA users. Though limited in scope, studies in MDMA users have shown that MDMA has the potential to induce neuronal injury in discrete areas of the brain, such as cortex (CTX), hippocampus (HIP), striatum and *raphe nuclei* (Quednow *et al.*, 2006; Capela *et al.*, 2009; Adamaszek *et al.*, 2010; Tai *et al.*, 2011; Carvalho *et al.*, 2012; Parrott, 2012), additionally to the reduction of several serotonergic biochemical markers (McCann *et al.*, 1994; Parrott, 2012; Schouw *et al.*, 2012). Studies comparing “ecstasy” users and nonusers support an association between long-lasting neurocognitive impairments, including learning and memory deficits and mood disturbances, and “ecstasy” use (Quednow *et al.*, 2006; Roberts *et al.*, 2009; Adamaszek *et al.*, 2010; Tai *et al.*, 2011; Di Iorio *et al.*, 2012). Furthermore, MDMA shares the common trait that is rewarding, which is generally accompanied by a state of addiction and dependence to the drug after repeated exposure (Büttner, 2011). Research on the neurobiology of drug addiction has shown that the reinforcing properties associated with drug abuse are mainly mediated by activation of HIP (Fernàndez-Castillo *et al.*, 2012), the mesolimbic dopaminergic system and the extended amygdala (Hyman *et al.*, 2006; Nakagawa and Kaneko, 2008; Koob and Volkow, 2009). In fact, many lines of evidence suggest that chronic MDMA consumption leads to the enhancement of the mesocorticolimbic dopaminergic neurons from the ventral tegmental area to the *nucleus accumbens* and the medial prefrontal CTX. The neural adaptation of dopaminergic-glutamatergic system is considered to be critically implicated in neuropsychotoxic effects of this drug of abuse (Nakagawa and Kaneko, 2008).

Emerging studies in the MDMA’s research field have emphasize a promising role to monoaminergic system, metabolism and hyperthermia in developing neurotoxic actions (Alves *et al.*, 2007; Capela *et al.*, 2007b; Alves *et al.*, 2009b; Capela *et al.*, 2009; Carvalho *et al.*, 2012), in which mitochondrial-dependent pathways have been suggested as key players (Quinton and Yamamoto, 2006; Alves *et al.*, 2007; Alves *et al.*, 2009b; Puerta *et*

al., 2010). However, it is reasonable to note that the truly acute- and long-lasting neuronal effects of MDMA exposure remain largely unknown. Despite this, the understanding of the mechanisms involved in MDMA-induced neurotoxic actions is extremely important, not only in addressing the brain targets of MDMA's action, but also to develop putative treatments for the drug abuse and toxicity in humans. Thus, to a better integration and understanding of the studies performed in the scope of this thesis, in the introduction section we provide an overview of the following subjects:

► Neurotoxicity of "ecstasy", with special focus on the role of the monoaminergic system, metabolism and hyperthermia;

► *In vitro* neurotoxicity assessment, including the main advantages and limitations and models, with particular attention to the systems used in our studies (synaptosomes, SH-SY5Y differentiated cells and cultured hippocampal neurons);

► Mitochondrial dynamics, which, being critical for proper neuronal functioning and survival, may constitute an important target in developing neurotoxicity.

Thus, this background allows a harmonious integration of the studies included in this thesis, as highlighted by its title: "Ecstasy's neurotoxicity: *in vitro* findings from mitochondria to the cell".

I.1.1 Neurotoxicity

Neurotoxicity can be defined as any adverse effect on the chemistry, structure or function of the nervous system, during development or at maturity, induced by chemical, biological or physical influences (Costa, 1998a). A large number of compounds have been shown to cause neurotoxicity, including metals (e.g. lead) (Baranowska-Bosiacka *et al.*, 2013), industrial chemicals (e.g. acrylamide) (Erkekoglu and Baydar, 2013), solvents (e.g. toluene) (Win-Shwe and Fujimaki, 2010), natural toxins (e.g. domoic acid) (Hogberg and Bal-Price, 2011), pharmaceutical drugs (e.g. doxorubicin) (Pal *et al.*, 2012), drugs of abuse (e.g. MDMA) (Capela *et al.*, 2009) and pesticides (e.g. organophosphates) (Flaskos, 2012). The nervous system is particularly sensitive to toxic insults because of a number of intrinsic characteristics, such as dependence upon aerobic metabolism, the presence of axonal transport, or the processes of neurotransmission (Moser *et al.*, 2010). In addition, the developing nervous system, during which replication, migration, differentiation and myelination of neurons and synapse formation occur, is believed to be even more susceptible to neurotoxic chemicals. This is aggravated by the lack of a fully developed blood-brain barrier (BBB). A neurotoxic effect can be the direct alteration of the neuronal structure or activity or can be the result of a cascade of effects due to glia activation and glia-neuron interactions. Additionally, a neurotoxic effect can manifest immediately or only years later after the substance exposure, it can be permanent or reversible, and it can affect the whole nervous system, or only parts of it (Tabakman *et al.*, 2004; Coecke *et al.*, 2006; Moser *et al.*, 2010).

From a general mechanistic perspective, neurotoxicants can be divided into four groups: those which cause neuronopathies, those which target the axon and cause axonopathies, those inducing myelopathies, and those affecting neurotransmission (Costa, 1998a). A number of chemicals may cause toxicity that result in the loss of neurons (neuronopathy), either by necrosis or by apoptosis. Such neuronal loss is irreversible, and may result in a global encephalopathy or, whether only subpopulations of neurons are affected, in the loss of particular functions. An example is 1-methyl-4-phenyl-1,2,3,6-tetrahydropyridine (MPTP), which causes degeneration of dopaminergic neurons, resulting in Parkinson's disease-like symptoms (Yuan *et al.*, 2013a), or trimethyltin, which targets hippocampal, amygdala and pyriform cortical neurons, resulting in cognitive impairment (Feldman *et al.*, 1993). Chemicals can cause neuronal cell death by a variety of mechanisms, including disruption of the cytoskeleton, induction of oxidative stress, Ca^{2+} overload, or by damaging mitochondria. A large number of neurotoxic chemicals mainly target the axon, and cause axonopathies. The axon degenerates, and with it the myelin sheath surrounding the axon. In this case, the cell body remains intact. Additionally, the

chemical may cause a chemical section of the axon at some point along its length, and the axon distal to the section, which is separated from the cell body, degenerates. The result is most often the clinical condition of peripheral neuropathy, in which sensations and motor strength are first impaired in feet and hands. If the insult is not severe, there is good potential for regeneration and recovery (Moser *et al.*, 2010). An example of chemical that causes axonopathy is the solvent n-hexane (Graham *et al.*, 1995). Other chemicals may target myelin, causing intramyelinic edema or demyelination. While neurons are structurally unaffected, their functions are altered. Triethyltin (Stahnke and Richter-Landsberg, 2004) and hexachlophene (Amacher and Schomaker, 1994) are examples of chemicals that cause intramyelinic edema, leading to the formation of vacuoles and spongiosis in the brain. Finally, there are neurotoxicants that interfere with neurotransmission (Costa, 1988; Moser *et al.*, 2010). They can inhibit the release of neurotransmitters, such as the botulin toxin, which inhibits acetylcholine (ACh) release, act as agonist or antagonist of specific receptors, such as the marine neurotoxin domoic acid, which activates a subtype of glutamate (GLU) receptors, or atropine, which blocks muscarinic receptors, thus interfering with signal transduction processes. These effects are usually reversible, but nevertheless of toxicological relevance, as they may lead to severe acute toxicity or death (Costa, 1998b; Tilson *et al.*, 1998).

I.1.1.1 MDMA's neurotoxicity

The potential neurotoxic risk associated with MDMA use has received particular attention following a study published in 1986, in which Schmidt and co-workers (Schmidt *et al.*, 1986) reported damage to serotonergic system after MDMA administration to rats. Following this study, data from both neurochemical and functional studies have clearly demonstrated widespread and long-lasting degeneration of the serotonergic neuronal system, without any major or consistent effects on catecholaminergic neurons, after *in vivo* administration of MDMA, both in rats and non-human primates (O'Hearn *et al.*, 1988; Hatzidimitriou *et al.*, 1999; Bai *et al.*, 2001). Though deficits on the serotonergic system is the most studied neurotoxic event associated with MDMA, several reports emphasize that MDMA-induced neuronal injury is observed in other brain areas. In fact, studies that analyzed the location of MDMA-induced neuronal degeneration throughout the entire rat brain have reported neuronal deficits in different brain areas, such as parietal CTX, insular/perirhinal CTX, ventromedial/ventrolateral thalamus and the *tenia tecta* (Commins *et al.*, 1987; Schmued, 2003; Armstrong and Noguchi, 2004; Tamburini *et al.*, 2006; Warren *et al.*, 2007). Similar to rats, in non-human primates, serotonergic depletion and neuronal injury after exposure to MDMA is well documented (Ali *et al.*, 1993; Fischer *et al.*, 1995; Hatzidimitriou *et al.*, 1999). In this experimental laboratory animal, other studies have demonstrated a dose-dependent reduction of the serotonin (5-HT) content in several brain areas, such as CTX, *caudate nucleus*, *putamen*, HIP, hypothalamus, and thalamus (Ricaurte *et al.*, 1988b). Interestingly, non-human primates appear to be much more vulnerable to the neurotoxic actions of MDMA, since their 5-HT nerve endings were found to degenerate if only 1/10 of the MDMA-dose required to produce degenerative effects in rats was given (Ricaurte and McCann, 1992). Moreover, the route of drug administration also seems to largely affect the degree of serotonergic neurotoxicity. Oral administration has been reported to be less toxic than subcutaneous (s.c.) injection. MDMA administration to non-human primates in a dose of 5 mg/kg, twice daily, for four consecutive days, produced 86% depletion of 5-HT content in the frontal CTX when given by s.c. injection, compared with 42% depletion when given orally (Ricaurte *et al.*, 1988a). Monkeys seem to be very susceptible towards MDMA's neurotoxicity. Since a single 5 mg/kg oral dose in monkeys has been proposed to be equivalent to a 1.4 mg/kg dose in a 70 kg human, based on interspecies dose scaling, these data may indicate a possible risk of serotonergic damage in humans even after a single dose (Ricaurte *et al.*, 1988a; Ricaurte *et al.*, 2000). Additionally, plasmatic levels of MDMA in squirrel monkeys were highly correlated with regional brain 5-HT deficits observed two weeks after administration (2.4 to 6.4 mg/kg, oral, three times, at 3-h intervals) (Mechan *et al.*, 2005). Therefore,

these observations indicate that the plasmatic concentrations of MDMA shown to produce long-lasting serotonergic deficits in squirrel monkeys, overlap those reported by other research groups in some recreational “ecstasy” users and are two to three times higher than those found in humans administrated with a single dose of MDMA (100 to 150 mg) in a controlled setting (Mechan *et al.*, 2005).

Unlike rats and non-human primates, the mice model, which corresponds to a regular experimental animal model, has proven to be a notable exception regarding the pattern of MDMA-induced neurotoxicity. In mice, MDMA presents a different toxicity profile, producing essentially dopaminergic neurotoxicity in contrast to serotonergic neurotoxicity observed in rats or non-human primates. Though several brain areas may be affected, MDMA administration to mice particularly results in long-term degeneration of striatal dopaminergic nerve terminals (Stone *et al.*, 1987; Cadet *et al.*, 2001; O'Shea *et al.*, 2001; Johnson *et al.*, 2004; Granado *et al.*, 2008; Granado *et al.*, 2011). However, depending on the MDMA dosage and mouse strain, it can cause dual dopaminergic/serotonergic neurotoxicity (Fornai *et al.*, 2001; Itzhak *et al.*, 2003; Fornai *et al.*, 2004). Mice administrated with MDMA [2 x 50 mg/kg, intraperitoneal (i.p.), 2h apart] presented, 1 week later, both 5-HT and dopamine depletion in several brain regions, namely cerebellum, frontal CTX, HIP, striatum, hypothalamus, and *substantia nigra* (Fornai *et al.*, 2001). A neurotoxic regimen of MDMA (2 x 15 mg/kg, i.p., 8h apart, for 2 days) in Swiss-Webster mice was shown to cause marked depletion of striatal dopamine and dopamine transporter (DAT)-binding sites, as well as depletion of striatal and hippocampal 5-HT, and depletion of serotonin transporter (5-HTT) binding sites in the frontal CTX. Additionally, the depletion of striatal DAT and frontocortical 5-HTT binding sites in mice was demonstrated to be long-lasting, as it was observed 82 days following exposure to MDMA (2 x 15 mg/kg, i.p., 8h apart, for 2 days or 2 x 30 mg/kg, i.p., 8h apart) (Itzhak *et al.*, 2003).

In humans, MDMA-associated neuronal deficits have also been documented (McCann *et al.*, 1994; Quednow *et al.*, 2006; Roberts *et al.*, 2009; Adamaszek *et al.*, 2010; Parrott, 2012). In a post-mortem study performed in a 26-year-old male, who had taken MDMA regularly for 9 years, it was observed severe depletions (50-80%) of striatal 5-HT and 5-hydroxyindoleacetic acid (5-HIAA, 5-HT metabolite) (measured 21 h post-mortem). However, the subject studied had also taken cocaine and heroin before his death. Therefore, since none of these drugs has previously been demonstrated to alter striatal 5-HT concentration, it was suggested that this effect was most likely due to chronic use of MDMA, rather than cocaine or heroin (Kish *et al.*, 2000). Other studies, evaluating the long-lasting effects of MDMA on serotonergic neurotransmission in humans, demonstrated that recreational MDMA users (intake of MDMA more than 25 times) presented lower levels of 5-HIAA in the cerebrospinal fluid (CSF), compared to control

subjects. Furthermore, this effect was more pronounced in females rather than in males (46 and 20% of reduction, respectively). Also, there was no correlation between CSF 5-HIAA levels and the duration or frequency of MDMA use (McCann *et al.*, 1994; McCann *et al.*, 1999). Additionally, gray matter reduction in the neocortical, bilateral cerebellum and midline brainstem brain regions was shown in MDMA users, potentially accounting for previously reported neuropsychiatric impairments in MDMA users (Cowan *et al.*, 2003).

Studies performed by positron emission tomography found a lower density of brain 5-HTT sites in MDMA users (McCann *et al.*, 2008) and reduced 5-HTT activity following MDMA exposure (Thomasius *et al.*, 2006). Additionally, there are indications that the observed 5-HTT reductions play a role in memory deficits in individuals with a history of recreational MDMA use (McCann *et al.*, 2008). By single photon emission computed tomography it was also observed that human MDMA users have reductions in 5-HT binding sites (Reneman *et al.*, 2001). Another study, evaluating the effects of MDMA on cortical serotonin 2A (5-HT_{2A}) receptors, showed lower postsynaptic receptor density in all cortical areas studied in human MDMA users (Reneman *et al.*, 2002). Importantly, many studies have demonstrated that females are more sensitive to the MDMA neurotoxicity than human male subjects. Female MDMA users show higher depression scores than male users or male/female control subjects, several days after an acute dose of MDMA (Verheyden *et al.*, 2002). Furthermore, it was demonstrated lower brain 5-HTT density in female heavy MDMA users than in male heavy MDMA users or control subjects, which was not related to greater MDMA use (Reneman *et al.*, 2001). In addition to studies on brain serotonergic markers, several reports showed long-lasting impairments in memory and learning of human MDMA abusers, which persisted by a long time after cessation of drug use (McCann *et al.*, 1994; McCann *et al.*, 1996; Bolla *et al.*, 1998; McCann *et al.*, 1999; Gouzoulis-Mayfrank *et al.*, 2003; Zakzanis *et al.*, 2003; Jacobsen *et al.*, 2004; Quednow *et al.*, 2006; Schilt *et al.*, 2007). Verbal and visual memory have also been shown to be impaired by MDMA use and were related to the CSF concentration of 5-HIAA, thus indicating that serotonergic damage may be the cause of these deficits (Bolla *et al.*, 1998). In adolescence, MDMA use appears to be associated with cognitive impairments and dysfunction of inhibitory circuits in the HIP, thus indicating the particular vulnerability of this brain area to the MDMA's actions (Jacobsen *et al.*, 2004). Indeed, in heavy MDMA users, studies have indicated that the primary memory dysfunction, which is more associated with heavy "ecstasy" use rather than recreational use, may be related to a particularly high vulnerability of the HIP to the neurotoxic effects of MDMA (Gouzoulis-Mayfrank *et al.*, 2003).

In addition to studies conducted in experimental laboratory animals and human users, many *in vitro* studies have reported that MDMA could induce neuronal death in several

neuronal models, like cultured rat cortical (Capela *et al.*, 2006a; Capela *et al.*, 2006b; Capela *et al.*, 2007a; Capela *et al.*, 2007b), hippocampal (Capela *et al.*, 2013) or cerebellar granule neurons (Jiménez *et al.*, 2004), and SH-SY5Y differentiated cells (Ferreira *et al.*, 2013).

Despite the increase number of data relating the potential of MDMA to induce neuronal dysfunction and degeneration, the cellular and molecular mechanisms involved are still not completely understood at present. However, several factors are known to contribute to MDMA-induced neurotoxicity, namely inhibition of neurotransmitter synthesis (Schmidt and Taylor, 1987; Stone *et al.*, 1987; Arrue *et al.*, 2003), monoamine oxidase (MAO)-dependent metabolism of neurotransmitters (Alves *et al.*, 2007; Alves *et al.*, 2009b), over-stimulation of receptors (Schmidt *et al.*, 1990a; Capela *et al.*, 2006b), hyperthermia (Capela *et al.*, 2006a; Takamatsu *et al.*, 2011) and hepatic formation of reactive metabolites (Capela *et al.*, 2006a; Capela *et al.*, 2007b), among others. A common outcome of these factors is oxidative stress, which appears contribute to the pathogenesis of MDMA (Capela *et al.*, 2009; Carvalho *et al.*, 2012), though the relative contribution of each of these factors for the neurotoxic actions associated with MDMA remains to be elucidated.

I.1.1.1.1 MDMA and the monoaminergic system: implications on drug´s neurotoxicity

The brain consists of a network of neurotransmitter systems that execute complex brain functions. It is generally believed that MDMA's effects in the central nervous system (CNS) and peripheral nervous system (PNS) result from its action on the monoaminergic system. Though limited, both in non-human primates and humans, data obtained from laboratory animals, namely from rats, have demonstrated that MDMA acts mainly as an indirect monoaminergic agonist (Schmidt *et al.*, 1987). In this way, MDMA exposure is known to increase the extracellular brain levels of several neurotransmitters, both *in vivo* and *in vitro*. Detailed mechanisms of action of MDMA into the serotonergic terminal and synapse are represented in Figure 1. The best characterized effect of MDMA is the acute increase in brain levels of 5-HT and dopamine following drug exposure, which is observed both in humans and in laboratory animals (Baumann *et al.*, 2004; Capela *et al.*, 2009; Kehr *et al.*, 2011). In fact, initial studies showed that MDMA stimulates the efflux of pre-loaded 5-HT, [^{3}H]5-HT and, in a lesser extension [^{3}H]dopamine and dopamine, in rat brain (Johnson *et al.*, 1986; Schmidt *et al.*, 1987). Subsequent findings also revealed that MDMA interacts with monoamine transporters, thus stimulating non-excitotoxic release not only of 5-HT and dopamine, but also noradrenaline (NA) (Crespi *et al.*, 1997).

Neurotransmitter release occurs by two mechanisms: (1) neurotransmitter molecules exit the cell along their concentrations gradient via reversal of the function of neurotransmitter reuptake systems and, (2) cytoplasmic concentrations of neurotransmitters are increased due to drug-induced disruption of vesicular storage. An involvement of the 5-HTT on MDMA´s actions has been suggested by some studies, presumably by a inhibition and/or reversal mechanism, since the MDMA-induced release and depletion of 5-HT was suppressed *in vitro* by drugs that inhibit the 5-HTT activity (Rudnick and Wall, 1992; Crespi *et al.*, 1997; Verrico *et al.*, 2007) and *in vivo,* in 5-HTT knockout mice (Renoir *et al.*, 2008).

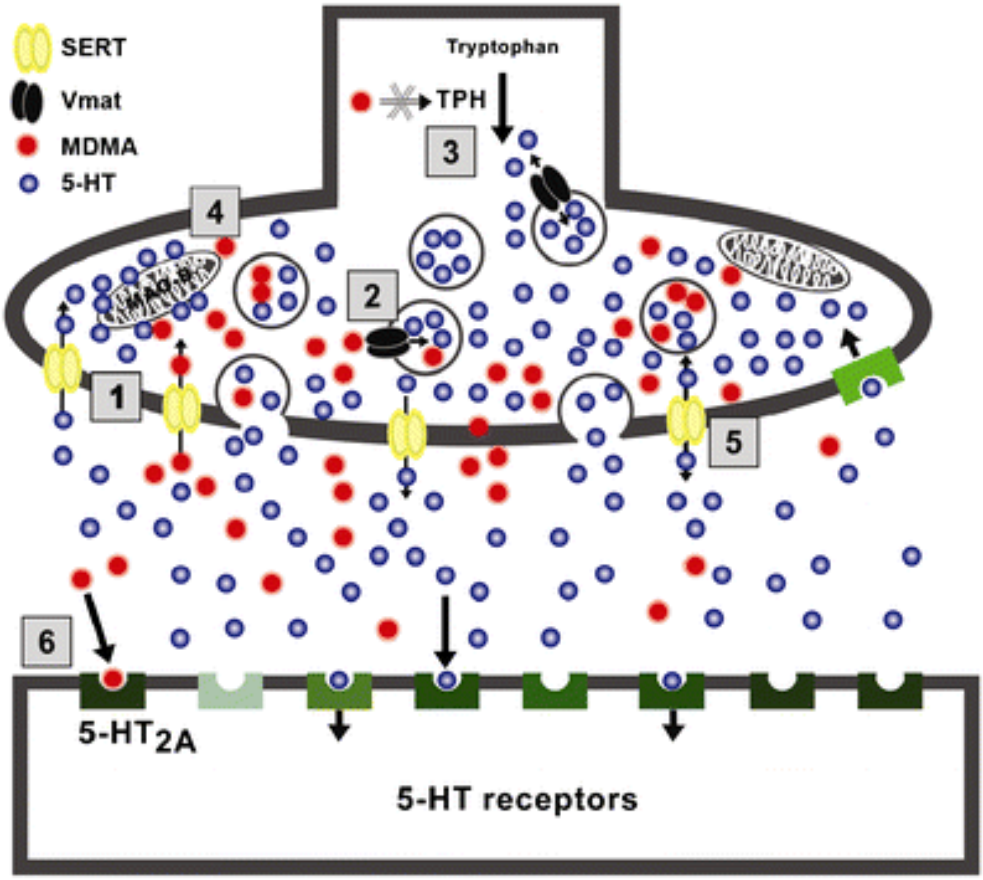


Figure 1. Pharmacological mechanism of action of MDMA at the neuronal serotonergic terminal and synapse. MDMA, such as serotonin (5-HT), is a substrate of the serotonin transporter (5-HTT), using the transporter to enter inside the presynaptic terminal (1), though at high concentration, it may also enter by diffusion. Inside of the presynaptic terminal, MDMA induces an acute and rapid release of 5-HT from the storage vesicles, possibly by entering the vesicles via the vesicular monoamine transporter (VMAT) and depletes vesicular neurotransmitter stores via a carrier-mediated exchange mechanism (2). MDMA also inhibits tryptophan hydroxylase (TPH), the rate-limiting enzyme for 5-HT synthesis (3). Monoamine oxidase (MAO)-B, which is located in the outer mitochondrial membrane, is involved on the 5-HT metabolism, being its activity partially inhibited by MDMA (4). As a result of the increased free cytoplasmic pool of 5-HT, MDMA promotes a rapid release of intracellular 5-HT to the neuronal synapse via reversal of the 5-HTT activity (5). The agonist activity on the serotonin 2A (5-HT_{2A}) receptor is involved in MDMA's hallucinogenic and neurotoxic properties (6). Scheme from (Capela *et al.*, 2009).

Data from microdialysis studies also indicate that MDMA enhances the release of 5-HT *in vivo* in numerous brain regions. Indeed, the administration of MDMA to rats has been reported to result in a dose-dependent increase in the extracellular 5-HT content in the striatum, HIP and CTX (Gough *et al.*, 1991; Gudelsky and Nash, 1996). Consistent with results from *in vitro* studies, inhibition of the 5-HTT with fluoxetine suppressed MDMA-induced 5-HT release *in vivo* (Gudelsky and Nash, 1996; Mechan *et al.*, 2002), thereby indicating that MDMA facilitates the transporter-mediated release of 5-HT. MDMA, acting as a substract of the vesicular monoamine transporter (VMAT), enters into the vesicles, through VMAT, and deplete the vesicular neurotransmitters storage, by reversion of the transporter activity (Mlinar and Corradetti, 2003; Partilla *et al.*, 2006). Inhibition or reversal of VMAT will increase cytosolic 5-HT levels, thereby possibly contributing to the MDMA-induced increase in extracellular 5-HT levels by 5-HTT reversal. Similarly, though in a lesser magnitude, it has been demonstrated that MDMA increases the extracellular dopamine content in several brain areas, such as striatum (Gudelsky and Nash, 1996; Nair and Gudelsky, 2004; Vanattou-Saïfoudine *et al.*, 2011), HIP (Shankaran and Gudelsky, 1998; Breier *et al.*, 2006), *nucleus accumbens* (Bankson and Yamamoto, 2004; Cadoni *et al.*, 2005; Amato *et al.*, 2006) and prefrontal CTX (Nair and Gudelsky, 2004; Pehek *et al.*, 2005).

By using voltamperometric studies, Yamamoto and Spanos (Yamamoto and Spanos, 1988) were the first to demonstrate, in rats, the potential of MDMA to induce dopamine release *in vivo*, an effect observed at behaviorally relevant doses (5-10 mg/kg). Though with a lower potency, MDMA also inhibits DAT and induces DAT reversal, thus increasing brain extracellular dopamine levels (Schmidt *et al.*, 1987; Nash and Brodkin, 1991; Verrico *et al.*, 2007). In this way, MDMA-induced increases in extracellular dopamine levels and serotonergic neurotoxicity was attenuated by the DAT inhibitors GBR 12909 and mazindol (Stone *et al.*, 1988; Shankaran *et al.*, 1999b). Though other studies indicate that vesicular dopamine release could also contribute to increased dopamine brain levels (Schmidt *et al.*, 1987; Nash and Brodkin, 1991), a direct effect of MDMA on vesicular dopamine secretion was not mechanistically demonstrated, since, in PC12 cells, MDMA inhibited dopamine exocytosis via indirect inhibition of Ca^{2+} influx (Hondebrink *et al.*, 2011).

In addition to its serotonergic and dopaminergic effects, MDMA also induces NA release due to inhibition and reversal of the noradrenaline transporter (NAT). Consequently, NA levels are increased following MDMA exposure, as revealed by human controlled studies (Rothman *et al.*, 2001; Hysek *et al.*, 2011). Notably, the stimulant effects of MDMA in humans were attenuated with the NAT inhibitor reboxetine (Hysek *et al.*, 2011), thus highlighting a role for NAT in MDMA-induced brain effects.

Apart from interferences on neurotransmitter reuptake systems, MDMA has also been reported to interfere with the synthesis and metabolism of neurotransmitters. The rate-limiting reaction in the 5-HT biosynthesis is the hydroxylation of tryptophan, which is catalyzed by tryptophan hydroxylase (TPH) (Roberts and Fitzpatrick, 2013). In rats, MDMA exposure was shown to decrease TPH activity within hours, which can last up to several weeks (Stone *et al.*, 1986; Schmidt and Taylor, 1987). Possibly, MDMA metabolites are involved in reducing TPH activity, since the decrease in TPH activity was not observed *in vitro* (Schmidt and Taylor, 1987). Therefore, as TPH is the rate-limitant enzyme involved in 5-HT biosynthesis, a decrease in enzyme activity may contribute to MDMA-induced 5-HT deficits.

Tyrosine hydroxylase (TH) is the rate-limiting enzyme in the biosynthesis of dopamine and NA. It converts *L*-tyrosine to *L*-3,4-dihydroxyphenylalanine (L-Dopa), which is posteriorly decarboxylated to dopamine by aromatic *L*-amino acid decarboxylase. Subsequently, dopamine is hydroxylated to NA by dopamine-β-hydroxylase (Meiser *et al.*, 2013). In rats, varying MDMA-induced effects on TH activity were observed, ranging from small decreases (Arrue *et al.*, 2003) to no effect (Stone *et al.*, 1986) or even increases (Nash *et al.*, 1990), thus suggesting that changes in TH activity may play a role in MDMA-mediated effects.

MAO is an enzyme of the outer mitochondrial membrane involved in the metabolism of neurotransmitters, such as 5-HT, dopamine or NA, which, in rat brain tissue, is reported to be partially inhibited by MDMA (Leonardi and Azmitia, 1994; Scorza *et al.*, 1997), thus contributing to the acute increase in extracellular levels of neurotransmitters observed after MDMA exposure. One of the major consequences of MAO metabolism is the generation of high levels of hydrogen peroxide (H_2O_2) (Alves *et al.*, 2007; Alves *et al.*, 2009b), which may contribute to the oxidative stress-related neuronal injury. Additionally, MAO metabolism of 5-HT and dopamine generates reactive aldehyde intermediates, such as 5-hydroxyindole-3-acetaldehyde (5-HIAL) and 3,4-dihydroxyphenylacetaldehyde (DOPAL), respectively, being the last described to contribute to MAO-related injury (Marchitti *et al.*, 2007). In this way, inhibition of MAO-B with deprenyl was shown to attenuate the MDMA-induced deleterious effects in rat brain mitochondria *in vivo* (Alves *et al.*, 2007). Furthermore, MDMA-induced serotonergic neurotoxicity in rats was also attenuated by MAO-B inhibition with deprenyl (Sprague and Nichols, 1995) and through the use of an antisense oligonucleotide targeted to MAO-B (Falk *et al.*, 2002). In addition, MAO-B knockout mice was shown to be protected against MDMA-induced serotonergic neurotoxicity, compared to wild-type animals (Fornai *et al.*, 2001), thus supporting a role for MAO in MDMA-induced neurotoxic effects.

I.1.1.1.2 The role of metabolism on MDMA's neurotoxicity

One of the notorious features of MDMA metabolism is its potential involvement in the development of mid- to long-lasting neurotoxic effects, as a result of progressive neurodegeneration of the serotonergic and/or dopaminergic neurotransmission systems. MDMA metabolism leads to the production of several highly reactive metabolites (Capela *et al.*, 2009). Therefore, it is expected that these metabolites can mediate neurotoxic actions. Indeed, several studies failed to demonstrate neurotoxicity when MDMA or 3,4-methylenedioxyamphetamine (MDA) were injected directly into the rat brain (Paris and Cunningham, 1992; Bai *et al.*, 1999; Esteban *et al.*, 2001). Furthermore, since both MDMA and MDA could mediate neurotoxic effects after peripheral administration (de la Torre and Farré, 2004; Monks *et al.*, 2004), suggests that metabolism may be involved in the occurrence of neurotoxic effects. In agreement, an attenuation in MDMA-mediated depletions in 5-HT levels in rat brain was observed by inhibition of cytochrome P450 (CYP450) (Gollamudi *et al.*, 1989). Additionally, MDMA metabolites have been identified in rat brain after peripheral administration of MDMA (Chu *et al.*, 1996; Jones *et al.*, 2005; Erives *et al.*, 2008), thus supporting a role for metabolism in the context of MDMA-induced neurotoxicity.

A schematic representation of MDMA metabolism is illustrated in Figure 2. Hepatic metabolism of MDMA involves *N*-demethylation to MDA, which is also another drug of abuse. Both MDMA and MDA may be *O*-demethylenated to the catechol metabolites *N*-methyl-α-methyldopamine (N-Me-α-MeDA) and α-methyldopamine (α-MeDA), respectively (Capela *et al.*, 2009; Carvalho *et al.*, 2012). Different metabolic profiles between species are described. While in humans and rats N-Me-α-MeDA is the major MDMA metabolite, in mice the rate of α-MeDA formation is higher, compared to N-Me-α-MeDA (de la Torre and Farré, 2004; Escobedo *et al.*, 2005; Easton and Marsden, 2006; de la Torre *et al.*, 2009). Though a direct relationship between metabolic profile and neurotoxicity was never established, this metabolic difference between species may justify the higher serotonergic toxicity observed in humans and rats, compared to both serotonergic and dopaminergic deficits observed in mice. Both catechol MDMA metabolites can undergo oxidation to the corresponding highly redox-active *ortho*-quinones, which, after redox cycling, may originate semi-quinone radicals and lead to the generation of reactive oxygen and nitrogen species (ROS and RNS, respectively). Moreover, as the reactive *ortho*-quinone intermediates are electrophilic compounds, cellular damage may occur by alkylation of crucial cellular macromolecules, such as proteins, lipids and/or deoxyribonucleic acid (DNA) (Capela *et al.*, 2009; Carvalho *et al.*, 2012). However, in the presence of GSH, *ortho*-quinones may be conjugated to form glutathionyl adducts (Hiramatsu *et al.*, 1990).

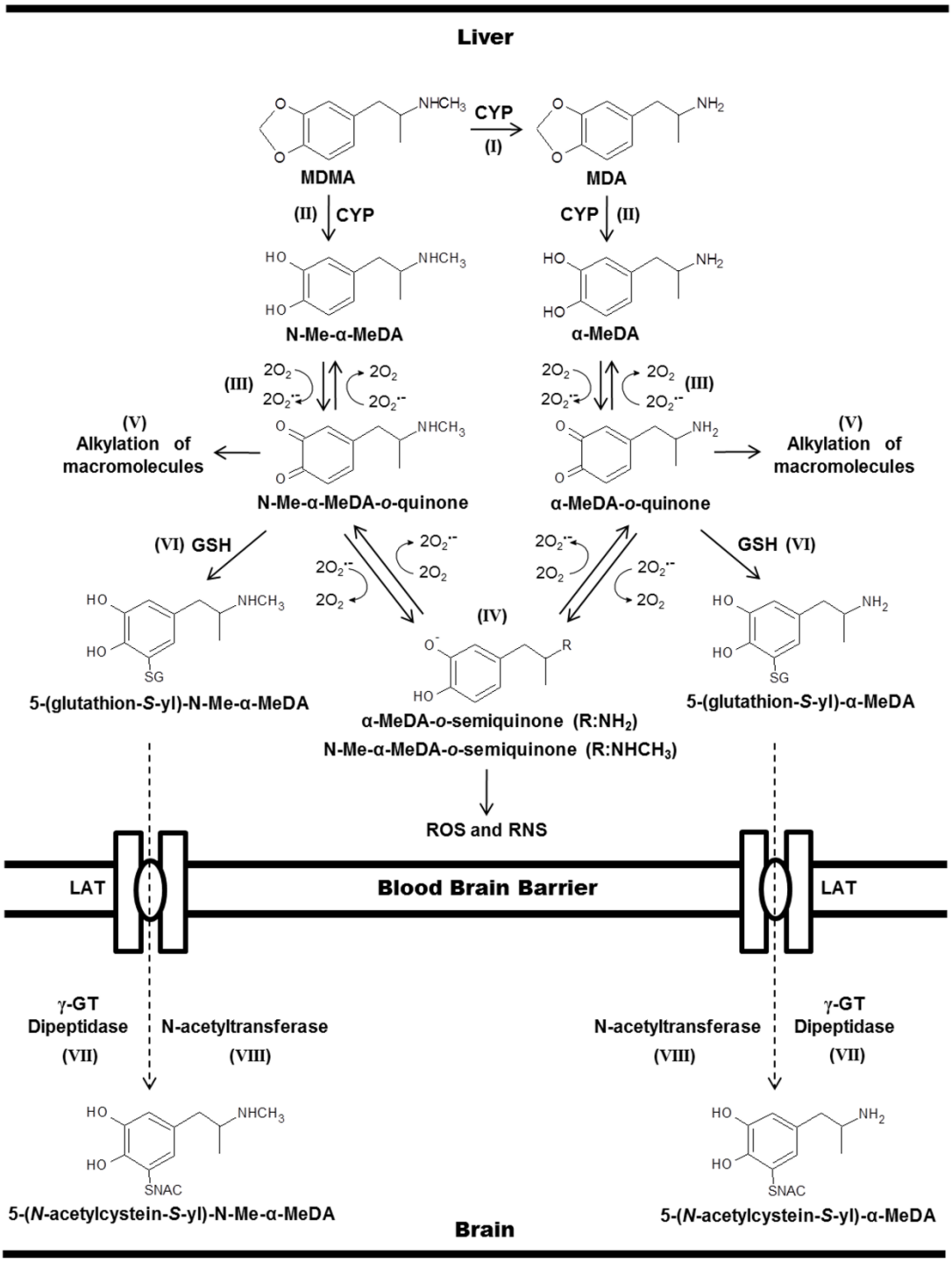


Figure 2. Major pathways of MDMA metabolism.
The parent compound MDMA is *N*-demethylated to form 3,4-methylenedioxyamphetamine (MDA) (I). Both MDMA and MDA may be *O*-demethylenated to the catechol metabolites *N*-methyl-α-methyldopamine (N-Me-α-MeDA) and α-methyldopamine α-MeDA (II). In rats, *N*-demethylation to MDA is one of the main metabolic pathways, whereas in humans, *O*-demethylation to N-Me-α-MeDA predominates. Isoenzymes of the cytochrome P450 (CYP450) are involved in the *N*-demethylation and *O*-demethylation metabolic reactions (I, II). Both N-Me-α-MeDA and α-MeDA can undergo oxidation to the corresponding *ortho*-quinones (III), which can enter in redox-cycle and generate semiquinone radicals (IV), thus leading to the formation of reactive oxygen and nitrogen species (ROS and RNS, respectively). Alternatively, *ortho*-quinones can undergo adduction with nucleophiles, such as cellular macromolecules [deoxyribonucleic acid (DNA), lipids or proteins] (V) or reduced glutathione (GSH) (VI). GSH conjugates 5-(glutathion-*S*-yl)-*N*-methyl-α-methyldopamine [5-(GSH)-N-Me-α-MeDA] and 5-(glutathion-*S*-yl)-α-methyldopamine [5-(GSH)-α-MeDA] can be transported into the brain by *L*-transporter for neutral amino acids (LAT), located in the capillaries of blood-brain barrier (BBB).

These conjugates can be metabolized by γ-glutamyltransferase (γ-GT) and dipeptidase (VII) to their corresponding cysteine derivates, which, by *N*-acetyltransferase action (VIII), can be further metabolized to their corresponding *N*-acetylcysteine (NAC) conjugates. NAC-conjugated metabolites appear to be slowly eliminated and, consequently, persist into the brain. Created by the author based in the reference (Capela *et al.*, 2009).

MDMA metabolites can either be monoconjugated with GSH or undergo the addition of a second molecule of GSH, yielding, thus, a 2,5-bis-glutathionyl conjugate. Conjugation of GSH with electrophiles, such as *ortho*-quinones, can preserve or enhance their biological reactivity (Monks *et al.*, 2004; Jones *et al.*, 2005; Erives *et al.*, 2008). Importantly, glutathionyl adducts of MDMA metabolites are known to cause irreversible inhibition of enzymes that possess either GSH-binding sites or cysteine residues critical for the enzymatic activity (Monks and Lau, 1997).

The systemically formed metabolites may be transported across the BBB, by the *L*-transporter for neutral amino acids, which is involved in the transport of cysteine and GSH-conjugated compounds (Miller *et al.*, 1996; Kühne *et al.*, 2007; del Amo *et al.*, 2008), as proved by their presence in the brain after MDMA administration to rats (Jones *et al.*, 2005; Erives *et al.*, 2008). In the brain, GSH-conjugated metabolites of MDMA can be further metabolized via the marcapturic acid pathway (Esteban *et al.*, 2001). Initially, GSH conjugates are metabolized by γ-glutamyltransferase (γ-GT) and dipeptidase to the corresponding cysteine conjugates. Additionally, these cysteine conjugates may be further metabolized by *N*-acetyltransferase to their corresponding *N*-acetylcysteine (NAC) adducts. However, GSH-conjugated metabolites can also be metabolized, by dipeptidase and γ-GT, to their corresponding cysteine derivates in the capillary lumen and then transported into the brain through the *L*-transporter for neutral amino acids (Patel *et al.*, 1993; Erives *et al.*, 2008). Despite existence of metabolic conversion, NAC-conjugated metabolites of MDMA retain the toxicity of their GSH precursors (Jones *et al.*, 2005). However, contrary to GSH conjugates, in which their brain accumulation may be counteracted by multidrug resistance protein (MRP) 1 and MRP2 localized in the BBB (Slot *et al.*, 2008; Ballatori *et al.*, 2009), NAC-conjugated metabolites appear to be slowly eliminated and, consequently, persist in the brain (Jones *et al.*, 2005; Erives *et al.*, 2008), given the absence of active transporter from the brain. In agreement, some studies have demonstrated that, in rat brain, NAC-conjugated metabolites of MDMA present higher half-life than GSH conjugates, after s.c. injection of MDMA (Jones *et al.*, 2005). Still, it was observed that, after multiple administrations of MDMA to rats, these metabolites tend to accumulate in the brain (Erives *et al.*, 2008).

To clarify the role of metabolism on MDMA´s neurotoxicity, other studies have been conducted through direct administration of the MDMA metabolites to laboratory animals.

Injection of MDMA catechol metabolites α-MeDA and N-Me- α-MeDA directly in rat brain did not elicit neurotoxicity (McCann *et al.*, 1994; Miller *et al.*, 1996; Escobedo *et al.*, 2005), thus suggesting that peripheral metabolism of these compounds is required for metabolism-related MDMA-induced neurotoxicity. Indeed, when peripherally administrated, these metabolites exhibit neurotoxic properties. Subcutaneous injection of α-MeDA caused decreases in 5-HT concentration in rat frontal CTX (Yeh and Hsu, 1991). In addition, in mice, i.p. administration of N-Me- α-MeDA elicited long-term dopamine and 5-HT depletions (Escobedo *et al.*, 2005). Contrary to catechol MDMA metabolites, *in vivo* studies performed with thioether metabolites of MDMA have revealed neurotoxic effects when directly injected into rat brain (Miller *et al.*, 1996; Miller *et al.*, 1997; Bai *et al.*, 1999; Jones *et al.*, 2005). Intracerebroventricular (i.c.v.) administration of 5-(glutathion-*S*-yl)-α-methyldopamine [5-(GSH)-α-MeDA] in rats produced neurobehavioral changes and acute increases of dopamine and 5-HT levels, such as observed after peripheral administration of MDMA or MDA (Miller *et al.*, 1996). Furthermore, direct injection of 5-(GSH)-α-MeDA and 5-(*N*-acetylcysteine-*S*-yl)-α-methyldopamine [5-(NAC)-α-MeDA] into striatum, CTX or HIP of rats induced prolonged depletions in 5-HT levels (Bai *et al.*, 1999). Also, i.c.v. injection of 2,5-bis(glutathion-*S*-yl)-α-methyldopamine [2,5-(GSH)-α-MeDA] decreased 5-HT levels in rat striatum, CTX and HIP (Miller *et al.*, 1997). In addition, intrastriatal administration of the MDMA metabolite 5-(*N*-acetylcysteine-*S*-yl)-*N*-methyl-α-methyldopamine [5-(NAC)-N-Me-α-MeDA] caused acute behavioral changes in rats (Jones *et al.*, 2005) similar to those seen after peripheral administration of MDMA or MDA, or following i.c.v. injection of other thioether conjugates of α-MeDA [5-(GSH)-α-MeDA and 2,5-(GSH)-α-MeDA] (Miller *et al.*, 1996; Miller *et al.*, 1997). Still, intrastriatal administration of the MDMA metabolite 5-(NAC)-N-Me-α-MeDA was also associated with decreased striatal and cortical concentrations of 5-HT and its metabolite 5-HIAA (Jones *et al.*, 2005).

Though metabolism appear to contribute to MDMA-induced neurotoxicity, it is likely that MDMA itself has some neurotoxic potential. In fact, after oral administration of MDMA to rats, the neurotoxicity observed was most closely related to plasma and brain concentrations of MDMA rather than its metabolites (Mueller *et al.*, 2009), thus suggesting that MDMA may be the initiator of the neurotoxic process (Green *et al.*, 2012). Accordingly, no changes in serotonergic neurotoxicity were observed by inhibiting MDMA metabolism in rats (Mueller *et al.*, 2011). However, it is important to consider that parent compound and its metabolites are present simultaneously in the brain after administration of MDMA (Chu *et al.*, 1996; Jones *et al.*, 2005; Erives *et al.*, 2008; Mueller *et al.*, 2009), thus suggesting the existence of a synergic or additive effect at low concentrations. Therefore, more than MDMA or its metabolites, by itself, the neurotoxic effects mediated

by this drug of abuse may result from a dynamic interaction between parent compound and metabolites.

Results obtained in animal models are very important for the prediction of the neurotoxic potential of MDMA in humans, though the pharmacological differences between species make difficult the extrapolation of data (de la Torre and Farré, 2004; Easton and Marsden, 2006). Since MDMA metabolism in humans occurs mainly by *O*-demethylation rather than *N*-demethylation, in the human plasma N-Me-α-MeDA is the major MDMA metabolite (de la Torre and Farré, 2004; Green *et al.*, 2012). Therefore, neurotoxicity studies with the conjugated metabolites of N-Me-α-MeDA might be of high relevance for the extrapolation of data to the human scenario (Easton and Marsden, 2006; Verrico *et al.*, 2007).

I.1.1.1.3 The role of hyperthermia on MDMA's neurotoxicity

One of the most relevant particularities of the MDMA-induced neurotoxicity is the thermoregulation impairment. Since the use of MDMA as a recreational drug in the early 1980's (Shulgin, 1986; Parrott, 2004a), reports of hyperthermia associated with the comsumption of this drug have emerged. Indeed, it has been demonstrated impaired thermoregulation in rats exposed to a neurotoxic dose of MDMA, when maintained at high ambient temperature, which can be a consequence of 5-HT-mediated effects (Dafters and Lynch, 1998; Mechan *et al.*, 2001; Jaehne *et al.*, 2008). Similarly, impaired thermoregulation has been demonstrated in humans, in both warm (30ºC) or cold (18ºC) conditions (Freedman *et al.*, 2005). At present, hyperthermia is probably the most widely known acute adverse event after intake of MDMA by recreational users. The first reports of fatalities associated with the recreational use of MDMA involved overheating, with core body temperatures over 40ºC (Henry *et al.*, 1992; Chadwick *et al.*, 2001), though these extreme thermal reactions were noted to be rare. The first published study reporting the effects of MDMA on body temperature in humans was a phase-1 pilot study (Grob *et al.*, 1996). It was demonstrated that oral administration of MDMA (0.5 to 1.5 mg/kg) did not result in any overt evidence of hyperthermia, though only low doses of MDMA were used (Grob *et al.*, 1996). From this, many other studies have shown the potential of MDMA to induce acute hyperthermia in humans (McCann *et al.*, 1996; Freedman *et al.*, 2005; Farré *et al.*, 2007), which in many cases was fatal (Mallick and Bodenham, 1997; Kunitz *et al.*, 2003; Patel *et al.*, 2005).

The acute and sustained hyperthermia produced by MDMA in humans is one of the few effects that can be directly compared to experimental data from laboratory animals. In fact, MDMA was shown to cause acute dose-dependent hyperthermia in mice (Colado *et*

al., 2001; Pontes *et al.*, 2008a; Bexis and Docherty, 2009; Granado *et al.*, 2011; Takamatsu *et al.*, 2011), rats (Blessing *et al.*, 2003; Alves *et al.*, 2007; Alves *et al.*, 2009b; Hrometz *et al.*, 2011; Shen *et al.*, 2011; Nisijima *et al.*, 2012), rabbits (Pedersen and Blessing, 2001; Blessing and Seaman, 2003; Blessing *et al.*, 2003), guinea pigs (Saadat *et al.*, 2004) and pigs (Fiege *et al.*, 2003; Schütte *et al.*, 2013). Furthermore, in non-human primates, MDMA also increased body temperature in a dose-dependent manner, leading to hyperthermia (Crean *et al.*, 2006; Taffe *et al.*, 2006; Von Huben *et al.*, 2006; Taffe, 2012).

Considering that MDMA produces an acute and sustained release of 5-HT from nerve endings in the brain, it has often been assumed that the hyperthermic response results from the release of this amine (Shankaran and Gudelsky, 1999). In agreement with this hypothesis, a marked increase in 5-HT release and hyperthermia were found after administration of tryptophan (5-HT precursor) and MAO inhibition (Grahame-Smith, 1971). However, there is now considerable evidence suggesting that 5-HT plays little or no role in the acute hyperthermic response. Indeed, repeated administration of low doses of MDMA to rats (4 mg/kg, twice daily, for 4 days) did not produce hyperthermia, but was associated with long-term depletion of 5-HT (O'Shea *et al.*, 1998). In accordance, pre-treatment with a variety of selective and non-selective 5-HT receptors' antagonists was found to have no effect on MDMA-induced hyperthermia in rats (Mechan *et al.*, 2002). It has also been observed that the pre-treatment with the 5-HT uptake inhibitors fluoxetine (Schmidt *et al.*, 1990b; Malberg *et al.*, 1996) or citalopram (Piper *et al.*, 2007) has no effect on MDMA-induced hyperthermia in rats. Notably, Mechan and co-workers (Mechan *et al.*, 2002) showed, in rats, through the use of *in vivo* microdialysis, that fluoxetine almost completely inhibited MDMA-induced 5-HT release in the brain, though the hyperthermic response in the same animals was the same as that seen in control rats. Recently, Rodsiri and co-workers (Rodsiri *et al.*, 2011) also failed to find any correlation between the hyperthermic response and the increase in extracellular 5-HT in rats given low doses of MDMA. Similarly, in humans, Liechti and Vollenweider (Liechti and Vollenweider, 2000) observed that neither citalopram nor haloperidol attenuated the MDMA-induced hyperthermic effect. However, by using the 5-HT_{2A} antagonist ketanserin, it was reported an attenuation in MDMA-induced hyperthermia in healthy human volunteers (Liechti *et al.*, 2000). In mice, the role of 5-HT in the temperature effects following MDMA administration is less clear. Indeed, O'Shea and co-workers (O'Shea *et al.*, 2001) found no correlation between the temperature change and the alteration in cerebral 5-HT concentration. However, fluoxetine blocked the MDMA-induced hyperthermia. Therefore, though 5-HT appears to play a major role in MDMA-induced hyperthermia in mice, its exact role remains unclear.

Despite the apparent dissociation between MDMA-induced monoamines release and hyperthermia, many studies have established that hyperthermia plays a major role in the acute- and long-lasting neurotoxicity induced by MDMA. However, other studies have demonstrated that neurotoxic effects can still occur even under normothermic or hypothermic conditions (O'Shea *et al.*, 2006; Walker *et al.*, 2007). Furthermore, in rats, an attenuation of the neurotoxicity elicited by MDMA was observed at low ambient temperature (Schmidt *et al.*, 1990b; Broening *et al.*, 1995), while under elevated ambient temperature its neurotoxicity was exacerbated (Broening *et al.*, 1995; Sanchez *et al.*, 2004). In addition, it was shown that small changes in ambient temperature produced marked changes in the degree of serotonergic neurotoxicity. Therefore, though neurotoxicity associated with MDMA may occur in the absence of a hyperthermic response, in general there is a close correlation between the hyperthermic response and the degree of neurotoxic injury (Malberg and Seiden, 1998). In addition, in contrast to rats, where MDMA can induce hypothermia or hyperthermia depending on the ambient room temperature in which the animals are housed, in humans (Freedman *et al.*, 2005) and monkeys (Von Huben *et al.*, 2006) MDMA administration is always associated with an increase in core body temperature, regardless of ambient temperature. Thus, these findings provide evidences for interspecies differences regarding to thermic response induced by MDMA. Supporting a role for hyperthermia in the context of MDMA-induced neurotoxicity, Malberg and co-workers (Malberg *et al.*, 1996) and Farfel and co-workers (Farfel and Seiden, 1995) showed lower neurotoxicity by preventing the hyperthermia induced by MDMA. Furthermore, many drugs that protect animals against MDMA-induced serotonergic neurotoxicity also decrease the body temperature. Additionally, in experimental animals, compounds with neuroprotective effects against MDMA-induced neurotoxicity confirmed to afford protection by lowering body temperature as an indirect effect, but not by a specific neurochemical action (Malberg *et al.*, 1996; Colado *et al.*, 1998).

5-HT_{2A} receptor antagonists, like ketanserin (Malberg *et al.*, 1996) or ritanserin (Schmidt *et al.*, 1990a; Johnson *et al.*, 1993) and also α-methyl-*p*-tyrosine (AMPT) (Stone *et al.*, 1988; Malberg *et al.*, 1996) protected against MDMA-induced injury to 5-HT nerve terminals in rats. However, it was also shown that in co-administration with MDMA, ketanserin, ritanserin, AMPT or even risperidone, all 5-HT_{2A} receptor antagonists, inhibited the MDMA-induced hyperthermia in rats (Malberg *et al.*, 1996; Shioda *et al.*, 2008). When the temperatures of ketanserin- or AMPT-administrated animals were kept elevated, the neuroprotective effect of these drugs against MDMA's serotonergic neurotoxicity was lost (Malberg *et al.*, 1996). The *N*-methyl-*D*-aspartate (NMDA) receptor antagonist dizocilpine (MK-801) was also reported to protect against MDMA-induced injury to serotonergic nerve

endings (Farfel *et al.*, 1992; Colado *et al.*, 1993; Hewitt and Green, 1994), though the co-administration of MK-801 and MDMA was associated with a hypothermic response. However, when the temperatures of these animals were maintained elevated, the neuroprotective effect of MK-801 was lost (Farfel and Seiden, 1995; Malberg *et al.*, 1996). Furthermore, another NMDA antagonist, *S*-(+)-α-phenyl-2-pyridine ethanamide dihydrochloride (AR-R15896AR), did not attenuate MDMA-induced hyperthermia in rats and, consequently, did not confer any neuroprotective effect (Colado *et al.*, 1998). Nevertheless, it may be assumed that by blocking the hyperthermic response, the MDMA's neurotoxicity can be attenuated or prevented.

On the other hand, drugs or environments that promote MDMA-induced hyperthermia can enhance its neurotoxicity. MDMA abuse by humans commonly occurs in hot overcrowded environments and in combination with caffeine. Co-administration of caffeine with MDMA or MDA to rats resulted in an enhanced hyperthermic response, which promoted the acute and long-term serotonergic toxicity associated with MDMA and MDA (Camarasa *et al.*, 2006; McNamara *et al.*, 2006).

Another mechanism implicated in MDMA-induced hyperthermia that can contribute to the neuronal injury is the enhanced production of free radicals in the brain. Several studies have measured brain ROS formation after MDMA administration (Colado *et al.*, 1997; Colado *et al.*, 1999; Shankaran *et al.*, 1999a). Administration of MDMA to Dark Agouti rats (15 mg/kg, i.p.) increased the formation of 2,3-dihydroxybenzoic (2,3-DHBA), an indicator of ROS formation, in the HIP for at least 6h, which was prevented by the free radical scavenging agent alpha-phenyl-N-tert-butyl nitrone (PBN), when given 10 min before and 120 min after MDMA administration (Colado *et al.*, 1997). In the same line, MDMA (15 mg/kg, i.p.) produced a sustained rise of approximately 50% in the concentration of 2,3-DHBA and 2,5-dihydroxybenzoic (2,5-DHBA) in rat brain (Colado *et al.*, 1999). The drug clomethiazole, an agonist of gamma-aminobutyric acid (GABA)-A receptors devoid of free radical scavenging properties, when administrated either prior or after MDMA, prevented both the acute hyperthermia and radical formation induced by MDMA. However, it was also demonstrated that in rats administrated with MDMA plus clomethiazole and kept under elevated temperature conditions, there was no prevention of the radical formation induced by MDMA. Therefore, this suggest that the inhibition of MDMA-induced hyperthermia decreases ROS formation (Colado *et al.*, 1999). However, drugs that do not interfere with MDMA-induced hyperthermia, such as ethanol, can increase MDMA-induced ROS formation in the brain of animals, thus indicating further mechanisms of free radical formation. Rats pre-exposed to ethanol (4-day ethanol regimen leading to plasma ethanol levels of around 450 mg/dl) presented a more marked increase in hydroxyl radical production in the HIP following MDMA administration (5

mg/kg, i.p.), which was correlated with extended long-lasting serotonergic neurotoxicity (Izco *et al.*, 2007). Similarly, in rats, it was also shown that the co-administration of MDMA (2 x 10 mg/kg, i.p., 6h apart) and ethanol (2 x 1.5 g/kg, i.p., 6h apart) significantly decreased 5-bromodeoxyuridine labeling in the dentate gyrus, thus indicating reduced survival of neuronal precursors (Hernandez-Rabaza *et al.*, 2010). Notably, memory impairment was correlated with granule cell depletion. However, in animals administrated with MDMA or ethanol alone, none of this effects were observed (Hernandez-Rabaza *et al.*, 2010). In addition, co-administration of ethanol (1.5 mg/kg, i.p.) potentiated the hyperactivity associated with MDMA (6.6 or 10 mg/kg, i.p.) and increased brain and blood concentrations of MDMA, thus leading to enhanced MDMA-related neurotoxicity (Hamida *et al.*, 2009).

Despite these reports, it should be considered that animal experiments performed in the regular laboratory might increase the core temperature up to 1°C due to the handling of the animals, thus introducing a variable of error in predicting the exact role of hyperthermia in MDMA-induced neurotoxicity (Gordon and Fogelson, 1994). Furthermore, modifications on body temperature are accompanied and/or associated with several physiological changes (Capela *et al.*, 2009). Therefore, in animal studies, researchers are faced with a variety of factors affecting body temperature, which is a variable of major importance in interpreting experimental results regarding MDMA´s neurotoxicity.

Recent studies have been also conducted simulating *in vitro* the hyperthermic conditions that are attained *in vivo* (Capela *et al.*, 2006a; Capela *et al.*, 2006b; Capela *et al.*, 2007b). This condition has the advantage of tight temperature control throughout the whole experiment, without the interference of other factors that are observed in *in vivo* experiments. In primary neuronal cortical cultures, MDMA and its metabolites induced a time- and concentration-dependent neuronal apoptotic death, which was potentiated by hyperthermia (Capela *et al.*, 2006a; Capela *et al.*, 2006b; Capela *et al.*, 2007b). As the abuse of MDMA as a recreational drug (particularly in crowded and hot environments) can induce hyperthermia, the obtained results corroborate the serious concern previously reported in the literature. Furthermore, these studies demonstrated that several drugs that attenuated the MDMA-induced serotonergic neurotoxicity *in vivo,* by modulating the hyperthermic response, also attenuated MDMA-induced toxicity *in vitro*, in a temperature-independent manner. A protective effect was observed for the selective 5-HT_{2A} receptor antagonist ketanserin, the NMDA receptor antagonist MK-801, and the nitric oxide synthase (NOS) inhibitor *N*-nitro-*L*-arginine (L-NNA) against MDMA-induced cortical neuronal death, which was observed at both normothermic and hyperthermic conditions (Capela *et al.*, 2006b; Capela *et al.*, 2007a).

In addition, it has already been reported that the core temperature can alter the pharmacokinetic parameters and metabolism of MDMA, both in rats (Goni-Allo *et al.*, 2008) and monkeys (Banks et al., 2007), thus suggesting that the different neurotoxicity patterns observed under normothermic or hyperthermic ambient conditions may result from differences on MDMA's metabolism.

In conclusion, though is clear that hyperthermia potentiates the MDMA's neurotoxicity, not all agents that prevent MDMA-induced neurotoxicity necessarily do so by blocking the hyperthermic response. Thus, this suggests that the long-lasting neurotoxicity that follows MDMA neurotoxic regimens goes well beyond its hyperthermic effects.

I.1.2 Neurotoxicity assessment

Prediction of neurotoxic effects is a key feature in the toxicological profile of many compounds and, therefore, is required by regulatory testing schemes. Nowadays, neurotoxicity assessment required by guidelines is solely based on *in vivo* testing, evaluating mainly neurobehavioral and neuropathological effects, which is expensive, time consuming and unsuitable for screening large number of chemicals. Additionally, such *in vivo* tests are not always sensitive enough to predict human neurotoxicity and often do not provide information that facilitates regulatory decision-making processes (Bal-Price *et al.*, 2008).

In the field of neurobiology and neurotoxicology, *in vitro* neuronal models have been successfully developed and employed to address specific questions of cell biology and nervous system functioning, and provide a means to systematically study the complexicity of the nervous system. Additionally, *in vitro* studies may provide the most appropriate approach when in many cases these studies cannot or are difficult to be conducted in live animals. For example, the study of mechanistic pathways and target molecules for neurotoxicants is difficult to performe in the whole animal. *In vitro* studies, by allowing to work with a specific cell/tissue target enable the elucidation of such pathways or disclosure of target molecules. However, it is generally recognized that *in vitro* systems often provide only partial answers to more complex situations. Therefore, though *in vitro* studies rarely replace *in vivo* situation, they can supplement investigations with whole animals. Additionally, the information obtained may also be used in the refinement of future *in vivo* studies to facilitate predictions of neurotoxicity (Bal-Price *et al.*, 2008; Council, 2012; Visan *et al.*, 2012).

A range of *in vitro* systems of increasing biological complexity is available for neurotoxicity testing, from subcellular systems (e.g. isolated mitochondria and synaptosomes), single cell types (e.g. immortalized cell lines) to systems that preserve some aspects of tissue structure and function (e.g. primary mixed neuronal and glial cultures, aggregated cultures or organotypic brain slices). The selection of any particular system depends on the question addressed, the intended use of the data and available information on the suspected mechanism of neurotoxicity (Costa, 1998a; Bal-Price *et al.*, 2008). By using *in vitro* approaches, neurotoxicity may be assessed through evaluation of cell viability, general but critical cell functions (e.g. energy metabolism, oxidative stress or Ca^{2+} homeostasis) and neuronal specific functions (e.g. neurite outgrowth and axonal transport, neurotransmission and vesicular release, signaling between various types of neurons and glia, receptor pharmacology, ion-channel activation or electrical activity) (Bal-Price et al., 2008).

I.1.2.1 Use of *in vitro* systems in evaluating neurotoxicity

The rationale for the use of *in vitro* procedures to assess neurotoxicological effects is based in the clear understanding of mechanistic processes underlying normal nervous system functioning and some forms of dysfunction. Prior to the1990's, neurotoxicological studies generally lacked any mechanistic consideration. However, the mechanistic information is critical for assessing the potential neurotoxicological effect of compounds. Since *in vitro* systems allow the examination of mechanistic processes in isolated conditions, they facilitate the characterization of the modes of action in target tissues by elucidating information in cellular and molecular alterations caused by neurotoxicant exposure. Mechanistic understandings are also valuable in designing directed, hypothesis-driven, *in vivo* experiments (Tiffany-Castiglioni, 2004). When applied to chemical-induced perturbations of the nervous system, knowledge of biological mechanisms led to the examination of more advanced and subtle biologically based expressions of neurotoxicity. This advance has been seen in all levels of examination, from the integrative functioning of the nervous system, as manifested by behavioral alterations, to morphological and biochemical alterations in the intact animal, to the molecular mechanisms associated with injury response or development, and to the intricate cellular changes examined by *in vitro* methodologies (Tiffany-Castiglioni, 2004).

Though the assessment of neurotoxic endpoints in the whole animal are presumed to be causally related to those initiated at cellular level, in many cases the cascade of effects is not well-understood. Chemicals rarely affect all neurons indiscriminately, but induce selective damage, since the neuronal toxicity depends on the specific sensitivity of the cell, as well as on the extracellular concentration of the compound to be tested. However, either *in vivo* or *in vitro*, the effects observed may not be due to the primary toxicant that is been tested, but may result from its bioactivation, with subsequent response to its metabolites (Capela *et al.*, 2009; Schildknecht *et al.*, 2009; Valente *et al.*, 2012; Bajpai *et al.*, 2013; Rossato *et al.*, 2013). In addition, toxic responses of neurons *in vivo* may be the result of toxicity to neuronal or non-neuronal cells. Observed responses may also be due to a systemic biological process activated by the exposure or may be observed only during the maturation or aging of the system. These features create a major problem in selecting an *in vitro* system that will model the nervous system target site or process for any particular drug. With the use of *in vitro* systems, it must be kept in mind that there is no an ideal *in vitro* system that allows the evaluation of all toxic effects induced by chemicals. This limitation is partly due to the lack of all possible target sites and the interaction between the cell types. Furthermore, the limited lifespan of *in vitro* systems may not allow the appearance of delayed responses or allow the discrimination between

transient and persistent neurotoxic effects. Still, mechanistic *in vitro* studies, when conducted correctly, may help to construct and validate pharmacokinetic analyses and dose-response models, which play a pivotal role in the risk assessment of neurotoxic compounds. Nevertheless, dose-response data obtained from *in vitro* studies must be used with caution, because of significant differences in the pharmacokinetic and behavior of chemicals observed *in vivo* and *in vitro*. In addition, effects observed *in vitro* are not necessarily predictive of those that may occur in the *in vivo* scenario. However, the mechanisms of neurotoxicity identified using *in vitro* studies may contribute to determine whether an effect observed *in vitro* may also result in an adverse effect in animals or humans following exposure to neurotoxins (Tiffany-Castiglioni, 2004).

I.1.2.1.1 Advantages and limitations in using *in vitro* systems for neurotoxicity assessment

Much of the studies with *in vitro* systems for neurotoxicity testing lie in maximizing their potential for yielding valid mechanistic responses. Experimental systems for the understanding of toxicant-induced damage to the nervous system are often reductionist in nature, in order to increase the specificity and sensitivity of endpoints measured.

The main advantages and limitations in using *in vitro* neuronal models for neurotoxicological studies are summarized in Table 1. Among the advantages in using these systems is the option to study a single cell type of interest, thus facilitating the direct observation and measurement of cellular responses to toxicants, under a defined extracellular environment, and direct interactions of the toxicant with test cells. Moreover, another significant advantage of *in vitro* systems for neurotoxicological research is the ability to create and compare concentration-response curves. Furthermore, *in vitro* systems may provide an economic advantage of a reduced requirement for test compounds. However, though *in vitro* methods are associated with limitations and drawbacks, which must be considered when designing studies and extrapolating data to the dose-response paradigm, they play an important role in experimental research and provide valuable opportunities for more mechanistic based risk assessments. Additionally, when combined with *in vivo* approaches, they allow a better understanding of the mechanistic basis of a neurotoxic effect.

Table 1. Advantages and limitations in using *in vitro* neuronal systems for neurotoxicological studies.

Advantages	
Reduced cost	Easy to maintain and manipulate
Tight control of the neurotoxicant concentration	Control of the exposure time
Control of the extracellular environment	Study of a single cell type of interest
Fewer ethical issues, except for human embryonic cells	Higher reproducibility between independent experiments
Direct observation and measurement of cellular responses to neurotoxicants	Observation of direct interactions between neurotoxicant and test system
Ability to create and compare concentration-response curves for different compounds	Ability to address questions of interspecies selective toxicity
Study of toxicants' effects at different maturation and differentiation stages	Precise temporal analysis of the sequence of events
Limitations	
Lack of integrated functions	Lack of ability to assess behavioral endpoints
Lack of the BBB function	Unknown target concentration
Absence of systemic endocrine control	Limited ability for mimicking heterogeneous cell-cell interactions
Difficult to determine and reproduce the compensatory mechanisms observed *in vivo*	Lack of the nutritional support provided by the blood circulation
Fail to account for the route of administration, distribution and biotransformation of the neurotoxicant in the body	The *in vitro* conditions that neuronal systems grow are a poor substitute for the intricate neuronal environment of the whole animal brain

On the other hand, *in vitro* systems lack the ability to assess behavioral endpoints, which is a major neurotoxic outcome of concern. Lacking this ability, the value of *in vitro* systems lies in their potential capacity to respond mechanistically to a toxicant in a manner similar to that occurring from *in vivo* exposure. Furthermore, *in vitro* studies fail to account for the route of administration, distribution and biotransformation of the toxicant in the body. The *in vitro* conditions in which cells grow are a poor substitute for the intricate neuronal environment of the whole animal. In addition, *in vitro* systems have limited capacities for mimicking heterogeneous cell-cell interactions, systemic endocrine control, or metabolism of xenobiotics. The appropriate age and development state of the nervous system at the time of exposure have been extremely difficult to approximate in culture. Other limitations include the lack of integrated functions and the BBB function, unknown target concentration and the existence of compensatory mechanisms that cannot be determined and reproduced *in vitro*.

I.1.2.1.1.1 Acess to the cellular environment

The physicochemical environment of cells may be easily manipulated *in vitro*. Chemicals can be added or removed from the culture medium, allowing precise temporal analysis of the sequence of events. The concentration of the test compound can be controlled in terms of the amount being delivered to the entire cell population or to an individual target cell. However, this concentration must be consistent with the *in vivo* level of exposure to be meaningful.

Physicochemical properties of compounds, such as solubility, volatility, pH, binding to components of the culture medium, including protein binding, and osmolality are critical for predicting their toxic effect in an *in vitro* system. Therefore, a tight control of their concentration is required over time. On the other hand, it is difficult to evaluate *in vitro* compounds that are either insoluble in aqueous systems or at neutral pH, thus forming insoluble particules or precipitate over time. To expose neuronal systems to such insoluble compounds, additives (e.g. dimethylsulfoxide or ethanol) are often added to the culture medium. However, the presence of these additives may modify the neurotoxicological response to the tested compound. To overcome these problems, compounds may be solubilized using physiological carriers, such as albumin or lipoproteins. Therefore, the chemical nature of the substance to be studied must be considered. Alterations in the osmolality or pH shifts in the culture medium can occur, which may affect the stability of the cellular system or may stimulate the precipitation of nutrients from the culture media. The addition of the chemical under study to the medium can result in a direct reaction between the test compound and a component of the culture medium (e.g. protein denaturation or precipitation), thus affecting the availability of the toxicant or essential nutrients, and modifying signals to the cultured cells. Any protein-binding properties of test drugs can directly alter the microenvironment of cultured cells in a fashion that may not occur *in vivo* (Harry *et al.*, 1998).

I.1.2.1.1.2 Toxicokinetics

Toxicokinetics consists of absorption, distribution, metabolism and excretion of toxicants and their metabolites following exposure. The dose needed to induce toxic effects depends on these pharmacokinetic parameters. For example, the route by which a compound enters into the body can substantially alter the quantity absorbed and, consequently, modify the dose required to cause neurotoxicity. Metabolism of xenobiotics usually serves detoxification in the organism, but for some compounds metabolism generates neurotoxic metabolites (Capela *et al.*, 2009; Bajpai *et al.*, 2013). This process can take place in non-neural tissue (e.g. liver) (Capela *et al.*, 2009; Carvalho *et al.*, 2012),

but also in the brain (Capela *et al.*, 2009; Bajpai *et al.*, 2013). Nevertheless, whereas non-neuronal cells possess xenobiotic inactivation systems (Gradinaru *et al.*, 2012), neuronal cells presented a lower metabolic activity (Ferguson and Tyndale, 2011). Within the organism, the compound may be bioactivated and/or detoxified before its release back into the blood circulation, being posteriorly distributed throughout the body by the circulatory system. However, metabolism of such compounds may be affected by several enzymatic processes, being the specificity and velocity of each enzymatic process strongly dependent on the animal species. For example, in humans and rats, N-Me-α-MeDA is the main plasma metabolite of MDMA. However, in mice, the rate of α-MeDA formation is higher, compared to N-Me-α-MeDA (de la Torre and Farré, 2004).

Differences in drug metabolism and excretion are widely considered to be an important determinant for the large species' differences regarding both toxic dose and type of neurotoxic response following drug or chemical exposure (de la Torre and Farré, 2004; Mueller *et al.*, 2013). For example, in culture, a test compound either remains unaltered or is relatively slowly modified, and one can examine the intrinsic toxicity of a substance to a cell-based system in the absence of any metabolites. Thus, *in vitro* test systems lacking metabolizing activity can overestimate or underestimate the toxicity that a compound would have *in vivo*. For example, in the field of "ecstasy"-induced neurotoxicity, hepatic formation of neurotoxic metabolites, followed by their uptake into the brain, is thought to contribute to the neurotoxic actions of this drug (Capela *et al.*, 2009), as demonstrated by studies in which the direct injection of MDMA into the brain did not produce the neurotoxic effects observed after its peripheral administration (Paris and Cunningham, 1992; Bai *et al.*, 1999; Esteban *et al.*, 2001; de la Torre and Farré, 2004; Monks *et al.*, 2004). On the other hand, there are also compounds that following peripheral administration do not cause neurotoxicity *in vivo*, but are neurotoxic *in vitro*. One such example is the metabolite of MPTP, *N*-methyl-4-phenylpyridinium ion (MPP^+). Whereas MPTP easily crosses the BBB *in vivo*, MPP^+ cannot reach the brain, since it does not cross the BBB, and, therefore, its peripheral administration is not associated with neurotoxicity (Schildknecht *et al.*, 2009; Bajpai *et al.*, 2013). However, in an *in vitro* system containing dopaminergic neurons expressing DAT, it will be highly toxic (Schildknecht *et al.*, 2009; Gao *et al.*, 2013). Additionally, in the brain, the metabolism of MPTP to MPP^+ is catalyzed by the astrocytic enzyme MAO-B, thus indicating that in systems lacking the above mentioned metabolic ability, MPTP will not produce neurotoxic effects (Schildknecht *et al.*, 2009; Bajpai *et al.*, 2013). Therefore, the use of *in vitro* models for predicting the neurotoxic potential of compounds with recognized metabolism-dependent toxicity will not be the best approach. However, many metabolic enzymes may be introduced into the *in vitro* system through the serum supplementation or growth media. Thus, the combined effect of these variables can

lead to lower concentrations of the tested compounds and, therefore, modify their neurotoxic effects. Additionally, it is critical to understand the *in vivo* metabolism, distribution, and effects of potential metabolites on the nervous system, in order to interpret the data obtained from both *in vivo* studies and *in vitro* systems. When the neurotoxic potential of a chemical *in vivo* is largely dependent upon metabolic parameters, such as metabolism, lipid-aqueous partitioning and distribution, then the expression of toxicity in an *in vitro* system may not be directly related to whole-animal studies.

To compensate the lack of metabolic competence of the *in vitro* neuronal systems, different approaches have been proposed. These include the addition of metabolic competent sources, such as S9 liver fractions (short-term experiments), hepatocyte-conditioned medium, or direct co-culture with hepatocytes from different species, and the transfection of cells with phase-I biotransformation enzymes (Bal-Price *et al.*, 2010; Yoon *et al.*, 2012). However, any artificial system used to simulate normal metabolism of compounds should preferably be comparable to the *in vivo* condition. Moreover, attention should be given to the differences between species in metabolic and kinetic ability, which is important for the extrapolation of results obtained in animal models to the human situation (Chen *et al.*, 2006; Bal-Price *et al.*, 2010). S9 liver fractions should be used with caution, since the amounts of S9 fraction that is generally needed for the occurrence of metabolic convertion may exhibit toxicity to neuronal cultures. However, this problem may be prevented by using tissue culture inserts, which allow the separation between cultured cells and S9 fraction by a microporous membrane (Kohn and Durham, 1993). Alternatively, for compounds in which the glial cells-mediated metabolism is critical for their neuronal toxicity (Schildknecht *et al.*, 2009; Bajpai *et al.*, 2013), co-cultures of neuronal and glial cells may be a good approach. However, the use of biotransformation processes may be incomplete or proceed by pathways different from those operating in whole organisms. Furthermore, the metabolic pattern is determined by the type of metabolic system, as well as by the species and gender from which the metabolic competent cells are isolated.

Other reports have shown that polymorphic effects might play a role in inter-individual variability to acute- or long-term degenerative effects of xenobiotics in the human brain (Bal-Price *et al.*, 2010). Indeed, it should be taken into account that polymorphisms reported for some enzymes, such as CYP450 or MAO-B, which metabolizes several classes of therapeutic drugs, endogenous neurochemicals and toxicants, may be relevant to the development of neurotoxicity. Particularly, microsomal CYP450 isoenzymes are determinant for phase-I oxidative metabolism of MDMA (Capela *et al.*, 2009). Many of the phase-I metabolites are subsequently conjugated by catechol-*O*-methyl transferase (COMT), sulfotransferase (SULT), or UDP-glucuronosyltransferase (UGT) phase-II

enzymes and preferentially excreted as the respective conjugates (Meyer *et al.*, 2008; Schwaninger *et al.*, 2012). Therefore, being these enzymes polymorphically expressed (Capela *et al.*, 2009; Pardo-Lozano *et al.*, 2012), it is expected an influence on the biokinetics parameters and, consequently, on the neurotoxic potential of MDMA.

In many cases, the neurotoxic potential of several compounds is critically dependent on brain metabolism. For example, there is evidence that glial cells are necessary to produce the neurotoxic metabolite MPP^+ from the parent compound MPTP (Bajpai *et al.*, 2013) and to convert GLU to glutamine (Stobart and Anderson, 2013) (see section I.1.2.1.1.6). In the same way, it is generally believed that the biotransformation of glutathione reduced (GSH)-monoconjugated metabolites of MDMA into their corresponding NAC conjugates occurs in the brain by action of the γ-GT, dipeptidase and *N*-acetyltransferase. These NAC conjugates, being slowly eliminated, persist into the brain (Jones *et al.*, 2005; Erives *et al.*, 2008) and, consequently, present a higher neurotoxic potential than their GSH precursors (Capela *et al.*, 2006a; Capela *et al.*, 2007b). Thus, *in vitro* models for the study of xenobiotics are often deficient in competent metabolic systems operating in the whole organism. Though *in vitro* systems allow a precise control of the concentration of compound delivered to the experimental model, they also present a difficulty in defining a toxicologically relevant dose of the *in vivo* scenario. On the other hand, *in vivo* metabolism of xenobiotics may also be simulated *in vitro* by co-exposure of the *in vitro* system to the parent compound and its metabolites that are formed *in vivo*. However, for this approach, it is necessary to know whether the metabolites are present into the brain, which implicates previous *in vivo* studies. Furthermore, these previous *in vivo* studies are important to predict the target organ(s) and the range of concentrations that are really attained *in vivo,* for both parent compound and its metabolites and, thus, for the selection of the range of concentrations that may be tested *in vitro*.

I.1.2.1.1.3 Exposure time

The chemical-induced neurotoxic effects *in vivo* are largely dependent on the dose and time of exposure. Neurotoxic effects may be observed shortly after the initiation of exposure (acute effects) or only after days, months or years of exposure (long-lasting effects). In some cases, indicators of neurotoxicity may be observed only after repeated or prolonged exposure . The appearance of such effects may not only depend on the type of chemical and dose used, but may also depend upon the biological processes underlying the neurotoxic response. Certain compounds interact directly with accessible cellular components, such as the cellular membrane or vital enzymes. As a result, these structures will be functionally affected shortly after exposure (Abdollahi and Karami-

Mohajeri, 2012). For example, by inhibiting the acetylcholinesterase (AChE), organophosphorus compounds and carbamates lead to the accumulation of ACh at cholinergic synapses, causing the cholinergic syndrome characteristic of the compounds (Jokanović *et al.*, 2011). For these effects, the peak concentration and exposure schedule are of critical importance. On the other hand, a delay in the occurrence of neurotoxic effects may be due to the initiation of an irreversible cascade of reactions, which may culminate in cell death. As each step along the cascade needs time to initiate the subsequent step, the final result corresponds to a long-lasting appearance of a neurotoxic effect. For example, organophosphorus compounds can cause a delayed polyneuropathy, which is related to the irreversible inhibition of other esterase, the neuropathy target esterase (Grauer *et al.*, 2008; Jokanović *et al.*, 2011).

Depending on the type of *in vitro* system, neuronal cells may survive only a few hours or several months. Moreover, as the degree of cellular maturation and differentiation of the cultured cells in influenced by time, this will influence the exposure window among the different culture systems, as a result of differences in survival and differentiation state of the cells. Therefore, though the majority of *in vitro* neuronal systems employed are valuable for predicting acute responses, they are not readily conducive to examining any effects that are progressive or delayed in nature.

I.1.2.1.1.4 Lack of cellular homeostatic mechanisms

Considering the high functionality of the nervous system, perhaps one of the most important limitations of *in vitro* neuronal models is the lack of the homeostatic mechanisms that are observed *in vivo,* such as the nutritional support that is provided by the blood circulation, regulatory control of the neuroendocrine system, interactions with adjacent cells and the intercellular components that create a unique microenvironment (Harry *et al.*, 1998). For example, in the whole animal, the presence of an intact BBB constitutes an important factor influencing the drug's access to the brain (Daneman, 2012), as observed for MPTP (Schildknecht et al., 2009; Bajpai et al., 2013), thus limiting the extrapolation of *in vitro* results to the *in vivo* scenario. Therefore, the use of *in vitro* systems provides the ability to study a discrete nervous system area or cells isolated from the homeostatic mechanisms observed *in vivo*. However, *in vitro* systems offer much in the way of assessing mechanistic questions in a defined controlled system (Costa *et al.*, 2011b).

I.1.2.1.1.5 Multiple interspecies comparisons

One of the main advantages in using *in vitro* systems for neurotoxicological studies rely on the opportunity for the investigator to examine similar cell types from multiple animal species. For example, when immortalized cell lines are used, the effects in cells from different species may be easly measured. Furthermore, it is also possible to perform studies in human cells and then compare with the response observed in other species (Culbreth *et al.*, 2012). Therefore, this allows to address questions of selective toxicity among species. However, comparisons may be limited by the inherent differences in the origin and type of the cell lines that are totally unrelated to species origin. Additionally, since the manipulation of *in vitr*o models is easier than *in vivo* conditions, the use of such models facilitates the comparison of effects between species, becoming this approach more representative of the *in vivo* scenario.

This approach may be particularly useful to evaluate the neuroxic potential of new compounds to the human scenario. For example, if a compound exhibits neurotoxicity in *in vitro* systems derived from mouse or rat and also *in vivo*, but not in an *in vitro* system derived from humans, it suggests that this compound may have a low impact in the human health. As a good example, it is well-recognized that MDMA-induced neurotoxicity in humans and rats essentially affects serotonergic neurons (O'Hearn *et al.*, 1988; Bai *et al.*, 2001), whereas in mice MDMA induces both serotonergic and dopaminergic neurotoxicity (Stone *et al.*, 1987; Cadet *et al.*, 2001; Granado *et al.*, 2008). Therefore, the use of *in vitro* neuronal models from these species may help to understand the molecular and cellular basis of this phenomenon.

I.1.2.1.1.6 Heterogeneity of the nervous system

In vivo, the development and differentiation of the nervous system depend on the interaction between neuronal and non-neuronal cells (McManus *et al.*, 1999; Vaccarino *et al.*, 2007). In mediating a neurotoxic response, not all compounds directly interact with individual cells but may cause injury by indirect effects, such as modifications of cell-cell interactions (Vijayaraghavan, 2009). The ability to obtain a culture enriched in a particular cell type constitutes a major advantage of primary cell cultures. Much work has been focused in obtaining enriched cultures representative of neuronal populations in the brain. From this, it has been demonstrated that rarely a neuronal culture exists in the absence of some glial cells and that dynamic interactions exist between the cell types in culture. In fact, in many cases, neuronal survival is poor or improbable in the absence of astroglial cells (Hatten, 1985; Vaccarino *et al.*, 2007). When early postnatal cerebellar astroglial cells are cultured in the absence of neurons, they show a flat, undifferentiated morphology

and proliferate rapidly. However, the presence of neurons in such cultures rapidly arrests glial cell growth and induces glial morphological differentiation into profiles resembling cerebellar glia seen *in vivo* (Hatten, 1987; Gómez-Nicola et al., 2013). Additionally, it has been reported that the inhibition of glial cell proliferation by neurons may be modulated by the availability and type of serum in the culture media (Bruinink *et al.*, 1992).

Studies performed during the past few years have also established the existence of bidirectional signaling between neurons and astrocytes (Freeman, 2010), thus influencing the cellular differentiation. The anatomical organization of astrocytes and their ability to take up and metabolize synaptic neurotransmitters suggest multiple functions for astrocytes in synaptic transmission, thus potentially influencing the functionality of neurons (Nag, 2011; Nedergaard and Verkhratsky, 2012). Furthermore, by regulating glutamine-GLU cycle, glial cells play a major role in modulating the neuronal activity. Glial cells may play an important role in the maintenance of neuronal GLU metabolism in cells that use GLU as a neurotransmitter. Based upon the cellular location of glutamine synthase in glial cells and glutaminase in neurons, a cycle has been proposed in which GLU released by the neuron is taken up into astrocytes by a high-affinity uptake system. Once in the astrocyte, GLU is converted to glutamine by glutamine synthase and released. It is then taken up by the neuron and reconverted by glutaminase into GLU (Stobart and Anderson, 2013). Additionally, the activation of NMDA receptors by endogenous GLU levels controlled by astrocyte GLU transporters, evokes a transient and reversible potentiation of postsynaptic GABA-A receptors, thus playing a critical role in neuronal signaling (Potapenko *et al.*, 2013).

As a functional component of the tripartite synapse, along with pre- and postsynaptic neuronal elements, astrocytes also actively participate in synaptic transmission (Halassa *et al.*, 2007). Further, the clear spatiotemporal correlation between the onset of synaptogenesis and the appearance and association of immature astrocytes with neurons at CNS synapses (Ullian *et al.*, 2001), strongly suggests the possibility that extracellular signals from astrocytes can provide a signal necessary to trigger synapse formation. Indeed, astrocytes may release a large variety of other gliotransmitters, such as *D*-serine, adenosine 5'-triphosphate (ATP), adenosine, tumor necrosis factor alpha (TNF-α), brain-derived neurotrophic factor (BDNF), cholesterol or thrombospondins, which may modulate neuronal activity and synaptic physiology. For example, cholesterol is described as an essential component for synaptic vesicle production, and its presence serves as a limiting factor in vesicle formation (Goritz *et al.*, 2005). BDNF presents important modulatory effects on the growth, remodeling and stability of dendrites and axons (Elmariah *et al.*, 2005). Thrombospondins, astrocyte-secreted extracellular matrix proteins, also promote CNS synaptogenesis, both *in vitro* and *in vivo* (Risher and Eroglu, 2012). Additionally,

transforming growth factor- β2 (TGF-β2) was demonstrated to play an essential role in the functional maturation of both excitatory and inhibitory synapses in the CNS (Heupel *et al.*, 2008).

Therefore, though mixed cultures of neurons and glial cells make difficult the evaluation of a particular response of neurons to a neurotoxicant, the presence of glial cells is determinant to maintain a healthly neuronal population, a basic requesite to obtain valid results and representative of the *in vivo* scenario.

I.1.2.1.2 Use of *in vitro* systems for mechanistic studies

In vitro systems present high usefulness for understand the mechanistic basis of neurotoxic effects that occur at molecular or cellular level. Thus, they have been extensively used in neurotoxicological studies. Since nervous system presents a high complexity, generally no single *in vitro* preparation can be used to detect all possible endpoints. However, depending on the knowledge on the neurotoxicity of a certain compound, and of the specific questions that needs to be addressed, complementary studies with different models may be used (Costa *et al.*, 2011b).

In the context of mechanistic *in vitro* neurotoxicology, one can point out studies investigating mechanisms of neurotoxicant-induced neuronal cell death (Capela *et al.*, 2006b; Capela *et al.*, 2007a), inhibition of cell proliferation (Chen *et al.*, 2011), alterations of signal transduction pathways (Yuan *et al.*, 2013b), modulation of neurotoxicity by cell–cell interactions (Giordano *et al.*, 2009; Bajpai *et al.*, 2013), alterations of inhibitory or excitatory circuits (Xu *et al.*, 2012) and many others. Therefore, there is no doubt that *in vitro* systems play a most relevant role in addressing the mechanisms involved in compound-induced neurotoxicity. For example, neuroblastoma cell lines may be useful in addressing the interaction of neurotoxicants with ion channels or receptors. Slice cultures, due to their more complex organization may be useful to study whether neurotoxicants affect certain excitatory or inhibitory circuits. Additionally, cultures of Schwann cells represent a good model to study the effects of neurotoxicants on myelination. However, in all cases, the extrapolation of *in vitro* findings to *in vivo* scenario still requires important considerations, such as the dose selection (Goldoni *et al.*, 2003), the importance of metabolism and toxicokinetics for the development of neurotoxic effects (Capela *et al.*, 2009; Bajpai *et al.*, 2013), the BBB permeability (Bal-Price *et al.*, 2010), among other factors.

In some cases, the existence of a characteristic mechanistic knowledge, may lead to the selection of a specific *in vitro* neuronal system to assess particular endpoints of neurotoxicity. For example, by inhibiting the AChE, organophosphorus compounds and

carbamates lead to the accumulation of ACh at cholinergic synapses, causing the cholinergic syndrome characteristic of the compounds. On the other hand, these compounds also cause a delayed polyneuropathy, which is related to the irreversible inhibition of other esterase, the neuropathy target esterase (Jokanović *et al.*, 2011). Therefore, the selection of specific *in vitro* neuronal models with differential expression of these enzymes may be useful in assessing the mechanistic basis of their acute and delayed neurotoxicity.

I.1.2.1.3 Use of *in vitro* systems for neurotoxicity screening

As already mentioned, a second primary objective of *in vitro* systems is providing a rapid, relatively inexpensive and reliable way for screening chemicals for potential neurotoxicity. However, though the screening tests can provide much information about potential neurotoxicants, the study of these compounds is always followed by more specific and complex tests, both *in vitro* and *in vivo*. The criteria used to *in vitro* neurotoxicity screening are the same general criteria that are used for *in vitro* screening approaches for other endpoints of toxicity, namely low incidence of false positives and false negatives, high correlation with the data provided by *in vivo* studies, sensibility, simplicity, quickness, economy and versatility (Costa, 1998a).

The selection of a specific *in vitro* model for neurotoxicity screening is not always easy. However, this selection is primarily influenced by the endpoint of neurotoxicity that it will be measured. A common belief is that for screening purposes one should examine general cellular processes, such as cell viability or proliferation or axonal/dendritic growth. However, each possibility requires careful considerations. For example, basic tests for cytotoxicity and viability assessment, including measurements of cell death and proliferation, membrane permeability or mitochondrial function are common to most cell types. However, though a chemical can affect these endpoints, we cannot conclude that the chemical is neurotoxic, but only that it displays cytotoxicity in this model (Costa *et al.*, 2011b). Additionally, the use of different *in vitro* models may provide additional information whether the chemicals display differential effects, or present different potencies, in neuronal versus non-neuronal cells. For example, to evaluate the toxic effects of methylmercury and polychlorinated biphenyls, a total of 17 different *in vitro* models were used, including models of the nervous system [neuronal (PC12 rat pheocromocytoma cells, human SH-SY5Y cells, primary cultures of cortical, hippocampal or cerebellar neurons and primary cultures of cerebellar granule or purkinje cells) and astroglial (C6 glioma cells, 1321N1 human astrocytoma cells and primary cultures of cortical, hippocampal, cerebellar or brainstem astrocytes) and non-nervous system (NIH 3T3

mouse fibroblasts, PZ-HPV-7 human prostate cells, LNCaP human prostate carcinoma cells and TT human thyroid cells). With this simple approach methylmercury was identified as a potential neurotoxicant, since toxicity was greater in neuronal cells than in other cell types. On the other hand, though the polychlorinated biphenyls were also considered potential neurotoxicants, neurons and glial cells were similarly affected (Costa *et al.*, 2007). Additionally, the relative sensitivity of each *in vitro* model to the toxic effects of compounds, can provide additional information about the possible targets involved in compound-induced neurotoxicity (Costa *et al.*, 2011b).

In the field of the neurotoxicants screening, neurite outgrowth has been proposed as an important endpoint of neurotoxicity during the development stage. This parameter may be evaluated in cell lines, like SH-SY5Y (Jung *et al.*, 2009) and PC12 cells (Radio *et al.*, 2008; Takeshita *et al.*, 2011) or in primary cultures (Maekawa *et al.*, 2013). In fact, many studies have used the interference with the neurite outgrowth as measure to screening potential neurotoxicants (Radio *et al.*, 2008; Harrill *et al.*, 2013; Krug *et al.*, 2013). In one of these studies, using a subclone of PC12 cells (Neuroscreen-1 cells), the ability of several developmental neurotoxicants to inhibit neurite outgrowth was evaluated. It was observed that retinoic acid (RA) and methylmercury, at non-cytotoxic concentrations, inhibited neurite outgrowth. Similar results were found for dexamethasone and cadmium, though at concentrations that decreased cell viability. On the other hand, while amphetamine facilitated neurite outgrowth, valproic acid, diphenylhydantoin and lead were devoid of effects on this parameter (Radio *et al.*, 2008). In another study, performed with primary cortical neurons, the effect of classical developmental neurotoxicants on axon and dendrite outgrowth was also tested. It was demonstrated that RA and methylmercury affected growth of axons to a greater extension than dendrites. On the other hand, cadmium-induced neurite outgrowth inhibition was more pronounced in dendrites than in axons (Harrill *et al.*, 2013). Therefore, this study, compared to the study presented below, indicated that the growth axons and dendrites may be differently affected by neurotoxicants.

By evaluating interference with neurite outgrowth, differentiated human LUHMES cells were also recently proposed as potential model for developmental neurotoxicity testing. In this study, in which 40 compounds were screened, it was demonstrated that several compounds, such as colchicine, vincristine, narciclasine, rotenone and cicloheximide, at non-cytotoxic concentrations, inhibited the neurite extension in this cellular model. Moreover, it was found that neurite outgrowth was affected more potently than the integrity of developed neurites of mature neurons (Krug *et al.*, 2013). Furthermore, the authors concluded that, though LUHMES cells had a definitive neuronal phenotype, the use of a general cell death endpoint in these cultures did not allow specific identification of

neurotoxicants. In addition, a ratio of the EC_{50} values of neurite growth inhibition and cell death higher that 4 provided a robust classifier for compounds associated with a developmental neurotoxic hazard, while the unspecific toxicants screened always yielded ratio lower than 4. Therefore, the authors suggest that through the evaluation of functional endpoints, such as neurite outgrowth, it is possible specifically identify and characterize potential neurotoxicants (Krug *et al.*, 2013).

Besides the high utility of the neurite outgrowth evaluation in the screening of potential neurotoxicants, the assessment of chemical effects on neuronal network activity using microelectrode arrays has been also proposed as a screening tool for neurotoxicity assessment (Frega *et al.*, 2012; McConnell *et al.*, 2012; LeFew *et al.*, 2013). In fact, electrophysiological changes in neural activity can be detected before the occurrence of any morphological change, thus representing a promising and sensitive approach to detect early effects of chemicals (Köhling *et al.*, 2005). In one of these studies, 23 chemicals known to alter neuronal function *in vivo*, including 6 GABAergic and 3 glutamatergic antagonists/agonists, 4 pyrethroids, 3 metals, 2 cholinesterase inhibitors, 2 nicotinic acetylcholine receptor agonists, valproic acid, verapamil, and fluoxetine, and 7 chemicals without neurotoxic effects recognized (glyphosate, acetaminophen, salicylic acid, paraquat, saccharin, d-sorbitol and amoxicillin) were studied, using a microelectrode arrays system. Using this approach, the 7 chemicals without neurotoxic effects recognized were correctly classified as negative, while only 20 in 23 were positively classified as neurotoxicants. Based on these results, in which high sensitivity (87% identification of positive compounds) and specificity (100% identification of negative compounds) were found, the authors suggested that the evaluation of the neuronal network activity, using microelectrode arrays, may constitute an important research tool in screening compounds with neurotoxic potential, mediated by a broad variety of mechanisms (McConnell *et al.*, 2012). In another study, through the evaluation of acute (1h after the treatment) and chronic (3 days after the treatment) effects of agonists of the glutamatergic transmission in cortical neuronal cultures, this approach was also proposed for the screening of potential neurotoxicants. It was demonstrated that fine modulations (low concentrations of drug) of the excitatory synaptic transmission are reflected in the electrophysiological activation of the network, whereas the use of medium or high concentrations of drug, which lead to excessive direct stimulation of glutamatergic pathways, results in the abolishment of the electrophysiological activity and eventually cell death. Therefore, the authors concluded that an accurate characterization of the effects of metabotropic GLU receptor activation/blockade on neuronal network activity might extend potential usefulness of microelectrode arrays techniques for the assessment of endpoints to detect acute and

chronic neurotoxic effects of chemicals and drugs for predictive neurotoxicity testing (Frega *et al.*, 2012).

A test system, using multi-electrode arrays, based on the electrophysiological recordings from neural networks in re-aggregating brain cell cultures was also proposed to detect acute neurotoxic effects of chemicals. Initial experiments indicated that re-aggregated brain cell cultures displayed evoked field potentials and spontaneous neural activity involving glutamatergic and GABAergic synaptic transmission. It was demonstrated that trimethyltin, methylmercury and ethanol, at non cytotoxic concentrations, caused a decrease in field potential amplitude. However, though an irreversible loss of neuronal electric activity was observed for trimethyltin and methylmercury, the effect of ethanol was fully reversible upon wash-out. Despite this, the test method used cannot distinguish between pharmacological actions, such as block of receptors and interactions with neurotransmitters) and neurotoxicity, as traduced by a persistent structural damage. However, based in the simple observation of loss/recovery of electrical function, it is possible to establish a differentiation between neurotoxic or acute pharmacological effects. Therefore, this approach appears to be suitable for the assessment of toxic insults specifically interfering with nervous system function, thus representing a valuable tool for the mechanistic assessment of neurotoxic effects (van Vliet *et al.*, 2007).

By combining rat primary reaggregated brain cell cultures with a mass spectrometry-based metabolomics approach, van Vliet and co-workers (van Vliet *et al.*, 2008) developed another method for neurotoxicity screening. In this study it was demonstrated that the classical neurotoxicant methylmercury chloride, at subtoxic concentrations, produced significant alterations in the levels of GABA, choline, glutamine, creatine and spermine. On the other hand, the brain stimulant caffeine only changed the levels of creatine and spermine. Additionally, the profile observed for methylmercury chloride was mimicked by other known neurotoxicants, trimethyltin or paraquat, whereas several other compounds without neurotoxic properties presented similar profile to that was observed in control cultures. Therefore, this study indicated that the levels of GABA, choline, glutamine, creatine and spermine may be used as biomarkers in neurotoxicity screening, and, additionally, in neuroprotection studies (van Vliet *et al.*, 2008).

The examples presented here suggest that several *in vitro* systems, such as cell lines, primary neuronal cultures or aggregated brain cell cultures, which present different complexity, and through different neurotoxicity endpoints, such as disruption of the neurite outgrowth or neuronal electrical activity, may be used in the screening of potential neurotoxicants.

I.1.2.2 Types of *in vitro* systems for neurotoxicity assessment

Several *in vitro* systems, including subcellular systems [e.g. isolated mitochondria (Cassarino *et al.*, 1999; Misiti *et al.*, 2004; Li *et al.*, 2012) and synaptosomes (Pubill *et al.*, 2005; Chipana *et al.*, 2006; Chipana *et al.*, 2008a; Chang and Wang, 2010; Elinos-Calderón *et al.*, 2010; Lu *et al.*, 2010; Mannangatti *et al.*, 2011; López-Arnau *et al.*, 2012; Martínez-Clemente *et al.*, 2012)], immortalized cell lines (Presgraves *et al.*, 2003; Ferreira *et al.*, 2013; Heusinkveld *et al.*, 2013; Im *et al.*, 2013; Zhou *et al.*, 2013), primary neuronal cultures (Capela *et al.*, 2006a; Capela *et al.*, 2006b; Cunha-Oliveira *et al.*, 2006; Capela *et al.*, 2007b), three-dimensional (3D) cultures (Hill *et al.*, 2008; Moors *et al.*, 2009; Schreiber *et al.*, 2010; Choi *et al.*, 2013) and brain slices (Rump *et al.*, 2010; Torres-Altoro *et al.*, 2011; Rozas *et al.*, 2012; Yamazaki *et al.*, 2013) are routinely used for predicting toxic effects to the nervous system. In addition, the increased scientific interest in the biology of the stem cells has attributed to the neural stem cells (NSCs) an emerging role in the field of the neurotoxicology (Fujita *et al.*, 2008; Ceccatelli *et al.*, 2013). Despite this, here, we focused in three experimental models, synaptosomes, the SH-SY5Y immortalized cell line and primary neuronal cultures, the models used in the studies accomplished in the scope of this thesis.

Synaptosomes are obtained by homogenization and fractionation of brain tissue. They are isolated terminals that break away from axon terminals when the neuronal tissue is homogenized. The synaptosomes retain pre- and postsynaptic characteristics, which make them useful in the study of synaptic transmission. They retain the molecular machinery used in neuronal signaling and are able of uptake, storage, and release of neurotransmitters (Dunkley *et al.*, 2008; Westmark *et al.*, 2011).

Immortalized cell lines provide a homogeneous cell population that is often well characterized and controlled. Generically, they are easily cultured, divide rapidly, and can be derived from different species, including humans. Compared with primary cells, cell lines readily allow the incorporation of exogenous genes. Additionally, some of these cells can be differentiated into different neuronal subtypes (Costa *et al.*, 2011a; de Groot *et al.*, 2013). However, their genetic stability decreases with increasing number of passages, neurites do not always represent true axons or dendrites and functional synapses are often absent. Additionally, transformed cell lines may represent only a subset of cells and may not have the same (functional) phenotype as primary cells (Breier *et al.*, 2010; Astashkina *et al.*, 2012).

Primary cultures usually have the same phenotype as brain cells *in vivo* and maintain most neurodevelopmental processes. They can be isolated relatively easily from distinct brain areas and at different developmental stages (Breier *et al.*, 2010; Costa *et al.*,

2011a). However, these cultures often contain populations of postmitotic neurons, which implicate that these cells do not multiplicate in culture. Among the most frequent limitations of this system are the relatively short lifespan, the variability that exists between cultures and the limited availability of tissue (Breier *et al.*, 2010; Costa *et al.*, 2011a).

I.1.2.2.1 Uses and limitations of *in vitro* models

For evaluation of altered nervous system functioning, isolated models have been selected based on key biochemical and morphological features, which are specifically targeted by neurotoxicants *in vivo*. The use of *in vitro* models for predicting neurotoxic events offers several advantages including reduced costs, ease of use, fewer ethical issues and better control over experimental variables (Kumaria and Tolias, 2008). Primary cultures allow for visualization of individual living cells and for monitoring both morphological and electrophysiological features. It is believed that neuronal and glial cells migrate to re-arrange themselves on the substratum and differentiate according to their function and abilities. However, the tissue organization is lost as a result of the dissociation procedure needed to obtain the isolated brain cells. Additionally, *in vivo*-like structures cannot be obtained by this technique. Despite these limitations, primary cultures are more accessible to experimental manipulation than slice cultures, apart from the fact thatthey are easier to obtain and maintain. It is possible to obtain and correlate biochemical, morphological, electrophysiological, and molecular data from a single cell. Additional purification methods can be used to enrich a particular cell type in a cell preparation obtained by dissociation, but it is difficult to obtain and define pure cultures of any one cell type (Banker and Goslin, 1998; Tiffany-Castiglioni, 2004).

On the other hand, cell lines of tumoral origin provide homogeneous cell populations in large quantities in a very reproducible manner. Usually the common cell lines of choice are those that continue to express, in culture, the properties of their normal adult cell counterpart. It must be noted, again, that these cell culture systems represent cells that are no longer part of an integrated neural network and may develop an altered appearance, metabolism and response to chemicals. Some believe that these concerns can be addressed by experimental design and choice of endpoints. No such efforts, however, will fully compensate for the isolation of a system from the natural neural environment and all of the systemic influences on that environment. In addition, the ability of *in vitro* neuronal systems to predict the neurotoxicity of a chemical *in situ* or the potency of a series of structurally related analogs can depend on whether they express the molecular/cellular target for neurotoxicants (Banker and Goslin, 1998; Tiffany-Castiglioni, 2004).

Below, for each *in vitro* neuronal model use n the scope of this thesis, its particular advantages and limitations, as well as its main characteristics, are described.

I.1.2.2.2 Subcellular systems

Despite the extended use of cell based systems as *in vitro* models in neurotoxicological research, in the last decades, sub-cellular systems have been extensively used in evaluating signaling pathways and receptor-mediated signal transduction, as well as to study specific points that may be addressed out of the cellular environment.

I.1.2.2.2.1 Synaptosomes

One of the most used subcellular systems in neuropharmacological and neurotoxicological studies is the synaptosome model. More than 50 years ago, Gray and Whittaker (Gray and Whittaker, 1962) and De Robertis and co-workers (De Robertis *et al.*, 1962) introduced the preparation of nerve-ending particles, also called synaptosomes. Understanding the function of nerve terminals at physiological and molecular level has been dramatically enhanced by the development of procedures to isolate nerve terminals from the brain (Dunkley *et al.*, 2008). It should be emphasized that the *in situ nerve* terminal functions, which are largely autonomously from the distant cell body, require only the electrical signal from the axonal action potential to trigger release and the replenishment of materials via axonal transport mechanisms for long-term survival (Erecinska *et al.*, 1996). Representative images of synaptosomes with their mitochondria labeled with tetramethylrhodamine methyl ester (TMRM) are shown Figure 3.

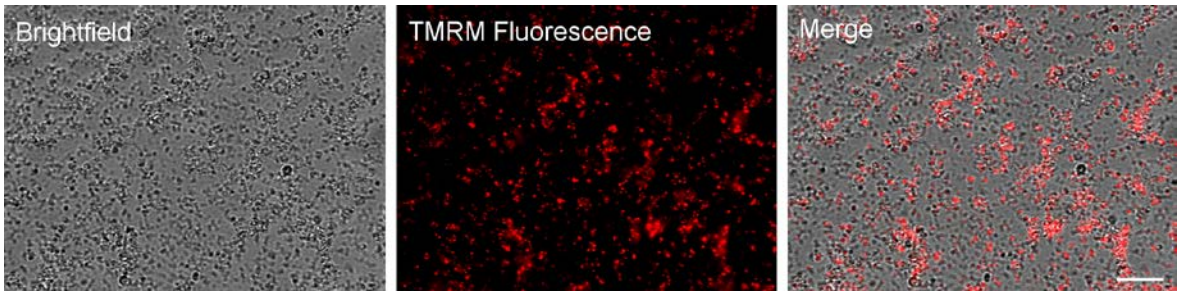


Figure 3. Representative images of synaptosomes with their mitochondria labeled with tetramethylrhodamine methyl ester (TMRM). Scale bar: 20 µM.

The main characteristics of the synaptosome model are summarized in Table 2. Synaptosomes are a subcellular fraction, derived from neurons, prepared from brain tissue by homogenization and function as small anucleated cells that retain neuronal

vesicles and enzymes (Nicholls, 1993). In addition, synaptosomes can be partially purified by gradient centrifugation, thus eliminating portions of axons that are frequently present in unpurified synaptosomal preparations (Dunkley *et al.*, 1986). Usually, synaptosome size range from 0.5 to 1 µm, it has one or more mitochondria and possess extremely active ion transport systems across its membrane (Nicholls, 1993; Whittaker, 1993).

Table 2. Characteristics of synaptosomes.

0.5 to 1 µm of size	Metabolic ability
High respiratory control	Possess one or more mitochondria
Reduced protein synthesis	Prepared from brain tissue by homogenization
Function as small anucleated cells that retain neuronal vesicles and enzymes	Maintain a plasma membrane potential ranging from -60 to -80 mV
Highly labile structures, especially after osmication	Present an average cytoplasmic free Ca^{2+} concentration of about 0.1-0.2 µM
Possess extremely active ion transport systems across their membranes	Maintain intact mechanisms involved in neurotransmitter uptake, storage and release
Not able to use GLU and aspartate as energy sources	Can use glucose both aerobically and anaerobically and pyruvate as an oxidative metabolite

Biochemically, synaptosomes can use glucose, either aerobically or anaerobically and pyruvate, as an oxidative metabolite. Despite the high content in GLU and aspartate in the synaptosomal cytoplasm, these are not readily utilizable as energy sources. (Nicholls, 1993). When maintained at 37ºC, the ATP produced is rapidly degraded, thus leading to a fast decrease in synaptosomal viability. However, when kept on ice and with availability of nutrients, their functionality is maintained for several hours (Dunkley *et al.*, 1988; Dunkley *et al.*, 2008). Carefully prepared synaptosomes retain a high respiratory control, maintain a plasma membrane potential ranging from -60 to -80 mV, in low K^+ medium (Agoston *et al.*, 1983), with an average cytoplasmic free Ca^{2+} concentration of about 0.1-0.2 µM (Kauppinen *et al.*, 1988). It may, thus, be concluded that the synaptosome model is energetically viable (Nicholls, 1993). The metabolic specialization of the nerve terminals, as result of their long distance from cell body, allows to maintain intact the mechanisms involved in neurotransmitter uptake and release. On the other hand, also determines the synaptosomal viability, given their reduced protein synthesis, since only proteins of the mitochondrial electron transport chain (ETC) are synthetized in synaptosomes, which are codified by mitochondrial deoxyribonucleic acid (mtDNA). Therefore, methodologies

involving transference of DNA or genetic silencing [ribonucleic acid (RNA) interference] cannot be performed in this model (Dunkley *et al.*, 2008). Although the nerve endings originating synaptosomes are more resistant to liquid shear forces than other parts of neurons they are highly labile structures, especially after osmication (Gray and Whittaker, 1962).

The synaptosomal model presents particular advantages and limitations, which are summarized in Table 3. The major advantage of this model consists in its simple preparation. Moreover, synaptosomes retain all the machinery for the uptake, storage and release of neurotransmitters present in terminal nerve. However, it is largely depleted of functional glial and neuronal cell body elements. Although electron micrographs of synaptosomal preparations sometimes look unpleasantly heterogeneous, the non-synaptosomal membrane fragments are generally dead from a functional point of view, and do not interfere with studies which require an intact membrane, glycolytic pathway, mitochondria and ion gradients. One of the major limitation of synaptosome model is the inherently heterogeneous neurotransmitters content, since even the most closely defined anatomical region contains a wide variety of neurotransmitters (Nicholls, 1993; Erecinska *et al.*, 1996).

Table 3. Advantages and limitations in using synaptosomes as *in vitro* model for neurotoxicological studies.

Advantages	
Simple preparation	Easy to maintain *in vitro*
Absence of functional glial and neuronal cell body elements	Ability to perform studies of synaptic transmission, as they are capable of uptake, storage, and release of neurotransmitters
Limitations	
Loss of cell to cell interactions	Heterogeneity in terms of type of neurotransmitters and content
Not possible to work with methodologies involving transference of DNA or genetic silencing	

Synaptosome model has been routinely used in the field of the neurobiology to study metabolic pathways (Jankowska-Kulawy *et al.*, 2010), energy production and ion movements (Choi *et al.*, 2009), neurotransmitters storage and synthesis (Escubedo *et al.*, 2011; López-Arnau *et al.*, 2012), and mechanisms involved in neurotransmitters release (Chang and Wang, 2010; Lu *et al.*, 2010; Mannangatti *et al.*, 2011; López-Arnau *et al.*, 2012; Martínez-Clemente *et al.*, 2012), as well as oxidative injury to macromolecules (Pubill *et al.*, 2005; Chipana *et al.*, 2006; Chipana *et al.*, 2008a; Elinos-Calderón *et al.*,

2010) and neuronal mitochondria (Bains *et al.*, 2009; Choi *et al.*, 2009; Telford *et al.*, 2010). By using the synaptosome model, it was demonstrated that alterations in ACh release from thiamine deficient nerve terminals, resulting from the inhibition of mitochondrial acetyl-coenzyme A (acetyl-CoA) and citrate synthesis, and inhibition of acetyl-CoA transport to the synaptoplasmic compartment, through ATP-citrate lyase pathway, may yield deficits of cholinergic functions observed in thiamine deficiency-evoked cholinergic encephalopathies (Jankowska-Kulawy *et al.*, 2010). As presynaptic mitochondrial dysfunction is implicated in a variety of neurodegenerative disorders, synaptosomes may be also used to mimetize the mitochondrial deficits found in neurodegenerative diseases (Chinopoulos and Adam-Vizi, 2001; Colle *et al.*, 2013), in order to understand the basis of the neurodegenerative process. Working with this model, a few studies have recently evaluated the influence of several drugs on GLU homeostasis (Chang and Wang, 2010; Lu *et al.*, 2010), as well as alterations in neurotransmitter transporters' functions elicited by psychostimulant drugs with neurotoxic properties (Mannangatti *et al.*, 2011; López-Arnau *et al.*, 2012; Martínez-Clemente *et al.*, 2012). Furthermore, in mouse brain synaptosomes, increased ROS production, as well as mitochondrial dysfunction, has been proved to be useful indexes for the evaluation of neurotoxicity induced by several drugs (Chipana *et al.*, 2006; Chipana *et al.*, 2008a; Bains *et al.*, 2009). In addition, synaptosomes have been widely used as *in vitro* model to study the function and activity of the neuronal Na^+- and K^+-activated adenosine 5'-triphosphatase (Na^+/K^+ ATPase) under several experimental settings (Bersier *et al.*, 2011; Pendyala *et al.*, 2012; Pimentel *et al.*, 2013).

Therefore, though the synaptosome model does not present many of the mechanisms found at cellular level, given its simplicity and functionality, it constitutes an important *in vitro* model for neurotoxicological studies that does not require the functionality of the intact cells.

I.1.2.2.3 Cellular systems

With the development of new approaches to study the nervous system, cell culture began to gain a more prominent and important position in the neurobiology and neurotoxicology fields. Since 1907, studies of the nervous system in tissue culture have provided invaluable insights into the embryological origins of nerve cells, the development of their cytological and biochemical identities, their functional connectivity and their interactions with glia and other cell types within nervous system (Banker and Goslin, 1998).

I.1.2.2.3.1 Immortalized cell lines

Similarly to other tissues, several approaches have been developed for establishing cell lines from neuronal tissue. Cell lines of limited lifespan often undergo genetic changes, after which their growth potential is modified and, consequently, their lifespan becomes unlimited. These cell lines are termed immortalized cell lines (Banker and Goslin, 1998).

The main advantages and limitations in using immortalized cell lines as *in vitro* models for neurotoxicological studies are summarized in Table 4. The major attributes of immortalized cell lines are their homogeneity, making them appropriate to study the selectivity of neurotoxicants. However, this homogeneity can limit the cellular interactions, which implicates that cells are not exposed to the complex network of messages typical for neuronal circuits. In addition, another remarkable advantage consists in the large quantity of cells that can be used. Also, cell lines offer the possibility to perform biochemical studies with homogenous populations of neuronal cells devoid of glia (Banker and Goslin, 1998). Immortalized cell lines can be stored indefinitely in liquid nitrogen and grown up whenever needed. Additionally, when properly handled, the cells will exhibit identical properties time after time, year after year. However, it has been observed quite often that the cells will drift with regard to physiological responsiveness with increased passages. Other features of established cell lines include the ability to undergo an unlimited number of cell divisions, altered cell and colony morphology and loss of anchorage dependence (Banker and Goslin, 1998; Breier *et al.*, 2010; Astashkina *et al.*, 2012).

One of the major limitations of immortalized cell lines is the difficulty in inhibiting cell division experimentally to obtain a stable population of differentiated cells. This contrasts with the *in vivo* situation, where the end cell in a differentiation sequence usually does not divide. In many cases, differentiation is induced by chemicals and drugs. However, it is not known if this differentiation process is comparable to the differentiation that occurs *in vivo*. Furthermore, there are two important recognized problems associated with the use of immortalized cell line cultures. The first is the genetic transformation and sub-culturing procedures to isolate cells that have escaped senescence, and exhibit up-regulated telomerase activity, thus producing cells with significant changes in their differentiation potential. Second, the majority of transformed immortalized cell lines have not been studied in depth to identify all the idiosyncratic changes imposed by genetic manipulation and multiple passages (Astashkina *et al.*, 2012). In general, cell lines are more resistant than primary cell cultures to neurotoxic insults (LePage *et al.*, 2005). Still, genetic stability of any given phenotype is critical for the reproducibility of experimental findings. However,

in vitro differentiation of neuronal cell lines constitutes another contributing factor for phenotypic variability, as a result of differences in the effectiveness of the differentiation process. Additionally, after increased number of passages, cell lines may also suffer changes in their phenothype (Banker and Goslin, 1998; Breier *et al.*, 2010; Astashkina *et al.*, 2012).

Table 4. Advantages and limitations in using immortalized cell lines as *in vitro* models for neurotoxicological studies.

Advantages	
A large quantity of cells can be easily grown	High homogeneity of the cell populations
Retain their main properties along the time	Can be stored indefinitely in liquid nitrogen and used when needed
Proliferation in culture for long periods without contamination	Possibility to obtain and correlate biochemical, morphological, electrophysiological, and molecular data from a single cell
Enable studies with homogenous populations of neuronal cells uncontaminated with glia	
Limitations	
Lack the growth regulation seen *in vivo*	Possible development of phenotypic alterations
Limited cellular interactions resulting from the high homogeneity	Do not possess all the features of adult differentiated cells
In general, cell lines are more resistant than primary cell cultures to neurotoxic insults	Difficulty in inhibiting experimentally cell division to obtain a stable population of differentiated cells
The genetic amenability and response to a neurotoxicant may be changed, as compared to primary cells	The majority of immortalized cell lines have not been studied in depth to identify all the idiosyncratic changes imposed by genetic manipulation and multiple passages

Cell lines are such a mainstay of research in other areas of cell biology that someone coming to neurobiology from another discipline must find it peculiar that anyone still works with primary cultures (LePage *et al.*, 2005). The problem is that the cell lines presently available for neurobiological and neurotoxicological research do not express some key aspects of neuronal differentiation. Though there are cell lines that express many of the individual characteristics of differentiated neurons, including neurotransmitters, ion channels, receptors and other neuron-specific proteins, they are not good models for all specific neuronal phenothypes (LePage *et al.*, 2005). For example, PC12 cells, which can come as close as any cell line to mimicking a specific population of differentiated nerve cells, do not develop distinct axons and dendrites or form synapses like the sympathetic

neurons they otherwise resemble (Westerink and Ewing, 2008). The suitability of available cell lines as models for neurons from the CNS is even more limiting. Presumably this reflects the complexity of the developmental processes that lead to the acquisition of a specific neuronal identity in a tissue with hundreds or thousands of distinguishable neuronal phenotypes (LePage *et al.*, 2005).

Cell lines exist that are representative of neurons, including neuroblastomas cell lines (e.g. SH-SY5Y, Neuro-2A or IMR-32 cell lines) (Shastry *et al.*, 2001), and glia, such as oligodendrocyte cell lines (e.g. CG4, OLN-93 or HOG cell lines), Schwann cell lines (e.g. 33B, IMS32 or NF1T cell lines) astrocyte cell lines (e.g. C6, BALB SFME or U87MG cell lines) or microglia cell lines (e.g. HAPI, BV-2 or CHME-5 cell lines) (De Vries and Boullerne, 2010). With some rapidly dividing cell types, such as glia, a large cell population can be derived from the progeny of a single cell. Though cell lines lack the growth regulation seen *in vivo*, the critical point for experimental use is whether the cells express the differentiated characteristic of interest identical to those *in vivo*. If they do, information on the binding characteristics of the tested compound to the target receptor or binding site molecule may be studied as an important first step in the neurotoxicity evaluation. However, the use of cell lines for neurotoxicological studies, even if they express the differentiated characteristic of interest, should be exercised with caution. As the genetic amenability and response to a test compound may be dramatically changed in cell lines, as compared to the original primary cells, unforeseen cell line specific effects may occur. Thus, the data may not be directly applicable for extrapolation to the *in vivo* condition (Banker and Goslin, 1998; Astashkina *et al.*, 2012).

I.1.2.2.3.1.1 Cell lines of neuronal origin

I.1.2.2.3.1.1.1 Neuroblastoma cell lines

Neuroblastomas are neuro-endocrine solid tumors of childhood that show undifferentiated cell phenotypes and poor prognosis. These tumors arise from the neural crest and occasionally show spontaneous regression following differentiation into benign ganglioneuromas. The first neuroblastoma cell line emerged over 50 years ago. Human neuroblastoma cell lines correspond to adrenal neuroblasts, arrested at different levels during the morphogenesis of the adrenal medulla (Shastry *et al.*, 2001). The differentiation of sympathoadrenal precursor cells toward either sympathetic neurons or chromaffin cells may be promoted by several factors and hormones. Particularly, glucocorticoids are involved in the differentiation of the precursor cells toward chromaffin cells (Cooper *et al.*, 1990). This finding is indicative of the sensitivity and of dependency of neural crest-

derived cells to steroid hormones. Cell lines derived from human neuroblastomas represent a good model of human immature neurons and have been widely used for the study of mechanisms involved in neuronal function and differentiation (Påhlman *et al.*, 1990; Shastry *et al.*, 2001). They form homogenous populations, proliferate rapidly in chemically defined media and extend neuritic-like processes. These cell lines also synthesize *in vitro* proteins unique to the neuronal phenotype [e.g. neuron-specific enolase (NSE) and neurofilaments (NFs)], receptors for neuroactive factors, as well as enzymes required for the biosynthesis of several neurotransmitters [choline acetyltransferase, TH and dopamine-β-hydroxylase]. In addition, they form homogenous populations and proliferate rapidly in chemically defined media (Sadée *et al.*; Biedler *et al.*, 1978; Påhlman *et al.*, 1983; Ciccarone *et al.*, 1989). Neuroblastoma cells may be differentiated *in vitro*, from immature into mature neuronal cells, by different natural and chemical agents, allowing, thus, to study the evolution of several biologic processes at different stages of cellular development and differentiation. However, when neuroblastoma cell lines are being used, it is important, and at times difficult, to distinguish between morphologic differentiation and cytotoxicity (Påhlman *et al.*, 1990; Shastry *et al.*, 2001). A large part of the data present in the literature using neuroblastoma cells has been performed with the human SH-SY5Y cell line.

I.1.2.2.3.1.1.1.1 SY-SY5Y cells: a human neuroblastoma cell line

The SH-SY5Y neuroblastoma cell line is a thrice cloned subline of SK-N-SH cells which were originally established from a bone marrow biopsy of a neuroblastoma patient with sympathetic adrenergic ganglial origin in the early 1970's (Biedler *et al.*, 1973). This cell line has been widely used as a neuronal model since the early 1980's, as these cells possess many biochemical and functional properties of neurons (Presgraves *et al.*, 2003; Ferreira *et al.*, 2013).

The main characteristics of the SH-SY5Y cell line are summarized in Table 5. This cell line exhibits enzymatic neuronal markers (TH and dopamine-β-hydroxylase), specific uptake of NA and expresses one or more proteins of the NFs. These cells also express opioid, muscarinic and nerve growth factor receptors (Takeuchi *et al.*, 2009). SH-SY5Y cells may differentiate upon treatment with a variety of agents, including RA (Presgraves *et al.*, 2003; Cheung *et al.*, 2009), 12-*O*-tetradecanoylphorbol-13-acetate (TPA) (Presgraves *et al.*, 2003; Ferreira *et al.*, 2013), BDNF (Cernaianu *et al.*, 2008), dibutyryl cyclic adenosine 5'-monophosphate (dBcAMP) (Kume *et al.*, 2008) or staurosporine (Mollereau *et al.*, 2007). Consequently, the SH-SY5Y cell line has been widely used in experimental neurotoxicological studies (Presgraves *et al.*, 2003; Wang and Xu, 2005;

Shavali and Sens, 2008; Lopes *et al.*, 2010; Ferreira *et al.*, 2013). Although SH-SY5Y cells have been widely used either in their undifferentiated or differentiated state, use of undifferentiated cells involves some limitations. One of the most important limitation is the proliferation during the course of the experiment, which makes difficult to distinguish whether neurotoxic agents influence the proliferation rate or the rate of cell death (Datki *et al.*, 2003). Furthermore, SH-SY5Y cells in culture are unsynchronized and do not always exhibit the typical markers of mature neurons, which leads to uncertainty in experiments. Moreover, undifferentiated cells do not express high levels DAT, apart from that they exhibit less sensitivity to neurotoxins and neuroprotective agents than primary neurons (Presgraves *et al.*, 2003). In addition, though SH-SY5Y cells express dopamine-β-hydroxylase and TH, catecholamines (dopamine and NA) synthesis is limited as result of a deficiency in dihydroxyphenylalanine decarboxylase (Ikeda *et al.*, 1994).

Table 5. Characteristics of the SH-SY5Y cell line.

Thrice cloned subline of SK-N-SH cells	Exhibits specific uptake of NA
Expresses DAT	Expresses proteins of NFs
Expresses dopamine-β-hydroxylase and TH	Expresses opioid, muscarinic, and nerve growth factor (NGF) receptors
After differentiation, presents a functionally mature neuronal phenotype	May differentiate upon treatment with a variety of agents
Limited synthesis of catecholamines (dopamine and NA) as a result of the deficiency in dihydroxyphenylalanine decarboxylase	

Differentiation of SH-SY5Y cells lead to a functionally mature neuronal phenotype. In fact, upon differentiation, cells stop proliferating, become a more stable population (Presgraves *et al.*, 2003), and show extensive neurite outgrowth (Ferreira *et al.*, 2013) with morphological similarity to living neurons in the brain. In addition, SH-SY5Y differentiated cells possess more biochemical, ultrastructural, morphological and electrophysiological similarity to neurons and express a variety of neuronal-specific markers, including receptors for neurotrophic factors, growth-associated protein 43 (GAP-43), NSE, neuronal nuclei (NeuN) synaptophysin, and neuronal-specific cytoskeletal proteins, including microtubule-associated protein (MAP) Tau. In fact, Tau, GAP-43, NeuN, and synaptophysin are classical markers of mature neurons (Cheung *et al.*, 2009). However, according to the differentiation agent used, cells may acquire different phenotypes. SH-SY5Y cells differentiated with RA present a mature cholinergic phenothype, with no significant differences in DAT and TH expression (Presgraves *et al.*,

2003; Cheung *et al.*, 2009). However, they present higher expression of choline acetyl transferase (ChAT) (Adem *et al.*, 1987) and VMAT (Presgraves *et al.*, 2003), thus confirming the enhancement of a cholinergic phenothype. On the other hand, SH-SY5Y cells differentiated with TPA acquire a more characteristically adrenergic neuronal phenothype, as observed by increased expression of TH, neuropeptide Y (NPY), as well as NSE, and increased NA biosynthesis. Indeed, both NA and NPY are two important neurotransmitters produced in adrenergic neurons of the sympathetic nervous system (Jalava *et al.*, 1992; Presgraves *et al.*, 2003). Despite this, SH-SY5Y cells differentiated with RA followed by TPA specially develop a dopaminergic phenotype, expressing higher levels of DAT and TH, though lower levels of VMAT, compared to their undifferentiated state. Furthermore, RA/TPA-differentiation increases the density of dopamine 2 (D2) and dopamine 3 (D3) receptors in cell surface (Presgraves *et al.*, 2003). Additionally, it was shown a higher ability of RA/TPA-differentiated SH-SY5Y cells to uptake and retain dopamine, compared to their undifferentiated state (Presgraves *et al.*, 2003; Ferreira *et al.*, 2013) and lower resistance to the neurotoxic actions of dopaminergic toxins, such as MPP^+ (Presgraves *et al.*, 2003), thus confirming the enhancement of a dopaminergic phenothype. Representative images of undifferentiated or RA/TPA-differentiated SH-SY5Y cells are shown in Figure 4.

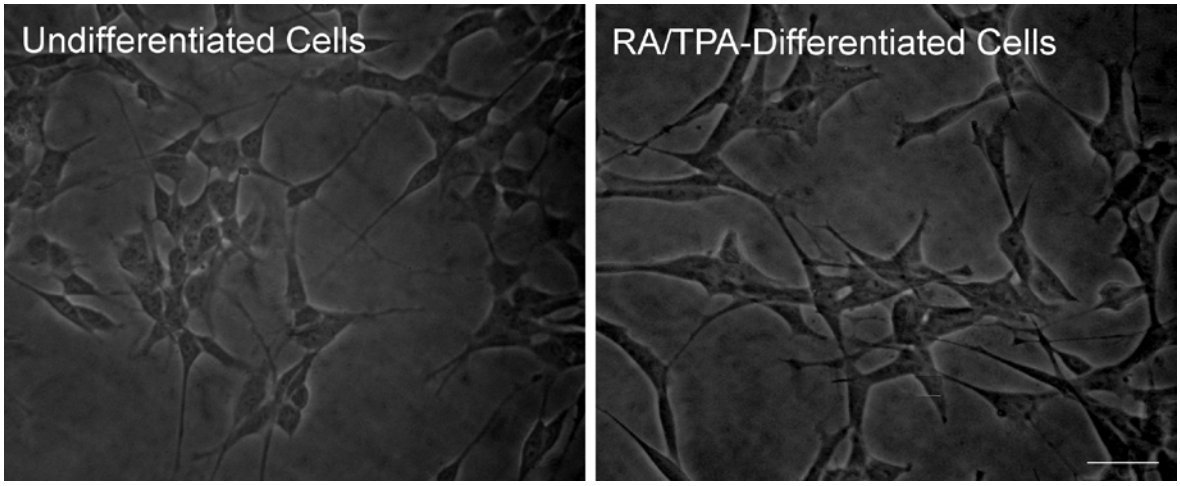


Figure 4. Brightfield images of SH-SY5Y cells in their undifferentiated state or after differentiation with RA/TPA (3 days with 10 µM RA followed by additional 3 days with 80 nM TPA). Scale bar: 50 µm.

Among the different agents that can be used to differentiate SH-SY5Y cells are also included compounds of the family of neurotrophins, including NGF and BDNF (Cernaianu *et al.*, 2008). In addition, several other growth factors, including basic fibroblast growth factor (bFGF), insulin-like growth factor I (IGF1), glial cell line-derived neurotrophic factor

(GDNF) and ciliary neurotrophic factor (CNTF) also induce differentiation of SH-SY5Y cells (Weiss *et al.*, 2001; Yang *et al.*, 2008). However, SH-SY5Y cells generally lack functional neurotrophin receptors. Nevertheless, pre-treatment with RA up-regulates the neurotrophin receptors, making, thus, SH-SY5Y cell responsive to differentiation by neurotrophins (Cernaianu *et al.*, 2008). Despite the well-known effectiveness of neurotrophins as differentiation agents, the neuronal phenothype that is promoted remains unclear. Reports indicate that SH-SY5Y cells differentiated with RA and BDNF increase the expression of general neuronal markers and cholinergic markers [NPY, vesicular acetylcholine transporter (VAChT) and ChAT], thus suggesting that after differentiation cells acquire a typically cholinergic neuronal phenothype (Edsjö *et al.*, 2003). However, other reports indicate that SH-SY5Y cells differentiated with RA and BDNF exhibit a characteristically dopaminergic phenothype, with high TH and DAT activity and functional uptake and release of dopamine (Mastroeni *et al.*, 2009). Therefore, further studies in SH-SY5Y cells differentiated with RA and BDNF are needed to a better characterization of their phenothype.

Staurosporine is another agent used to differentiate SH-SY5Y cells, inducing a mature adrenergic phenotype characterized by up-regulation of TH, DAT and NPY activities and increased NA content (Jalava *et al.*, 1993; Mollereau *et al.*, 2007). SH-SY5Y cells differentiated with guanosine and guanosine 5'-triphosphate (GTP) presented a dual dopaminergic/adrenergic phenothype characterized by cell-cycle arrest and increased TH and DAT expression (Guarnieri *et al.*, 2009). On the other hand, dBcAMP differentiate SH-SY5Y into an adrenergic neuronal phenothype, characterized by increased NA synthesis and TH expression (Kume *et al.*, 2008).

As previously stated, after differentiation, SH-SY5Y cells present a modified susceptibility to neurotoxins. These changes appear to be most closely related with the differentiation agent used. Reports indicate that SH-SY5Y cells differentiated with RA are more resistant to certain neurotoxins, like MPP^+, 6-hydroxydopamine or β-amyloid protein, than undifferentiated cells (Cecchi *et al.*, 2008; Cheung *et al.*, 2009; Wszelaki and Melzig, 2011). Other reports indicate that differentiation with RA followed by TPA make SH-SY5Y cells less prone to the neurotoxic actions of dopamine (Ferreira *et al.*, 2013). However, compared to cells differentiated with RA, RA/TPA-differentiated SH-SY5Y cells appear to be more sensitive to the neurotoxic effects of the MPP^+ (Presgraves *et al.*, 2003). On the other hand, staurosporine-differentiated SH-SY5Y cells are more susceptible to the neurotoxic actions of several agents, than in their undifferentiated state (Tieu *et al.*, 1999), which emphasizes the similarity of RA/TPA- or staurosporine-differentiated SH-SY5Y cells to primary neurons. These changes of vulnerability might be attributed to various biochemical changes evoked by different differentiating agents, such as over-expression

and down-regulation of anti- and pro-apoptotic proteins (Tieu *et al.*, 1999; Jantas *et al.*, 2008) or alterations in signaling pathways, including protein kinase B (Akt) and tropomyosin receptor kinase B (TrkB) pathways (Ho *et al.*, 2002; Wenker *et al.*, 2010). Nevertheless, SH-SY5Y differentiated cells, given their similarity to primary neurons in drug-induced toxic actions, remain valuable research tools.

The SH-SY5Y cell line has been extensively used to establish the neurotoxic potential of several compounds, namely MDMA (Ferreira *et al.*, 2013), classical neurotoxicants, like MPP^+ (Presgraves *et al.*, 2003) and 6-hydroxydopamine (Tirmenstein *et al.*, 2005; Tsushima *et al.*, 2012), or organic pollutants (Jung *et al.*, 2009; Chen *et al.*, 2013). Additionally, different mechanisms have been explored, such as disruption in intracellular Ca^{2+} levels (Hettiarachchi *et al.*, 2012), mitochondrial dysfunction (Tirmenstein *et al.*, 2005), oxidative stress (Tirmenstein *et al.*, 2005; Tsushima *et al.*, 2012; Ferreira *et al.*, 2013) or disruptions in neurite outgrowth (Jung *et al.*, 2009; Chen *et al.*, 2013), thus making this cell line an important *in vitro* model in the field of the neurotoxicology.

I.1.2.2.3.2 Primary cultures

I.1.2.2.3.2.1 Dissociated primary cultures

The dissociated primary culture is one of the most widely used *in vitro* system in the field of the neurotoxicity research. The dissociated primary cultures, as indicate by their name, are prepared from suspensions of individual cells, obtained by dissociation of the brain tissue (Capela *et al.*, 2007b; López-Doménech *et al.*, 2012; Capela *et al.*, 2013). When plated onto an appropriate surface, the neurons begin to extend processes within several hours, ultimately forming a dense network. The plating efficiency is dependent on the dissociation technique, the type of substratum, the culture medium composition, and the type of tissue. The presence and amount of serum and trophic factors, oxygen tension, the composition of the substratum and seeding density strongly affect the viability and differentiation of the cell culture (dedifferentiation, transdifferentiation, differentiation inhibition or induction of differentiation) (Banker and Goslin, 1988). However, under favorable conditions, it is possible to maintain such cultures for long periods of time, during which cells acquire most of the properties of mature neurons. They develop distinct axons and dendrites, form synapses with other neurons, and express the receptors and ion channels characteristic of the corresponding cell type *in situ* (Radio and Mundy, 2008). Frequently, cells develop considerable spontaneous electrical activity, including synaptic potentials. When co-cultured with Schwann cells or oligodendrocytes, axons become myelinated. Importantly, neurons obtained by dissociation appear to retain their individual

identities, presumably as a result of their postmitotic nature and committed in their differentiation at the time that they are introduced in culture. Motor neurons express properties reminiscent of motor neurons, Purkinje cells of Purkinje cells, and so on. In a few cases, it has been possible to demonstrate this directly by labeling specific populations of embryonic cells *in situ*, then examining their properties in culture (Huang *et al.*, 2012). Therefore, in general, the morphological and physiological properties of the cell populations present in culture correspond closely to the characteristics of the cell populations present in the tissue of origin.

The main advantages and limitations in using dissociated primary cultures for neurotoxicological studies are summarized in Table 6. The most obvious advantage of the dissociated primary cultures is that they render accessibility to individual living cells. During the first few days in culture, before the neural network becomes too dense, individual neurons can be easily visualized in their entirety. This allows a direct observation of growing axons, their mode of branching and the behavior of their growth cones. Importantly, dissociated cells in culture permit a remarkably precise experimental analysis of these events. Additionally, primary dissociated neuronal cultures are particularly amenable to study using morphological and physiological techniques, which may be applied on a cell-by-cell basis. However, these cultures are less suited to traditional biochemical approaches, since the amount of biological material obtainable from these cultures usually is limited. Another inherent limitation of the dissociated primary cultures is the homogeneous population of cells. In specific cases, cultures may be prepared whose cellular composition is much simple than that of the tissues from which they derive. However, more commonly, cultures are as complex as the tissue from which they are originated. The heterogeneity of the culture also complicates studies using morphological and physiological techniques, since consistent results require the identification of specific cell populations. Developing approaches to deal with the heterogeneity of cell types is critical to the successful use of dissociated primary cultures. Such considerations begin with the choice of tissue to culture. Some regions of the nervous system are simply more complicated than others. There is also a general belief that cells in primary culture may be more sensitive to the effects of neurotoxicants. Though this is true at times, it is not always the case, because these differences of susceptibility may also be often due to different culturing conditions (Banker and Goslin, 1998; Radio and Mundy, 2008; Astashkina *et al.*, 2012).

Table 6. Advantages and limitations in using dissociated primary cultures as *in vitro* models for neurotoxicological studies.

Advantages	
Individual living cell is accessible	Possibility of a direct observation of growing axons, their mode of branching and the behavior of their growth cones
These cultures allow the monitorization of both morphological and electrophysiological features, which may be applied on a cell-by-cell basis	Possibility to obtain and correlate biochemical, morphological, electrophysiological and molecular data from a single cell
Limitations	
Heterogeneity of the cellular population	Limited amount of biological material, compared to the immortalized cell lines
The tissue organization is lost as a result of the dissociation procedure	Higher susceptibility to the effects of neurotoxicants

I.1.2.2.3.2.1.1 Neuronal primary cultures

Much work has focused on obtaining cultures representative of neuronal populations. Usually primary neuronal cultures are derived from many different brain regions, such as HIP (López-Doménech *et al.*, 2012; Capela *et al.*, 2013), CTX (Capela *et al.*, 2007b; Xu *et al.*, 2012; Yuan *et al.*, 2013b), striatum (Oliveira *et al.*, 2006) or cerebellum (Jiménez *et al.*, 2004; Giordano *et al.*, 2009), or from peripheral nervous system (PNS) (Söderström and Ebendal, 1995), of rat (Capela *et al.*, 2007b; Xu *et al.*, 2012; Yuan *et al.*, 2013b) or mouse (Oliveira *et al.*, 2006; López-Doménech *et al.*, 2012) fetal brain tissue. However, fetal brain tissue from humans (Rahman *et al.*, 2011) or chicken (Söderström and Ebendal, 1995; Windisch *et al.*, 2003) has also been used. The use of fetal tissue is required, because neurons are much less susceptible to damage during dissociation, since their soma are still small, and before they have developed extensive axonal and dendritic arbors, and have become highly innervated. Additionally, at early stages of development, neurons may also be less dependent on their target cells for trophic support (Banker and Goslin, 1998). Even within a brain region, such as the cerebellum, individual cell types require distinct donor ages. While cerebellar granule cells are generally isolated from postnatal day 6 to 8 brains (Jiménez *et al.*, 2004; Giordano *et al.*, 2009), for a successful Purkinje cell cultures, usually fetal tissue is used (Wagner *et al.*, 2011). Therefore, as the age of the donor is critical for successful culturing of each cell type from different brain regions, it is important to maintain a consistency in donor age between different experiments. Moreover, different brain regions present different neuronal populations.

While primary cultures of cortical neurons are mainly constituted by GABAergic and glutamatergic neurons, primary cultures of cerebellar granule cells are mainly constituted by glutamatergic neurons (Suñol *et al.*, 2008). Thus, according to the endpoint of neurotoxicity that will be measured, there are brain areas that may be more appropriated than others.

On the other hand, it is difficult to obtain pure cultures of dissociated primary neurons, since these cultures are generally contaminated with glial cells, thus difficulting to discern pharmacological or toxicological phenomena that are specific of neurons (Viviani *et al.*, 1998). To circumvent this limitation, primary cultures may be added of cytosine arabinose, generally 24 to 48h after seeding, which, by inhibiting the glial proliferation, allows to obtain neuron-enriched primary cultures (Zhang *et al.*, 2010; Liu *et al.*, 2011; Wang *et al.*, 2012a).

In vitro, neurons extend neurites rapidly, with minimal requirement for extracellular matrix proteins, neural cell adhesion molecules or NGF. Though brain tissue constitutes the most widely used source for culture of dissociated neuronal cells, cultures of sympathetic ganglion cells (Koike and Ninomiya, 2000) and dorsal root ganglion cells (Misko *et al.*, 2010; Misko *et al.*, 2012) have also been made. In these cells, neurite outgrowth can be enhanced by the presence of various growth factors, including NGF. On the other hand, neurons in culture differ from neurons *in vivo* for a number of reasons, which must be considered when interpreting data from *in vitro* systems. Primary neurons in culture are metabolically, physiologically and morphologically stunted. Furthermore, they are not subject to normal excitatory or inhibitory inputs that are observed *in vivo*. Therefore, the susceptibility of these cells to toxic insult may be different. Another limitation of the use of primary neuronal culture is that these cells do not divide *in vitro* and survive during a limited time. In addition, it is difficult to obtain homogenous, well-defined and reproducible cultures (Radio *et al.*, 2008; Astashkina *et al.*, 2012).

Despite all these limitations, primary neuronal cultures have proved to be a useful system for measuring neurotoxicity *in vitro*. In fact, many studies have used primary neuronal cultures to study the neurotoxic potential of several compounds, namely drugs of abuse, such as MDMA (Capela *et al.*, 2007b; Capela *et al.*, 2013), amphetamine (Cunha-Oliveira *et al.*, 2006) or cocaine (Cunha-Oliveira *et al.*, 2006), methylmercury (Meacham *et al.*, 2005), lead (Hogberg *et al.*, 2010), organic pollutants (Meacham *et al.*, 2005), neuropharmacological agents (Hogberg *et al.*, 2010), among other compounds. Several endpoints of neurotoxicity have been assessed, such as cell death (Capela *et al.*, 2007b; Capela *et al.*, 2013) interference with neurite outgrowth (Söderström and Ebendal, 1995; Maekawa *et al.*, 2013) or disruption of the mitochondrial function (Cunha-Oliveira *et al.*, 2006). Additionally, this model, in association with other research tools, has provided

valuable insights in screening the neurotoxic potential of several compounds (Hogberg *et al.*, 2010; Hogberg *et al.*, 2011).

I.1.2.2.3.2.1.1.1 Hippocampal primary cultures

The HIP is brain area that has received special attention along the years, as a result of its anatomical organization, which is strikingly precise and exhibits a remarkable ability for activity-dependent changes in synaptic function, such as long-term potentiation (Epp *et al.*, 2013). Many of these characteristics are believed to reflect the specific endogenous properties of hippocampal neurons. For example, hippocampal neurons have the ability for plasticity and exhibit higher susceptibility to anoxia. This feature appears to be related to the unique properties of NMDA receptors, which are expressed at particularly high levels by hippocampal neurons (Legendre *et al.*, 1993).

The HIP presents a relatively homogeneous population of neurons with well-characterized properties typical of CNS neurons in general. Pyramidal neurons, the principal cell type in the HIP, have been estimated to account for 85 to 90% of the total neuronal population. The CA1 and CA3 regions of the HIP contain pyramidal neurons that differ from one another in some of their physiological properties and in some aspects of their connectivity. Therefore, these neurons may be cultured separately. However, they are similar in many fundamental aspects. A variety of interneurons have also been described in the HIP, though they are few in number, compared with pyramidal neurons. Additionally, hippocampal primary cultures may present a low content of dentate granule cells (Fath *et al.*, 2009; Herculano-Houzel, 2011). Representative confocal images of hippocampal primary cells obtained from mouse embryos at embryonic day (E) 16 are shown in Figure 5.

In the HIP, neurons of the try-synaptic circuit, granule and pyramidal cells are glutamatergic excitatory, whereas inhibitory interneurons are GABAergic. This mode of separation of synaptic activity is at the basis of the functioning of the nervous system as a network. Excitatory neuronal cells produce synaptic inputs that stimulate target cells and, in turn, receive inhibitory inputs that govern their excitability Despite this, hippocampal pyramidal neurons and dentate granule cells express GABA receptors, thus indicating that these cells may be modulated by GABA neurotransmission. (Lambert *et al.*, 1989; McBain *et al.*, 1999). Therefore, primary hippocampal cultures are mainly constituted by glutamatergic neurons.

Hippocampal pyramidal neurons exhibit many features of interest for neurobiology and neurotoxicology studies, which are summarized in Table 7. For example, these neurons have a characteristic, well-defined shape. Furthermore, such as most neurons of the CNS,

they exhibit a single axon and innumerous dendrites. Also, their dendritic arbor is distinctive, consisting of a single long apical dendrite and several shorter basilar dendrites, all highly branched and studded with dendritic spines. Additionally, hippocampal pyramidal neurons establish direct connections with other neurons and with the population of endogenous interneurons. Therefore, in culture, hippocampal neurons still can make extensive and establish synaptic connections with one another (Kaech and Banker, 2006; Fath *et al.*, 2009).

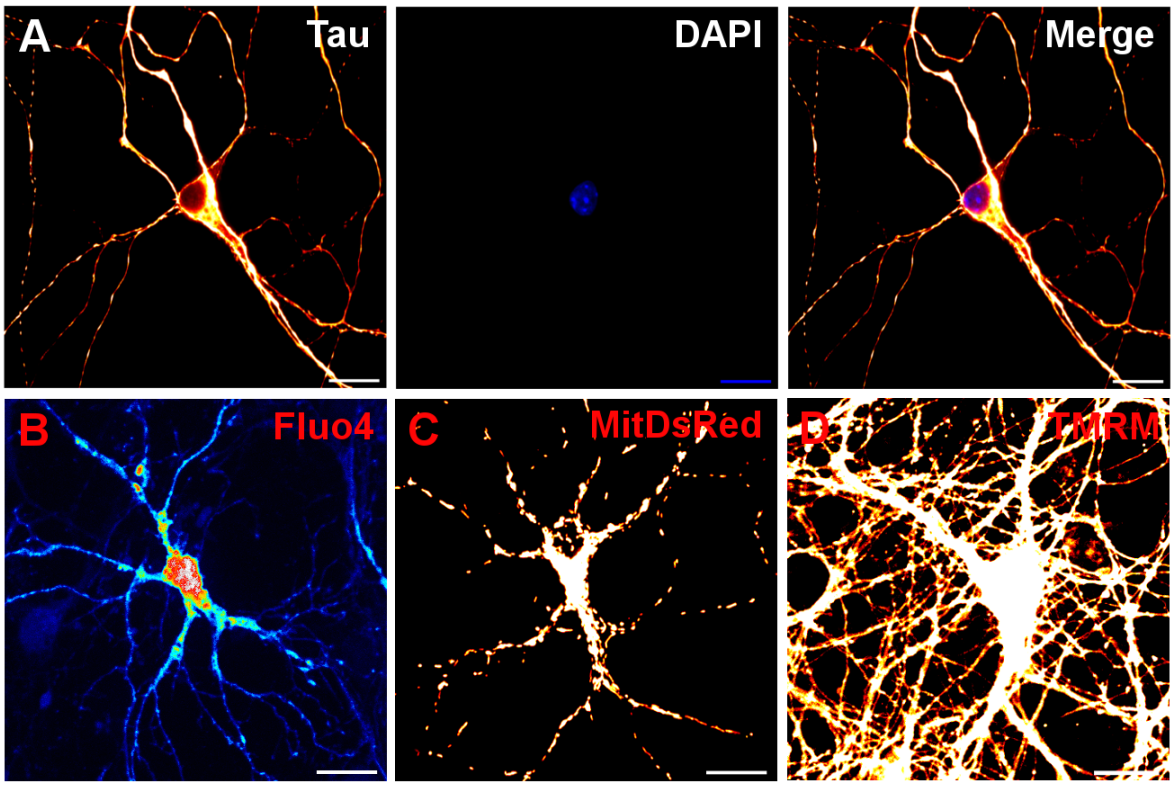


Figure 5. Hippocampal primary cells isolated from mouse embryos at embryonic day (E) 16.
(A) Confocal images of a hippocampal primary neuron, at 6 days *in vitro* (DIV), colabelled with anti-Tau antibody and the nuclear marker 4',6-diamidino-2-phenylindole (DAPI). (B-D) Confocal images of live hippocampal primary cells, at 6DIV, labeled with Fluo4 (intracellular calcium staining) (B), over-expressing the mitochondrial tagged protein MitDsRed (mitochondrial staining) (C) or labeled with tetramethylrhodamine methyl ester (TMRM, mitochondrial staining) (D). Scale bar: 20 µm.

Generally, hippocampal primary cultures are prepared from E17 to E19 rat embryos (Chen *et al.*, 2007b; Chen *et al.*, 2010; Capela *et al.*, 2013) or from mice embryos at a comparable stage of development (E15 to E17) (Llorens-Martín *et al.*, 2011; López-Doménech *et al.*, 2012). At this stage, the generation of pyramidal neurons, which begins in the rat at about E15, is essentially complete, though the generation of dentate granule cells, which largely occurs postnatally, scarcely has begun (Epp *et al.*, 2013). Therefore, hippocampal primary cultures prepared from embryos at this stage are essentially

constituted by pyramidal neurons. This characteristic allows to obtain a more homogeneous experimental response.

Table 7. Characteristics of hippocampal primary cultures.

High content of pyramidal neurons	Low content of interneurons and dentate granule cells
Pyramidal neurons have a characteristic, well-defined shape	Pyramidal neurons exhibit a single axon and innumerous dendrites
Pyramidal neurons establish direct connections with other neurons and with the population of endogenous interneurons	Dendritic arbor is distinctive, consisting of a single long apical dendrite and several shorter basilar dendrites, all highly branched and studded with dendritic spines
Since hippocampal primary cultures prepared from rodent embryos are essentially constituted by pyramidal neurons, they allow to obtain a more homogeneous experimental response	

Hippocampal primary cultures have been extensively used to establish the neurotoxic potential of several compounds (Sanchez *et al.*, 2008; Capela *et al.*, 2013; Godoi *et al.*, 2013), thus making them an important *in vitro* model in the field of the neurotoxicology. Additionally, hippocampal cultures have also been widely used for visualizing the subcellular location of endogenous or expressed proteins, for imaging protein trafficking (Chen *et al.*, 2007b; Chen *et al.*, 2010; Llorens-Martín *et al.*, 2011; López-Doménech *et al.*, 2012) and for defining the molecular mechanisms underlying the development of neuronal polarity, dendritic growth and synapse formation (Geissler *et al.*, 2013; Sapir *et al.*, 2013). For these proposes cultures conditions must permit the growth of cells at low density, to allow the easy observation of individual cells.

I.1.3 The pivotal role of mitochondria in neurons

The name mitochondrion was first coined by Benda (Benda, 1898), and it comes from two Greek words, “mitos” (thread) and “condros” (granule), which describe the appearance of mitochondria. In the following years, many investigators speculated on the role of mitochondria in cells, with Warburg (Warburg, 1913) recognizing the association between mitochondria and respiration. Many years of biochemical studies characterized this organelle as the site of energy production and cellular respiration, leading to consider mitochondria as the “powerhouses” of the cell.

The critical dependence of neurons on mitochondria is determined by three interconnected functions:

► **Energy production -** While the brain is only 2% of the body weight, it consumes approximately 20% of the energy produced in the body. Most brain energy is generated by mitochondria (mitochondria are thought to produce more than 90% of the cellular ATP), organelles highly efficient in utilizing oxygen and substrates, mainly derived from glucose, to produce cellular energy in the form of ATP. Mitochondria provide ATP via oxidative phosphorylation, which occurs on the ETC, localized in the inner mitochondrial membrane (Ho et al., 2012; Van Laar and Berman, 2013). Oxidation of pyruvic acid in the Krebs cycle supplies high-energy electrons, in the form of nicotinamide adenine dinucleotide reduced form (NADH) or flavin-adenine dinucleotide reduced form ($FADH_2$), to undergo oxidative phosphorylation. This process involves the flow of these electrons along the ETC, from complex I (NADH ubiquinone oxidoreductase) and complex II (succinate dehydrogenase) to complex IV (cytochrome c oxidase) and, finally, to molecular oxygen, which is subsequently converted to water. Along with the flow of electrons through the ETC, there is a concomitant pumping of protons in complexes I, III (ubiquinol cytochrome c oxidoreductase) and IV, from the mitochondrial matrix to the mitochondrial inter-membrane space, creating an electrochemical gradient, also known as proton-motive force, across the inner membrane. Complex V, also called ATP synthase, utilizes this electrochemical gradient to drive adenosine 5’-diphosphate (ADP) phosphorylation and generate ATP by channeling the protons back to the matrix. The proton-motive force has two components: the mitochondrial membrane potential ($\Delta\Psi_m$), which arises from the net movement of positive charge across the inner mitochondrial membrane, and the pH gradient. At any given time, the $\Delta\Psi_m$ (typically between -150 and -180 mV) reflects the balance between processes that contribute to the generation of the proton gradient and those that consume it (Ho *et al.*, 2012; Vafai and Mootha, 2012). Mitochondrial-dependent ATP production is critical to support many important neuronal functions, including the generation of axonal and synaptic membrane potentials, mobilization of synaptic vesicles

during intensive neuronal activity and assembly of the actin cytoskeleton among synapses, and for proper mitochondrial distribution along neuronal processes (Attwell and Laughlin, 2001; Verstreken *et al.*, 2005).

► **Ca^{2+} handling -** The mitochondrial potential is used to accumulate cytosolic Ca^{2+}. Ca^{2+} is taken up by the Ca^{2+} uniporter. Once inside the mitochondria it can either be buffered [probably by converting it to an insoluble $(Ca)_x(PO_4)_y(OH)_z$ salt by reaction with PO_4^{3-} supplied by the Pi carrier) or it can be transported back out of the mitochondria via a Na^+/Ca^{2+} antiporter. This is powered by a Na^+ gradient, set up by a Na^+/H^+ antiporter (Szabadkai and Duchen, 2008). This ability of mitochondria to undertake Ca^{2+} buffering plays a major role in neuronal signaling, since Ca^{2+} acts as an key regulator of neurotransmission and as secondary messenger (Billups and Forsythe, 2002; Michaelsen and Lohmann, 2010).

► **Apoptotic cell death -** The mitochondrial stage of apoptosis control is upstream of caspase activation. One well understood role of mitochondria in caspase activation is to regulate the release of proteins from the space between the inner and outer mitochondrial membranes to the cytosol, such as cytochrome c, apoptosis inducing factor (AIF) or SMAC/Diablo, thus leading to apoptotic neuronal death (Danial and Korsmeyer, 2004; Franklin, 2011).

I.1.4 Mitochondrial transport in neurons

In the nervous system, neurons are extremely polarized cells that present three distinct functional and subcellular domains, the cell body or soma, the axon, and dendrites. While the soma and dendrites receive and process the information provided from another cell, the axon is responsible for transfers it, by generating action potentials. Essential materials and mitochondria, which are generally synthesized or generated in the cell body, are delivered through the neuronal processes to their final destination, the synaptic terminals. Owing to their unique metabolic requirements, these areas do not display a uniform mitochondrial distribution. The large size of many neurons (up to 1 m in humans), which precludes rapid diffusion of ATP from one end of the cell to the other, implies, therefore, that the energy production must be spatially matched to local energy usage. In neurons, areas with high energy requirements, such as presynaptic and postsynaptic terminals, active growth cones and axonal branches, myelination boundaries, sites of axonal protein synthesis and nodes of Ranvier are enriched in mitochondria, compared to other cellular domains (Sheng and Cai, 2012). Furthermore, though mitochondrial biogenesis may occur locally in the axon, generation of new organelles mainly occurs within the cell body. Additionally, as the degradation of organelles, such as mitochondria, ensues in the cell body, dysfunctional mitochondria need to return to the soma for an efficient degradation (mitophagy) through the autophagy-lysosomal system (Ashrafi and Schwarz, 2013). Therefore, neurons require highly efficient mechanisms for mitochondrial transport regulation from and to the cell body to enable the rapid redistribution of mitochondria to different areas, in order to supply increased metabolic requirements.

In neurons, mitochondria are highly dynamic organelles with bidirectional transport along neuronal processes, frequently changing direction, pausing or switching to persistent docking (Kang *et al.*, 2008; López-Doménech *et al.*, 2012; Plucińska *et al.*, 2012). The cytoskeleton is responsible for the maintenance of the highly specialized structure of neurons, also allowing axonal growth and coordinated transport and stable docking events (Sau *et al.*, 2011). Microtubules, the main component of the cytoskeleton, which are formed by polymers of α- and β-tubulin, are polarized structures with the “plus” end toward to the terminal and the “minus” end toward to the cell body. However, dendrites presented a mixed polarity (Sau *et al.*, 2011; Saxton and Hollenbeck, 2012). Actin filaments, which are enriched in nerve terminals, are composed of monomers forming flexible helical polymers with fast-growing and slow-growing ends that generate explosive growth during neurite extension. This allows the extrusion of the axonal growth cone (Sau *et al.*, 2011; Millecamps and Julien, 2013). NFs, also called intermediate filaments, are the most abundant component in neuronal cytoskeleton. NFs lack any

polarity and assemble from three subunit polypeptides, such as NF-L (light-chain NF), NF-M (medium-chain NF) and NF-H (high-chain NF). Additionally, NFs are much more stable than actin or microtubules, and primarily provide structural stabilization to neurons and regulate the radial axonal growth, axonal calibre and speed of impulse conduction (Sau *et al.*, 2011; Millecamps and Julien, 2013). Of note, cytoskeletal filaments are linked to MAPs, such as Tau protein, which permit their stabilization. However, though microtubules, actin, and IFs are three major components of the axonal cytoskeleton, only microtubules and actin filaments play critical roles in mitochondrial transport and docking. A schematic representation of the mitochondrial transport along axons and dendrites are illustrated in Figure 6.

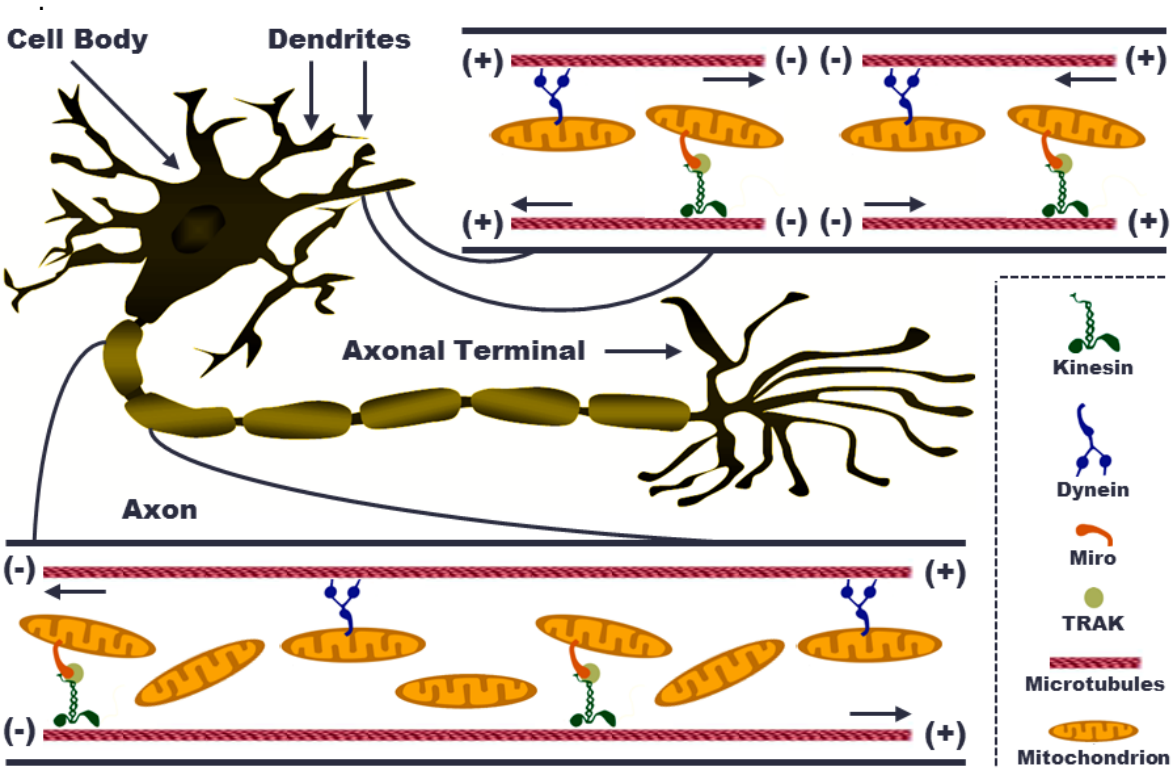


Figure 6. Mitochondrial transport in neurons.
In axons, microtubules are uniformly organized with the "plus" ends (+) facing toward the axonal terminals and the "minus" ends (-) toward to the cell body. However, the organization of microtubules in dendrites show mixed orientation. Polarity and organization of microtubules in axons and dendrites are critical for the targeted transport of synaptic cargoes and organelles by microtubule-associated motor proteins. While kinesin motors are mostly "plus"-end directed, dyneins travel toward the "minus" ends of microtubules. Therefore, in the axonal compartment, kinesin motors mediate anterograde transport of mitochondria and dynein drives retrograde mitochondrial transport. In dendrites, both kinesin and dynein motors may drive mitochondria in both anterograde and retrograde directions, depending on the microtubule polarity.

Mitochondrial transport in neurons occurs through motor proteins, which move mitochondria along the microtubules, whereas the actin cytoskeleton is much more important for mitochondrial anchor and for short-range movements (MacAskill and Kittler,

2010; Sheng and Cai, 2012). These highly coordinated processes involved in mitochondrial mobility result from the coupling of mitochondria to anterograde and retrograde motor proteins and to docking and anchoring machinery. Kinesin superfamily and cytoplasmic dyneins are the major motor proteins involved in mitochondrial transport along microtubules. Additionally, mitochondria are linked to the motor proteins through adaptor proteins or mitochondrial receptors (López-Doménech *et al.*, 2012). The mitochondrial transport between the soma and distal axonal and dendritic regions depends on the polarity of the microtubules. Thus, the anterograde transport involves translocation toward microtubule "plus" ends, using kinesin motors, while retrograde transport requires translocation toward "minus" ends, using dynein motors, being the motor proteins functions highly dependent on the ATP hydrolysis. However, in dendritic processes, as microtubules present mixed polarity in the proximal regions, both kinesin and dynein motors may drive mitochondria in both anterograde and retrograde directions, depending on the microtubule polarity (MacAskill and Kittler, 2010; Sheng and Cai, 2012; Schwarz, 2013).

I.1.4.1 Motor proteins

I.1.4.1.1 Kinesin motors

Microtubule "plus" end directed anterograde axonal transport of mitochondria is mediated by kinesin motors. At least 45 different kinesin motor genes have been identified in humans and mice, which are classified into 14 families. However, the best characterized molecular motors are the members of the kinesin-1 family, also known as KIF5 (Hirokawa *et al.*, 2010).

KIF5 motor protein contains two kinesin heavy chains and two kinesin light chains. The KIF5 heavy chains are constituted by an amino-terminal motor domain that has adenosine 5'-triphosphatase (ATPase) activity and binds directly to microtubules, and a carboxyl-terminal domain that mediates the association with the kinesin light chain or interacts directly with cargoes or adaptor molecules, such as mitochondrial adaptor proteins (Sheng and Cai, 2012). In mammalians there are 3 KIF5 isoforms (KIF5A, KIF5B and KIF5C). KIF5B is expressed in many cell types, though KIF5A and KIF5C are only found in neurons (Cho *et al.*, 2007). The role of kinesin motors in regulating anterograde axonal transport of mitochondria has been demonstrated by several studies. For example, the over-expression of a dominant negative construct of KIF5 in cultured hippocampal neurons disrupted the axonal transport of mitochondria (Cai *et al.*, 2005). Similarly, in KIF5A (-/-) mouse cultured motor neurons the maximum and average velocity of

mitochondrial transport was reduced in both anterograde and retrograde directions (Karle *et al.*, 2012). In addition, kinesin-mediated mitochondrial transport may occur by direct attach of motor protein to the lipid bilayer of the mitochondrial membrane, or via adaptor proteins that themselves can bind lipids or have transmembrane domains (Macaskill *et al.*, 2009b; Wang and Schwarz, 2009).

I.1.4.1.1.1 Adaptor proteins for kinesin motors

The *Drosophila melanogaster* proteins Milton and mitochondrial Rho guanosine 5'-triphosphatase (GTPase) Miro (dMiro) are described to be crucial for anterograde transport of mitochondria in flies. In this model, Milton is linked indirectly to mitochondria through an interaction with dMiro, a protein located in the outer mitochondrial membrane. Therefore, Miro serves as a membrane anchor that links Milton and, thus, kinesin to the mitochondrial surface (Stowers *et al.*, 2002; Guo *et al.*, 2005; Glater *et al.*, 2006). Since the initial identification of these adaptor proteins in flies, two mammalian orthologous of Milton, TRAK1 and TRAK2, also known as OIP106 and OIP98/Grif-1, respectively (Brickley *et al.*, 2005), and two mammalian orthologous of dMiro, Miro1 and Miro2 (Fransson *et al.*, 2006), were identified. A schematic representation of Miro protein structure is illustrated in Figure 7.

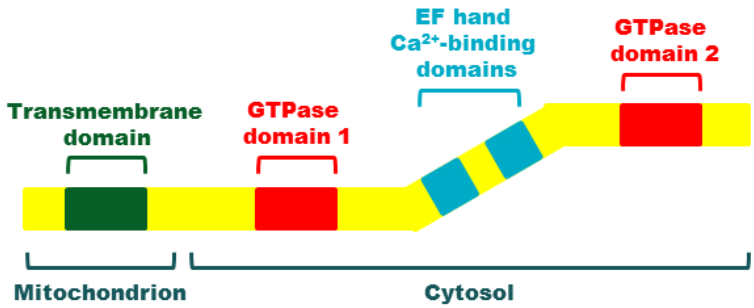


Figure 7. Primary structure of Miro protein.
Miro contains two guanosine 5'-triphosphatase (GTPase) domains, which bind and hydrolyze guanosine 5'-triphosphate (GTP), and two EF hand Ca^{2+}-binding domains. Miro is anchored in the mitochondrial outer membrane by a carboxyl-terminal transmembrane domain. Created by the author based in the references (Fransson *et al.*, 2006; Glater *et al.*, 2006; Macaskill *et al.*, 2009b; Wang and Schwarz, 2009; MacAskill and Kittler, 2010).

Miro protein contains two EF hand Ca^{2+}-binding domains, flanked by two GTPase domains, and a carboxyl-terminal transmembrane domain that sits in the outer mitochondrial membrane (Fransson *et al.*, 2006; Glater *et al.*, 2006). In hippocampal neurons, Miro1 acts as the major mitochondrial acceptor site for TRAK2, as demonstrated by the key regulator role of this complex in controlling mitochondrial transport (MacAskill

et al., 2009a). In agreement, a recruitment of TRAK2 to mitochondria and enhanced organelle's transport was observed by increasing Miro1 expression (MacAskill *et al.*, 2009a). Additionally, impaired axonal movement of mitochondria was observed in hippocampal neurons over-expressing a dominant negative construct of TRAK1 (Brickley and Stephenson, 2011), thus providing additional evidence for an important role of TRAK and Miro proteins in mediating mitochondrial transport.

Three additional motor adaptor proteins, syntabulin, fasciculation and elongation protein-ζ1 (FEZ1) and Ran-binding protein 2 (RANBP2) were also implicated in kinesin-dependent transport of mitochondria.

Syntabulin is a membrane-associated protein that binds directly to the cargo-binding domain of KIF5 and targets to mitochondria through its carboxyl-terminal tail (Cai *et al.*, 2005). Knockdown of syntabulin expression with targeted small interfering RNA or interference with the syntabulin-kinesin-1 heavy chain interaction reduced mitochondrial density within axonal processes by impairing anterograde movement of mitochondria (Cai *et al.*, 2005). In addition, syntabulin loss-of-function in cultured superior cervical ganglion neurons was associated with reduced mitochondrial distribution along neuronal processes (Ma *et al.*, 2009), thus indicating an important role for syntabulin in mitochondrial transport in neurons.

FEZ1, a brain-specific protein involved in axonal outgrowth, has also been implicated in neuronal mitochondrial transport. Silencing of FEZ1 by RNA interference efficiently reduced NGF-induced neurite elongation and the anterograde movement of mitochondria in PC12 cells (Fujita *et al.*, 2007). Similarly, in hippocampal neurons, silencing of FEZ1 by RNA interference repressed the axonal formation and retarded the anterograde mitochondrial movement in neurites (Ikuta *et al.*, 2007), thus suggesting that FEZ1 participates in the establishment of neuronal polarity by controlling the mitochondrial motility along axon.

The other kinesin adaptor RanBP2, a large scaffold protein associated with nucleocytoplasmic transport, protein biogenesis, mitosis and trafficking, has been shown to mediate the interaction between mitochondria and KIF5B and KIF5C, but not KIF5A (Cho *et al.*, 2009). However, though in non-neuronal cells RanBP2 was described to regulate kinesin-dependent mitochondrial transport (Patil *et al.*, 2013), its role in mitochondrial transport in neurons remain unclear.

I.1.4.1.2 Dynein motors

Microtubule “minus” end-directed retrograde axonal transport of mitochondria is mediated by cytoplasmic dynein motors (Hirokawa *et al.*, 2010). In agreement, as demonstrated in *Drosophila melanogaster*, retrograde axonal transport of mitochondria, velocity and run length, was altered by mutations in dynein heavy chain genes, thus elucidating the role of dyneins in regulating “minus” end-directed transport (Pilling *et al.*, 2006).

Dynein motors are constituted by two dynein heavy chains and several dynein intermediate chains, dynein light intermediate chains and dynein light chains. Such as dynein light-chain 1 (LC), Roadblock and T-complex testis-specific protein 1 homolog (Tctex1) constitute other dynein light chain proteins. Dynein heavy chains, which have ATPase activity, function as motors, but the existence of a large numbers of accessory proteins, such as dynein light chains, appears to allow selectivity between dynein motors and different cargoes (Hirokawa *et al.*, 2010). On the other hand, dynein is associated with the protein dynactin, a multi-subunit complex necessary for dynein activity (King and Schroer, 2000). Both dynein and dynactin have been shown to be essential in mediating retrograde mitochondrial transport (Pilling *et al.*, 2006).

Contrary to kinesin superfamily, few dynein heavy chains have been identified, and the mechanisms that link dynein to mitochondria are not well understood. One model suggests that dyneins link to mitochondrial membrane-associated proteins via their light and intermediate chains. T-complex testis-specific protein 1 homolog (Tctex1), which is a dynein light chain protein capable to support dynein-mediated transport, was shown to interact with mitochondria by binding to the voltage-dependent anion-selective channel 1 (VDAC1), located in the outer mitochondrial membrane (Schwarzer *et al.*, 2002). Furthermore, in flies, mutations in the gene of the protein β-amyloid precursor protein-like protein interacting protein 1 (APLIP1), a neuronally expressed *Drosophila melanogaster* orthologous of mammalian c-Jun *N*-terminal kinase (JNK)-interacting protein-1 (JIP1), decreased the transport of mitochondria only in retrograde direction (Horiuchi *et al.*, 2005), thus suggesting inhibition of the “minus” end-directed transport by cytoplasmic dynein. However, at present, a role for the vertebrate APLIP orthologous JIP1-3 in regulating dynein-mediated mitochondrial transport is not established. Furthermore, Snapin was reported as a possible dynein motor adaptor that contributes to dynein-mediated retrograde transport of late endocytic organelles in neurons (Cai *et al.*, 2010), though its involvement in mitochondrial transport is not established.

Studies in *Drosophila melanogaster* neurons demonstrated that dMiro protein also regulates retrograde mitochondrial transport (Russo *et al.*, 2009). Recently, biochemical

evidences confirmed that the dynein motor indeed interacts with the TRAK/Miro complex (van Spronsen *et al.*, 2013). Moreover, potential TRAK-binding partners were identified, such as several components of dynein and dynactin complexes, including dynein heavy-chain 1, dynein light-chain 1 (LC8), p150Glued, and p50/dynamitin (van Spronsen *et al.*, 2013), thus suggesting that this kinesin adaptor protein may also regulate dynein-mediated retrograde mitochondrial transport.

I.1.4.1.3 Myosin motors

While long range transport of mitochondria in neuronal processes is mediated by kinesin and dynein motors along microtubules, short range movements in nerve terminals and growth cones, in which actin filaments form the major cytoskeletal architecture, are probably mediated by myosin motors (Adikes *et al.*, 2013). At least 18 classes of myosin motor proteins are identified, though the best characterized is the myosin V (Foth *et al.*, 2006).

Myosin V motor protein is constituted by two heavy chains and two light chains. Myosin heavy chain is constituted by a motor domain, which has ATPase activity and binds directly to actin, and a terminal domain that mediates the association with cargoes (Hirokawa *et al.*, 2010; Sheng and Cai, 2012).

Though several evidences report the involvement of myosin motors in mitochondrial movement in many systems, mitochondrial association with myosin motors and myosin-driven mitochondrial transport have not been directly demonstrated in mammalian neurons (Valiathan and Weisman, 2008; Adikes *et al.*, 2013). However, it has been shown that cargoes associated with myosin V move along axons at a rate that is markedly slower than that of most axonal organelles, but similar to mitochondria (Alami *et al.*, 2009; Macaskill *et al.*, 2009b; Wang and Schwarz, 2009; MacAskill and Kittler, 2010; López-Doménech *et al.*, 2012; Nalavadi *et al.*, 2012). Thus, myosin motors may drive short-range mitochondrial movement in certain regions where actin filaments are enriched (Sheng and Cai, 2012).

Notably, myosin V can form hetero-motor complexes by interacting with a dynein light chain (Naisbitt *et al.*, 2000). Thus, considering that actin is required for mitochondrial docking along axons (Chada and Hollenbeck, 2004) and that mitochondrial movement is enhanced in the absence of actin (Morris and Hollenbeck, 1995), it was suggested that a coupled dual motor complex may coordinate mitochondrial movement. In this motor complex, myosin V may compete with dynein for binding to mitochondria, thus causing displaced mitochondrial transport between microtubule tracks and actin filaments during retrograde movements. In agreement with this hypothesis, a recent study using

Drosophila melanogaster neurons demonstrated that myosin V and VI modulate axonal transport of mitochondria (Pathak *et al.*, 2010). Additionally, in axons, myosin V depletion increased mitochondrial transport in both directions, whereas depletion of myosin VI selectively increased retrograde mitochondrial transport (Pathak *et al.*, 2010), thus suggesting that myosin V and VI may compete with microtubule‑based motor proteins. Nevertheless, myosin II depletion produced no phenotype (Pathak *et al.*, 2010). Alternatively, by moving mitochondria away from microtubule tracks, myosins may promote mitochondrial docking along the actin-based cytoskeleton. According to this model, fine and dynamic coordination of microtubule‑ and actin-based motor proteins, as well as of docking and anchoring receptors, probably contributes to the complex saltatory mobility of neuronal mitochondria (Sheng and Cai, 2012). Though these two models are certainly interesting, further investigation is needed to determine how myosin motors regulate microtubule‑based motor activity and whether they are required for mitochondrial transport directed to the synapses or for mitochondrial docking at regions of axons and dendrites with high metabolic demands.

Myosin XIX, a newly identified mitochondria-associated myosin, was involved in actin-based mitochondrial movement in vertebrate cells (Quintero *et al.*, 2009). Expression of full-length GFP-myosin XIX in A549 cells led to a remarkable gain of function, where the majority of the mitochondria move continuously (Quintero *et al.*, 2009). Additionally, since myosin XIX is targeted to mitochondria by its tail domain, which is widely expressed, including in neurons, suggests that myosin XIX may also mediate mitochondrial transport along neuronal processes and at synaptic terminals (Quintero *et al.*, 2009; Adikes *et al.*, 2013).

I.1.4.2 Regulation of mitochondrial transport

As reported above, mitochondria accumulate in areas with high energy requirements, such as presynaptic and postsynaptic terminals, active growth cones and branches in developing neurons, myelination boundaries, sites of axonal protein synthesis and nodes of Ranvier (Sheng and Cai, 2012). Furthermore, in axons, mitochondria undergo anterograde transport directed to the distal portions of axons and retrograde movement in the opposite direction (to the soma). Additionally, these transport events are tightly regulated in response to changes in the local energetic state and metabolic demand. Therefore, mitochondrial transport requires the existence of highly coordinated mechanisms to regulate the movement of these organelles along neuronal processes and their docking to supply specific biological needs.

I.1.4.2.1 Regulation of mitochondrial transport by cytosolic Ca^{2+}

Cytosolic Ca^{2+} is one of the best studied regulators of mitochondrial transport. Ca^{2+} influx occurs at presynaptic and postsynaptic terminals, where mitochondria are retained to maintain Ca^{2+} homeostasis by providing ATP to pump Ca^{2+} across the plasmatic membrane or by direct intramitochondrial Ca^{2+} buffering. Indeed, increased cytosolic Ca^{2+} is described to inhibit both anterograde and retrograde movement of mitochondria in neurons (Rintoul *et al.*, 2003; Chang *et al.*, 2006; Macaskill *et al.*, 2009b; Wang and Schwarz, 2009; Chang *et al.*, 2011). Recent studies have identified Miro as a Ca^{2+} sensor in regulating mitochondrial mobility (Saotome *et al.*, 2008; Macaskill *et al.*, 2009b; Wang and Schwarz, 2009). As presented above, Miro is a subfamily of the mitochondrial Rho GTPases, located in the outer mitochondrial membrane, which has two EF hand Ca^{2+}-binding domains (Fransson *et al.*, 2006) (see section I.1.4.1.1.1). In these studies, it was shown that the KIF5/Milton/dMiro or KIF5/TRAK2/Miro1 motor complexes allowed mitochondrial movement along dendrites (Macaskill *et al.*, 2009b) or axons (Wang and Schwarz, 2009) of hippocampal neurons, or along microtubules in the H9c2 heart cell line (Saotome *et al.*, 2008). Additionally, an increase on cytosolic Ca^{2+} efficiently inhibited mitochondrial movement.

Though these studies converge on similar final conclusion, the proposed mechanisms underlying Ca^{2+}-dependent regulation of motor-adaptor coupling are different. MacAskill and co-workers (Macaskill *et al.*, 2009b) proposed that Miro1 mediates mitochondrial transport by linking mitochondria to KIF5. Ca^{2+} binding to the EF hand domains of Miro1 dissociates it from KIF5, being that TRAK2 remains bound to Miro1, thus retaining mitochondria at synapses (Figure 8A). On the other hand, Wang and Schwarz (Wang and Schwarz, 2009) proposed a motor-adaptor switch model. They showed that, in the absence of Ca^{2+}, the carboxyl-terminal tail of KIF5 was bound to the mitochondrion by interacting with the Milton/dMiro complex, remaining its amino-terminal motor domain free to engage with microtubules, thus allowing anterograde transport. However, Ca^{2+} binding to the EF hand domains results in a conformational change, in which the amino-terminal motor domain of KIF5 binds to dMiro, thus preventing KIF5-microtubules interaction (Figure 8B). Despite these small mechanistic differences, both studies demonstrated, in neurons, that the over-expression of a Miro construct with the EF hand domains mutated, to prevent Ca^{2+} binding, efficiently blocked the Ca^{2+}-induced impairment of mitochondrial mobility (Macaskill *et al.*, 2009b; Wang and Schwarz, 2009), thus confirming the important role of Miro protein in regulating mitochondrial transport in neurons. A surprise from these studies was that the EF hand Ca^{2+}-binding domains of Miro mediated Ca^{2+}-dependent impairment of mitochondrial transport in both anterograde and retrograde directions.

However, recent evidences indicating that dMiro protein also regulates retrograde mitochondrial transport in *Drosophila melanogaster* neurons (Russo *et al.*, 2009), and that dynein motors interacts with the TRAK/Miro complex (van Spronsen *et al.*, 2013), may add important knowledge how Ca^{2+}-regulated Miro-dependent mechanism may control dynein-mediated retrograde movement of mitochondria.

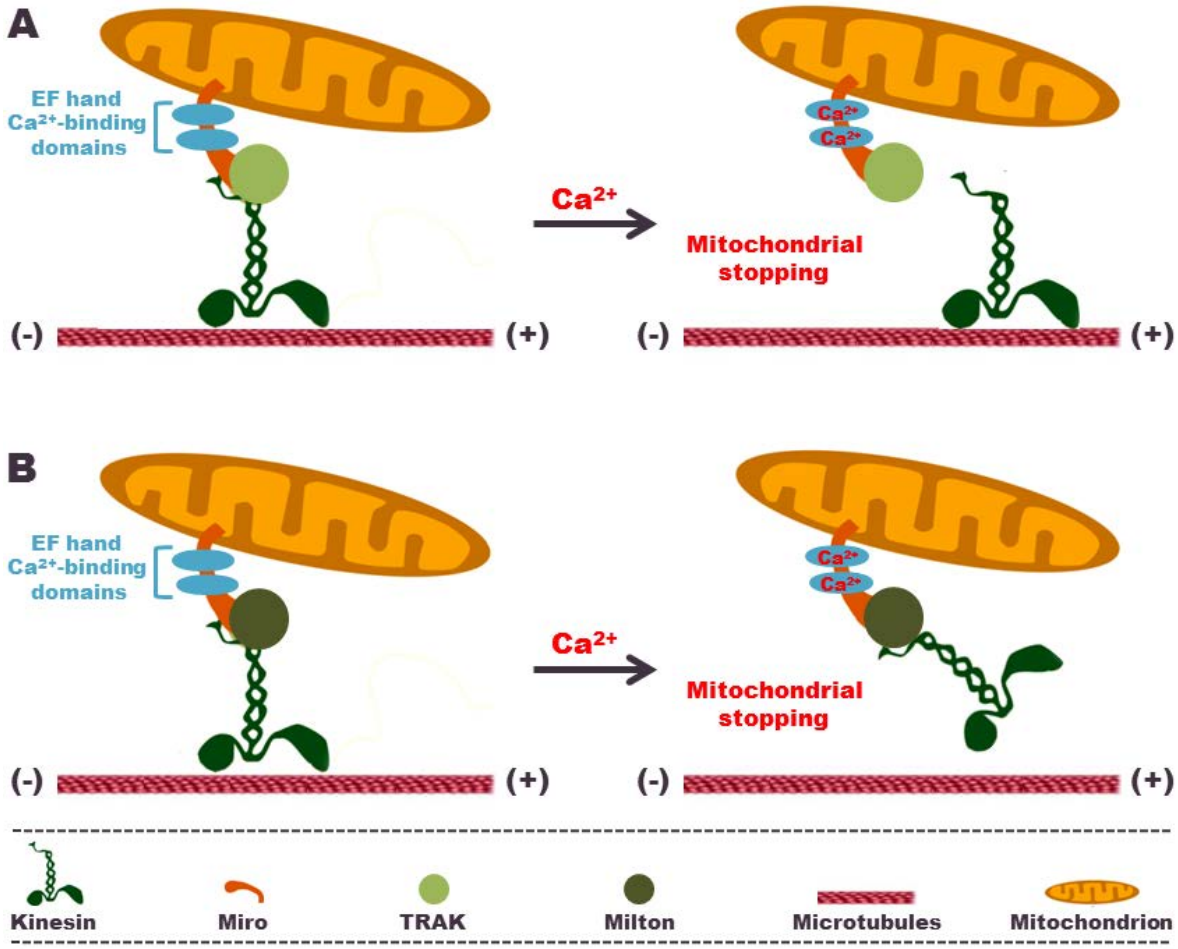


Figure 8. Models of Miro as a Ca^{2+} sensor in regulating mitochondrial motility.
High levels of Ca^{2+} inhibit mitochondrial movement via Ca^{2+} binding to the EF hand domains of Miro. (A) In mammalian neurons, Ca^{2+} binding to the EF hand domains of Miro dissociates Miro from KIF5 (kinesin), while KIF5-binding protein Grif-1/TRAK2 remains bound to Miro, thus leading to KIF5 detachment from mitochondria with consequent mitochondrial stopping. (B) In *Drosophila melanogaster* neurons, the tail of KIF5 is linked to Miro via Milton in a Ca^{2+}-independent manner, thus leaving its motor domain to engage with microtubules. Ca^{2+} binding to the EF hand domains of Miro detaches KIF5 from microtubules with consequent mitochondrial stopping. Created by the author based in the references (Macaskill *et al.*, 2009b; Wang and Schwarz, 2009; MacAskill and Kittler, 2010).

I.1.4.2.2 Regulation of mitochondrial transport by microtubule-associated proteins

Microtubules are dynamic structures stabilized by MAPs, including MAP1B and Tau, which are mainly distributed in axons, and MAP2, which is specially located in dendrites. Apart from stabilizing axonal microtubules, Tau protein has been shown to contribute to the regulation of the axonal transport of membranar organelles, including mitochondria (Ebneth *et al.*, 1998; Stamer *et al.*, 2002). Over-expression of Tau, in several neuronal cell types, inhibited mitochondrial transport (Ebneth *et al.*, 1998; Stamer *et al.*, 2002; Dubey *et al.*, 2008; Stoothoff *et al.*, 2009). Additionally, in another study using Tau mutant neurons [Tau (-/-) or Tau (-/+)], the dependence on Tau protein for the β-amyloid protein-induced mitochondrial transport impairment (Vossel *et al.*, 2010), support, therefore, the notion that Tau protein plays a major role in regulating an efficient axonal transport of mitochondria.

Since Tau is a phosphoprotein, its functions may be regulated by phosphorylation (Mandelkow *et al.*, 2004; Darios *et al.*, 2005; Morel *et al.*, 2010; Llorens-Martín *et al.*, 2011). Many of the phosphorylation sites are proline-directed (Serine/Threonine)-Pro sequences, though these sites are moderately phosphorylated in healthy neurons. Many studies have associated increased Tau phosphorylation with improved mitochondrial transport (Mandelkow *et al.*, 2004; Llorens-Martín *et al.*, 2011). One of these studies demonstrated that Tau-mediated inhibition of axonal transport of mitochondria was rescued by increasing Tau phosphorylation through MARK expression (MARK causes the phosphorylation of Tau in its KXGS motifs, thus leading to the detachment of Tau from microtubules) (Mandelkow *et al.*, 2004). Similarly, over-expression of glycogen synthase 3β (GSK3β), in cultured hippocampal neurons, resulted in increased mitochondrial motility, whereas a decrease in GSK3β activity decreased mitochondrial transport. These effects were dependent on Tau protein, as Tau (-/-) neurons did not respond to distinct GSK3β levels (Llorens-Martín *et al.*, 2011). Therefore, from these observations it was suggested that Tau protein preferentially competes with mitochondrial motor proteins for binding to microtubules, as previously reported (Hagiwara *et al.*, 1994), thus regulating mitochondrial transport. Additionally, the observations indicating that, neither Tau (Trinczek *et al.*, 1999), nor GSK3β over-expression (Llorens-Martín *et al.*, 2011) affected mitochondrial transport velocity, support the existence of a competition between motor proteins and Tau to interact with the microtubule surface.

Despite this, other studies have indicated that the hyperactivation of Tau kinases reduces mitochondrial movement in neurons (Darios *et al.*, 2005; Morel *et al.*, 2010). In GSK3β- and p25 [activator of cyclin-dependent kinase 5 (Cdk5)]-transfected neurons, the high levels of hyperphosphorylated Tau were correlated with impaired mitochondrial

movement (Morel *et al.*, 2010). Moreover, rotenone-induced microtubule destabilization in SH-SY5Y cells was suppressed by inhibiting GSK3β activity (Hongo *et al.*, 2012). Therefore, from these observations, it was suggested another model for the regulation of mitochondrial transport by Tau: increased Tau phosphorylation impairs mitochondrial transport by microtubule destabilization.

Several other models have been proposed for Tau-mediated inhibition of mitochondrial transport (Thies and Mandelkow, 2007; Shemesh *et al.*, 2008; Seeger and Rice, 2010). One mechanism involves the inhibition of motor protein access to microtubules. Using fluorescence anisotropy methodologies, it was demonstrated that the human Tau construct hTau-40 competitively inhibited the interaction between kinesin-1 tail and microtubules (Seeger and Rice, 2010), thus indicating that the kinesin-1 tail and hTau-40 compete for the same binding site on tubulin. Therefore, since mitochondria are transported along microtubules by motor proteins, the inhibition of motor protein access to microtubules by Tau may block mitochondrial movement in neuritic processes. Another mechanism proposed involves the reorganization of microtubules. The impairment of the mitochondrial transport induced by over-expression of human Tau was associated with substantial reorganization of microtubules polar orientation along the main axon of cultured *Aplysia* neurons (Shemesh *et al.*, 2008). Considering that mitochondrial transport along microtubules by motor proteins depends on the microtubule polarity, the existence of points of microtubule polarity discontinuation or polarity mismatching may disrupt mitochondrial movement along axons. The last mechanism proposed involves the distance between microtubules. After Tau over-expression in hippocampal neurons, tubulin synthesis was up-regulated and microtubules became more numerous and densely packed, resulting in inhibition of mitochondrial movement (Thies and Mandelkow, 2007). Though this effect was reported in dendrites, similar outcomes were recently described in axons of cultured hippocampal neurons (Sudo and Baas, 2010). Similarly, Tau over-expression increased the number of microtubules and reduced the inter-microtubule spaces in neurites of PC12 cells (Shahpasand *et al.*, 2012). Therefore, considering that neuronal mitochondria are transported within microtubule bundles (Rochlin *et al.*, 1996), limited spacing between microtubules may block mitochondrial movement in neuritic processes.

In addition to Tau protein, MAP1B was also described to regulate axonal transport of mitochondria (Jiménez-Mateos *et al.*, 2006). In comparison to wild-type neurons, the rates of retrograde mitochondrial movement and velocity were increased in MAP1B (-/-) hippocampal neurons. Additionally, the fraction of mitochondria that did not constantly move, because they stop or pause, was significantly decreased in MAP1B (-/-) hippocampal neurons, compared to wild-type neurons (Jiménez-Mateos *et al.*, 2006).

Therefore, these results suggest that MAP1B may act as a key regulator of retrograde mitochondrial transport.

I.1.4.2.3 Regulation of mitochondrial transport by phosphatase and tensin homolog-induced putative kinase 1/Parkin

Recent studies have attributed to phosphatase and tensin homolog-induced putative kinase 1 (PINK1) and Parkin an important role in regulating mitochondrial transport. PINK1 is a protein kinase and Parkin an E3 ubiquitin ligase, which are involved in the autophagic clearance of mitochondria (mitophagy) with lower membrane potential (Narendra *et al.*, 2012). Additionally to the autophagy regulation, the PINK1/Parkin pathway was also described regulate mitochondrial morphology (Poole *et al.*, 2008), but, though the relationship between these actions remain unclear, it appears to be mediated, at least in part, by targeting mitofusins (Mfns) for degradation (Tanaka *et al.*, 2010; Chan *et al.*, 2011).

The biochemical association demonstrated for PINK1 and the Milton/Miro complex constituted the first indication that this pathway may regulate mitochondrial transport (Weihofen *et al.*, 2009). Subsequently, it was found that Parkin may also binds to this complex and that PINK1 may phosphorylate Miro in several sites, which is important for a subsequent stimulation of the Parkin function and mitochondrial stop (Wang *et al.*, 2011b). Furthermore, Miro is also a substrate for Parkin (Wang *et al.*, 2011b; Liu *et al.*, 2012). The activation of this pathway led to the proteasome-dependent degradation of Miro with consequent release of kinesin from mitochondrial surface (Chan *et al.*, 2011; Wang *et al.*, 2011b), thus resulting in mitochondrial stopping. In addition, the observations indicating reduced mitochondrial occupancy in neuronal processes of hippocampal neurons over-expressing PINK1 or Parkin, and increased mitochondrial movement in *Drosophila melanogaster* axons expressing either PINK1 or Parkin RNA interference (Yu *et al.*, 2011) corroborate this hypothesis.

I.1.4.2.4 Other regulators of mitochondrial transport

Though cytosolic Ca^{2+}, MAPs and PINK1/Parkin are, perhaps, the best characterized regulators of mitochondrial transport, many other regulatory proteins/pathways have been described.

I.1.4.2.4.1 Mitochondrial Ca^{2+}

Mitochondrial Ca^{2+} was recently suggested as another important regulator of mitochondrial transport. In hippocampal neurons, it was shown an inverse correlation between the speed of mitochondrial movement and the mitochondrial Ca^{2+} levels (moving mitochondria have lower Ca^{2+} content, compared to stationary mitochondria). However, mitochondrial Ca^{2+} did not influence the directionality of mitochondrial movement (Chang *et al.*, 2011). Furthermore, a major role for Miro protein in controlling mitochondrial Ca^{2+} levels was established. In hippocampal neurons, mutations in the EF hand Ca^{2+}-binding domains of Miro1 protein reduced Ca^{2+} entry into the mitochondria, resulting in persistent mitochondrial movement (Chang *et al.*, 2011). Therefore, it is plausible to consider that the blockage of mitochondrial Ca^{2+} influx by Miro1 EF mutants also contributes to failure in mitochondrial movement arrest in neurons, as reported previously (Saotome *et al.*, 2008; Macaskill *et al.*, 2009b; Wang and Schwarz, 2009). These results suggest, thus, that Miro protein may also regulate mitochondrial transport throught the regulation of the mitochondrial Ca^{2+} content (Miro protein are described to have a key role in regulating mitochondrial transport through cytosolic Ca^{2+} - see section I.1.4.2.1).

On the other hand, it was also demonstrated that the blockage of the mitochondrial Ca^{2+} uniporter (Baughman *et al.*, 2011; De Stefani *et al.*, 2011), in the presence of high cytosolic Ca^{2+}, delayed ion entry into the mitochondria and, consequently, preserved mitochondrial movement. In the same line, activation of the mitochondrial Ca^{2+} uniporter elevated mitochondrial Ca^{2+}, with consequent mitochondrial stopping. However, in neurons transfected either with wild-type Miro1 or with Miro1 EF mutant, an activation of the mitochondrial Ca^{2+} uniporter produced similar increases in mitochiondral Ca^{2+} content, and consequent mitochondrial stopping (Chang *et al.*, 2011). Therefore, these data suggest that the role of Miro1 in controlling mitochondrial Ca^{2+} content, and consequently mitochondrial transport, may not result from an influence in mitochondrial Ca^{2+} uniporter opening.

I.1.4.2.4.2 Mitofusin 2

Mfn2, a component of the mitochondrial fusion machinery, such as Mfn1 and the dynamin-related protein optic atrophy 1 (OPA1), was previously reported to regulate mitochondrial movement in neurons (Misko *et al.*, 2010; Misko *et al.*, 2012). In Mfn2-null neurons or in neurons over-expressing a Mfn2 mutant (Mfn2 R94Q), axonal mitochondria spend more time paused and undergo slower anterograde and retrograde movements, thus indicating an alteration in attachment to microtubule-based transport systems (Misko *et al.*, 2010; Misko *et al.*, 2012). In contrast, disruption of mitochondrial fusion via

knockdown of OPA1 had no effect on mitochondrial motility, indicating, therefore, that loss of fusion does not inherently alter mitochondrial transport (Misko *et al.*, 2010). Furthermore, both Mfn1 and Mfn2 were shown to interact with mammalian Miro (Miro1/Miro2) and Milton (TRAK1/TRAK2) proteins (Misko *et al.*, 2010). Additionally, knockdown of Miro2 produced axonal mitochondrial transport deficits in a similar extension to the loss of Mfn2 (Misko *et al.*, 2010). These results indicate that both proteins (Mfns and Miro) must be present at the outer mitochondrial membrane to mediate axonal transport of mitochondria. Nevertheless, if Mfns regulate mitochondrial transport directly or by interacting with Miro functioning remain unclear (to a better understanding about the role of Mfn2 and Miro proteins in regulating fusion/fission events and transport see section I.1.6).

I.1.4.2.4.3 Serotonin and Dopamine

Monoamine neurotransmitters, namely 5-HT and dopamine, have been shown to alter mitochondrial movement in hippocampal neurons. Acting through the serotonin 1A (5-HT_{1A}) receptor subtype, 5-HT increased Akt activity, and consequently decreased GSK3β activity, thus promoting axonal transport of mitochondria (Chen *et al.*, 2007b). Although the molecular targets of the Akt-GSK3β signaling pathway are not clear, this observation highlights the possibility that 5-HT may act as an extracellular modulator in regulating neuronal ATP distribution by controlling axonal mitochondrial trafficking. By contrast, another study showed that dopamine or dopamine D2 receptor agonists inhibited mitochondrial movement via the same Akt-GSK3β signaling cascade (Chen *et al.*, 2008). Therefore, this result indicates that the distribution of neuronal mitochondria may occur through a conserved regulatory mechanism. Additionally, the Akt-GSK3β signaling pathway likely achieves this through the regulation of kinesin-cargo interactions (Morfini *et al.*, 2002; Pigino *et al.*, 2003).

I.1.4.2.4.4 Histone deacetylases

Histone deacetylases (HDACs) are another class of regulators of mitochondrial transport in neurons. HDAC6 was found to interact with Tau protein, a key regulator of mitochondrial transport. Furthermore, tubacin, a selective inhibitor of tubulin deacetylation activity of HDAC6, did not disrupt HDAC6-Tau interaction, but attenuated site-specific Tau phosphorylation, as did RNA silencing-mediated knockdown of HDAC6 (Ding *et al.*, 2008). Furthermore, in hippocampal neurons, specific inhibition of HDAC6 with tubacin dramatically enhanced mitochondrial movement, in both anterograde and retrograde directions, improved tubulin acetylation and increased the amount of kinesin-1 associated

with mitochondria. Nevertheless, niltubacin, an inactive tubacin analog, produced no effect (Chen *et al.*, 2010). Indeed, inhibition of HDAC6, with consequent increase in tubulin acetylation levels, was previously reported as an interesting approach to compensate the trafficking deficits in Huntington's disease (Dompierre *et al.*, 2007). Furthermore, HDAC6 inhibition rescued the mitochondrial transport deficits caused by mutations in heat-shock protein gene (d'Ydewalle *et al.*, 2011) and significantly restored the velocity and motility of mitochondria in both anterograde and retrograde axonal transports compromised by β-amyloid protein (Kim *et al.*, 2012). Similarly, a recent study reported significant increases in α-tubulin acetylation in HDAC6 (-/-) mice and rescue of β-amyloid protein-induced impairment of mitochondrial trafficking in primary hippocampal neurons lacking HDAC6 (Govindarajan *et al.*, 2013). Additionally, GSK3β inhibition reduced HDAC6 phosphoryation at Serine22, increased tubulin acetylation and enhanced mitochondrial transport, thus suggesting that HDAC6 functions in regulating mitochondrial mobility may rely on GSK3β-regulated pathways (Chen *et al.*, 2010). Therefore, it may be supposed that GSK3β may regulate HDAC6 activity by a phosphorylation dependent-mechanism, and, thus, control mitochondrial movement by modulating tubulin acetylation and kinesin-1 association with mitochondria.

HDAC1 was also reported to modulate mitochondrial transport in neurons. Formation of complexes between HDAC1 (exported from nucleus) and members of the kinesin family of motor proteins inhibited mitochondrial movement by hindering the interaction of kinesin motors with cargo molecules. Additionally, a rescue of this phenotype was achieved by inhibiting HDAC1 nuclear export with leptomycin B, HDAC1 activity or by HDAC1 silencing, thus identifying nuclear export as a critical event for mitochondrial transport regulation by HDAC1 (Kim *et al.*, 2010).

Recently, in non-neuronal cells, HDAC inhibition was associated with increased mitochondrial elongation, characterized by reduced expression of the mitochondrial fission protein 1 (Fis1) and reduced mitochondrial translocation of the dynamin-related protein 1 (Drp1) (Lee *et al.*, 2012a). Therefore, these results suggest that HDACs may indirectly regulate mitochondrial movement by modulating fusion/fission events (to a better understanding of the cross-talk between mitochondrial fusion/fission and transport see section I.1.6).

I.1.4.2.4.5 Adenosine 5'-diphosphate/adenosine 5'-triphosphate

ADP is another regulator of mitochondrial motility. Since mitochondrial transport was more sensitive to increases in intracellular ADP than to ATP depletions, it was proposed that the consumption of synaptic ATP may produce local increases in ADP, thus

facilitating the targeting of mitochondria where they are most needed, the synapses, to supply specific energetic needs (Mironov, 2007).

I.1.4.2.4.6 Nitric oxide

Nitric oxide (NO) has a number of physiological effects in the nervous system, though targeting mitochondria may inhibit respiration and ATP synthesis. In primary cultures of forebrain neurons NO caused a rapid cessation of mitochondrial movement, by a mechanism independent on cyclic guanosine 5'-monophosphate (cGMP)-regulated pathways (NO is a potent activator of the soluble guanylate cyclase (sGC), resulting in the elevation of cGMP), which was associated with dissipation of the $\Delta\Psi_m$ (Rintoul *et al.*, 2006). In cultured cortical neurons, either hypoxia/re-oxygenation or NO insults resulted in impaired mitochondrial movement and morphology. Furthermore, inhibition of the NOS with Nω-nitro-*L*-arginine methyl ester (*L*-NAME) partially rescued the hypoxia-induced decrease in mitochondrial movement, thus suggesting the involvement of NO-mediated pathways in this effect (Zanelli *et al.*, 2006). Therefore it is likely to assume that NO may modulate mitochondrial movement by inhibiting mitochondrial function.

I.1.4.2.4.7 Nerve growth factor

Another mechanism involved in mitochondrial transport control is regulated by NGF, which can cause a local accumulation of mitochondria where an NGF-coupled bead makes contact with a sensory axon. Mitochondria that enter in the portion of the axon closest to the bead tend to stop their movement and, therefore, tend to accumulate in these regions. Actin-based mechanisms seem to have a role in NGF-stimulates mitochondrial stopping. Inhibition of phosphoinositide 3-kinase (PI3K) or latrunculin B, an agent that destabilizes filamentous actin, inhibits mitochondrial recruitment to the NGF-stimulated site, thus highlighting a crucial role for this signaling cascade in the regulation of mitochondrial movement by NGF (Chada and Hollenbeck, 2004). However, it remains unclear whether the NGF signaling pathway cause a local accumulation of mitochondria through a mitochondria-actin interaction or indirectly through an unidentified docking receptor (Sheng and Cai, 2012).

I.1.4.2.4.8 Proteins of the Armcx family

The proteins of the Armcx family, including Alex3, were also recently described as regulators of the mitochondrial motility. This protein localizes in mitochondria, and its over-expression caused mitochondrial aggregation near the nucleus. Additionally, Alex3 was

described to interact with TRAK2/Miro complex and its over-expression in cultured hippocampal neurons decreased axonal transport of mitochondria in both anterograde ad retrograde directions (López-Doménech *et al.*, 2012). Thus, these data suggest that Alex3 may regulate mitochondrial transport by modulating the interaction between TRAK2/Miro complex and microtubule-based motor proteins.

I.1.4.2.4.9 Hypoxia up-regulated mitochondrial movement regulator and β *O*-linked *N*-acetylglucosamine transferase

Proteins that associate with the TRAK/Miro or Milton/dMiro complexs, including the hypoxia up-regulated mitochondrial movement regulator (HUMMR), whose expression is induced by hypoxic conditions, and β *O*-linked *N*-acetylglucosamine transferase (OGT), an enzyme that catalyzes the transfer of single *N*-acetylglucosamine sugars to Serine and Threonine residues of intracellular proteins, may also act as regulators of mitochondrial transport. The first was described to interact with Miro1 and Miro2. Furtermore, loss of HUMMR function in hypoxia diminished the percentage of motile mitochondria moving in the anterograde direction and enhanced the percentage moving in the retrograde direction. (Li *et al.*, 2009). OGT, though generally has only low-affinity interactions with its many substrates, it was shown to bind strongly to Milton, which is also a substrate (Iyer *et al.*, 2003). In COS-7 cells, OGT was shown to from a ternary complex with KIF5 and TRAK1/2 and its over-expression resulted in altered distribution of mitochondria (Brickley *et al.*, 2011). Therefore, it is likely to consider that both HUMMR, as a sensor of hypoxic stress, and OGT, as a sensor of metabolic state (Lazarus *et al.*, 2009), may help mitochondria to redistribute themselves, in response to changes in environmental and energetic conditions.

I.1.4.2.4.10 RhoA/lysophosphatidic acid

A potentially related pathway that regulates mitochondrial motility is activated by the growth factor lysophosphatidic acid (LPA) and mediated by the small GTPase RhoA (Minin *et al.*, 2006). RhoA was described to regulate the interactions between myosin motors and actin. Furthermore, via Rho-kinase, RhoA can lead to the activation of myosin motors (Kimura *et al.*, 1996) and, thus, potentially remove mitochondria from their microtubule tracks. Additionally, RhoA was also described to activate the actin-regulatory formin-like protein mDia, a protein involved in the regulation of the cell morphology, adhesion and cytokinesis through the actin cytoskeleton (Watanabe *et al.*, 1997). This last pathway was described to be necessary and sufficient to explain the inhibitory effects of

RhoA and LPA on mitochondrial transport, by a mechanism involving the anchoring of mitochondria to the actin cytoskeleton (Minin *et al.*, 2006).

I.1.5 Mitochondrial fusion/fission

Mitochondria are highly dynamic and complex organelles that, as well as undergoing regulated movement throughout the cell, continuously alter their shape, ranging between two opposite processes, fusion and fission, in response to several stimuli and metabolic demands of the cell. These opposite processes are crucial in sustaining the robust structure and function of mitochondria (Saxton and Hollenbeck, 2012). Mitochondrial shapes can range from punctuate structures to tubular networks, which are probably physically contiguous structures constructed via fusion of single bean-like shaped mitochondria (Popov *et al.*, 2005). Continuous movements of mitochondria allow a physical contact that facilitates their fusion, thus creating single large mitochondria. Mitochondrial fusion allows the exchange of mtDNA and other matrix components between neighboring mitochondria, including damaged or senescent mitochondria, thus conferring protection against mtDNA mutations and maintaining a healthy oxidative phosphorylation (Chan, 2006; Ranieri *et al.*, 2013). Fission events permit mitochondrial separation to daughter cells during mitosis (Taguchi *et al.*, 2007), control organelle size and shape for an efficient mitochondrial distribution in neuronal processes (Ishihara *et al.*, 2009; Kageyama *et al.*, 2012), allow the recovery of damaged mitochondria for degradation by mitophagy (Twig *et al.*, 2008a) and regulate apoptosis through segregation of the most critically injured mitochondria (Youle and van der Bliek, 2012).

I.1.5.1 Mitochondrial fusion

Mitochondrial fusion is a multi-step process that requires the coordinated fusion of both outer and inner mitochondrial membranes, ultimately resulting in mixing of matrix contents. In mammalian cells, three large GTPases mediate mitochondrial fusion. Mfn1 and Mfn2, located in the outer membranes of adjacent mitochondria, induce outer-membrane fusion, whereas OPA1, a protein residing in the intermembrane space, mediates fusion of the inner membranes (Song et al., 2009). A schematic representation of the mitochondrial fusion is illustrated in Figure 9.

Mfns are highly homologous GTPases anchored to the outer membrane, with their amino- and carboxyl-terminals directed to the cytosol (Rojo et al., 2002), which forming homo- or hetero-protein complexes allow mitochondrial tethering and fusion throught GTP hydrolysis (Koshiba et al., 2004). The amino-terminal GTPase domain of Mfns is required for fusion activity, while carboxyl-terminal domain coordinates the docking of mitochondria to one another through antiparallel binding to the carboxyl-terminal domains of Mfn molecules on adjacent mitochondria. Additionally, Mfn1 appears to mediate tethering of mitochondria more efficiently than Mfn2 (Ishihara et al., 2004). OPA1 acts as a hetero-

oligomeric complex, formed by a larger size OPA1 (L-OPA1) and the smaller size OPA1 (S-OPA1), in the fusion of the inner mitochondrial membrane (Cipolat et al., 2004). Furthermore, to mediate mitochondrial fusion, OPA1 functionality appears to require Mfn1, but not Mfn2 (Cipolat et al., 2004). Additionally, OPA1 was also described to play a key role in cristae organization of the inner mitochondrial membrane (Cipolat *et al.*, 2006; Frezza *et al.*, 2006), by a mechanism independent on the mitochondrial fusion (Frezza *et al.*, 2006).

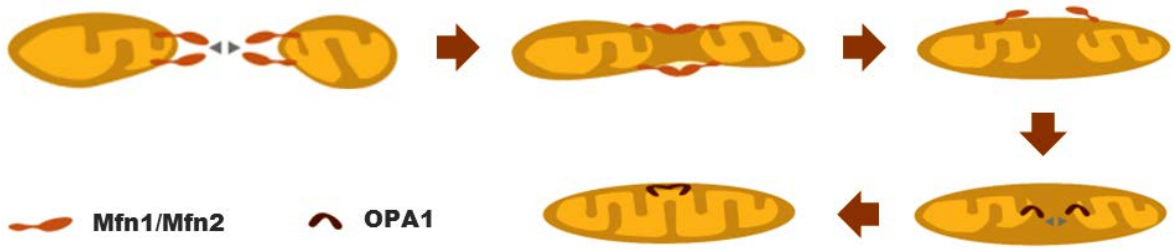


Figure 9. Mitochondrial fusion.
Mitochondrial fusion of the outer mitochondrial membrane involves trans-dimerization of mitofusin 1 (Mfn1) and its homologous mitofusin 2 (Mfn2), allowing mitochondrial tethering and fusion through guanosine 5'-triphosphate (GTP) hydrolysis. Optic atrophy 1 (OPA1), a protein residing in the intermembrane space, mediates fusion of the inner membranes, in an equivalent manner involving its trans-dimerization. Created by the author based in the references (Koshiba *et al.*, 2004; Song *et al.*, 2009; MacAskill and Kittler, 2010).

Mutations in the mitochondrial fusion proteins Mfn2 and OPA1 have been associated with neurodegenerative disorders, such as Charcot-Marie-Tooth neuropathy 2A (CMT2A) and dominant optic atrophy 1, respectively (Delettre et al., 2000; Lv et al., 2013). Mfns are subjected to ubiquitination processes (Gegg et al., 2010) and proteosomal degradation (Tanaka et al., 2010). OPA1 may also be proteolytically regulated by different mitochondrial proteases (Ehses et al., 2009; Head et al., 2009), thus controlling its activity.

Since knockout of Mfn1 or Mfn2 resulted in the formation of small fragmented mitochondria (Chen *et al.*, 2007a), and cells lacking Mfns exhibited several cellular defects, including poor cell growth, heterogeneity of inner mitochondrial membrane potential and decreased respiration (Chen *et al.*, 2003), indicates that mitochondrial fusion plays an important role in maintaining mitochondrial functionality.

I.1.5.2 Mitochondrial fission

Mitochondrial fission is mediated by Drp1, a member of the dynamin family of GTPases. A schematic representation of the mitochondrial fission is illustrated in Figure 10. When mitochondrial fission is stimulated, Drp1 translocates from the cytosol to specific sites on the mitochondrial outer membrane and homo-oligomerizes, forming spiral chains

around mitochondria, which, using GTP hydrolysis, constrict and twist tubule to initiate mitochondrial fission (Smirnova *et al.*, 2001; Ingerman *et al.*, 2005). The translocation of Drp1 from the cytosol to mitochondria depends on a direct interaction with actin (DuBoff *et al.*, 2013). Nevertheless, it has been suggested that tubules of the endoplasmic reticulum wrap around and squeeze mitochondria at the early stage of division, prior to the assembly of Drp1 filaments on mitochondria (Friedman *et al.*, 2011). After mitochondrial fission, Drp1 spirals likely disassemble from mitochondria for future rounds of mitochondrial fission (Smirnova *et al.*, 2001; Ingerman *et al.*, 2005). Several different post-translational modifications, including phosphorylation, ubiquitination, and sumoylation, of Drp1 regulate its interactions with mitochondria (Chang and Blackstone, 2010; Wilson *et al.*, 2013).

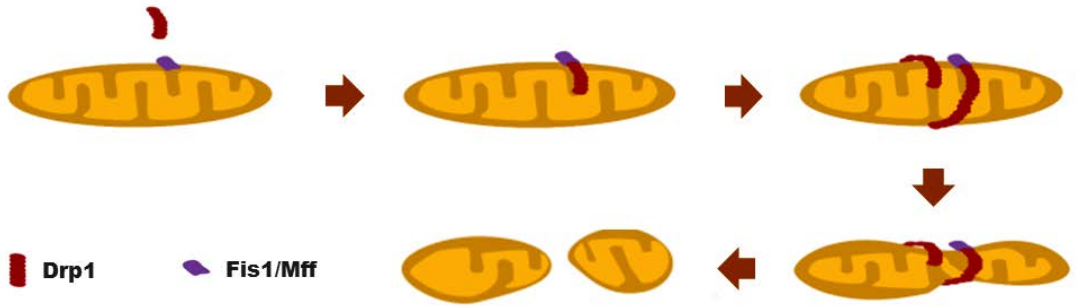


Figure 10. Mitochondrial fission.
Mitochondrial fission is mediated by dynamin-related protein 1 (Drp1), which is recruited to mitochondria via adaptors mitochondrial fission protein 1 (Fis1) or mitochondrial fission factor (Mff). This recruitment allows the homo-oligomerization of Drp1 into spiral chains around mitochondria, which, through guanosine 5'-triphosphate (GTP) hydrolysis, constrict and twist tubule to initiate mitochondrial fission. Created by the author based in the references (Yoon *et al.*, 2003; MacAskill and Kittler, 2010; Otera *et al.*, 2010).

In yeast, Drp1 attaches to mitochondria by binding to Fis1, a protein anchored to the mitochondrial outer membrane, through the adaptor protein Mdv1 (or its paralogue Caf4) (Mozdy *et al.*, 2000). However, in mammalians, though a yeast Fis1 orthologous has been identified (hFis1) (James *et al.*, 2003), orthologous for Mdv1 and Caf4 are not described, and the evidences supporting a role for hFis1 in mitochondrial fission are mixed. Supporting a role in fission events, over-expression of Fis1 in mammalian cells promoted mitochondrial fragmentation, and Fis1 inhibition resulted in mitochondrial elongation (Yoon *et al.*, 2003). Furthermore, a recent study demonstrated that mitochondria in Fis1-null cells presented an elongated and interconnected morphology, when compared to mitochondria from wild-type cells, thus indicating that Fis1 plays a role in mitochondrial fission (Losón *et al.*, 2013). However, in another study, it was shown that conditional knockdown of Fis1 in colon carcinoma cells did not disrupt mitochondrial morphology or Drp1 recruitment to

mitochondria (Otera *et al.*, 2010). In addition, in Hela cells, Fis1 was shown to regulate mitochondrial fission independently of Drp1 (Onoue *et al.*, 2013). Therefore, the exact role of Fis1 in mediating mitochondrial fission remains unclear, though it is possible that the relative importance of Fis1 depends on the cell type.

Despite this, other molecules have been described to play a role in mitochondrial fission. Gandre-Babbe and van der Bliek (Gandre-Babbe and van der Bliek, 2008) showed that the knockdown of the mitochondrial fission factor (Mff) resulted in mitochondrial elongation. Subsequently, the observations that Mff and Drp1 colocalize in puncta on mitochondria, and that the exogenous expression of Mff increased the amount of Drp1 recruited to mitochondria and induced extensive mitochondrial fission (Otera *et al.*, 2010), led to consider Mff as a strong candidate for Drp1 receptor in the outer mitochondrial membrane. In accordance, a further study confirmed that Mff plays a major role in mitochondrial fission, since mitochondria in Mff-null cells presented severely elongated and interconnected (Losón *et al.*, 2013). Furthermore, the expression of Fis1 in Mff-null cells or the expression of Mff in Fis1-null cells only partialy rescued the mitochondrial morphology (Losón *et al.*, 2013), thus indicating that Fis1 and Mff can act independently and partially replace each other to regulate mitochondrial morphology.

Alternatively, mitochondrial elongation factor 1 (MIEF1) (Zhao *et al.*, 2011), also identified as MiD49/51 (Palmer *et al.*, 2011), appears to block GTP binding to the GTPase domain of Drp1. Consequently, since the conformational change of Drp1 multimers required for membrane fission is inhibited, MIEF1 promotes fusion instead of fission (Zhao *et al.*, 2011). However, it remains unclear why MiD49/51 causes mitochondrial elongation instead of fission. According to one model, Fis1 can partially reverse the elongated mitochondrial phenotype by sequestering MIEF1 and, consequently, unblocking Drp1 GTP hydrolysis, thus leading to organelle fission (Zhao *et al.*, 2011; Oettinghaus *et al.*, 2012). On the other hand, a recent study demonstrated that MiD49/51over-expression enhanced mitochondrial recruitment of Drp1, though an increased inhibitory phosphorylation of Drp1 on Serine637 was observed [decreased phosphorylation of Drp1 at Serine637 facilitates its recruitment to mitochondria (Cereghetti *et al.*, 2008)]. However, after carbonyl cyanide m-chlorophenyl hydrazone (CCCP) treatment, this phosphorylation was reduced, and mitochondrial fission ensues (Losón *et al.*, 2013). Therefore, this model suggests that MiD49/51 may recruit Drp1 to mitochondria, but maintain it in an inactive state until a cellular signal triggers fission (Losón *et al.*, 2013).

In addition, the observation that B-cell lymphoma-extra large (Bcl-xL) caused a significant increase in Drp1 GTPase activity in cultured hippocampal neurons, also suggests that Bcl-xL may act as a GTPase-activating protein for Drp1 in mediating mitochondrial fission (Li *et al.*, 2008).

Recently, in mammalian cells, Fis1 was also proposed to act as a mitochondrial receptor in the recruitment of the GTPase regulator protein TBC1D15, thus modulating mitochondrial morphology independently of Drp1 (Onoue *et al.*, 2013). Therefore, though Drp1, Fis1, Mff and MIEF1 appear to be key regulators of fission events, whether and how they interplay is not perfectly understood.

I.1.6 Interplay between mitochondrial fusion/fission and transport

Mitochondria in neuronal cell bodies form reticular networks (Popov *et al.*, 2005), whereas in axons are discrete organelles (ranging from 100 nm to several micrometers of length) (Pilling *et al.*, 2006), being this morphology determined by the balance between fusion and fission events. Though in *Drosophila melanogaster* neurons the different lengths of axonal mitochondria are not correlated with different transport velocities (Russo *et al.*, 2009; Pathak *et al.*, 2010), extremely long axonal mitochondria, resulting from a perturbation of fusion/fission processes, do not move (Amiri and Hollenbeck, 2008). Therefore, this observation suggests that a correct balance between fusion and fission generates discrete mitochondria that may be transported over long distances, thus providing an important explanation for the cross-talk between fusion/fission events and transport. On the other hand, fusion/fission processes may occur in the axonal compartment (Amiri and Hollenbeck, 2008), a local in which mitochondria are often widely spaced. This spacing makes difficult the occurrence of fusion events between isolated stationary mitochondria. However, this problem may be resolved by transport. Indeed, studies with non-neuronal cells have shown that transported mitochondria may mixture their contents substantially during contacts, which are as brief as 2 seconds, and that moving mitochondria are more likely to fuse (Liu *et al.*, 2009; Twig *et al.*, 2010), thus suggesting that, perhaps, transport supports fusion/fission events in axons.

Despite this, other functional connections between mitochondrial fission/fusion events and transport have been suggested. With regard to fission, inhibition of Drp1 greatly reduced the number of mitochondria in synaptic terminals, thus suppressing synaptic formation and function (Li *et al.*, 2004; Verstreken *et al.*, 2005; Li *et al.*, 2008). In agreement, Drp1 deletion in cerebellar postmitotic Purkinje cells became mitochondrial tubules elongated due to excess fusion and, therefore, as oxidative damage accumulated in mitochondria due to impaired mitophagy, they formed large spheres whose diameters were higher than those of the dendrites (Kageyama *et al.*, 2012). Thus, as in Drp1-null neurons these large and spherical mitochondria localized exclusively in the cell body (Kageyama *et al.*, 2012), it may be assumed that these mitochondria are difficult to transport along neuritic processes (Figure 11). Other reports indicate enhanced mitochondrial fusion following over-expression of Miro (Fransson *et al.*, 2006; Saotome *et al.*, 2008; MacAskill *et al.*, 2009a) or Milton/TRAK (Koutsopoulos *et al.*, 2010). However, at high cytosolic Ca^{2+} concentrations, Miro over-expression promoted mitochondrial fragmentation (Saotome *et al.*, 2008). Additionally, it was shown that dynein/dynactin complex regulated the subcellular distribution of mitochondria by controlling the

recruitment of Drp1 to the outer mitochondrial membrane (Varadi *et al.*, 2004), and the depletion of myosin V increased mitochondrial length (Pathak *et al.*, 2010).

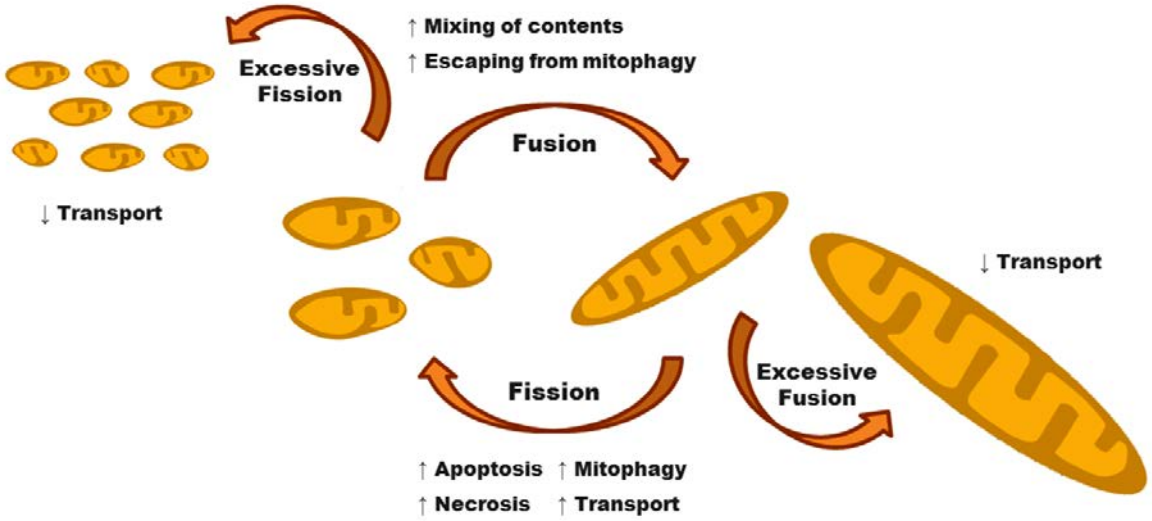


Figure 11. Cellular and physiological roles of mitochondrial fusion/fission.
A correct balance between fusion and fission generates discrete mitochondria that may be transported over long distances. Additionally, fission events facilitate cell death, through apoptotic or necrotic features and mitophagy, whereas fusion allows content mixing and can block mitophagy. However, an excessive mitochondrial fusion or fragmentation generate mitochondria that present defective transport. Created by the author based in the reference (Itoh *et al.*, 2013).

Mfns, which are well-known for having a central role in outer mitochondrial membrane fusion, are also important for mitochondrial transport and movement, though distinct mechanisms appear to be involved. In Mfn1- or Mfn2-null mouse embryonic fibroblasts, mitochondria display a dramatic alteration in their movement (Chen *et al.*, 2003). In neurons, lack of Mfn2 was associated with decreased number of mitochondria within their highly branched dendrites (Chen *et al.*, 2007a) and impaired mitochondrial transport in axons (Misko *et al.*, 2010). Furthermore, over-expression of a CMT2A Mfn2 mutant, Mfn2 R94Q, disrupted axonal transport of mitochondria in both anterograde and retrograde directions (Misko *et al.*, 2010; Misko *et al.*, 2012), thus suggesting that uncontrolled fission may result in decreased mitochondrial movement (Figure 11). In agreement, Mfn1 and Mfn2 were found to interact with mammalian Miro (Miro1/Miro2) and Milton (TRAK1/TRAK2) proteins, members of the molecular complex that links mitochondria to kinesin motors (Misko *et al.*, 2010), thus facilitating the axonal transport of mitochondria in both directions (Baloh *et al.*, 2007; Misko *et al.*, 2010). Threfore, the association between Mfns and Miro could also allow Miro to regulate mitochondrial fusion events. Indeed, the over-expression of constitutively active Miro1 increased mitochondrial length in hippocampal neurons (MacAskill *et al.*, 2009a) and H9c2 cells (at resting cytosolic Ca^{2+}

concentrations) (Saotome *et al.*, 2008), and the over-expression of dMiro in *Drosophila melanogaster* neurons also increased the mean length of axonal mitochondria (Russo *et al.*, 2009). Thus, these results suggest that Miro protein, apart from its role in regulating mitochondrial transport, may also play a major role in controlling fusion events. Therefore, these findings indicate that an interplay between mitochondrial transport and fusion/fission machineries may regulate mitochondrial shape, function and distribution.

Main Goals of the Thesis

I.2 Main Goals of the Thesis

"Ecstasy" is a powerful stimulant, entactogenic and hallucinogenic drug, which has raised concern worldwide because of its high abuse liability and potential toxicity. An increased number of studies have established that MDMA may elicit acute- and long-term neurotoxic effects, which have been described both in laboratory animals and humans, such as documented by hundreds of case reports of adverse events in illicit "ecstasy" users. Nevertheless, though emerging studies have attributed a promising role to monoaminergic system, metabolism and hyperthermia, involving mitochondrial-dependent pathways, it is reasonable to note that the molecular and cellular mechanisms behind MDMA-induced neuronal degeneration and neurotoxicity remain largely unknown. Consequently, the understanding of such mechanisms is extremely important not only in addressing the brain targets of MDMA's action, but also to develop putative treatments for the drug abuse and toxicity in humans. This thesis aimed to study and clarify the putative contribution of the monoaminergic system, metabolism and hyperthermia, with special focus on mitochondrial-dependent trails, in "ecstasy"-elicited neurotoxicity. Therefore, the following specific objectives were explored:

► To evaluate the putative deleterious effects of MDMA, its metabolites and monoamine neurotransmitters in mouse brain synaptosomes;

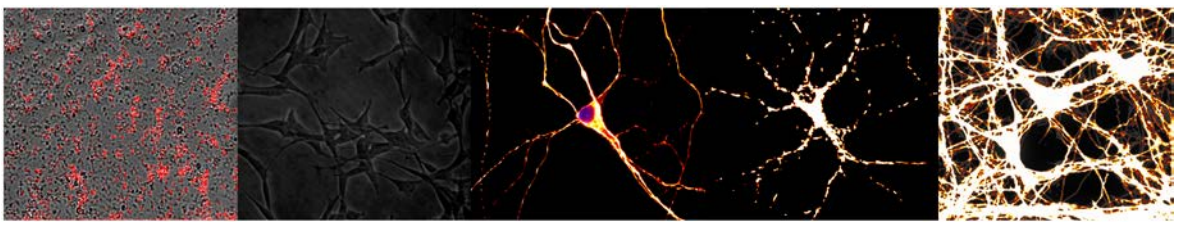
► To evaluate the putative effects of MDMA, its metabolites and monoamine neurotransmitters on the Na^+/K^+ ATPase activity in mouse brain synaptosomes;

► To evaluate the putative deleterious effects of MDMA and its metabolites, singly or as a mixture, in human SH-SY5Y differentiated cells;

► To evaluate the putative disrupting effects of MDMA and its metabolites on mitochondrial trafficking in cultured hippocampal neurons;

► To evaluate the mechanisms by which MDMA and its metabolites impar mitochondrial trafficking in cultured hippocampal neurons;

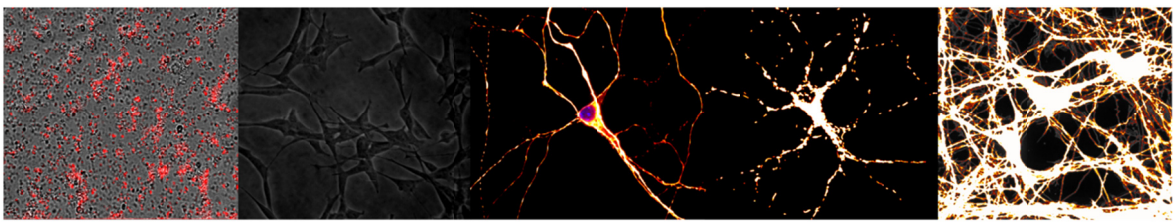
Chapter II



1.

Pro-oxidant effects of Ecstasy and its metabolites in mouse brain synaptosomes

Reprinted from ***British Journal of Pharmacology***,
volume 165, issue 4b, pages 1017 to 1033
Copyright © ***The British Pharmacological Society*** 2012



British Journal of Pharmacology

DOI:10.1111/j.1476-5381.2011.01453.x
www.brjpharmacol.org

RESEARCH PAPER

Pro-oxidant effects of Ecstasy and its metabolites in mouse brain synaptosomes

Daniel José Barbosa[1], João Paulo Capela[1,2], Jorge MA Oliveira[3], Renata Silva[1], Luísa Maria Ferreira[4], Filipa Siopa[4], Paula Sério Branco[4], Eduarda Fernandes[5], José Alberto Duarte[6], Maria de Lourdes Bastos[1] and Félix Carvalho[1]

[1]*REQUIMTE (Rede de Química e Tecnologia), Laboratório de Toxicologia, Departamento de Ciências Biológicas, Faculdade de Farmácia, Universidade do Porto, Porto, Portugal,* [2]*Faculdade de Ciências da Saúde, Universidade Fernando Pessoa, Porto, Portugal,* [3]*REQUIMTE, Laboratório de Farmacologia, Departamento de Ciências do Medicamento, Faculdade de Farmácia, Universidade do Porto, Porto, Portugal,* [4]*REQUIMTE/CQFB (Centro de Química Fina e Biotecnologia), Departamento de Química, Faculdade de Ciências e Tecnologia, Universidade Nova de Lisboa, Caparica, Portugal,* [5]*REQUIMTE, Laboratório de Química Analítica e Físico-Química, Departamento de Ciências Químicas, Faculdade de Farmácia, Universidade do Porto, Porto, Portugal, and* [6]*CIAFEL, Departamento de Biologia do Desporto, Faculdade de Desporto, Universidade do Porto, Porto, Portugal*

Correspondence
Félix Carvalho and Daniel Barbosa, REQUIMTE (Rede de Química e Tecnologia), Laboratório de Toxicologia, Departamento de Ciências Biológicas, Faculdade de Farmácia, Universidade do Porto, Rua Aníbal Cunha 164, 4050-047 Porto, Portugal. E-mail: felixdc@ff.up.pt and daniel.barbosa@ff.up.pt

Keywords
3,4-methylenedioxymethamphetamine (MDMA or 'Ecstasy'); MDMA metabolites; monoamine oxidase; mitochondria; synaptosomes; oxidative stress; neurotoxicity

Received
1 February 2011
Revised
23 March 2011
Accepted
10 April 2011

BACKGROUND AND PURPOSE

3,4-Methylenedioxymethamphetamine (MDMA or 'Ecstasy') is a worldwide major drug of abuse known to elicit neurotoxic effects. The mechanisms underlying the neurotoxic effects of MDMA are not clear at present, but the metabolism of dopamine and 5-HT by monoamine oxidase (MAO), as well as the hepatic biotransformation of MDMA into pro-oxidant reactive metabolites is thought to contribute to its adverse effects.

EXPERIMENTAL APPROACH

Using mouse brain synaptosomes, we evaluated the pro-oxidant effects of MDMA and its metabolites, α-methyldopamine (α-MeDA), N-methyl-α-methyldopamine (N-Me-α-MeDA) and 5-(glutathion-*S*-*yl*)-α-methyldopamine [5-(GSH)-α-MeDA], as well as those of 5-HT, dopamine, L-DOPA and 3,4-dihydroxyphenylacetic acid (DOPAC).

KEY RESULTS

5-HT, dopamine, L-DOPA, DOPAC and MDMA metabolites α-MeDA, N-Me-α-MeDA and 5-(GSH)-α-MeDA, concentration- and time-dependently increased H_2O_2 production, which was significantly reduced by the antioxidants N-acetyl-L-cysteine (NAC), ascorbic acid and melatonin. From experiments with MAO inhibitors, it was observed that H_2O_2 generation induced by 5-HT was totally dependent on MAO-related metabolism, while for dopamine, it was a minor pathway. The MDMA metabolites, dopamine, L-DOPA and DOPAC concentration-dependently increased quinoproteins formation and, like 5-HT, altered the synaptosomal glutathione status. Finally, none of the compounds modified the number of polarized mitochondria in the synaptosomal preparations, and the compounds' pro-oxidant effects were unaffected by prior mitochondrial depolarization, excluding a significant role for mitochondrial-dependent mechanisms of toxicity in this experimental model.

CONCLUSIONS AND IMPLICATIONS

MDMA metabolites along with high levels of monoamine neurotransmitters can be major effectors of neurotoxicity induced by Ecstasy.

© 2011 The Authors
British Journal of Pharmacology © 2011 The British Pharmacological Society

Abbreviations

BSO, buthionine sulphoximine; DMSO, dimethylsulphoxide; DOPAC, 3,4-dihydroxyphenylacetic acid; DTNB, 5,5-dithio-bis(2-nitrobenzoic acid); FCCP, carbonyl cyanide 4-(trifluoromethoxy)phenylhydrazone; GR, glutathione reductase; GSH, reduced glutathione; 5-(GSH)-α-MeDA, 5-(glutathion-*S*-yl)-α-methyldopamine; GSSG, oxidized glutathione; HBSS/glucose, HBSS with glucose; HRP, horseradish peroxidase; MDA, 3,4-methylenedioxyamphetamine; MDMA, 3,4-methylenedioxymethamphetamine, Ecstasy; α-MeDA, α-methyldopamine; mFU, milliunits of fluorescence; NAC, N-acetyl-L-cysteine; β-NADPH, β-nicotinamide adenine dinucleotide phosphate reduced form; NBT, nitro blue tetrazolium; N-Me-α-MeDA, N-methyl-α-methyldopamine; RNS, reactive nitrogen species; ROS, reactive oxygen species; TBA, thiobarbituric acid; TBARS, thiobarbituric acid reactive substances; TBS, Tris-buffered saline solution; TBS-T, Tris-buffered saline solution with Tween 20; TCA, trichloroacetic acid; TMRM, tetramethylrhodamine methyl ester

Introduction

3,4-Methylenedioxymethamphetamine (MDMA or 'Ecstasy') is a strong psychoactive and mild hallucinogenic substance, which has become a major drug of abuse worldwide, over the last three decades (Hrometz *et al.*, 2004; Capela *et al.*, 2009). MDMA consumption has received particular attention because several studies have documented its potential neurotoxicity (see Capela *et al.*, 2009). MDMA-mediated neurotoxicity in rats essentially affects 5-hydroxytryptaminergic neurons (O'Hearn *et al.*, 1988; Bai *et al.*, 2001). On the other hand, high doses of MDMA administered to mice result in both dopaminergic and 5-hydroxytryptaminergic neurotoxicity (Stone *et al.*, 1987; Cadet *et al.*, 2001; Granado *et al.*, 2008). Several factors are thought to contribute to MDMA-induced neurotoxicity, namely hyperthermia, sustained receptor stimulation, inhibition of neurotransmitter synthesis, monoamine oxidase (MAO)-related metabolism of dopamine and 5-HT, dopamine oxidation and formation of neurotoxic metabolites of MDMA (Capela *et al.*, 2009). Oxidative stress is a common outcome of these factors and has an important role in the pathogenesis of MDMA, both in peripheral organs (Ninković *et al.*, 2008; Carvalho *et al.*, 2010; Shenouda *et al.*, 2010) and in the CNS (Sanchez *et al.*, 2003; Capela *et al.*, 2007; Alves *et al.*, 2009). However, the relative contribution of each of these factors to the neurotoxicity of MDMA remains to be elucidated.

It is well known that MDMA induces an acute and rapid release of both 5-HT and dopamine from nerve endings, which may undergo oxidative deamination by MAO, leading to the formation of deleterious amounts of hydrogen peroxide (H_2O_2) (Alves *et al.*, 2007). On the other hand, several studies failed to demonstrate 5-hydroxytryptaminergic neurotoxicity when MDMA or 3,4-methylenedioxyamphetamine (MDA) were injected directly into the brain, suggesting an important role for systemic metabolism in the neurotoxicity induced by these amphetamine derivatives (Bai *et al.*, 1999; Esteban *et al.*, 2001). The hepatic metabolism of MDMA involves N-demethylation to MDA, which is also a well-known drug of abuse. MDMA and MDA are *O*-demethylenated to N-methyl-α-methyldopamine (N-Me-α-MeDA) and α-methyldopamine (α-MeDA), respectively, both of which are catechols that can undergo oxidation to the corresponding *o*-quinones (Lim and Foltz, 1988; Pizarro *et al.*, 2004). In humans, N-Me-α-MeDA is the main plasma metabolite of MDMA, while α-MeDA is the main plasma metabolite in mice (de la Torre and Farré, 2004). These *o*-quinones are highly redox active molecules that can undergo redox cycling, generating semiquinone radicals and leading to the formation of reactive oxygen species (ROS) and reactive nitrogen species (RNS) (Erives *et al.*, 2008). In addition, as the reactive *o*-quinone intermediates are electrophilic compounds, cellular damage can occur through alkylation of crucial cellular proteins and/or DNA (Capela *et al.*, 2009). In the presence of reduced glutathione (GSH), *o*-quinones may be conjugated to form a glutathionyl adduct (Hiramatsu *et al.*, 1990). This GSH conjugate remains redox active and is readily oxidized to the quinone-thioether, which can undergo further reaction with GSH and/or protein thiols (Miller *et al.*, 1997). The systemic formation of GSH conjugates of α-MeDA and N-Me-α-MeDA is followed by uptake and further metabolism in the brain, as GSH conjugates of N-Me-α-MeDA are present in the brain of rats given MDMA by s.c. injection (Jones *et al.*, 2005; Erives *et al.*, 2008). Therefore, MDMA metabolites can be major effectors of MDMA neurotoxic effects, though the mechanisms behind their toxicity remain to be clarified.

The present study used mouse brain synaptosomes as an experimental model to further clarify the mechanisms of MDMA-induced neurotoxicity. Synaptosomes are a subcellular fraction, derived from neurons, prepared from brain tissue by homogenization and function as small anucleated cells that retain neuronal vesicles and enzymes. Usually, synaptosomes have one or more mitochondria and possess extremely active ion transport systems across their membranes (Nicholls, 1993; Whittaker, 1993). Synaptosomes have been used successfully to study metabolic pathways, relationships between energy production and ion movements, neurotransmitter storage and synthesis, and mechanisms involved in neurotransmitters release, as well as oxidative damage to macromolecules and neuronal mitochondria (Nicholls, 1993; Erecinska *et al.*, 1996). Increased ROS formation in mouse brain synaptosomes proved to be a useful index of the neurotoxicity induced by MDMA (Chipana *et al.*, 2006). Also, several studies have been conducted in synaptosomes to assess the effects on neurotransmitter uptake induced by amphetamine derivatives (Kim *et al.*, 2000; Pubill *et al.*, 2005).

In the present study, the pro-oxidant effects of MDMA and its metabolites α-MeDA, N-Me-α-MeDA and 5-(glutathion-*S*-*yl*)-α-methyldopamine [5-(GSH)-α-MeDA], as well as those of 5-HT, dopamine, L-DOPA and 3,4-dihydroxyphenylacetic acid (DOPAC), were evaluated in mouse brain synaptosomes through the assessment of H_2O_2 production, oxidative stress biomarkers and formation of protein quinones. We also assessed the role of mitochondria and MAO metabolism in the neurotoxic process.

Methods

Animals

All procedures were designed to minimize the number of animals used and their suffering, and were approved by the Portuguese Agency for Animal Welfare (general board of Veterinary Medicine in compliance with the Institutional Guidelines and the European Convention).

Adult male Swiss CD-1 mice (Charles River, Barcelona, Spain) weighting 30–40 g were used in all experiments. Animals were maintained under a 12 h light/dark cycle, in a temperature- and humidity-controlled room and given *ad libitum* access to food and water.

Preparation of mouse brain synaptosomes

Mouse brain synaptosomes were obtained as described elsewhere (Pubill *et al.*, 2005; Chipana *et al.*, 2006) with minor modifications. Briefly, on the morning of each assay, after weighing and anaesthetizing (sodium thiopental, 60 mg·kg^{-1}, i.p.) the animal, the brain was rapidly removed, weighed and placed in 20 volumes of cold homogenization buffer (5 mM Tris–HCl and 320 mM sucrose, pH 7.4). The mouse brain was homogenized using a borosilicate glass homogenizing tube fitted with a motor-driven Teflon pestle (10 strokes on ice). The homogenate was centrifuged at 1000× *g*, for 10 min, at 4°C. The supernatant was recovered, its volume was measured, and 1.6 M sucrose buffer (containing 5 mM Tris–HCl, pH 7.4) was added to a final sucrose concentration of 0.8 M. Samples were then centrifuged at 16 000× *g*, for 30 min, at 4°C, which gave a myelin-rich supernatant and a pellet (P2) consisting of mitochondria (brown-coloured) covered by a layer of synaptosomes (white). The supernatant was discarded, and the synaptosome layer was separated by carefully adding 1 mL of ice-cold 320 mM sucrose buffer (pH 7.4) and gently shaking the suspension. Finally, the synaptosome fraction was diluted in HBSS/glucose. All experiments were performed at a final protein concentration of 0.1 mg·mL^{-1}, except in assessment of mitochondrial damage, in which synaptosomes were used at a final protein concentration of 0.5 mg·mL^{-1}. Protein concentration was determined using the Bio-Rad DC protein assay kit, according to the manufacturer's specifications and using BSA solutions as standards.

Assessment of H_2O_2 production

The formation of synaptosomal H_2O_2 was measured by fluorescence, using amplex red (25 μM) in the presence of 0.25 U·mL^{-1} horseradish peroxidase (HRP), as previously described (Tretter and Adam-Vizi, 2007), with some adaptations. The method is based in the fact that H_2O_2 reacts with amplex red, a colourless and non-fluorescent compound, at a stoichiometry of 1:1, in a reaction catalysed by HRP to generate the highly fluorescent product resorufin. The fluorescence intensity is proportional to the H_2O_2 generation. Resorufin exhibits a maximum of fluorescence emission at a wavelength of 587 nm and maximum excitation at 563 nm. This is a very sensitive method for low concentrations of H_2O_2 (this procedure allows detection of 5 pmol H_2O_2 in a 96-well fluorescence assay microplate) (Zhou *et al.*, 1997). The synaptosomes were exposed to the drugs under study (6.25, 12.5, 25, 50, 100 and 200 μM) and fluorescence intensities of the reaction mixtures were measured at 37°C during 15 min, using a 96-well microplate in a fluorescence microplate reader (Synergy HT; Bio-Tek Instruments, VT) with a filter set for excitation and emission at 530 ± 25 and 590 ± 35 nm respectively. Each well contained 250 μL of synaptosomal suspension, 15 μL of HRP, 15 μL of amplex red and 10 μL of compound solution. The final volume in the well was fixed with HBSS/glucose to 300 μL. In the experiments conducted in the presence of MAO inhibitors (clorgyline 100 nM and deprenyl 10 nM), antioxidants (NAC 10 and 100 μM, ascorbic acid 10 and 100 μM and melatonin 0.5 and 1 mM) and FCCP (1 μM), synaptosomes were pre-incubated with these compounds in water bath, at 37°C, for 30 min. Based on the results obtained for H_2O_2 production, the effects of antioxidants and FCCP were evaluated after incubation of synaptosomes with the drugs at a fixed concentration (50 μM). The MAO inhibitors' concentrations used in this study were selected from previous studies of MAO inhibition (Youdim *et al.*, 2001; Aubin *et al.*, 2004). The FCCP concentration used here was selected from studies of maximal mitochondrial depolarization in neurons (Oliveira and Gonçalves, 2009) and synaptosomes (Tretter *et al.*, 1998). Mean fluorescence values of each experimental condition are presented in milliunits of fluorescence [mFU (arbitrary units)] or by the slope of the reading [mFU (arbitrary units)·min^{-1}, from 10 to 15 min].

Assessment of lipid peroxidation

Lipid peroxidation was assessed by measuring malondialdehyde equivalents, using the thiobarbituric acid (TBA) assay (as TBA reactive substances – TBARS). After incubation of synaptosomes with different concentrations of compounds (6.25, 12.5, 25, 50, 100 and 200 μM) in a water bath, at 37°C, samples of 150 μL were removed at selected time points (15, 30, 60, 120 and 180 min) and 300 μL of 10% trichloroacetic acid (TCA) (w/v) were added. The mixture was allowed to incubate on ice for 30 min before centrifugation at 16 000× *g*, for 10 min, at 4°C. After centrifugation, 250 μL of the supernatant was incubated with 250 μL of TBA reagent [1% TBA (w/v) in distilled water]. The mixture was heated at 95°C, for 10 min, and allowed to cool at room temperature. The malondialdehyde levels were estimated by spectrophotometric determination (PowerWaveX; Bio-Tek Instruments) at 535 nm. The effect promoted by 100 μM of NAC against lipid peroxidation was evaluated after incubating synaptosomes with the MDMA metabolite 5-(GSH)-α-MeDA, at the concentration of 200 μM. The amount of malondialdehyde equivalents was calculated using a molar extinction coefficient of 1.56 × 10^5 mol·cm^{-1}, and the final result was expressed as nmol malondialdehyde Eq·mg^{-1} protein.

Assessment of protein-bound quinones (quinoproteins)

Protein-bound quinones were assessed by the NBT/glycinate colorimetric assay, as previously described (Capela *et al.*, 2007), with a few adaptations. After incubation of synaptosomes with different concentrations of drugs (6.25, 12.5, 25, 50, 100 and 200 μM) in water bath, at 37°C, sample aliquots (1 mL) were collected at selected time points (20, 30 and

60 min) and centrifuged at 16 000× *g*, for 15 min, at 37°C. The supernatant was carefully discarded, and the pellet was lysed in ice-cold RIPA buffer [50 mM Tris–HCl, 150 mM NaCl, 1% Igepal CA-630 (v/v), 0.5% sodium deoxycholate (w/v) and 0.1% SDS (w/v), pH 7.4], supplemented with 0.5 mM of PMSF. The samples were vortexed and placed in the ultrasonic bath for 10 min. Subsequently, 70 µL of the lysates in RIPA buffer were added to 180 µL of 2 M sodium glycinate solution (pH 10). The protein containing solution was added to 500 µL of NBT reagent (0.24 mM NBT in 2 M sodium glycinate, pH 10). The reaction was performed for 2 h, with agitation, at room temperature, after which the absorbance of the blue-purple colour was read at 530 nm in a 96-well plate reader (PowerWaveX; Bio-Tek Instruments). Whole protein content was quantified using the Bio-Rad DC protein assay kit and BSA solutions as standards. Results are expressed as optical density arbitrary units (OD 530 nm·mg^{-1} protein).

Assessment of protein carbonylation

Protein carbonyls, an index of protein oxidation, were determined as previously described (Magalhães *et al.*, 2007), with adaptations. After incubation of synaptosomes with 200 µM of the different compounds in a water bath at 37°C, for 2 h, 2 mL sample aliquots were removed and centrifuged at 16 000× *g*, for 15 min, at 4°C. The supernatant was discarded, and the pellet was dispersed in 300 µL of phosphate buffer (50 mM KH_2PO_4 and 1 mM EDTA, pH 6.7), sonicated and again centrifuged at 10 000× *g*, for 15 min, at 4°C. Protein concentrations of all samples were determined using the Bio-Rad DC protein assay kit, and all samples were diluted down to a final protein concentration of 0.1 mg·mL^{-1}. Samples containing 20 µg of protein (200 µL) were incubated with 400 µL of 20 mM 2,4-dinitrophenylhydrazine [in 10% trifluroacetic acid (v/v)] in the presence of 200 µL of 12% SDS (w/v), for 30 min at room temperature in the dark, after which were neutralized with 300 µL of neutralization solution [18% β-mercaptoethanol (v/v) in 2 M Tris] and diluted down to a final protein concentration of 2 µg·mL^{-1}. Derivatized proteins (0.2 µg) were loaded into nitrocellulose membrane under vacuum using a slot blot apparatus. Then, after washing in Tris-buffered saline solution (TBS:10 mM Tris–HCl, 150 mM NaCl, pH 8.0), the membrane was blocked in blocking buffer [5% non-fat powdered skim milk (w/v) in TBS with 0.05% Tween 20 (v/v) (TBS-T)] overnight, at 4°C. The membrane was then incubated with primary antibody (rabbit polyclonal anti-DNP, 1:1000) for 1.5 h. After incubation with the primary antibody, membranes were rinsed two times with TBS-T and added with the secondary antibody (anti-rabbit IgG-peroxidase, 1:2000) for 1 h. Antibodies were diluted in blocking buffer. Following two washes in TBS-T, bands were visualized by treating the immunoblots with ECL Plus chemiluminescence reagents (Amersham Pharmacia Biotech), according to the supplier's instructions, and developed on high performance chemiluminescence films (Amersham Pharmacia Biotech) with Kodak Film Developer and Kodak Fixer (Sigma-Aldrich). Bands in the films were quantified using the Image J software (National Institutes of Health). Optical density results were expressed as % of control values.

Assessment of glutathione levels

The GSH and GSSG levels of the synaptosomes were determined by the DTNB-GSH reductase recycling assay as previously described (Carvalho *et al.*, 2004a), with adaptations. After exposure of the synaptosomes to the tested compounds at the concentrations of 50 and 200 µM in water bath, at 37°C, 2 mL sample aliquots were collected at selected time points (1 and 2 h) and centrifuged at 16 000× *g*, for 15 min, at 4°C. The supernatant (600 µL) was collected, and 200 µL $HClO_4$ 20% (w/v) was added. The pellet was dispersed in 250 µL of $HClO_4$ 5% (w/v) and again centrifuged at 16 000× *g*, for 5 min, at 4°C. In sample aliquots, the perchloric acid pellet was dissolved in 250 µL of NaOH 0.3 M, and the protein content was assayed by the Lowry method (Lowry *et al.*, 1951), using BSA solutions as standards. The supernatants (200 µL) were neutralized with an equimolar solution of $KHCO_3$ (0.76 M) and centrifuged at 16 000× *g*, for 5 min, at 4°C. For GSSG quantification, aliquots (200 µL) of acidic supernatant were added of 10 µL 2-vinylpyridine and shaked continuously during 1 h to block free SH groups. In 96-well plates, 100 µL of sample, standard or blank were added in triplicate and mixed with 65 µL of fresh reagent solution containing 1.3 mM 5,5-dithio-bis(2-nitrobenzoic acid) (DTNB) and 0.24 mM β-NADPH dissolved in phosphate buffer (71.5 mM Na_2HPO_4, 71.5 mM NaH_2PO_4 and 0.63 mM EDTA, pH 7.5). Plates were then incubated in a plate reader (PowerWaveX; Bio-Tek Instruments) at 30°C during 15 min prior to the addition of 40 µL of fresh GR solution per well (10 U·mL^{-1} in phosphate buffer). The stoichiometric formation of 5-thio-2-nitrobenzoic acid (TNB) was followed for 3 min at 415 nm and compared with a standard curve. GSH and GSSG standard solutions were prepared in $HClO_4$ 5% (w/v). The effect of buthionine sulphoximine (BSO) on GSH levels was evaluated after incubating synaptosomes with the drugs, at the concentration of 200 µM, for 1 h. GSH and GSSG contents were normalized to the total protein content, and the final result was expressed as nmol GSH or GSSG·mg^{-1} protein or µM GSH in the supernatant.

Assessment of mitochondrial integrity

To assess mitochondrial integrity, synaptosomes exposed to drugs, at the concentration of 200 µM, for 1 h, were subsequently incubated with 50 nM tetramethylrhodamine methyl ester (TMRM) and imaged by fluorescence microscopy as previously described (Oliveira and Gonçalves, 2009), during 2 h. The imaging system consisted of an inverted epifluorescence microscope (Eclipse TE300; Nikon, Tokyo, Japan) equipped with a 60× air objective, a monochromator (Polychrome II; TILL Photonics, Martinsried, Germany) and a CCD camera (C6790; Hamamatsu Photonics, Hamamatsu, Japan). In each experiment, synaptosomal preparations were sampled in triplicate, by placing 20 µL of the synaptosomal suspension between glass slide and coverslip and processed with the automated acquisition of 20 random fields. The number of mitochondria (TMRM-labelled puncta, as confirmed by FCCP-induced fluorescence decay) was quantified by particle analysis using custom built macros in Image J (National Institutes of Health). Results (average number of polarized mitochondria per field) are presented as % of control.

Statistical analysis

Results are presented as mean ± SD from four to six independent experiments, with synaptosomes derived from the same number of different animals. All data were analysed using parametric tests. Statistical comparisons between groups were performed with one-way ANOVA followed by the Newman–Keuls multiple comparison *post hoc* test, for experiments with one variable. Two-way ANOVA followed by the Bonferroni's multiple comparison *post hoc* test, was used in experiments with two variables. Details of the statistical analysis are described in each figure legend. Differences were considered to be statistically significant at *P*-values lower than 0.05. All analyses were performed using GraphPad Prism 5.0 for Windows (GraphPad Software, San Diego, CA).

Materials

All reagents used in this study were of analytical grade or of the highest grade available. The following reagents were obtained from Sigma-Aldrich (St. Louis, MO): N-acetyl-3,7-dihydroxyphenoxazine (amplex red), horseradish peroxidase (HRP), 5-HT hydrochloride, dopamine hydrochloride, L-DOPA, DOPAC, *R*-(–)-deprenyl hydrochloride, N-methyl-*N*-propargyl-3-(2,4-dichlorophenoxy)propylamine hydrochloride (clorgyline), N-acetyl-l-cysteine (NAC), ascorbic acid, melatonin, carbonyl cyanide 4-(trifluoromethoxy)phenylhydrazone (FCCP), thiobarbituric acid (TBA), PMSF, nitro blue tetrazolium (NBT), sodium glycinate, GSH, oxidized glutathione (GSSG), β-NADPH, 5,5-dithio-bis(2-nitrobenzoic acid) (DTNB), glutathione reductase (GR), buthionine sulphoximine (BSO) and bovine serum albumin (BSA). Rabbit polyclonal anti-DNP antibody and tetramethylrhodamine methyl ester (TMRM) were obtained from Invitrogen (Carlsbad, CA). Anti-rabbit IgG-peroxidase antibody was purchased from Amersham Pharmacia Biotech (Buckinghamshine, United Kingdom). Bio-Rad DC protein assay kit was purchased from Bio-Rad Laboratories (Hercules, CA). $HClO_4$, NaOH, absolute ethanol, dimethylsulphoxide (DMSO) and Folin reagent were obtained from Merck (Darmstadt, Germany). Sodium thiopental was obtained from B. Braun (Lisbon, Portugal). MDMA (hydrochloride salt) was extracted and purified from high-purity MDMA tablets that were kindly provided by the Portuguese Criminal Police Department. The obtained salt was pure and fully characterized by NMR and mass spectrometry methodologies. The MDMA metabolites α-MeDA, N-Me-α-MeDA and 5-(GSH)-α-MeDA were synthesized and fully characterized by NMR and mass spectrometry methodologies by REQUIMTE/CQFB (Centro de Química Fina e Biotecnologia), Departamento de Química, Faculdade de Ciências e Tecnologia, Universidade Nova de Lisboa, according to methods previously published by our group (Capela *et al.*, 2006; Macedo *et al.*, 2007). All other chemicals were purchased from Sigma-Aldrich. 5-HT, dopamine, DOPAC, MAO inhibitors clorgyline and deprenyl, NAC and ascorbic acid were dissolved in HEPES-buffered salt solution with glucose (HBSS/glucose: 140 mM NaCl, 5.37 mM KCl, 1.26 mM $CaCl_2$, 0.44 mM KH_2PO_4, 0.49 mM $MgCl_2{\cdot}6H_2O$, 0.41 mM $MgSO_4(7H_2O$, 4.17 mM $NaHCO_3$, 0.34 mM $Na_2HPO_4{\cdot}7H_2O$, 20 mM HEPES-Na and 5.5 mM glucose, pH 7.4). HRP, BSO, MDMA and MDMA metabolites were dissolved in distilled water. L-DOPA was solubilized in 10 mM HCl. Amplex red and TMRM were dissolved in DMSO. PMSF and melatonin were solubilized in absolute ethanol. FCCP was dissolved in 95% of ethanol. Controls received an equivalent amount of vehicle.

Results

MDMA metabolites, monoamine neurotransmitters, L-DOPA and DOPAC induced H_2O_2 generation in a concentration- and time-dependent manner

Mouse brain synaptosomes were exposed to growing concentrations of the different compounds (6.25–200 μM) and assayed for H_2O_2 generation, using an amplex red method. Incubation of synaptosomes with MDMA metabolites α-MeDA, N-Me-α-MeDA and 5-(GSH)-α-MeDA, as well as 5-HT, dopamine, L-DOPA and DOPAC significantly increased H_2O_2 production (Figure 1) in a concentration- and time-dependent manner. On the other hand, MDMA did not significantly increase the H_2O_2 formation at any of the evaluated concentrations during the time course of the experiment (Figure 1A). For N-Me-α-MeDA, 5-HT, L-DOPA and DOPAC, there was a statistically significant amount of H_2O_2 at the lowest concentration studied (6.25 μM) (Figure 1C,E,G,H). The other compounds generated a significant amount of H_2O_2 only at 12.5 μM or above (Figure 1B,D,F). The MDMA metabolite 5-(GSH)-α-MeDA was the most effective generator of H_2O_2, under our conditions. In experiments conducted in the absence of amplex red, no auto-fluorescence was observed for all studied compounds (data not shown).

DA- and 5-HT-induced H_2O_2 production was dependent on MAO-related metabolism

Figure 2 presents the results for H_2O_2 production, expressed by the slope of the reading [mFU (arbitrary units)·min^{-1}, from 10 to 15 min], when synaptosomes were pre-incubated with MAO-A and/or MAO-B selective inhibitors clorgyline (100 nM) and deprenyl (10 nM), respectively. There were no significant differences in basal H_2O_2 production between synaptosomes pre-incubated with MAO inhibitor(s) and non pre-incubated synaptosomes. Pre-incubation of synaptosomes with clorgyline blocked H_2O_2 production for all concentrations of 5-HT tested (Figure 2A). However, for dopamine (Figure 2B), clorgyline decreased H_2O_2 generation only at the highest dopamine concentration tested (200 μM) ($P < 0.001$), with similar effects for deprenyl ($P < 0.05$) (Figure 2B). On the other hand, MAO-B inhibition with deprenyl did not affect H_2O_2 generation by 5-HT (Figure 2A). In another set of experiments, the results of pre-incubation with clorgyline and deprenyl were similar to those obtained with clorgyline alone (Figure 2C–D). For the other compounds, pretreatment of synaptosomes with MAO inhibitors had no effect on H_2O_2 production (data not shown).

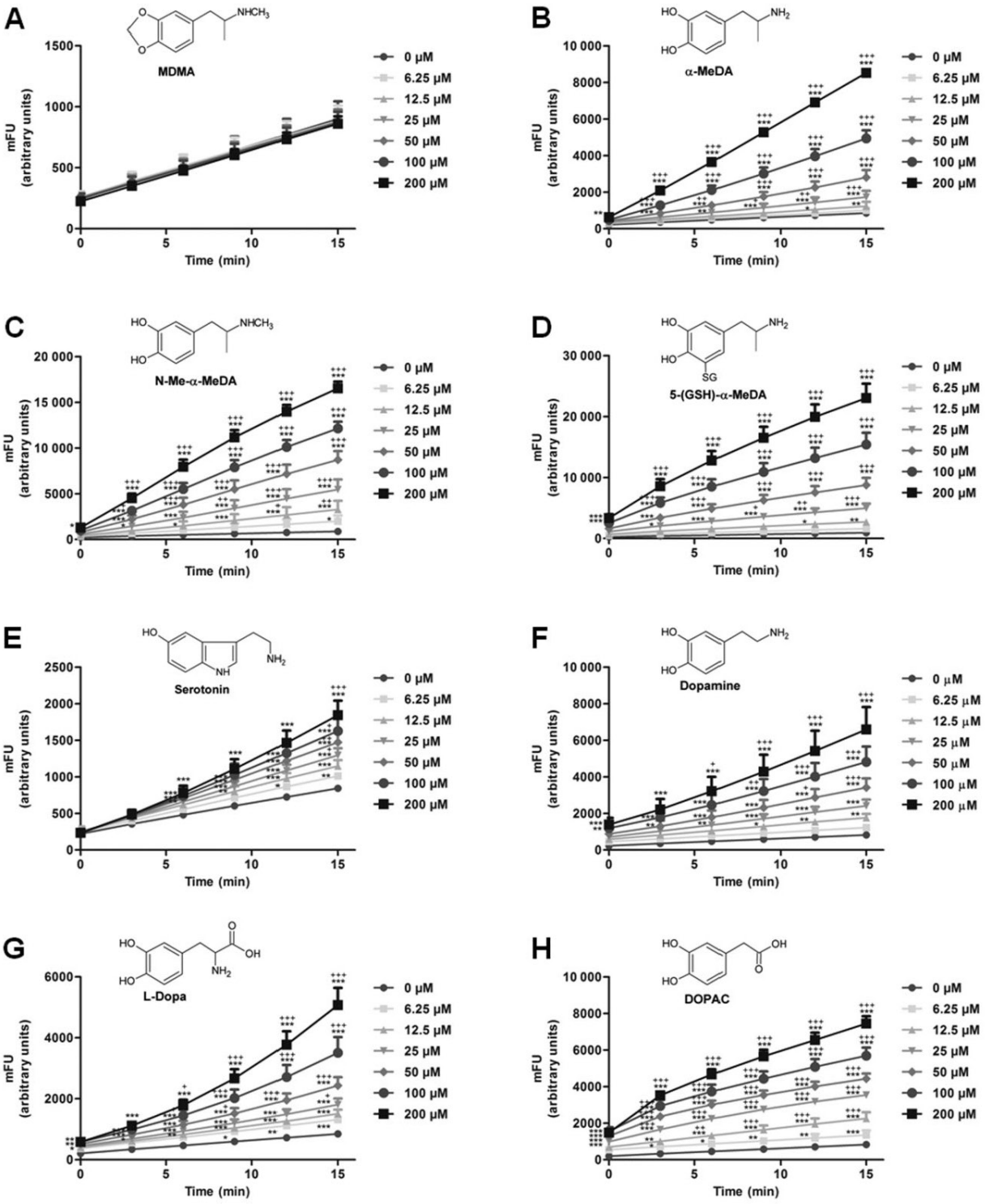


Figure 1

H_2O_2 generation induced by MDMA (A), its metabolites α-MeDA (B), N-Me-α-MeDA (C) and 5-(GSH)-α-MeDA (D), monoamine neurotransmitters 5-HT (E) and dopamine (F), as well as the dopamine precursor L-DOPA (G) and dopamine metabolite DOPAC (H), in mouse brain synaptosomes, evaluated by the amplex red method. Synaptosomes were exposed, for 15 min, to increasing concentrations (6.25, 12.5, 25, 50, 100 and 200 µM) of the compounds, and measurements were made at six different time points. Results are presented as mean ± SD from 5 independent experiments for panel A and 6 independent experiments for panels B–H, expressed in mFU (arbitrary units). Statistical comparisons were made using two-way ANOVA with repeated measures followed by the Bonferroni's multiple comparison *post hoc* test [$^{*}P < 0.05$, $^{**}P < 0.01$, $^{***}P < 0.001$ concentration vs. control (0 µM); $^{+}P < 0.05$, $^{++}P < 0.01$, $^{+++}P < 0.001$ concentration vs. prior concentration].

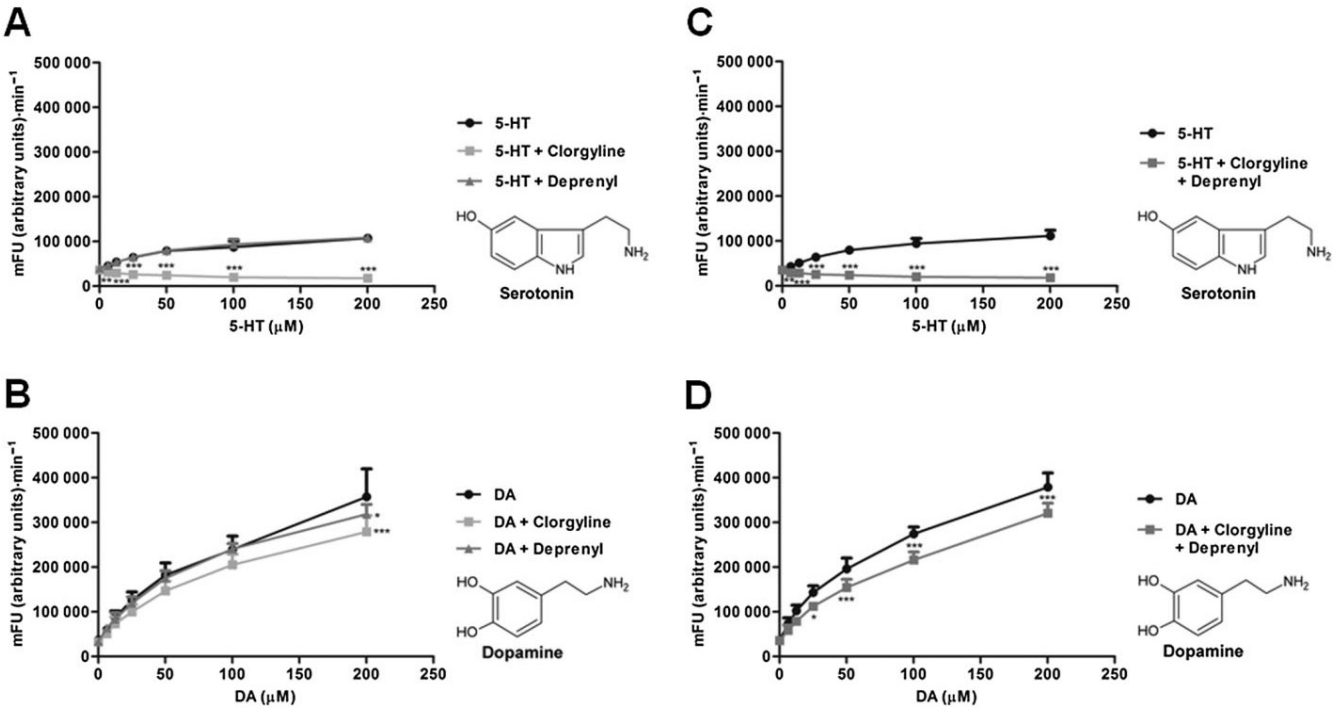


Figure 2

Effect of clorgyline (MAO-A inhibitor) or deprenyl (MAO-B inhibitor) on H_2O_2 generation induced by 5-HT and dopamine, in mouse brain synaptosomes, evaluated by the amplex red method. Synaptosomes were exposed, for 15 min, to increasing concentrations (6.25, 12.5, 25, 50, 100 and 200 μM) of 5-HT (A) or dopamine (B) either with or without clorgyline (100 nM) or deprenyl (10 nM) pre-incubation. On another set of experiments, synaptosomes were pre-incubated with clorgyline (100 nM) plus deprenyl (10 nM) before exposure to 5-HT (C) and dopamine (D). Results are presented as mean ± SD from 6 independent experiments, expressed by the slope of the reading [mFU (arbitrary units)·min^{-1}, from 10 to 15 min]. Statistical comparisons were made using two-way ANOVA followed by the Bonferroni's multiple comparison *post hoc* test [*P < 0.05, **P < 0.01, ***P < 0.001 monoamine plus MAO inhibitor(s) vs. monoamine].

NAC, ascorbic acid and melatonin prevented H_2O_2 generation induced by MDMA metabolites, 5-HT, dopamine, L-DOPA and DOPAC

Figure 3 shows the antioxidant effects of 10 μM NAC, 10 μM ascorbic acid and 0.5 mM melatonin, on H_2O_2 production. Ascorbic acid, by itself, increased H_2O_2 generation. For the MDMA metabolite α-MeDA, (Figure 3A), NAC (P < 0.05), ascorbic acid (P < 0.001) and melatonin (P < 0.001) decreased H_2O_2 production. Ascorbic acid decreased H_2O_2 production by N-Me-α-MeDA (Figure 3B) more effectively. On the other hand, for the MDMA metabolite 5-(GSH)-α-MeDA (Figure 3C) and 5-HT (Figure 3D), only melatonin decreased H_2O_2 levels (P < 0.001). Both ascorbic acid and melatonin decreased (P < 0.001) H_2O_2 levels generated by dopamine (Figure 3E). All three antioxidants decreased H_2O_2 levels resulting from incubation with L-DOPA (P < 0.001 for all antioxidants) (Figure 3F). In contrast with all other studied compounds, for DOPAC (Figure 3G), only ascorbic acid was able to decrease H_2O_2 levels (P < 0.001) but with NAC, there was actually an abrupt increase. When higher concentrations (100 μM) of the antioxidants were tested, only NAC and ascorbic acid inhibited H_2O_2 production induced by N-Me-α-MeDA (P < 0.001), while in the case of L-DOPA, only 100 μM of NAC significantly decreased H_2O_2 levels (P < 0.001) (data not shown). Also, the effects elicited by a higher concentration of melatonin (1 mM) were not significantly different from 0.5 mM for all compounds tested (data not shown). Thus, among the antioxidants studied, melatonin showed the highest antioxidant effects against H_2O_2 production induced by the different compounds.

H_2O_2 production induced by the tested compounds was unaffected by prior mitochondrial depolarization

To investigate if H_2O_2 production induced by the different compounds had a mitochondrial source, we used the protonophore FCCP that depolarizes mitochondria by collapsing the proton gradient across the mitochondrial inner membrane and dissipating mitochondrial membrane potential. Table 1 shows that FCCP (1 μM) did not affect either the basal H_2O_2 production or that induced by any of the evaluated compounds. In experiments conducted by real-time fluorescence videomicroscopy, we confirmed that the FCCP concentration used in this study was able to completely collapse the mitochondrial membrane potential (data not shown). Thus, in our experimental conditions, the H_2O_2 production induced by all tested compounds was independent of the mitochondrial polarization status,

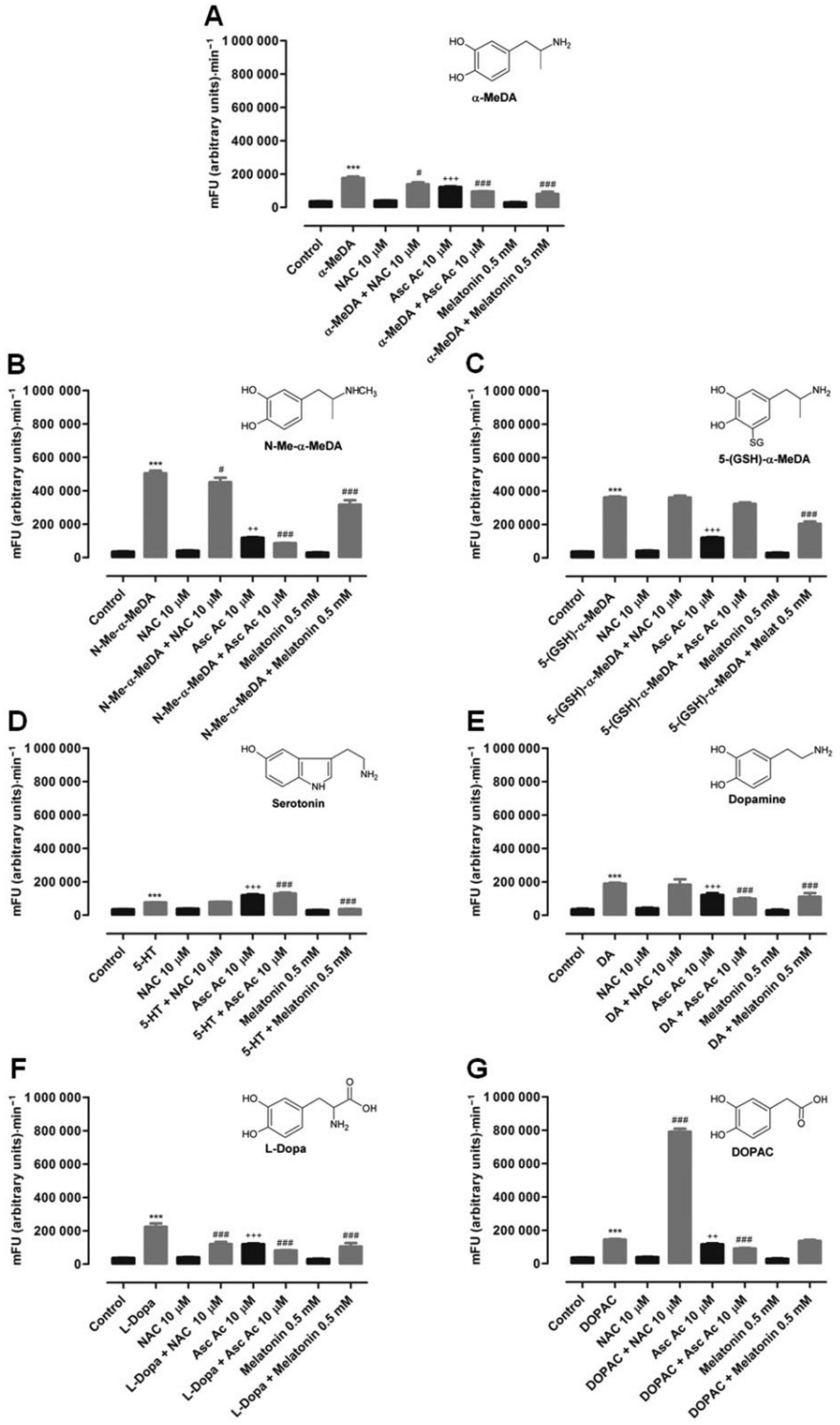


Figure 3

Protective effect of NAC, ascorbic acid and melatonin against H_2O_2 generation induced by the MDMA metabolites α-MeDA (A), N-Me-α-MeDA (B) and 5-(GSH)-α-MeDA (C), 5-HT (D), dopamine (E), L-DOPA (F) and DOPAC (G) in mouse brain synaptosomes, evaluated by the amplex red method. Synaptosomes, with or without antioxidant pre-incubation (10 μM of NAC and ascorbic acid or 0.5 mM of melatonin), were exposed for 15 min to the compounds, at the concentration of 50 μM. Results are presented as mean ± SD from 6 independent experiments, expressed by the slope of the reading [mFU (arbitrary units)·min^{-1}, from 10 to 15 min]. Statistical comparisons were made using one-way ANOVA followed by the Newman–Keuls multiple comparison *post hoc* test (***$P < 0.001$ compound vs. control; $^{++}P < 0.01$, $^{+++}P < 0.001$ antioxidant vs. control; $^{\#}P < 0.05$, $^{\#\#\#}P < 0.001$ compound plus antioxidant vs. compound).

Table 1

Effect of mitochondrial depolarization with FCCP (1 μM) on H_2O_2 generation induced by MDMA metabolites, as well as by 5-HT, dopamine, L-DOPA and DOPAC

Compound	Control	FCCP 1 μM	50 μM	50 μM + FCCP 1 μM
α-MeDA	3.97 ± 0.16	4.06 ± 0.20	9.96 ± 2.06	10.85 ± 1.92
N-Me-α-MeDA	3.99 ± 0.15	4.04 ± 0.17	13.69 ± 3.49	16.83 ± 4.18×
5-(GSH)-α-MeDA	4.17 ± 0.38	4.14 ± 0.36	10.82 ± 2.29	11.54 ± 2.16
5-HT	3.85 ± 0.16	3.98 ± 0.22	7.39 ± 0.48	7.32 ± 0.52
DA	3.88 ± 0.16	3.96 ± 0.20	18.28 ± 2.09	18.17 ± 1.85
L-DOPA	3.96 ± 0.20	4.04 ± 0.23	8.50 ± 1.57	9.62 ± 1.84
DOPAC	3.86 ± 0.25	3.95 ± 0.25	15.32 ± 1.40	15.88 ± 1.49

Synaptosomes, with or without FCCP (1 μM) pretreatment were exposed for 15 min to MDMA metabolites (α-MeDA, N-Me- α-MeDA and 5-(GSH)-α-MeDA), 5-HT, dopamine, L-DOPA or DOPAC, all at 50 μM, and H_2O_2 generation was evaluated by the amplex red method. Results are presented as mean ± SD from 6 independent experiments, expressed by the slope of the reading [10^4mFU (arbitrary units)·min^{-1}, from 10 to 15 min]. Statistical comparisons were made using one-way ANOVA followed by the Newman–Keuls multiple comparison *post hoc* test.

excluding a significant role of the organelle's respiratory chain in the H_2O_2-generating mechanism.

MDMA metabolite 5-(GSH)-α-MeDA concentration- and time-dependently induced lipid peroxidation, an effect prevented by NAC

Lipid peroxidation induced by the compounds in mouse brain synaptosomes was evaluated by the TBA assay. As shown in Figure 4, the MDMA metabolite 5-(GSH)-α-MeDA induced lipid peroxidation in a concentration- and time-dependent manner, reaching significance at 120 min (Figure 4A). For the remaining compounds, we did not observe significant differences from control at any of concentrations and incubation times studied (data not shown). Experiments were conducted to verify the ability of this metabolite to react directly with the TBA. After exposure of the MDMA metabolite directly with TBA in HBSS/glucose, we verified the absence of any reaction, excluding also the possibility of reaction with the final products of the lipid peroxidation (data not shown).

Pre-incubation of synaptosomes with NAC (100 μM), inhibited lipid peroxidation mediated by 5-(GSH)-α-MeDA (200 μM) (Figure 4B). Other antioxidant treatments (NAC 10 μM, ascorbic acid 10 and 100 μM, or melatonin 0.5 and 1 mM) did not change lipid peroxidation induced by 5-(GSH)-α-MeDA (data not shown).

MDMA metabolites α-MeDA, N-Me-α-MeDA and 5-(GSH)-α-MeDA, as well as dopamine, L-DOPA and DOPAC increased the formation of protein-bound quinones, in a concentration-dependent manner

To assess the role of quinones in the deleterious potential of the different studied compounds, we evaluated the levels of protein-bound quinones (quinoproteins). Although different incubation times were tested (20, 30 and 60 min), formation of protein-bound quinones was not time-dependent, and, thus, only the results obtained at 30 min time point are presented (Figure 5). MDMA and 5-HT did not generate quinoproteins, at any of the concentrations studied (data not shown). The other compounds increased quinoprotein levels, in a concentration-dependent manner (Figure 5), and the most effective was the MDMA metabolite N-Me-α-MeDA, with a significant formation of quinoproteins at the lowest concentration studied (6.25 μM) ($P < 0.05$) (Figure 5B). The antioxidants NAC (10 and 100 μM), ascorbic acid (10 and 100 μM) and melatonin (0.5 and 1 mM) did not prevent the formation of quinoproteins (data not shown).

The MDMA metabolite 5-(GSH)-α-MeDA and DOPAC induced a significant carbonylation of synaptosomal proteins

To evaluate possible oxidative effects to synaptosomal proteins, we also studied the protein carbonylation by an immunoblotting method. As presented in Figure 6, the levels of protein carbonyls in the synaptosomes were raised by incubation with the MDMA metabolite 5-(GSH)-α-MeDA or DOPAC (200 μM), for 2 h ($P < 0.05$) but not by the other compounds (data not shown).

Incubation of synaptosomes with MDMA metabolites α-MeDA, N-Me-α-MeDA and 5-(GSH)-α-MeDA, as well as 5-HT, dopamine, L-DOPA and DOPAC altered the intra-synaptosomal glutathione status

Figure 7 shows the glutathione status in synaptosomes after incubation with 50 and 200 μM of the tested compounds for 1 and 2 h. Incubation of synaptosomes, for 1 h, with 50 μM of MDMA metabolites α-MeDA, N-Me-α-MeDA and 5-(GSH)-α-MeDA and dopamine increased total GSH levels ($P < 0.001$, $P < 0.01$, $P < 0.01$ and $P < 0.01$ respectively) (Figure 7A), without affecting GSSG levels (Figure 7E). After 2 h, there was also a significant increase in total GSH levels, only for the MDMA metabolite α-MeDA and dopamine ($P < 0.01$) (Figure 7B), without changing GSSG levels (Figure 7F).

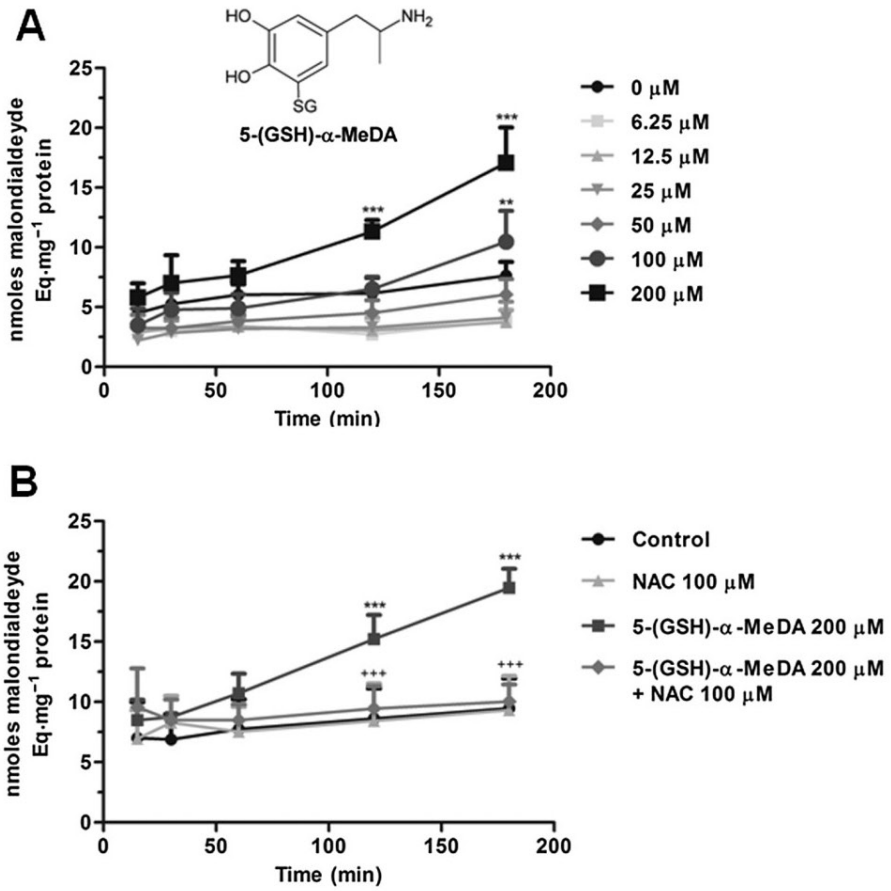


Figure 4

(A) Lipid peroxidation induced by the MDMA metabolite 5-(GSH)-α-MeDA in mouse brain synaptosomes, evaluated by the TBA assay (TBARS). Synaptosomes were exposed, for 3 h, to increasing concentrations (6.25, 12.5, 25, 50, 100 and 200 μM) of MDMA metabolite 5-(GSH)-α-MeDA, and measurements were made at 5 different time-points (15, 30, 60, 120 and 180 min). (B) Protective effect of NAC against lipid peroxidation induced by the MDMA metabolite 5-(GSH)-α-MeDA, in mouse brain synaptosomes, evaluated by the TBA assay (TBARS). Synaptosomes were exposed for 3 h to MDMA metabolite 5-(GSH)-α-MeDA, at the concentration of 200 μM, in the presence or absence of NAC (100 μM). Results are presented as mean ± SD from $n = 6$ independent experiments, expressed in nmol malondialdehyde Eq·mg^{-1} protein. Statistical comparisons were made using two-way ANOVA followed by the Bonferroni's multiple comparison *post hoc* test [$^{**}P < 0.01$, $^{***}P < 0.001$ concentration vs. control (0 μM); $^{+++}P < 0.001$ 5-(GSH)-α-MeDA plus NAC vs. 5-(GSH)-α-MeDA].

However, for the MDMA metabolite 5-(GSH)-α-MeDA, GSSG levels were significantly increased at this time point ($P < 0.05$) (Figure 7F). When synaptosomes were incubated with 200 μM of the different compounds, for 1 h, it was observed a significant increase in total GSH levels for all compounds, except for MDMA and DOPAC ($P < 0.05$ for α-MeDA, N-Me-α-MeDA, 5-(GSH)-α-MeDA, 5-HT and dopamine, and $P < 0.01$ for L-DOPA) (Figure 7C). For N-Me-α-MeDA, 5-(GSH)-α-MeDA and dopamine, the increase in total GSH levels were accompanied by significant elevations of GSSG levels ($P < 0.01$, $P < 0.001$ and $P < 0.001$, respectively) (Figure 7G). Incubation of synaptosomes with the different compounds at a concentration of 200 μM, for 2 h, resulted in significant increases in total GSH levels only after exposure to 5-HT ($P < 0.05$) and L-DOPA ($P < 0.001$) (Figure 7D), which were accompanied by increased GSSG levels ($P < 0.001$ and $P < 0.01$ respectively) (Figure 7H). At the same time point, 200 μM N-Me-α-MeDA, 5-(GSH)-α-MeDA, dopamine and DOPAC also promoted a significant increase in GSSG levels ($P < 0.01$, $P < 0.001$, $P < 0.001$ and $P < 0.01$, respectively) (Figure 7H).

In order to explain the increase of total GSH levels without concomitant elevations in the GSSG levels, we used BSO, a selective and potent inhibitor of γ-glutamylcysteine ligase (the enzyme catalysing the rate limiting step in GSH biosynthesis), and measured total GSH levels in the incubation medium after incubation with the different compounds (200 μM; 1 h). Pre-incubation of synaptosomes with BSO (Figure 8A) did not modify the basal GSH content of synaptosomes or that after incubation with the compounds. However, in the supernatant, total GSH levels decreased ($P < 0.05$ for N-Me-α-MeDA, $P < 0.01$ for 5-HT and L-DOPA and $P < 0.001$ for α-MeDA, 5-(GSH)-α-MeDA, dopamine and DOPAC) (Figure 8B), but GSSG levels remained below the detection limit of the method. Thus, the increase in total GSH levels observed did not result from an increase in its synthesis, as ascertained by the use of BSO, but rather to the uptake from the incubation medium.

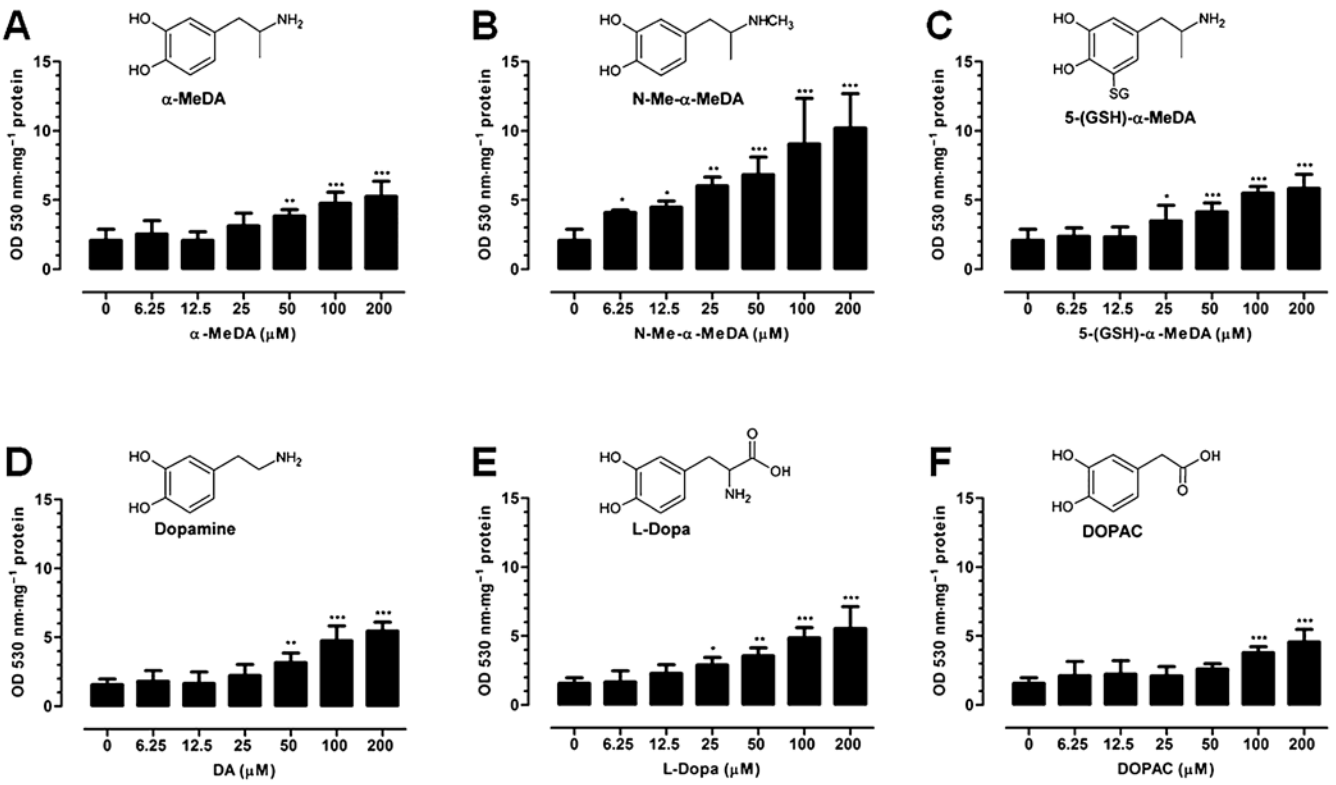


Figure 5

Protein-bound quinones (quinoproteins) induced by the MDMA metabolites α-MeDA (A), N-Me-α-MeDA (B) and 5-(GSH)-α-MeDA (C), as well as by dopamine (D), L-DOPA (E) and DOPAC (F), in mouse brain synaptosomes, evaluated by the NBT/glycinate colorimetric assay. Synaptosomes were exposed to increasing concentrations of the compounds (6.25, 12.5, 25, 50, 100 and 200 μM), and measurements were made after 30 min. Results are presented as mean ± SD from 6 independent experiments, expressed as OD 530 nm·mg^{-1} protein. Statistical comparisons were made using one-way ANOVA followed by the Newman–Keuls multiple comparison *post hoc* test [*P < 0.05, **P < 0.01, ***P < 0.001 concentration vs. control (0 μM)].

Oxidative stress induced by MDMA metabolites N-Me-α-MeDA and 5-(GSH)-α-MeDA and 5-HT did not alter the number of polarized mitochondria

To evaluate possible effects of 5-HT, N-Me-α-MeDA and 5-(GSH)-α-MeDA on mitochondrial integrity, we quantified the number of polarized mitochondria labelled with TMRM (50 nM). Representative images of the synaptosomes and their mitochondria are depicted in Figure 9A (bright field) and Figure 9B (TMRM fluorescence). As shown in Figure 9C, the number of polarized mitochondria after incubation of the synaptosomes, for 1 h, with 200 μM of 5-HT, N-Me-α-MeDA or 5-(GSH)-α-MeDA, was not different from the controls.

Discussion

Key findings of our study in synaptosomes were as follows: (i) MDMA metabolites α-MeDA, N-Me-α-MeDA and 5-(GSH)-α-MeDA, as well as 5-HT, dopamine, L-DOPA and DOPAC induced extensive H_2O_2 generation, in a concentration- and time-dependent manner; (ii) H_2O_2 production induced by 5-HT was fully dependent on MAO-A metabolism, while for dopamine, it was partly dependent on both MAO-A and MAO-B; (iii) NAC, ascorbic acid and melatonin decreased H_2O_2 levels in synaptosomes exposed to MDMA metabolites, as well as 5-HT, dopamine, L-DOPA and DOPAC; (iv) H_2O_2 production promoted by the tested compounds was independent of mitochondrial polarization status; (v) the MDMA metabolite 5-(GSH)-α-MeDA induced lipid peroxidation in a concentration- and time-dependent manner, an effect prevented by NAC; (vi) formation of protein-bound quinones (quinoproteins) induced by the studied compounds, except MDMA and 5-HT, was concentration-dependent but time-independent; (vii) MDMA metabolite 5-(GSH)-α-MeDA and DOPAC induced protein carbonylation; (viii) all studied compounds, except MDMA, altered the synaptosomal glutathione status; and (ix) MDMA metabolites presented a higher toxic potential than the parent compound MDMA, with 5-(GSH)-α-MeDA promoting higher oxidative stress.

Although MDMA is known to promote brain oxidative stress in laboratory animals (Alves *et al.*, 2007; 2009; Granado *et al.*, 2008), the underlying mechanisms remain largely unknown. MDMA metabolites can be major contributors (Capela *et al.*, 2006; 2007), and there is a role for dopamine

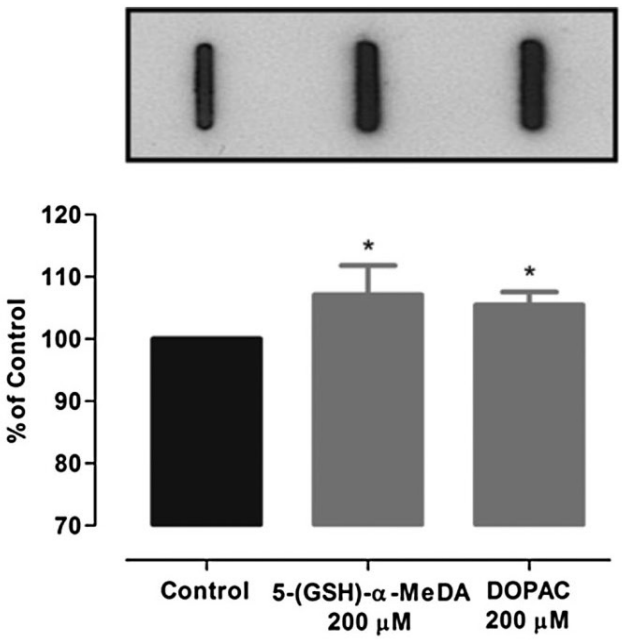


Figure 6

Protein carbonylation induced by 200 μM of the MDMA metabolite 5-(GSH)-α-MeDA and DOPAC, after exposure of synaptosomes for 2 h, evaluated by an immunoblotting method. Results are presented as mean ± SD from 4 independent experiments, expressed in percentage of control, which values were set to 100%. Statistical comparisons were made using one-way ANOVA followed by the Newman–Keuls multiple comparison *post hoc* test (*P < 0.05 compound vs. control).

and 5-HT in MDMA-induced neurotoxicity (Hrometz *et al.*, 2004). We found that the monoamine neurotransmitters 5-HT and dopamine, as well as the dopamine precursor (L-DOPA) and its metabolite (DOPAC), increased H_2O_2 production (Figure 1E–H).

After MDMA administration to experimental animals, there is an abrupt increase in the extravesicular levels of monoamine neurotransmitters inside nerve endings, which are metabolized by MAO (Alves *et al.*, 2007) and a byproduct of MAO action is H_2O_2, which subsequently may be converted into the hydroxyl radical, a highly cytotoxic ROS (Nagatsu, 2004). In mouse brain synaptosomes, H_2O_2 generation induced by dopamine and 5-HT was MAO-dependent, MAO-A being the only source of H_2O_2 for 5-HT (Figure 2). Previous studies from our group established that MAO-dependent metabolism contributed to MDMA-induced mitochondrial neurotoxicity (Alves *et al.*, 2007; 2009). Although 5-HT has been shown to be metabolized *in vitro* both by MAO-A (K_m = 178 ± 2 μM) and MAO-B (K_m = 1170 ± 432 μM), metabolism by MAO-B is minimal in the presence of MAO-A (Shih *et al.*, 1999). However, MAO-B is fully effective in the absence of MAO-A, as when metabolism occurs inside 5-hydroxytryptaminergic nerves (Alves *et al.*, 2009). Thus, our results agree with previously published studies in which 5-HT metabolism is associated with MAO-A, while dopamine metabolism is both MAO-A- and MAO-B-dependent (Nagatsu, 2004).

MAO-catalysed dopamine metabolism has DOPAC as a final product. Here, DOPAC induced extensive H_2O_2 formation that may be involved in dopamine-associated MDMA neurotoxicity. Accordingly, DOPAC and its aldehyde precursor 3,4-dihydroxyphenylacetaldehyde were described as possible neurotoxic agents in MAO-associated oxidative damage (Burke *et al.*, 2003).

5-HT is readily oxidized and, simultaneously, acts as a ROS scavenger (Uemura *et al.*, 1980). The dimer 5,5′-dihydroxy-4,4′-bitryptamine is the major product of 5-HT auto-oxidation at physiological pH and temperature, being formed in the presence of H_2O_2 and peroxidase (Wrona and Dryhurst, 1988). In the presence of MAO-A inhibitor clorgyline, we observed lower H_2O_2 levels after exposure of synaptosomes to 5-HT, relative to that of control values, which can be explained by H_2O_2 consumption during the formation of 5-HT dimers in control conditions, as previously observed in cultured rat microglia (Huether *et al.*, 1997).

As demonstrated by several studies (Gollamudi *et al.*, 1989; Bai *et al.*, 1999; Esteban *et al.*, 2001), metabolism is required for MDMA neurotoxicity. Our results showed that MDMA metabolites, in mouse brain synaptosomes, induce a significant production of H_2O_2 in a concentration- and time-dependent manner, an effect that was not observed for the parent compound MDMA (Figure 1A–D). According to these results, MDMA metabolites exhibit higher neurotoxic potential than MDMA, as previously observed in rat cortical neurons (Capela *et al.*, 2006; 2007). Also, in other cell types, like rat cardiomyocytes (Carvalho *et al.*, 2004c), rat hepatocytes (Carvalho *et al.*, 2004b) and rat and human renal proximal tubular cells (Carvalho *et al.*, 2002), MDMA metabolites presented a higher toxic potential than the parent compound MDMA. Other reports indicate that peripheral metabolism of N-Me-α-MeDA and α-MeDA is required for neurotoxic events (Miller *et al.*, 1996). In fact, the conjugate 5-(GSH)-α-MeDA, which can be transported into the brain (Miller *et al.*, 1996), was the most potent H_2O_2 generator. Thus, our findings are consistent with previous studies, in which we demonstrated that conjugated metabolites of the catechols exhibited a higher neurotoxic potential in rat cortical neurons (Capela *et al.*, 2006; 2007).

The mechanism underling the toxicity of MDMA metabolites is thought to involve the inherent reactivity of their catechol moiety (Carvalho *et al.*, 2004b). MDMA metabolites α-MeDA, N-Me-α-MeDA and 5-(GSH)-α-MeDA, as well as dopamine, L-DOPA and DOPAC are prone to the oxidation to the corresponding *o*-quinones (Spencer *et al.*, 1998; Macedo *et al.*, 2007), which may further undergo redox cycling and generate the extensive H_2O_2 production observed in our studies. Therefore, antioxidants are expected to reduce not only *o*-quinones-related injury, but also the deleterious effects mediated by ROS and RNS. Accordingly, we observed that the antioxidants NAC, ascorbic acid and melatonin partially prevented the increase of H_2O_2 levels induced by MDMA metabolites α-MeDA, N-Me-α-MeDA and 5-(GSH)-α-MeDA, as well as by 5-HT, dopamine, L-DOPA and DOPAC (Figure 3).

ROS, being normal products of mitochondrial respiration (Adam-Vizi, 2005), are assumed to play a key role in the MDMA-related neurotoxicity (Cadet *et al.*, 1995;

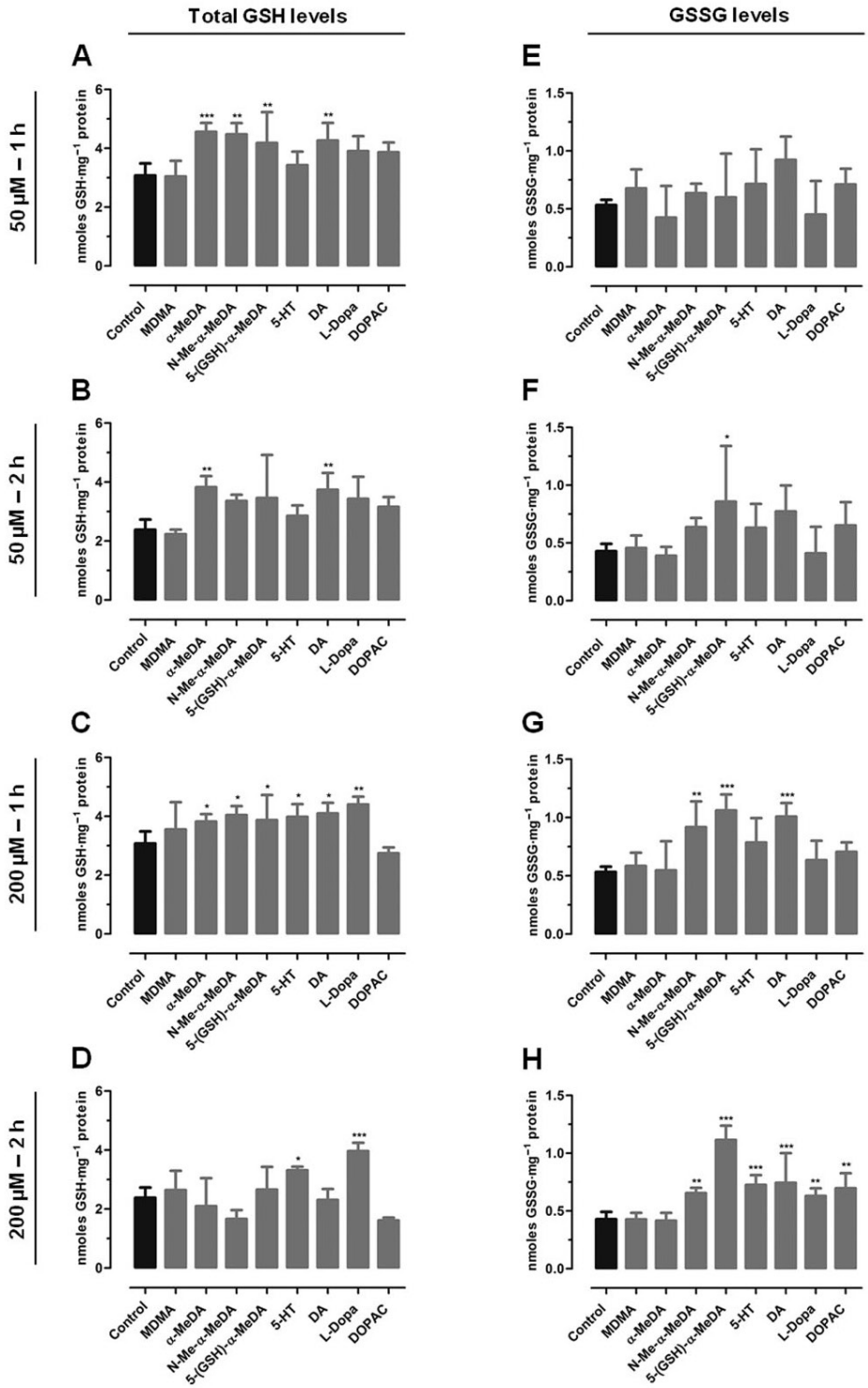


Figure 7

Effects of MDMA, its metabolites α-MeDA, N-Me-α-MeDA and 5-(GSH)-α-MeDA, as well as 5-HT, dopamine, L-DOPA and DOPAC, on total GSH and GSSG levels, in mouse brain synaptosomes, evaluated by the DTNB/GSH reductase recycling assay. Intra-synaptosomal total GSH (A, B, C and D) and GSSG levels (E, F, G and H) are presented. Synaptosomes were exposed to MDMA, its metabolites α-MeDA, N-Me-α-MeDA and 5-(GSH)-α-MeDA, as well as 5-HT, dopamine, L-DOPA and DOPAC, for 1 h (A, C, E and G) and 2 h (B, D, F and H), at the concentrations of 50 (A, B, E and F) and 200 µM (C, D, G and H). Results are presented as mean ± SD from 6 independent experiments, expressed in nmol GSH or GSSG·mg^{-1} protein. Statistical comparisons were made using one-way ANOVA followed by the Newman–Keuls multiple comparison *post hoc* test (*$P < 0.05$, **$P < 0.01$, ***$P < 0.001$ compound vs. control).

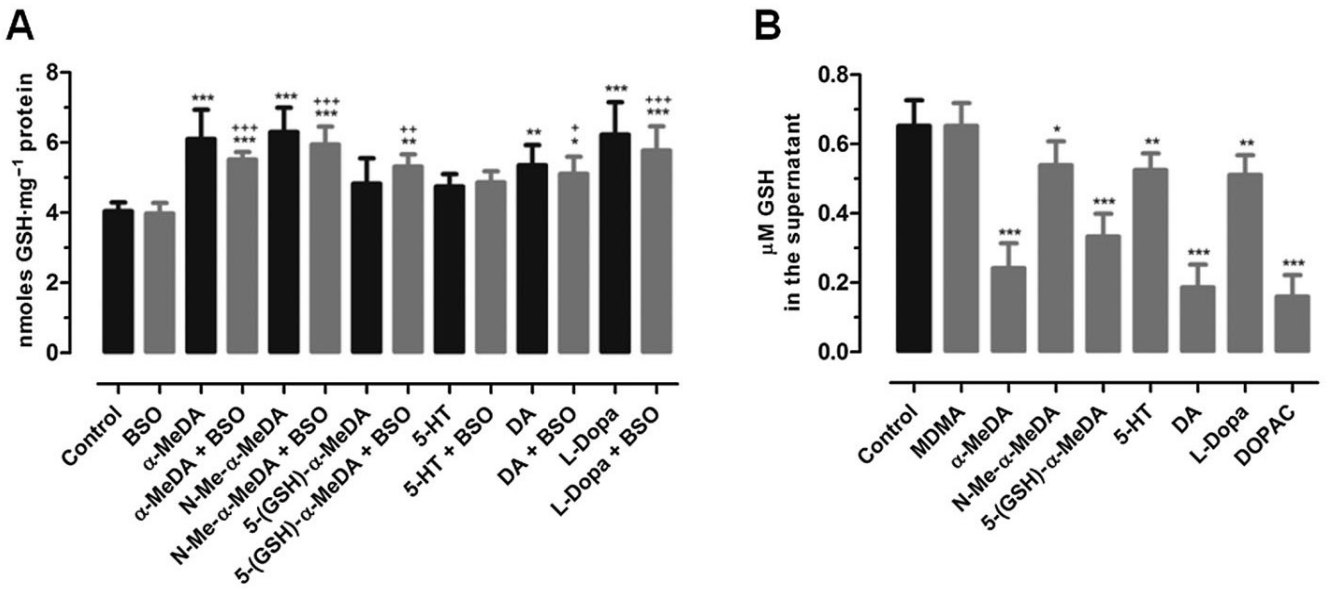


Figure 8

(A) Effect of pre-incubation with BSO (25 μM) on intra-synaptosomal total GSH levels elevation when synaptosomes were exposed to 200 μM of MDMA metabolites α-MeDA, N-Me-α-MeDA and 5-(GSH)-α-MeDA, as well as 5-HT, dopamine and L-DOPA for 1 h. (B) Total GSH levels in the supernatant after 1 h of incubation with 200 μM of MDMA, its metabolites α-MeDA, N-Me-α-MeDA and 5-(GSH)-α-MeDA, as well as 5-HT, dopamine, L-DOPA and DOPAC. Results are presented as mean ± SD from 6 independent experiments, expressed in nmol GSH·mg^{-1} protein (A) or μM GSH in the supernatant (B). Statistical comparisons were made using one-way ANOVA followed by the Newman–Keuls multiple comparison *post hoc* test (*P < 0.05, **P < 0.01, ***P < 0.001 treatment vs. control; ^{+}P < 0.05, ^{++}P < 0.01, ^{+++}P < 0.001 compound + BSO vs. BSO).

Sanchez *et al.*, 2003). Although studies on isolated mitochondria have identified complex I and complex III as possible sites of ROS generation in the respiratory chain, complex I is likely to be a physiologically more relevant site (Votyakova and Reynolds, 2001). Therefore, interference with these mitochondrial complexes may increase ROS production. In this study, mitochondrial depolarization with the protonophore FCCP did not modify H_2O_2 generation induced by any of the tested compounds (Table 1). Although a recent *in vivo* study suggests that MDMA may inhibit mitochondrial complex I (Puerta *et al.*, 2010), the absence of effects in our experimental conditions is probably due to the fact that the whole brain synaptosome model lacks *in vivo* factors, like hyperthermia, inflammation, cell signalling and excitotoxicity.

MDMA can increase lipid peroxidation in the mouse striatum (Camarero *et al.*, 2002) and mitochondria from whole rat brain (Alves *et al.*, 2007; 2009). Though MAO-B strongly contributes to this effect *in vivo* (Alves *et al.*, 2007; 2009), in the present study, only the MDMA metabolite 5-(GSH)-α-MeDA significantly increased lipid peroxidation, in a concentration- and time-dependent manner (Figure 4A). It is noteworthy that during the preparation of synaptosomes, a significant proportion of brain mitochondria are lost, which may explain the absence of lipid peroxidation for 5-HT and dopamine, since MAO enzymes are located at the outer membrane of mitochondria. Lipid peroxidation induced by 5-(GSH)-α-MeDA was completely prevented by NAC (Figure 4B). Thus, the protective effect exerted by NAC on this process and in previous studies on MDMA metabolites (Capela *et al.*, 2006; 2007) suggests that this antioxidant may be an interesting drug to prevent MDMA-induced neurotoxicity.

MDMA metabolite-related *o*-quinones may arylate macromolecules and thus lead to gross structural and functional modifications including protein fragmentation, protein carbonylation, generation of protein peroxides and enzyme inactivation (Carvalho *et al.*, 2004a; 2004b; 2004c). In accordance, we found a significant increase in protein carbonylation, not only with the MDMA metabolite 5-(GSH)-α-MeDA, but also with DOPAC. Also, an increase in quinoprotein levels was observed when synaptosomes were exposed to the MDMA metabolites α-MeDA, N-Me-α-MeDA and 5-(GSH)-α-MeDA, as previously observed in rat cortical neurons (Capela *et al.*, 2007), as well as dopamine, L-DOPA and DOPAC, in a concentration-dependent but time-independent manner (Figure 5). The presence of the catechol group in these six compounds allows them to undergo redox cycling and the corresponding formation of *o*-quinones and subsequent binding to synaptosomal proteins. Likewise, the absence of the catechol group in the MDMA and 5-HT molecules explains the absence of increased quinoprotein levels for these compounds. Of note, the lower oxidation potential of these metabolites, when compared with the parent compound, correlated with a higher toxicity of these catechols to rat cortical neurons (Macedo *et al.*, 2007). Thus, the results herein shown for the H_2O_2 production, lipid peroxidation, quinoproteins

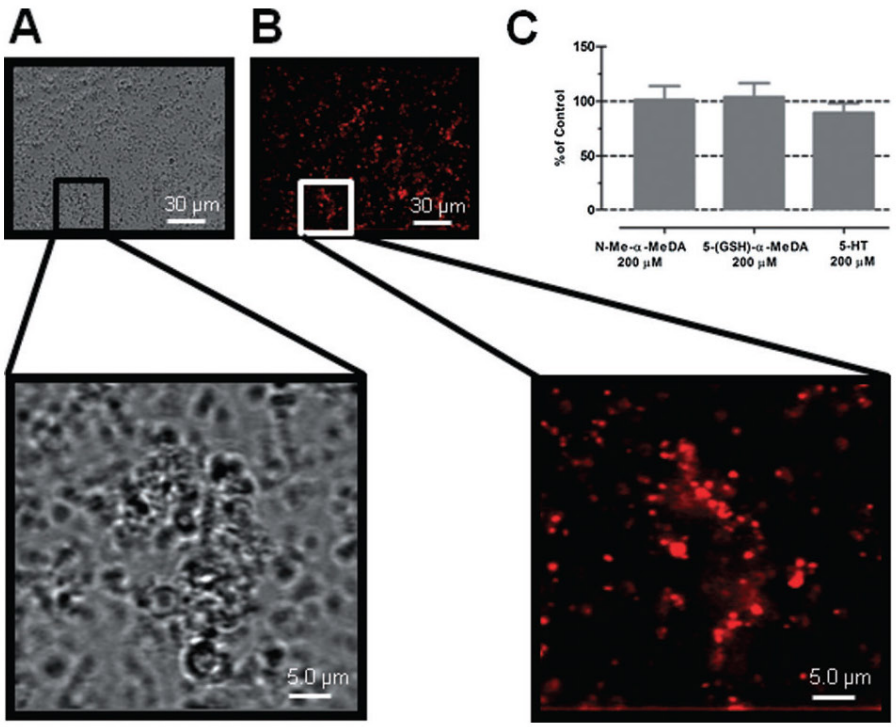


Figure 9

Microphotographs of control synaptosomes using bright field microscopy (A) and TMRM fluorescence (B) at 60× magnification. (C) Effects of MDMA metabolites N-Me-α-MeDA and 5-(GSH)-α-MeDA as well as 5-HT on the number of polarized mitochondria. Synaptosomes were exposed to 200 μM of MDMA metabolites N-Me-α-MeDA and 5-(GSH)-α-MeDA as well as 5-HT, for 1 h, then incubated with 50 nM TMRM and imaged as described under Methods during 2 h. Results are presented as mean ± SD from 6 independent experiments, expressed in percentage of control (number of polarized mitochondria per field, set to 100%). Statistical comparisons were made using one-way ANOVA followed by the Newman–Keuls multiple comparison *post hoc* test.

and protein carbonylation clearly demonstrate the high toxic potential of the MDMA metabolites, in particular 5-(GSH)-α-MeDA.

GSH, the most abundant intracellular antioxidant, plays a major role in protecting biological systems against oxidative stress. Incubation of synaptosomes with the tested compounds, except MDMA and its metabolite α-MeDA, significantly increased GSSG levels and decreased intrasynaptosomal total GSH levels from the first to the second hour of exposure, which can be a direct consequence of the pro-oxidant activity promoted by these compounds. However, as we previously reported, for the MDMA metabolites, decreased GSH levels may, as well, be due to GSH conjugation with reactive *o*-quinones and/or aminochromes produced during oxidation of these compounds (Carvalho *et al.*, 2004c; Capela *et al.*, 2007).

Administration of MDMA to rats causes oxidative stress in brain mitochondria (Alves *et al.*, 2007; 2009). With this in mind, and considering that MAO is located at the outer membrane of mitochondria, we evaluated possible consequences of 5-HT (MAO substrate) and the MDMA metabolites N-Me-α-MeDA and 5-(GSH)-α-MeDA on mitochondrial integrity. As observed, in this experimental model, the oxidative stress mediated by 5-HT, N-Me-α-MeDA and 5-(GSH)-α-MeDA did not induce detectable mitochondrial dysfunction, as monitored by the average number of polarized mitochondria.

In conclusion, our study in mouse brain synaptosomes demonstrated that there was an increase in ROS generation associated with damage to cellular macromolecules promoted by MDMA metabolites. Moreover, the increase in monoamine neurotransmitters promoted by MDMA, namely 5-HT and dopamine, or their metabolites, such as DOPAC, can equally promote oxidative stress and contribute to MDMA neurotoxicity.

Acknowledgements

This work received financial support from 'Fundação para a Ciência e a Tecnologia (FCT)', Portugal (Project PTDC/SAU-FCF/102958/2008), under the frame of 'Programa Operacional Temático Factores de Competitividade (COMPTE) do Quadro Comunitário de Apoio III' and 'Fundo Comunitário Europeu (FEDER)'.

DJB, RS and JPC acknowledge 'Fundação para a Ciência e a Tecnologia' for their PhD grants (SFRH/BD/64939/2009 and SFRH/BD/29559/2006), and Post-doc grant (SFRH/BPD/30776/2006), respectively.

Silvana Araújo MSc, Vânia Vilas Boas MSc and Vera Marisa Costa PhD are gratefully acknowledged for their help in this work.

Conflict of interest

None.

References

Adam-Vizi V (2005). Production of reactive oxygen species in brain mitochondria: contribution by electron transport chain and non-electron transport chain sources. Antioxid Redox Signal 7: 1140–1149.

Alves E, Summavielle T, Alves CJ, Gomes-da-Silva J, Barata JC, Fernandes E *et al.* (2007). Monoamine oxidase-B mediates ecstasy-induced neurotoxic effects to adolescent rat brain mitochondria. J Neurosci 27: 10203–10210.

Alves E, Summavielle T, Alves CJ, Custódio JB, Fernandes E, Lourdes Bastos M *et al.* (2009). Ecstasy-induced oxidative stress to adolescent rat brain mitochondria in vivo: influence of monoamine oxidase type A. Addict Biol 14: 185–193.

Aubin N, Barneoud P, Carter C, Caille D, Sontag N, Marc C *et al.* (2004). SL25.1131 [3(S),3a(S)-3-methoxymethyl-7-[4,4,4-trifluorobutoxy]-3,3a,4,5-tetrahydro-1,3-oxazolo[3,4-a]quinolin-1-one], a new, reversible, and mixed inhibitor of monoamine oxidase-A and monoamine oxidase-B: biochemical and behavioral profile. J Pharmacol Exp Ther 310: 1171–1182.

Bai F, Lau SS, Monks TJ (1999). Glutathione and N-acetylcysteine conjugates of α-methyldopamine produce serotonergic neurotoxicity: possible role in methylenedioxyamphetamine-mediated neurotoxicity. Chem Res Toxicol 12: 1150–1157.

Bai F, Jones DC, Lau SS, Monks TJ (2001). Serotonergic neurotoxicity of 3,4-(±)-methylenedioxyamphetamine and 3,4-(±)-methylendioxymethamphetamine (ecstasy) is potentiated by inhibition of γ-glutamyl transpeptidase. Chem Res Toxicol 14: 863–870.

Burke WJ, Li SW, Williams EA, Nonneman R, Zahm DS (2003). 3,4-Dihydroxyphenylacetaldehyde is the toxic dopamine metabolite in vivo: implications for Parkinson's disease pathogenesis. Brain Res 989: 205–213.

Cadet JL, Ladenheim B, Hirata H, Rothman RB, Ali S, Carlson E *et al.* (1995). Superoxide radicals mediate the biochemical effects of methylenedioxymethamphetamine (MDMA): evidence from using CuZn-superoxide dismutase transgenic mice. Synapse 21: 169–176.

Cadet JL, Thiriet N, Jayanthi S (2001). Involvement of free radicals in MDMA-induced neurotoxicity in mice. Ann Med Interne 152: IS57–IS59.

Camarero J, Sanchez V, O'Shea E, Green AR, Colado MI (2002). Studies, using in vivo microdialysis, on the effect of the dopamine uptake inhibitor GBR 12909 on 3,4-methylenedioxymethamphetamine ('ecstasy')-induced dopamine release and free radical formation in the mouse striatum. J Neurochem 81: 961–972.

Capela JP, Meisel A, Abreu AR, Branco PS, Ferreira LM, Lobo AM *et al.* (2006). Neurotoxicity of ecstasy metabolites in rat cortical neurons, and influence of hyperthermia. J Pharmacol Exp Ther 316: 53–61.

Capela JP, Macedo C, Branco PS, Ferreira LM, Lobo AM, Fernandes E *et al.* (2007). Neurotoxicity mechanisms of thioether ecstasy metabolites. Neuroscience 146: 1743–1757.

Capela JP, Carmo H, Remião F, Bastos ML, Meisel A, Carvalho F (2009). Molecular and cellular mechanisms of ecstasy-induced neurotoxicity: an overview. Mol Neurobiol 39: 210–271.

Carvalho M, Hawksworth G, Milhazes N, Borges F, Monks TJ, Fernandes E *et al.* (2002). Role of metabolites in MDMA (ecstasy)-induced nephrotoxicity: an in vitro study using rat and human renal proximal tubular cells. Arch Toxicol 76: 581–588.

Carvalho M, Milhazes N, Remiao F, Borges F, Fernandes E, Amado F *et al.* (2004a). Hepatotoxicity of 3,4-methylenedioxyamphetamine and alpha-methyldopamine in isolated rat hepatocytes: formation of glutathione conjugates. Arch Toxicol 78: 16–24.

Carvalho M, Remiao F, Milhazes N, Borges F, Fernandes E, Carvalho F *et al.* (2004b). The toxicity of N-methyl-alpha-methyldopamine to freshly isolated rat hepatocytes is prevented by ascorbic acid and N-acetylcysteine. Toxicology 200: 193–203.

Carvalho M, Remião F, Milhazes N, Borges F, Fernandes E, Monteiro MC *et al.* (2004c). Metabolism is required for the expression of ecstasy-induced cardiotoxicity *in vitro*. Chem Res Toxicol 17: 623–632.

Carvalho M, Pontes H, Remião F, Bastos ML, Carvalho F (2010). Mechanisms underlying the hepatotoxic effects of ecstasy. Curr Pharm Biotechnol 11: 476–495.

Chipana C, Camarasa J, Pubill D, Escubedo E (2006). Protection against MDMA-induced dopaminergic neurotoxicity in mice by methyllycaconitine: involvement of nicotinic receptors. Neuropharmacology 51: 885–895.

Erecinska M, Nelson D, Silver IA (1996). Metabolic and energetic properties of isolated nerve ending particles (synaptosomes). Biochim Biophys Acta 1277: 13–34.

Erives GV, Lau SS, Monks TJ (2008). Accumulation of neurotoxic thioether metabolites of 3,4-(±)-methylenedioxymethamphetamine in rat brain. J Pharmacol Exp Ther 324: 284–291.

Esteban B, O'Shea E, Camarero J, Sanchez V, Green AR, Colado MI (2001). 3,4-Methylenedioxymethamphetamine induces monoamine release, but not toxicity, when administered centrally at a concentration occurring following a peripherally injected neurotoxic dose. Psychopharmacology 154: 251–260.

Gollamudi R, Ali SF, Lipe G, Newport G, Webb P, Lopez M *et al.* (1989). Influence of inducers and inhibitors on the metabolism in vitro and neurochemical effects in vivo of MDMA. Neurotoxicology 10: 455–466.

Granado N, O'Shea E, Bove J, Vila M, Colado MI, Moratalla R (2008). Persistent MDMA-induced dopaminergic neurotoxicity in the striatum and substantia nigra of mice. J Neurochem 107: 1102–1112.

Hiramatsu M, Kumagai Y, Unger SE, Cho AK (1990). Metabolism of methylenedioxymethamphetamine: formation of dihydroxymethamphetamine and a quinone identified as its glutathione adduct. J Pharmacol Exp Ther 254: 521–527.

Hrometz SL, Brown AW, Nichols DE, Sprague JE (2004). 3,4-Methylenedioxymethamphetamine (MDMA, ecstasy)-mediated production of hydrogen peroxide in an in vitro model: the role of dopamine, the serotonin-reuptake transporter, and monoamine oxidase-B. Neurosci Lett 367: 56–59.

Huether G, Fettkötter I, Keilhoff G, Wolf G (1997). Serotonin acts as a radical scavenger and is oxidized to a dimer during the respiratory burst of activated microglia. J Neurochem 69: 2096–2101.

Jones DC, Duvauchelle C, Ikegami A, Olsen CM, Lau SS, de la Torre R *et al.* (2005). Serotonergic neurotoxic metabolites of ecstasy identified in rat brain. J Pharmacol Exp Ther 313: 422–431.

Kim S, Westphalen R, Callahan B, Hatzidimitriou G, Yuan J, Ricaurte GA (2000). Toward development of an in vitro model of methamphetamine-induced dopamine nerve terminal toxicity. J Pharmacol Exp Ther 293: 625–633.

Lim HK, Foltz RL (1988). In vivo and in vitro metabolism of 3,4-(methylenedioxy)methamphetamine in the rat: identification of metabolites using an ion trap detector. Chem Res Toxicol 1: 370–378.

Lowry OH, Rosebrough NJ, Farr AL, Randall RJ (1951). Protein measurement with the folin phenol reagent. J Biol Chem 193: 265–275.

Macedo C, Branco PS, Ferreira LM, Lobo AM, Capela JP, Fernandes E *et al.* (2007). Sinthesis and cyclic voltammetry studies of3,4-methylenedioxymetamphetamine (MDMA) human metabolites. J Health Sci 53: 31–42.

Magalhães J, Ferreira R, Marques F, Olivera E, Soares J, Ascensão A (2007). Indoor climbing elicits plasma oxidative stress. Med Sci Sports Exerc 39: 955–963.

Miller RT, Lau SS, Monks TJ (1996). Effects of intracerebroventricular administration of 5-(glutathion-*S*-yl)-α-methyldopamine on brain dopamine, serotonin, and norepinephrine concentrations in male Sprague-Dawley rats. Chem Res Toxicol 9: 457–465.

Miller RT, Lau SS, Monks TJ (1997). 2,5-bis-(glutathion-*S*-yl)-[alpha]-methyldopamine, a putative metabolite of (±)-3,4-methylenedioxyamphetamine, decreases brain serotonin concentrations. Eur J Pharmacol 323: 173–180.

Nagatsu T (2004). Progress in monoamine oxidase (MAO) research in relation to genetic engineering. Neurotoxicology 25: 11–20.

Nicholls DG (1993). The glutamatergic nerve terminal. Eur J Biochem 212: 613–631.

Ninković M, Selaković V, Dukić M, Milosavljević P, Vasiljević I, Jovanović M *et al.* (2008). Oxidative stress in rat kidneys due to 3,4-methylenedioxymetamphetamine (ecstasy) toxicity. Nephrology 13: 33–37.

O'Hearn E, Battaglia G, De Souza EB, Kuhar MJ, Molliver ME (1988). Methylenedioxyamphetamine (MDA) and methylenedioxymethamphetamine (MDMA) cause selective ablation of serotonergic axon terminals in forebrain: immunocytochemical evidence for neurotoxicity. J Neurosci 8: 2788–2803.

Oliveira JMA, Gonçalves J (2009). *In situ* mitochondrial Ca^{2+} buffering differences of intact neurons and astrocytes from cortex and striatum. J Biol Chem 284: 5010–5020.

Pizarro N, Farre M, Pujadas M, Peiro AM, Roset PN, Joglar J *et al.* (2004). Stereochemical analysis of 3,4-methylenedioxymethamphetamine and its main metabolites in human samples including the catechol-type metabolite (3,4-dihydroxymethamphetamine). Drug Metab Dispos 32: 1001–1007.

Pubill D, Chipana C, Camins A, Pallàs M, Camarasa J, Escubedo E (2005). Free radical production induced by methamphetamine in rat striatal synaptosomes. Toxicol Appl Pharmacol 204: 57–68.

Puerta E, Hervias I, Goñi-Allo B, Zhang SF, Jordán J, Starkov AA *et al.* (2010). Methylenedioxymethamphetamine inhibits mitochondrial complex I activity in mice: a possible mechanism underlying neurotoxicity. Br J Pharmacol 160: 233–245.

Sanchez V, Camarero J, O'Shea E, Green AR, Colado MI (2003). Differential effect of dietary selenium on the long-term neurotoxicity induced by MDMA in mice and rats. Neuropharmacology 44: 449–461.

Shenouda SK, Carvalho F, Varner KJ (2010). The cardiovascular and cardiac actions of ecstasy and its metabolites. Curr Pharm Biotechnol 11: 470–475.

Shih JC, Grimsby J, Chen K (1999). Molecular biology of monoamine oxidase A and B: their role in the degradation of serotonin. In: Baumgarten HG, Gothert M (eds). Serotoninergic Neurons and 5-HT Receptors in the SNC. Springer: Berlim, pp. 655–670.

Spencer JPE, Jenner P, Daniel SE, Lees AJ, Marsden DC, Halliwell B (1998). Conjugates of catecholamines with cysteine and GSH in Parkinson's disease: possible mechanisms of formation involving reactive oxygen species. J Neurochem 71: 2112–2122.

Stone DM, Hanson GR, Gibb JW (1987). Differences in the central serotonergic effects of methylenedioxymethamphetamine (MDMA) in mice and rats. Neuropharmacology 26: 1657–1661.

de la Torre R, Farré M (2004). Neurotoxicity of MDMA (ecstasy): the limitations of scaling from animals to humans. Trends Pharmacol Sci 25: 505–508.

Tretter L, Adam-Vizi V (2007). Uncoupling is without an effect on the production of reactive oxygen species by *in situ* synaptic mitochondria. J Neurochem 103: 1864–1871.

Tretter L, Chinopoulos C, Adam-Vizi V (1998). Plasma Membrane Depolarization and Disturbed Na+Homeostasis induced by the Protonophore Carbonyl Cyanide-p-trifluoromethoxyphenyl-hydrazon in isolated Nerve Terminals. Mol Pharmacol 53: 734–741.

Uemura T, Shimazu T, Miura R, Yamano T (1980). NADPH-dependent melanin pigment formation from 5-hydroxyindolealkylamines by hepatic and cerebral microsomes. Biochem Biophys Res Commun 93: 1074–1081.

Votyakova TV, Reynolds IJ (2001). ΔΨm-Dependent and -independent production of reactive oxygen species by rat brain mitochondria. J Neurochem 79: 266–277.

Whittaker VP (1993). Thirty years of synaptosome research. J Neurocytol 22: 735–742.

Wrona MZ, Dryhurst G (1988). Further insights into the oxidation chemistry of 5-hydroxytryptamine. J Pharm Sci 77: 911–917.

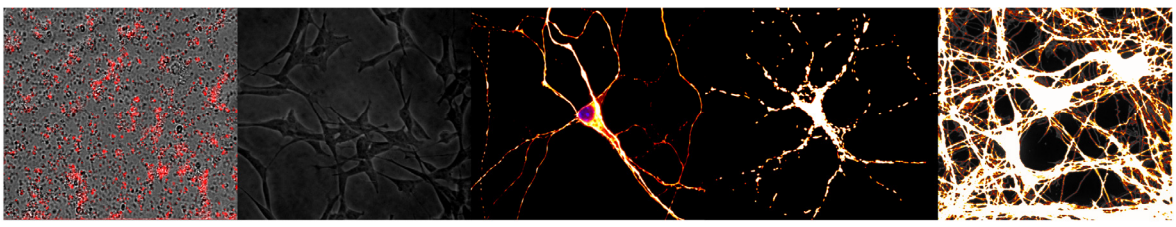
Youdim MBH, Gross A, Finberg JPM (2001). Rasagiline [N-propargyl-1R(+)-aminoindan], a selective and potent inhibitor of mitochondrial monoamine oxidase B. Br J Pharmacol 132: 500–506.

Zhou M, Diwu Z, Panchuk-Voloshina N, Haugland RP (1997). A stable nonfluorescent derivative of resorufin for the fluorometric determination of trace hydrogen peroxide: applications in detecting the activity of phagocyte NADPH oxidase and other oxidases. Anal Biochem 253: 162–168.

2.

MDMA metabolites and monoamine neurotransmitters stimulate the Na^+/K^+ ATPase activity in mouse brain synaptosomes

Manuscript under preparation



MDMA metabolites and monoamine neurotransmitters stimulate the Na^+/K^+ ATPase activity in mouse brain synaptosomes

Authors

Daniel José Barbosa[1], João Paulo Capela[1,2], Luísa Maria Ferreira[3], Paula Sério Branco[3], Eduarda Fernandes[4], Maria de Lourdes Bastos[1] and Félix Carvalho[1]

Affiliations

[1]REQUI*M*TE (Rede de Química e Tecnologia), Toxicology Laboratory, Department of Biological Sciences, Faculty of Pharmacy, University of Porto, Rua Jorge Viterbo Ferreira 228, 4050-313 Porto, Portugal.

[2]Faculty of Health Sciences, University Fernando Pessoa, Rua Carlos da Maia 296, 4200-150 Porto, Portugal.

[3]REQUI*M*TE, CQFB (Centro de Química Fina e Biotecnologia), Chemistry Department, Faculdade de Ciências e Tecnologia, Universidade Nova de Lisboa, 2829-516 Caparica, Portugal.

[4]REQUI*M*TE, Laboratory of Applied Chemistry, Department of Chemical Sciences, Faculty of Pharmacy, University of Porto, Rua Jorge Viterbo Ferreira 228, 4050-313 Porto, Portugal.

Corresponding Authors

Daniel José Barbosa

E-mail: daniel.barbosa@ff.up.pt

Phone: (+351) 220 428 500

Fax: (+351) 226 093 390

Félix Carvalho

E-mail: felixdc@ff.up.pt

Phone: (+351) 220 428 500

Fax: (+351) 226 093 390

Abbreviations

5-(GSH)-α-MeDA	5-(glutathion-*S*-yl)-α-methyldopamine
5-HT	serotonin; 5-hydroxytryptamine
ATP	adenosine 5'-triphosphate
DOPAC	3,4-dihydroxyphenylacetic acid
HEPES	4-(2-Hydroxyethyl)piperazine-1-ethanesulfonic acid
L-Dopa	3,4-dihydroxy-*L*-phenylalanine
MDMA	3,4-methylenedioxymethamphetamine; "ecstasy"
α-MeDA	α-methyldopamine
Na^+/K^+ ATPase	Na^+- and K^+-activated adenosine 5'-triphosphatase
NAC	*N*-acetylcysteine
N-Me-α-MeDA	*N*-methyl-α-methyldopamine
PMS	phenazine methosulfate

Abstract

3,4-Methylenedioximethamphetamine (MDMA; “ecstasy”) is a worldwide major drug of abuse with well documented stimulant, addictive and neurotoxic properties. Though the mechanisms involved in MDMA´s brain effects remain poor understood, hepatic formation of reactive metabolites and monoamine oxidase (MAO)-metabolism of serotonin (5-HT) and dopamine is thought to contribute for MDMA´s actions. In neuronal cells, the Na^+- and K^+-activated adenosine 5’-triphosphatase (Na^+/K^+ ATPase) plays a major role in regulating neuronal excitability. Therefore, a disruption of its activity might lead to neuronal dysfunction. However, at present, the putative effect of MDMA on the Na^+/K^+ ATPase functioning remains unclear. Here, using mouse brain synaptosomes, we studied the effect of MDMA and its metabolites α-methyldopamine (α-MeDA), *N*-methyl-α-methyldopamine (N-Me-α-MeDA) and 5-(glutathion-*S*-yl)-α-methyldopamine [5-(GSH)-α-MeDA], as well as of 5-HT, dopamine, 3,4-dihydroxy-*L*-phenylalanine (L-Dopa) and 3,4-dihydroxyphenylacetic acid (DOPAC) on synaptosomal Na^+/K^+ ATPase. MDMA metabolites, 5-HT, dopamine, L-Dopa and DOPAC significantly increased the Na^+/K^+ ATPase activity in a concentration-dependent manner. The antioxidant *N*-acetylcysteine (NAC) partially rescued the reported effect for MDMA metabolites, dopamine and L-Dopa. Additionally, increased Na^+/K^+ ATPase activity was also found in synaptosomes exposed to the chemical generator of superoxide radicals phenazine methosulfate (PMS), thus suggesting the involvement of reactive species-regulated pathways on the reported effect.

In conclusion, our study demonstrated that MDMA metabolites significantly increased the Na^+/K^+ ATPase activity. Additionally, considering the critical role of this pump in regulating neuronal function, these results suggest a new mechanism of action for MDMA metabolites into the brain, which may contribute to the stimulant and/or neurotoxic actions of MDMA.

Keywords

3,4-Methylenedioxymethamphetamine (MDMA; “ecstasy”); MDMA metabolites; Monoamine neurotransmitters; Na^+/K^+ ATPase; Synaptosomes.

Introduction

3,4-methynedioxymethamphetamine (MDMA; “ecstasy”), a worldwide major drug of abuse with stimulant and hallucinogenic properties, is known to elicit acute and long lasting effects in brain function, which result from its stimulant, addictive and toxic properties (Capela *et al.*, 2009; Robledo, 2010). In humans, MDMA induces an entactogenic state with increased self-confidence, emotional excitation and sensorimotor activation, as well as several physiological changes (Orejarena *et al.*, 2011; Ribeiro Do Couto *et al.*, 2012). Many studies have documented the potential of MDMA to induce neurotoxicity (Capela *et al.*, 2009; Roberts *et al.*, 2009; Carvalho *et al.*, 2012), though the effects at molecular and cellular level are not completely understood. MDMA’s effects into the brain appear to result from a complexity of mechanisms, in which increased extravesicular and extracellular levels of monoamine neurotransmitters serotonin (5-HT) and dopamine are involved. This effect is associated with increased formation of H_2O_2, as a result of monoamine oxidase (MAO)-mediated metabolism (Alves *et al.*, 2007; Capela *et al.*, 2009; Barbosa *et al.*, 2012). Additionally, increased evidences have attributed to MDMA metabolism a pivotal role in the context of MDMA-induced neurotoxicity (Capela *et al.*, 2007; Capela *et al.*, 2009; Barbosa *et al.*, 2012).

In specialized cells, the maintenance of Na^+ and K^+ gradients between the intracellular and extracellular compartments is a prerequisite for basic cellular homeostasis and other diverse functions (Azarias *et al.*, 2013; Doğanlı *et al.*, 2013). Na^+- and K^+-activated adenosine 5-triphosphatase (Na^+/K^+ ATPase), also termed Na^+ pump or Na^+/K^+ pump, is an ubiquitous membrane transport protein in mammalian cells essential to establish and maintain high K^+ and low Na^+ concentration in the cytoplasm (Stahl, 1986). In each transport sequence, this pump imports 2 K^+ and extrudes 3 Na^+ ions against the electrochemical gradient, being, therefore, crucial in maintaining the Na^+/K^+ equilibrium through cellular membranes. This mechanism plays a key role in controlling the normal cell cycle, cell volume, osmotic balance, as well as in the maintenance and restoration of the resting membrane potential in excitable cells. The most important and unique characteristic property of neurons is their excitable nature needed to conduct electrical signals. This excitability property of neurons, as compared to other somatic cells, is due to higher potential gradient across their membranes. An action potential is generated due to influx of Na^+ followed by efflux of K^+. In this process, there is a reversion of potential across the membrane, which is consequently restored by Na^+/K^+ ATPase (Skou, 1965). Given its important role in regulating neuronal excitability, an impairment of the Na^+/K^+ ATPase activity might lead to neuronal dysfunction (Clapcote *et al.*, 2009; Benarroch,

2011). However, to the best of our knowledge, the putative effect of MDMA on the Na^+/K^+ ATPase functioning was never studied.

Isolated nerve endings (synaptosomes), prepared from brain homogenates, are characterized to possess extremely active ion transport systems across their membranes (Nicholls, 1993; Whittaker, 1993). For that reason, this neuronal model has been used successfully to study metabolic pathways, relationships between energy production and ion movements, neurotransmitter storage and synthesis, mechanisms involved in neurotransmitters release and oxidative damage to macromolecules and neuronal mitochondria (Nicholls, 1993; Erecinska *et al.*, 1996). In addition, synaptosomes have been widely used as *in vitro* model to study the function and activity of the neuronal Na^+/K^+ ATPase under several experimental settings (Bersier *et al.*, 2011; Pendyala *et al.*, 2012; Pimentel *et al.*, 2013).

In the present study, the putative effects of MDMA and its metabolites α-methyldopamine (α-MeDA), *N*-methyl-α-methyldopamine (N-Me-α-MeDA) and 5-(glutathion-*S*-yl)-α-methyldopamine [5-(GSH)-α -MeDA], as well as of 5-HT, dopamine, 3,4-dihydroxy-*L*-phenylalanine (L-Dopa) and 3,4-dihydroxyphenylacetic acid (DOPAC), on synaptosomal Na^+/K^+ ATPase was studied, using synaptosomes as *in vitro* neuronal model.

Materials and Methods

Animals

Adult male Swiss CD-1 mice (Charles River, Barcelona, Spain) weighting 30-40 g were used in all experiments. Animals were maintained under a 12h light/dark cycle, in a temperature- and humidity-controlled room and given *ad labitum* access to food and water. Institutional guidelines concerning animal experimentation were followed. All procedures used were approved by the Portuguese Agency for Animal Welfare (general board of Veterinary Medicine in compliance with the Institutional Guidelines and the European Convention). All procedures were taken to minimize the number of animals used and their suffering.

Materials

All reagents used in this study were of analytical grade or of the highest grade available. The following reagents were obtained from Sigma-Aldrich (St. Louis, MO, USA): dopamine hydrochloride, 5-HT hydrochloride, L-Dopa, DOPAC, ouabain, adenosine 5′-triphosphate (ATP) disodium salt hydrate, ethylene glycol-bis(2-aminoethylether)-N,N,N′,N′-tetraacetic acid (EGTA), 4-(2-Hydroxyethyl)piperazine-1-ethanesulfonic acid (HEPES), *N*-acetylcysteine (NAC), phenazine methosulfate (PMS), nicotinamide adenine dinucleotide reduced (NADH) disodium salt hydrate and bovine serum albumin (BSA). Bio-Rad DC protein assay kit was purchased from Bio-Rad Laboratories (Hercules, CA, USA). MDMA (hydrochloride salt) was extracted and purified from high purity MDMA tablets kindly provided by the Portuguese Criminal Police Department. The obtained salt was pure and fully characterized by NMR and mass spectrometry methodologies. The MDMA metabolites α-MeDA, N-Me-α-MeDA and 5-(GSH)-α-MeDA were synthesized and fully characterized by NMR and mass spectrometry methodologies by REQUI*M*TE (Centro de Química Fina e Biotecnologia), Chemistry Department, Faculty of Science and Technology, University Nova de Lisboa, according previously published methods by our group (Capela *et al.*, 2006; Capela *et al.*, 2007). All other chemicals were purchased from Sigma-Aldrich.

Preparation of mouse brain synaptosomes

Mouse brain synaptosomes were obtained as described elsewhere (Barbosa *et al.*, 2012). Briefly, after anesthesia with sodium thiopental, whole brain was rapidly removed, weighed, and placed in 20 volumes of cold homogenization buffer (5 mM Tris-HCl and 320 mM sucrose, pH 7.4). The mouse brain was homogenized using a borosilicate glass

homogenizing tube fitted with a motor-driven teflon pestle (10 strokes on ice). The homogenate was centrifuged at 1,000*g*, for 10 min, at 4ºC. The supernatant was recovered, its volume was measured, and 1.6 M sucrose buffer (containing 5 mM Tris-HCl, pH 7.4) was added to a final sucrose concentration of 0.8 M. Samples were then centrifuged at 16,000*g*, for 30 min, at 4ºC, which gave a myelin-rich supernatant and a pellet (P2) consisting of mitochondria (brown-colored) covered by a layer of synaptosomes (white). The supernatant was discarded and the synaptosomal layer was separated by carefully adding 1 ml of ice-cold 320 mM sucrose buffer (pH 7.4) and gently shaking the suspension. Finally, the synaptosome fraction was diluted in HEPES-buffered salt solution with glucose (HBSS/glucose: 140 mM NaCl, 5.37 mM KCl, 1.26 mM $CaCl_2$, 0.44 mM KH_2PO_4, 0.49 mM $MgCl_2.6H_2O$, 0.41 mM $MgSO_4.7H_2O$, 4.17 mM $NaHCO_3$, 0.34 mM $Na_2HPO_4.7H_2O$, 5.5 mM glucose and 20 mM HEPES-Na, pH 7.4). Protein concentration was determined using the Bio-Rad DC protein reagent assay kit, according to the manufacturer's specifications, and using BSA as standard.

Study design

To assess the effects of MDMA and its metabolites α-MeDA and N-Me-α-MeDA, as well as of 5-HT, dopamine, L-Dopa and DOPAC on Na^+/K^+ ATPase activity, synaptosomes (0.5 mg protein/mL) were incubated with the compounds (6.25, 12.5, 25, 50, 100 and 200 μM), for 3h, in water bath at 37ºC. Particularly, the effect of MDMA metabolite 5-(GSH)-α-MeDA on Na^+/K^+ ATPase activity was studied at concentrations of 0.0625, 0.125, 0.25, 0.5, 1, 2, 6.25, 12.5, 25, 50, 100 and 200 μM. The concentrations of MDMA and its metabolites, as well as 5-HT, dopamine, L-Dopa and DOPAC used were selected according to our previously published study in mouse brain synaptosomes (Barbosa *et al.*, 2012). Preliminary experiments demonstrated a time-dependent effect of the tested compounds on the Na^+/K^+ ATPase activity (data not shown). Therefore, the 3h time-point was selected for all the subsequent studies. To assess the effect of the NADH/PMS system (chemical generator of superoxide radicals) on the Na^+/K^+ ATPase activity, synaptosomes (0.5 mg protein/mL) were incubated with 166 μM NADH in the presence of growing concentrations of PMS (0.01, 0.1, 1, 10, 50 and 250 μM). To evaluate the putative effect of NAC (1 mM) in the stimulant effect induced by MDMA metabolites, 5-HT, dopamine, L-Dopa and DOPAC, on the Na^+/K^+ ATPase activity, the 50 μM concentration was selected. Stock solution of NAC, PMS and NADH solutions were prepared in distilled water.

Na^+/K^+ ATPase activity

Na^+/K^+ ATPase activity was measured as the difference between total ATPase activity and Mg^{2+} ATPase activity (the ouabain-insensitive component). Synaptosomes (0.5 mg/mL) were incubated with different concentrations of the studied compounds and placed in a water bath at 37ºC during 3h. At this time, samples of 200 µL were removed and added to 795 µL (total ATPase activity) or 770 µL (Mg^{2+} ATPase activity) of reaction medium (128 mM NaCl, 5 mM KCl, 3 mM $MgCl_2$, 0.1 mM EGTA and 10 mM HEPES-Na, pH 7.4). To determine the Mg^{2+} ATPase activity, 25 µL of ouabain 20 mM (dissolved in reaction medium) was added. The final protein concentration was 0.1 mg/mL. ATPase activity measurements were started by the addition of 5 µL of ATP 200 mM (dissolved in reaction medium), followed by 5 min of incubation at 37°C, and subsequently stopped by addition of 250 µL trichloroacetic acid (TCA) 20 % (w/v). The reaction mixture was allowed to incubate on ice for 30 min and centrifuged at 16,000*g*, for 2 min, at 4ºC. In 96-well plates, 150 µL of sample, standard or blank were added in triplicate and mixed with 150 µL of ammonium heptamolybdate reagent [$FeSO_4$ 5% (w/v) and ammonium heptamolybdate 1% (w/v), in 0.5 M H_2SO_4]. After 15 min of reaction at room temperature, in the dark, the inorganic phosphate concentration was measured at 620 nm in a 96-well plate reader (PowerWaveX, Bio-Tek Instruments, VT, USA). KH_2PO_4 solutions (0, 10, 25, 50, 100, 200, 400 and 600 µM), prepared in reaction medium, were used as standards. The Na^+/K^+ ATPase activity was expressed as nmol of Pi released per mg protein per minute (nmol Pi/mg protein/min).

Data analysis

Values in figures and text are presented as mean ± SD of the indicated number of independent experiments, with synaptosomes derived from the same number of different animals. Normality of the data distribution was assessed by the Kolmogorov-Smirnov normality test. Statistical comparisons between groups were performed with one-way ANOVA followed by the Newman-Keuls multiple comparison *post-hoc* test. Details of the statistical analysis performed are described in each figure legend. Differences were considered to be significant at *p* values lower than 0.05. All analysis were performed using SigmaStat 3.5 (Systat Software, San Jose, CA, USA) and GraphPad Prism 6.0 for Windows (GraphPad Software, San Diego, CA, USA).

Results

MDMA metabolites, 5-HT, dopamine, L-Dopa and DOPAC significantly increased synaptosomal Na^+/K^+ ATPase activity in a concentration-dependent manner

By regulating the Na^+/K^+ equilibrium through cellular membranes, Na^+/K^+ ATPase plays a major role in the maintenance and restoration of the resting membrane potential in neurons, thus controlling a correct neuronal function (Azarias *et al.*, 2013). Therefore, disruptions on intracellular ionic balance are thought to mediate a large number of cellular events, which may lead, ultimately, to neurotoxicity and, consequently, to neuronal cell death (Xu *et al.*, 2013).

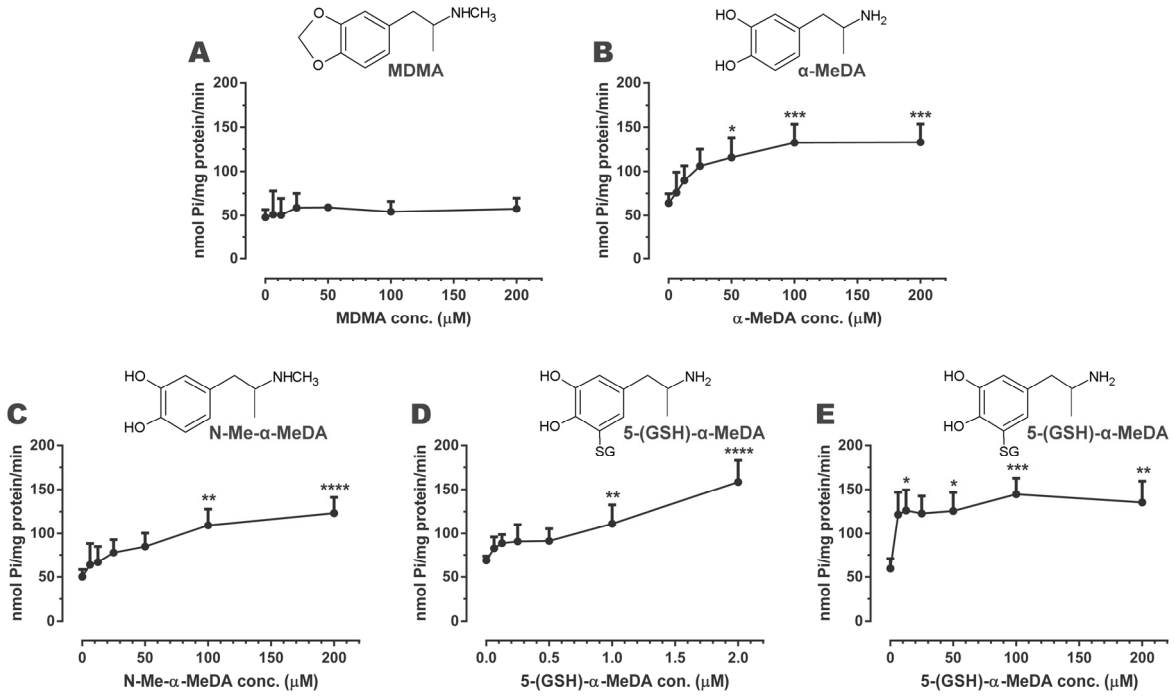


Figure 1. Effect of MDMA and its metabolites on Na^+/K^+ ATPase activity, in mouse brain synaptosomes. Synaptosomes were exposed to increasing concentrations (6.25, 12.5, 25, 50, 100 or 200 μM) of MDMA (A) or its metabolites α-MeDA (B) and N-Me-α-MeDA (C) for 3h, at 37ºC, and Na+/K+ ATPase activity was then evaluated. Particularly, MDMA metabolite 5-(GSH)-α-MeDA (D and E) was studied at concentrations ranging from 0.0625 to 200 μM. Results are present as mean ± SD, from 6 independents experiments, and expressed as nmol Pi released per mg of protein per minute (nmol Pi/mg protein/min). Statistical comparisons were performed using one-way ANOVA, followed by the Newman-Keuls multiple comparison *post-hoc* test [**p*<0.05, ***p*<0.01, ****p*<0.001, *****p*<0.0001 concentration vs. control (0 μM)].

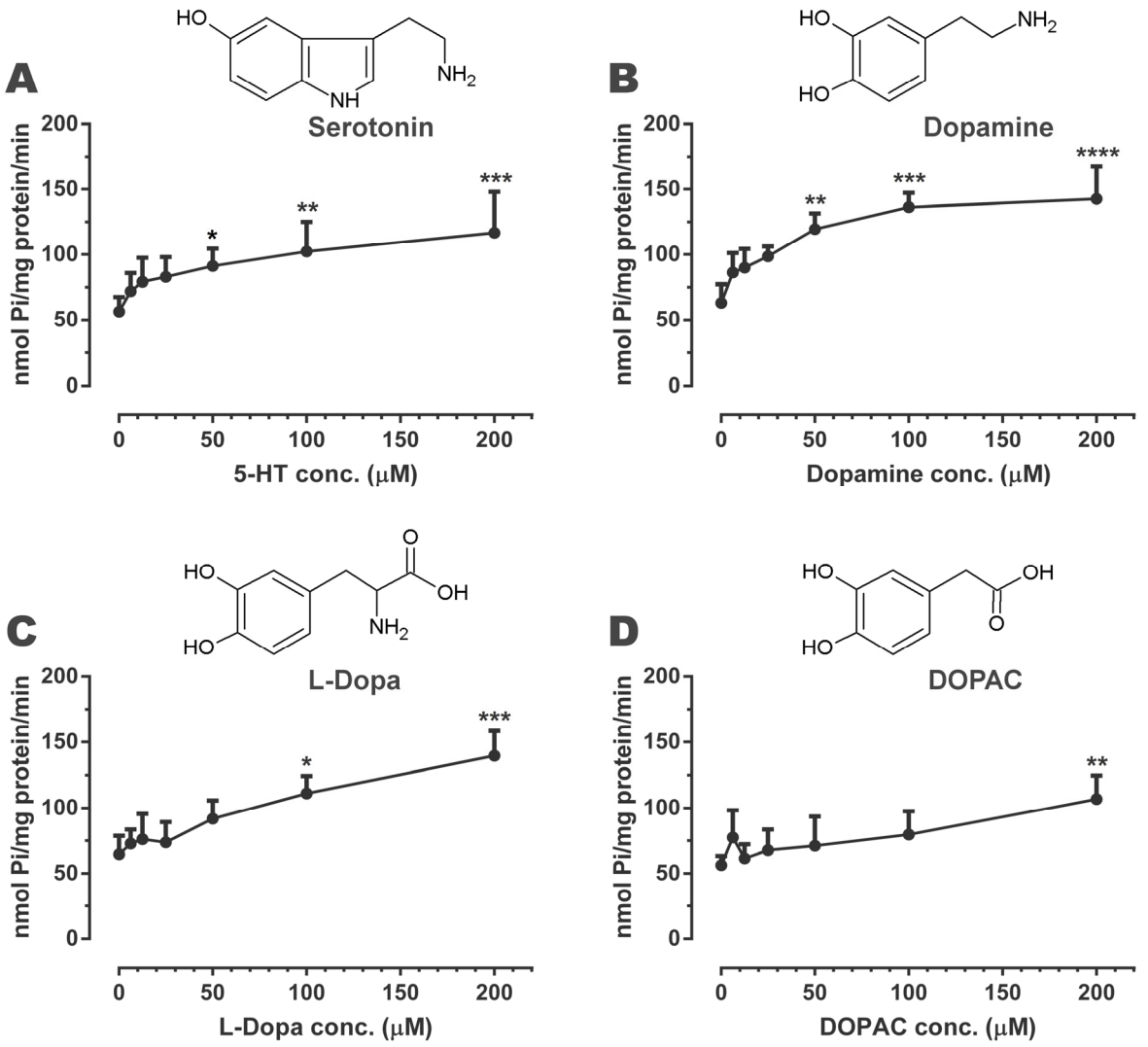


Figure 2. Effect of monoamine neurotransmitters 5-HT and dopamine, L-Dopa and DOPAC on Na^+/K^+ ATPase activity, in mouse brain synaptosomes. Synaptosomes were exposed to increasing concentrations (6.25, 12.5, 25, 50, 100 or 200 μM) of 5-HT (A), dopamine (B), L-Dopa (C) or DOPAC (D) for 3h, at 37ºC, and Na^+/K^+ ATPase activity was then evaluated. Results are present as mean ± SD, from 6 independents experiments, and expressed as nmol Pi released per mg of protein per minute (nmol Pi/mg protein/min). Statistical comparisons were performed using one-way ANOVA, followed by the Newman-Keuls multiple comparison *post-hoc* test [**p*<0.05, ***p*<0.01, ****p*<0.001, *****p*<0.0001 concentration *vs.* control (0 μM)].

Through the evaluation of the Na^+/K^+ ATPase activity, many studies have focused on synaptosome model to elucidate either mechanisms involved in regulating pump activity (Tian and Xie, 2008; Bersier *et al.*, 2011) or toxic effects mediated by stressor stimulus into the brain (Pendyala *et al.*, 2012; Pimentel *et al.*, 2013). Thus, by using synaptosomes from whole mouse brain, we studied the effects of MDMA and its metabolites, as well as of monoamine neurotransmitters 5-HT and dopamine, L-Dopa and DOPAC on the Na^+/K^+ ATPase activity. As shown in Figure 1A, MDMA did not significantly modify the Na^+/K^+ ATPase activity, at the range of concentrations studied. However in synaptosomes exposed to MDMA metabolites α-MeDA, N-Me-α-MeDA and 5-(GSH)-α-MeDA, as well as to monoamine neurotransmitters 5-HT and dopamine, L-Dopa and DOPAC, it was

observed a significant increase on the Na^+/K^+ ATPase activity, in a concentration-dependent manner (Figure 1B-E and Figure 2). Interestingly, for the MDMA metabolite 5-(GSH)-α-MeDA this effect was significant at concentrations from 1 μM (Figure 1D-E). For all the remaining compounds tested, a significant increase on the Na^+/K^+ ATPase activity was only observed at higher concentrations (50 μM or above) (Figure 1B-C and Figure 2). Therefore, in our experimental conditions, the MDMA metabolite 5-(GSH)-α-MeDA was the most potent stimulant of the Na^+/K^+ ATPase activity.

NAC partially rescued the stimulation of the Na^+/K^+ ATPase activity induced by MDMA metabolites, as well as by dopamine and L-Dopa

It has been suggested that oxidative stress can activate Na^+/K^+ ATPase signaling pathways (Liu *et al.*, 2012). In accordance, both H_2O_2 and exogenously added glucose oxidase (which generates a sustained low level of H_2O_2 by consuming glucose) were implicated in Na^+/K^+ ATPase signaling activation in cardiac myocytes (Liu *et al.*, 2006). Furthermore, it was shown that the pre-incubation with the antioxidant NAC prevented the ouabain-Na^+/K^+ ATPase signaling and its downstream effects (Liu *et al.*, 2006). Interestingly, in a previous work we showed that increased reactive oxygen species (ROS) production, namely H_2O_2, was implicated on the oxidative stress-related modifications triggered by MDMA metabolites, 5-HT, dopamine, L-Dopa and DOPAC in mouse brain synaptosomes (Barbosa *et al.*, 2012). Therefore, by using the antioxidant NAC, we next investigated the involvement of oxidative stress-related mechanisms in the increased Na^+/K^+ ATPase activity observed in synaptosomes exposed to MDMA metabolites, 5-HT, dopamine, L-Dopa and DOPAC. Pre-incubation of synaptosomes with NAC partially prevented the stimulant effects of MDMA metabolites α-MeDA, N-Me-α-MeDA and 5-(GSH)-α-MeDA, as well as of dopamine and L-Dopa on the Na^+/K^+ ATPase activity (Figure 3A-C, E-F). However, the effects of 5-HT and DOPAC on pump activity were not significantly modified by NAC (Figure 4D, G). Therefore, these results suggest that oxidative stress-related pathways may be involved, at least partially, in the stimulant effects elicited by the studied compounds on the Na^+/K^+ ATPase activity.

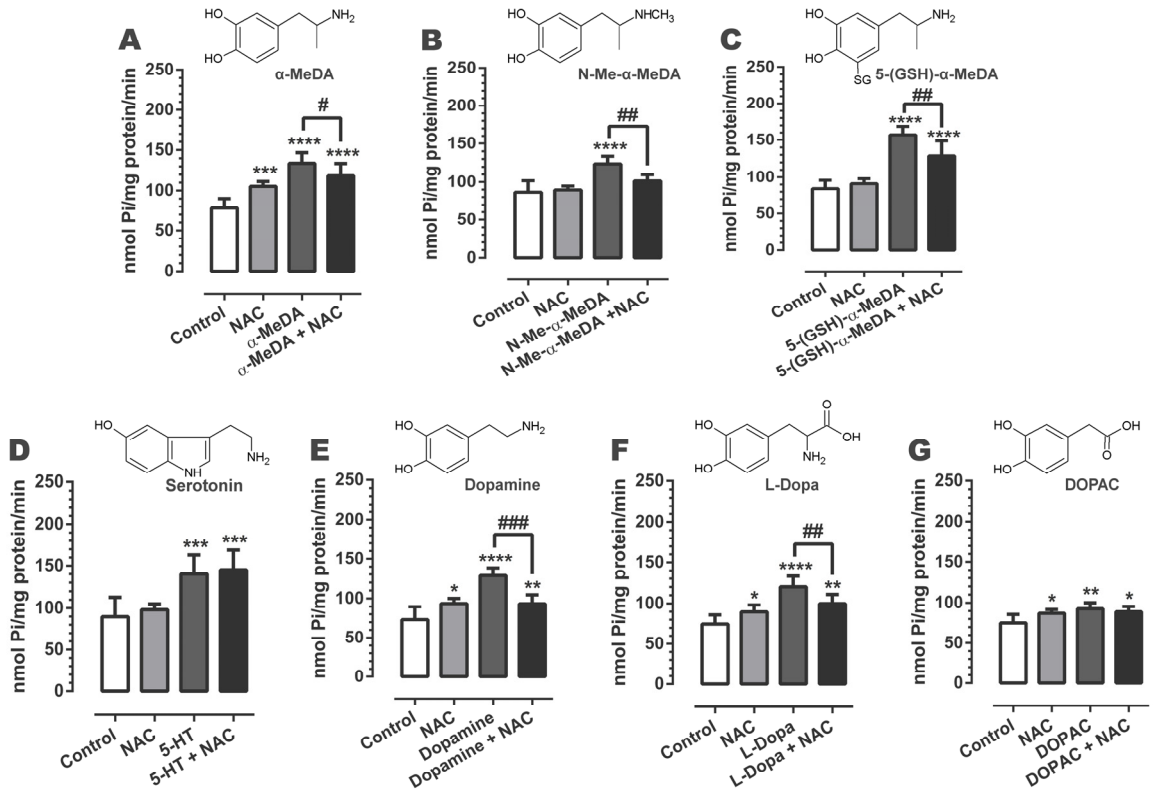


Figure 3. Effect of NAC on the stimulation of the Na^+/K^+ ATPase activity induced by MDMA metabolites, 5-HT, dopamine, L-Dopa and DOPAC, in mouse brain synaptosomes. Synaptosomes, with or without NAC (1 mM) pre-incubation, were exposed to MDMA metabolites α-MeDA (A), N-Me-α-MeDA (B) or 5-(GSH)-α-MeDA (C), as well as to 5-HT (D), dopamine (E), L-Dopa (F) or DOPAC (G), at the concentration of 50 μM, for 3h, at 37ºC, and Na^+/K^+ ATPase activity was then evaluated. Results are present as mean ± SD, from 6 independents experiments, and expressed as nmol Pi released per mg of protein per minute (nmol Pi/mg protein/min). Statistical comparisons were performed using one-way ANOVA, followed by the Newman-Keuls multiple comparison *post-hoc* test [$^*p$<0.05, $^{**}p$<0.01, $^{***}p$<0.001, $^{****}p$<0.0001 condition *vs.* control; $^{\#}p$<0.05, $^{\#\#}p$<0.01, $^{\#\#\#}p$<0.001 compound plus NAC *vs.* compound].

PMS, a chemical generator of superoxide radicals, significantly increased the Na^+/K^+ ATPase activity

Following the previous results observed in the presence of NAC, we next used a chemical generator of superoxide radicals to confirm the involvement of reactive species-related pathways on the reported effects under the Na^+/K^+ ATPase activity. As shown in Figure 4, PMS, at the concentrations of 1, 10 and 50 μM, induced a significant increase on the Na^+/K^+ ATPase activity. However, for the higher concentration tested, 250 μM, the stimulant effect of PMS on the Na^+/K^+ ATPase activity was lost. This effect may result from an oxidative modification of the pump, as a consequence of the high levels of ROS that are expected to be generated by PMS at this concentration. Therefore, PMS mimetized the stimulant effects induced by MDMA metabolites and monoamine neurotransmitters on the Na^+/K^+ ATPase activity.

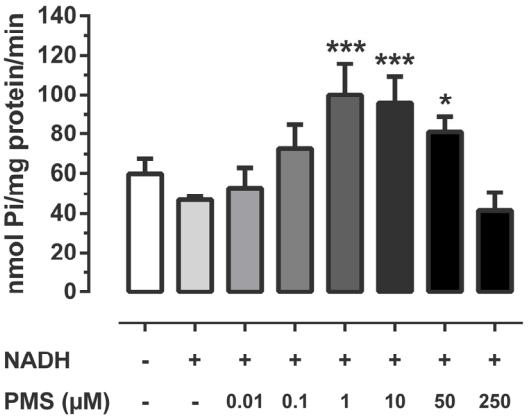


Figure 4. Effect of the chemical generator of superoxide radicals PMS on Na^+/K^+ ATPase activity, in mouse brain synaptosomes. Synaptosomes were exposed to increasing concentrations (0.01, 0.1, 1, 10, 50 and 250 µM) of PMS (combined with 166 µM NADH) for 3h, at 37ºC, and the Na^+/K^+ ATPase activity was then evaluated. Results are present as mean ± SD, from 4 independents experiments, and expressed as nmol Pi released per mg of protein per minute (nmol Pi/mg protein/min). Statistical comparisons were performed using one-way ANOVA, followed by the Newman-Keuls multiple comparison *post-hoc* test [**p*<0.05, ****p*<0.001 concentration *vs.* control (0 µM)].

Discussion

Previous studies have suggested that changes in Na^+/K^+ ATPase activity play a role in drug-evoked deregulation of brain function (Pendyala *et al.*, 2012; Rambo *et al.*, 2012), which, ultimately, may lead to neurotoxicity. Though the neurotoxic potential of MDMA is well established, the mechanisms underlying its toxicity remain largely unknown. Therefore, it was our propose to evaluate whether MDMA may interfere with the Na^+/K^+ ATPase activity. We found that MDMA metabolites, as well as 5-HT, dopamine, L-Dopa and DOPAC significantly increased the activity of the Na^+/K^+ ATPase. Furthermore, the antioxidant NAC partially rescued the reported effect for MDMA metabolites, as well as for dopamine and L-Dopa. Additionally, by using a chemical generator of superoxide radicals, PMS, a significant increase on the Na^+/K^+ ATPase activity was also revealed, thus suggesting that reactive species-mediated pathways may be key players on the effects triggered by MDMA metabolites and monoamine neurotransmitters on the Na^+/K^+ ATPase activity.

Neurons are highly specialized and polarized cells with large energy dependence. Importantly, neuronal transmission is tightly regulated by Na^+/K^+ ATPase activity, whose function is critical in maintaining intracellular homeostasis (Azarias *et al.*, 2013; Doğanlı *et al.*, 2013). Though MDMA is known to elicit acute and long lasting effects in brain function, which appear to result from its toxic and stimulant properties (Capela *et al.*, 2009; Robledo, 2010), the involvement of an abnormal Na^+/K^+ ATPase functioning on these effects was never studied and, therefore, is hitherto completely unknown. Here, we showed that MDMA metabolites, unlike the parent compound MDMA, significantly increased the synaptosomal Na^+/K^+ ATPase activity, in a concentration dependent-manner. In line with these results, several studies have demonstrated that metabolism appears to be required for MDMA-induced neurotoxic actions *in vivo* (Gollamudi *et al.*, 1989; Bai *et al.*, 1999; Esteban *et al.*, 2001). Additionally, *in vitro* studies have also established that MDMA metabolites presented higher neurotoxic potential than their parent compound MDMA (Capela *et al.*, 2006; Capela *et al.*, 2007; Barbosa *et al.*, 2012; Ferreira *et al.*, 2013). Therefore, our results suggest that a mechanism involving the modulation of the Na^+/K^+ ATPase function may contribute to the MDMA's effects into the brain.

Apart from MDMA metabolism, other studies have suggested that 5-HT and dopamine may also play an important role in MDMA-induced changes in brain function and neurotoxicity (Hrometz *et al.*, 2004; Alves *et al.*, 2007; Alves *et al.*, 2009b; Barbosa *et al.*, 2012). Indeed, it is well known that MDMA abuse is associated with behavioral excitation. In rodents, this effect persists for many months after the last administration, thus

mimicking the long lasting sensitivity observed in human MDMA's addicts (Ciudad-Roberts *et al.*, 2013). Additionally, studies in laboratory animals have also linked the MDMA's locomotor stimulant effects to the activation of both dopaminergic and serotonergic systems (Scearce-Levie *et al.*, 1999). Here, we found that, in addition to MDMA metabolites, also the monoamine neurotransmitters 5-HT and dopamine, as well as dopamine precursor L-Dopa and dopamine metabolite DOPAC, significantly increased the activity of the Na^+/K^+ ATPase. Of note, it was previously postulated that decreased dopamine levels in the brain may be, at least in part, responsible for the decreased Na^+/K^+ ATPase activity in the striatum of newborn piglets during a post-hypoxic reoxygenation insult (Zaitseva *et al.*, 2002). Furthermore, increased activity of the serotonergic system was previously associated with increased Na^+/K^+ ATPase activity (Hernández-Rodríguez and Chagoya, 1986). Additionally, a concentration-dependent increase in Na^+/K^+ ATPase activity in rat brain homogenate was found following incubation with varying concentrations of 5-HT, with cerebral cortex and cerebellum showing the largest response (Hernández, 1987). Therefore, as the psychomotor stimulant and neurotoxic effects of MDMA are considered to be a consequence of the extravesicular and extracellular increase in monoamine neurotransmitter levels (Bankson and Cunningham, 2001; Alves *et al.*, 2007; Alves *et al.*, 2009a; Alves *et al.*, 2009b; Barbosa *et al.*, 2012), our results suggest that 5-HT and dopamine may also contribute to the stimulant and neurotoxic effects of MDMA, through the regulation of the Na^+/K^+ ATPase activity.

Oxidative stress has been described as a key regulator of the Na^+/K^+ ATPase functioning (Liu *et al.*, 2012). Accumulating evidences also suggest that ROS, which may be generated as byproducts of some metabolic pathways, are essential players in regulating cell function and survival. In fact, in the last years, ROS have emerged as important components of membrane receptor signaling (Forman and Torres, 2002; Yin *et al.*, 2008). Notably, in a previous work published by our group, it was demonstrated that the oxidative injury elicited by MDMA metabolites, as well as by 5-HT, dopamine, L-Dopa and DOPAC, in mouse brain synaptosomes, involved increased H_2O_2 production, which was partially attenuated by the antioxidant NAC (Barbosa *et al.*, 2012). Here, we found that the co-incubation of synaptosomes with NAC partially prevented the stimulant effect of MDMA metabolites, as well as dopamine and L-Dopa, on the Na^+/K^+ ATPase activity. Looking for reports in the literature studying the same ROS paradigm, we verified that it was previously demonstrated, in MDCK cells, that the suppression of ROS activity by NAC blocked low K^+-induced increased activity, protein abundance and cell surface localization of the Na^+/K^+ ATPase (Zhou *et al.*, 2003). Furthermore, recently, a prominent role for H_2O_2 was described in CD95-induced internalization of the Na^+/K^+ ATPase in human T cells. (Yin *et al.*, 2007). Additionally, another specific regulatory function of H_2O_2,

namely the stimulation of the *de novo* synthesis of Na^+/K^+-ATPase, was also reported (Yin *et al.*, 2007). In accordance, here, a significant increase on the Na^+/K^+ ATPase activity was also observed for the chemical generator of superoxide radicals PMS, thus supporting a role for reactive species-regulated pathways on the reported effects. Since the Na^+/K^+ ATPase plays a remarkable role in regulating the neuronal Na^+/K^+ equilibrium, an increase in its activity, by allowing a more rapid restoration of the membrane potential, may render neurons more prone to excitability, a critical event contributing to neuronal dysfunction and death (Szydlowska and Tymianski, 2010).

Despite these emerging data, the exact role of ROS in regulating the Na^+/K^+ ATPase function remains unknown. In a previous study published by our group, using the same compounds that were evaluated in the present study, it was found that the MDMA metabolite 5-(GSH)-α-MeDA was the most potent generator of H_2O_2 (Barbosa *et al.*, 2012). Here, we found that the same MDMA metabolite was the most potent stimulant of the Na^+/K^+ ATPase activity (significant effect at concentrations form 1 μM). Therefore, our postulated mechanism is that the ROS generated by MDMA metabolites. 5-HT, dopamine, L-Dopa and DOPAC may damage synaptosomal membranes. Consequently, the electrochemical gradient of Na^+ and K^+ across the synaptosomal membranes is lost, thus leading to a Na^+/K^+ ATPase functioning in its maximal activity. However, more studies are needed to address the real mechanisms involved in the effects.

In conclusion, our study demonstrated, for the first time, that MDMA metabolites and monoamine neurotransmitters stimulated the synaptosomal Na^+/K^+ ATPase activity, which seemed to involve reactive species-regulated pathways. Considering the critical role of the Na^+/K^+ ATPase in regulating neuronal function, our study suggests a new mechanism of action for MDMA metabolites into the brain, which may contribute to the stimulant and/or neurotoxic effects of MDMA.

Acknowledgements

This work was supported by “Fundação para a Ciência e a Tecnologia” (FCT), Portugal (Project PTDC/SAU-FCF/102958/2008), under the framework of the “Programa Operacional Temático Factores de Competitividade (COMPTE) do Quadro Comunitário de Apoio III” and “Fundo Comunitário Europeu (FEDER)” (FCOMP-01-0124-FEDER-011079). The NMR spectrometers are part of “The National NMR Facility”, supported by FCT (RECI/BBB-BQB/0230/2012). DJB was supported by a fellowship (SFRH/BD/64939/2009) from FCT, Portugal.

References

Alves E, Binienda Z, Carvalho F, Alves CJ, Fernandes E, de Lourdes Bastos M, et al. (2009a). Acetyl-l-carnitine provides effective *in vivo* neuroprotection over 3,4-methylenedioximethamphetamine-induced mitochondrial neurotoxicity in the adolescent rat brain. Neuroscience 158:514-523.

Alves E, Summavielle T, Alves CJ, Custódio JB, Fernandes E, Lourdes Bastos M, et al. (2009b). Ecstasy-induced oxidative stress to adolescent rat brain mitochondria *in vivo*: influence of monoamine oxidase type A. Addict Biol 14:185-193.

Alves E, Summavielle T, Alves CJ, Gomes-da-Silva J, Barata JC, Fernandes E, et al. (2007). Monoamine oxidase-B mediates ecstasy-induced neurotoxic effects to adolescent rat brain mitochondria. J Neurosci 27:10203-10210.

Azarias G, Kruusmägi M, Connor S, Akkuratov EE, Liu X, Lyons D, et al. (2013). A specific and essential role for Na,K-ATPase α3 in neurons co-expressing α1 and α3. J Biol Chem 288:2734-2743.

Bai F, Lau SS, Monks TJ (1999). Glutathione and N-acetylcysteine conjugates of α-methyldopamine produce serotonergic neurotoxicity: possible role in methylenedioxyamphetamine-mediated neurotoxicity. Chem Res Toxicol 12:1150-1157.

Bankson MG, Cunningham KA (2001). 3,4-Methylenedioxymethamphetamine (MDMA) as a unique model of serotonin receptor function and serotonin-dopamine interactions. J Pharmacol Exp Ther 297:846-852.

Barbosa DJ, Capela JP, Oliveira JMA, Silva R, Ferreira LM, Siopa F, et al. (2012). Pro-oxidant effects of Ecstasy and its metabolites in mouse brain synaptosomes. Br J Pharmacol 165:1017-1033.

Benarroch EE (2011). Na^+, K^+-ATPase: functions in the nervous system and involvement in neurologic disease. Neurology 76:287-289.

Bersier MG, Peña C, Rodríguez de Lores Arnaiz G (2011). Changes in Na^+, K^+-ATPase activity and alpha 3 subunit expression in CNS after administration of Na^+, K^+-ATPase inhibitors. Neurochem Res 36:297-303.

Capela JP, Carmo H, Remião F, Bastos ML, Meisel A, Carvalho F (2009). Molecular and cellular mechanisms of ecstasy-induced neurotoxicity: an overview. Mol Neurobiol 39:210-271.

Capela JP, Macedo C, Branco PS, Ferreira LM, Lobo AM, Fernandes E, et al. (2007). Neurotoxicity mechanisms of thioether ecstasy metabolites. Neuroscience 146:1743-1757.

Capela JP, Meisel A, Abreu AR, Branco PS, Ferreira LM, Lobo AM, et al. (2006). Neurotoxicity of ecstasy metabolites in rat cortical neurons, and influence of hyperthermia. J Pharmacol Exp Ther 316:53-61.

Carvalho M, Carmo H, Costa VM, Capela JP, Pontes H, Remião F, et al. (2012). Toxicity of amphetamines: an update. Arch Toxicol 86:1167-1231.

Ciudad-Roberts A, Camarasa J, Pubill D, Escubedo E (2013). Heteromeric nicotinic receptors are involved in the sensitization and addictive properties of MDMA in mice. Prog Neuropsychopharmacol Biol Psychiatry 44:201-209.

Clapcote SJ, Duffy S, Xie G, Kirshenbaum G, Bechard AR, Schack VR, et al. (2009). Mutation I810N in the α3 isoform of Na^+,K^+-ATPase causes impairments in the sodium pump and hyperexcitability in the CNS. Proc Natl Acad Sci U S A 106:14085-14090.

Doğanlı C, Beck HC, Ribera AB, Oxvig C, Lykke-Hartmann K (2013). α3Na^+/K^+-ATPase deficiency causes brain ventricle dilation and abrupt embryonic motility in zebrafish. J Biol Chem 288:8862-8874.

Erecinska M, Nelson D, Silver IA (1996). Metabolic and energetic properties of isolated nerve ending particles (synaptosomes). Biochim Biophys Acta 1277:13-34.

Esteban B, O'Shea E, Camarero J, Sanchez V, Green AR, Colado MI (2001). 3,4-Methylenedioxymethamphetamine induces monoamine release, but not toxicity, when administered centrally at a concentration occurring following a peripherally injected neurotoxic dose. Psychopharmacology 154:251-260.

Ferreira PS, Nogueira TB, Costa VM, Branco PS, Ferreira LM, Fernandes E, et al. (2013). Neurotoxicity of “ecstasy” and its metabolites in human dopaminergic differentiated SH-SY5Y cells. Toxicol Lett 216:159-170.

Forman HJ, Torres M (2002). Reactive oxygen species and cell signaling. Am J Respir Crit Care Med 166:4-8.

Gollamudi R, Ali SF, Lipe G, Newport G, Webb P, Lopez M, et al. (1989). Influence of inducers and inhibitors on the metabolism *in vitro* and neurochemical effects *in vivo* of MDMA. Neurotoxicology 10:455-466.

Hernández-Rodríguez J, Chagoya G (1986). Brain serotonin synthesis and Na^+,K^+-ATPase activity are increased postnatally after prenatal administration of L-tryptophan. Brain Res 390:221-226.

Hernández J (1987). Brain Na^+,K^+-ATPase activity possibly regulated by a specific serotonin receptor. Brain Res 408:399-402.

Hrometz SL, Brown AW, Nichols DE, Sprague JE (2004). 3,4-Methylenedioxymethamphetamine (MDMA, ecstasy)-mediated production of hydrogen peroxide in an *in vitro* model: the role of dopamine, the serotonin-reuptake transporter, and monoamine oxidase-B. Neurosci Lett 367:56-59.

Liu J, Kennedy DJ, Yan Y, Shapiro JI (2012). Reactive oxygen species modulation of Na/K-ATPase regulates fibrosis and renal proximal tubular sodium handling. Int J Nephrol 381320.

Liu L, Li J, Liu J, Yuan Z, Pierre SV, Qu W, et al. (2006). Involvement of Na^+/K^+-ATPase in hydrogen peroxide-induced hypertrophy in cardiac myocytes. Free Radic Biol Med 41:1548-1556.

Nicholls DG (1993). The glutamatergic nerve terminal. Eur J Biochem 212:613-631.

Orejarena MJ, Lanfumey L, Maldonado R, Robledo P (2011). Involvement of 5-HT2A receptors in MDMA reinforcement and cue-induced reinstatement of MDMA-seeking behaviour. Int J Neuropsychopharmacol 14:927-940.

Pendyala G, Buescher JL, Fox HS (2012). Methamphetamine and inflammatory cytokines increase neuronal Na^+/K^+-ATPase Isoform 3: relevance for HIV associated neurocognitive disorders. PLoS ONE 7:e37604.

Pimentel VC, Zanini D, Cardoso AM, Schmatz R, Bagatini MD, Gutierres JM, et al. (2013). Hypoxia–ischemia alters nucleotide and nucleoside catabolism and Na^+,K^+-ATPase activity in the cerebral cortex of newborn rats. Neurochem Res 38:886-894.

Rambo LM, Ribeiro LR, Schramm VG, Berch AM, Stamm DN, Della-Pace ID, et al. (2012). Creatine increases hippocampal Na^+,K^+-ATPase activity via NMDA–calcineurin pathway. Brain Res Bull 88:553-559.

Ribeiro Do Couto B, Daza-Losada M, Rodríguez-Arias M, Nadal R, Guerri C, Summavielle T, et al. (2012). Adolescent pre-exposure to ethanol and 3,4-methylenedioxymethylamphetamine (MDMA) increases conditioned rewarding effects of MDMA and drug-induced reinstatement. Addict Biol 17:588-600.

Roberts GMP, Nestor L, Garavan H (2009). Learning and memory deficits in ecstasy users and their neural correlates during a face-learning task. Brain Res 1292:71-81.

Robledo P (2010). Cannabinoids, opioids and MDMA: neuropsychological interactions related to addiction. Curr Drug Targets 11:429-439.

Scearce-Levie K, Viswanathan SS, Hen R (1999). Locomotor response to MDMA is attenuated in knockout mice lacking the 5-HT1B receptor. Psychopharmacology 141:154-161.

Skou JC (1965). Enzymatic basis for active transport of Na^+ and K^+ across cell membrane. Physiol Rev 45:596-617.

Stahl WL (1986). The Na,K-ATPase of nervous tissue. Neurochem Int 8:449-476.

Szydlowska K, Tymianski M (2010). Calcium, ischemia and excitotoxicity. Cell Calcium 47:122-129.

Tian J, Xie Z (2008). The Na-K-ATPase and calcium-signaling microdomains. Physiology 23:205-211.

Whittaker VP (1993). Thirty years of synaptosome research. J Neurocytol 22:735-742.

Xu B, Xu Z, Deng Y, Liu W, Yang H, Wei Y (2013). MK-801 protects against intracellular Ca^{2+} overloading and improves N-methyl-D-aspartate receptor expression in cerebral cortex of methylmercury-poisoned rats. J Mol Neurosci 49:162-171.

Yin W, Cheng W, Shen W, Shu L, Zhao J, Zhang J, et al. (2007). Impairment of Na^+,K^+-ATPase in CD95(APO-1)-induced human T-cell leukemia cell apoptosis mediated by glutathione depletion and generation of hydrogen peroxide. Leukemia 21:1669-1678.

Yin W, Yin F, Shen W, Cai B, Hua Z (2008). Requirement of hydrogen peroxide and Sp1 in the stimulation of Na,K-ATPase by low potassium in MDCK epithelial cells. Int J Biochem Cell Biol 40:942-953.

Zaitseva T, Shen J, Schears G, Creed J, Wilson DF, Pastuszko A (2002). Effect of catecholamines on activity of Na^+, K^+-ATPase in neonatal piglet brain during posthypoxic reoxygenation. Comp Biochem Physiol A Mol Integr Physiol 132:139-145.

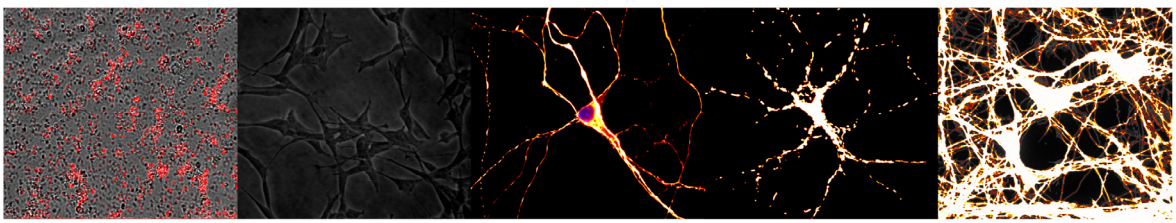
Zhou X, Yin W, Doi SQ, Robinson SW, Takeyasu K, Fan X (2003). Stimulation of Na,K-ATPase by low potassium requires reactive oxygen species. Am J Physiol Cell Physiol 285:319-326.

3.

"Ecstasy"-induced toxicity in SH-SY5Y differentiated cells: role of hyperthermia and metabolites

Accepted manuscript

Archives of Toxicology, DOI 10.1007/s00204-013-1147-9



"Ecstasy"-induced toxicity in SH-SY5Y differentiated cells: role of hyperthermia and metabolites

Authors

Daniel José Barbosa[1], João Paulo Capela[1,2], Renata Silva[1], Luísa Ferreira[3], Paula Sério Branco[3], Eduarda Fernandes[4], Maria Lourdes Bastos[1] and Félix Carvalho[1]

Affiliations

[1]REQUI*M*TE (Rede de Química e Tecnologia), Toxicology Laboratory, Department of Biological Sciences, Faculty of Pharmacy, University of Porto, Rua Jorge Viterbo Ferreira 228, 4050-313 Porto, Portugal.

[2]Faculty of Health Sciences, University Fernando Pessoa, Rua Carlos da Maia 296, 4200-150 Porto, Portugal.

[3]REQUI*M*TE/CQFB (Centro de Química Fina e Biotecnologia), Department of Chemistry, Faculty of Science and Technology, University Nova de Lisboa, 2829-516 Caparica, Portugal.

[4]REQUI*M*TE, Laboratory of Applied Chemistry, Department of Chemical Sciences, Faculty of Pharmacy, University of Porto, Rua Jorge Viterbo Ferreira 228, 4050-313 Porto, Portugal.

Corresponding Authors

Daniel José Barbosa

E-mail: daniel.barbosa@ff.up.pt)

Phone: (+351) 220 428 500

Fax: (+351) 226 093 390

Félix Carvalho

E-mail: felixdc@ff.up.pt

Phone: (+351) 220 428 500

Fax: (+351) 226 093 390

Abstract

3,4-Methylenedioxymethamphetamine (MDMA; “ecstasy”) is a recreational hallucinogenic drug of abuse known to elicit neurotoxic properties. Hepatic formation of neurotoxic metabolites is thought to plays a major role in MDMA-related neurotoxicity, though the mechanisms involved are still unclear. Here, we studied the neurotoxicity mechanisms and stability of MDMA and 6 of its major human metabolites, namely α-methyldopamine (α-MeDA) and *N*-methyl-α-methyldopamine (N-Me-α-MeDA) and their corresponding glutathione (GSH) and *N*-acetylcysteine (NAC) conjugates, under normothermic (37ºC) or hyperthermic conditions (40ºC), using cultured SH-SY5Y differentiated cells. We showed that MDMA metabolites exhibited toxicity to SH-SY5Y differentiated cells, being the GSH and NAC conjugates more toxic than their catechol precursors and MDMA. Furthermore, whereas the toxicity of the catechol metabolites was potentiated by hyperthermia, NAC-conjugated metabolites revealed higher toxicity under normothermia and GSH-conjugated metabolites-induced toxicity was temperature-independent. Moreover, a time-dependent decrease in extracellular concentration of MDMA metabolites was observed, which was potentiated by hyperthermia. The antioxidant NAC significantly protected against the neurotoxic effects of MDMA metabolites. MDMA metabolites increased intracellular glutathione levels, though depletion in thiol content was observed in MDMA-exposed cells. Finally, the neurotoxic effects induced by MDMA metabolite N-Me-α-MeDA involved caspase 3 activation.

In conclusion, this study evaluated the stability of MDMA metabolites *in vitro*, and demonstrated that the catechol MDMA metabolites and their GSH and NAC conjugates, rather than MDMA itself, exhibited neurotoxic actions in SH-SY5Y differentiated cells, which were differently affected by hyperthermia, thus highlighting a major role for the metabolism and hyperthermia on MDMA´s neurotoxicity.

Keywords

3,4-Methylenedioxymethamphetamine (MDMA; “ecstasy”); MDMA metabolites; Hyperthermia; SH-SY5Y differentiated cells; Neurotoxicity.

Introduction

3,4-Methylenedioxymethamphetamine (MDMA; ”ecstasy”) is a worldwide major drug of abuse known to elicit neurotoxic effects, which are well documented in laboratory animals (Bai *et al.*, 2001; Granado *et al.*, 2011), nonhuman primates (Hatzidimitriou *et al.*, 1999), as well as in humans (McCann *et al.*, 1994; Quednow *et al.*, 2006; Roberts *et al.*, 2009; Tai *et al.*, 2011). Notably, long-term effects of MDMA in nonhuman primates occur at doses that are comparable to those that are used by human MDMA users (Ricaurte *et al.*, 1988). Though in humans the neurotoxic effects of MDMA are believed to affect more the serotonergic system (Kish *et al.*, 2010a; Kish *et al.*, 2010b; Erritzoe *et al.*, 2011), a recent study described a potential risk of long-lasting dopaminergic deficits in MDMA users (Tai *et al.*, 2011). Likewise, by using *in vitro* models of dopaminergic neurons, it has been documented a high potential of MDMA and its catechol metabolites to affect the dopaminergic system (Ferreira *et al.*, 2013).

It is well-known that MDMA induces an acute and rapid release of serotonin (5-HT) and dopamine from nerve endings, which may undergo oxidative deamination by monoamine oxidase (MAO), leading to the formation of deleterious amounts of hydrogen peroxide. While this pharmacological pathway may explain part of the neurotoxic effects of MDMA, other mechanisms are also suggested to contribute to its neurotoxic properties. Indeed, recent studies have highlighted the formation of reactive hepatic metabolites as another major contributing factor to the MDMA´s neurotoxicity (Monks *et al.*, 2004; Capela *et al.*, 2006a; Capela *et al.*, 2007; Barbosa *et al.*, 2012). Notably, some studies failed to demonstrate serotonergic neurotoxicity when MDMA was injected directly into the brain (Bai *et al.*, 1999; Esteban *et al.*, 2001). In agreement, an attenuation in MDMA-mediated depletions in 5-HT brain content was observed under CYP450 inhibition (Gollamudi *et al.*, 1989), thus supporting an important role for metabolism in the context of “ecstasy”-induced neurotoxicity. The hepatic metabolism of MDMA is mainly mediated by CYP450, involving *N*-demethylation to 3,4-methylenedioxyamphetamine (MDA). MDMA and MDA may be further *O*-demethylated to the catechol metabolites *N*-methyl-α-methyldopamine (N-Me-α-MeDA) and α-methyldopamine (α-MeDA), respectively, both of which can undergo oxidation to corresponding *ortho*-quinones. In humans and rats N-Me-α-MeDA is the main catechol metabolite of MDMA, being α-MeDA the major metabolite in mice. Since the *ortho*-quinones formed are highly redox-active molecules, they can undergo redox cycling, generating semiquinone radicals, as well as reactive oxygen (ROS) and nitrogen (RNS) species. In addition, since the reactive *ortho*-quinones intermediates are electrophilic compounds, cellular damage may occur through the alkylation of crucial cellular proteins and/or DNA. In the presence of reduced glutathione (GSH), *ortho*-

quinones may be conjugated to form glutathionyl adducts (Hiramatsu *et al.*, 1990). Conjugation of GSH with electrophiles, such as *ortho*-quinones, can preserve or enhance their biological reactivity (Monks *et al.*, 2004; Jones *et al.*, 2005; Erives *et al.*, 2008). The systemically formed GSH-conjugated metabolites of MDMA may be transported across the blood-brain barrier (BBB) (Miller *et al.*, 1996), as proved by their presence in the brain after MDMA administration to rats (Jones *et al.*, 2005; Erives *et al.*, 2008). In the brain, GSH conjugates can be further metabolized via the marcapturic acid pathway (Esteban *et al.*, 2001). Initially, GSH conjugates are metabolized by γ-glutamyltransferase and dipeptidase to their corresponding cysteine conjugates. Additionally, these cysteine conjugates may be further metabolized by *N*-acetyltransferase to their corresponding *N*-acetylcysteine (NAC) conjugates (Patel *et al.*, 1993; Erives *et al.*, 2008). However, despite metabolic conversion, NAC-conjugated metabolites of MDMA retain the toxicity of their GSH precursors (Jones *et al.*, 2005). Furthermore, contrary to GSH conjugates, where the brain accumulation may be counteracted by multidrug resistant protein transports 1 and 2 localized in the BBB (Slot *et al.*, 2008; Ballatori *et al.*, 2009), NAC conjugates appear to be slowly eliminated and, consequently, persist in the brain (Jones *et al.*, 2005; Erives *et al.*, 2008). In agreement, recent studies have demonstrated that, in rat brain, NAC-conjugated metabolites of MDMA present a longer half-life than GSH conjugates after subcutaneous injection of MDMA (Jones *et al.*, 2005). Still, it was observed that, after multiple administrations of MDMA, both GSH and NAC metabolites tend to accumulate in the brain (Erives *et al.*, 2008). Though GSH- and NAC-conjugated metabolites of MDMA are described to play a major role in MDMA-induced neurotoxicity (Miller *et al.*, 1996; Bai *et al.*, 1999; Capela *et al.*, 2007), catechol metabolites, which are also detected in the brain after MDMA administration (Chu *et al.*, 1996; Jones *et al.*, 2005; Erives *et al.*, 2008), may also contribute to MDMA's deleterious effects. Indeed, catechol MDMA metabolites were proven to induce neurotoxic effects in an *in vitr*o dopaminergic system (Ferreira *et al.*, 2013). Another factor that may exacerbate the toxic effects of MDMA and its metabolites is hyperthermia, since it may increase the production of ROS by itself, or by increasing the metabolism of MDMA (Ádori *et al.*, 2006). In accordance, by preventing the hyperthermic response, a decrease in the neurotoxic effects associated with MDMA was observed (Farfel and Seiden, 1995), clearly demonstrating the role of hyperthermia in MDMA's neurotoxicity.

The aim of the present study was to evaluate the mechanisms involved in MDMA-related neurotoxicity, using human SH-SY5Y differentiated cells as *in vitro* dopaminergic neuronal model, specifically evaluating the role of MDMA metabolites and hyperthermia in MDMA's neurotoxic actions.

Human neuroblastoma cell line SH-SY5Y is a suitable neuronal model, as it bears biochemical properties of human neurons *in vivo* (Constantinescu *et al.*, 2007). Furthermore, being a tumor-derived cell line, SH-SY5Y cells continuously divide without exhibiting a large phenotypic variability (Presgraves *et al.*, 2003). Therefore, since these cells can acquire a dopaminergic phenotype after differentiation with retinoic acid (RA) and 12-O-tetradecanoylphorbol-13-acetate (TPA) (Presgraves *et al.*, 2003; Barbosa *et al.*, 2013; Ferreira *et al.*, 2013), they constitute a suitable *in vitro* model to study the mechanisms involved in MDMA-induced dopaminergic deficits.

Materials and Methods

Materials

All reagents used in this study were of analytical grade or of the highest grade available. Dulbecco's modified Eagle's medium (DMEM) with 4.5 g/L glucose and GlutMAX^{TM}, nonessential amino acids (NEAA), heat inactivated fetal bovine serum (FBS), 0.25% trypsin/ethylenediaminetetraacetic acid (EDTA) and Dulbecco's phosphate buffered saline (DPBS) were purchased from Gibco Laboratories (Lenexa, KS, USA). Penicillin (10,000 U/mL) and streptomycin (10,000 µg/mL) were purchased from Biochrom AG (Berlin, Germany). Trypan blue solution [0.4% (w/v)], RA, TPA, 3-(4,5-dimethyl-2-thiazolyl)-2,5-diphenyl-2H-tetrazolium bromide (MTT), sodium dodecyl sulfate (SDS), *L*-lactic dehydrogenase (LDH), sodium pyruvate, nicotinamide adenine dinucleotide reduced form (NADH), triton X-100, GSH, nicotinamide adenine dinucleotide phosphate reduced form (NADPH), 5,5-dithio-bis(2-nitrobenzoic acid) (DTNB), glutathione reductase (GR), *N*-acetyl-Asp-Glu-Val-Asp-*p*-nitroaniline (Ac-DEVD-pNA), 4-(2-hydroxyethyl)piperazine-1-ethanesulfonic acid (HEPES), 3-[(3-cholamidopropyl)dimethylammonio]-1-propanesulfonate hydrate (Chaps), dithiothreitol (DTT), Tris-HCl, NAC, and bovine serum albumin (BSA) were obtained from Sigma-Aldrich (St. Louis, MO, USA). Bio-Rad DC protein assay was purchased from Bio-Rad Laboratories (Hercules, CA, USA). EDTA, KH_2PO_4, $K_2HPO_4.3H_2O$, KCl, $MgCl_2.6H_2O$, dimethylsulfoxide (DMSO), HCl, $HClO_4$, NaOH, $KHCO_3$ and Folin reagent were obtained from Merck (Darmstadt, Germany). MDMA (hydrochloride salt) was extracted and purified from high-purity MDMA tablets that were provided by the Portuguese Criminal Police Department. The obtained salt was pure and fully characterized by NMR and mass spectrometry methodologies, as previously described by our group (Capela *et al.*, 2007). The MDMA metabolites α-MeDA, N-Me-α-MeDA, 5-(glutathion-*S*-yl)-α-methyldopamine [5-(GSH)-α-MeDA], 5-(glutathion-*S*-yl)-*N*-methyl-α-methyldopamine [5-(GSH)-N-Me-α-MeDA], 5-(*N*-acetylcysteine-*S*-yl)-α-methyldopamine [5-(NAC)-α-MeDA] and 5-(*N*-acetylcysteine-*S*-yl)-*N*-methyl-α-methyldopamine [5-(NAC)-N-Me-α-MeDA] were synthesized and fully characterized by nuclear magnetic resonance and mass spectrometry methodologies by REQUI*M*TE (Centro de Química Fina e Biotecnologia), Chemistry Department, Faculty of Science and Technology, University Nova de Lisboa, according to previously published methods (Capela *et al.*, 2006a; Capela *et al.*, 2007; Macedo *et al.*, 2007). All other chemicals were purchased from Sigma-Aldrich.

Cell culture and differentiation

SH-SY5Y cells are a neuroblastoma cell line cloned from SK-N-SH cells with a human origin. This cell line has been widely used as *in vitro* neuronal model, since the early 1980's as these cells possess many biochemical and functional properties of neurons (Takeuchi *et al.*, 2009). SH-SY5Y cells (ATCC, Manassas, VA, USA) were routinely cultured in 25-cm^2 flasks (Costar, Corning, NY, USA) using DMEM with GlutMAX™ and 4.5 g/L glucose, supplemented with 10% heat inactivated FBS (v/v), 1% NEAA (v/v), 100 U/mL penicillin, and 100 µg/mL streptomycin. Cells were maintained at 37ºC in a humidified atmosphere of 95% air/5% CO_2. Cultures were sub-cultivated weekly by trypsinization (0.25% trypsin/EDTA). The SH-SY5Y cells used for all the experiments were taken between the 25^{th} and 34^{th} passages, in order to avoid phenotypic changes. To increase the dopaminergic neuronal phenotype, SH-SY5Y cells were differentiated as described previously by our group (Barbosa *et al.*, 2013; Ferreira *et al.*, 2013). Cells were counted in a Fuchs-Rosenthal camera (using a trypan blue solution), seeded at the initial density of 25,000 cells/cm^2, in complete medium containing 10 µM RA, and cultured for 3 days. After seeding, the final volume of medium in the 48-well and 6-well cultures plates (Corning Costar, Corning) was 250 µL and 2 mL, respectively. After 3 *days in vitro*, 50 or 400 µL of medium containing 480 nM of TPA were added to each well of the 48- or 6-well culture plates (final concentration of TPA 80 nM), respectively, and cells were cultured for another 3 days. Stock solutions of RA (10 mM) and TPA (80 µM) were prepared in DMSO. Final concentration of DMSO in each well was 0.2% (v/v). For MTT reduction and LDH assays, SH-SY5Y differentiated cells were cultured onto 48-well culture plates. For GSH measurement and caspase 3 activity assay, SH-SY5Y differentiated cells were cultured onto 6-well culture plates.

Study design

After conclusion of the differentiation protocol, the medium of each well was removed and replaced by new medium containing MDMA or its metabolites, at concentrations ranging from 50 to 200 µM. Incubations were performed for a period of 24 or 48h, under normothermic (37ºC) or hyperthermic (40ºC) conditions, in a humidified atmosphere of 95% air/5% CO_2. In experiments using the antioxidant NAC (1 mM), it was added to the cultures 30 min prior exposure to MDMA metabolites. In humans, the first reports of fatalities associated with the recreational use of MDMA involved overheating, with core body temperatures over 40ºC (Henry *et al.*, 1992; Chadwick *et al.*, 2001). Therefore, based in previous published works by our group (Capela *et al.*, 2006a; Capela *et al.*, 2006b; Capela *et al.*, 2007), the temperature of 40ºC was then selected for the

hyperthermic experiments. Stock solutions of MDMA, MDMA metabolites and NAC were prepared in distilled water. Stock solutions were at least 50 times more concentrated than the concentration tested, in order to avoid media dilution. All stock solutions were stored at -20 ºC.

MTT reduction assay

The MTT reduction assay was used to measure mitochondrial dysfunction (decrease in mitochondrial dehydrogenase activity) in SH-SY5Y differentiated cells exposed to MDMA or its 6 metabolites, as previously described (Barbosa *et al.*, 2013). The signal generated is dependent on the degree of activation of the MTT tetrazolium salt (water soluble) to MTT formazan (water insoluble) by the cellular dehydrogenases within metabolically active cells. Following exposure to the putative deleterious conditions, the medium was removed and 200 µL of new medium containing 0.5 mg/mL MTT was added to each well and incubated for 3h, at 37ºC. MTT stock solution (5 mg/mL) was prepared in DPBS without Ca^{2+} and Mg^{2+} [DPBS (-/-)]. After this incubation period, the reaction was stopped by adding 200 µL of SDS 10% (w/v) in 0.01 M hydrochloric acid, followed by overnight incubation at 37ºC. After pipetting, in duplicate, 150 µL of the content from each well of the 48-well plate to a 96-well plate, the rate of MTT reduction was measured spectrophotometrically, in a multi-well plate reader (PowerWaveX; Bio-Tek Instruments, VT, USA), at 550 nm. Final results from 6 independent experiments (each experiment was performed at least in triplicate) are expressed as percentage of absorbance in control cells [MTT reduction (% of control)].

LDH assay

The integrity of the plasma membrane in SH-SY5Y differentiated cells exposed to MDMA or its metabolites was assessed biochemically by measuring the cellular leakage of the cytosolic enzyme LDH. LDH is a soluble cytosolic enzyme present in most eukaryotic cells, released into the culture medium upon cell death due to the damage of plasma membrane. Thus, the increase in the LDH activity in the culture supernatant is proportional to the number of cells with disrupted membrane. LDH activity in the culture medium was determined spectrophotometrically by measuring the decrease of NADH absorbance during the reduction of pyruvate to lactate, as previously described (Barbosa *et al.*, 2013). After conclusion of the incubation periods, 50 µL of the cellular medium was removed from each well and transferred to a 96-well plate (to measure extracellular LDH), in duplicate. After removing the medium to evaluate the extracellular LDH, 75 µL of new medium plus 25 µL of triton X-100 5% solution (v/v) (final concentration of 0.5%) were

added to the cells, and the plates were incubated for 30 min, at 37ºC, to allow cellular lyses. After this time, 25 µL of medium from each well were transferred to a new 96-well plate (to measure the LDH after the full kill), also in duplicate. Thus, in the 96-well plates, the collected medium was mixed with 200 µL of reagent solution containing 0.21 mM NADH, dissolved in LDH buffer (33.3 mM KH_2PO_4 and 66.7 mM $K_2HPO_4.3H_2O$, pH 7.4). The reaction was started with 25 µL sodium pyruvate (22.7 mM, prepared in LDH buffer) and the kinetic formation of nicotinamide adenine dinucleotide oxidized form (NAD^+) from NADH was followed for 5 min, at 340 nm, in a 96-well plate reader (PowerWaveX, Bio-Tek Instruments). The final reaction volume in each well was fixed with LDH buffer to 275 µL. Thus, to measure LDH after the full kill, 25 µL of LDH buffer were added to each well before sodium pyruvate addition. Final results of LDH released into the extracellular medium (LDH leakage), from 6 independent experiments (each experiment was performed at least in triplicate), are expressed as percentage of cell death (% cell death) according to the equation: % cell death = (extracellular LDH/total LDH) x 100, considering total LDH = extracellular LDH removed + LDH after full kill.

Assessment of glutathione levels

Total intracellular glutathione levels in SH-SY5Y differentiated cells exposed to MDMA or its 6 metabolites were evaluated by the DTNB-GSH reductase recycling assay, as previously described (Barbosa *et al.*, 2012), with some adaptations. After conclusion of the exposure periods, the medium was removed and cells were scraped in 1 mL of cold DPBS with Ca^{2+} and Mg^{2+} [DPBS (+/+)], and then harvested (1 well per condition). After centrifugation at 2,376 *g*, for 5 min, at 4ºC, the supernatant was discarded and the cellular pellet was dispersed in 400 µL $HClO_4$ 5% (w/v) and centrifuged again at 16,000 *g*, for 10 min, at 4ºC. The perchloric acid pellet was dissolved in 400 µL NaOH 0.3 M and the protein content was assayed by the Lowry method (Lowry *et al.*, 1951), using BSA as standard. The supernatants (200 µL) were neutralized with 200 µL of an equimolar solution of $KHCO_3$ (0.76 M) and centrifuged at 16,000 *g*, for 2 min, at 4ºC. In 96-well plates, 100 µL of sample or standard were added in triplicate and mixed with 65 µL of freshly prepared reagent solution containing 3.96 mM DTNB and 0.68 mM NADPH prepared in a mixture of 40.5% H_2O/59.5% phosphate buffer (71.5 mM Na_2HPO_4, 71.5 mM NaH_2PO_4 and 0.63 mM EDTA, pH 7.5). Plates were then incubated in a 96-well microplate reader (PowerWaveX; Bio-Tek Instruments) at 30ºC, during 15 min, prior to the addition of 40 µL of fresh GR solution per well (10 U/mL in phosphate buffer). The stoichiometric formation of 5-thio-2-nitrobenzoic acid (TNB) was followed for 3 min, at 415 nm, and compared with the standard GSH curve. GSH standard solutions (0, 0.25, 0.5,

1.25, 2.5, 5, 10 and 15 μM) were prepared in $HClO_4$ 5% (w/v) and kept at -20ºC until use. Intracellular total glutathione levels were normalized to the total protein content and the final results from 6 independent experiments (each experiment was performed in duplicate) are expressed as nmol of GSH per milligram of protein (nmol GSH/mg protein). Intracellular levels of oxidized glutathione (GSSG) were found to be below the detection limit of the method. Therefore, only intracellular total glutathione results are presented.

Caspase 3 activity assay

The activation of caspase 3 was assessed in SH-SY5Y differentiated cells exposed to MDMA metabolites, as previously described (Capela *et al.*, 2007; Barbosa *et al.*, 2013), with some modifications. The hydrolysis of the peptide substrate Ac-DEVD-pNA by caspase 3 results in the release of the *p*-nitroaniline (pNA) moiety, which presents high absorbance at 405 nm. After conclusion of the exposure periods, the medium was removed and the cells were scraped in 750 μL of cold DPBS (+/+), and then harvested (2 wells per condition). After centrifugation at 855 *g*, for 4 min, at 4ºC, the supernatant was discarded and the cellular pellet was lysed in 75 μL of ice cold lysis buffer [50 mM Hepes, 0.1 mM EDTA and 0.1% Chaps (w/v), pH 7.4, supplemented with 1 mM DTT (no protease inhibitors)]. After vortexing, the cell lysates were allowed to incubate on ice for 10 min before centrifugation at 16,000 *g*, for 10 min, at 4ºC. Whole protein content in the supernatants was determined using the Bio-Rad DC protein assay and BSA as standard. In a 96-well plate, 50 μL of the supernatant were mixed with 200 μL of assay buffer [100 mM NaCl, 50 mM Hepes, 1 mM EDTA, 0.1% Chaps (w/v) and 10% glycerol (v/v), pH 7.4, supplemented with 10 mM DTT (no protease inhibitors)]. The reaction was started by adding 5 μL of caspase 3 substrate Ac-DEVD-pNA (final concentration of 80 μM), and subsequent incubation at 37ºC, for 24h, after which the formation of pNA was measured spectrophotometrically, at 405 nM, in a 96-well plate reader (PowerWaveX; Bio-Tek Instruments). Caspase 3 substrate Ac-DEVD-pNA (stock solution at 4 mM) and DTT were prepared in DMSO. The absorbance of blanks, used as non-enzymatic control, was subtracted from each value of absorbance. Final results of caspase 3 activity from 8 independent experiments are expressed as optical density at 405 nm per milligram of protein (OD 405 nm/mg protein).

HPLC analysis of MDMA metabolites

The stability of MDMA metabolites α-MeDA, N-Me-α-MeDA, 5-(GSH)-α-MeDA and 5-(NAC)-α-MeDA under normothermic (37ºC) and hyperthermic (40ºC) conditions was evaluated by HPLC analysis with electrochemical detection, according to previously

published methods (Silva *et al.*, 2007), with some modifications. Briefly, MDMA metabolites α-MeDA, N-Me-α-MeDA, 5-(GSH)-α-MeDA or 5-(NAC)-α-MeDA were incubated in cell culture medium with or without cells (starting concentration of 50 μM) under normothermic (37ºC) or hyperthermic (40ºC) conditions and, at selected time-points, 150 μL of medium were removed and added to 50 μL $HClO_4$ 20% (w/v). After centrifugation at 13,000 *g*, for 10 min, at 4ºC, the supernatant was used for HPLC analysis. To determine the intracellular concentration of metabolites, cells were washed with cold DPBS (+/+), scraped in 400 μL $HClO_4$ 5% (w/v) and then harvested (1 well per condition). After centrifugation at 16000 *g*, for 10 min, at 4ºC, the supernatant was used for HPLC analysis and the cellular pellet was dissolved in 400 μL NaOH 0.3 M to quantify the protein content by the Lowry method (Lowry *et al.*, 1951), using BSA as standard. MDMA metabolites' concentrations was evaluated in a HPLC system equipped with a Waters 2,690 separations module (Waters, Milford, MA, USA) and a commercially pre-packed reverse phase cartridge of 250 mm × 4.6 mm, Waters Spherisorb RP-18 (5 μm) ODS2 column. The mobile phase [10% methanol (v/v) in 50 mM citric acid and 0.46 mM octanesulfonic acid, pH 3.0] was filtered through a 0.45 μm membrane (Millipore, Madrid, Spain) and degassed under a nitrogenium stream. Solvent was delivered at a flow rate of 1 mL/min, at room temperature, under isocratic conditions. Electrochemical analysis was performed using a Colouchem II detector (ESA, Chelmsford, USA) equipped with a guard cell (ESA 5020) and an analytical cell (ESA 5011A). The electrochemical potential settings of the Coulochem II detector were: guard cell, +0.5V; detector 1, -0.075V; detector 2 (analytical detector), +0.45V. A Compaq computer fitted with Millenium^{32} software (Waters) was used to process the chromatographic data. Final results, from 3-7 independent experiments are expressed in concentration (μM) of MDMA metabolites or in nmole of MDMA metabolites per milligram of protein (nmole/mg proten).

Data analysis

Values in figures and text are presented as mean ± SD of the indicated number of independent experiments (n). Each independent experiment was performed with SH-SY5Y differentiated cells proceeding from different passages. Normality of the data distribution was assessed by three tests (KS normality test, D'Agostino and Pearson omnibus normality test and Shapiro-Wilk normality test). Statistical comparisons between groups were performed with two-way ANOVA, followed by the Bonferroni multiple comparison post-hoc test. Particularly, to analyze the data presented in Figure 3, relative to the stability of MDMA metabolites α-MeDA, N-Me-α-MeDA, 5-(GSH)-α-MeDA and 5-(NAC)-α-MeDA in cell culture medium, time-response curves (MDMA metabolite

concentration decrease over time) were compared by using one phase or plateau followed by one phase exponential decay models and least squares as a fitting methods. Comparisons between curves were performed using the extra sun-of-squares F test. Details of the performed statistical analysis are described in each figure legend. Differences were considered to be significant at *p* values lower than 0.05. All analyses were performed using GraphPad Prism 6.0 for Windows (GraphPad Software, San Diego, CA, USA).

Results

MDMA metabolites were toxic to SH-SY5Y differentiated cells. Temperature and time of exposure differently affected the neurotoxic outcome

SH-SY5Y differentiated cells were incubated with growing concentrations (50 to 200 μM) of MDMA or its metabolites. Mitochondrial dysfunction and cell death were evaluated by the MTT reduction and LDH release assays, respectively. MDMA, at both time and temperatures of incubation studied, did not induce significant mitochondrial dysfunction or cell death, at any of the tested concentrations (Figures 1Ai and 2Ai, respectively). In contrast, all the MDMA metabolites studied significantly decreased the mitochondrial function and increased cell death, in a concentration-dependent manner, at both temperatures studied (Figures 1Ai-Gi and 2Ai-Gi). Since the differences promoted by the factor time and temperature of exposure were higher at 100 μM, this concentration was then selected to evaluate the role of those two factors in the toxic effect induced by MDMA and its metabolites in SH-SY5Y differentiated cells. As observed in Figure 1Bii, the mitochondrial dysfunction induced by the catechol MDMA metabolite α-MeDA was independent on the time of exposure. However, after 24h of exposure the toxic effect was potentiated by hyperthermia (p<0.05). The catechol MDMA metabolite N-Me-α-MeDA induced mitochondrial dysfunction in a time- and temperature-dependent manner (Figure 1Cii). Unlike mitochondrial dysfunction, the cell death induced by these two MDMA metabolites did not reveal a time dependency, but hyperthermia potentiated the toxicity after 48h of exposure (Figures 2Bii and 2Cii, p<0.05). Following a different pattern observed for the catechol MDMA metabolites, the mitochondrial dysfunction and cell death induced by 100 μM of the metabolites 5-(GSH)-α-MeDA (Figures 1Dii and 2Dii, respectively) and 5-(GSH)-N-Me-α-MeDA (Figures 1Eii and 2Eii, respectively) revealed to be independent on the time and temperature of exposure. NAC-conjugated metabolites 5-(NAC)-α-MeDA (Figures 1Fii and 2Fii, respectively) and 5-(NAC)-N-Me-α-MeDA (Figures 1Gii and 2Gii, respectively) induced mitochondrial dysfunction and cell death in a time-independent manner, but dependent on the temperature. Surprisingly, for these two NAC metabolites, at the 100 μM concentration, the toxicity was significantly higher under normothermia, as revealed by the mitochondrial dysfunction at both times of exposure (Figures 1Fii and 1Gii), and by the cell death after 24h of exposure (Figures 2Fii and 2Gii).

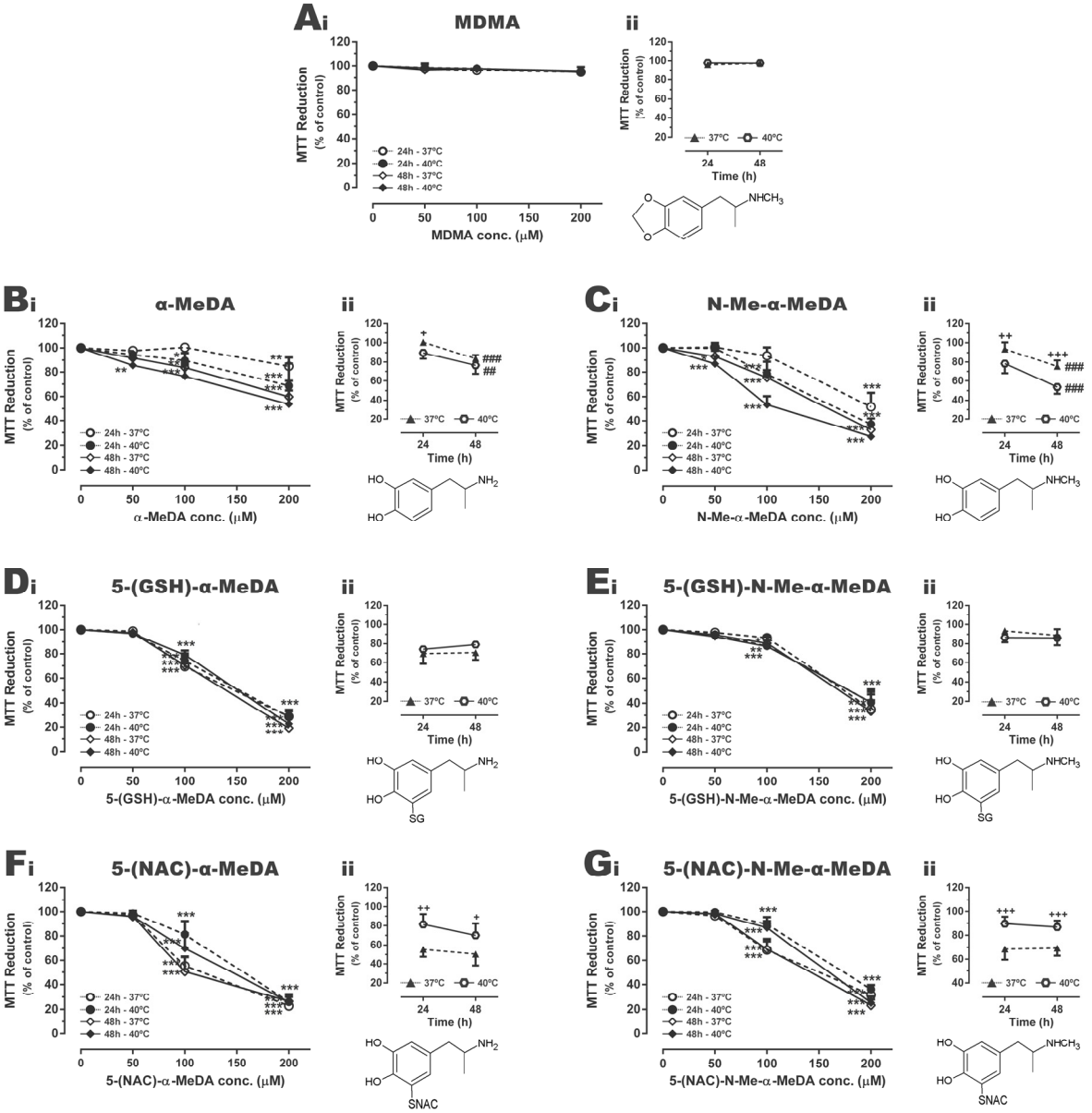


Figure 1. Mitochondrial dysfunction induced by MDMA and its metabolites in SH-SY5Y differentiated cells. Cells were exposed to growing concentrations (0, 50, 100 or 200 μM) of MDMA (Ai), α-MeDA (Bi), N-Me-α-MeDA (Ci), 5-(GSH)-α-MeDA (Di), 5-(GSH)-N-Me-α-MeDA (Ei), 5-(NAC)-α-MeDA (Fi) or 5-(NAC)-N-Me-α-MeDA (Gi), for 24 or 48h, under normothermic (37ºC) or hyperthermic conditions (40ºC), and mitochondrial dysfunction was then evaluated by the MTT reduction assay. The concentration of 100 μM was selected to evaluate the role of time and temperature of exposure on the mitochondrial dysfunction induced by MDMA or its metabolites (ii). Results are presented as mean ± SD, from 6 independent experiments (each experiment was performed at least in triplicate), and expressed as percentage of MTT reduction relative to control cells [MTT reduction (% of control)]. Statistical comparisons were performed with two-way ANOVA, followed by the Bonferroni's multiple comparison *post-hoc* test (*p<0.05, **p<0.01, ***p<0.001 compound *vs.* control; ^{+}p<0.05, ^{++}p<0.01, ^{+++}p<0.001 40ºC *vs.* 37ºC, for the same time-point; $^{\#\#}p$<0.01, $^{\#\#\#}p$<0.001 48h *vs.* 24h, for the same temperature).

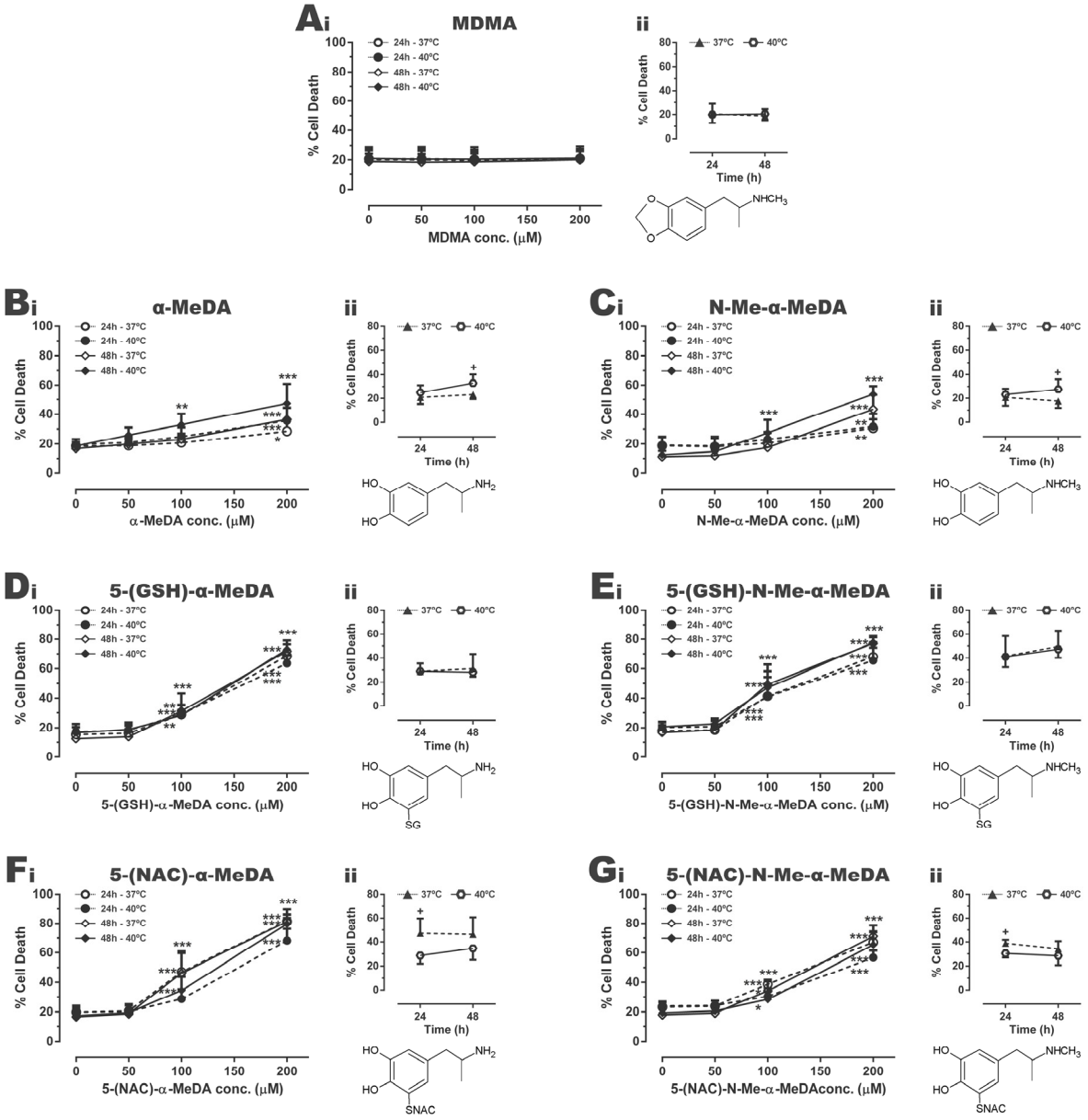


Figure 2. Cell death induced by MDMA and its metabolites in SH-SY5Y differentiated cells. Cells were exposed to growing concentrations (0, 50, 100 or 200 μM) of MDMA (Ai), α-MeDA (Bi), N-Me-α-MeDA (Ci), 5-(GSH)-α-MeDA (Di), 5-(GSH)-N-Me-α-MeDA (Ei), 5-(NAC)-α-MeDA (Fi) or 5-(NAC)-N-Me-α-MeDA (Gi), for 24 or 48h, under normothermic (37ºC) or hyperthermic conditions (40ºC), and cell death was then evaluated by the LDH assay. The concentration of 100 μM was selected to evaluate the role of time and temperature of exposure on the cell death induced by MDMA or its metabolites (ii). Results are presented as mean ± SD, from 6 independent experiments (each experiment was performed at least in triplicate), and expressed as percentage of cell death (% cell death). Statistical comparisons were performed with two-way ANOVA, followed by the Bonferroni's multiple comparison *post-hoc* test (**p*<0.05, ***p*<0.01, ****p*<0.001 compound *vs.* control; ^{+}p<0.05, 40ºC *vs.* 37ºC, for the same time-point).

The extracellular concentration of MDMA metabolites decreased over time, an effect potentiated under hyperthermic conditions

Previously, it was demonstrated an over time decrease in the concentration of MDMA metabolites α-MeDA and N-Me-α-MeDA in biological medium (Carvalho *et al.*, 2004b). In order to verify the effect of temperature and time of exposure on the concentration of the MDMA metabolites, we compared their stability in cell culture medium without cells, under normothermic and hyperthermic conditions.

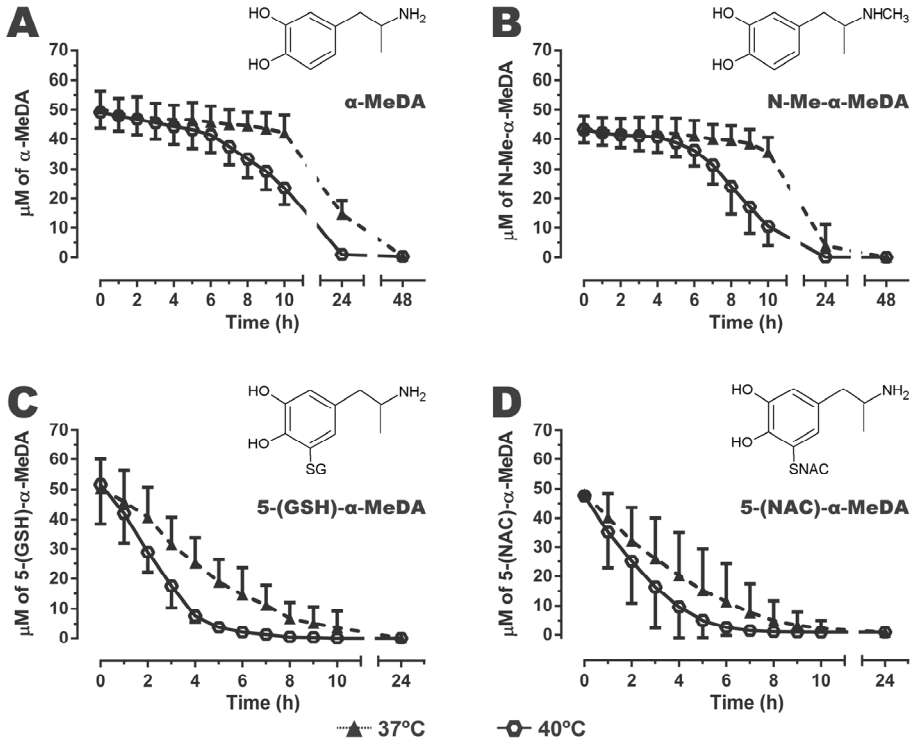


Figure 3. Comparative stability of MDMA metabolites over time in culture medium (without cells). MDMA metabolites α-MeDA (A), N-Me-α-MeDA (B), 5-(GSH)-α-MeDA (C) or 5-(NAC)-α-MeDA (D), at the concentration of 50 μM, were incubated in cell culture medium, under normothermic (37ºC) or hyperthermic (40ºC) conditions and their concentration was then evaluated hourly until 10h and after 24 or 48h of incubation, by HPLC with electrochemical detection, as described under Methods. Results are presented as mean ± SD, from 5-7 independent experiments, and expressed as μM of MDMA metabolite. Time-concentration curves, representing the decrease of MDMA metabolites concentration over time, were fitted with plateau followed by one-phase (A and B) or one-phase (C and D) exponential decay models, and the curves obtained at 37ºC and 40ºC were compared with the extra sun-of-squares *F* test ($p<0.0001$, curve obtained under normothermia *vs.* curve obtained under hyperthermia, for all metabolites represented). In all cases, no significant differences were observed in Y0 (concentration of MDMA metabolites at 0h time-point) and plateau values (base of the curves) obtained from normothermic and hyperthermic conditions.

Figure 3 shows the time-concentration curves obtained for the metabolites studied. For the studied compounds no significant differences were observed in Y0 (concentration of MDMA metabolites at 0h time-point) and plateau values (base of the curves) obtained from normothermic and hyperthermic conditions (data not shown), thus becoming possible

a comparison between curves. Furthermore, in cell culture medium without cells, either under normothermic or hyperthermic conditions, an over time decrease in compounds concentration in cell culture medium was observed for all the MDMA metabolites studied (Figure 3A-D). In addition, the time-concentration curves obtained under normothermia and hyperthermia were significantly different, being that the degradation of the MDMA metabolites was faster under hyperthermic conditions (Figure 3A-D). Importantly, the catechol MDMA metabolites (Figure 3A-B) presented higher stability in cell culture medium, comparared to the conjugates (Figure 3C-D). For the MDMA-conjugated metabolites (Figure 3C-D), since a low concentration was observed after 24h of incubation, the concentration at 48h time-point was below of the detection limit and, therefore, was not calculated.

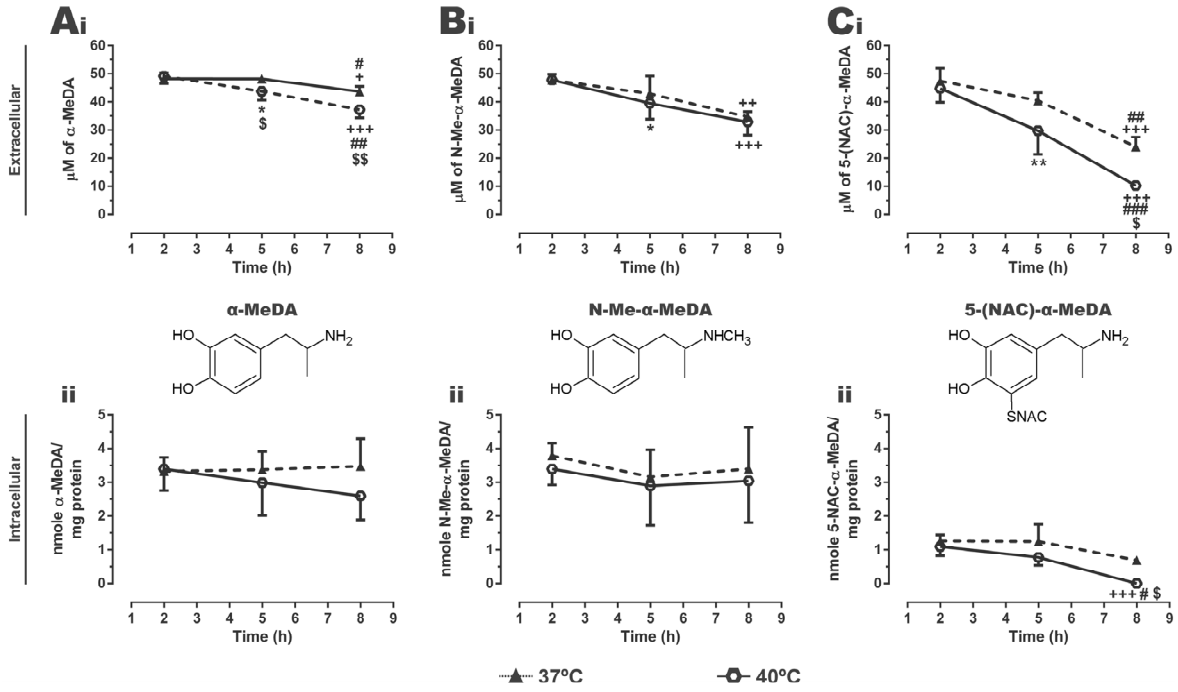


Figure 4. Comparative stability of MDMA metabolites over time on the extra- and intracellular compartment (with cells). SH-SY5Y cells were exposed to MDMA metabolites α-MeDA (A), N-Me-α-MeDA (B) or 5-(NAC)-α-MeDA (C), at the concentration of 50 µM, under normothermic (37ºC) or hyperthermic (40ºC) conditions and their extra- (i) and intracellular (ii) content was evaluated after 2, 5 and 8h of exposure, by HPLC with electrochemical detection, as described under Methods. Results are presented as mean ± SD, from 3-4 independent experiments (each experiment was performed in duplicate), and expressed as µM of MDMA metabolite (extracellular) or nmole MDMA metabolite per milligram of protein (nmole MDMA metabolite/mg protein - intracellular). Statistical comparisons were performed with two-way ANOVA, followed by the Bonferroni´s multiple comparison *post-hoc* test (**p*<0.05, ***p*<0.01 5h *vs.* 2h, ^{+}p<0.05, ^{++}p<0.01, ^{+++}p<0.001 8h *vs.* 2h, $^{\#}p$<0.05, $^{\#\#}p$<0.01, $^{\#\#\#}p$<0.001 8h *vs.* 5h, for the same temperature; $^{\$}p$<0.05, $^{\$\$}p$<0.01 40ºC *vs.* 37ºC, for the same time-point).

Next, it was also evaluated whether the temperature of incubation affected the intracellular metabolites' concentrations. To this end, we exposed SH-SY5Y differentiated cells to the MDMA metabolites α-MeDA, N-Me-α-MeDA and 5-(NAC)-α-MeDA, at the

concentration of 50 μM, and their intra- and extracellular levels were then evaluated after 2, 5 or 8h of exposure (these time-points were selected based on the results of stability in cell culture medium without cells, in which for periods beyond 8h the amount of metabolites was low, thus difficulting their quantification). Similarly to the results obtained in culture medium without cells, in SH-SY5Y differentiated cells exposed to the MDMA metabolites α-MeDA, N-Me-α-MeDA and 5-(NAC)-α-MeDA, an over time decrease in metabolites' concentrations was found in the cell culture medium (Figure 4Ai-Ci). Furthermore, the extracellular decrease in the concentration of the MDMA metabolites α-MeDA (Figure 4Ai) and 5-(NAC)-α-MeDA (Figure 4Ci) was faster under hyperthermic conditions, as revealed by the existence of significant differences in their extracellular content after 5 and 8h of exposure. For the MDMA metabolite N-Me-α-MeDA, the over time decrease of its concentration in the cell culture medium was similar under normothermic and hyperthermic conditions (Figure 4Bi). An over time decrease in the intracellular concentration of the MDMA metabolite 5-(NAC)-α-MeDA was observed, which was also faster under hyperthermic conditions, as observed by the existence of significant differences after 8h of exposure (Figure 4Cii). On the other hand, the intracellular concentration of catechol MDMA metabolites remained stable along the time-points studied (Figure 4Aii-Bii).

NAC differentially prevented the mitochondrial dysfunction induced by MDMA metabolites

Several *in vitro* studies have shown a protective role of NAC against the toxicity mediated by several toxic compounds (Capela *et al.*, 2007; Barbosa *et al.*, 2012). Therefore, we evaluate the putative effect of NAC (1mM) against mitochondrial dysfunction induced by 200 μM of the MDMA metabolites under normothermic conditions. As shown in Figure 5A-B, NAC significantly prevented the mitochondrial dysfunction induced by the catechol MDMA metabolites α-MeDA and N-Me-α-MeDA, respectively, at both exposure times studied. In fact, at the 24h time-point, the toxicity of both metabolites was fully prevented. However, the percentage of protection was higher for N-Me-α-MeDA (50% and 71%, after 24 and 48h of exposure, respectively) (Figure 5B), compared to α-MeDA (18% and 13%, after 24 and 48h of exposure, respectively) (Figure 5A). Regarding the MDMA metabolites 5-(NAC)-α-MeDA (Figure 5E) and 5-(NAC)-N-Me-α-MeDA (Figure 5F), NAC fully prevented the mitochondrial dysfunction observed after 24h of exposure to these compounds. After 48h of exposure, no protection was afforded by NAC. A minor protective effect of NAC was also observed for MDMA metabolite 5-(GSH)-α-MeDA (Figure 5C), once again significant after 24h of exposure. However, the protection

observed for this compound was much more lower, compared to the effect observed for the NAC conjugates (% of protection: 5-(GSH)-α-MeDA = 8%, 5-(NAC)-α-MeDA = 71% and 5-(NAC)-N-Me-α-MeDA = 84%) (Figure 5C, E-F). Differently, NAC did not confer any significant protection against the mitochondrial dysfunction induced by the MDMA metabolite 5-(GSH)-N-Me-α-MeDA, at both times of exposure tested (Figure 5D).

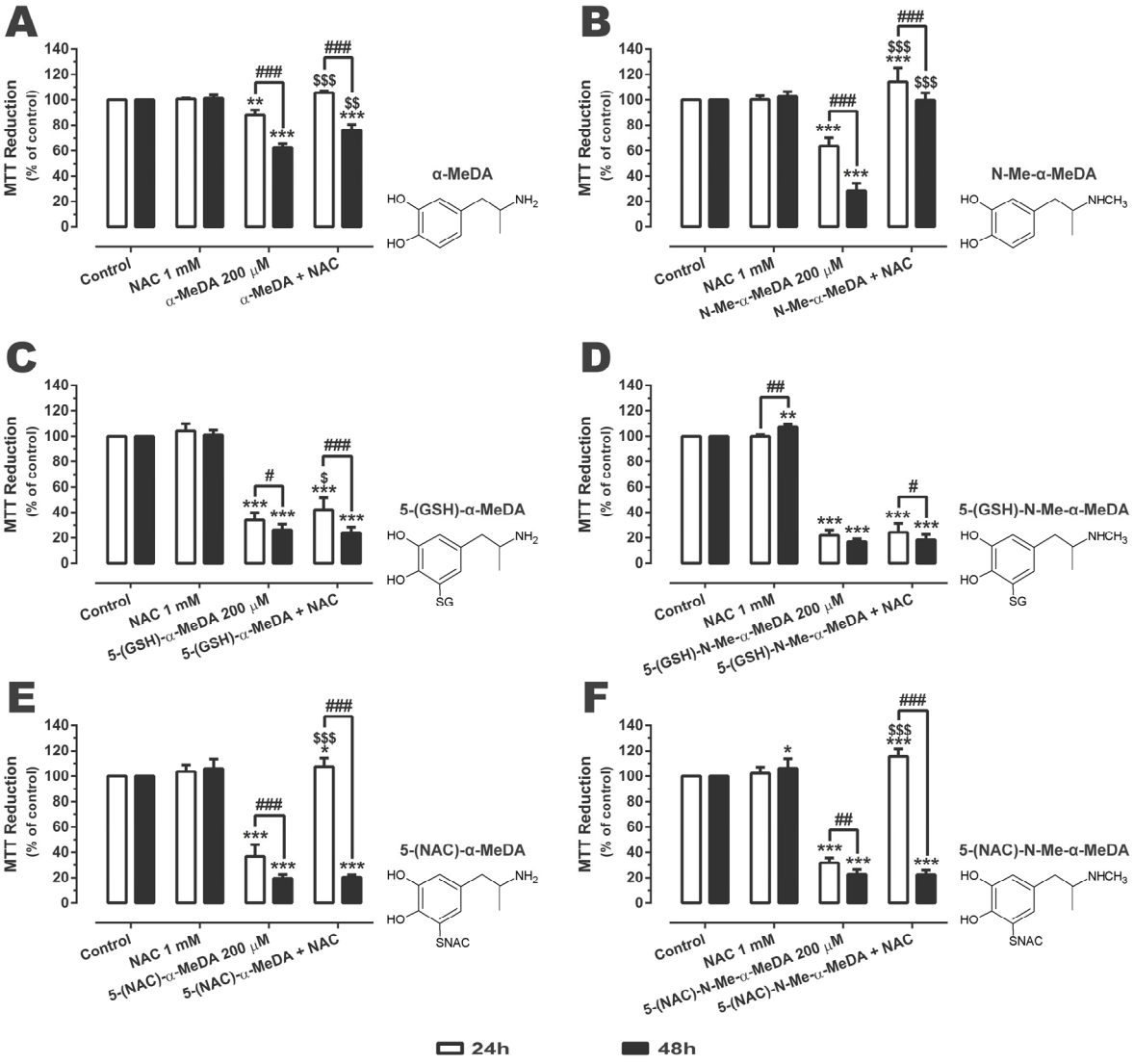


Figure 5. Protective effect of NAC against the mitochondrial dysfunction induced by MDMA metabolites in SH-SY5Y differentiated cells. Cells were pre-incubated with 1 mM NAC for 30 minutes, after which 200 μM of MDMA metabolites α-MeDA (A), N-Me-α-MeDA (B), 5-(GSH)-α-MeDA (C), 5-(GSH)-N-Me-α-MeDA (D), 5-(NAC)-α-MeDA (E) or 5-(NAC)-N-Me-α-MeDA (F) were added to the cultures and mitochondrial dysfunction was then evaluated after 24 or 48h of exposure, under normothermic (37ºC) conditions, by the MTT reduction assay. Results are presented as mean ± SD, from 6 independent experiments (each experiment was performed at least in triplicate), and expressed as percentage of MTT reduction relative to control cells [MTT reduction (% of control)]. Statistical comparisons were performed with two-way ANOVA, followed by the Bonferroni's multiple comparison *post-hoc* test [$^{*}p<0.05$, $^{**}p<0.01$, $^{***}p<0.001$ condition *vs.* control; $^{\#}p<0.05$, $^{\#\#}p<0.01$, $^{\#\#\#}p<0.001$ 48h *vs.* 24h, for the same experimental condition; $^{\$}p<0.05$, $^{\$\$}p<0.01$, $^{\$\$\$}p<0.001$ metabolite plus NAC *vs.* metabolite, for the same time-point].

MDMA and its metabolites induced significant changes in the intracellular total glutathione levels in SH-SY5Y differentiated cells

In order to evaluate the putative role of glutathione in the toxic effects mediated by MDMA and its metabolites in SH-SY5Y differentiated cells, intracellular total glutathione levels were evaluated after exposure to 100 μM of the studied compounds, under normothermic or hyperthermic conditions.

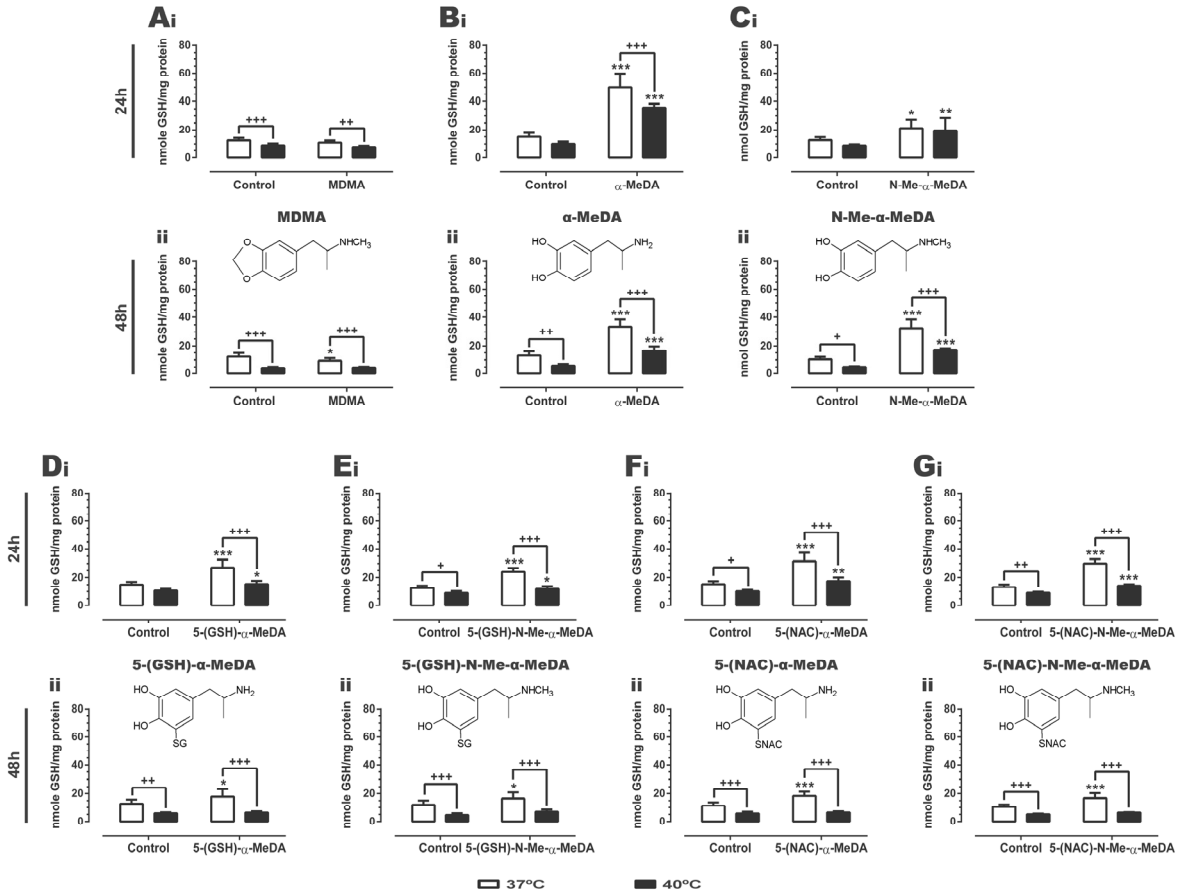


Figure 6. Effects of MDMA and its metabolites in intracellular total GSH levels, in SH-SY5Y differentiated cells. Cells were exposed to 100 μM of MDMA (A) or its metabolites α-MeDA (B), N-Me-α-MeDA (C), 5-(GSH)-α-MeDA (D), 5-(GSH)-N-Me-α-MeDA (E), 5-(NAC)-α-MeDA (F) and 5-(NAC)-N-Me-α-MeDA (G), for 24 (i) or 48h (ii), under normothermic (37ºC) or hyperthermic (40ºC) conditions, and intracellular total GSH levels were then evaluated by the DTNB/GSH reductase recycling assay. Results are presented as mean ± SD, from 6 independent experiments (each experiment was performed in duplicate), and expressed in nmol GSH per mg of protein (nmol GSH/mg protein). Statistical comparisons were performed with two-way ANOVA, followed by the Bonferroni's multiple comparison *post-hoc* test (**p*<0.05, ***p*<0.01, ****p*<0.001 compound *vs.* control, for the same temperature; ^{+}p<0.05, ^{++}p<0.01, ^{+++}p<0.001 40ºC *vs.* 37ºC).

SH-SY5Y differentiated cells exposed to hyperthermia presented lower levels of glutathione relative to their counterparts at 37ºC, an effect more pronounced at the time-point of 48h (Figure 6). MDMA, unlike all its metabolites, significantly decreased the intracellular total glutathione levels after 48h of exposure, and under normothermic

conditions (Figure 6Aii). However, after 24h of exposure to MDMA, at both normothermic and hyperthermic conditions (Figure 6Ai), and after 48h under hyperthermia (Figure 6Aii), there were no significant changes in the intracellular glutathione content. For all the MDMA metabolites studied, 24h of exposure significantly increased the intracellular total glutathione levels, at both normothermic and hyperthermic conditions (Figure 6Bi-Gi). SH-SY5Y differentiated cells exposed to all MDMA metabolites for 48h and under normothermic conditions presented a significant increase in intracellular total glutathione levels (Figure 6Bii-Gii). However, only the catechol MDMA metabolites α-MeDA (Figure 6Bii) and N-Me-α-MeDA (Figure 6Cii) significantly increased the intracellular total glutathione levels after 48h of exposure under hyperthermic conditions. Additionally, in all cases, the increases in total glutathione levels promoted by MDMA metabolites under hyperthermia were less pronounced than those observed under normothermic conditions.

Cell death induced by the catechol MDMA metabolite N-Me-α-MeDA in SH-SY5Y differentiated cells was accompanied by caspase 3 activation

To evaluate the involvement of apoptotic mechanisms on the toxic effects induced by MDMA metabolites, caspase 3 activity was evaluated after exposure of SH-SY5Y differentiated cells to MDMA metabolites, at the concentration of 100 μM, for 24h, under normothermic or hyperthermic conditions. Catechol MDMA metabolite N-Me-α-MeDA induced a significant increase in caspase 3 activity under hyperthermic conditions (Figure 7). For the remaining MDMA metabolites, there were no significant effects on caspase 3 activity, under our experimental conditions (data not shown).

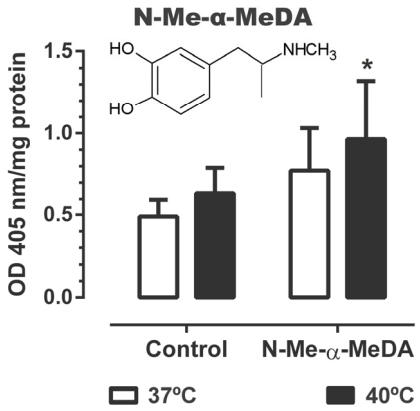


Figure 7. Caspase 3 activity in SH-SY5Y differentiated cells exposed to the catechol MDMA metabolite N-Me-α-MeDA. Cells were exposed to 100 μM of MDMA metabolite N-Me-α-MeDA, for 24h, under normothermic (37ºC) or hyperthermic (40ºC) conditions, and caspase 3 activity was then evaluated by a colorimetric assay. Results are presented as mean ± SD, from 8 independent experiments, and expressed in optical density at 405 nm per mg of protein (OD 405 nm/mg protein). Statistical comparisons were performed with two-way ANOVA, followed by the Bonferroni's multiple comparison *post-hoc* test (**p*<0.05 N-Me-α-MeDA *vs.* control, for the same temperature).

Discussion

Despite the increased number of data, the molecular and cellular mechanisms involved in MDMA-related neurotoxicity are still not completely understood. Previous works suggest an important role for systemic metabolism (Carvalho *et al.*, 2004b; Monks *et al.*, 2004; Capela *et al.*, 2007; Barbosa *et al.*, 2012). Nevertheless, hyperthermia, which is often associated with MDMA abuse (Capela *et al.*, 2009; Docherty and Green, 2010), is thought to contribute to MDMA's neurotoxicity (Capela *et al.*, 2006a; Capela *et al.*, 2006b; Capela *et al.*, 2009; Carvalho *et al.*, 2012). Though *in vivo* studies can provide a more realistic approximation of the effects associated with MDMA use by humans, *in vitro* models may be useful in understanding the events at molecular and cellular level. In the present study, MDMA metabolites were shown to be toxic to SH-SY5Y differentiated cells, being that both GSH and NAC conjugates revealed to be more toxic than their catechol precursors α-MeDA and N-Me-α-MeDA, as weel as the parent compound MDMA. Furthermore, it was shown that the temperature of exposure differently affected the neurotoxic potential of the MDMA metabolites. However, the antioxidant NAC conferred significant protection against the toxic effects mediated by MDMA metabolites. Therewithal, it was shown a time-dependent decrease in the concentration of MDMA metabolites in cell culture medium, an effect also potentiated by hyperthermia. Additionally, it was observed that MDMA and its metabolites differentially modulated the intracellular glutathione status, with the MDMA metabolites promoting an increase in the intracellular glutathione levels, whereas MDMA decreased it. Finally, it was demonstrated that the cell death induced by the MDMA metabolite N-Me-α-MeDA was associated with caspase 3 activation.

MDMA-associated neurotoxicity has been reported *in vitro* and *in vivo*, though the role of systemic metabolism and hyperthermia is not completely elucidated. As demonstrated by some studies (Gollamudi *et al.*, 1989; Bai *et al.*, 1999; Esteban *et al.*, 2001), metabolism seems to be required for MDMA-induced neurotoxicity. Furthermore, MDMA was shown to cause acute hyperthermia in laboratory animals (Green *et al.*, 2003; Capela *et al.*, 2009), which has been related to the acute- and long-lasting effects of this drug into the brain (Malberg and Seiden, 1998; Touriño *et al.*, 2010). In humans, MDMA-induced hyperthermia can be fatal (Capela *et al.*, 2009). Moreover, by preventing MDMA-induced hyperthermia, a decrease in acute- and long-term neurotoxic effects of MDMA was observed (Johnson and Yamamoto, 2010; Touriño *et al.*, 2010). In our experimental conditions, no toxic effects were observed for the parent compound MDMA. In accordance, several studies failed to demonstrate neurotoxicity when MDMA was directly injected into the rat brain (Bai *et al.*, 1999; Esteban *et al.*, 2001). However, neurotoxic

effects were observed after its peripheral administration (de la Torre and Farré, 2004; Monks *et al.*, 2004). Furthermore, the observations indicating that MDMA metabolites are found in the brain (Chu *et al.*, 1996; Jones *et al.*, 2005; Erives *et al.*, 2008) and that the inhibition of the CYP450 metabolism attenuates MDMA-mediated depletion in brain neurotransmitters (Gollamudi *et al.*, 1989), suggest a major role for metabolism in MDMA-induced neurotoxicity. Here, the 6 MDMA metabolites studied presented higher neurotoxic potential than MDMA, which was differently influenced by the time and temperature of exposure. Furthermore, both mitochondrial dysfunction and cell death were more pronounced with the GSH- and NAC-conjugated metabolites than with their two catechol precursors. A higher neurotoxic potential for the MDMA metabolites was also previously shown in rat cultured cortical neurons (Capela *et al.*, 2006a; Capela *et al.*, 2007) and also for the two catechol MDMA metabolites in SH-SY5Y differentiated cells (Ferreira *et al.*, 2013). Similar results were also previously reported in non-neuronal cells, such as rat cardiomyocytes (Carvalho *et al.*, 2004b; Shenouda *et al.*, 2009), rat hepatocytes (Carvalho *et al.*, 2004a) and rat and human renal proximal tubular cells (Carvalho *et al.*, 2002).

Other reports indicate that peripheral metabolism of N-Me-α-MeDA and α-MeDA is required for the development of metabolism-associated neurotoxic events (Miller *et al.*, 1996), since their direct injection in the brain did not elicit neurotoxicity (McCann *et al.*, 1994; Escobedo *et al.*, 2005). Indeed, the GSH-conjugated metabolites of N-Me-α-MeDA and α-MeDA, which can be transported into the brain (Miller *et al.*, 1996; Erives *et al.*, 2008), were highly toxic to SH-SY5Y differentiated cells. Moreover, their respective NAC conjugates, which are slowly eliminated and, consequently, persistent in the brain (Jones *et al.*, 2005; Erives *et al.*, 2008), presented also high toxicity, in agreement with previous studies published in rat cultured cortical neurons (Capela *et al.*, 2006a; Capela *et al.*, 2007). Notably, we observed that the temperature and time of exposure differently affected the toxicity profile of MDMA metabolites. The catechol MDMA metabolites presented a time-dependent toxicity, which was potentiated by hyperthermia. Recently, in the same experimental model, our group demonstrated that these two catechol metabolites of MDMA induced mitochondrial dysfunction in a time-dependent manner, though the role of temperature was not studied (Ferreira *et al.*, 2013). Furthermore, in rat cultured cortical neurons, the two catechol MDMA metabolites used in this study showed a time- and temperature-dependent toxicity after 24h of exposure (Capela *et al.*, 2006a). The present study used 6 MDMA metabolites, including the GSH- and NAC-conjugated, and extended the findings of previous studies, using a human dopaminergic neuronal model.

A factor many times neglected in *in vitro* studies is the potential decay of compounds when placed in biological medium, at 37ºC, during large periods of exposure. Indeed, MDMA metabolites can undergo auto-oxidation processes and also react with compounds present in biological matrices, thus promoting their concentration decrease over time. Therefore, we studied the stability of these compounds over time in cell culture medium. Here, we show an over time decrease in MDMA metabolites concentration in cell medium, not only for the catechol precursors, but also for the GSH and NAC conjugates of α-MeDA, which was accelerated by hyperthermia. However, the catechol metabolites were more stable in cell culture medium than the GSH and NAC conjugates. Indeed, previous *in vitro* studies demonstrated an over time decrease in N-Me-α-MeDA and α-MeDA concentrations in biological media, which was associated with oxidation to the corresponding aminochromes (Carvalho *et al.*, 2004b). Therefore, the results demonstrating potentiation of the neurotoxic effect under hyperthermia and higher amount of metabolite in culture medium under normothermic conditions, comparatively to hyperthermia, suggest that a degradation product may be involved in the toxic effect. Indeed, in the chromatograms obtained for the catechol MDMA metabolite α-MeDA, it was observed an increased amount over time of a compound with similar retention time to α-MeDA (data not shown). Therefore, knowing that MDMA metabolites may be converted to aminochromes (Carvalho *et al.*, 2004b), it is expected that these oxidation products may play a role in metabolism-related neurotoxicity of MDMA. The reactive intermediates produced during the oxidation of these catechol metabolites into reactive *ortho*-quinones and/or aminochromes can be conjugated with GSH to form the corresponding glutathionyl adducts (Hiramatsu *et al.*, 1990). Therefore, the higher neurotoxic potential of these compounds under hyperthermia suggest that hyperthermia may, perhaps, accelerate the formation of these conjugates, which, in this study, were demonstrated to be more toxic than their catechol precursors.

It was previously demonstrated that the exposure of rat cultured cortical neuronal cultures to GSH and NAC-conjugated metabolites of MDMA, for a short period of 6h, led to mitochondrial dysfunction in a time- and temperature-dependent manner (Capela *et al.*, 2007). In this study, NAC-conjugated metabolites were more toxic under normothermic conditions, whereas the neurotoxic effect mediated by GSH conjugates was independent of the temperature of exposure. However, similarly to the catechol metabolites, faster over time decrease in the concentration of both GSH- and NAC-conjugated metabolites was observed under hyperthermic conditions. Here, the apparent contradictory results observed for these metabolites may result from the longer periods of exposure tested (24 and 48h). Furthermore, variations in receptors and/or transporters, or in intracellular regulatory mechanisms between neuronal models, may also contribute to the observed

results. Additionally, considering the results of stability of the GSH- and NAC-conjugated metabolites in culture medium without cells, the independence on the exposure time for the neurotoxic effects may result from the low concentration that was already observed after 24h of incubation, which, therefore, is unable to potentiate the toxicity when cells are further exposed to metabolites for 48h.

Interestingly, though the intracellular amount of the studied metabolites was lower than the content in the extracellular compartment, the catechol metabolites presented higher intracellular content (ranging from 3 to 4 nmole/mg protein) than the 5-(NAC)-α-MeDA (intracellular concentrations lower than 1.5 nmole/mg protein). However, whereas the intracellular concentration of the catechol metabolites remained stable during the time courses studied, an over time decrease of the 5-(NAC)-α-MeDA concentration was observed, though in all cases, its intracellular levels were not significantly affected by the temperature of exposure. Therefore, these results suggest that extracellular mechanisms may greatly contribute to the toxic effects mediated by these compounds. In fact, other findings demonstrated a DAT-independent mechanism of uptake for the neurotoxic effects elicited by the mixture of MDMA and its 6 metabolites (the same used in the present study) (Barbosa *et al.*, 2013), as well as by the catechol MDMA metabolites (Ferreira *et al.*, 2013), in this experimental model.

Among the different factors that have been implicated in MDMA-induced neurotoxicity, such as hyperthermia, sustained receptor stimulation, MAO-related metabolism of 5-HT and dopamine, and hepatic formation of neurotoxic metabolites (Capela *et al.*, 2009; Carvalho *et al.*, 2012), oxidative stress constitutes a common outcome. Furthermore, the mechanisms underlying the toxicity of MDMA metabolites is thought to involve the reactivity of their catechol moiety (Carvalho *et al.*, 2004a). In agreement, increased ROS production after exposure to MDMA metabolites, which was proved to occur in mouse brain synaptosomes (Barbosa *et al.*, 2012) and rat cultured cortical neurons (Capela *et al.*, 2007), was implicated on their neurotoxic effects. Therefore, we evaluated the effects of an antioxidant against the toxic effects induced by MDMA metabolites. The antioxidant NAC protected against the mitochondrial dysfunction induced by MDMA metabolites. Indeed, after 24h of exposure, the toxicity of the two catechol metabolites and respective NAC conjugates was blunted at normothermic conditions. These findings are in line with previous published studies from our group (Carvalho *et al.*, 2004a; Capela *et al.*, 2007; Barbosa *et al.*, 2012; Ferreira *et al.*, 2013). Previously, it was demonstrated that the conjugation of MDMA metabolites with GSH and NAC increased their reactivity (Macedo *et al.*, 2007) and, consequently, their toxicity (Capela *et al.*, 2007). In accordance, the MDMA-conjugated metabolites revealed to be more toxic than their catechol precursors and parent compound MDMA. In fact, the protective effect mediated by NAC against the

toxicity of the GSH-conjugated metabolites of MDMA was lower, compared to the protection observed in the presence of the catechol precursors. Additionally, these differences on the protection conferred by NAC against the neurotoxic effects mediated by NAC- and GSH-conjugated metabolites support the notion that these metabolites present different toxic potential, which, at least in part, may justify the differential effect of the exposure temperature in their toxic effect.

Many conditions are known to change glutathione homeostasis, namely oxidative stress, which has been frequently associated with a cellular response leading to increased cellular GSH levels (Godwin *et al.*, 1992; Shi *et al.*, 1994). Here, we found that the MDMA metabolites induced a significant increase in intracellular glutathione content. In the same line, similar results were found in previous studies performed in the same experimental model, after exposure to neurotoxic insults mediating oxidative stress (Núñez *et al.*, 2004; Aguirre *et al.*, 2007), by a mechanism involving the up-regulation of γ-GCL activity. Moreover, and using the same experimental model, previous studies showed increased intracellular glutathione levels after exposure to the catechol MDMA metabolites (Ferreira *et al.*, 2013) or to the mixture of the same metabolites tested here (Barbosa *et al.*, 2013), which were demonstrated to result from a *de novo* synthesis. Therefore, we are confident to state that a *de novo* synthesis of GSH may be involved on the modulatory effects of MDMA metabolites in intracellular glutathione levels in this cellular model. In contrast to its metabolites, MDMA decreased the intracellular glutathione levels in SH-SY5Y differentiated cells (48h of exposure, under normothermia). Glutathione depletion has already been reported in non-neuronal cells, including isolated rat (Beitia *et al.*, 1999; Carvalho *et al.*, 2004a) and mouse (Carvalho *et al.*, 2001) hepatocytes, exposed to MDMA.

In vivo studies have demonstrated the potential of MDMA to induce cell death in several brain regions of laboratory animals (Commins *et al.*, 1987; Hatzidimitriou *et al.*, 1999; Schmued, 2003). Though limited in scope, studies in MDMA users have also showed the potential of MDMA to induce neuronal injury in discrete areas of the brain, such as cortex, striatum, raphe nuclei, and hippocampus (Capela *et al.*, 2009; Carvalho *et al.*, 2012; Parrott, 2012). The neurotoxic effect mediated by the catechol MDMA metabolite N-Me-α-MeDA involved caspase 3 activation, though for the remaining metabolites studied there were no significant differences in caspase 3 activity, when compared with the control. Notably, it was previously reported increased caspase 3 activity after exposure of SH-SY5Y undifferentiated cells to the same catechol metabolite (0.1 to 1 mM) (Felim *et al.*, 2009). However, in another recent study, no changes in caspase 3 activity were found in SH-SY5Y differentiated cells exposed either to N-Me-α-MeDA (400 μM) or α-MeDA (400 μM) for 24 or 48h (Ferreira *et al.*, 2013). In the present

study we used a lower concentration of 100 μM. Therefore, our results suggest that low concentrations of MDMA metabolites may elicit a more apoptotic death profile, meanwhile higher concentrations may trigger a more necrotic process. Though an apoptotic death profile accompanied by caspase 3 activation was previously demonstrated in rat cultured cortical neurons exposed to the NAC-conjugated metabolites of MDMA for 6h (Capela *et al.*, 2007), these differences among studies may result from the different times of exposure tested or variations in intracellular regulatory mechanisms between neuronal models.

In conclusion, this study evaluated the neurotoxicity of 6 MDMA metabolites, in a human dopaminergic neuronal model, and showed that MDMA metabolites may be major effectors in MDMA-induced neurotoxicity. Furthermore, it was established the time-course of stability for some MDMA metabolites in the cellular medium, a factor often neglected in *in vitro* studies. Additionally, it was further confirmed that hyperthermia, a common outcome associated with "ecstasy" consumption, may differentially affect the stability and neurotoxicity of MDMA metabolites.

Acknowledgements

This work was supported by "Fundação para a Ciência e a Tecnologia" (FCT), Portugal (Project PTDC/SAU-FCF/102958/2008), under the framework of the "Programa Operacional Temático Factores de Competitividade (COMPTE) do Quadro Comunitário de Apoio III" and "Fundo Comunitário Europeu" (FEDER) (FCOMP-01-0124-FEDER-011079). The NMR spectrometers are part of "The National NMR Facility", supported by FCT (RECI/BBB-BQB/0230/2012). DJB was supported by a fellowship (SFRH/BD/64939/2009) from FCT, Portugal.

Conflict of Interest

The authors declare that they have no conflict of interest.

References

Ádori C, Andó RD, Kovács GG, Bagdy G (2006). Damage of serotonergic axons and immunolocalization of Hsp27, Hsp72, and Hsp90 molecular chaperones after a single dose of MDMA administration in Dark Agouti rat: Temporal, spatial, and cellular patterns. J Comp Neurol 497:251-269.

Aguirre P, Valdés P, Aracena-Parks P, Tapia V, Núñez MT (2007). Upregulation of γ-glutamate-cysteine ligase as part of the long-term adaptation process to iron accumulation in neuronal SH-SY5Y cells. Am J Physiol Cell Physiol 292:2197-2203.

Bai F, Jones DC, Lau SS, Monks TJ (2001). Serotonergic neurotoxicity of 3,4-(±)-methylenedioxyamphetamine and 3,4-(±)-methylendioxymethamphetamine (ecstasy) is potentiated by inhibition of γ-glutamyl transpeptidase. Chem Res Toxicol 14:863-870.

Bai F, Lau SS, Monks TJ (1999). Glutathione and N-acetylcysteine conjugates of α-methyldopamine produce serotonergic neurotoxicity: possible role in methylenedioxyamphetamine-mediated neurotoxicity. Chem Res Toxicol 12:1150-1157.

Ballatori N, Krance SM, Marchan R, Hammond CL (2009). Plasma membrane glutathione transporters and their roles in cell physiology and pathophysiology. Mol Aspects Med 30:13-28.

Barbosa DJ, Capela JP, Oliveira JMA, Silva R, Ferreira LM, Siopa F, et al. (2012). Pro-oxidant effects of Ecstasy and its metabolites in mouse brain synaptosomes. Br J Pharmacol 165:1017-1033.

Barbosa DJ, Capela JP, Silva R, Vilas-Boas V, Ferreira LM, Branco PS, et al. (2013). The mixture of “ecstasy” and its metabolites is toxic to human SH-SY5Y differentiated cells at *in vivo* relevant concentrations. Arch Toxicol.

Beitia G, Cobreros A, Sainz L, Cenarruzabeitia E (1999). 3,4-Methylenedioxymethamphetamine (ecstasy)-induced hepatotoxicity: effect on cytosolic calcium signals in isolated hepatocytes. Liver 19:234-241.

Capela JP, Carmo H, Remião F, Bastos ML, Meisel A, Carvalho F (2009). Molecular and cellular mechanisms of ecstasy-induced neurotoxicity: an overview. Mol Neurobiol 39:210-271.

Capela JP, Macedo C, Branco PS, Ferreira LM, Lobo AM, Fernandes E, et al. (2007). Neurotoxicity mechanisms of thioether ecstasy metabolites. Neuroscience 146:1743-1757.

Capela JP, Meisel A, Abreu AR, Branco PS, Ferreira LM, Lobo AM, et al. (2006a). Neurotoxicity of ecstasy metabolites in rat cortical neurons, and influence of hyperthermia. J Pharmacol Exp Ther 316:53-61.

Capela JP, Ruscher K, Lautenschlager M, Freyer D, Dirnagl U, Gaio AR, et al. (2006b). Ecstasy-induced cell death in cortical neuronal cultures is serotonin 2A-receptor-dependent and potentiated under hyperthermia. Neuroscience 139:1069-1081.

Carvalho M, Carmo H, Costa VM, Capela JP, Pontes H, Remião F, et al. (2012). Toxicity of amphetamines: an update. Arch Toxicol 86:1167-1231.

Carvalho M, Carvalho F, Bastos ML (2001). Is hyperthermia the triggering factor for hepatotoxicity induced by 3,4-methylenedioxymethamphetamine (ecstasy)? An *in vitro* study using freshly isolated mouse hepatocytes. Arch Toxicol 74:789-793.

Carvalho M, Hawksworth G, Milhazes N, Borges F, Monks TJ, Fernandes E, et al. (2002). Role of metabolites in MDMA (ecstasy)-induced nephrotoxicity: an *in vitro* study using rat and human renal proximal tubular cells. Arch Toxicol 76:581-588.

Carvalho M, Remiao F, Milhazes N, Borges F, Fernandes E, Carvalho F, et al. (2004a). The toxicity of N-methyl-alpha-methyldopamine to freshly isolated rat hepatocytes is prevented by ascorbic acid and N-acetylcysteine. Toxicology 200:193-203.

Carvalho M, Remião F, Milhazes N, Borges F, Fernandes E, Monteiro MC, et al. (2004b). Metabolism is required for the expression of ecstasy-induced cardiotoxicity *in vitro*. Chem Res Toxicol 17:623-632.

Chadwick IS, Curry PD, Linsley A, Freemont AJ, Doran B (2001). Ecstasy, 3-4 methylenedioxymethamphetamine (MDMA), a fatality associated with coagulopathy and hyperthermia. J R Soc Med 84:371.

Chu T, Kumagai Y, DiStefano EW, Cho AK (1996). Disposition of methylenedioxymethamphetamine and three metabolites in the brains of different rat strains and their possible roles in acute serotonin depletion. Biochem Pharmacol 51:789-796.

Commins DL, Vosmer G, Virus RM, Woolverton WL, Schuster CR, Seiden LS (1987). Biochemical and histological evidence that methylenedioxymethylamphetamine (MDMA) is toxic to neurons in the rat brain. J Pharmacol Exp Ther 241:338-345.

Constantinescu R, Constantinescu AT, Reichmann H, Janetzky B (2007). Neuronal differentiation and long-term culture of the human neuroblastoma line SH-SY5Y. J Neural Transm Suppl 72:17-28.

de la Torre R, Farré M (2004). Neurotoxicity of MDMA (ecstasy): the limitations of scaling from animals to humans. Trends Pharmacol Sci 25:505-508.

Docherty JR, Green AR (2010). The role of monoamines in the changes in body temperature induced by 3,4-methylenedioxymethamphetamine (MDMA, ecstasy) and its derivatives. Br J Pharmacol 160:1029-1044.

Erives GV, Lau SS, Monks TJ (2008). Accumulation of neurotoxic thioether metabolites of 3,4-(±)-methylenedioxymethamphetamine in rat brain. J Pharmacol Exp Ther 324:284-291.

Erritzoe D, Frokjaer VG, Holst KK, Christoffersen M, Johansen SS, Svarer C, et al. (2011). *In vivo* imaging of cerebral serotonin transporter and serotonin2a receptor binding in 3,4-methylenedioxymethamphetamine (mdma or “ecstasy”) and hallucinogen users. Arch Gen Psychiatry 68:562-576.

Escobedo I, O’Shea E, Orio L, Sanchez V, Segura M, de la Torre R, et al. (2005). A comparative study on the acute and long-term effects of MDMA and 3,4-dihydroxymethamphetamine (HHMA) on brain monoamine levels after i.p. or striatal administration in mice. Br J Pharmacol 144:231-241.

Esteban B, O'Shea E, Camarero J, Sanchez V, Green AR, Colado MI (2001). 3,4-Methylenedioxymethamphetamine induces monoamine release, but not toxicity, when administered centrally at a concentration occurring following a peripherally injected neurotoxic dose. Psychopharmacology 154:251-260.

Farfel GM, Seiden LS (1995). Role of hypothermia in the mechanism of protection against serotonergic toxicity. I. Experiments using 3,4-methylenedioxymethamphetamine, dizocilpine, CGS 19755 and NBQX. J Pharmacol Exp Ther 272:860-867.

Felim A, Herrera G, Neudörffer A, Blanco M, O’Connor J, Largeron M (2009). Synthesis and *in vitro* cytotoxicity profile of the R-enantiomer of 3,4-dihydroxymethamphetamine (R-(−)-HHMA): comparison with related catecholamines. Chem Res Toxicol 23:211-219.

Ferreira PS, Nogueira TB, Costa VM, Branco PS, Ferreira LM, Fernandes E, et al. (2013). Neurotoxicity of “ecstasy” and its metabolites in human dopaminergic differentiated SH-SY5Y cells. Toxicol Lett 216:159-170.

Godwin AK, Meister A, O'Dwyer PJ, Huang CS, Hamilton TC, Anderson ME (1992). High resistance to cisplatin in human ovarian cancer cell lines is associated with marked increase of glutathione synthesis. Proc Natl Acad Sci U S A 89:3070-3074.

Gollamudi R, Ali SF, Lipe G, Newport G, Webb P, Lopez M, et al. (1989). Influence of inducers and inhibitors on the metabolism *in vitro* and neurochemical effects *in vivo* of MDMA. Neurotoxicology 10:455-466.

Granado N, Ares-Santos S, Oliva I, O´Shea E, Martin ED, Colado MI, et al. (2011). Dopamine D2-receptor knockout mice are protected against dopaminergic neurotoxicity induced by methamphetamine or MDMA. Neurobiol Dis 42:391-403.

Green AR, Mechan AO, Elliott JM, O'Shea E, Colado MI (2003). The pharmacology and clinical pharmacology of 3,4-methylenedioxymethamphetamine (MDMA, "ecstasy"). Pharmacol Rev 55:463-508.

Hatzidimitriou G, McCann UD, Ricaurte GA (1999). Altered serotonin innervation patterns in the forebrain of monkeys treated with (+/-)3,4-methylenedioxymethamphetamine seven years previously: factors influencing abnormal recovery. J Neurosci 19:5096-5107.

Henry JA, Jeffreys KJ, Dawling S (1992). Toxicity and deaths from 3,4-methylenedioxymethamphetamine ("ecstasy"). Lancet 340:384-387.

Hiramatsu M, Kumagai Y, Unger SE, Cho AK (1990). Metabolism of methylenedioxymethamphetamine: formation of dihydroxymethamphetamine and a quinone identified as its glutathione adduct. J Pharmacol Exp Ther 254:521-527.

Johnson BN, Yamamoto BK (2010). Chronic stress enhances the corticosterone response and neurotoxicity to +3,4-methylenedioxymethamphetamine (MDMA): the role of ambient temperature. J Pharmacol Exp Ther 335:180-189.

Jones DC, Duvauchelle C, Ikegami A, Olsen CM, Lau SS, de la Torre R, et al. (2005). Serotonergic neurotoxic metabolites of ecstasy identified in rat brain. J Pharmacol Exp Ther 313:422-431.

Kish SJ, Fitzmaurice PS, Chang LJ, Furukawa Y, Tong J (2010a). Low striatal serotonin transporter protein in a human polydrug MDMA (ecstasy) user: a case study. J Psychopharmacol 24:281-284.

Kish SJ, Lerch J, Furukawa Y, Tong J, McCluskey T, Wilkins D, et al. (2010b). Decreased cerebral cortical serotonin transporter binding in ecstasy users: a positron emission tomography/[11C]DASB and structural brain imaging study. Brain 133:1779-1797.

Lowry OH, Rosebrough NJ, Farr AL, Randall RJ (1951). Protein measurement with the folin phenol reagent. J Biol Chem 193:265-275.

Macedo C, Branco PS, Ferreira LM, Lobo AM, Capela JP, Fernandes E, et al. (2007). Sinthesis and cyclic voltammetry studies of 3,4-methylenedioxymethamphetamine (MDMA) human metabolites. J Health Sci 53:31-42.

Malberg JE, Seiden LS (1998). Small Changes in Ambient Temperature Cause Large Changes in 3,4-Methylenedioxymethamphetamine (MDMA)-Induced Serotonin Neurotoxicity and Core Body Temperature in the Rat. J Neurosci 18:5086-5094.

McCann UD, Ridenour A, Shaham Y, Ricaurte GA (1994). Serotonin neurotoxicity after (+/-)3,4-methylenedioxymethamphetamine (MDMA; "Ecstasy"): a controlled study in humans. Neuropsychopharmacology 10:129-138.

Miller RT, Lau SS, Monks TJ (1996). Effects of intracerebroventricular administration of 5-(glutathion-*S*-yl)-α-methyldopamine on brain dopamine, serotonin, and norepinephrine concentrations in male Sprague-Dawley rats. Chem Res Toxicol 9:457-465.

Monks TJ, Jones DC, Fengju B, Lau SS (2004). The role of metabolism in 3,4-Methylenodioxyamphetamine and 3,4-Methylenodioxymethamphetamine (Ecstasy) toxicity. Ther Drug Monit 26:132-136.

Núñez MT, Gallardo V, Muñoz P, Tapia V, Esparza A, Salazar J, et al. (2004). Progressive iron accumulation induces a biphasic change in the glutathione content of neuroblastoma cells. Free Radic Biol Med 37:953-960.

Parrott AC (2012). MDMA and 5-HT neurotoxicity: the empirical evidence for its adverse effects in humans – no need for translation. Br J Pharmacol 166:1518-1520.

Patel NJ, Fullone JS, Anders MW (1993). Brain uptake of S-(1,2-dichlorovinyl)glutathione and S-(1,2-dichlorovinyl)-L-cysteine, the glutathione and cysteine S-conjugates of the neurotoxin dichloroacetylene. Brain Res Mol Brain Res 17:53-58.

Presgraves S, Ahmed T, Borwege S, Joyce J (2003). Terminally differentiated SH-SY5Y cells provide a model system for studying neuroprotective effects of dopamine agonists. Neurotox Res 5:579-598.

Quednow BB, Jessen F, Kühn K, Maier W, Daum I, Wagner M (2006). Memory deficits in abstinent MDMA (ecstasy) users: neuropsychological evidence of frontal dysfunction. J Psychopharmacol 20:373-384.

Ricaurte GA, DeLanney LE, Irwin I, Langston JW (1988). Toxic effects of MDMA on central serotonergic neurons in the primate: importance of route and frequency of drug administration. Brain Res 446:165-168.

Roberts GMP, Nestor L, Garavan H (2009). Learning and memory deficits in ecstasy users and their neural correlates during a face-learning task. Brain Res 1292:71-81.

Schmued LC (2003). Demonstration and localization of neuronal degeneration in the rat forebrain following a single exposure to MDMA. Brain Res 974:127-133.

Shenouda SK, Varner KJ, Carvalho F, Lucchesi PA (2009). Metabolites of MDMA induce oxidative stress and contractile dysfunction in adult rat left ventricular myocytes. Cardiovasc Toxicol 9:30-38.

Shi MM, Kugelman A, Iwamoto T, Tian L, Forman HJ (1994). Quinone-induced oxidative stress elevates glutathione and induces gamma-glutamylcysteine synthetase activity in rat lung epithelial L2 cells. J Biol Chem 269:26512-26517.

Silva R, Boldt S, Costa VM, Carmo H, Carvalho M, Carvalho F, et al. (2007). Evaluation of GSH adducts of adrenaline in biological samples. Biomed Chromatogr 21:670-679.

Slot AJ, Wise DD, Deeley RG, Monks TJ, Cole SPC (2008). Modulation of human multidrug resistance protein (MRP) 1 (ABCC1) and MRP2 (ABCC2) transport activities by endogenous and exogenous glutathione-conjugated catechol metabolites. Drug Metab Dispos 36:552-560.

Tai YF, Hoshi R, Brignell CM, Cohen L, Brooks DJ, Curran HV, et al. (2011). Persistent nigrostriatal dopaminergic abnormalities in ex-users of MDMA ("Ecstasy"): an 18F-dopa PET study. Neuropsychopharmacology 36:735-743.

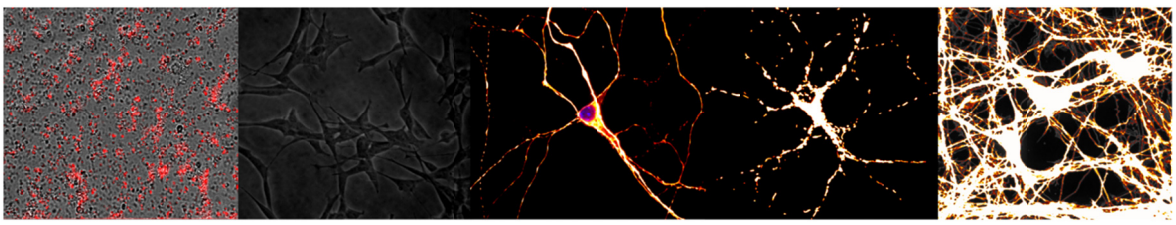
Takeuchi H, Yanagida T, Inden M, Takata K, Kitamura Y, Yamakawa K, et al. (2009). Nicotinic receptor stimulation protects nigral dopaminergic neurons in rotenone-induced Parkinson's disease models. J Neurosci Res 87:576-585.

Touriño C, Zimmer A, Valverde O (2010). THC prevents MDMA neurotoxicity in mice. PLoS ONE 5:e9143.

4.

The mixture of “ecstasy” and its metabolites is toxic to human SH-SY5Y differentiated cells at *in vivo* relevant concentrations

Reprinted from ***Archives of Toxicology***,
[Epub ahead of print]
Copyright © ***Springer-Verlag Berlin Heidelberg*** 2013



Arch Toxicol
DOI 10.1007/s00204-013-1120-7

ORGAN TOXICITY AND MECHANISMS

The mixture of "ecstasy" and its metabolites is toxic to human SH-SY5Y differentiated cells at in vivo relevant concentrations

Daniel José Barbosa · João Paulo Capela · Renata Silva · Vânia Vilas-Boas · Luísa Maria Ferreira · Paula Sério Branco · Eduarda Fernandes · Maria de Lourdes Bastos · Félix Carvalho

Received: 24 May 2013 / Accepted: 22 August 2013
© Springer-Verlag Berlin Heidelberg 2013

Abstract The neurotoxicity of "ecstasy" (3,4-methylenedioxymethamphetamine, MDMA) is thought to involve hepatic metabolism, though its real contribution is not completely understood. Most in vitro neurotoxicity studies concern isolated exposures of MDMA or its metabolites, at high concentrations, not considering their mixture, as expected in vivo. Therefore, our postulate is that combined deleterious effects of MDMA and its metabolites, at low micromolar concentrations that may be attained into the brain, may elicit neurotoxicity. Using human SH-SY5Y differentiated cells as dopaminergic neuronal model, we studied the neurotoxicity of MDMA and its MDMA metabolites α-methyldopamine and *N*-methyl-α-methyldopamine and their correspondent glutathione and *N*-acetylcysteine monoconjugates, under isolated exposure and as a mixture, at normothermic or hyperthermic conditions. The results showed that the mixture of MDMA and its metabolites was toxic to SH-SY5Y differentiated cells, an effect potentiated by hyperthermia and prevented by *N*-acetylcysteine. As a mixture, MDMA and its metabolites presented a different toxicity profile, compared to each compound alone, even at equimolar concentrations. Caspase 3 activation, increased reactive oxygen species production, and intracellular Ca^{2+} raises were implicated in the toxic effect. The mixture increased intracellular glutathione levels by increasing its de novo synthesis. In conclusion, this study demonstrated, for the first time, that the mixture of MDMA and its metabolites, at low micromolar concentrations, which represents a more realistic approach of the in vivo scenario, elicited toxicity to human SH-SY5Y differentiated cells, thus constituting a new insight into the context of MDMA-related neurotoxicity.

Keywords 3,4-Methylenedioxymethamphetamine (MDMA or "ecstasy") · MDMA metabolites · SH-SY5Y differentiated cells · Oxidative stress · Neurotoxicity

D. J. Barbosa (✉) · J. P. Capela · R. Silva · V. Vilas-Boas · M. L. Bastos · F. Carvalho (✉)
REQUIMTE (Rede de Química e Tecnologia), Toxicology Laboratory, Department of Biological Sciences, Faculty of Pharmacy, University of Porto, Rua Jorge Viterbo Ferreira 228, 4050-313 Porto, Portugal
e-mail: daniel.barbosa@ff.up.pt

F. Carvalho
e-mail: felixdc@ff.up.pt

J. P. Capela
Faculty of Health Sciences, University Fernando Pessoa, Rua Carlos da Maia 296, 4200-150 Porto, Portugal

L. M. Ferreira · P. S. Branco
REQUIMTE/CQFB (Centro de Química Fina e Biotecnologia), Department of Chemistry, Faculty of Science and Technology, University Nova de Lisboa, 2829-516 Caparica, Portugal

E. Fernandes
REQUIMTE, Laboratory of Applied Chemistry, Department of Chemical Sciences, Faculty of Pharmacy, University of Porto, Rua Jorge Viterbo Ferreira 228, 4050-313 Porto, Portugal

Introduction

3,4-Methylenedioxymethamphetamine (MDMA or "ecstasy"), a psychoactive substance with hallucinogenic properties, is a worldwide major recreational drug with high abuse liability (Capela et al. 2009; Carvalho et al. 2012). The potential neurotoxic risk associated with its use has received particular attention following a study published in 1986, in which Schmidt et al. (1986) reported MDMA-associated damage to the serotonergic system after administration to rats. Following this study, many others have described the

Published online: 08 October 2013

potential neurotoxicity of MDMA to serotonergic and/or dopaminergic neurons, both in humans (Adamaszek et al. 2010; Roberts et al. 2009) and in laboratory animals (Bai et al. 2001; Granado et al. 2011). MDMA administration to rats results essentially in serotonergic toxicity (Bai et al. 2001; Jones et al. 2005), whereas in mice MDMA-induced neurotoxicity affects fundamentally the dopaminergic system (Cadet et al. 2001; Escobedo et al. 2005; Granado et al. 2008, 2011). Though limited in scope, studies with MDMA users have shown that MDMA has the potential to induce neuronal injury in discrete areas of the brain, such as cortex, striatum, raphe nuclei and hippocampus, thus affecting both serotonergic and dopaminergic neurons (for a comprehensive review, see Capela et al. 2009 and Carvalho et al. 2012).

Several factors have been shown to contribute for MDMA-induced neurotoxicity, namely hyperthermia, increased release of neurotransmitters from storage vesicles, monoamine oxidase-related metabolism of dopamine and serotonin (5-HT), auto-oxidation of dopamine, sustained receptors' stimulation, and formation of neurotoxic metabolites (Capela et al. 2009; Carvalho et al. 2012). It is generally believed that metabolism of MDMA into reactive intermediates is a major factor mediating its neurotoxic effects, since the direct local injection of MDMA into rat brain fails to produce the neurotoxic effects observed following its peripheral administration (Bai et al. 1999; Esteban et al. 2001). Despite this, it is likely that MDMA itself can promote neurotoxicity, especially because, in rats, neurotoxicity was most closely related to plasma and brain concentrations of MDMA, rather than its metabolites (Mueller et al. 2009b). Nevertheless, to evaluate MDMA neurotoxicity in vitro, most studies focus on MDMA or its metabolites under isolated exposures (Barbosa et al. 2012; Capela et al. 2007b; Carvalho et al. 2004a), rather than in mixture, at more realistic concentrations.

The hepatic metabolism of MDMA is mainly mediated by cytochrome P450 (CYP450) enzymes by *N*-demethylation, originating 3,4-methylenedioxyamphetamine (MDA). Both MDMA and MDA are then *O*-demethylenated to the catechol compounds *N*-methyl-α-methyldopamine (N-Me-α-MeDA) and α-methyldopamine (α-MeDA), respectively, which can undergo oxidation to the correspondent highly redox active *ortho*-quinones (Pizarro et al. 2004). While in humans and rats N-Me-α-MeDA is the main plasma metabolite of MDMA, in mice the rate of α-MeDA formation is higher, compared to N-Me-α-MeDA (de la Torre and Farré 2004). The *ortho*-quinones formed may undergo redox cycling, producing semiquinone radicals, which may lead to the generation of reactive oxygen species (ROS) or, additionally, may be conjugated with reduced glutathione (GSH), originating glutathionyl adducts (Erives et al. 2008). The systemic formation of 5-(glutathion-*S*-yl)-*N*-methyl-α-methyldopamine [5-(GSH)-N-Me-α-MeDA] and 5-(glutathion-*S*-yl)-α-methyldopamine [5-(GSH)-α-MeDA] is followed by their uptake into the brain (Erives et al. 2008; Jones et al. 2005). Furthermore, GSH conjugates may undergo further metabolism to *N*-acetylcysteine (NAC) conjugates, which are slowly eliminated and, consequently, persistent in the brain (Jones et al. 2005). Supporting the role of metabolism in MDMA-induced neurotoxicity is the study of Gollamudi et al. (1989), in which attenuation in MDMA-mediated depletions in 5-HT levels was observed by CYP450 metabolism inhibition.

In rats, after oral administration (20 mg/kg), high concentrations of MDMA were found in the brain (17.17 nmol/g brain) (Mueller et al. 2009b). Similarly, after subcutaneous injection (from 5 to 20 mg/kg), brain concentrations of MDMA ranged from 0.74 to 147.65 nmol/g brain, and plasma concentrations ranged from 0.00 to 15.78 μM (Chu et al. 1996), showing, therefore, that the brain accumulation of MDMA is clearly favored. Notably, in human-controlled studies, using doses similar to those consumed by recreational MDMA users, high plasmatic concentrations of MDMA were found (2.41 μM), after oral administration of the drug (2 mg/kg, which is equivalent to 10 and 20 mg/kg doses in rat and mice, respectively; Mueller et al. 2009a) (De La Torre et al. 2000; Morefield et al. 2011). Moreover, it was also shown the presence of the catechol MDMA metabolites (Chu et al. 1996) and their correspondent GSH and NAC conjugates (Erives et al. 2008; Jones et al. 2005) in the brain after subcutaneous administration of MDMA (20–40 mg/kg) to rats. Interestingly, the combined concentration of the four thioether metabolites in the rat brain striatal dialysate reached a maximum of 13 μM, which remained relatively unchanged for approximately 4 h after exposure to MDMA (4 × 20 mg/kg subcutaneous, at 12-h interval) (Erives et al. 2008). Therefore, it is expected that the neurotoxicity associated with MDMA may result from the combined effects of the parent compound and its metabolites.

From the above rationale, the hypothesis tested in the present study was that the combined deleterious effects of MDMA and its metabolites may contribute to the neurotoxicity of this drug, in a way that low micromolar concentrations, as observed in vivo, may elicit toxicity. For this purpose, the toxicity of MDMA and its metabolites was evaluated in human SH-SY5Y differentiated cells, either for each compound alone or as a mixture. Human SH-SY5Y cells are frequently used as in vitro neuronal model. Although they do not present all the characteristics of adult neurons in the brain (Takeuchi et al. 2009), these cells may acquire a neuronal dopaminergic phenotype after stimulation with several agents (Presgraves et al. 2003; Ferreira et al. 2013), making them a useful research tool to elucidate the toxicity mechanisms of several drugs (Presgraves

et al. 2003; Takeuchi et al. 2009). Since dopaminergic deficits have been linked to MDMA (Cadet et al. 2001; Granado et al. 2008; Ferreira et al. 2013), in vitro dopaminergic neuronal models may be useful to elucidate the molecular and cellular mechanisms involved in MDMA-related neurotoxicity.

Methods

Materials

All reagents used in this study were of analytical grade or of the highest grade available. Dulbecco's modified Eagle's medium (DMEM) with 4.5 g/L glucose and GlutaMAX™, DMEM without phenol red, Dulbecco's phosphate-buffered saline (DPBS), nonessential amino acids (NEAA), heat-inactivated fetal bovine serum (FBS), 0.25 % trypsin/ethylenediaminetetraacetic acid (EDTA), 0.05 % trypsin/EDTA, and Fluo3 acetoxymethyl ester (Fluo3/AM) were purchased from Gibco Laboratories (Lenexa, KS, USA). Penicillin (10,000 U/mL) and streptomycin (10,000 μg/mL) were purchased from Biochrom AG (Berlin, Germany). Trypan blue solution [0.4 % (w/v)], retinoic acid (RA), 12-*O*-tetradecanoylphorbol-13-acetate (TPA), phenylmethylsulfonyl fluoride (PMSF), complete protease inhibitor cocktail, rabbit polyclonal anti-dopamine transporter (DAT) N-terminal antibody, 3-(4,5-dimethyl-2-thiazolyl)-2,5-diphenyl-2H-tetrazolium (MTT) bromide, sodium dodecyl sulfate (SDS), L-lactic dehydrogenase (LDH), sodium pyruvate, nicotinamide adenine dinucleotide reduced form (NADH), triton X-100, caspase 3 subtract *N*-acetyl-Asp-Glu-Val-Asp-*p*-nitroaniline (Ac-DEVD-pNA), 4-(2-hydroxyethyl)piperazine-1-ethanesulfonic acid (HEPES), 3-[(3-cholamidopropyl)dimethylammonio]-1-propanesulfonate hydrate (Chaps), dithiothreitol (DTT), Tris–HCl, dichlorodihydrofluorescein diacetate (DCFH-DA), NAC, GSH, nicotinamide adenine dinucleotide phosphate reduced form (NADPH), 5,5-dithio-bis(2-nitrobenzoic acid (DTNB), glutathione reductase (GR), L-buthionine-sulfoximine (BSO), propidium iodide (Pi), ethylene glycol-bis(2-aminoethylether)-*N*,*N*,*N*′,*N*′-tetraacetic acid (EGTA), BAPTA acetoxymethyl ester (BAPTA/AM), and bovine serum albumin (BSA) were obtained from Sigma-Aldrich (St. Louis, MO, USA). Mouse anti-tyrosine hydroxylase (TH) antibody was purchased from Merck Millipore (Merck KGaA, Darmstadt, Germany). Rabbit anti-β-actin antibody was obtained from Santa Cruz Biotechnology (Santa Cruz, CA, USA). Anti-rabbit and anti-mouse IgG-peroxidase polyclonal antibodies were purchased from Amersham Pharmacia Biotech (Buckinghamshine, United Kingdom). Bio-Rad DC protein assay was obtained from Bio-Rad Laboratories (Hercules, CA, USA). EDTA, KH_2PO_4, $K_2HPO_4.3H_2O$, KCl, $MgCl_2.6H_2O$, dimethylsulfoxide (DMSO), HCl, $HClO_4$, NaOH, $KHCO_3$, and Folin reagent were obtained from Merck (Darmstadt, Germany). MDMA (hydrochloride salt) was extracted and purified from high-purity MDMA tablets, kindly provided by the Portuguese Criminal Police Department. The obtained salt was pure and fully characterized by nuclear magnetic resonance (NMR) and mass spectrometry methodologies, as previously described (Capela et al. 2007b). The MDMA metabolites α-MeDA, N-Me-α-MeDA, 5-(GSH)-α-MeDA, 5-(GSH)-N-Me-α-MeDA, 5-(*N*-acetylcysteine-*S*-yl)-α-methyldopamine [5-(NAC)-α-MeDA], and 5-(*N*-acetylcysteine-*S*-yl)-*N*-methyl-α-methyldopamine [5-(NAC)-N-Me-α-MeDA] were synthesized and fully characterized by NMR and mass spectrometry methodologies by REQUIMTE (Centro de Química Fina e Biotecnologia), Chemistry Department, Faculty of Science and Technology, University Nova de Lisboa, according to the methods previously published by our group (Capela et al. 2006a, 2007b). All other chemicals were purchased from Sigma-Aldrich.

Cell culture and differentiation

SH-SY5Y cells are a neuroblastoma cell line cloned from SK-N-SH cells. This cell line has been widely used as neuronal model since the early 1980s as these cells possess many biochemical and functional properties of neurons (Takeuchi et al. 2009). SH-SY5Y cells (ATCC, Manassas, VA, USA) were routinely cultured in 25-cm^2 flasks (Corning Costar, Corning, NY, USA) using DMEM with 4.5 g/L glucose and GlutaMAX™, supplemented with 10 % heat-inactivated FBS (v/v), 1 % NEAA (v/v), 100 U/mL penicillin, and 100 μg/mL streptomycin. Cells were maintained at 37 °C in a humidified atmosphere of 95 % air/5 % CO_2. Cultures were subcultivated weekly by trypsinization (0.25 % trypsin/EDTA). The cells used for all the experiments were taken between the 25th and 34th passages, in order to avoid phenotypic changes. SH-SY5Y undifferentiated cells may be differentiated upon treatment with a variety of agents, including RA and TPA (Lopes et al. 2010; Presgraves et al. 2003). To induce an increase in dopaminergic neuronal phenotype, SH-SY5Y cells were differentiated as described previously by our group (Ferreira et al. 2013). Thus, after counting the cells in a Fuchs-Rosenthal camera (using a trypan blue solution), SH-SY5Y cells were seeded at the density of 25,000 cells/cm^2, in complete medium containing 10 μM RA, and cultured for 3 days at 37 °C. After 3 days, 80 nM of TPA was added to the cultures, and cells were cultured for another 3 days at 37 °C. Stock solutions of RA (10 mM) and TPA (80 μM) were prepared in DMSO. Final concentration of DMSO in each well was 0.2 % (v/v). To confirm the enhancement of the dopaminergic phenotype, undifferentiated and differentiated SH-SY5Y cells

were seeded at the same time and conditions, and Western blotting analysis of DAT and TH expression was performed in both cell types. For MTT reduction and LDH assays and measurement of ROS production, SH-SY5Y differentiated cells were cultured onto 48-well culture plates (Corning Costar, Corning). For caspase 3 activity assay, assessment of intracellular glutathione levels, flow cytometry analysis of intracellular Ca^{2+} levels, and Western blotting analysis, SH-SY5Y differentiated cells were cultured onto 6-well culture plates (Corning Costar, Corning).

Western blotting analysis

In order to confirm the enhancement of the dopaminergic phenotype in SH-SY5Y cells differentiated with RA and TPA, Western blotting analyses against two important dopaminergic neuronal markers, DAT and TH, were performed, according to previously published protocols (Perry et al. 2010; Presgraves et al. 2003), with some modifications. Sister cultures of SH-SY5Y cells were seeded on 6-well culture plates, at a density of 25,000 cells/cm^2. A portion of cells were differentiated, as described above, and another part was maintained in culture in their undifferentiated state. After 6 days in culture, the time needed to perform the differentiation protocol, the medium was removed and the cells were scraped in 700 μL of cold DPBS with Ca^{2+} and Mg^{2+} [DPBS (+/+)] and then harvested (3 wells per condition). After centrifugation at 2,376*g* for 5 min at 4 °C, the supernatant was discarded and the resulting cellular pellet was stored at −80 °C until Western blotting analysis. To extract the proteins, cells were lysed in 125 μL of ice-cold lysis buffer [10 mM Tris–HCl, 5 mM EDTA, 150 mM NaCl, and 0.5 % triton X-100 (v/v), pH 7.4], supplemented with 1 mM DTT, 0.25 mM PMSF, and 1 % complete protease inhibitor cocktail (v/v), followed by incubation on ice for 30 min and centrifugation at 16,000*g* for 20 min at 4 °C. DTT (stock solution at 200 mM) was prepared in DMSO, and PMSF (stock solution at 50 mM) was prepared in absolute ethanol. After determination of the total protein concentration in the supernatant, using the Bio-Rad DC protein assay and BSA as standard, samples were diluted to equal protein concentration, and 50 μL was mixed with 25 μL SDS–PAGE reducing buffer [4 % SDS (w/v), 87.5 mM Tris base (pH 6.8), 22.5 % glycerol (v/v), 1 % bromophenol blue (w/v), and 20 % β-mercaptoethanol (v/v)]. Sixty micrograms of protein were loaded and separated on 10 % SDS/polyacrylamide gels, at a constant voltage of 150 mV, using a running buffer [25 mM Tris Base, 192 mM glycine, and 0.1 % SDS (w/v), pH 8.6]. Gels were allowed to equilibrate in transfer buffer [20 % methanol (v/v) in 25 mM Tris base and 192 mM glycine, pH 8.3] and then transferred to nitrocellulose membranes (Hybond ECL, Amersham Pharmacia Biotech) at a constant current of 200 mA for 2.5 h in a Bio-Rad semidry transfer apparatus (Bio-Rad Laboratories), according to the manufacturer's protocol. DAT was found to be extremely sensitive to the effects of heating the lysates, as this appeared to alter the conformation of critical epitopes sufficiently to prevent DAT antibody binding (Perry et al. 2010). Therefore, the lysates were not heated before loading the gel. Then, membranes were rinsed in Tris-buffered saline solution (TBS: 20 mM Tris base and 300 mM NaCl, pH 8.0), and nonspecific sites were blocked overnight in blocking buffer [5 % nonfat powdered skim milk (w/v) in Tris-buffered saline solution with 0.05 % Tween 20 (v/v) (TBS-T)] at 4 °C. Membranes were then incubated with primary antibodies: rabbit polyclonal anti-DAT (N-terminal) (1:500), mouse monoclonal anti-TH (1:1,000), or rabbit monoclonal anti-β-actin antibody (1:400) overnight, at 4 °C. After incubation with the primary antibodies, membranes were washed three times (10 min each) with TBS-T and incubated with the secondary antibodies [anti-rabbit or anti-mouse IgG-peroxidase polyclonal antibodies (1:2,000)] for 2 h at room temperature. All antibodies were diluted in blocking buffer. Following two washes in TBS-T (10 min each), bands were visualized with ECL Plus chemiluminescence reagents (Amersham Pharmacia Biotech), according to the supplier's instructions, and developed on high-performance chemiluminescence films (Amersham Pharmacia Biotech) with Kodak Film Developer and Kodak Fixer (Sigma-Aldrich). Bands in the films were quantified using the Quantity One software (Bio-Rad Laboratories). β-Actin was used as loading control. To normalize DAT and TH immunoreactivity, OD ratio of the DAT/β-actin and TH/β-actin was calculated. Final results, from three independent experiments (each experiment was performed in duplicate), are expressed as percentage of DAT or TH expression compared to undifferentiated cells [DAT or TH expression (% of undifferentiated cells)].

Studies on differentiated cells

After conclusion of the differentiation protocol, the medium of each well was removed and replaced by new medium containing a single compound, MDMA or its metabolites α-MeDA, N-Me-α-MeDA, 5-(GSH)-α-MeDA, 5-(GSH)-N-Me-α-MeDA, 5-(NAC)-α-MeDA, and 5-(NAC)-N-Me-α-MeDA, at the concentrations of 10, 20, 70, or 140 μM, or the mixture of the seven drugs (each compound at 10 or 20 μM). Cultures were incubated for a period of 24 or 48 h, under normothermic (37 °C) or hyperthermic (40 °C) conditions, in a humidified atmosphere of 95 % air/5 % CO_2. Temperature for the hyperthermic experiments was selected according to previous studies published by our group (Capela et al. 2006a, b, 2007b). Particularly, to assess the

ROS production, measurements were taken hourly, during 6 h. The concentration of NAC was selected from studies in rat cortical neurons (Capela et al. 2007b). DAT inhibitor (GBR 12909) concentration was in accordance with a previous study showing complete inhibition of DAT-mediated transport (Shavali and Sens 2008). BSO concentration used was selected from studies showing high GSH depletion (Ferreira et al. 2013). The concentrations of DCFH-DA (Sun et al. 2011), Fluo3/AM (Wang and Xu 2005), and BAPTA/AM (Nguyen et al. 2002) were selected according to the previous studies published with SH-SY5Y cells. Stock solutions of MDMA, MDMA metabolites, GBR 12909, NAC, and BSO were prepared in distilled water. DCFH-DA, Fluo3/AM, and BAPTA/AM were solubilized in DMSO. In experiments using the antioxidant NAC or the Ca^{2+} chelator BAPTA/AM, these compounds were added to the cultures 30 min prior to incubation with the mixture of MDMA and its metabolites. All stock solutions of drugs were stored at −20 °C.

MTT reduction assay

The MTT proliferation assay was used to measure mitochondrial dysfunction (decrease in mitochondrial dehydrogenase activity) in SH-SY5Y differentiated cells exposed to MDMA and/or its metabolites, as previously described (Capela et al. 2006a), with some adaptations. The signal generated is dependent on the degree of reduction of the MTT tetrazolium salt (water soluble) to MTT formazan (water insoluble) by cellular dehydrogenases within metabolically active cells. NADPH quinone oxidoreductase is an important cytosolic enzyme that can reduce the MTT tetrazolium salt. However, as previously demonstrated (Haefeli et al. 2011), this enzyme presents a low expression in SH-SY5Y cells. Therefore, in this cell line, MTT tetrazolium salt is essentially metabolized by mitochondrial enzymes. After conclusion of exposure periods, the medium was removed and 200 μL of new medium containing 0.5 mg/mL MTT was added to each well and incubated for 3 h at 37 °C. MTT stock solution (5 mg/mL) was prepared in DPBS without Ca^{2+} and Mg^{2+} [DPBS (−/−)]. After this incubation time, the reaction was stopped by adding 200 μL SDS 10 % (w/v) in 0.01 M hydrochloric acid, followed by overnight incubation at 37 °C. After pipetting, in duplicate, 150 μL of the content from each well to a 96-well plate (APTACA, Cannelli, Italy), the MTT reduction was measured spectrophotometrically in a 96-well plate reader (PowerWaveX, Bio-Tek Instruments, VT, USA) at 550 nm. Final results of MTT reduction, from three to six independent experiments (each experiment was performed at least in triplicate), are expressed as the percentage of the absorbance of the respective control cells [MTT reduction (% of control)].

LDH assay

The integrity of the plasma membrane in SH-SY5Y differentiated cells exposed to MDMA and/or its metabolites was assessed biochemically by measuring the cellular leakage of the cytosolic enzyme LDH. LDH is a soluble cytosolic enzyme present in most eukaryotic cells, released into the culture medium upon cell death due to the damage of plasma membrane. Thus, the increase in the LDH activity in the culture supernatant is proportional to the number of cells with disrupted membrane. LDH activity in the culture medium was determined spectrophotometrically by measuring the decrease in absorbance of NADH during the reduction of pyruvate to lactate, as previously described (Capela et al. 2006b), with adaptations. After conclusion of the incubation periods, 50 μL of the incubation medium from each well was transferred to a 96-well plate (to measure extracellular LDH), in duplicate, after which 75 μL of new medium plus 25 μL of triton X-100 5 % (v/v) (final concentration of 0.5 %) were added to the cells (to lyse all cells) and the plates were incubated again for 30 min at 37 °C. After this time, 25 μL of medium from each well was transferred again to a new 96-well plate (to measure the LDH after the full kill), also in duplicate. LDH was determined spectrophotometrically by following the rate of conversion of NADH to nicotinamide adenine dinucleotide oxidized form (NAD^+) at 340 nm. Thus, in the 96-well plates, the collected medium was mixed with 200 μL of reagent solution containing 0.21 mM NADH, (dissolved in LDH buffer: 33.3 mM KH_2PO_4 and 66.7 mM $K_2HPO_4{\cdot}3H_2O$, pH 7.4). The reaction was started with 25 μL sodium pyruvate (22.7 mM, prepared in LDH buffer), and the kinetic formation of NAD^+ from NADH was followed for 5 min at 340 nm in a 96-well plate reader (PowerWaveX, Bio-Tek Instruments). The final volume of reaction in each well was fixed with LDH buffer to 275 μL. Thus, to measure LDH after the full kill, 25 μL of LDH buffer was added to each well before sodium pyruvate addition. Final results of LDH released into the extracellular medium (LDH leakage), from three to six independent experiments (each experiment was performed at least in triplicate), are expressed as the percentage of cell death (% cell death) according to the equation: % cell death = (extracellular LDH/total LDH) × 100, considering total LDH = extracellular LDH removed + LDH after full kill.

Caspase 3 activity assay

The activation of caspase 3, which occurs in cells during the programmed cell death (apoptotic cell death), was assessed in SH-SY5Y differentiated cells exposed to the mixture of MDMA and its metabolites, as previously

described (Capela et al. 2007b), with some modifications. The hydrolysis of the peptide substrate (Ac-DEVD-pNA) by caspase 3 results in the release of the *p*-nitroaniline (pNA) moiety, which presents a high absorbance at 405 nm. SH-SY5Y differentiated cells exposed to the mixture of MDMA and its metabolites, at 10 or 20 μM, for 24 h, under normothermic or hyperthermic conditions, were scraped in 750 μL of cold DPBS (+/+) and then harvested (2 wells per condition). After centrifugation at 855 *g* for 4 min at 4 °C, the supernatant was discarded and the cellular pellet lysed in 75 μL of ice-cold lysis buffer [50 mM HEPES, 0.1 mM EDTA, and 0.1 % Chaps (w/v), pH 7.4], supplemented with 1 mM DTT. After vortexing, cell lysates were allowed to incubate on ice for 10 min before centrifugation at 16,000*g* for 10 min at 4 °C. Whole protein content in the supernatants was determined using the Bio-Rad DC protein assay and BSA as standard. In a 96-well plate, 50 μL of the supernatant was mixed with 200 μL of assay buffer [100 mM NaCl, 50 mM HEPES, 1 mM EDTA, 0.1 % Chaps (w/v), and 10 % glycerol (v/v), pH 7.4], supplemented with 10 mM DTT. The reaction was started by adding 5 μL of caspase 3 substrate Ac-DEVD-pNA (final concentration 80 μM) and subsequent incubation at 37 °C for 24 h, after which the formation of pNA was measured spectrophotometrically at 405 nm in a 96-well plate reader (PowerWaveX, Bio-Tek Instruments). Caspase 3 substrate Ac-DEVD-pNA (stock solution at 4 mM) and DTT (stock solution at 200 mM) were prepared in DMSO. The absorbance of blanks, used as nonenzymatic control, was subtracted from each sample absorbance. Final results of caspase 3 activity, from seven independent experiments, are expressed as optical density at 405 nm per milligram of protein (OD 405 nm/mg protein).

Measurement of reactive oxygen species production

The formation of ROS in SH-SY5Y differentiated cells exposed to the mixture of MDMA and its six metabolites was quantified by a fluorescence method, using DCFH-DA, according to previously published methods (Sun et al. 2011), with minor adaptations. After uptake by live cells, DCFH-DA is enzymatically hydrolyzed by intracellular esterases to nonfluorescent dichlorodihydrofluorescein (DCFH). In the presence of ROS, namely H_2O_2, DCFH may be oxidized to form a fluorescent compound dichlorodihydrofluorescein (DCF). After conclusion of the differentiation protocol, SH-SY5Y cells were washed with heated DPBS (+/+) and subsequently incubated with 10 μM DCFH-DA in culture medium for 30 min at 37 °C, to promote the intracellular accumulation of the probe. After washing with heated DPBS (+/+), cells were incubated with the mixture of MDMA and its six metabolites (each compound at 10 or 20 μM) in fresh cell culture medium, under normothermic conditions. Fluorescence intensities were measured hourly, during 6 h, using a multiwell microplate fluorescence reader (Synergy HT, Bio-Tek Instruments) with a filter set for excitation and emission at 485 ± 20 and 530 ± 25, respectively. Final results of ROS formation, from six independent experiments (each experiment was performed in triplicate), are expressed in percentage of DCFH fluorescence intensity relative to control conditions [DCFH fluorescence (% of control)].

Assessment of intracellular glutathione levels

The intracellular total glutathione content in SH-SY5Y differentiated cells exposed to the mixture of MDMA and its metabolites was evaluated by the DTNB/GSH reductase recycling assay, as previously described (Barbosa et al. 2012), with some adaptations. After conclusion of the differentiation protocol, cells were exposed to the mixture of MDMA and its metabolites (each compound at 10 or 20 μM), in fresh cell culture medium, for 24 or 48 h under normothermic or hyperthermic conditions. After these exposure times, the medium was removed and the cells were scraped in 1 mL of cold DPBS (+/+) and then harvested (1 well per condition). After centrifugation at 2,376*g* for 5 min at 4 °C, the supernatant was discarded and cellular pellet was dispersed in 400 μL $HClO_4$ 5 % (w/v) and again centrifuged at 16,000*g* for 10 min at 4 °C. The perchloric acid pellet was dissolved in 400 μL NaOH 0.3 M, and the protein content was assayed by the Lowry method (Lowry et al. 1951), using BSA as standard. The supernatants (200 μL) were neutralized with 200 μL of an equimolar solution of $KHCO_3$ (0.76 M) and centrifuged at 16,000*g* for 2 min at 4 °C. In 96-well plates, 100 μL of sample or standard were added in triplicate and mixed with 65 μL of freshly prepared reagent solution containing 3.96 mM DTNB and 0.68 mM NADPH prepared in a mixture of 40.5 % H_2O/59.5 % phosphate buffer (71.5 mM Na_2HPO_4, 71.5 mM NaH_2PO_4, and 0.63 mM EDTA, pH 7.5). Plates were then incubated in a 96-well microplate reader (PowerWaveX, Bio-Tek Instruments) for 15 min at 30 °C, prior to the addition of 40 μL of fresh GR solution per well (10 U/mL in phosphate buffer). The stoichiometric formation of 5-thio-2-nitrobenzoic acid (TNB) was followed for 3 min at 415 nm and compared with a standard GSH curve. GSH standard solutions (0, 0.25, 0.5, 1.25, 2.5, 5, 10, and 15 μM) were prepared in $HClO_4$ 5 % (w/v) and kept at −20 °C until use. Intracellular total glutathione levels were normalized to the total protein content, and the final results from six independent experiments (each experiment was performed in duplicate) are presented as nmol of glutathione per milligram of protein (nmol glutathione/mg protein). Intracellular levels of oxidized glutathione (GSSG) were found to be below the detection limit of the

method. Therefore, only intracellular total glutathione results are presented.

Flow cytometry analysis of intracellular Ca^{2+} levels

Intracellular Ca^{2+} levels in SH-SY5Y differentiated cells exposed to the mixture of MDMA and its six metabolites were evaluated using the Ca^{2+}-sensitive fluorochrome Fluo3/AM, as previously described (Carvalho et al. 2004b; Wang and Xu 2005), with adaptations. After uptake by live cells, Fluo3/AM is enzymatically hydrolyzed by intracellular esterases to Fluo3, which binds Ca^{2+} exhibiting an increase in fluorescence (approximately 40-fold). SH-SY5Y differentiated cells exposed to the mixture of MDMA and its metabolites at 10 or 20 μM for 24 h and under normothermic or hyperthermic conditions were harvested by trypsinization (0.05 % trypsin/EDTA). After centrifugation at 300*g* for 5 min at 4 °C, cells were then loaded with 5 μM Fluo3/AM in 200 μL of heated serum-free DMEM without phenol red, for 30 min, at 37 °C, in a water bath with shake. After this incubation period, cells were centrifuged at 300 *g* for 5 min at 4 °C, resuspended in 400 μL of heated DPBS (+/+), centrifuged again at 300*g* for 5 min at 4 °C, and kept on ice until flow cytometry analysis. In all experiments, a portion of cell suspension (with or without exposure to the drugs) was not incubated with the dye. Sample analysis was performed in a FACSCalibur™ flow cytometer (Becton–Dickinson, Mountain View, CA, USA), equipped with a 488-nm argon ion laser, using CellQuest software (BD Biosciences). The green fluorescence of Fluo3 was measured by a 530 ± 15-nm band-pass filter (FL1). After resuspending the cellular pellet in DPBS (+/+) with 0.5 μg/mL Pi (after enter in death cells, Pi interlaces with the nucleic acid helix with consequent increase in fluorescence intensity emission at 615 nm) and 0.57 mM EGTA, data from at least 15,000 viable cells (based on Pi incorporation) were collected from each condition. In order to detect a possible contribution from cells' autofluorescence to the analyzed fluorescence signals, the portions of cell suspension (with or without exposure to the drugs) that were not incubated with Fluo3/AM were analyzed in the 530 ± 15-nm band-pass filter (FL1). Final results of intracellular Ca^{2+} levels, from six independent experiments (each experiment was performed in duplicate), are presented as median values of Fluo3 fluorescence intensity [Fluo3 fluorescence (arbitrary units)].

Data analysis

Values in figures and text are presented as mean ± SD of the indicated number of independent experiments. Each independent experiment was performed with SH-SY5Y differentiated cells proceeding from different passages. Normality of the data distribution was assessed by three tests, KS normality test, D'Agostino and Pearson omnibus normality test, and Shapiro–Wilk normality test. Statistical comparisons between groups were performed with unpaired Student's *t* test or one-way analysis of variance (ANOVA) followed by Tukey's multiple-comparison test, for experiments with one variable. Two-way ANOVA, followed by Bonferroni's multiple-comparison post hoc test, was used in experiments with two variables. Particularly, the data concerning ROS production were analyzed using two-way ANOVA with repeated measures, followed by Bonferroni's multiple-comparison post hoc test. The detailed statistical analysis performed for each graph is described in each figure legend. Differences were considered to be significant at p values lower than 0.05. All analyses were performed using GraphPad Prism 6.0 for Windows (GraphPad Software, San Diego, CA, USA).

Results

RA and TPA effectively differentiated SH-SY5Y cells into a dopaminergic phenotype

The SH-SY5Y cell line, derived from neuroblastoma, expresses several dopaminergic markers (Cheung et al. 2009), including DAT and TH, two important proteins involved on neurotransmitter transport and biosynthesis, respectively. SH-SY5Y cells are, therefore, frequently used as in vitro model of dopaminergic neurons. However, in their undifferentiated state, SH-SY5Y cells do not display certain features found in primary neurons (Lopes et al. 2010). Therefore, it is necessary to stimulate their differentiation using various agents, such as RA and TPA, into a more characteristically dopaminergic neuronal phenotype (Presgraves et al. 2003). Under our experimental conditions, these agents induced an increase in the dopaminergic phenotype, as observed by both morphological and biochemical criteria (Fig. 1). After 6 days of differentiation with RA/TPA, it was observed an extension of neurites and a more elongated cellular form (Fig. 1a–c). Biochemically, after 6 days of differentiation, Western blotting analysis showed a significant increase in DAT (Fig. 1d, e, $p < 0.05$) and TH expression (Fig. 1f, g, $p < 0.001$).

Low micromolar mixture of MDMA and its metabolites was toxic to SH-SY5Y differentiated cells

Neurons are recognized to have a low metabolic activity, namely oxidative metabolism catalyzed by CYP450 (Ferguson and Tyndale 2011). However, numerous compounds produced by hepatic metabolism, such as MDMA metabolites, can be transported across the blood-brain-barrier

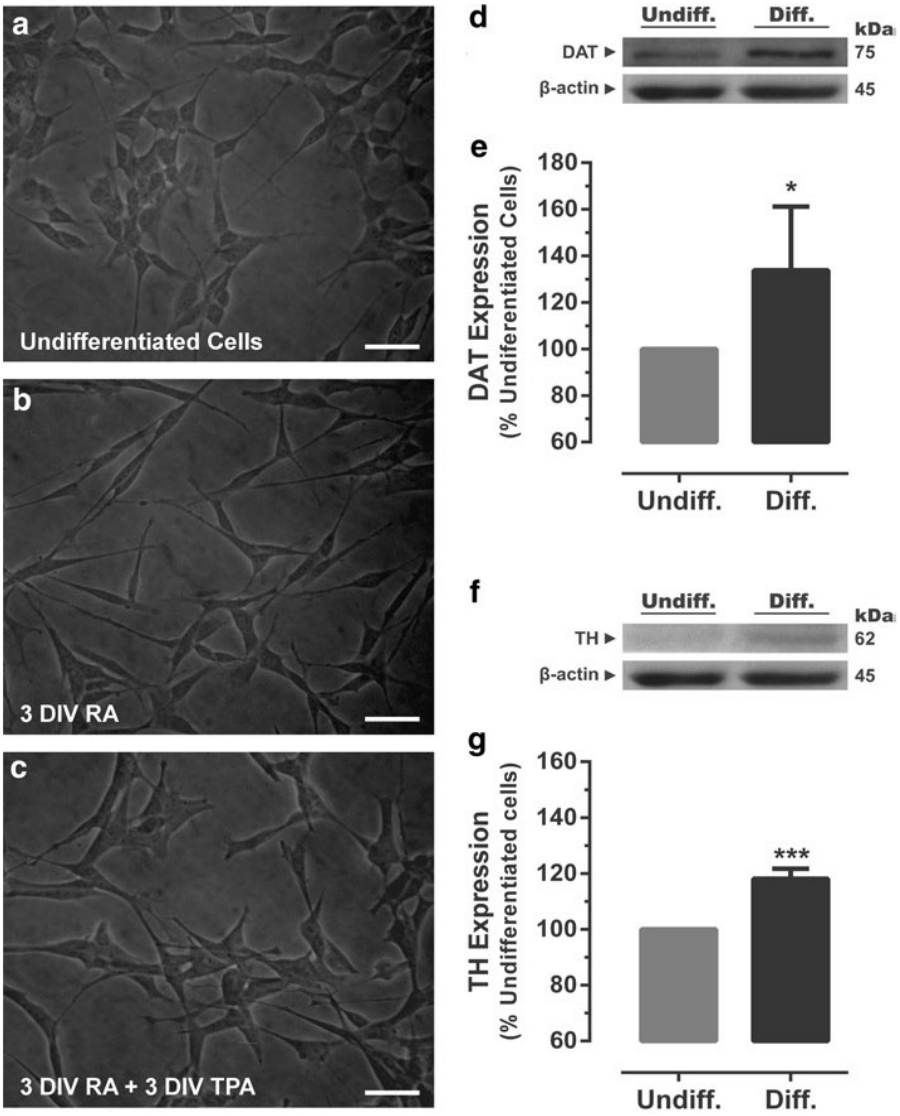


Fig. 1 Differentiation of SH-SY5Y cells with RA and TPA enhanced the dopaminergic phenotype. **a–c** Bright-field images of SH-SY5Y undifferentiated cells (**a**), or SH-SY5Y cells, after 3 days in vitro (DIV) with 10 μM RA (**b**), or after 3 DIV with 10 μM RA followed by additional 3 DIV in the presence of 80 nM TPA (**c**). *Scale bar* 50 μm. **d–g** Western blotting analysis of DAT and TH immunocontent in sister cultures of SH-SY5Y undifferentiated cells and after differentiation with RA and TPA. To avoid any potential inter-gel variation, equal amounts of protein (60 μg) from the different conditions were loaded on the same gel. Representative images of Western blotting analyses for DAT (75 kD) (**d**) and TH (62 kD) (**f**) immunocontent in SH-SY5Y undifferentiated and differentiated cells, and respective densitometric analyses (**e** and **g**, respectively) are shown. β-Actin was used as loading control. Results are presented as mean ± SD, from three independent experiments (each experiment was performed in duplicate), and expressed as percentage of DAT or TH expression compared to undifferentiated cells [DAT or TH expression (% undifferentiated cells)]. Statistical comparisons were made using unpaired Student's *t* test (*$p < 0.05$, ***$p < 0.001$ differentiated vs. undifferentiated cells)

(Erives et al. 2008; Jones et al. 2005). Therefore, one of the most important limitations of the in vitro studies with neuronal models is the lack of metabolism, which implies that the co-exposure to parent compounds and its metabolites is rarely tested. Thus, considering that metabolism can be an important factor contributing to MDMA-induced neurotoxicity (Barbosa et al. 2012; Capela et al. 2006a), one of the main aims of this work was to investigate the potential toxicity of MDMA and its metabolites, as a mixture, and the possible mechanisms involved. As shown in Fig. 2, the mixture of MDMA and its metabolites induced toxicity to SH-SY5Y differentiated cells, as evaluated by the MTT reduction (Fig. 2a, b) and LDH release (Fig. 2c, d) assays. The mixture of all compounds, each at 10 μM, induced mitochondrial dysfunction accompanied by cell death, only after 48 h of exposure and under hyperthermic conditions

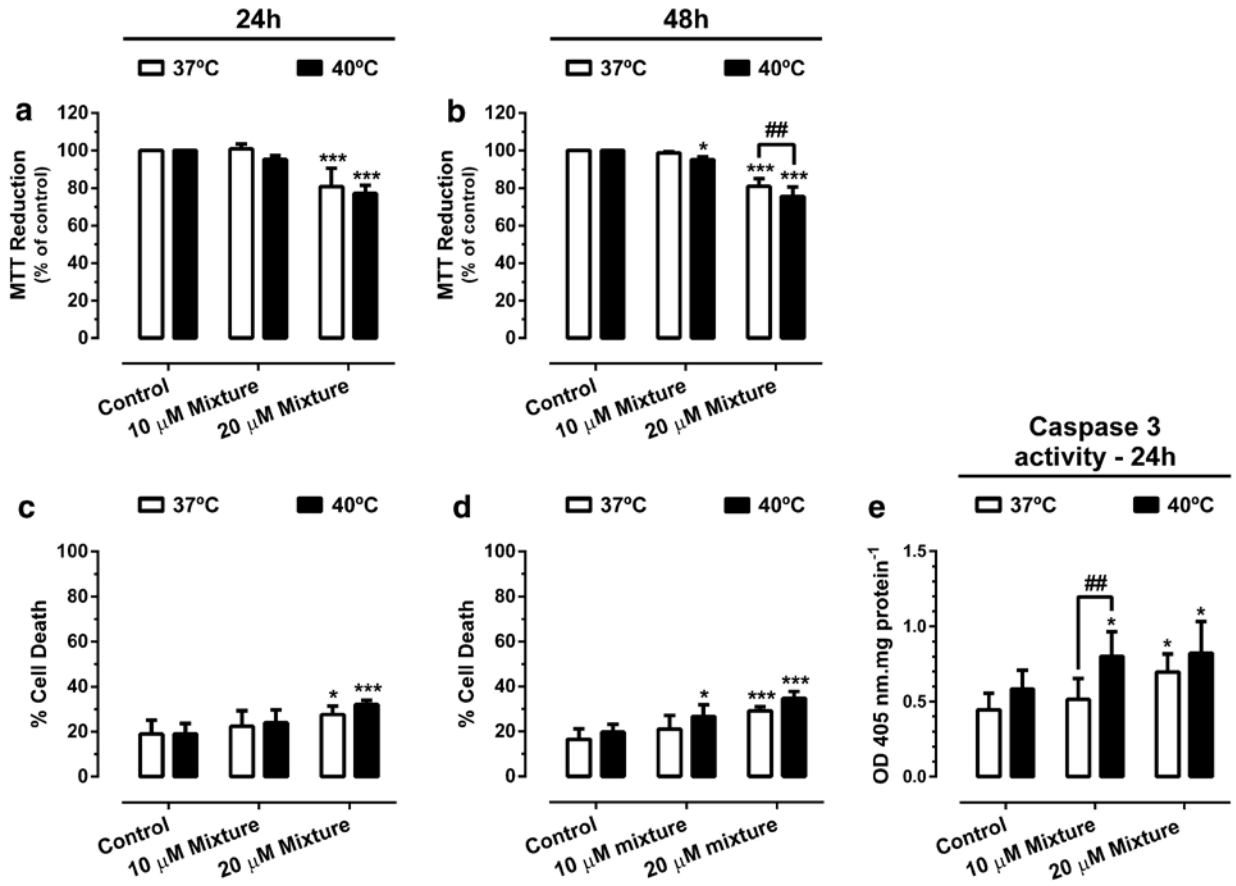


Fig. 2 Cytotoxic effects of the mixture of MDMA and its six metabolites α-MeDA, N-Me-α-MeDA, 5-(GSH)-α-MeDA, 5-(GSH)-N-Me-α-MeDA, 5-(NAC)-α-MeDA, and 5-(NAC)-N-Me-α-MeDA, in SH-SY5Y differentiated cells. SH-SY5Y differentiated cells were exposed to the mixture of MDMA and its six metabolites, each compound at 10 or 20 μM, for 24 (**a**, **c**) or 48 h (**b**, **d**), under normothermic (37 °C) or hyperthermic (40 °C) conditions, and the toxicity was evaluated by the MTT reduction (**a**, **b**) and LDH assays (**c**, **d**). Results are presented as mean ± SD, from six independent experiments (each experiment was performed at least in triplicate), and expressed as the percentage of the absorbance of the respective control cells [MTT reduction (% of control)] (**a**, **b**), or in percentage of cell death (% cell death) (**c**, **d**). Statistical comparisons were made using two-way ANOVA, followed by Bonferroni's multiple-comparison post hoc test (*$p < 0.05$, ***$p < 0.001$ treatment vs. control; $^{\#\#}p < 0.01$, 40 vs. 37 °C, for the same time-point). **e** Caspase 3 activation induced by the mixture of MDMA and its metabolites, evaluated by a colorimetric assay. SH-SY5Y differentiated cells were exposed to the mixture of MDMA and its six metabolites, each compound at 10 or 20 μM, for 24 h, under normothermic (37 °C) or hyperthermic (40 °C) conditions, and caspase 3 activity was then evaluated. Results are presented as mean ± SD, from seven independent experiments, and expressed as optical density at 405 nm per mg of protein (OD 405 nm/mg protein). Statistical comparisons were made using two-way ANOVA, followed by Bonferroni's multiple-comparison post hoc test (*$p < 0.05$ treatment vs. control; $^{\#\#}p < 0.01$, 40 vs. 37 °C)

(Fig. 2b, d). Meanwhile, for the mixture of all compounds at 20 μM, a significant decrease in mitochondrial metabolic activity (Fig. 2a, b) and increased cell death (Fig. 2c, d) were observed, at both times and temperatures of exposure. Notably, the mitochondrial dysfunction induced by the 20 μM mixture was potentiated by hyperthermia (Fig. 2b). Importantly, the decrease in mitochondrial function induced by the mixture of MDMA and its metabolites was clearly associated with increased cell death. Thus, this study demonstrates, for the first time, that the mixture of MDMA and its metabolites induced toxicity in an in vitro neuronal model, at low micromolar concentrations, which constitutes a more real estimation of the in vivo experimental scenario.

The neurotoxicity of the mixture of MDMA and its metabolites involved caspase 3 activation

It is known that the activation of a specific class of proteases, the caspase proteins, namely caspase 3, is involved in the apoptotic cascade, leading to cell death (Bernardi and von Stockum 2012). As observed in Fig. 2e, the mixture of MDMA and its metabolites induced a significant increase in caspase 3 activity after 24 h of exposure. For

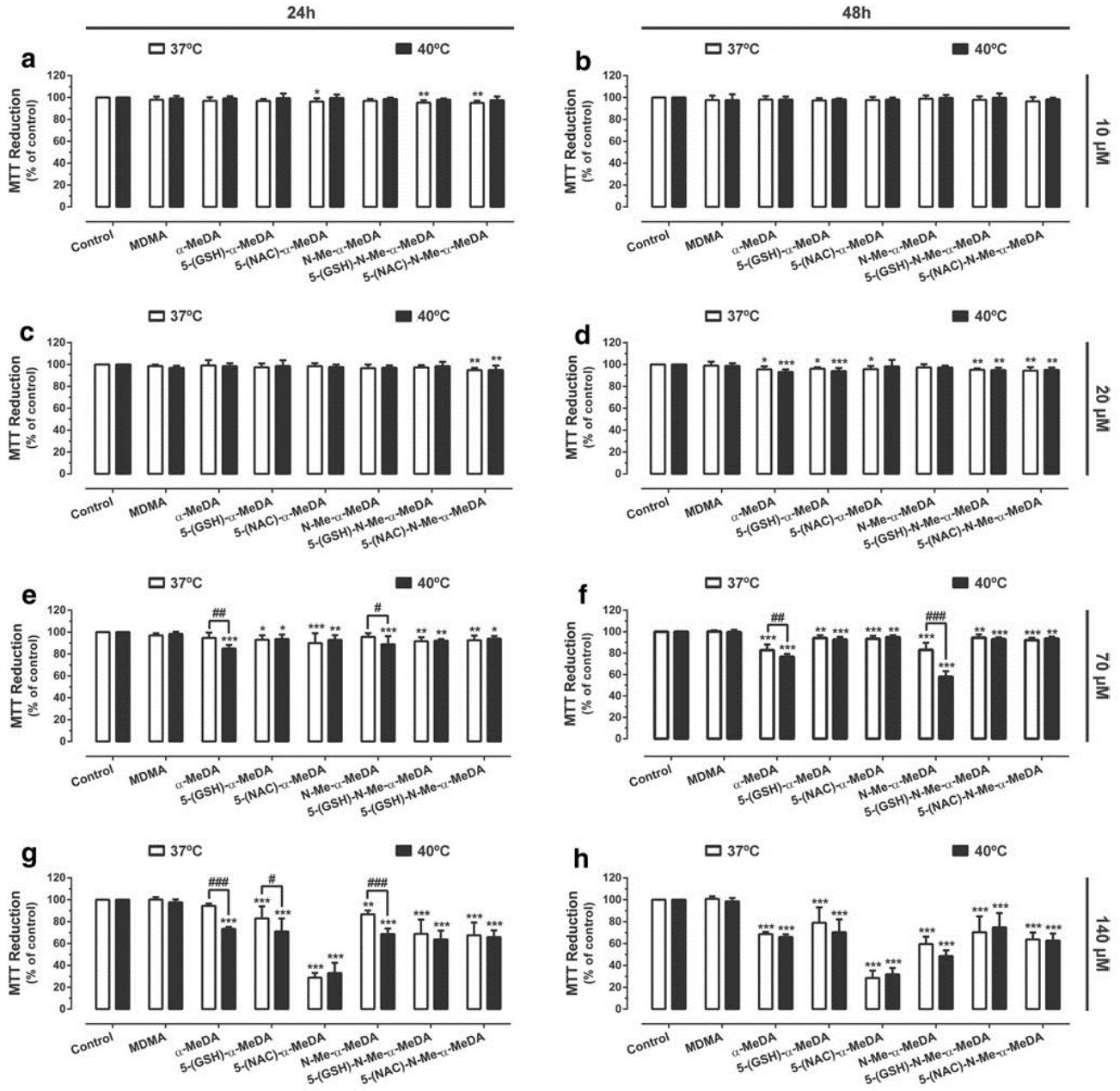


Fig. 3 Mitochondrial dysfunction induced by MDMA and its six metabolites α-MeDA, N-Me-α-MeDA, 5-(GSH)-α-MeDA, 5-(GSH)-N-Me-α-MeDA, 5-(NAC)-α-MeDA, and 5-(NAC)-N-Me-α-MeDA, in SH-SY5Y differentiated cells, evaluated by the MTT reduction assay. SH-SY5Y differentiated cells were exposed to MDMA or its six metabolites, at the concentrations of 10 μM (**a**, **b**), 20 μM (**c**, **d**), 70 μM (**e**, **f**), or 140 μM (**g**, **h**), for 24 (**a**, **c**, **e**, **g**) or 48 h (**b**, **d**, **f**, **h**), under normothermic (37 °C) or hyperthermic (40 °C) conditions, and mitochondrial dysfunction was then evaluated. Results are presented as mean ± SD, from six independent experiments (each experiment was performed at least in triplicate), and expressed as the percentage of the absorbance of the respective control cells [MTT reduction (% of control)]. Statistical comparisons were made using two-way ANOVA, followed by Bonferroni's multiple-comparison post hoc test (*$p < 0.05$, **$p < 0.01$, ***$p < 0.001$ treatment vs. control; $^{\#}p < 0.05$, $^{\#\#}p < 0.01$, $^{\#\#\#}p < 0.001$, 40 vs. 37 °C, for the same time-point)

the 10 μM mixture, the increase in caspase 3 activity was only observed under hyperthermic conditions, while for the 20 μM mixture, the increase in caspase 3 activity was observed at both temperatures tested. Therefore, hyperthermia potentiated caspase 3 activity for the 10 μM mixture.

MDMA and its metabolites, as a mixture, present a different toxicity profile, compared to each compound alone

As mentioned above, one of the most important limitations of in vitro neuronal models is the lack of metabolism.

Knowing this, and considering the toxicity of the mixture of MDMA and its metabolites to SH-SY5Y differentiated cells, we studied the toxicity of each compound alone, at the same concentrations present in the mixture. As observed in Fig. 3a–d, at the concentration of 10 or 20 μM, some of the tested compounds elicited minor effects, though significant, on mitochondrial function. Twenty four hours of exposure to 10 μM of the MDMA metabolites 5-(NAC)-α-MeDA, 5-(GSH)-N-Me-α-MeDA, or 5-(NAC)-N-Me-α-MeDA, under normothermia, induced a minor, but significant, decrease in mitochondrial function (Fig. 3a). Similarly, 20 μM of MDMA metabolite 5-(NAC)-N-Me-α-MeDA promoted a significant decrease in mitochondrial function, at both times and temperatures of exposure tested (Fig. 3c, d). Also, after 48 h of exposure, MDMA metabolites α-MeDA, 5-(GSH)-α-MeDA, and 5-(GSH)-N-Me-α-MeDA, at 20 μM, reduced significantly the rate of MTT reduction, at both temperatures studied (Fig. 3d). Particularly, 48 h of exposure to MDMA metabolite 5-(NAC)-α-MeDA, at 20 μM, under normothermic conditions, resulted also in a significant decrease in mitochondrial function (Fig. 3d). Contrary to mitochondrial dysfunction, at the concentration of 10 or 20 μM, none of the tested compounds alone elicited significant cell death, at any times or temperatures of exposure (Fig. 4a–d).

Next, we tested the toxicity of the different compounds at the equimolar concentrations of 70 and 140 μM, which represent the total concentration of all compounds in both mixtures of 10 and 20 μM, respectively. As shown in Figs. 3e–h and 4e–h, MDMA, at 70 or 140 μM, respectively, did not induce significant toxicity to SH-SY5Y differentiated cells. Contrariwise, at 70 μM, all the MDMA metabolites tested induced a significant reduction in mitochondrial function, at both times and temperatures studied (Fig. 3e, f), except the MDMA metabolites α-MeDA and N-Me-α-MeDA, which after 24 h of exposure only elicited toxicity under hyperthermic conditions (Fig. 3e). However, for these two compounds, at both time-points studied, hyperthermia potentiated the toxic effect (Fig. 3e, f). Differently, after 24 h of exposure, only the MDMA metabolite α-MeDA, under hyperthermic conditions, and 5-(NAC)-α-MeDA, under normothermic conditions, induced a significant increase in cell death (Fig. 4e). However, after 48 h of exposure, 70 μM of MDMA metabolites α-MeDA and N-Me-α-MeDA significantly increased the cell death (Fig. 4f), which was potentiated by hyperthermia. At the concentration of 140 μM, all the MDMA metabolites induced significant mitochondrial dysfunction, at both times and temperatures studied (Fig. 3g, h), except the MDMA metabolite α-MeDA, after 24 h of exposure, and under normothermic conditions (Fig. 3g). Also, after 24 h of exposure, hyperthermia potentiated the mitochondrial dysfunction induced by 140 μM of MDMA metabolites α-MeDA, 5-(GSH)-α-MeDA, and N-Me-α-MeDA (Fig. 3g). A significant increase in cell death was observed for the MDMA metabolites 5-(GSH)-α-MeDA, 5-(NAC)-α-MeDA, 5-(GSH)-N-Me-α-MeDA, or 5-(NAC)-N-Me-α-MeDA at 140 μM after 24 h of exposure at both temperatures tested (Fig. 4g). At the same time-point, a significant increase in cell death was observed for the MDMA metabolite α-MeDA at 140 μM, under hyperthermic conditions (Fig. 4g). A significant increase in cell death was observed for all MDMA metabolites at 140 μM, after 48 h of exposure, at both temperatures tested (Fig. 4h). Importantly, for the MDMA metabolite 5-(NAC)-N-Me-α-MeDA, after 24 h of exposure, and for catechol MDMA metabolites α-MeDA and N-Me-α-MeDA, after 48 h of exposure, hyperthermia potentiated the cell death (Fig. 4g, h). Therefore, these results suggest that MDMA and its metabolites, as a mixture, present a different toxicity profile, compared to each compound alone.

Dopamine uptake system was not implicated on the toxic effect mediated by the mixture of MDMA and its metabolites

Dopamine transporter (DAT) plays a critical role in neurotransmitter uptake, thus regulating an efficient synaptic transmission (Sulzer 2011). Additionally, MDMA is known to modulate DAT function (Capela et al. 2009). Therefore, considering the structural similarity between MDMA metabolites and dopamine, it was evaluated the possible involvement of DAT in the neurotoxic effects mediated by the mixture of MDMA and its metabolites. As shown in Fig. 5, the DAT inhibitor GBR 12909 (1 μM) (Ferreira et al. 2013; Shavali and Sens 2008), by itself, did not induce any significant mitochondrial dysfunction, at both temperatures studied. Following DAT inhibition, the toxicity of the 20 μM mixture of MDMA and its metabolites was not significantly modified, as evaluated by the MTT reduction assay, thus indicating a DAT-independent mechanism for the reported toxic effect.

Increased ROS production was involved on the toxic effect induced by the mixture of MDMA and its metabolites

Previous studies have shown increased ROS formation in the brain after MDMA administration to rats (Colado et al. 1997). Moreover, recently, it was also demonstrated increased ROS formation in rat cortical neurons (Capela et al. 2007b) and mouse brain synaptosomes (Barbosa et al. 2012) after exposure to MDMA metabolites. As observed in Fig. 6a, the mixture of MDMA and its metabolites induced a significant increase in ROS formation in SH-SY5Y differentiated cells, under normothermic conditions.

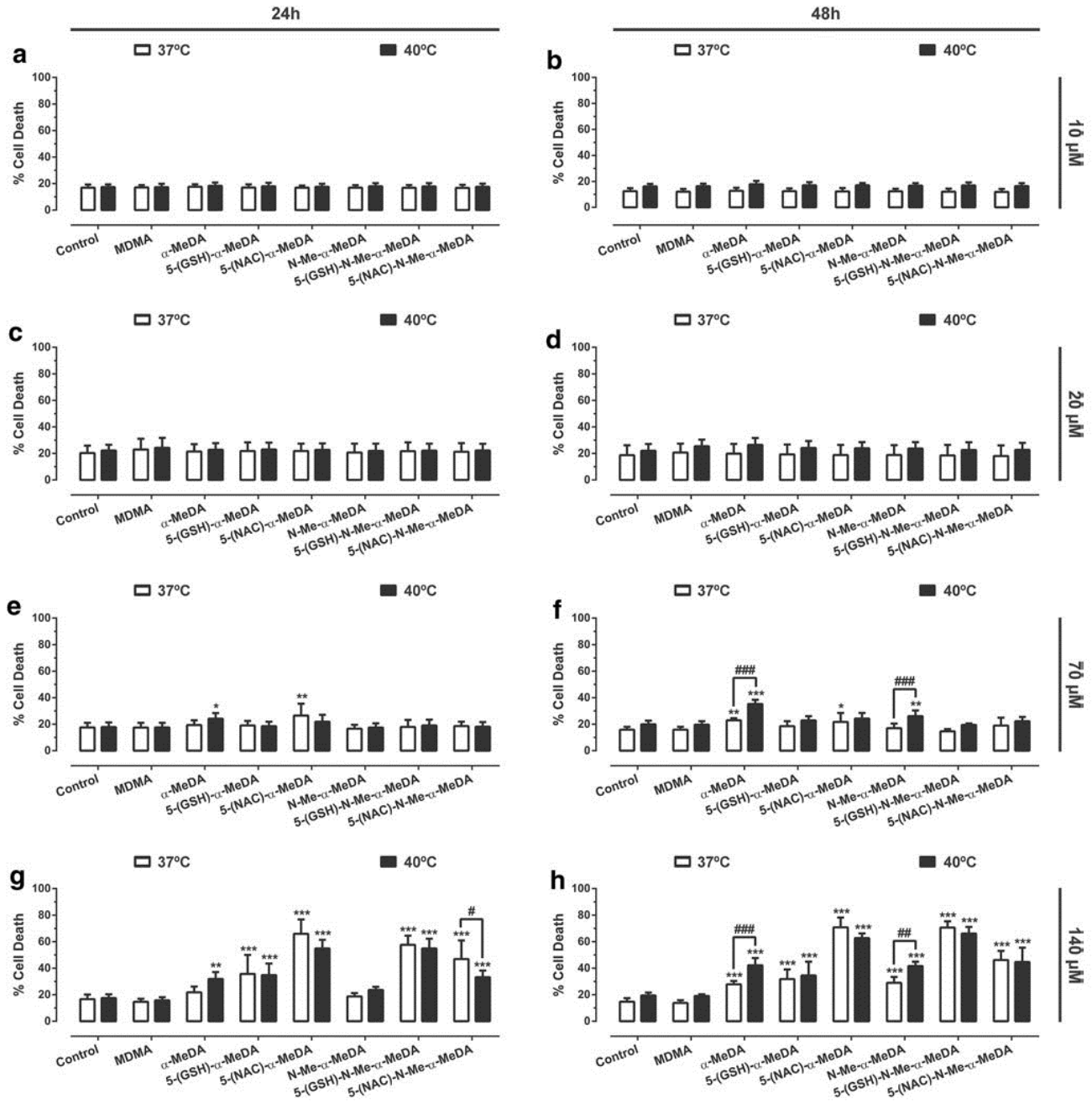


Fig. 4 Cytotoxic effects of MDMA and its six metabolites α-MeDA, N-Me-α-MeDA, 5-(GSH)-α-MeDA, 5-(GSH)-N-Me-α-MeDA, 5-(NAC)-α-MeDA, and 5-(NAC)-N-Me-α-MeDA, in SH-SY5Y differentiated cells, evaluated by the LDH assay. SH-SY5Y differentiated cells were exposed to MDMA or its six metabolites, at the concentrations of 10 μM (**a**, **b**), 20 μM (**c**, **d**), 70 μM (**e**, **f**), or 140 μM (**g**, **h**), for 24 (**a**, **c**, **e**, **g**) or 48 h (**b**, **d**, **f**, **h**), under normothermic (37 °C) or hyperthermic (40 °C) conditions, and cell death was then evaluated. Results are presented as mean ± SD, from three to six independent experiments (each experiment was performed at least in triplicate), and expressed in percentage of cell death (% cell death). Statistical comparisons were made using two-way ANOVA, followed by Bonferroni's multiple-comparison post hoc test (*$p < 0.05$, **$p < 0.01$, ***$p < 0.001$ treatment vs. control; $^{\#}p < 0.05$, $^{\#\#}p < 0.01$, $^{\#\#\#}p < 0.001$, 40 vs. 37 °C, for the same time-point)

While for the 10 μM mixture ROS formation reached significance only after 6 h of incubation ($p < 0.05$), for the 20 μM mixture this effect became significant as early as 2 h after exposure. Moreover, after 2 h of exposure, it was observed a significant difference in ROS production between the mixtures tested.

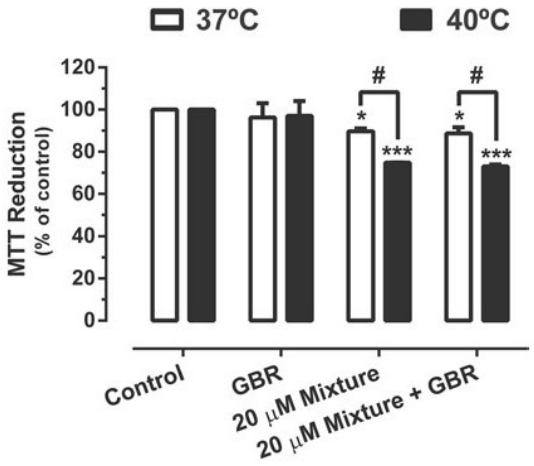


Fig. 5 Involvement of DAT-mediated transport on the toxic effect induced by the 20 μM mixture of MDMA and its six metabolites α-MeDA, N-Me-α-MeDA, 5-(GSH)-α-MeDA, 5-(GSH)-N-Me-α-MeDA, 5-(NAC)-α-MeDA, and 5-(NAC)-N-Me-α-MeDA, in SH-SY5Y differentiated cells, evaluated by the MTT reduction assay. SH-SY5Y differentiated cells were preincubated with 1 μM GBR 12909 for 30 min, after which the mixture of MDMA and its metabolites, each compound at 20 μM, was added to the cultures and mitochondrial dysfunction evaluated after 24 h of exposure, under normothermic (37 °C) or hyperthermic (40 °C) conditions. Results are presented as mean ± SD, from three independent experiments (each experiment was performed in triplicate), and expressed as the percentage of the absorbance of the respective control cells [MTT reduction (% of control)]. Statistical comparisons were made using two-way ANOVA, followed by Bonferroni's multiple-comparison post hoc test (*$p < 0.05$, ***$p < 0.001$ treatment vs. control; $^{\#}p < 0.05$, 40 vs. 37 °C)

NAC prevented the mitochondrial dysfunction induced by the mixture of MDMA and its metabolites

N-acetylcysteine, an antioxidant and GSH precursor, has been reported to be an important protective agent against the toxicity induced by MDMA and/or its metabolites in several in vitro neuronal models (Barbosa et al. 2012; Capela et al. 2007b; Ferreira et al. 2013). Knowing that oxidative stress is an important factor contributing to MDMA-induced neurotoxicity (Capela et al. 2009), the use of antioxidants constitutes an important approach to elucidate the putative mechanisms involved. As shown in Fig. 6b, c, 1 mM NAC (Capela et al. 2007b), by itself, did not induce any significant changes in mitochondrial function, at both times and temperatures of exposure tested. However, NAC fully prevented the mitochondrial dysfunction elicited by the 20 μM mixture of MDMA and its metabolites in SH-SY5Y differentiated cells, at both time-points and temperatures of exposure studied (Fig. 6b, c). Considering that hyperthermia is an important effect associated with MDMA consumption (Capela et al. 2009; Carvalho et al. 2012), which is known to potentiate the toxicity induced by MDMA and its metabolites (Capela et al. 2006a, 2007b), this result constitutes the first report indicating that this antioxidant is also able to prevent the neurotoxicity of the mixture of MDMA and its metabolites under hyperthermic conditions.

The mixture of MDMA and its metabolites altered the intracellular glutathione status

Glutathione, the most important intracellular antioxidant, plays a major role in protecting biological systems against oxidative stress (Marí et al. 2013). As previously demonstrated by our group (Barbosa et al. 2012; Capela et al. 2007b; Carvalho et al. 2004a; Ferreira et al. 2013), MDMA and/or its metabolites are known to induce important changes in intracellular glutathione status in several in vitro models. As observed in Fig. 7a, b, the mixture of MDMA and its metabolites, at low concentrations, significantly increased the intracellular glutathione content in SH-SY5Y differentiated cells. For the 10 μM mixture, a significant increase in intracellular glutathione levels was only observed under normothermic conditions, at both time-points tested (Fig. 7a, b). The 20 μM mixture significantly increased the intracellular glutathione levels at both times and temperatures studied, being again more pronounced under normothermic than under hyperthermic conditions (Fig. 7a, b). Since the increase in glutathione levels was more pronounced for the 20 μM mixture, after 24 h of exposure, and under normothermic conditions, we tested whether pretreatment with BSO, a potent γ-glutamylcysteine ligase inhibitor, could prevent the observed effect. Previously, we showed that 48 h of exposure to 25 μM BSO reduced dramatically the intracellular glutathione content to about 15 % of control levels (Ferreira et al. 2013). As shown in Fig. 7c, BSO completely prevented the increase in intracellular total glutathione levels elicited by the 20 μM mixture of MDMA and its metabolites, thus suggesting a contribution of pathways involving de novo GSH synthesis for the observed effect.

The mixture of MDMA and its metabolites increased intracellular Ca^{2+} levels

Intracellular Ca^{2+} homeostasis is critical in maintaining the normal function of the cell, in that variations in the concentration of Ca^{2+} in cells can determine cell survival or death (Oliveira and Gonçalves 2009). As shown in Fig. 8a, SH-SY5Y differentiated cells exposed to the mixture of MDMA and its metabolites at 20 μM for 24 h presented a significant increase in intracellular Ca^{2+} levels, at both temperature conditions studied. Previous studies have demonstrated the involvement of calcium-regulated pathways in the neurotoxic effects triggered by MDMA in primary

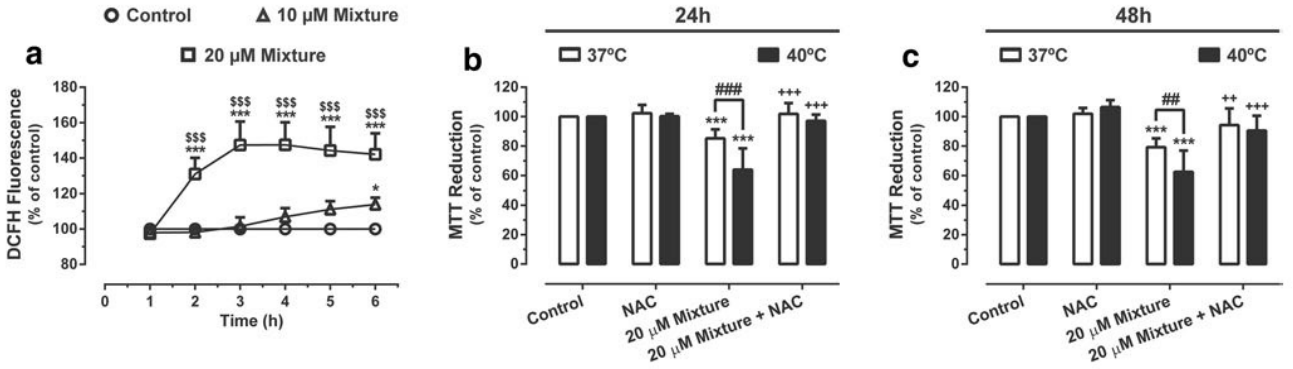


Fig. 6 Involvement of oxidative stress-related mechanisms on the toxic effect induced by the mixture of MDMA and its six metabolites α-MeDA, N-Me-α-MeDA, 5-(GSH)-α-MeDA, 5-(GSH)-N-Me-α-MeDA, 5-(NAC)-α-MeDA, and 5-(NAC)-N-Me-α-MeDA in SH-SY5Y differentiated cells. **a** ROS production induced by the mixture of MDMA and its metabolites, evaluated by a fluorescence method. SH-SY5Y differentiated cells, preloaded with 10 μM DCFH-DA for 30 min, were incubated with the mixture of MDMA or its six metabolites, each compound at 10 or 20 μM, under normothermic (37 °C) conditions, and ROS production was then evaluated. Fluorescence intensities were recorded hourly, during 6 h. Results are presented as mean ± SD from six independent experiments (each experiment was performed in triplicate) and expressed in percentage of DCFH fluorescence intensity relative to control conditions [DCFH fluorescence (% control)]. Statistical comparisons were made using two-way ANOVA, followed by Bonferroni's multiple-comparison post hoc test ($^{*}p < 0.05$, $^{***}p < 0.001$ mixture vs. control, for the same time-point, $^{\$\$\$}p < 0.001$ 20 μM mixture vs. 10 μM mixture, for the same time-point). **b**, **c** Protective effect of NAC against the toxicity induced by the 20 μM mixture of MDMA and its six metabolites, evaluated by the MTT reduction assay. SH-SY5Y differentiated cells were pre-incubated with 1 mM NAC for 30 min, after which the mixture of MDMA and its metabolites, each compound at 20 μM, was added to the cultures and mitochondrial dysfunction evaluated after 24 (**b**) or 48 h (**c**) of exposure, under normothermic (37 °C) or hyperthermic (40 °C) conditions. Results are presented as mean ± SD, from six independent experiments (each experiment was performed at least in triplicate), and expressed as the percentage of the absorbance of the respective control cells [MTT reduction (% of control)]. Statistical comparisons were made using two-way ANOVA, followed by Bonferroni's multiple-comparison post hoc test ($^{***}p < 0.001$ treatment vs. control; $^{\#\#}p < 0.01$, $^{\#\#\#}p < 0.001$, 40 vs. 37 °C, for the same time-point; $^{++}p < 0.01$, $^{+++}p < 0.001$ 20 μM mixture plus NAC vs. 20 μM mixture, for the same time-point)

cerebrocortical cultures (Warren et al. 2007) and PC12 cells (Garcia-Ratés et al. 2010). Therefore, to elucidate the involvement of Ca^{2+} on the toxic effect observed, we used the cell-permeable selective chelator of intracellular Ca^{2+}, BAPTA/AM. As shown in Fig. 8b, 20 μM BAPTA/AM (Nguyen et al. 2002), by itself, did not induce any significant mitochondrial dysfunctions, at both temperatures of exposure tested. Preincubation with BAPTA/AM did not modify the toxicity induced by the mixture of MDMA and its metabolites, as evaluated by the MTT reduction assay.

Discussion

The present study is the first to evaluate the in vitro neurotoxicity of the mixture of MDMA and its metabolites, at low micromolar concentrations, which represents a more realistic approach to the in vivo exposure to MDMA. It was demonstrated that the mixture of MDMA and its major metabolites was toxic to human SH-SY5Y differentiated cells, an effect fully prevented by NAC. Furthermore, the reported neurotoxic effects were potentiated by hyperthermia and accompanied by caspase 3 activation. Additionally, it was observed that the toxicity induced by this mixture was associated with increased ROS production and increased intracellular Ca^{2+} levels. Finally, this mixture increased intracellular glutathione levels by modulating GSH biosynthesis.

Though the majority of the studies have been focused on the MDMA-induced toxicity to the serotonergic system, dopaminergic deficits are also well documented, particularly in the mice model (Cadet et al. 2001; Escobedo et al. 2005; Granado et al. 2008, 2011). Therefore, in the present study, we used human SH-SY5Y differentiated cells to elucidate the putative mechanisms by which MDMA and its metabolites induce neurotoxicity. Under our experimental conditions, SH-SY5Y cells differentiated with RA and TPA showed higher expression of TH and DAT, thus presenting a more characteristic dopaminergic phenotype, as previously reported (Ferreira et al. 2013; Pennypacker et al. 1989; Presgraves et al. 2003).

Accordingly, we studied the toxicity mechanisms of MDMA and its metabolites, as a mixture, using concentrations within the range of those found in the rat brain after subcutaneous (Chu et al. 1996; Erives et al. 2008) or oral (Mueller et al. 2009b) administration of MDMA (from 5 to 20 mg/kg). We found that the mixture of MDMA and its metabolites induced significant mitochondrial dysfunction and cell death in SH-SY5Y differentiated cells. Moreover, we demonstrated that the toxicity of this mixture was

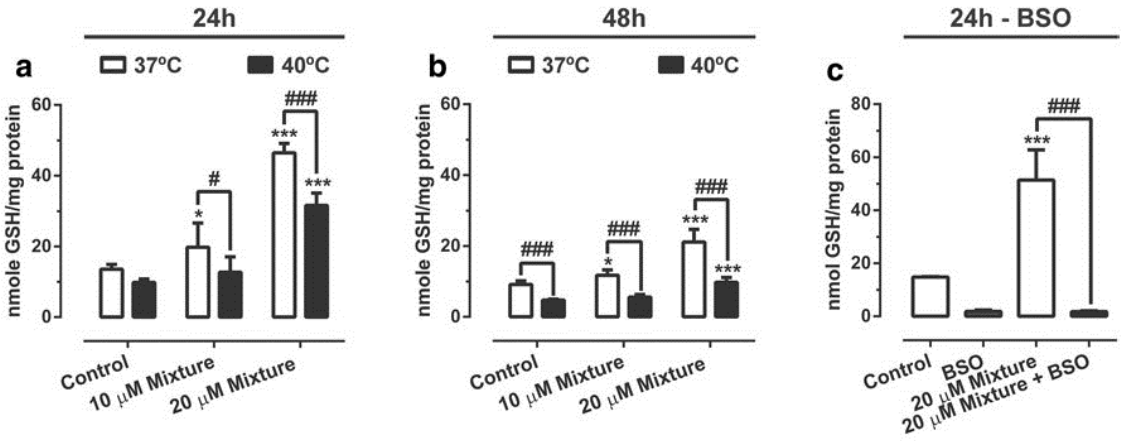


Fig. 7 Effects of the mixture of MDMA and its six metabolites α-MeDA, N-Me-α-MeDA, 5-(GSH)-α-MeDA, 5-(GSH)-N-Me-α-MeDA, 5-(NAC)-α-MeDA, and 5-(NAC)-N-Me-α-MeDA on intracellular glutathione status, in SH-SY5Y differentiated cells, evaluated by the DTNB/GSH reductase recycling assay. SH-SY5Y differentiated cells were incubated with the mixture of MDMA and its metabolites, each compound at 10 μM or 20 μM, for 24 (**a**) or 48 h (**b**), under normothermic (37 °C) or hyperthermic (40 °C) conditions, and total intracellular glutathione levels were then evaluated. Results are presented as mean ± SD, from six independent experiments (each experiment was performed in duplicate), and expressed in nmol GSH per mg of protein (nmol GSH/mg protein). Statistical comparisons were made using two-way ANOVA, followed by Bonferroni's multiple-comparison post hoc test (*$p < 0.05$, ***$p < 0.001$ treatment vs. control; $^{\#}p < 0.05$, $^{\#\#\#}p < 0.001$, 40 vs. 37 °C). **c** Effect of BSO on intracellular total glutathione levels elevation induced by the 20 μM mixture of MDMA and its metabolites. SH-SY5Y differentiated cells, preincubated with 25 μM BSO for 30 min, were exposed to the mixture of MDMA and its six metabolites, each compound at 20 μM, for 24 h, under normothermic (37 °C) conditions, and total intracellular glutathione levels were then evaluated. Results are presented as mean ± SD, from three independent experiments (each experiment was performed in duplicate), and expressed in nmol GSH per mg of protein (nmol GSH/mg protein). Statistical comparisons were made using one-way ANOVA, followed by Tukey's multiple-comparison post hoc test (***$p < 0.001$ treatment vs. control; $^{\#\#\#}p < 0.001$ 20 μM mixture plus BSO vs. 20 μM mixture)

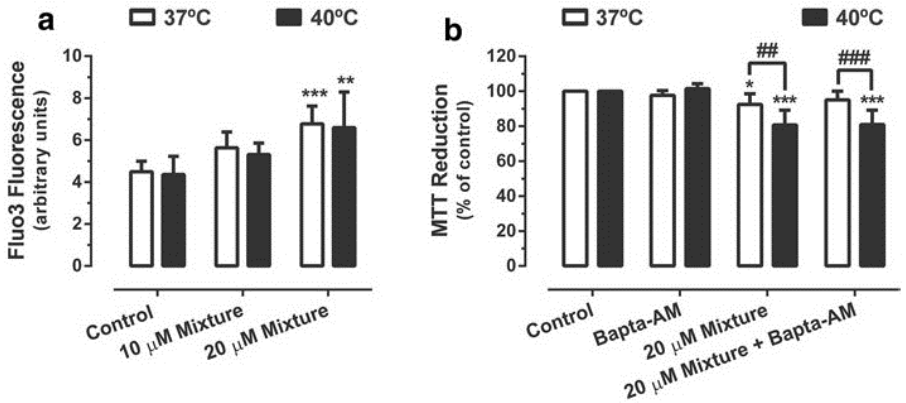


Fig. 8 The role of intracellular Ca^{2+} on the toxic effects induced by the mixture of MDMA and its six metabolites α-MeDA, N-Me-α-MeDA, 5-(GSH)-α-MeDA, 5-(GSH)-N-Me-α-MeDA, 5-(NAC)-α-MeDA, and 5-(NAC)-N-Me-α-MeDA in SH-SY5Y differentiated cells. **a** Effects of the mixture of MDMA and its six metabolites on intracellular Ca^{2+} levels, evaluated by flow cytometry. After exposure to the mixture of MDMA and its six metabolites, each compound at 10 or 20 μM, for 24 h, under normothermic (37 °C) or hyperthermic (40 °C) conditions, SH-SY5Y differentiated cells were loaded with 5 μM Fluo3-AM, for 30 min, at 37 °C, and intracellular Ca^{2+} levels were then evaluated. Results are presented as mean ± SD, from six independent experiments (each experiment was performed in duplicate), and expressed as median values of Fluo3 fluorescence intensity [Fluo3 fluorescence (arbitrary units)]. Statistical comparisons were made using two-way ANOVA, followed by Bonferroni's multiple-comparison post hoc test (**$p < 0.01$, ***$p < 0.001$ treatment vs. control). **b** Effect of the cell-permeable Ca^{2+} chelator BAPTA/AM on the toxicity induced by the mixture of MDMA and its six metabolites, evaluated by the MTT reduction assay. SH-SY5Y differentiated cells, preincubated with 20 μM BAPTA/AM for 30 min, were exposed to the mixture of MDMA and its six metabolites, each compound at 20 μM, for 24 h, under normothermic (37 °C) or hyperthermic (40 °C) conditions, and mitochondrial dysfunction was then evaluated. Results are presented as mean ± SD, from six independent experiments (each experiment was performed in triplicate), and expressed as the percentage of the absorbance of the respective control cells [MTT reduction (% of control)]. Statistical comparisons were made using two-way ANOVA, followed by Bonferroni's multiple-comparison post hoc test (*$p < 0.05$, ***$p < 0.001$ treatment vs. control; $^{\#\#}p < 0.01$, $^{\#\#\#}p < 0.001$, 40 vs. 37 °C)

potentiated by hyperthermia. This is an important finding, as MDMA was shown to cause acute hyperthermia in laboratory animals (Capela et al. 2009; Carvalho et al. 2012), which has been related to its acute and long-term effects in the brain (Malberg and Seiden 1998; Touriño et al. 2010). Additionally, by preventing MDMA-induced hyperthermia, a decrease in acute and long-term neurotoxic effects of MDMA in mice (Touriño et al. 2010) and rats (Johnson and Yamamoto 2010) was observed. Therefore, using a human cell line differentiated to acquire the dopaminergic phenotype, this study represents the first report showing toxicity for the mixture of low micromolar concentrations of MDMA and its metabolites, which is more representative of the in vivo scenario, and highlighting the important role of hyperthermia in "ecstasy"-induced neurotoxicity.

As mentioned before, most in vitro studies are performed for each compound alone, not considering that, in the organism, the parent compound and its metabolites usually coexist. Therefore, the toxic effects may be a result of a dynamic interaction among all the compounds. Here, we show that MDMA and its metabolites, as a mixture, presented a different toxicity profile, compared to each compound alone. Therefore, studies conducted with parent compound and its metabolites, as a mixture, constitute important approaches to elucidate the neurotoxicity mechanisms of drugs, in particular of "ecstasy" and its metabolites.

Previous in vitro studies showed the activation of neuronal apoptotic pathways in the toxicity mediated by MDMA or its metabolites in rat cortical neurons (Capela et al. 2006b, 2007a), undifferentiated PC12 cells (Escubedo et al. 2011; Milhazes et al. 2006), and SH-SY5Y cells (Felim et al. 2009). Here, we also showed that the neurotoxic effects mediated by the mixture of MDMA and its metabolites were accompanied by increased caspase 3 activation, which corroborates that apoptotic features may be involved in brain injury associated with MDMA. Using higher concentrations of the MDMA catechol metabolites, our group reported that caspase 3 activation was not involved in the neurotoxicity promoted by these two compounds in SH-SY5Y differentiated cells (Ferreira et al. 2013). Therefore, our results suggest that low concentrations of MDMA metabolites may elicit a more apoptotic death profile; meanwhile, higher concentrations may trigger a necrotic process.

In the present study, by inhibiting DAT-mediated transport, the toxicity of the mixture of MDMA and its metabolites was not significantly modified, thus indicating a DAT-independent mechanism for the toxicity induced by this mixture. This corroborates previous in vitro studies, using the same experimental model, in which the toxicity elicited by the MDMA catechol metabolites, at higher concentrations, was independent of DAT-uptake system (Ferreira et al. 2013). Therefore, these data suggests that MDMA metabolites may access the cell through other means or even promote the generations of toxic reactive species outside the cell that will culminate in intracellular damage.

The inherent reactivity of catechol moiety of MDMA metabolites constitutes an important mechanism underlying their toxicity (Barbosa et al. 2012; Carvalho et al. 2004a). Further, MDMA metabolites can undergo oxidation to the corresponding *ortho*-quinones (Pizarro et al. 2004), which after generation of semiquinones may lead to ROS production (Erives et al. 2008) and cellular damage (Capela et al. 2009). These mechanisms contribute to the oxidative stress that is usually associated with MDMA-induced neurotoxicity (Barbosa et al. 2012; Capela et al. 2009; Carvalho et al. 2012). Accordingly, we showed increased ROS production in SH-SY5Y differentiated cells exposed to the mixture of MDMA and its metabolites. Therefore, antioxidants are expected to reduce not only *ortho*-quinones-related injury, but also the deleterious effects mediated by ROS that can be generated by MDMA metabolites. NAC, a powerful antioxidant that scavenges radicals and acts as cysteine donor for GSH synthesis, completely prevented the toxicity induced by the mixture of MDMA and its metabolites, reinforcing, thus, the role of pro-oxidant reactive species in the neurotoxicity induced by MDMA.

In biological systems, GSH is the most important antioxidant, conferring protection against reactive compounds and oxidative stress. Its biosynthesis, which occurs in the cytosol, involves two enzymes: γ-glutamylcysteine ligase and GSH synthase, the first catalyzing the rate-limiting step of this biosynthetic pathway (Marí et al. 2013). As previously observed, GSH plays an important role in protecting neuronal system against the toxicity induced by MDMA and its metabolites (Barbosa et al. 2012; Capela et al. 2007b). Here, we found that the mixture of MDMA and its metabolites induced a significant increase in intracellular glutathione levels. This corroborates previous findings, since we have previously reported an increase in intracellular glutathione levels after exposure of SH-SY5Y differentiated cells to high concentrations of MDMA metabolite α-MeDA (Ferreira et al. 2013). Additionally, the increase in GSH levels was more pronounced under normothermic than under hyperthermic conditions. This might be related to the fact that control cells after 48 h under hyperthermia have lower GSH levels, which can be viewed as a differential behavior of cells under hyperthermic conditions. The activation of intracellular pathways and consequent GSH increase were shown to be redox sensitive and particularly to the presence of electrophiles (Satoh and Lipton 2007). Other studies conducted with SH-SY5Y cells also reported an increase in glutathione levels using other experimental paradigms (Aguirre et al. 2007; Tirmenstein et al. 2005). We also demonstrated that

the mechanism behind the increase in intracellular glutathione content elicited by the mixture of MDMA and its metabolites involved de novo synthesis of GSH, since BSO, a potent γ-glutamylcysteine ligase inhibitor, completely prevented this effect. Therefore, we can postulate that the increase in intracellular glutathione content observed is probably a reflection of the activation of intracellular pathways promoted by the oxidative stress of the mixture.

Ca^{2+} homeostasis is critical in regulating neuronal function and survival (Oliveira and Gonçalves 2009). Increases in intracellular Ca^{2+} levels are thought to mediate a large number of cellular events, such as calpain activation, leading ultimately to neurotoxicity (Xu et al. 2013) and, consequently, to neuronal cell death (Bernardi and von Stockum 2012). In the present study, we observed increases in intracellular Ca^{2+} levels after exposure of SH-SY5Y differentiated cells to the mixture of MDMA and its metabolites. In accordance, MDMA was shown to induce increased cytosolic Ca^{2+} levels in PC12 cells, in a concentration-dependent manner (Garcia-Ratés et al. 2010). Furthermore, previous data indicated that MDMA triggers cell death through concerted proteolytic attacks of the structural proteins by calpain family of proteases (Warren et al. 2007). Therefore, to verify the role of intracellular Ca^{2+} as a key second messenger in the toxicity induced by the mixture of MDMA and its metabolites, cells were preloaded with BAPTA/AM for 30 min. As shown, by chelating intracellular Ca^{2+} with BAPTA/AM, the toxicity induced by the mixture of MDMA and its metabolites was not significantly modified. Therefore, these data suggest that a Ca^{2+}-regulated mechanism, such as calpain activation, which may lead to cell death, was not implicated on the toxicity induced by the mixture of MDMA and its metabolites in SH-SY5Y differentiated cells.

In conclusion, this study presents, for the first time, data indicating that low concentrations of MDMA and its metabolites, as a mixture, representing a more real scenario of the in vivo exposition to MDMA, were toxic to human SH-SY5Y differentiated cells. These findings come after several mechanistic studies using high concentrations of MDMA or of its metabolites in single exposure models and provide a new breakthrough in the study of MDMA neurotoxicity.

Acknowledgments This work was supported by "Fundação para a Ciência e a Tecnologia," Portugal (Project PTDC/SAU-FCF/102958/2008), under the framework of the "Programa Operacional Temático Factores de Competitividade (COMPTE) do Quadro Comunitário de Apoio III" and "Fundo Comunitário Europeu (FEDER) (FCOMP-01-0124-FEDER-011079)." The NMR spectrometers are part of the National NMR Facility, supported by FCT (RECI/BBB-BQB/0230/2012). DJB and RS were supported by fellowships (SFRH/BD/64939/2009 and SFRH/BD/29559/2006, respectively) from FCT, Portugal.

Conflict of interest The authors declare that they have no conflict of interest.

References

Adamaszek M, Khaw AV, Buck U, Andresen B, Thomasius R (2010) Evidence of neurotoxicity of ecstasy: sustained effects on electroencephalographic activity in polydrug users. PLoS One 5:e14097

Aguirre P, Valdés P, Aracena-Parks P, Tapia V, Núñez MT (2007) Upregulation of γ-glutamate-cysteine ligase as part of the long-term adaptation process to iron accumulation in neuronal SH-SY5Y cells. Am J Physiol Cell Physiol 292:2197–2203

Bai F, Lau SS, Monks TJ (1999) Glutathione and *N*-acetylcysteine conjugates of α-methyldopamine produce serotonergic neurotoxicity: possible role in methylenedioxyamphetamine-mediated neurotoxicity. Chem Res Toxicol 12:1150–1157

Bai F, Jones DC, Lau SS, Monks TJ (2001) Serotonergic neurotoxicity of 3,4-(±)-methylenedioxyamphetamine and 3,4-(±)-methylendioxymethamphetamine (ecstasy) is potentiated by inhibition of γ-glutamyl transpeptidase. Chem Res Toxicol 14:863–870

Barbosa DJ, Capela JP, Oliveira JMA et al (2012) Pro-oxidant effects of Ecstasy and its metabolites in mouse brain synaptosomes. Br J Pharmacol 165:1017–1033

Bernardi P, von Stockum S (2012) The permeability transition pore as a Ca^{2+} release channel: new answers to an old question. Cell Calcium 52:22–27

Cadet JL, Thiriet N, Jayanthi S (2001) Involvement of free radicals in MDMA-induced neurotoxicity in mice. Ann Med Interne 152:57–59

Capela JP, Meisel A, Abreu AR et al (2006a) Neurotoxicity of ecstasy metabolites in rat cortical neurons, and influence of hyperthermia. J Pharmacol Exp Ther 316:53–61

Capela JP, Ruscher K, Lautenschlager M et al (2006b) Ecstasy-induced cell death in cortical neuronal cultures is serotonin 2A-receptor-dependent and potentiated under hyperthermia. Neuroscience 139:1069–1081

Capela JP, Fernandes E, Remiao F, Bastos ML, Meisel A, Carvalho F (2007a) Ecstasy induces apoptosis via 5-HT_{2A}-receptor stimulation in cortical neurons. Neurotoxicology 28:868–875

Capela JP, Macedo C, Branco PS et al (2007b) Neurotoxicity mechanisms of thioether ecstasy metabolites. Neuroscience 146:1743–1757

Capela JP, Carmo H, Remião F, Bastos ML, Meisel A, Carvalho F (2009) Molecular and cellular mechanisms of ecstasy-induced neurotoxicity: an overview. Mol Neurobiol 39:210–271

Carvalho M, Remiao F, Milhazes N et al (2004a) The toxicity of *N*-methyl-alpha-methyldopamine to freshly isolated rat hepatocytes is prevented by ascorbic acid and *N*-acetylcysteine. Toxicology 200:193–203

Carvalho M, Remião F, Milhazes N et al (2004b) Metabolism is required for the expression of ecstasy-induced cardiotoxicity in vitro. Chem Res Toxicol 17:623–632

Carvalho M, Carmo H, Costa VM et al (2012) Toxicity of amphetamines: an update. Arch Toxicol 86:1167–1231

Cheung Y, Lau WK, Yu M et al (2009) Effects of all-trans-retinoic acid on human SH-SY5Y neuroblastoma as in vitro model in neurotoxicity research. Neurotoxicology 30:127–135

Chu T, Kumagai Y, DiStefano EW, Cho AK (1996) Disposition of methylenedioxymethamphetamine and three metabolites in the brains of different rat strains and their possible roles in acute serotonin depletion. Biochem Pharmacol 51:789–796

Colado MI, O'Shea E, Granados R, Murray TK, Green AR (1997) In vivo evidence for free radical involvement in the degeneration of rat brain 5-HT following administration of MDMA ("ecstasy")

and *p*-chloroamphetamine but not the degeneration following fenfluramine. Br J Pharmacol 121:889–900

de la Torre R, Farré M (2004) Neurotoxicity of MDMA (ecstasy): the limitations of scaling from animals to humans. Trends Pharmacol Sci 25:505–508

De La Torre R, Farré M, Ortuño J et al (2000) Non-linear pharmacokinetics of MDMA ('ecstasy') in humans. Br J Clin Pharmacol 49:104–109

Erives GV, Lau SS, Monks TJ (2008) Accumulation of neurotoxic thioether metabolites of 3,4-(±)-methylenedioxymethamphetamine in rat brain. J Pharmacol Exp Ther 324:284–291

Escobedo I, O'Shea E, Orio L et al (2005) A comparative study on the acute and long-term effects of MDMA and 3,4-dihydroxymethamphetamine (HHMA) on brain monoamine levels after i.p. or striatal administration in mice. Br J Pharmacol 144:231–241

Escubedo E, Abad S, Torres I, Camarasa J, Pubill D (2011) Comparative neurochemical profile of 3,4-methylenedioxymethamphetamine and its metabolite alpha-methyldopamine on key targets of MDMA neurotoxicity. Neurochem Int 58:92–101

Esteban B, O'Shea E, Camarero J, Sanchez V, Green AR, Colado MI (2001) 3,4-Methylenedioxymethamphetamine induces monoamine release, but not toxicity, when administered centrally at a concentration occurring following a peripherally injected neurotoxic dose. Psychopharmacology 154:251–260

Felim A, Herrera G, Neudörffer A, Blanco M, O'Connor J, Largeron M (2009) Synthesis and in vitro cytotoxicity profile of the R-enantiomer of 3,4-dihydroxymethamphetamine (R-(−)-HHMA): comparison with related catecholamines. Chem Res Toxicol 23:211–219

Ferguson CS, Tyndale RF (2011) Cytochrome P450 enzymes in the brain: emerging evidence of biological significance. Trends Pharmacol Sci 32:708–714

Ferreira PS, Nogueira TB, Costa VM et al (2013) Neurotoxicity of "ecstasy" and its metabolites in human dopaminergic differentiated SH-SY5Y cells. Toxicol Lett 216:159–170

Garcia-Ratés S, Camarasa J, Sánchez-García AI, Gandía L, Escubedo E, Pubill D (2010) The effects of 3,4-methylenedioxymethamphetamine (MDMA) on nicotinic receptors: Intracellular calcium increase, calpain/caspase 3 activation, and functional upregulation. Toxicol Appl Pharmacol 244:344–353

Gollamudi R, Ali SF, Lipe G et al (1989) Influence of inducers and inhibitors on the metabolism in vitro and neurochemical effects in vivo of MDMA. Neurotoxicology 10:455–466

Granado N, O'Shea E, Bove J, Vila M, Colado MI, Moratalla R (2008) Persistent MDMA-induced dopaminergic neurotoxicity in the striatum and substantia nigra of mice. J Neurochem 107:1102–1112

Granado N, Ares-Santos S, Oliva I et al (2011) Dopamine D2-receptor knockout mice are protected against dopaminergic neurotoxicity induced by methamphetamine or MDMA. Neurobiol Dis 42:391–403

Haefeli RH, Erb M, Gemperli AC et al (2011) NQO1-dependent redox cycling of idebenone: effects on cellular redox potential and energy levels. PLoS One 6:e17963

Johnson BN, Yamamoto BK (2010) Chronic stress enhances the corticosterone response and neurotoxicity to +3,4-methylenedioxymethamphetamine (MDMA): the role of ambient temperature. J Pharmacol Exp Ther 335:180–189

Jones DC, Duvauchelle C, Ikegami A et al (2005) Serotonergic neurotoxic metabolites of ecstasy identified in rat brain. J Pharmacol Exp Ther 313:422–431

Lopes FM, Schröder R, Júnior MLC et al (2010) Comparison between proliferative and neuron-like SH-SY5Y cells as an in vitro model for Parkinson disease studies. Brain Res 1337:85–94

Lowry OH, Rosebrough NJ, Farr AL, Randall RJ (1951) Protein measurement with the folin phenol reagent. J Biol Chem 193:265–275

Malberg JE, Seiden LS (1998) Small changes in ambient temperature cause large changes in 3,4-methylenedioxymethamphetamine (MDMA)-induced serotonin neurotoxicity and core body temperature in the rat. J Neurosci 18:5086–5094

Marí M, Morales A, Colell A, García-Ruiz C, Kaplowitz N, Fernández-Checa JC (2013) Mitochondrial glutathione: features, regulation and role in disease. Biochim Biophys Acta 1830:3317–3328

Milhazes N, Cunha-Oliveira T, Martins P et al (2006) Synthesis and cytotoxic profile of 3,4-methylenedioxymethamphetamine ("Ecstasy") and its metabolites on undifferentiated PC12 cells: a putative structure–toxicity relationship. Chem Res Toxicol 19:1294–1304

Morefield KM, Keane M, Felgate P, White JM, Irvine RJ (2011) Pill content, dose and resulting plasma concentrations of 3,4-methylendioxymethamphetamine (MDMA) in recreational 'ecstasy' users. Addiction 106:1293–1300

Mueller M, Kolbrich EA, Peters FT et al (2009a) Direct comparison of (±) 3,4-methylenedioxymethamphetamine ("Ecstasy") disposition and metabolism in squirrel monkeys and humans. Ther Drug Monit 31:367–373

Mueller M, Yuan J, Felim A et al (2009b) Further studies on the role of metabolites in (±)-3,4-methylenedioxymethamphetamine-induced serotonergic neurotoxicity. Drug Metab Dispos 37:2079–2086

Nguyen HN, Wang C, Perry DC (2002) Depletion of intracellular calcium stores is toxic to SH-SY5Y neuronal cells. Brain Res 924:159–166

Oliveira JMA, Gonçalves J (2009) In situ mitochondrial Ca^{2+} buffering differences of intact neurons and astrocytes from cortex and striatum. J Biol Chem 284:5010–5020

Pennypacker KR, Kuhn DM, Billingsley ML (1989) Changes in expression of tyrosine hydroxylase immunoreactivity in human SMS-KCNR neuroblastoma following retinoic acid or phorbol ester-induced differentiation. Brain Res Mol Brain Res 5:251258

Perry SW, Barbieri J, Tong N et al (2010) Human immunodeficiency virus-1 tat activates calpain proteases via the ryanodine receptor to enhance surface dopamine transporter levels and increase transporter-specific uptake and Vmax. J Neurosci 30:14153–14164

Pizarro N, Farre M, Pujadas M et al (2004) Stereochemical analysis of 3,4-methylenedioxymethamphetamine and its main metabolites in human samples including the catechol-type metabolite (3,4-dihydroxymethamphetamine). Drug Metab Dispos 32:1001–1007

Presgraves S, Ahmed T, Borwege S, Joyce J (2003) Terminally differentiated SH-SY5Y cells provide a model system for studying neuroprotective effects of dopamine agonists. Neurotox Res 5:579–598

Roberts GMP, Nestor L, Garavan H (2009) Learning and memory deficits in ecstasy users and their neural correlates during a face-learning task. Brain Res 1292:71–81

Satoh T, Lipton SA (2007) Redox regulation of neuronal survival mediated by electrophilic compounds. Trends Neurosci 30:37–45

Schmidt CJ, Wu L, Lovenberg W (1986) Methylenedioxymethamphetamine: a potentially neurotoxic amphetamine analogue. Eur J Pharmacol 124:175–178

Shavali S, Sens DA (2008) Synergistic neurotoxic effects of arsenic and dopamine in human dopaminergic neuroblastoma SH-SY5Y cells. Toxicol Sci 102:254–261

Sulzer D (2011) How addictive drugs disrupt presynaptic dopamine neurotransmission. Neuron 69:628–649

Sun F, Zhang L, Zhang R, Li L (2011) Tetrahydroxystilbene glucoside protects human neuroblastoma SH-SY5Y cells against MPP+-induced cytotoxicity. Eur J Pharmacol 660:283–290

Takeuchi H, Yanagida T, Inden M et al (2009) Nicotinic receptor stimulation protects nigral dopaminergic neurons in rotenone-induced Parkinson's disease models. J Neurosci Res 87:576–585

Tirmenstein MA, Hu CX, Scicchitano MS et al (2005) Effects of 6-hydroxydopamine on mitochondrial function and glutathione status in SH-SY5Y human neuroblastoma cells. Toxicol In Vitro 19:471–479

Touriño C, Zimmer A, Valverde O (2010) THC prevents MDMA neurotoxicity in mice. PLoS One 5:e9143

Wang X, Xu J (2005) Possible involvement of Ca^{2+} signaling in rotenone-induced apoptosis in human neuroblastoma SH-SY5Y cells. Neurosci Lett 376:127–132

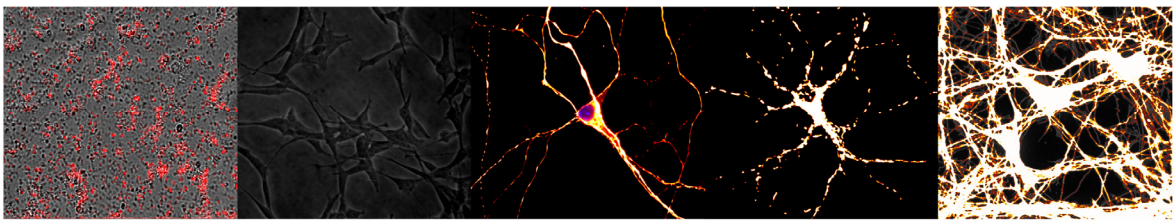
Warren MW, Zheng W, Kobeissy FH et al (2007) Calpain- and caspase-mediated alphaII-spectrin and tau proteolysis in rat cerebrocortical neuronal cultures after ecstasy or methamphetamine exposure. Int J Neuropsychopharmacol 10:479–489

Xu B, Xu Z, Deng Y, Liu W, Yang H, Wei Y (2013) MK-801 protects against intracellular Ca^{2+} overloading and improves *N*-methyl-D-aspartate receptor expression in cerebral cortex of methylmercury-poisoned rats. J Mol Neurosci 49:162–171

5.

MDMA impairs mitochondrial neuronal trafficking in a Tau- and Mitofusin 2/Drp1-dependent manner

Manuscript submitted for publication



MDMA impairs mitochondrial neuronal trafficking in a Tau- and Mitofusin 2/Drp1-dependent manner

Abbreviated title

MDMA impairs mitochondrial neuronal trafficking

Authors

Daniel José Barbosa[1,2,*], Romàn Serrat[2,*], Serena Mirra[2], Martí Quevedo[2], Elena Gómez de Barreda[3], Jesús Àvila[3], Eduarda Fernandes[4], Maria de Lourdes Bastos[1], João Paulo Capela[1,5], Félix Carvalho[1,$] and Eduardo Soriano[2,$]

Affiliations

[1]REQUI*M*TE (Rede de Química e Tecnologia), Toxicology Laboratory, Department of Biological Sciences, Faculty of Pharmacy, University of Porto, Rua Jorge Viterbo Ferreira 228, 4050-313 Porto, Portugal.

[2]Developmental Neurobiology and Regeneration Lab, Department of Cell Biology, University of Barcelona; Institute for Research in Biomedicine, Barcelona Science Park. Centro de Investigación Biomédica en Red sobre Enfermedades Neurodegenerativas (CIBERNED, ISCIII). C/Baldiri Reixac 10-12, 08028 Barcelona, Spain.

[3]Centro de Investigación Biomédica en Red sobre Enfermedades Neurodegenerativas (CIBERNED, ISCIII). Center of Molecular Biology Severo Ochoa (CSIC-UAM), C/Nicolás Cabrera 1, Campus de la Universidad Autónoma de Madrid, 28049, Madrid, Spain.

[4]REQUI*M*TE, Laboratory of Applied Chemistry, Department of Chemical Sciences, Faculty of Pharmacy, University of Porto, Rua Jorge Viterbo Ferreira 228, 4050-313 Porto, Portugal.

[5]Faculty of Health Sciences, University Fernando Pessoa, Rua 9 de Abril 349, 4249-004 Porto, Portugal.

Footnotes

[*]These authors contributed equally

[$]FC and ES are co-senior authors

Corresponding Authors

Félix Carvalho

E-mail: felixdc@ff.up.pt

Phone: (+351) 220 428 500

Fax: (+351) 226 093 390

Eduardo Soriano

E-mail: esoriano@ub.edu

Phone: (+34) 93 4037117

Fax: (+34) 93 4037116

Abstract

Identification of the mechanisms by which addictive drugs cause neuronal dysfunction is essential for understanding the biological bases of their acute and long lasting addictive and toxic effects. Here, we performed real-time functional experiments of axonal transport of mitochondria to explore the role of *in situ* mitochondrial dysfunction in 3,4-methylenedioxymethamphetamine (MDMA; "ecstasy")-related brain actions. We show that MDMA dramatically reduced mitochondrial trafficking in hippocampal neurons in a Tau-dependent manner, in which glycogen synthase 3β (GSK3β)-dependent phosphorylation was implicated. Furthermore, we found that these trafficking abnormalities were rescued by over-expression of mitofusin 2 (Mfn2) and dynamin-related protein 1 (Drp1), but not of Miro1. Given the relevance of mitochondrial targeting for neuronal function and neurotransmission, our data underscore a novel mechanism of action of MDMA that may contribute to our understanding of how drugs of abuse alter neuronal function.

Keywords

3,4-Methylenedioxymethamphetamine (MDMA; "ecstasy"); Mitochondrial fusion/fission; Mitochondrial trafficking; Mitochondrial dysfunction; Neurotoxicity.

Introduction

Addictive drugs cause a variety of complex cellular events, including changes in membrane excitability and neurotransmission, activation of complex signalling pathways, altered synaptic physiology and structural changes, and drug-evoked synaptic plasticity and neurotoxicity, which mediate both acute and long-term effects and addiction (Capela *et al.*, 2009; Kenny, 2011; Lüscher and Malenka, 2011). 3,4-Methylenedioxymethamphetamine (MDMA; "ecstasy") is a major drug of abuse with addictive and neurotoxic properties well documented both in humans and laboratory animals (Bai *et al.*, 2001; Capela *et al.*, 2009; Granado *et al.*, 2011). Though the molecular and cellular mechanisms behind MDMA-induced addiction and neurotoxicity remain unclear, recent studies have attributed a pivotal role to mitochondria (Alves *et al.*, 2007; Alves *et al.*, 2009; Puerta *et al.*, 2010).

In neurons, the high dependence on mitochondria for local adenosine 5'-triphosphate (ATP) supply and Ca^{2+} buffering in neurotransmission requires highly regulated mitochondrial trafficking and targeting (López-Doménech *et al.*, 2012; Sheng and Cai, 2012). Axonal transport of mitochondria is mediated by motor proteins. Members of the kinesin family mediate anterograde transport, while cytoplasmic dyneins mediate retrograde transport, processes that are highly dependent on ATP produced locally by mitochondria (MacAskill and Kittler, 2010; Shahpasand *et al.*, 2012; Sheng and Cai, 2012). Kinesin-1, the principal plus-end directed motor is linked to the outer mitochondrial membrane proteins Miro1/2 by the adaptor proteins Milton/TRAK (Macaskill *et al.*, 2009; Wang and Schwarz, 2009). Miro1/2, GTPase proteins with two Ca^{2+}-binding domains (EF hands), regulate the integrity of this complex, by a Ca^{2+}-dependent mechanism (Macaskill *et al.*, 2009; Wang and Schwarz, 2009; Byun *et al.*, 2012).

Microtubule-associated protein Tau, which is primarily localized within the axonal compartment of neurons (Rintoul and Reynolds, 2010), binds to microtubules resulting in the formation of microtubule bundles. In neurons, Tau phosphorylation has been proposed to decrease mitochondrial transport (Rintoul and Reynolds, 2010; Vossel *et al.*, 2010). MDMA has been associated with ATP depletion (Darvesh and Gudelsky, 2005) and increased Tau phosphorylation (Busceti *et al.*, 2008), which suggests a possible interference of MDMA on mitochondrial trafficking.

Disruption of mitochondrial trafficking or of the dynamic equilibrium between mitochondrial fusion and fission may contribute to important neuronal deficits and herald neuronal injury or death (Perier and Vila, 2012; Wang *et al.*, 2013). Furthermore, mitochondrial dysfunction, including trafficking, has been linked to several psychiatric diseases (Shao *et al.*, 2008; MacAskill *et al.*, 2010; Atkin *et al.*, 2013). In the present

study, we evaluated whether mitochondrial dynamics, namely mitochondrial neuronal trafficking, is affected by MDMA. We show that acute MDMA incubation substantially altered mitochondrial trafficking in neurons. These findings underscore a novel mechanism of action of MDMA that may have important consequences in neuronal function.

Materials and Methods

Materials

All reagents used were of analytical grade or of the highest grade available. Neurobasal medium, B27 supplement, penicillin/streptomycin 10,000 U/mL, GlutaMAX™ supplement, 0.5% trypsin/1 mM ethylenediaminetetraacetic acid (EDTA) without phenol red, horse serum, Opti-MEM medium, Lipofectamine 2000 and Dulbecco's phosphate-buffered saline (DPBS) were purchased from Gibco Laboratories (Lenexa, KS, USA). Poly-*L*-lysine (PLL), triton X-100, Na_3VO_4, NaF, Tris-HCl, bromophenol blue and β-mercaptoethanol were obtained from Sigma-Aldrich (St. Louis, MO, USA). DNAse recombinant I and complete protease inhibitor cocktail were from Roche Diagnostics (Mannheim, Germany). Fluo4/AM was purchased from Molecular Probes (Invitrogen Inc, Carlsbad, CA, USA). Swine anti-rabbit and goat anti-mouse IgG-peroxidase polyclonal antibodies were from DAKO (Glostrup, Denmark). Mouse anti-α-actin monoclonal antibody was supplied by Calbiochem (Darmstadt, Germany). MDMA (hydrochloride salt) was extracted and purified from high purity MDMA tablets kindly provided by the Portuguese Police Department. The salt obtained was pure and fully characterized by NMR and mass spectrometry methodologies.

Animals, cell culture and transfection

All procedures were approved by the Barcelona Science Park's Animal Experimentation Committee and performed in compliance with the "Guide for the Care and Use of Laboratory Animals" of the Institute for Laboratory Animal Research (Research, 2011), and the European Community Council directive and the National Institute of Health guidelines for the care and use of laboratory animals. Wt OF1 embryos and C57BL/6 Tau (-/-) embryos (de Barreda *et al.*, 2010) aged E15-16 (the mating day was E0) were used. Primary hippocampal cultures were prepared following previously published methods (Llorens-Martín *et al.*, 2011; López-Doménech *et al.*, 2012). Briefly, embryos were placed in ice-cold DPBS (-/-) containing 0.6% glucose, and the hippocampi were dissected out. Following trypsinization (0.05% trypsin/EDTA) and DNAse I treatment, tissue pieces were dissociated, and cells were seeded at a density of 78 000 cells/cm^2 in 35-mm *Fluordish* plates (World Precision Instruments, Sarasota, FL, USA) pre-coated with 0.2 mg/mL PLL solution (prepared in 0.1 M borate buffer, pH 8.5). For western blotting, cells were seeded onto 6-well plates. To evaluate mitochondrial length, hippocampal cultures were seeded in 12 mm round pre-coated glass coverslips. Cultures were maintained at 37ºC in a 5% CO_2/95% air atmosphere. Transfection was performed at 4 days *in vitro* (DIV) using Lipofectamine 2000, and cultures were used at 6DIV. Cultures

were transfected with MitDsRed (a gift from Antonio Zorzano) and GFP, or co-transfected with one of the following constructs: Miro1, Miro1ΔEF (Macaskill *et al.*, 2009), GSK3β Aln9 (Byun *et al.*, 2012), mitofusin 2 (Mfn2), Mfn2 R94Q (Misko *et al.*, 2010) or dynamin-related protein 1 (Drp1) K38A (Zhao *et al.*, 2011). The lack of Tau protein in hippocampal cultures prepared from C57BL/6 Tau (-/-) embryos was confirmed by western blotting (data not shown).

Design of the study

Hippocampal cultures were initially exposed to MDMA (1.6 mM) for 45 to 120 min. The concentration of MDMA was selected in accordance with a previous study (Carvalho *et al.*, 2004) and did not induce significant toxicity in our experimental model, as evaluated by the MTT reduction assay (data not shown). Exposure to MDMA (1.6 mM) for 90 min was selected for all the remaining studies of mitochondrial transport. Tau phosphorylation levels and mitochondrial length were also evaluated after exposure to MDMA (1.6 mM) for 90 min.

Live-imaging of axonal transport of mitochondria and intracellular Ca^{2+} levels in hippocampal neurons

Live-imaging of hippocampal neurons was performed using a Olympus IX81 confocal microscope (Olympus Corporation, Tokyo, Japan), equipped with a 60x immersion objective, and a Andor Revolution® XD spinning disk confocal microscopy system composed by a iXonEM + EM-CCD camera (Andor Technology, Belfast, United Kingdom), and FRAPPA and solid-state laser combiner (ALC-UVP 350i, Andor Technology) with the renowned CSU-X1 confocal scanner (Yokogawa Electric Corporation, Tokyo, Japan). All cultures were kept at 37ºC, using a heating insert on the microscope stage and an incubating chamber. For measurements of axonal transport of mitochondria, axonal processes were identified following morphological criteria. Time-lapse series of image stacks composed of 151 images (512x512 pixels) were taken every 6 sec for 15 min. All 151 images obtained were processed mainly with Andor IQ2 software (Andor Technology). Further image processing, analysis and video compilation and edition was done with Fiji (Image JA v1.45b, Open source software, NIH, Bethesda, Maryland, USA). Kymographs were generated with MetaMorph Software (Molecular Devices - MDS Analytical Technologies, Sunnyvale, CA, USA). Velocities of moving mitochondria were measured from the corresponding kymographs. In all cases, mitochondria were considered motile when they moved more than 5 μm during the 15-min periods. When a

single mitochondrion moved in both the anterograde and retrograde directions, it was included in both groups.

For measurements of intracellular Ca^{2+} levels, primary hippocampal cultures were washed once with Krebs buffer (145 mM NaCl, 5 mM KCl, 2.5 mM $CaCl_2$, 1 mM $MgCl_2$, 5.6 mM glucose, 10 mM Hepes, pH 7.4), and subsequently loaded with 5 μM Fluo4/AM in Krebs buffer, containing 0.4% pluoronic acid (w/v), for 30 min, at 37ºC. Stock solution of Fluo4/AM (250 μM) was prepared in DMSO. After this incubation time, the cultures were incubated in fresh Krebs buffer for a further 5 min (to allow the Fluo4/AM desterification) and subsequently imaged. Time-lapse series of image stacks composed of 101 images (512x512 pixels) were taken every 1 min, during 100 min. After 10 min of imaging, MDMA was added to the cultures, and images were taken again for another 90 min (images were continuously acquired before and after drug exposure).

Measurements of mitochondrial length

Hippocampal cultures transfected with MitDsRed and GFP and incubated with MDMA for 90 min were then fixed in 4% paraformaldehyde, for 20 min, at room temperature. Stacks of images (1024x1024 pixels) were acquired in a Leica TCS SP2 confocal microscope (Leica Microsystems, Mannheim, Germany) equipped with a 60x immersion objective and a Leica Confocal Software (Leica Microsystems). Further image processing and analysis was done with Fiji (NIH) by determining mitochondrial-tagged MitDsRed. Mitochondrial length was estimated for each mitochondrion. To identify axonal processes GFP was excited at 488 nm, and fluorescence emission was collected at 508 nm. MitDsRed was excited a 561 nm and fluorescence intensities were collected at 592 nm.

Western blotting analysis of Tau phosphorylation

Cellular proteins were extracted with lysis buffer [50 mM Tris-HCl pH 7.5, 150 mM NaCl, 5 mM EDTA, 1% triton X-100 (v/v), 10% glycerol (v/v), complete protease inhibitor cocktail, 1 mM Na_3VO_4, 10 mM $Na_4P_2O_7$ and 10 mM NaF), followed by an incubation on ice for 30 min. After centrifugation at 16,000*g,* for 10 min, at 4ºC, a SDS-PAGE reducing buffer [150 mM Tris-HCl pH 6.8, 3% SDS (w/v), 30% glycerol (v/v), 0.075% bromophenol blue (w/v) and 15% β-mercaptoethanol (v/v)] was added to the samples (1:2 ratio), which were then boiled at 90 °C for 5 min. Proteins were loaded and separated in 10% SDS/polyacrylamide gels, at a constant voltage of 120 mV. Gels were transferred to nitrocellulose membranes (Whatman, Dassel, Germany) using a transfer buffer (20% methanol (v/v) in 20 mM Tris Base and 139 mM glycine), at 125 mV, for 1.5h. Membranes were then rinsed in Tris-buffered saline solution with Tween 20 [TBS-T: 10 mM Tris base,

140 mM NaCl and 0.1 % Tween 20 (v/v), pH 7.4], and non-specific sites were blocked for 1h, at room temperature, in blocking buffer [3% BSA (w/v) in TBS-T]. Membranes were incubated with primary antibodies (overnight at 4ºC): rabbit polyclonal anti-P-Tau Thr181 (1:5,000) or mouse monoclonal anti-α-actin (1:100,000). After washing 5 times (10 min each) with TBS-T membranes were then incubated with secondary antibodies (1h at room temperature): swine anti-rabbit or goat anti-mouse IgG-peroxidase antibodies (1:2,500). All antibodies were diluted in blocking buffer. Following 3 washes (10 min each) with TBS-T, bands were visualized using ECL chemiluminescence reagents (Amersham Pharmacia Biotech, Buckinghamshire, United Kingdom), according to the supplier`s instructions, and were quantified using the Quantity One software (Bio-Rad Laboratories).

Data analysis

Values are represented as mean ± SEM. 7-16 axons, from 3-7 independent experiments, were analyzed for each condition. Normality of the data distribution was assessed by three tests: KS normality test, D'Agostino and Pearson omnibus normality test and Shapiro-Wilk normality test. In experiments with only one variable, statistical comparisons between groups were performed with Mann-Whitney test or Unpaired Student's t-test (to compare two groups), or with Friedman test (non-parametric one-way ANOVA with repeated measures) to compare three or more groups. Dunn's test was used for *post-hoc* evaluations. To compare data from experiments with two variables, two-way ANOVA was used, followed by Bonferroni's test for *post-hoc* evaluations. Details of the statistical analysis performed are described in each figure legend. All analyses were performed using GraphPad Prism 6.0 for Windows (GraphPad Software, San Diego, CA, USA).

Results

To address whether MDMA alters mitochondrial dynamics, we transfected hippocampal neurons with MitDsRed, performed videorecordings of mitochondrial trafficking, and generated kymographs, which were analyzed as described elsewhere (López-Doménech *et al.*, 2012). Control neurons exhibited prominent mitochondrial trafficking (Figures 1 and 2) with an average of 70% of motile mitochondria, moving in both anterograde and retrograde directions at a speed of about 0.4 μm/sec (Figures 1 and 2 and Movie 1). Exposure to MDMA (1.6 mM) for 45, 90 or 120 min dramatically reduced the mitochondrial trafficking in a time-dependent manner (Figure 1).

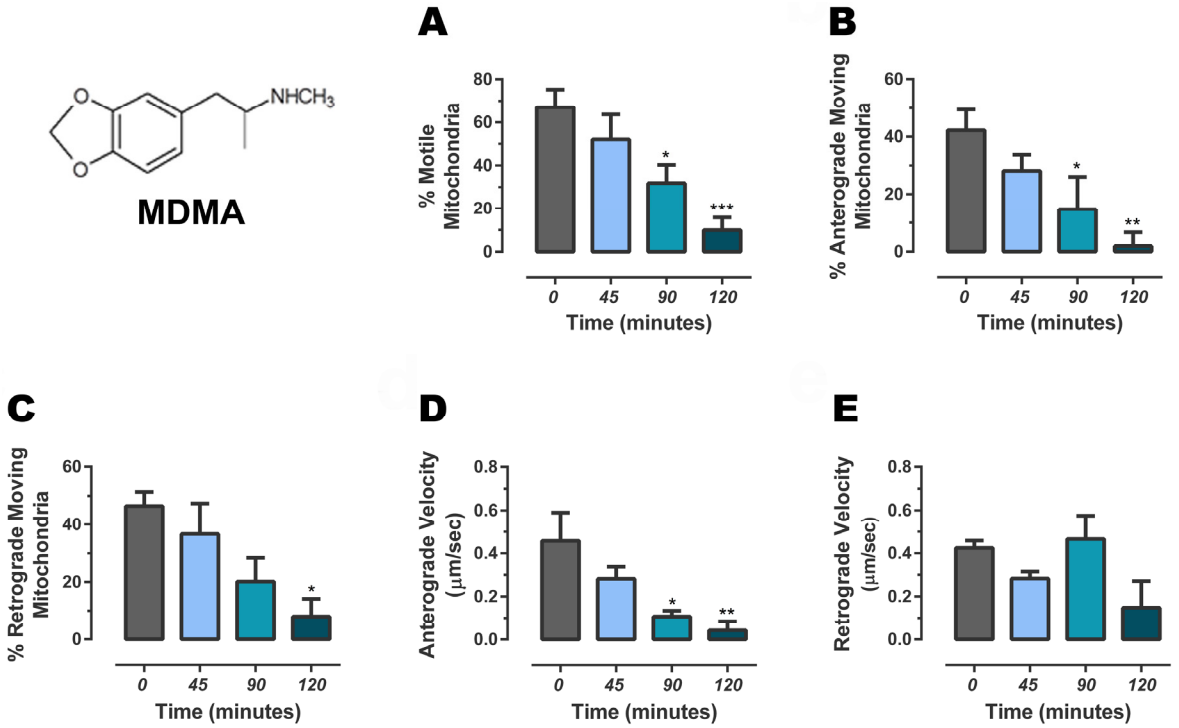


Figure 1. Effects of MDMA on axonal transport of mitochondria in hippocampal neurons. Hippocampal neuronal cultures were transfected with MitDsRed and GFP at 4DIV, and axonal transport of mitochondria was measured at 6DIV. After imaging under control conditions, MDMA (1.6 mM) was added to the cultures, and axons were imaged again after 45, 90 and 120 min of incubation. (A-E) Graphical representation of the percentage of motile mitochondria and velocities (both anterograde and retrograde directions) measured in kymographs obtained under control conditions and after exposure to MDMA. Data represent mean ± SEM (*p<0.05, **p<0.01, ***p<0.001 MDMA *vs.* control, Friedman test and Dunn's *post-hoc* test).

Movie 1 Axonal transport of mitochondria in a hippocampal neuron, at 6DIV, under control conditions.

According to these results, the 90 min time-point was selected for all the remaining studies of mitochondrial transport. Exposure to MDMA (1.6 mM) for 90 min dramatically reduced the percentage of motile mitochondria, in both anterograde and retrograde directions, as well as the anterograde velocity (Figure 2 and Movie 2).

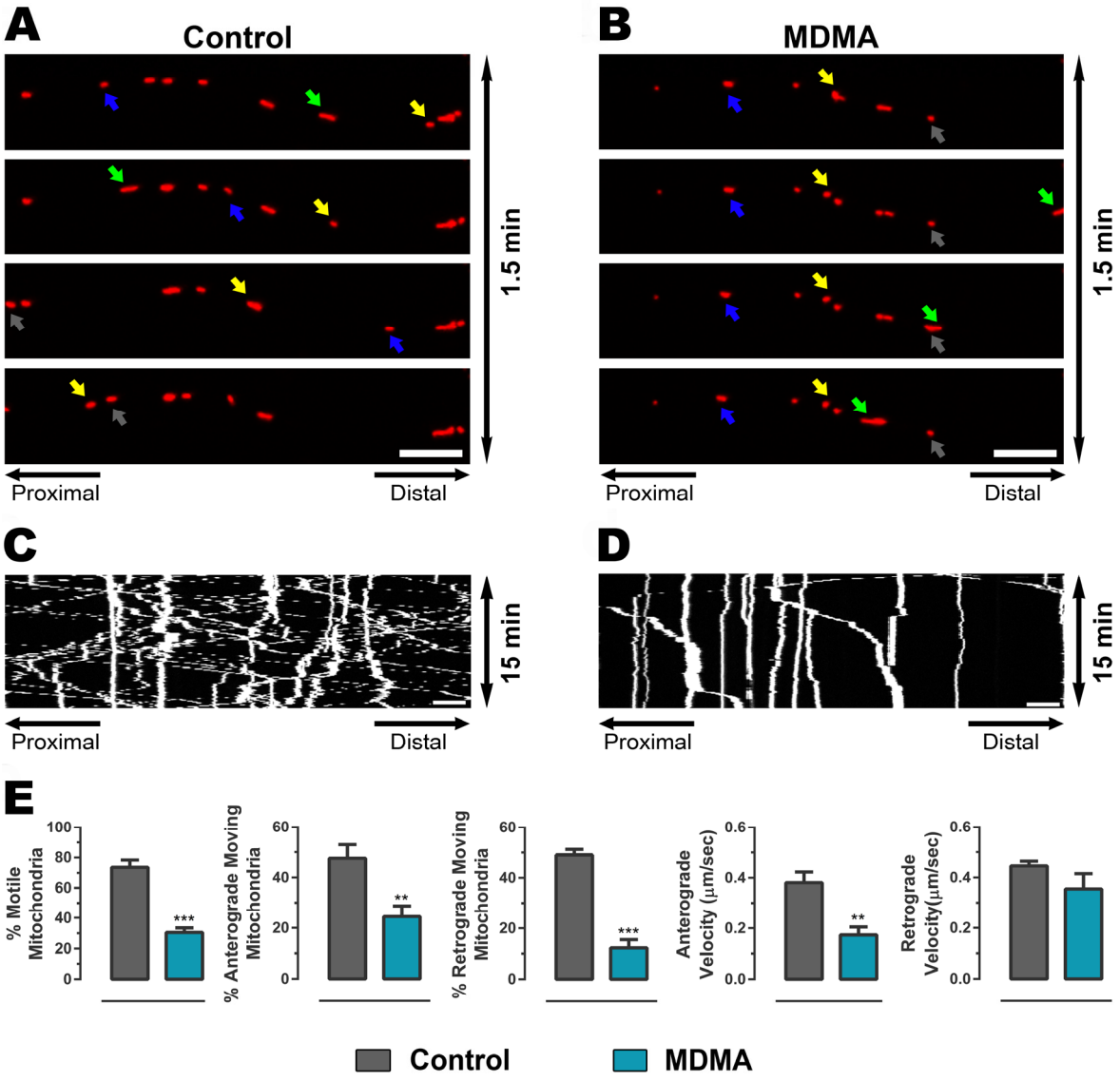


Figure 2. Mitochondrial neuronal trafficking impairment associated with MDMA. (A-B) Series of four representative confocal images, taken every 30 sec, of a live axon over-expressing MitDsRed under control conditions (A) or after 90 min of exposure to MDMA (1.6 mM) (B). Colored arrows indicate the same mitochondrion through the different acquisitions. (C-D) Representative kymographs of axons in control conditions (C) or after exposure to MDMA (D). (E) Graphical representation of the percentage of motile mitochondria and velocities, measured in kymographs obtained before and after exposure to MDMA (1.6 mM) for 90 min. Data represent mean ± SEM (**p<0.01; ***p<0.001 MDMA *vs.* control, Mann-Whitney test). Scale bar: 10 µm.

Movie 2 Axonal transport of mitochondria in a hippocampal neuron, after exposure to MDMA (1.6 mM), for 90 min.

Mitochondrial dynamics in neurons is exquisitely controlled by complex machinery involving the Miro/TRAK2 complex (Macaskill *et al.*, 2009; Wang and Schwarz, 2009; Sheng and Cai, 2012) and the GTPase proteins Mfns and Drp1 (Misko *et al.*, 2010; Misko *et al.*, 2012; Sheng and Cai, 2012), in a way that depends on Ca^{2+} concentration (Cereghetti *et al.*, 2008; Macaskill *et al.*, 2009; Wang and Schwarz, 2009). Exposure to 1.6 mM MDMA increased Ca^{2+} concentrations in the cell body and neuronal extensions

(Figure 3A). To address whether the Ca^{2+}-binding domains of Miro1 mediated MDMA's effects, we transfected hippocampal neurons with Miro1 and also with a Miro1 construct lacking the EF Ca^{2+}-binding domains (Miro1ΔEF), which acts as a dominant negative (Macaskill *et al.*, 2009). Neither the over-expression of Miro1 nor Miro1ΔEF reversed the effects of MDMA on neuronal mitochondrial trafficking (Figure 3B-D). This finding, therefore, indicates a Miro1-independent mechanism for the reported trafficking impairment induced by MDMA.

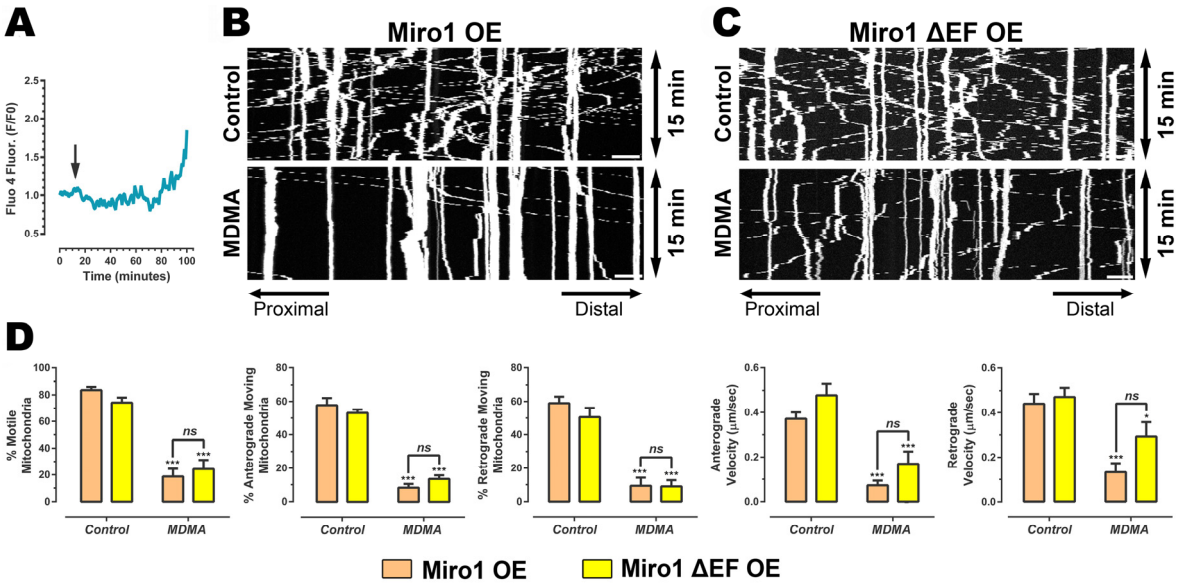


Figure 3. MDMA impaired mitochondrial neuronal trafficking by a Ca^{2+}-regulated Miro1-independent mechanism. (A) Graphical representation of individual changes in Fluo4 whole-cell F/F0 fluorescence ratios for a single neuron, pre-loaded with Fluo4/AM (5 µM), during 90 min of exposure to MDMA (1.6 mM), showing a time-dependent increase in intracellular Ca^{2+} concentration. The arrow indicates the onset of MDMA addition. (B-C) Representative kymographs from neurons transfected with Miro1 (B) or Miro1 ΔEF (C) under control conditions or after exposure to MDMA (1.6 mM) for 90 min. (D) Graphical representation of the percentage of motile mitochondria and velocities, measured in kymographs obtained under control conditions or after exposure to MDMA (1.6 mM) for 90 min. Data represent mean ± SEM (**p*<0.05, ****p*<0.001 MDMA *vs.* control, two-way ANOVA and Bonferroni's *post-hoc* test). Scale bar: 10 µm.

Exposure to neurotoxins (e.g. β-amyloid protein) causes Tau-dependent impairment of mitochondrial transport (Vossel *et al.*, 2010). We, thus, screened whether Tau was involved in MDMA-mediated effects on mitochondrial trafficking. Western blotting analysis showed increased Tau phosphorylation after exposure to MDMA (1.6 mM) for 90 min, particularly in Thr181 residue (Figure 4A-B). This observation is consistent with the findings of previous *in vivo* studies, in which increased Tau phosphorylation was observed in mice hippocampus after MDMA administration (Busceti *et al.*, 2008). By using Tau (-/-) neurons, we found that the lack of Tau protein partially abolished the MDMA-induced deficits on mitochondrial transport, thereby indicating a Tau-dependent mechanism (Figure 4D, F).

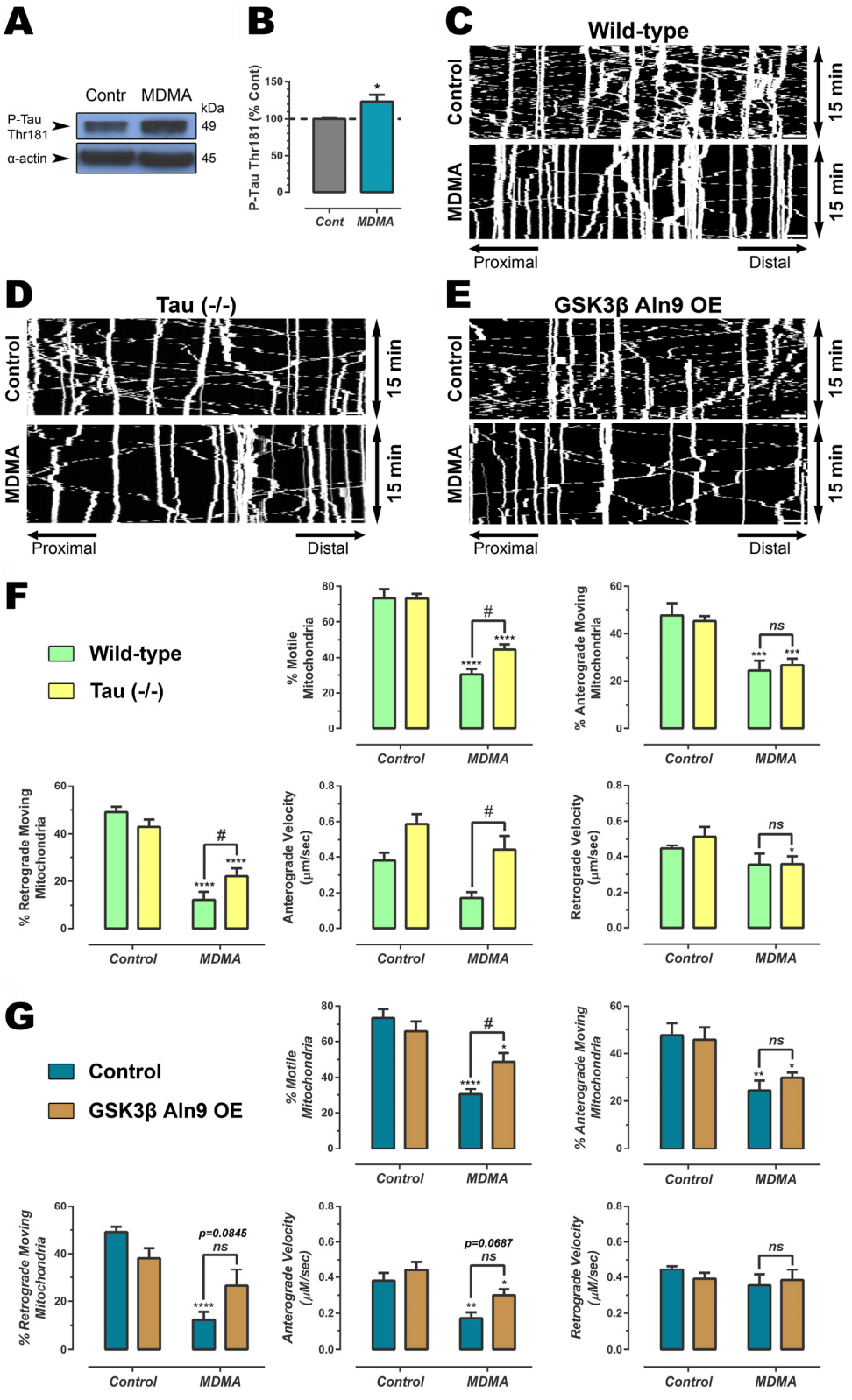


Figure 4. MDMA impaired mitochondrial neuronal trafficking by a Tau- and GSK3β-dependent mechanism. (A-B) Representative Western blot of Tau phosphorylation on residue Thr181 (A) and respective densitometric analysis (B) after exposure to MDMA (1.6 mM) for 90 min. Data represent mean ± SEM of 3 independent experiments (*p<0.05 MDMA *vs.* control, Unpaired Student's t-test). (C-E) Representative kymographs from wild-type (C), Tau (-/-) (D), or GSK3β Aln9 over-expressing (E) neurons. (F-G) Graphical representation of the percentage of motile mitochondria and velocities, measured in kymographs obtained from Tau (-/-) (F) or GSK3β Aln9-over-expressing neurons (G) after exposure to MDMA (1.6 mM) for 90 min. Data represent mean ± SEM [*p<0.05, **p<0.01, ***p<0.001, ****p<0.0001 MDMA *vs.* control; $^{\#}p$<0.05 Tau (-/-)/GSK3β Aln9-over-expressing *vs.* control neurons, two-way ANOVA and Bonferroni's *post-hoc* test]. Scale bar: 10 µm.

In neurons, Tau phosphorylation is largely dependent on glycogen synthase kinase 3β (GSK3β) activity (Busceti *et al.*, 2008; Llorens-Martín *et al.*, 2011; Park *et al.*, 2012). To evaluate the involvement of GSK3β on the trafficking deficits elicited by MDMA, hippocampal neurons were further transfected with the dominant negative construct GSK3β Aln9 that lacks kinase activity (Byun *et al.*, 2012). This experimental design resulted in a partial reversion of the MDMA-induced deficits on mitochondrial transport, comparable to those observed in Tau (-/-) neurons (Figure 4E, G). These observations indicate, therefore, that the trafficking deficits mediated by MDMA partially depend on Tau protein and GSK3β activity.

During the course of the experiments we noted that neurons exposed to MDMA exhibited smaller mitochondria than those of controls (Figure 5A), suggesting the involvement of mitochondrial fusion/fission machinery in the MDMA-induced impaired mitochondrial trafficking. The GTPases Mfns and Drp1 are known to mediate these processes (Misko *et al.*, 2010; Misko *et al.*, 2012; Sheng and Cai, 2012). Therefore, to evaluate the involvement of mitochondrial fission/fusion machinery on the trafficking deficits mediated by MDMA, hippocampal neurons were further transfected with Mfn2 or Drp1 constructs. As shown in Figure 5C-D, Mfn2 over-expression almost completely rescued the mitochondrial trafficking impairment induced by MDMA. In the same way, over-expression of the dominant negative Drp1 construct (Drp1 K38A), which down-regulates mitochondrial fission (Zhao *et al.*, 2011), also partially abolished the trafficking deficits caused by MDMA (Figure 5E, G). Finally, over-expression of the Mfn2 R94Q construct, a Charcot-Marie-Tooth Disease mutant with impaired fusion and transport properties (Detmer and Chan, 2007; Misko *et al.*, 2010), did not rescue the MDMA phenotypes (Figure 5F, H). Therefore, these experiments indicate that Mfn2 and Drp1 largely mediate the mitochondrial trafficking deficits induced by MDMA.

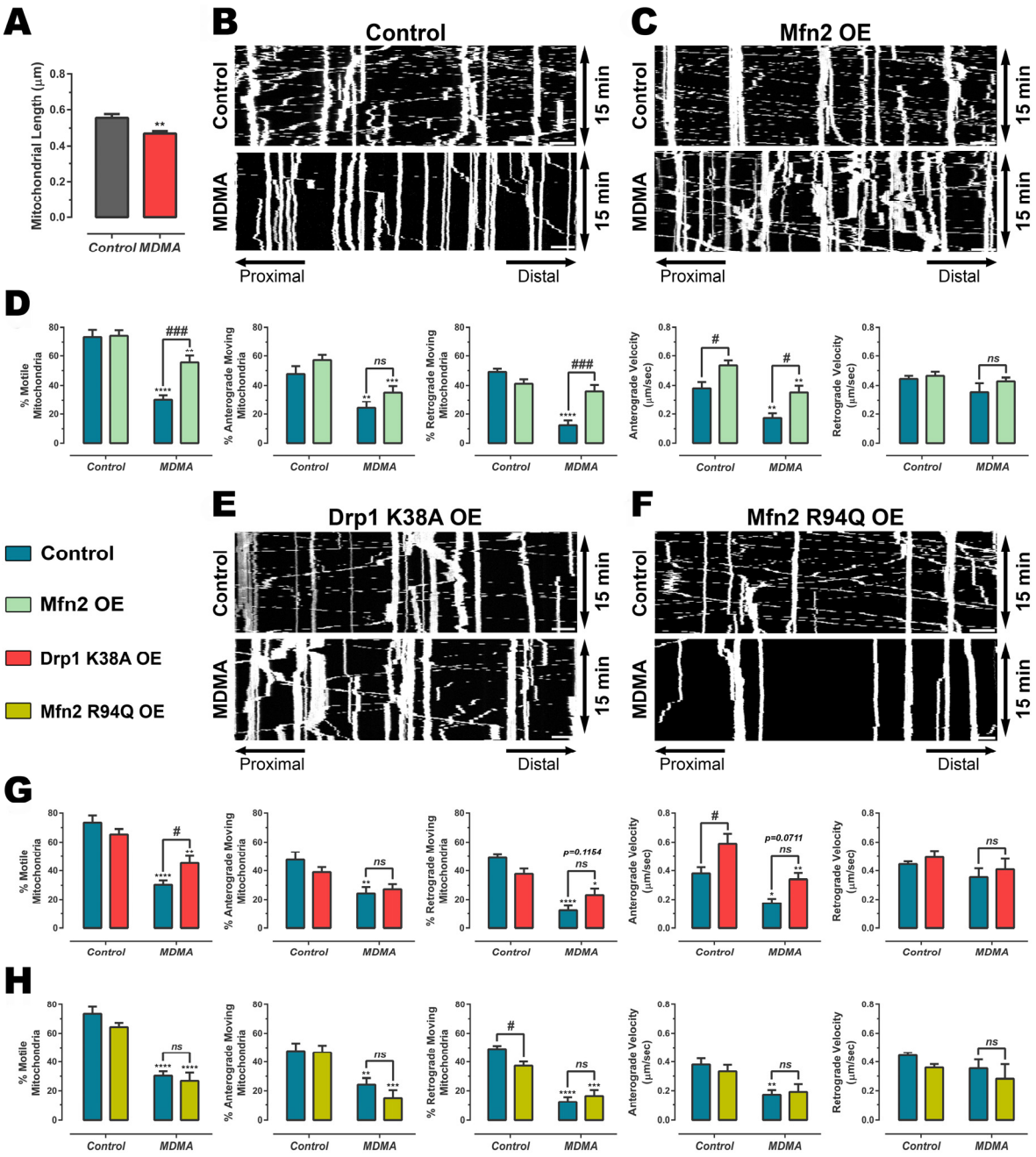


Figure 5. MDMA impaired mitochondrial neuronal trafficking by a mitochondrial fusion/fission machinery-dependent mechanism. (A) Graphical representation of mitochondrial length, showing increased mitochondrial fission after exposure to MDMA (1.6 mM) for 90 min. Data represent mean ± SEM of 126-131 individual mitochondria (29-31 axons) from 3 independent experiments, (***p*<0.01 MDMA *vs.* control, Mann-Whitney test). (B-C, E-F) Representative kymographs from control (B), Mfn 2 (C), Drp1 K38A (E) or Mfn2 R94Q (F) over-expressing neurons. (D, G-H) Graphical representation of the percentage of motile mitochondria and velocities, measured in kymographs obtained from neurons over-expressing Mfn2 (D), Drp1 K38A (G) or Mfn2 R94Q (H). Data represent mean ± SEM [**p*<0.05, ***p*<0.01, ****p*<0.001, *****p*<0.0001 MDMA *vs.* control; $^{\#}p$<0.05, $^{\#\#\#}p$<0.001 Mfn2/Drp1 K38A over-expression *vs.* control neurons, two-way ANOVA and Bonferroni´s *post-hoc* test]. Scale bar: 10 µm.

Discussion

Through *in situ* functional experiments we found that MDMA dramatically impaired axonal transport of mitochondria in hippocampal neurons. By using Tau (-/-) hippocampal neurons we also showed the involvement of Tau protein on the reported trafficking deficits, by a phosphorylation-dependent mechanism involving GSK3β. Moreover, we found that these trafficking abnormalities were strongly dependent on Mfn2 and Drp1 proteins, which regulate mitochondrial fission/fusion events, but not on Miro1.

Addictive drugs causes a variety of complex events, including changes in membrane excitability and neurotransmission, activation of signalling pathways and transcription, epigenetic regulation, altered synaptic structure, and drug-evoked synaptic plasticity and neurotoxicity, all of which contributing to both acute- and long-term neurotoxic effects and addiction (Lüscher and Malenka, 2011; Creed and Lüscher, 2013; Feng and Nestler, 2013; Lüscher, 2013). Recently, disrupted in schizophrenia-1 (DISC1), a candidate susceptibility gene for schizophrenia and major mental illness, which plays a role in brain development and synaptic function, has been shown to regulate intracellular trafficking of mitochondria in neurons (Atkin *et al.*, 2013). Furthermore, previous studies have reported mitochondrial deficits induced by MDMA, including ATP depletion, inhibition of mitochondrial proteins, oxidation of mitochondrial macromolecules and, notably, deletions on mitochondrial DNA, which have been mainly linked to neurotoxicity (Darvesh and Gudelsky, 2005; Alves *et al.*, 2007; Alves *et al.*, 2009; Puerta *et al.*, 2010). Here, we show, for the first time, that MDMA dramatically impaired axonal transport of mitochondria in hippocampal cultured neurons. High energy demands and the requirement to maintain cellular homeostasis at sites distant to the cell body make neurons particularly vulnerable to mitochondrial transport dysfunction (Deheshi *et al.*, 2013; Itoh *et al.*, 2013). Therefore, considering the critical dependence of neuronal activity on mitochondrial transport, energy supply and Ca^{2+} buffering (MacAskill and Kittler, 2010; Sheng and Cai, 2012), the present results provide a new, and important, insight in the context of MDMA-induced deleterious effects to the central nervous system, and suggest that alterations in mitochondrial trafficking may contribute to the acute- and long-lasting neurotransmission-related effects of MDMA.

Our results show that MDMA triggered an increase in intracellular Ca^{2+} levels. A Ca^{2+}-dependent arrest of mitochondrial motility has been described in neurons involving the EF hand containing mitochondrial outer membrane protein Miro (Macaskill *et al.*, 2009; Wang and Schwarz, 2009). However, our experiments over-expressing Miro1 protein or its mutant construct Miro1ΔEF, which lacks the EF Ca^{2+}-binding domains (Macaskill *et al.*, 2009), showed that the trafficking deficits induced by MDMA were not reversed.

Therefore, these results indicate that MDMA-induced impaired mitochondrial trafficking most likely rely on Miro1-independent mechanisms.

Some studies have suggested that increased expression or altered microtubule binding of Tau protein may compromise mitochondrial transport (Kopeikina *et al.*, 2011). Furthermore, the phosphorylation levels of Tau protein appear to be critical in regulating mitochondrial trafficking in neurons (Morel *et al.*, 2010; Vossel *et al.*, 2010; Llorens-Martín *et al.*, 2011). Here, we show that Tau protein was involved in the trafficking deficits elicited by MDMA, as confirmed by a partial reversion of mitochondrial deficits in Tau (-/-) neurons. Moreover, our results indicate that MDMA triggered Tau phosphorylation and that the main kinase for Tau protein, GSK3β, is likely to be also involved, as transfection with the GSK3β-kinase dead construct (GSK3β Aln9) reduced MDMA-induced trafficking alterations.

Here, we also found that the over-expression of Mfn2 almost completely rescued the trafficking deficits induced by MDMA. These results suggest that a deregulation on mitochondrial fission/fusion events, mediated by Mfn2, may be an important factor contributing to the reported trafficking deficits. Although it is clear that mitochondrial fission/fusion plays a major role in quality control regulation of dysfunctional mitochondria (Saxton and Hollenbeck, 2012; Itoh *et al.*, 2013; Shutt and McBride, 2013), an interplay between mitochondrial fission/fusion events and mitochondrial transport has also been described (Li *et al.*, 2004; Verstreken *et al.*, 2005; Misko *et al.*, 2010; Kageyama *et al.*, 2012; Misko *et al.*, 2012). Interestingly, the loss of Mfn2 causes abnormal mitochondrial morphology and transport, respiratory chain dysfunction and severe lack of dopaminergic terminals in the striatum (Lee *et al.*, 2012). The Mfn2 R94Q mutant is a CMT2A mutant with impaired fusion (Detmer and Chan, 2007) and transport properties (Misko *et al.*, 2010; Misko *et al.*, 2012). Since this mutant protein acts as a dominant negative, the physiological activity of Mfn2 is repressed, though endogenous fission machinery is not affected (Detmer and Chan, 2007). Thus, our over-expression experiments with the Mfn2 R94Q mutant, which did not rescue MDMA-mediated deficits, indicate that fully functional Mfn2 is required to reverse MDMA effects, and suggest that MDMA effects may alter the fusion mechanisms. Moreover, our data with the Drp1 K38A mutant, which inhibits endogenous fission without affecting mitochondrial fusion (Zhao *et al.*, 2011), supports also a role for fission events in MDMA-regulated phenotypes. Therefore, these experiments indicate that Mfn2 and Drp1 largely mediated the mitochondrial trafficking deficits induced by MDMA and suggest that MDMA may alter the fusion/fission mitochondrial equilibrium.

To the best of our knowledge, this study provides the first indication that an addictive drug dramatically alters mitochondrial neuronal trafficking and dynamics. As mitochondrial

transport and targeting to neuronal compartments and synapses is essential for many neuronal functions, including energy production and correct synaptic transmission (Wang and Schwarz, 2009; López-Doménech *et al.*, 2012; Sheng and Cai, 2012), our findings underscore a novel mechanism of action of MDMA. We postulate that this mechanism may contribute to the effects of MDMA, including its psycho-stimulant, addictive, and neurotoxic actions. It is thus tempting to propose that, in addition to their complex effects on neuronal function, addictive drugs target mitochondrial dynamics. Such targeting may represent a new mechanism underlying the neurotransmission and synaptic alterations caused by drugs of abuse.

Acknowlwdgements

We thank Luca Scorrano (University of Geneva) and Miquel Vila (VHIR, Barcelona) for providing the mitofusin and Drp1 constructs, and Isidre Ferrer (University of Barcelona) for providing the P-Tau Thr181 antibody. This study was supported by grant BFU2008-3980 ("Ministerio de Ciencia e Innovacion" (MICINN), Spain) and a grant from the "Plan Nacional de Drogas" to ES, and by the "Fundação para a Ciência e Tecnologia" (FCT), Portugal (Project PTDC/SAU-FCF/102958/2008), under the framework of the "Programa Operacional Temático Factores de Competitividade (COMPTE) do Quadro Comunitário de Apoio III" and "Fundo Comunitário Europeu (FEDER)" (FCOMP-01-0124-FEDER-011079). DJB's stay at IRB Barcelona was partially supported by FCT, Portugal. DJB was supported by a fellowship (SFRH/BD/64939/2009) from FCT, Portugal.

Conflict of interest

The authors declare that they have no conflict of interest.

References

Alves E, Summavielle T, Alves CJ, Custódio JB, Fernandes E, Lourdes Bastos M, et al. (2009). Ecstasy-induced oxidative stress to adolescent rat brain mitochondria *in vivo*: influence of monoamine oxidase type A. Addict Biol 14:185-193.

Alves E, Summavielle T, Alves CJ, Gomes-da-Silva J, Barata JC, Fernandes E, et al. (2007). Monoamine oxidase-B mediates ecstasy-induced neurotoxic effects to adolescent rat brain mitochondria. J Neurosci 27:10203-10210.

Atkin TA, MacAskill AF, Brandon NJ, Kittler JT (2013). Disrupted in Schizophrenia-1 regulates intracellular trafficking of mitochondria in neurons. Mol Psychiatry 16:122-124.

Bai F, Jones DC, Lau SS, Monks TJ (2001). Serotonergic neurotoxicity of 3,4-(±)-methylenedioxyamphetamine and 3,4-(±)-methylendioxymethamphetamine (ecstasy) is potentiated by inhibition of γ-glutamyl transpeptidase. Chem Res Toxicol 14:863-870.

Busceti CL, Biagioni F, Riozzi B, Battaglia G, Storto M, Cinque C, et al. (2008). Enhanced tau phosphorylation in the hippocampus of mice treated with 3,4-methylenedioxymethamphetamine ("ecstasy"). J Neurosci 28:3234-3245.

Byun J, Kim BT, Kim YT, Jiao Z, Hur E, Zhou F (2012). Slit2 inactivates GSK3β to signal neurite outgrowth inhibition. PLoS ONE 7:e51895.

Capela JP, Carmo H, Remião F, Bastos ML, Meisel A, Carvalho F (2009). Molecular and cellular mechanisms of ecstasy-induced neurotoxicity: an overview. Mol Neurobiol 39:210-271.

Carvalho M, Remiao F, Milhazes N, Borges F, Fernandes E, Carvalho F, et al. (2004). The toxicity of N-methyl-alpha-methyldopamine to freshly isolated rat hepatocytes is prevented by ascorbic acid and N-acetylcysteine. Toxicology 200:193-203.

Cereghetti GM, Stangherlin A, de Brito OM, Chang CR, Blackstone C, Bernardi P, et al. (2008). Dephosphorylation by calcineurin regulates translocation of Drp1 to mitochondria. Proc Natl Acad Sci U S A 105:15803-15808.

Creed MC, Lüscher C (2013). Drug-evoked synaptic plasticity: beyond metaplasticity. Curr Opin Neurobiol 23:553-558.

Darvesh AS, Gudelsky GA (2005). Evidence for a role of energy dysregulation in the MDMA-induced depletion of brain 5-HT. Brain Research 1056:168-175.

de Barreda EG, Pérez M, Ramos PG, de Cristobal J, Martín-Maestro P, Morán A, et al. (2010). Tau-knockout mice show reduced GSK3-induced hippocampal degeneration and learning deficits. Neurobiol Dis 37:622-629.

Deheshi S, Pasqualotto BA, Rintoul GL (2013). Mitochondrial trafficking in neuropsychiatric diseases. Neurobiol Dis 51:66-71.

Detmer SA, Chan DC (2007). Complementation between mouse Mfn1 and Mfn2 protects mitochondrial fusion defects caused by CMT2A disease mutations. J Cell Biol 176:405-414.

Feng J, Nestler EJ (2013). Epigenetic mechanisms of drug addiction. Curr Opin Neurobiol 23:521-528.

Granado N, Ares-Santos S, Oliva I, O´Shea E, Martin ED, Colado MI, et al. (2011). Dopamine D2-receptor knockout mice are protected against dopaminergic neurotoxicity induced by methamphetamine or MDMA. Neurobiol Dis 42:391-403.

Itoh K, Nakamura K, Iijima M, Sesaki H (2013). Mitochondrial dynamics in neurodegeneration. Trends Cell Biol 23:64-71.

Kageyama Y, Zhang Z, Roda R, Fukaya M, Wakabayashi J, Wakabayashi N, et al. (2012). Mitochondrial division ensures the survival of postmitotic neurons by suppressing oxidative damage. J Cell Biol 197:535-551.

Kenny PJ (2011). Common cellular and molecular mechanisms in obesity and drug addiction. Nat Rev Neurosci 12:638-651.

Kopeikina KJ, Carlson GA, Pitstick R, Ludvigson AE, Peters, Luebke JI, et al. (2011). Tau accumulation causes mitochondrial distribution deficits in neurons in a mouse model of tauopathy and in human alzheimer's disease grain. Am J Pathol 179:2071-2082.

Lee S, Sterky FH, Mourier A, Terzioglu M, Cullheim S, Olson L, et al. (2012). Mitofusin 2 is necessary for striatal axonal projections of midbrain dopamine neurons. Hum Mol Genet 21:4827-4835.

Li Z, Okamoto K, Hayashi Y, Sheng M (2004). The importance of dendritic mitochondria in the morphogenesis and plasticity of spines and synapses. Cell 119:873-887.

Llorens-Martín M, López-Doménech G, Soriano E, Avila J (2011). GSK3β is involved in the relief of mitochondria pausing in a tau-dependent manner. PLoS ONE 6:e27686.

López-Doménech G, Serrat R, Mirra S, D'Aniello S, Somorjai I, Abad A, et al. (2012). The Eutherian Armcx genes regulate mitochondrial trafficking in neurons and interact with Miro and Trak2. Nat Commun 3:814.

Lüscher C (2013). Cocaine-evoked synaptic plasticity of excitatory transmission in the ventral tegmental area. Cold Spring Harb Perspect Med 3:a012013.

Lüscher C, Malenka RC (2011). Drug-evoked synaptic plasticity in addiction: from molecular changes to circuit remodeling. Neuron 69:650-663.

MacAskill AF, Atkin TA, Kittler JT (2010). Mitochondrial trafficking and the provision of energy and calcium buffering at excitatory synapses. Eur J Neurosci 32:231-240.

MacAskill AF, Kittler JT (2010). Control of mitochondrial transport and localization in neurons. Trends Cell Biol 20:102-112.

Macaskill AF, Rinholm JE, Twelvetrees AE, Arancibia-Carcamo IL, Muir J, Fransson A, et al. (2009). Miro1 is a calcium sensor for glutamate receptor-dependent localization of mitochondria at synapses. Neuron 61:541-555.

Misko A, Jiang S, Wegorzewska I, Milbrandt J, Baloh RH (2010). Mitofusin 2 is necessary for transport of axonal mitochondria and interacts with the Miro/Milton complex. J Neurosci 30:4232-4240.

Misko AL, Sasaki Y, Tuck E, Milbrandt J, Baloh RH (2012). Mitofusin2 mutations disrupt axonal mitochondrial positioning and promote axon degeneration. J Neurosci 32:4145-4155.

Morel M, Authelet M, Dedecker R, Brion JP (2010). Glycogen synthase kinase-3β and the p25 activator of cyclin dependent kinase 5 increase pausing of mitochondria in neurons. Neuroscience 167:1044-1056.

Park H, Kam T, Kim Y, Choi H, Gwon Y, Kim C, et al. (2012). Neuropathogenic role of adenylate kinase-1 in Aβ-mediated tau phosphorylation via AMPK and GSK3β. Hum Mol Genet 21:2725-2737.

Perier C, Vila M (2012). Mitochondrial biology and Parkinson's disease. Cold Spring Harb Perspect Med 2:a009332.

Puerta E, Hervias I, Goñi-Allo B, Zhang SF, Jordán J, Starkov AA, et al. (2010). Methylenedioxymethamphetamine inhibits mitochondrial complex I activity in mice: a possible mechanism underlying neurotoxicity. Br J Pharmacol 160:233-245.

Research IfLA (2011) Guide for the care and use of laboratory animals. Washington DC, USA: The National Academies Press.

Rintoul GL, Reynolds IJ (2010). Mitochondrial trafficking and morphology in neuronal injury. Biochim Biophys Acta 1802:143-150.

Saxton WM, Hollenbeck PJ (2012). The axonal transport of mitochondria. J Cell Sci 125:2095-2104.

Shahpasand K, Uemura I, Saito T, Asano T, Hata K, Shibata K, et al. (2012). Regulation of mitochondrial transport and inter-microtubule spacing by tau phosphorylation at the sites hyperphosphorylated in alzheimer's disease. J Neurosci 32:2430-2441.

Shao L, Martin MV, Watson SJ, Schatzberg A, Akil H, Myers RM, et al. (2008). Mitochondrial involvement in psychiatric disorders. Ann Med 40:281-295.

Sheng Z, Cai Q (2012). Mitochondrial transport in neurons: impact on synaptic homeostasis and neurodegeneration. Nat Rev Neurosci 13:77-93.

Shutt TE, McBride HM (2013). Staying cool in difficult times: Mitochondrial dynamics, quality control and the stress response. Biochim Biophys Acta 1833:417-424.

Verstreken P, Ly CV, Venken KJT, Koh T, Zhou Y, Bellen HJ (2005). Synaptic mitochondria are critical for mobilization of reserve pool vesicles at drosophila neuromuscular junctions. Neuron 47:365-378.

Vossel KA, Zhang K, Brodbeck J, Daub AC, Sharma P, Finkbeiner S, et al. (2010). Tau reduction prevents Aβ-induced defects in axonal transport. Science 330:198.

Wang DB, Garden GA, Kinoshita C, Wyles C, Babazadeh N, Sopher B, et al. (2013). Declines in Drp1 and Parkin expression underlie DNA damage-induced changes in mitochondrial length and neuronal death. J Neurosci 33:1357-1365.

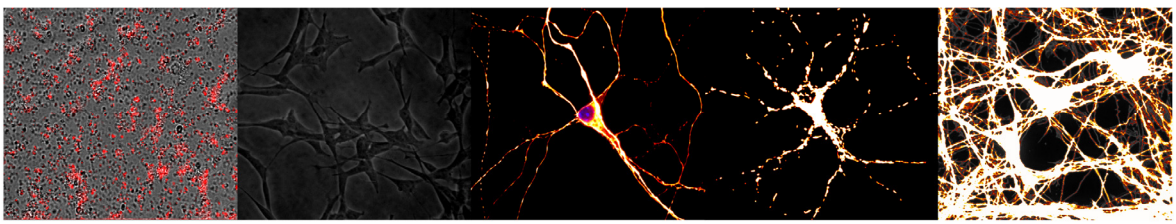
Wang X, Schwarz TL (2009). The mechanism of Ca^{2+}-dependent regulation of kinesin-mediated mitochondrial motility. Cell 136:163-174.

Zhao J, Liu T, Jin S, Wang X, Qu M, Uhlen P, et al. (2011). Human MIEF1 recruits Drp1 to mitochondrial outer membranes and promotes mitochondrial fusion rather than fission. EMBO J 30:2762-2778.

6.

The mixture of “ecstasy” and its metabolites, at *in vivo* relevant concentrations, impairs mitochondrial trafficking and increases organelle´s fragmentation in hippocampal neurons

Manuscript under submission



The mixture of "ecstasy" and its metabolites, at *in vivo* relevant concentrations, impairs mitochondrial trafficking and increases organelle's fragmentation in hippocampal neurons

Authors

Daniel José Barbosa[1,2,*], Romàn Serrat[2,*], Serena Mirra[2], Marti Quevedo[2], Elena Gómez de Barreda[3], Jesús Àvila[3], Luísa Maria Ferreira[4], Paula Sério Branco[4], Eduarda Fernandes[5], Maria de Lourdes Bastos[1], João Paulo Capela[1,6], Félix Carvalho[1,$] and Eduardo Soriano[2,$]

Affiliations

[1]REQUI*M*TE (Rede de Química e Tecnologia), Toxicology Laboratory, Department of Biological Sciences, Faculty of Pharmacy, University of Porto, Rua Jorge Viterbo Ferreira 228, 4050-313 Porto, Portugal.

[2]Developmental Neurobiology and Regeneration Lab, Department of Cell Biology, University of Barcelona; Institute for Research in Biomedicine, Barcelona Science Park. Centro de Investigación Biomédica en Red sobre Enfermedades Neurodegenerativas (CIBERNED, ISCIII). C/Baldiri Reixac 10-12, 08028 Barcelona, Spain.

[3]Centro de Investigación Biomédica en Red sobre Enfermedades Neurodegenerativas (CIBERNED, ISCIII). Center of Molecular Biology Severo Ochoa (CSIC-UAM), C/Nicolás Cabrera 1, Campus de la Universidad Autónoma de Madrid, 28049, Madrid, Spain.

[4]REQUI*M*TE, CQFB (Centro de Química Fina e Biotecnologia), Chemistry Department, Faculty of Science and Technology, University Nova de Lisboa, 2829-516 Caparica, Portugal.

[5]REQUI*M*TE, Laboratory of Applied Chemistry, Department of Chemical Sciences, Faculty of Pharmacy, University of Porto, Rua Jorge Viterbo Ferreira 228, 4050-313 Porto, Portugal.

[6]Faculty of Health Sciences, University Fernando Pessoa, Rua 9 de Abril 349, 4249-004 Porto, Portugal.

Footnotes

*These authors contributed equally.

[$]FC and ES are co-senior authors.

Corresponding Authors

Félix Carvalho

E-mail: felixdc@ff.up.pt

Phone: (+351) 220 428 500

Fax: (+351) 226 093 390

Eduardo Soriano

E-mail: esoriano@ub.edu

Phone: (+34) 93 4037117

Fax: (+34) 93 4037116

Abstract

3,4-Methylenedioxymethamphetamine (MDMA; “ecstasy”), is a potentially neurotoxic recreational drug of abuse. Though the mechanisms involved are still not completely understood, formation of reactive metabolites and mitochondrial dysfunction contribute to MDMA-related neurotoxicity. Mitochondrial neuronal trafficking, and their targeting to synapses, is essential for neuronal function and survival, rendering neurons particularly vulnerable to mitochondrial dysfunction. Indeed, MDMA-associated disruption on Ca^{2+} homeostasis and ATP depletions have been described in neurons, thus suggesting a direct interference of MDMA on mitochondrial dynamics. Here, we performed real-time functional experiments of axonal transport of mitochondria to explore the role of *in situ* mitochondrial dysfunction in MDMA-related neurotoxic actions. We show that the mixture of MDMA and its major *in vivo* metabolites, each compound at 10 μM, impaired axonal transport of mitochondria in cultured hippocampal neurons. Importantly, the mitochondrial trafficking deficits were associated with increased mitochondrial fragmentation. Furthermore, in transfected neurons, the over-expression of mitofusin 2 (Mfn2) or dynamin-related protein 1 (Drp1) K38A constructs almost completely rescued the trafficking deficits associated with this mixture. Finally, in hippocampal neurons over-expressing a mutant Mfn2 construct, Mfn2 R94Q, it was confirmed that a deregulation of the mitochondrial fission/fusion machinery greatly contributed to the reported trafficking phenotype. In conclusion, our study demonstrated that the mixture of MDMA and its metabolites, at *in vivo* relevant concentrations, impaired mitochondrial trafficking and increased mitochondrial fragmentation in hippocampal neurons, thus providing a new insight in the context of “ecstasy”-induced neuronal injury.

Keywords

3,4-Methylenedioxymethamphetamine (MDMA; “ecstasy”); MDMA metabolites; Mitochondrial trafficking; Mitochondrial dysfunction; Neurotoxicity.

Introduction

3,4-Methylenedioxymethamphetamine (MDMA; "ecstasy") is a worldwide major drug of abuse with well documented neurotoxic properties, both in humans (Roberts *et al.*, 2009; Tai *et al.*, 2011) and in laboratory animals (Bai *et al.*, 2001; Granado *et al.*, 2011). Though the molecular and cellular mechanisms behind MDMA-induced neurotoxicity remain unclear, recent studies have attributed a possible role to mitochondrial damage pathways (Alves *et al.*, 2007; Alves *et al.*, 2009; Puerta *et al.*, 2010). Hepatic formation of reactive metabolites, which is followed by their uptake into the brain (Jones *et al.*, 2005; Erives *et al.*, 2008), has been postulated to contribute to MDMA-related neurotoxicity (Capela *et al.*, 2009). Therefore, it is expected that the MDMA-mediated neurotoxic actions may result from a synergic or additive effect between parent compound and its metabolites, as they co-exist into the brain (Chu *et al.*, 1996; Jones *et al.*, 2005; Erives *et al.*, 2008; Mueller *et al.*, 2009). However, the mechanistic studies performed *in vitro* frequently have only taken into account each compound alone, which eludes the contribution of the mixture for the effects observed *in vivo*. Notably, previously, we demonstrated, for the first time, that the mixture of MDMA and its metabolites, at *in vivo* relevant concentrations, elicited cellular adaptations and toxicity in human SH-SY5Y differentiated cells, which provided a new breakthrough in the context of MDMA-induced neurotoxicity (Barbosa *et al.*, 2013).

Mitochondria are highly dynamic organelles that by undergoing fission and fusion can display significant variability in size and shape. In neurons, these opposing processes appear to play an important role in regulating mitochondrial distribution along the axons and dendrites, rendering, thus, neuronal cells critically dependent on mitochondrial dynamics (Sheng and Cai, 2012). Mitochondrial fission is mediated by an evolutionarily conserved soluble cytosolic dynamin-related guanosine 5'-triphosphatase (GTPase) protein, the dynamin-related protein 1 (Drp1), whose interaction with mitochondria is regulated by post-translational modifications (Itoh *et al.*, 2013) and Ca^{+2} (Cereghetti *et al.*, 2008). Mitochondrial fusion is also mediated by dynamin-related GTPase proteins, mitofusin 1 (Mfn1), mitofusin 2 (Mfn2), and optic dominant atrophy 1 (OPA1) (Itoh *et al.*, 2013). While Mfn1 and Mfn2 are involved in the outer mitochondrial membrane fusion, OPA1 mediates fusion of the inner membrane (Song *et al.*, 2009). A disruption of this dynamic equilibrium between mitochondrial fusion and fission may herald neuronal injury or death and may contribute to the development of neurodegenerative disorders (Wang *et al.*, 2013).

Axonal transport of mitochondria along microtubules is mediated by motor proteins, kinesins and dyneins. Kinesins, linked to the mitochondrial outer membrane protein Miro through the adaptor protein Milton/TRAK2, mediate anterograde transport, while

cytoplasmic dyneins mediate retrograde transport (MacAskill and Kittler, 2010), being their activity highly regulated by Ca^{2+} (Macaskill *et al.*, 2009; Wang and Schwarz, 2009) and critically dependent on ATP locally produced by mitochondria (Sheng and Cai, 2012). In *Drosophila melanogaster* neurons, a Miro-dependent regulation of retrograde axonal transport of mitochondria was also described (Russo *et al.*, 2009).

Microtubule-associated protein Tau, by assembly and maintenance of microtubules, also plays a major role on mitochondrial trafficking control (Vossel *et al.*, 2010; Kopeikina *et al.*, 2011; Llorens-Martín *et al.*, 2011), being its function largely dependent on the phosphorylation status (Llorens-Martín *et al.*, 2011; Shahpasand *et al.*, 2012). Importantly, MDMA was reported to promote intracellular Ca^{2+} raises in cultured hippocampal neurons (manuscript submitted for publication) and ATP depletion in rat striatum and hippocampus (Darvesh and Gudelsky, 2005), and also increased Tau phosphorylation in mice hippocampus (Busceti *et al.*, 2008), thus suggesting a possible direct interference of MDMA on mitochondrial dynamics.

By controlling organelle size, mitochondrial fission/fusion also regulates an efficient microtubule-mediated active transport in neurons (Itoh *et al.*, 2013). In fact, Mfn2 was recently described to be needed for neuronal transport of mitochondria by interaction with the Miro/TRAK complex (Misko *et al.*, 2010). Also, a Drp1-dependent regulation of mitochondrial density in dendrites (Li *et al.*, 2004) and a prevention of axonal transport of mitochondria in the absence of fission (Verstreken *et al.*, 2005) were reported, thus suggesting the existence of an interplay between fission/fusion machinery and mitochondrial transport.

Considering that MDMA and its metabolites co-exist into the brain, our hypothesis is that their mixture, at a range of concentrations with relevance to the *in vivo* scenario, may deregulate mitochondrial dynamics. To this end, by using real-time fluorescence microscopy at single-cell resolution, we evaluated the putative effects of the mixture of MDMA and its metabolites on mitochondrial fusion/fission and trafficking.

Materials and Methods

Materials

All reagents used were of analytical grade or of the highest grade available. Neurobasal medium, B27 supplement, penicillin/streptomycin 10,000 U/mL, GlutaMAX™ supplement, 0.5% trypsin/ethylenediaminetetraacetic acid (EDTA) without phenol red, horse serum heat inactivated, Opti-MEM medium, Lipofectamine 2000 and Dulbecco's phosphate buffered saline (DPBS) were purchased from Gibco Laboratories (Lenexa, KS, USA). Poly-*L*-lysine (PLL), triton X-100, Na_3VO_4, NaF, Tris-HCl, bromophenol blue and β-mercaptoethanol were obtained from Sigma-Aldrich (St. Louis, MO, USA). DNAse recombinant I and complete protease inhibitor cocktail were obtained from Roche Diagnostics (Mannheim, Germany). Swine anti-rabbit and goat anti-mouse IgG-peroxidase polyclonal antibodies were purchased from DAKO (Glostrup, Denmark). Mouse anti-Tau-1 and mouse anti-α-actin monoclonal antibodies were purchased from Merck Millipore (Merck KGaA, Darmstadt, Germany). MDMA (hydrochloride salt) was extracted and purified from high purity MDMA tablets kindly provided by the Portuguese Criminal Police Department. The obtained salt was pure and fully characterized by NMR and mass spectrometry methodologies. The MDMA metabolites α-methyldopamine (α-MeDA), *N*-methyl-α-methyldopamine (N-Me-α-MeDA), 5-(glutathion-*S*-yl)-α-methyldopamine [5-(GSH)-α-MeDA], 5-(glutathion-*S*-yl)-*N*-Me-α-methyldopamine [5-(GSH)-N-Me-α-MeDA], 5-(*N*-acetylcystein-*S*-yl)-α-methyldopamine [5-(NAC)-α-MeDA] and 5-(*N*-acetylcystein-*S*-yl)-*N*-methyl-α-methyldopamine [5-(NAC)-N-Me-α-MeDA] were synthesized and fully characterized by NMR and mass spectrometry methodologies by REQUI*M*TE (Centro de Química Fina e Biotecnologia), Chemistry Department, Faculty of Science and Technology, University Nova de Lisboa, according to previously published methods (Capela *et al.*, 2006; Capela *et al.*, 2007).

Animals

All procedures involving animals were approved by the Barcelona Scientific Park's Animal Experimentation Committee and were carried out in accordance with the "Guide for the Care and Use of Laboratory Animals" from the Institute for Laboratory Animal Research (Research, 2011), and the European Community Council directive and the National Institute of Health guidelines for the care and use of laboratory animals. Animals were allowed free access to a standard chow diet and water and maintained on a 12h/12h light/dark cycle under specific pathogen free conditions in the Animal Research Center at the Barcelona Scientific Park. To prepare primary hippocampal neuronal cultures, wild-type OF1 (Charles River, France) and C57BL/6 Tau (-/-) mice embryos were used, at

embryonic day 15 (E15) to E16, considering the mating day as E0. All procedures were taken to minimize the number of animals used and their suffering.

Cell culture and transfection

Primary neuronal cultures of hippocampus were prepared according to previously published methods (Llorens-Martín *et al.*, 2011; López-Doménech *et al.*, 2012), with few modifications. Pregnant mice were killed by cervical dislocation, and embryos were placed in ice-cold DPBS without Ca^{2+} and Mg^{2+} [DPBS (-/-)] containing 0.6% glucose during all dissection procedure. After brain isolation, meninges were removed, and hippocampus was dissected. Following a trypsinization (0.05% trypsin/EDTA) for 10 min, at 37ºC, a DNAse I treatment was applied, followed by another incubation period of 10 min, again at 37ºC. After dissociation of the tissue pieces by gently sweeping, cellular suspension was centrifuged at 127g, for 5 min, at 4ºC, and re-suspended in complete medium (neurobasal medium supplemented with 2% B27, 100 U/mL penicillin, 100 µg/mL streptomycin, and 2 mM Glutamax^{TM}). Cells were then seeded at the density of 78,000 cells/cm^2. For live imaging, hippocampal cultures were seeded in pre-coated 35 mm Fluordish plates (World Precision Instruments, Florida, USA), while for western blotting analysis, pre-coated 6-well plates (Nunc, Roskilde, Denmark), were used. To evaluate mitochondrial length, hippocampal cultures were seeded in 12 mm round pre-coated glass coverslips. Pre-coating was performed by overnight incubation, at 37ºC, with 0.2 mg/mL PLL solution (prepared in 0.1 M borate buffer, pH 8.5). Cultures were maintained at 37ºC, in an atmosphere of 5% CO_2/95% air and used for experiments at 5 *days in vitro* (DIV). Hippocampal cultures were transfected, at 4DIV, with MitDsRed (a gift from Antonio Zorzano) and GFP, or co-transfected with one of the following constructs: Mfn2 (Misko *et al.*, 2010), Mfn2 R94Q (Misko *et al.*, 2012) or Drp1 K38A (Zhao *et al.*, 2011), using Lipofectamine 2000 as transfection reagent and following the manufacturer's instructions.

Study design

Hippocampal neuronal cultures were incubated with the mixture of MDMA and its 6 metabolites α-MeDA, N-Me-α-MeDA, 5-(GSH)-α-MeDA, 5-(GSH)-N-Me-α-MeDA, 5-(NAC)-α-MeDA and 5-(NAC)-N-Me-α-MeDA, each compound at 10 µM, at 5DIV, and functional or biochemical experiments were performed at 6DIV (24h of exposure). The mixture composition was selected in accordance with a previous study published by us (Barbosa *et al.*, 2013).

Live-imaging of axonal transport of mitochondria in hippocampal neurons

Live-imaging of axonal transport of mitochondria in hippocampal neurons was performed using a Olympus IX81 confocal microscope (Olympus Corporation, Tokyo, Japan), equipped with a 60x immersion objective, and a Andor Revolution® XD spinning disk confocal microscopy system composed by a iXonEM + EM-CCD camera (Andor Tecnology, Belfast, United Kingdom), and FRAPPA and solid-state laser combiner (ALC-UVP 350i, Andor Tecnology) with the renowned CSU-X1 confocal scanner (Yokogawa Electric Corporation, Tokyo, Japan). All cultures were kept at 37ºC, using a heating insert on the microscope stage and an incubating chamber allowing circulation of a control CO_2 (5%)-air heated mixture for pH control. For measurements of axonal transport of mitochondria, axonal processes in transfected hippocampal neurons were identified following morphological criteria, and directionally were determined for each axon. Time-lapse series of image stacks composed of 151 images (512x512 pixels) were taken every 6 seconds, during 15 min. All 151 images obtained were processed mainly with Andor IQ2 software (Andor Technology). Further image processing, analysis and video compilation and edition was done with FIJI (Image JA v1.45b, Open source software, NIH, USA). Kymographs were generated with MetaMorph Software (Molecular Devices - MDS Analytical Technologies, Sunnyvale, CA, USA). In our presentation of kymographs, the vertical axis represents the time, and the horizontal axis is the distance along a slice. Stationary mitochondrial sites were identified as vertical lines on the kymographs. Motile mitochondria appeared as diagonal lines, and their slopes provided velocity. Distances and speeds of anterograde (from proximal to distal) and retrograde (from distal to proximal) motile mitochondria were measured separately from the corresponding kymographs. In all cases, a mitochondrion was considered motile when it moved more than 5 µm during the 15 min of recording. Mitochondrion motile in both anterograde and retrograde direction was considered a single mitochondrion, although it was included in both anterograde and retrograde moving mitochondria groups. For qualitative imaging of axonal transport of mitochondria, MitDsRed and GFP were excited at 561 and 488 nm and fluorescence emission was collected at 592 and 508 nm, respectively.

Western blotting analysis of Tau protein

Cellular proteins were extracted with lysis buffer [50 mM Tris-HCl pH 7.5, 150 mM NaCl, 5 mM EDTA, 1% triton X-100 (v/v), 10% glycerol (v/v), complete protease inhibitor cocktail, 1 mM Na3VO4, 10 mM Na4P2O7 and 10 mM NaF), followed by an incubation on ice for 30 min. After centrifugation at 16,000 g, for 10 min, at 4ºC, a SDS-PAGE reducing buffer [150 mM Tris-HCl pH 6.8, 3% SDS (w/v), 30% glycerol (v/v), 0.075% bromophenol

blue (w/v) and 15% β-mercaptoethanol (v/v)] was added to the samples (1:2 ratio), which were then boiled at 90 °C for 5 min. Proteins were loaded and separated in 10% SDS/polyacrylamide gels, at a constant voltage of 120 mV. Gels were transferred to nitrocellulose membranes (Whatman, Dassel, Germany) using a transfer buffer (20% methanol (v/v) in 20 mM Tris Base and 139 mM glycine), at 125 mV, for 1.5h. Membranes were then rinsed in Tris-buffered saline solution with Tween 20 [TBS-T: 10 mM Tris base, 140 mM NaCl and 0.1 % Tween 20 (v/v), pH 7.4], and non-specific sites were blocked for 1h at room temperature in blocking buffer [3% BSA (w/v) in TBS-T]. Membranes were incubated with primary antibodies (overnight at 4ºC): mouse monoclonal anti-Tau1 (1:50,000) or anti-α-actin (1:100,000). After washing 5 times (10 min each) with TBS-T membranes were then incubated with the anti-mouse IgG-peroxidase secondary antibody (1:2,500), for 1h, at room temperature. All antibodies were diluted in blocking buffer. Following 3 washes (10 min each) with TBS-T, bands were visualized using ECL chemiluminescence reagents (Amersham Pharmacia Biotech, Buckinghamshire, United Kingdom), according to the supplier`s instructions, and were quantified using the Quantity One software (Bio-Rad Laboratories).

Mitochondrial length measurements

Hippocampal cultures seeded in 12 mm round pre-coated glass coverslips, and transfected with MitDsRed and GFP, were incubated with the mixture of MDMA and its metabolites for 24h and then fixed in 4% paraformaldehyde, during 20 min, at room temperature. Images were acquired in a Leica TCS SP2 confocal microscope (Leica Microsystems, Mannheim, Germany), equipped with a 60x immersion objective. Stacks of images (1024x1024 pixels) were acquired with Leica Confocal Software (Leica Microsystems). Further image processing and analysis was done with Fiji (NIH). Mitochondria in axonal processes were visualized by mitochondrial targeted MitDsRed. Mitochondrial length was estimated individually for each mitochondrion. To identify axonal processes GFP was excited at 488 nm, and fluorescence emission was collected at 508 nm. MitDsRed was excited a 561 nm and fluorescence intensities were collected at 592 nm.

Data analysis

Values in the figures and text are presented as mean ± SEM of the indicated number of independent experiments. Each independent experiment was performed with hippocampal cultures proceeding from different pregnant mice. Normality of the data distribution was assessed by three tests (KS normality test, D'Agostino and Pearson

omnibus normality test and Shapiro-Wilk normality test). In experiments with only one variable, statistical comparisons between the two groups were performed with one-way ANOVA, followed by Bonferroni's test for *post-hoc* evaluations, or with Mann-Whitney test. Two-way ANOVA followed by Bonferroni *post-hoc* test was used to analyze the data from experiments with two variables. Details of the performed statistical analysis are described in each figure legend. Differences were considered to be significant at p values lower than 0.05. All analyses were performed using GraphPad Prism 6.0 for Windows (GraphPad Software, San Diego, CA, USA).

Results

The mixture of MDMA and its metabolites, at in vivo relevant concentrations, impaired axonal transport of mitochondria, in hippocampal neurons

Based in a recent study published by us (Barbosa *et al.*, 2013), in which it was demonstrated, for the first time, that the mixture of MDMA and its metabolites, at *in vivo* relevant concentrations, elicited cellular adaptations and toxicity in human SH-SY5Y differentiated cells, two different compositions of the mixture of MDMA and its metabolites, each compound at 10 μM or each compound at 20 μM, were tested. Twenty four hours of exposure to the 20 μM mixture resulted in significant toxicity to the culture, as evaluated by the MTT reduction assay (Figure 1). However, for the 10 μM mixture, not significant toxicity was observed after 24h of exposure (Figure 1). Therefore, the 10 μM mixture was selected for our functional and biochemical studies.

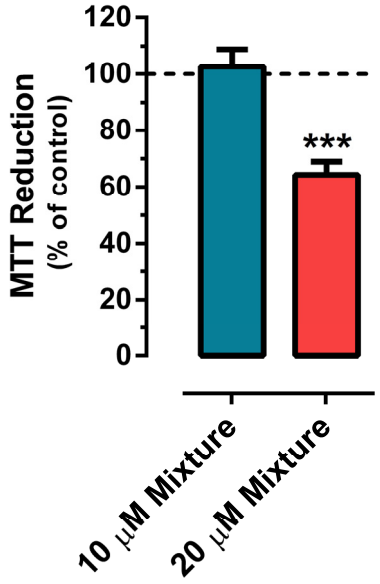


Figure 1. Toxic effect of the mixture of MDMA and its metabolites in primary hippocampal cultures. After 5DIV, hippocampal cultures were exposed to the mixture of MDMA and its metabolites α-MeDA, N-Me-α-MeDA, 5-(GSH)-α-MeDA, 5-(GSH)-N-Me-α-MeDA, 5-(NAC)-α-MeDA and 5-(NAC)-N-Me-α-MeDA, each compound at 10 or 20 μM, for 24h, and mitochondrial dysfunction was then evaluated by the MTT reduction assay. Data were analyzed using one-way ANOVA, followed by Bonferroni's test for *post-hoc* evaluations, and represent the mean ± SEM of four independent experiments (each experiment was performed in triplicate), being expressed as the percentage of the absorbance of the respective control cells [MTT reduction (% of control)] (***p<0.001 mixture *vs.* control).

In humans, MDMA-induced neuronal deficits have been reported in discrete areas of the brain, such as cortex, striatum, *raphe nuclei*, and hippocampus (Capela *et al.*, 2009; Carvalho *et al.*, 2012; Parrott, 2012). However, the memory and learning dysfunction in heavy "ecstasy" users appears to be related to the drug's actions on hippocampus, thus

agreeing with the particular vulnerability of this brain area observed in animals (Alves *et al.*, 2007; Alves *et al.*, 2009). Importantly, mitochondrial neuronal trafficking is a key regulator process in maintaining neuronal function and survival, since mitochondria need to be distributed from cell body, where occurs their biogenesis, to axons and dendrites, for a correct energy supply and Ca^{2+} buffering (Sheng and Cai, 2012). Therefore, by using cultured hippocampal neurons, we aimed at evaluating the effects of the mixture of MDMA and its metabolites, which represent a more real scenario of *in vivo* exposure to MDMA, on axonal transport of mitochondria. Control neurons exhibited a prominent mitochondrial neuronal trafficking, with an average of 65% of motile mitochondria, moving in both anterograde and retrograde directions, at velocity of about 0.4 μm/sec (Figure 2 and Movie 1). Exposure to the mixture of MDMA and its metabolites α-MeDA, N-Me-α-MeDA, 5-(GSH)-α-MeDA, 5-(GSH)-N-Me-α-MeDA, 5-(NAC)-α-MeDA and 5-(NAC)-N-Me-α-MeDA, each compound at 10 μM, for 24h, dramatically impaired mitochondrial neuronal trafficking (Figure 2 and Movie 2). Analysis of the data showed a significant reduction on mitochondrial motility (control = 65.27 ± 4.89%; mixture = 42.56 ± 5.90%, $p<0.05$), which was reflected in both anterograde (control = 43.37 ± 3.57%; mixture = 30.51 ± 4.62%, $p<0.05$) and retrograde (control = 40.01 ± 4.61%; mixture = 24.84 ± 4.72%, $p<0.05$) directions. Though anterograde velocity was unaffected (control = 0.394 ± 0.024 μm/sec; mixture = 0.330 ± 0.042 μm/sec, not significant), an impairment in retrograde velocity was observed (control = 0.474 ± 0.033 μm/sec; mixture = 0.264 ± 0.041 μm/sec, $p<0.01$). Thus, these results indicate that the mixture of MDMA and its metabolites impairs axonal transport of mitochondria.

Movie 1 Axonal transport of mitochondria in a hippocampal neuron, at 6DIV, under control conditions. Live-imaging of axonal mitochondria was performed in a hippocampal neuron transfected with MitDsRed.

Movie 2 Axonal transport of mitochondria in a hippocampal neuron, at 6DIV, after 24h of exposure to the mixture of MDMA and its metabolites. Hippocampal cultures were exposed to the mixture of MDMA and its metabolites at 5DIV and axonal transport of mitochondria measurements were performed at 6DIV. Live-imaging of axonal mitochondria was performed in a hippocampal neuron transfected with MitDsRed.

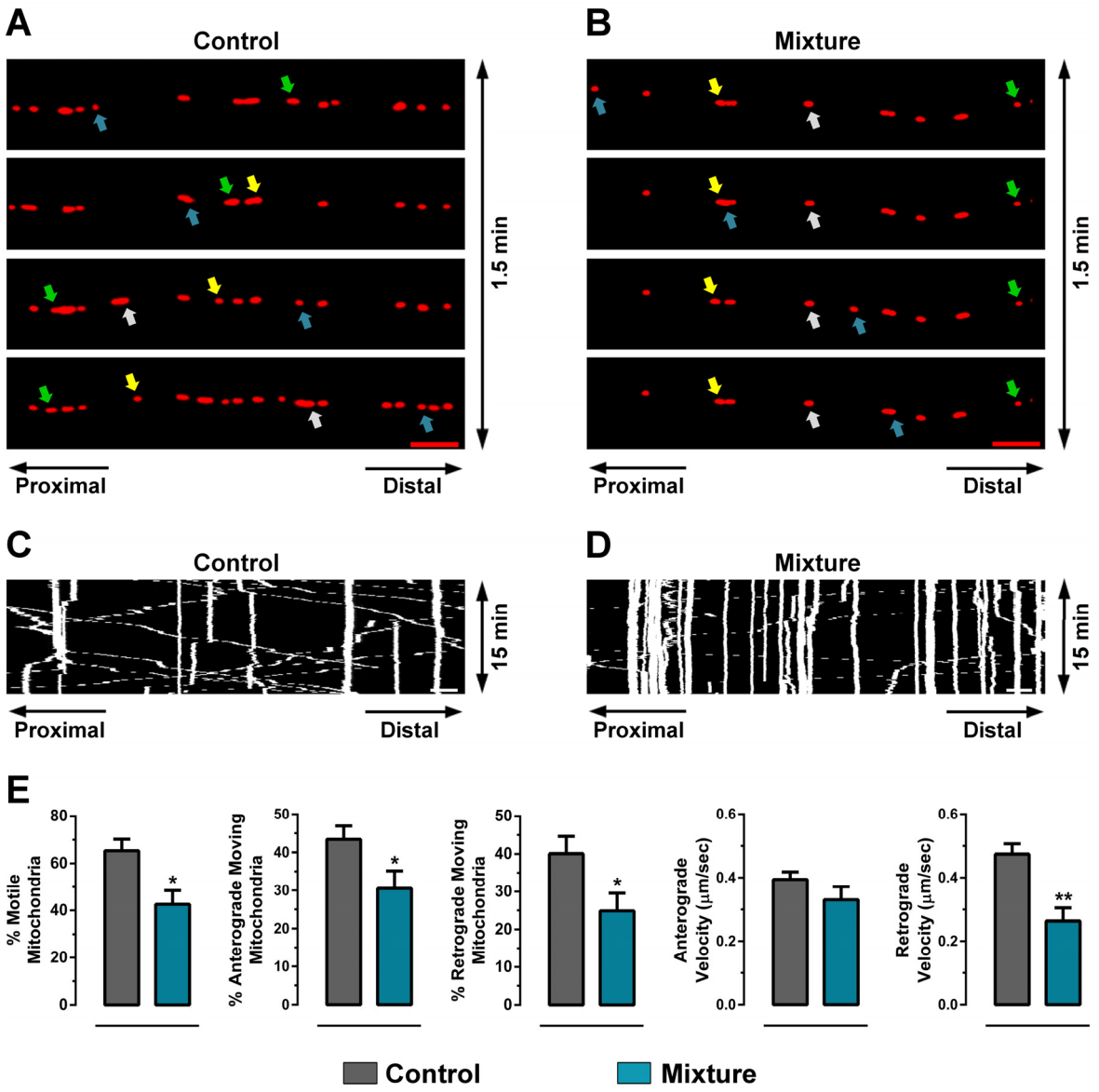


Figure 2. Effect of the mixture of MDMA and its metabolites on axonal transport of mitochondria, in cultured hippocampal neurons. Hippocampal neuronal cultures, transfected with MitDsRed and GFP, at 4DIV, were incubated with the mixture of MDMA and its metabolites α-MeDA, N-Me-α-MeDA, 5-(GSH)-α-MeDA, 5-(GSH)-N-Me-α-MeDA, 5-(NAC)-α-MeDA and 5-(NAC)-N-Me-α-MeDA, each compound at 10 µM, at 5DIV, and live-imaging of axonal transport of mitochondria was performed at 6DIV (24h of exposure). (A-B) Series of four representative confocal images of live axons, taken every 30 seconds, of neurons over-expressing the mitochondrial-tagged protein MitDsRed, under control conditions (A) or after 24h of exposure to the mixture of MDMA and its metabolites (B). Coloured arrows identify the same mitochondria through the different acquisitions. Up and down arrows represent mitochondria that move in anterograde or retrograde directions, respectively. (C-D) Representative kymographs showing the full-time acquisition periods (15 min of movie) of control (C) or mixture-incubated hippocampal neurons (D), which show decreased mitochondrial movement. All kymographs are arranged with the distal axonal end to the right. (E) Graphical representation of the percentage of total motile mitochondria, motile mitochondria in anterograde or retrograde directions, and velocity in both anterograde and retrograde directions, covered by individual mitochondria, and measured in kymograph. Data were analyzed using the Mann-Whitney test and represent the mean ± SEM of 18-19 axons (neurons) per experimental group, from four independent experiments (*p<0.05, **p<0.01 mixture *vs.* control). Scale bar: 10 µm.

Tau protein did not play a major role on the mitochondrial trafficking deficits triggered by the mixture of MDMA and its metabolites

Previous studies have attributed an important role of Tau protein in regulating axonal transport of mitochondria (Vossel *et al.*, 2010; Kopeikina *et al.*, 2011; Llorens-Martín *et al.*, 2011; Shahpasand *et al.*, 2012). However, anterograde and retrograde movements appear to be differently modulated by this protein (Dixit *et al.*, 2008). Furthermore, Tau protein functions in regulating mitochondrial trafficking are greatly dependent on protein phosphorylation ratio (Llorens-Martín *et al.*, 2011; Shahpasand *et al.*, 2012). By using Tau (-/-) neurons (Figure 3A) we studied the involvement of Tau protein on mitochondrial trafficking impairment associated with the mixture of MDMA and its metabolites. As shown in Figure 3, the lack of Tau protein significantly restored the deficits triggered by the mixture of MDMA and its metabolites in retrograde mitochondrial velocity. However, none of the remaining transport parameters evaluated were significantly modified, thus indicating a minor role for Tau protein on the reported trafficking deficits.

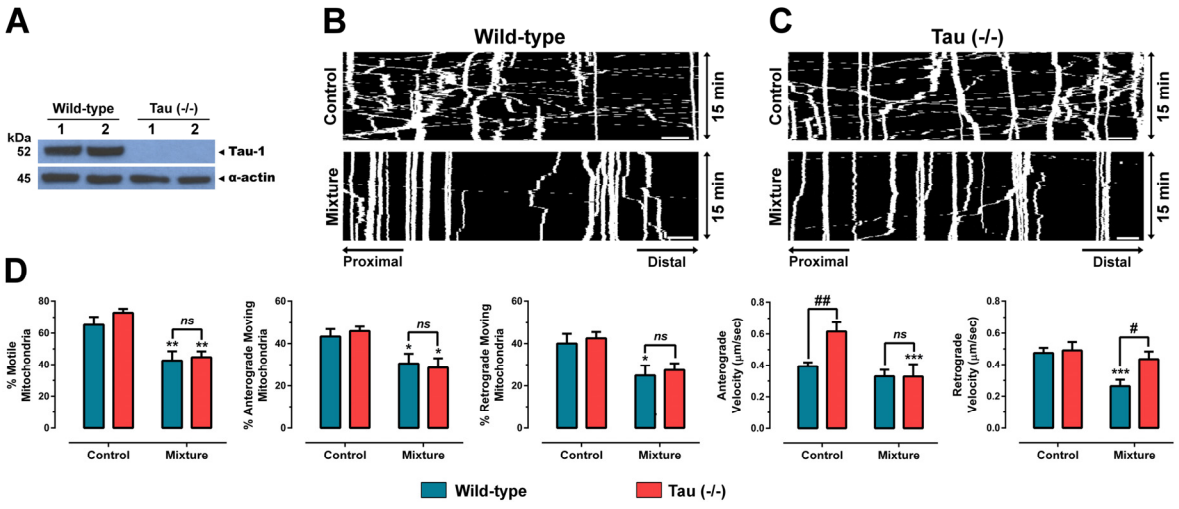


Figure 3. Involvement of Tau protein on mitochondrial trafficking impairment induced by the mixture of MDMA and its metabolites in cultured hippocampal neurons. Experiments were performed in wild-type and Tau (-/-) hippocampal neurons. (A) Western blot analysis of Tau protein expression in wild-type and Tau (-/-) hippocampal neurons at 6DIV. Wild-type neurons express Tau protein, whereas it is not expressed in Tau (-/-) neurons (anti-Tau1 antibody, 1:50,000). Equal protein loading was confirmed with α-actin antibody (1:100,000). (B-D) Hippocampal neuronal cultures, transfected with MitDsRed and GFP at 4DIV, were exposed to the mixture of MDMA and its metabolites α-MeDA, N-Me-α-MeDA, 5-(GSH)-α-MeDA, 5-(GSH)-N-Me-α-MeDA, 5-(NAC)-α-MeDA and 5-(NAC)-N-Me-α-MeDA, each compound at 10 μM, at 5DIV, and live-imaging of axonal transport of mitochondria was performed at 6DIV (24h of exposure). In (B) and (C), representative kymographs showing the full-time acquisition periods (15 min of movie) of wild-type (B) or Tau (-/-) hippocampal neurons (C), under control conditions or after 24h of exposure to the mixture of MDMA and its metabolites are presented. All kymographs are arranged with the distal axonal end to the right. In (D), the graphical representation of the percentage of total motile mitochondria, motile mitochondria in anterograde or retrograde directions, and velocity in both anterograde and retrograde directions, covered by individual mitochondria, and measured in kymographs are showed. Data were analyzed using two-way ANOVA, followed by Bonferroni's test for *post-hoc* evaluations, and represent the mean ± SEM of 10-19 axons (neurons) per experimental group, from at least three independent experiments [**p*<0.05, ***p*<0.01, ****p*<0.001 mixture *vs*. control; $^{\#}p$<0.05, $^{\#\#\#}p$<0.001 Tau (-/-) *vs.* wild-type; *ns*: not significant]. Scale bar: 10 μm.

Increased mitochondrial fragmentation was linked to the trafficking deficits induced by the mixture of MDMA and its metabolites

Neurons are critically dependent on mitochondrial dynamics to a correct ATP supply and Ca^{2+} homeostasis (Sheng and Cai, 2012). Emerging data suggest that a correct mitochondrial fusion/fission equilibrium is critical in regulating an efficient mitochondrial neuronal trafficking (Verstreken *et al.*, 2005; Misko *et al.*, 2010; Misko *et al.*, 2012). Therefore, to evaluate whether the mitochondrial trafficking deficits observed were associated with deregulations in mitochondrial fusion/fission events, we evaluate mitochondrial length on axonal extensions. Mitochondria from control neurons exhibited an average length of 0.555 ± 0.021 µm, whereas mitochondria from neurons exposed to the mixture of MDMA and its metabolites were significantly shorter, with an average length of 0.429 ± 0.011 µm (p<0.0001, Figure 4A). Therefore, the impairment of mitochondrial transport induced by the mixture of MDMA and its metabolites was associated with increased mitochondrial fragmentation.

Over-expression of mitofusin 2 or Drp1 K38A almost completely rescued the mitochondrial trafficking deficits triggered by the mixture of MDMA and its metabolites

Though a relationship between fusion proteins, namely Mfn2, and mitochondrial transport was recently described (Detmer and Chan, 2007; Misko *et al.*, 2010; Misko *et al.*, 2012), whether the effect of Mfn2 on mitochondrial transport is related to its fusion properties is not completely established. Furthermore, the previous involvement of Drp1 in regulating mitochondrial density in dendrites (Li *et al.*, 2004) and axonal transport of mitochondria (Verstreken *et al.*, 2005) suggests that a deregulation in mitochondrial fusion/fission events, as observed by increased mitochondrial fragmentation (Figure 4A), may be related to the observed trafficking phenotype. As shown in Figure 4B-D, over-expression of Mfn2 completely rescued the mitochondrial transport deficits elicited by the mixture of MDMA and its metabolites. Interestingly, a significant rescue in all transport parameters studied was observed.

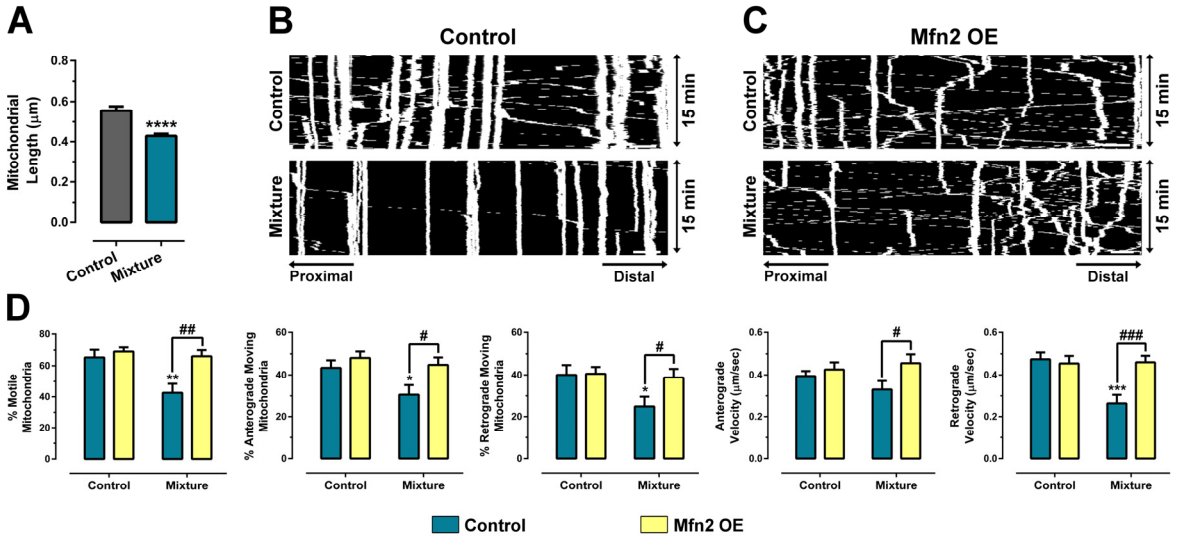


Figure 4. Contribution of mitochondrial fission/fusion-dependent mechanisms for the mitochondrial trafficking impairment induced by the mixture of MDMA and its metabolites in cultured hippocampal neurons. (A) Graphical representation of mitochondrial length, showing increased mitochondrial fragmentation following 24h of exposure to the mixture of MDMA and its metabolites α-MeDA, N-Me-α-MeDA, 5-(GSH)-α-MeDA, 5-(GSH)-N-Me-α-MeDA, 5-(NAC)-α-MeDA and 5-(NAC)-N-Me-α-MeDA, each compound at 10 µM. Data represent mean ± SEM of 126-171 individual mitochondria (29-30 different axons were analyzed) from 3 independent hippocampal cultures, and were analyzed using the Mann-Whitney test (****p<0.0001 mixture *vs.* control). (B-D) Effect of Mfn2 over-expression on mitochondrial trafficking impairment induced by the mixture of MDMA and its metabolites. Experiments were performed in control and Mfn2 over-expressing hippocampal neurons. Hippocampal neuronal cultures, transfected with MitDsRed and GFP or MitDsRed and GFP plus Mfn2 at 4DIV, were exposed to the mixture of MDMA and its metabolites, each compound at 10 µM, at 5DIV, and live-imaging of axonal transport of mitochondria was performed at 6DIV (24h of exposure). In (B) and (C), representative kymographs showing the full-time acquisition periods (15 min of movie) of control (B) or Mfn2 over-expressing neurons (C), under control conditions or after 24h of exposure to the mixture of MDMA and its metabolites are presented. All kymographs are arranged with the distal axonal end to the right. In (D), the graphical representation of the percentage of total motile mitochondria, motile mitochondria in anterograde or retrograde directions, and velocity in both anterograde and retrograde directions, covered by individual mitochondria, and measured in kymographs are showed. Data were analyzed using two-way ANOVA, followed by Bonferroni's test for *post-hoc* evaluations, and represent the mean ± SEM of 16-19 different axons (neurons) per experimental group, from four independent experiments (*p<0.05, **p<0.01, ***p<0.001 mixture *vs.* control; $^{\#}p$<0.05, $^{\#\#}p$<0.01, $^{\#\#\#}p$<0.001 Mfn2 over-expressing *vs.* control neurons). Scale bar: 10 µm.

Similarly, over-expression of Drp1 K38A, a dominant negative construct that lacks fission properties (Zhao *et al.*, 2011), almost completely rescued the reported trafficking impairment (Figure 5). Thus, these findings indicate that the mitochondrial fission/fusion machinery was greatly implicated on the trafficking impairment associated with the mixture of MDMA and its metabolites.

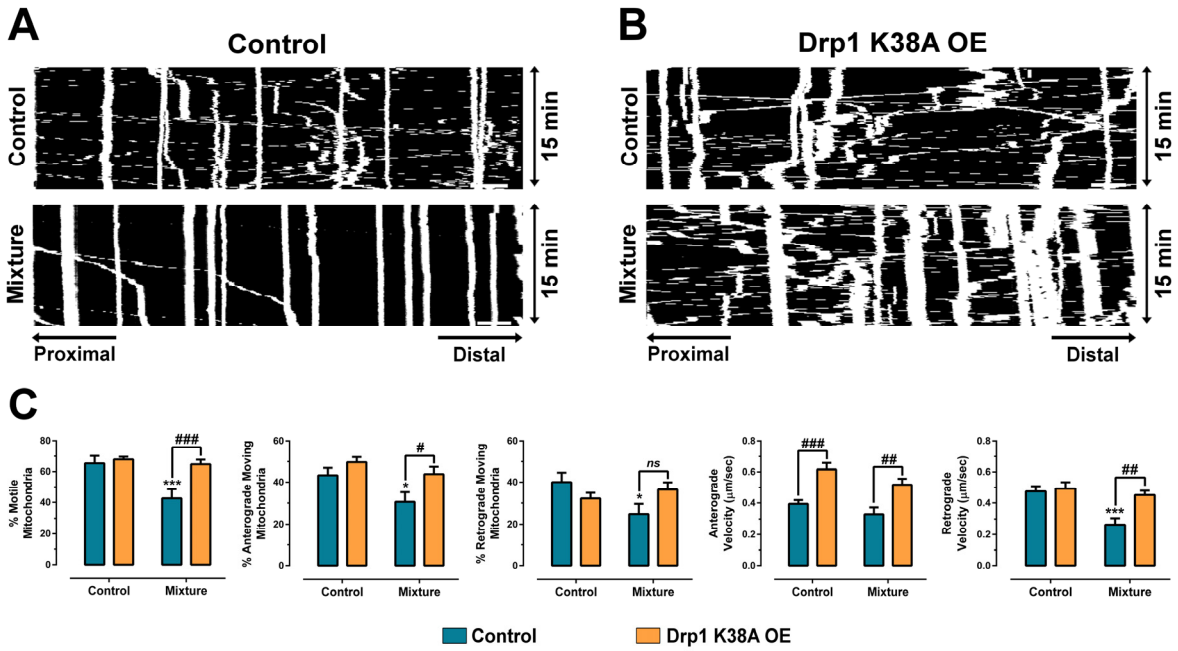


Figure 5. Effect of Drp1 K38A over-expression on mitochondrial trafficking impairment induced by the mixture of MDMA and its metabolites in cultured hippocampal neurons. Experiments were performed in control and Drp1 K38A over-expressing hippocampal neurons. Hippocampal neuronal cultures, transfected with MitDsRed and GFP or MitDsRed and GFP plus Drp1 K38A at 4DIV, were exposed to the mixture of MDMA and its metabolites α-MeDA, N-Me-α-MeDA, 5-(GSH)-α-MeDA, 5-(GSH)-N-Me-α-MeDA, 5-(NAC)-α-MeDA and 5-(NAC)-N-Me-α-MeDA, each compound at 10 µM, at 5DIV, and live-imaging of axonal transport of mitochondria was performed at 6DIV (24h of exposure). (A-B) Representative kymographs showing the full-time acquisition periods (15 min of movie) of control (A) or Drp1 K38A over-expressing neurons (B), under control conditions or after 24h of exposure to the mixture of MDMA and its metabolites. All kymographs are arranged with the distal axonal end to the right. (C) Graphical representation of the percentage of total motile mitochondria, motile mitochondria in anterograde or retrograde directions, and velocity in both anterograde and retrograde directions, covered by individual mitochondria, and measured in kymographs. Data were analyzed using two-way ANOVA, followed by Bonferroni's test for *post-hoc* evaluations, and represent the mean ± SEM of 18-19 different axons (neurons) per experimental group, from four independent experiments (*p<0.05, ***p<0.001 mixture *vs.* control; $^{\#}p$<0.05, $^{\#\#}p$<0.01, $^{\#\#\#}p$<0.001 Drp1 K38A over-expressing *vs.* control neurons; *ns*: not significant). Scale bar: 10 µm.

Charcot-Marie-Tooth Neuropathy 2A-associated mitofusin 2 mutant did not rescue the mitochondrial trafficking phenotype induced by the mixture of MDMA and its metabolites

Charcot-Marie-Tooth Neuropathy 2A (CMT2A), an autosomal dominant sensory-motor neuropathy, is associated with several mutations in Mfn2. One of these mutant forms is Mfn2 R94Q, which is described to present impaired mitochondrial fusion properties (Detmer and Chan, 2007). Moreover, associated with this mutant form, previous studies showed a marked decrease in overall mitochondrial motility in axons of cultured sensory neurons (Baloh *et al.*, 2007) and altered mitochondrial distribution and transport along the axons of dorsal root ganglion neurons (Misko *et al.*, 2010; Misko *et al.*, 2012). Therefore, we transfected hippocampal neurons with Mfn2 R94Q to elucidate the relative contribution of fission/fusion-dependent mechanisms for the mitochondrial trafficking deficits induced by the mixture of MDMA and its metabolites. As shown in Figure 6, over-expression of

Mfn2 R94Q did not modify the mitochondrial trafficking impairment elicited by the mixture of MDMA and its metabolites, compared to control neurons. Thus, and in line with our experiments performed with Mfn2 and Drp1 K38A over-expressing neurons, these results indicate a critical dependence on the mitochondrial fission/fusion machinery for the reported trafficking deficits.

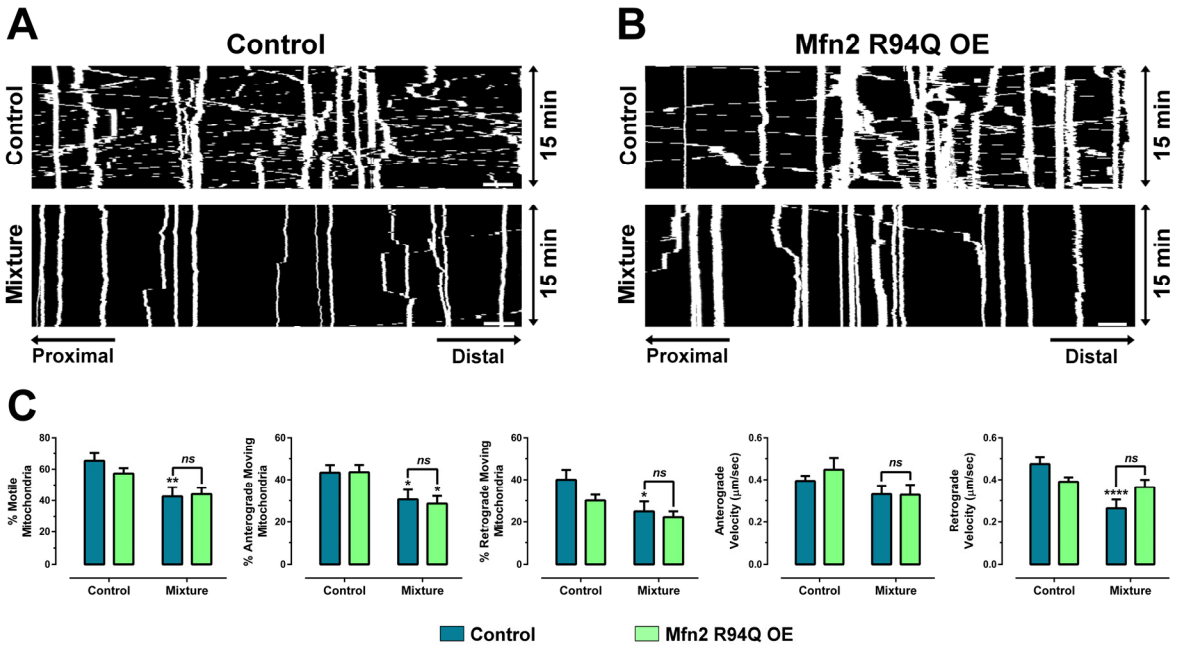


Figure 6. Effect of Mfn2 R94Q over-expression on mitochondrial trafficking impairment induced by the mixture of MDMA and its metabolites in cultured hippocampal neurons. Experiments were performed in control and Mfn2 R94Q over-expressing hippocampal neurons. Hippocampal neuronal cultures, transfected with MitDsRed and GFP or MitDsRed and GFP plus Mfn2 R94Q at 4DIV, were exposed to the mixture of MDMA and its metabolites α-MeDA, N-Me-α-MeDA, 5-(GSH)-α-MeDA, 5-(GSH)-N-Me-α-MeDA, 5-(NAC)-α-MeDA and 5-(NAC)-N-Me-α-MeDA, each compound at 10 µM, at 5DIV, and live-imaging of axonal transport of mitochondria was performed at 6DIV (24h of exposure). (A-B) Representative kymographs showing the full-time acquisition periods (15 min of movie) of control (A) or Mfn2 R94Q over-expressing neurons (B), under control conditions or after 24h of exposure to the mixture of MDMA and its metabolites. All kymographs are arranged with the distal axonal end to the right. (C) Graphical representation of the percentage of total motile mitochondria, motile mitochondria in anterograde or retrograde directions, and velocity in both anterograde and retrograde directions, covered by individual mitochondria, and measured in kymographs. Data were analyzed using two-way ANOVA, followed by Bonferroni's test for *post-hoc* test, and represent the mean ± SEM of 18-19 different axons (neurons) per experimental group, from four independent experiments (**p*<0.05, ***p*<0.01, *****p*<0.0001 mixture *vs.* control; *ns*: not significant). Scale bar: 10 µm.

Discussion

The present study clearly shows, for the first time, that the mixture of MDMA and its metabolites, at *in vivo* relevant concentrations, impaired axonal transport of mitochondria and increased organelle's fragmentation. Furthermore, by over-expressing wild-type or mutant proteins involved in mitochondrial fission/fusion events, a mechanism involved on the mitochondrial trafficking phenotype was unveiled. Lastly, by using Tau (-/-) neurons, it was demonstrated a minor involvement of Tau protein on the reported trafficking deficits.

High energy demands and the requirement to maintain cellular homeostasis at sites distant to the cell body make neurons particularly vulnerable to mitochondrial dysfunction (Itoh *et al.*, 2013). Furthermore, where extended arborization requires long-distance maneuvering of intracellular components, it has been suggested that disrupted mitochondrial translocation may contribute to the pathophysiology of neuronal injury (Deheshi *et al.*, 2013). In addition, there are emerging evidences suggesting that the damage of terminal axons may occur independently and by distinct mechanisms from those of cell bodies (Lee *et al.*, 2012). Importantly, selective damage to terminal axons is a characteristic marker of MDMA-associated neurotoxicity (Capela *et al.*, 2009). Likewise, mitochondrial-dependent mechanisms, including inhibition of mitochondrial proteins (Puerta *et al.*, 2010), oxidation of mitochondrial macromolecules (Alves *et al.*, 2007; Alves *et al.*, 2009) and deletions in mitochondrial DNA (Alves *et al.*, 2007) are likely to contribute to "ecstasy"-induced neurotoxicity. Furthermore, intracellular Ca^{2+} raises (manuscript submitted for publication) and ATP depletions (Darvesh and Gudelsky, 2005) were associated with MDMA-induced neuronal actions. Additionally, MDMA-associated increased reactive oxygen species (ROS) production in several *in vitro* neuronal models (Capela *et al.*, 2007; Barbosa *et al.*, 2012; Barbosa *et al.*, 2013) and alterations in oxygen consumption in rat liver mitochondria (Custódio *et al.*, 2010) were also previously reported. Therefore, it is expected that mitochondrial-dependent mechanisms may play a major role in mediating MDMA's neurotoxic effects. Of note, human studies have indicated that the memory and learning dysfunction in heavy "ecstasy" users may be related to the drug's actions on hippocampus (Gouzoulis-Mayfrank *et al.*, 2003). In accordance, animal studies revealed a high vulnerability of hippocampus to MDMA-induced deletions in mitochondrial DNA (Alves *et al.*, 2007), thus indicating a particular susceptibility of this brain area to the MDMA's actions.

Hepatic formation of reactive metabolites contributes to MDMA's neurotoxicity (Capela *et al.*, 2006; Capela *et al.*, 2007), though their role in MDMA-induced mitochondrial dysfunction is unknown. Moreover, the mitochondrial effects of the mixture of MDMA and its major metabolites, as it occurs *in vivo*, are unrevealed. In fact, one of the most

important limitations of *in vitro* neuronal models is the lack of drug metabolism mediated by cytochrome P450 (CYP450), which implies that the co-exposure to parent compound and its metabolites is rarely tested. The hepatic metabolism of MDMA is mainly regulated by CYP450 enzymes, originating, by *N*-demethylation, 3,4-methylenedioxyamphetamine (MDA). Both MDMA and MDA are then *O*-demethylenated to the catechol compounds N-Me-α-MeDA and α-MeDA respectively, which can undergo oxidation to the correspondent redox active *ortho*-quinones (Pizarro *et al.*, 2004). These *ortho*-quinones may be conjugated with reduced glutathione (GSH), originating glutathionyl adducts (Erives *et al.*, 2008). The systemic formation of 5-(GSH)-N-Me-α-MeDA and 5-(GSH)-α-MeDA is followed by their uptake into the brain (Jones *et al.*, 2005; Erives *et al.*, 2008), where they may undergo further metabolism to *N*-acetylcysteine (NAC) conjugates, which are slowly eliminated and, consequently, persist in the brain (Jones *et al.*, 2005). Supporting the role of metabolism in MDMA-induced neurotoxicity, Gollamudi *and* co-workers (Gollamudi *et al.*, 1989) showed an attenuation in MDMA-mediated depletions in 5-HT deficits after inhibition of MDMA's metabolism via CYP450. Therefore, in accordance with previous studies (Chu *et al.*, 1996; Jones *et al.*, 2005; Erives *et al.*, 2008) we selected the MDMA metabolites α-MeDA, N-Me-α-MeDA, 5-(GSH)-α-MeDA, 5-(GSH)-N-Me-α-MeDA, 5-(NAC)-α-MeDA and 5-(NAC)-N-Me-α-MeDA, to test the effects of their mixture with MDMA on mitochondrial dynamics. We demonstrated that this mixture, at *in vivo* relevant concentrations, dramatically impaired mitochondrial trafficking along axonal processes of cultured hippocampal neurons. Considering the critical dependence of neurons on mitochondrial transport to a correct energy supply and synaptic function (MacAskill and Kittler, 2010; Sheng and Cai, 2012), these results provide a new, and important, insight in the context of "ecstasy"-induced deleterious effects to the central nervous system.

A number of studies have suggested that increased expression or altered microtubule-binding of Tau may compromise axonal transport of mitochondria (Kopeikina *et al.*, 2011). Nevertheless, other studies have described a Tau-independent regulation of organelle's trafficking (Yuan *et al.*, 2008). Here, we showed that in Tau (-/-) neurons the trafficking impairment induced by the mixture of MDMA and its metabolites was comparable to the one found in wild-type neurons (only a partial rescue in retrograde velocity was found). In a previous work, we showed a partial dependence on Tau protein in MDMA-induced mitochondrial trafficking deficits by exposing cultured hippocampal neurons to a high concentration of MDMA (manuscript submitted for publication). In this study, the minor dependence on Tau protein for the reported effect suggests that other mechanisms prior to Tau involvement may play a critical role on the trafficking impairment associated with the mixture of MDMA and its metabolites, at lower concentrations. Indeed, other

mechanisms, instead of Tau protein, were demonstrated to play a major role in MDMA-induced mitochondrial trafficking impairment (manuscript submitted for publication).

Fission events fragment mitochondrial network into smaller units, thus allowing mitochondrial transport to different subcellular localizations, such as nerve terminals (Itoh *et al.*, 2013). Changes in mitochondrial morphology, resulting from excessive mitochondrial fission, have been associated with numerous neurodegenerative disorders (Rintoul and Reynolds, 2010; Wang *et al.*, 2013). Furthermore, oxidative stress, a common outcome in MDMA-related neuronal injury, appears to modify mitochondrial response to fission events (Mijaljica *et al.*, 2007). In this study, hippocampal neurons exposed to the mixture of MDMA and its metabolites presented mitochondria with smaller sizes, indicating, therefore, increased mitochondrial fragmentation. Importantly, increased organelle's fragmentation was recently linked to neurotoxicity (Wang *et al.*, 2013). In agreement, in a neuronal model of Parkinson's disease, the neuronal injury observed under oxidative stress conditions was prevented by chemical inhibition of mitochondrial fission (Qi *et al.*, 2012). Thus, the increase in mitochondrial fragmentation induced by the mixture of MDMA and its metabolites may be an important mechanism involved in MDMA-induced brain dysfunction. However, though it is clear that mitochondrial fission plays a major role in quality control regulation of dysfunctional mitochondria and mitochondrial transport (Verstreken *et al.*, 2005), if mitochondrial dysfunction is the cause or a consequence of impaired mitochondrial transport remains unknown.

Like fission, mitochondrial fusion is also required for proper mitochondrial distribution in neurons (Baloh *et al.*, 2007; Misko *et al.*, 2010; Misko *et al.*, 2012). Despite similar neuronal expression of Mfn1 and Mfn2, the lack of Mfn2 appears to be much more critical in regulating neuronal function than Mfn1. While the loss of Mfn2 causes abnormal mitochondrial morphology, respiratory chain dysfunction and severe lack of dopaminergic terminals in the striatum, loss of Mfn1 does not significantly affect neuronal function and survival (Lee *et al.*, 2012). Therefore, Mfn2 function appears to be critical on mitochondrial and neuronal functions maintenance. In neurons, as in other cell types, the mutant fission protein Drp1 K38A, acting as a dominant negative, inhibits endogenous fission activity without affecting the normal activity of fusion machinery (Zhao *et al.*, 2011). Therefore, to elucidate the involvement of mitochondrial fission/fusion-dependent mechanisms on the reported mitochondrial trafficking phenotype induced by the mixture of MDMA and its metabolites, we performed functional experiments with neurons over-expressing Mfn2 or Drp1 K38A. Over-expression of Mfn2 or Drp1 K38A almost completely rescued the trafficking deficits associated with the mixture of MDMA and its metabolites. However, Mfn2 was more effective than Drp1 K38A in preventing mitochondrial trafficking impairment. Thus, these results suggest that a deregulation of the mitochondrial

fission/fusion equilibrium may be a determinant factor contributing to the mitochondrial trafficking deficits observed. Additionally, in hippocampal neurons over-expressing Mfn2 R94Q, a CMT2A mutant construct with impaired fusion (Detmer and Chan, 2007) and transport properties (Misko *et al.*, 2010; Misko *et al.*, 2012), which acts as dominant negative, the mitochondrial trafficking impairment induced by the mixture of MDMA and its metabolites was not rescued. Therefore, these experiments indicate that Mfn2 and Drp1 largely mediated the reported mitochondrial trafficking deficits. In addition, these data also suggest that the mixture of MDMA and its metabolites may alter the fusion/fission mitochondrial equilibrium, as revealed by increased mitochondrial fragmentation.

In conclusion, our study demonstrated, for the first time, that the mixture of MDMA and its metabolites, at *in vivo* relevant concentrations, impaired axonal transport of mitochondria in hippocampal neurons. Furthermore, the trafficking deficits were linked to increased mitochondrial fragmentation, thus suggesting that interferences on mitochondrial dynamics may contribute to the neuronal injury associated with “ecstasy”.

Acknowledgements

We thank Luca Scorrano (University of Geneva) and Miquel Vila (VHIR, Barcelona) for providing the mitofusin and Drp1 constructs. This study was supported by grant BFU2008-3980 (“Ministerio de Ciencia e Innovacion” (MICINN), Spain) and a grant from the “Plan Nacional de Drogas”, and by the “Fundação para a Ciência e a Tecnologia” (FCT), Portugal (Project PTDC/SAU-FCF/102958/2008), under the framework of the “Programa Operacional Temático Factores de Competitividade (COMPTE) do Quadro Comunitário de Apoio III” and “Fundo Comunitário Europeu (FEDER)” (FCOMP-01-0124-FEDER-011079). The NMR spectrometers are part of “The National NMR Facility”, supported by FCT (RECI/BBB-BQB/0230/2012). DJB’s stay at IRB Barcelona was partially supported by FCT, Portugal. DJB was supported by a fellowship (SFRH/BD/64939/2009) from FCT, Portugal.

Conflit of Interest

The authors declare that they have no conflict of interest.

References

Alves E, Summavielle T, Alves CJ, Custódio JB, Fernandes E, Lourdes Bastos M, et al. (2009). Ecstasy-induced oxidative stress to adolescent rat brain mitochondria *in vivo*: influence of monoamine oxidase type A. Addict Biol 14:185-193.

Alves E, Summavielle T, Alves CJ, Gomes-da-Silva J, Barata JC, Fernandes E, et al. (2007). Monoamine oxidase-B mediates ecstasy-induced neurotoxic effects to adolescent rat brain mitochondria. J Neurosci 27:10203-10210.

Bai F, Jones DC, Lau SS, Monks TJ (2001). Serotonergic neurotoxicity of 3,4-(±)-methylenedioxyamphetamine and 3,4-(±)-methylendioxymethamphetamine (ecstasy) is potentiated by inhibition of γ-glutamyl transpeptidase. Chem Res Toxicol 14:863-870.

Baloh RH, Schmidt RE, Pestronk A, Milbrandt J (2007). Altered axonal mitochondrial transport in the pathogenesis of Charcot-Marie-Tooth disease from mitofusin 2 mutations. J Neurosci 27:422-430.

Barbosa DJ, Capela JP, Oliveira JMA, Silva R, Ferreira LM, Siopa F, et al. (2012). Pro-oxidant effects of Ecstasy and its metabolites in mouse brain synaptosomes. Br J Pharmacol 165:1017-1033.

Barbosa DJ, Capela JP, Silva R, Vilas-Boas V, Ferreira LM, Branco PS, et al. (2013). The mixture of “ecstasy” and its metabolites is toxic to human SH-SY5Y differentiated cells at *in vivo* relevant concentrations. Arch Toxicol.

Busceti CL, Biagioni F, Riozzi B, Battaglia G, Storto M, Cinque C, et al. (2008). Enhanced tau phosphorylation in the hippocampus of mice treated with 3,4-methylenedioxymethamphetamine ("ecstasy"). J Neurosci 28:3234-3245.

Capela JP, Carmo H, Remião F, Bastos ML, Meisel A, Carvalho F (2009). Molecular and cellular mechanisms of ecstasy-induced neurotoxicity: an overview. Mol Neurobiol 39:210-271.

Capela JP, Macedo C, Branco PS, Ferreira LM, Lobo AM, Fernandes E, et al. (2007). Neurotoxicity mechanisms of thioether ecstasy metabolites. Neuroscience 146:1743-1757.

Capela JP, Meisel A, Abreu AR, Branco PS, Ferreira LM, Lobo AM, et al. (2006). Neurotoxicity of ecstasy metabolites in rat cortical neurons, and influence of hyperthermia. J Pharmacol Exp Ther 316:53-61.

Carvalho M, Carmo H, Costa VM, Capela JP, Pontes H, Remião F, et al. (2012). Toxicity of amphetamines: an update. Arch Toxicol 86:1167-1231.

Cereghetti GM, Stangherlin A, de Brito OM, Chang CR, Blackstone C, Bernardi P, et al. (2008). Dephosphorylation by calcineurin regulates translocation of Drp1 to mitochondria. Proc Natl Acad Sci U S A 105:15803-15808.

Chu T, Kumagai Y, DiStefano EW, Cho AK (1996). Disposition of methylenedioxymethamphetamine and three metabolites in the brains of different rat strains and their possible roles in acute serotonin depletion. Biochem Pharmacol 51:789-796.

Custódio JBA, Santos MS, Gonçalves DIR, Moreno AJM, Fernandes E, Bastos ML, et al. (2010). Comparative effects of 3,4-methylenedioxymethamphetamine and 4-methylthioamphetamine on rat liver mitochondrial function. Toxicology 270:99-105.

Darvesh AS, Gudelsky GA (2005). Evidence for a role of energy dysregulation in the MDMA-induced depletion of brain 5-HT. Brain Research 1056:168-175.

Deheshi S, Pasqualotto BA, Rintoul GL (2013). Mitochondrial trafficking in neuropsychiatric diseases. Neurobiol Dis 51:66-71.

Detmer SA, Chan DC (2007). Complementation between mouse Mfn1 and Mfn2 protects mitochondrial fusion defects caused by CMT2A disease mutations. J Cell Biol 176:405-414.

Dixit R, Ross JL, Goldman YE, Holzbaur ELF (2008). Differential regulation of dynein and kinesin motor proteins by tau. Science 319:1086-1089.

Erives GV, Lau SS, Monks TJ (2008). Accumulation of neurotoxic thioether metabolites of 3,4-(±)-methylenedioxymethamphetamine in rat brain. J Pharmacol Exp Ther 324:284-291.

Gollamudi R, Ali SF, Lipe G, Newport G, Webb P, Lopez M, et al. (1989). Influence of inducers and inhibitors on the metabolism *in vitro* and neurochemical effects *in vivo* of MDMA. Neurotoxicology 10:455-466.

Gouzoulis-Mayfrank E, Thimm B, Rezk M, Hensen G, Daumann J (2003). Memory impairment suggests hippocampal dysfunction in abstinent ecstasy users. Prog Neuropsychopharmacol Biol Psychiatry 27:819-827.

Granado N, Ares-Santos S, Oliva I, O´Shea E, Martin ED, Colado MI, et al. (2011). Dopamine D2-receptor knockout mice are protected against dopaminergic neurotoxicity induced by methamphetamine or MDMA. Neurobiol Dis 42:391-403.

Itoh K, Nakamura K, Iijima M, Sesaki H (2013). Mitochondrial dynamics in neurodegeneration. Trends Cell Biol 23:64-71.

Jones DC, Duvauchelle C, Ikegami A, Olsen CM, Lau SS, de la Torre R, et al. (2005). Serotonergic neurotoxic metabolites of ecstasy identified in rat brain. J Pharmacol Exp Ther 313:422-431.

Kopeikina KJ, Carlson GA, Pitstick R, Ludvigson AE, Peters, Luebke JI, et al. (2011). Tau accumulation causes mitochondrial distribution deficits in neurons in a mouse model of tauopathy and in human alzheimer's disease grain. Am J Pathol 179:2071-2082.

Lee S, Sterky FH, Mourier A, Terzioglu M, Cullheim S, Olson L, et al. (2012). Mitofusin 2 is necessary for striatal axonal projections of midbrain dopamine neurons. Hum Mol Genet 21:4827-4835.

Li Z, Okamoto K, Hayashi Y, Sheng M (2004). The importance of dendritic mitochondria in the morphogenesis and plasticity of spines and synapses. Cell 119:873-887.

Llorens-Martín M, López-Doménech G, Soriano E, Avila J (2011). GSK3β is involved in the relief of mitochondria pausing in a tau-dependent manner. PLoS ONE 6:e27686.

López-Doménech G, Serrat R, Mirra S, D'Aniello S, Somorjai I, Abad A, et al. (2012). The Eutherian Armcx genes regulate mitochondrial trafficking in neurons and interact with Miro and Trak2. Nat Commun 3:814.

MacAskill AF, Kittler JT (2010). Control of mitochondrial transport and localization in neurons. Trends Cell Biol 20:102-112.

Macaskill AF, Rinholm JE, Twelvetrees AE, Arancibia-Carcamo IL, Muir J, Fransson A, et al. (2009). Miro1 is a calcium sensor for glutamate receptor-dependent localization of mitochondria at synapses. Neuron 61:541-555.

Mijaljica D, Prescott M, Devenish RJ (2007). Different fates of mitochondria: alternative ways for degradation? Autophagy 3:4-9.

Misko A, Jiang S, Wegorzewska I, Milbrandt J, Baloh RH (2010). Mitofusin 2 is necessary for transport of axonal mitochondria and interacts with the Miro/Milton complex. J Neurosci 30:4232-4240.

Misko AL, Sasaki Y, Tuck E, Milbrandt J, Baloh RH (2012). Mitofusin2 mutations disrupt axonal mitochondrial positioning and promote axon degeneration. J Neurosci 32:4145-4155.

Mueller M, Yuan J, Felim A, Neudörffer A, Peters FT, Maurer HH, et al. (2009). Further studies on the role of metabolites in (±)-3,4-methylenedioxymethamphetamine-induced serotonergic neurotoxicity. Drug Metab Dispos 37:2079-2086.

Parrott AC (2012). MDMA and 5-HT neurotoxicity: the empirical evidence for its adverse effects in humans – no need for translation. Br J Pharmacol 166:1518-1520.

Pizarro N, Farre M, Pujadas M, Peiro AM, Roset PN, Joglar J, et al. (2004). Stereochemical analysis of 3,4-methylenedioxymethamphetamine and its main metabolites in human samples including the catechol-type metabolite (3,4-dihydroxymethamphetamine). Drug Metab Dispos 32:1001-1007.

Puerta E, Hervias I, Goñi-Allo B, Zhang SF, Jordán J, Starkov AA, et al. (2010). Methylenedioxymethamphetamine inhibits mitochondrial complex I activity in mice: a possible mechanism underlying neurotoxicity. Br J Pharmacol 160:233-245.

Qi X, Qvit N, Su Y, Mochly-Rosen D (2012). Novel Drp1 inhibitor diminishes aberrant mitochondrial fission and neurotoxicity. J Cell Sci 126:789-802.

Research IfLA (2011) Guide for the care and use of laboratory animals. Washington DC, USA: The National Academies Press.

Rintoul GL, Reynolds IJ (2010). Mitochondrial trafficking and morphology in neuronal injury. Biochim Biophys Acta 1802:143-150.

Roberts GMP, Nestor L, Garavan H (2009). Learning and memory deficits in ecstasy users and their neural correlates during a face-learning task. Brain Res 1292:71-81.

Russo GJ, Louie K, Wellington A, Macleod GT, Hu F, Panchumarthi S, et al. (2009). Drosophila Miro Is Required for Both Anterograde and Retrograde Axonal Mitochondrial Transport. J Neurosci 29:5443-5455.

Shahpasand K, Uemura I, Saito T, Asano T, Hata K, Shibata K, et al. (2012). Regulation of mitochondrial transport and inter-microtubule spacing by tau phosphorylation at the sites hyperphosphorylated in alzheimer's disease. J Neurosci 32:2430-2441.

Sheng Z, Cai Q (2012). Mitochondrial transport in neurons: impact on synaptic homeostasis and neurodegeneration. Nat Rev Neurosci 13:77-93.

Song Z, Ghochani M, McCaffery JM, Frey TG, Chan DC (2009). Mitofusins and OPA1 mediate sequential steps in mitochondrial membrane fusion. Mol Biol Cell 20:3525-3532.

Tai YF, Hoshi R, Brignell CM, Cohen L, Brooks DJ, Curran HV, et al. (2011). Persistent nigrostriatal dopaminergic abnormalities in ex-users of MDMA ("Ecstasy"): an 18F-dopa PET study. Neuropsychopharmacology 36:735-743.

Verstreken P, Ly CV, Venken KJT, Koh T, Zhou Y, Bellen HJ (2005). Synaptic mitochondria are critical for mobilization of reserve pool vesicles at drosophila neuromuscular junctions. Neuron 47:365-378.

Vossel KA, Zhang K, Brodbeck J, Daub AC, Sharma P, Finkbeiner S, et al. (2010). Tau reduction prevents Aβ-induced defects in axonal transport. Science 330:198.

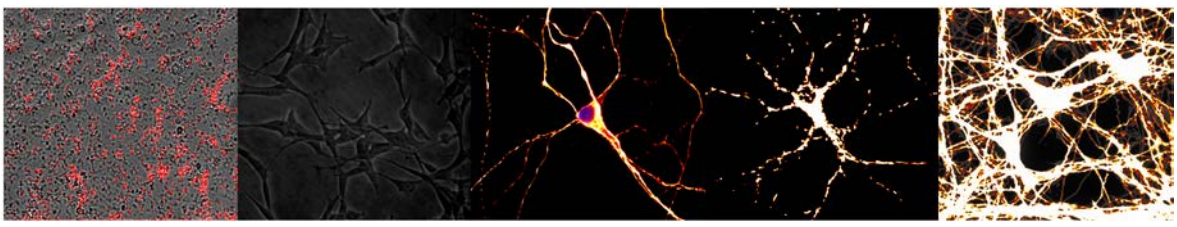
Wang DB, Garden GA, Kinoshita C, Wyles C, Babazadeh N, Sopher B, et al. (2013). Declines in Drp1 and Parkin expression underlie DNA damage-induced changes in mitochondrial length and neuronal death. J Neurosci 33:1357-1365.

Wang X, Schwarz TL (2009). The mechanism of Ca2+dependent regulation of kinesin-mediated mitochondrial motility. Cell 136:163-174.

Yuan A, Kumar A, Peterhoff C, Duff K, Nixon RA (2008). Axonal transport rates *in vivo* are unaffected by tau deletion or overexpression in mice. J Neurosci 28:1682-1687.

Zhao J, Liu T, Jin S, Wang X, Qu M, Uhlen P, et al. (2011). Human MIEF1 recruits Drp1 to mitochondrial outer membranes and promotes mitochondrial fusion rather than fission. EMBO J 30:2762-2778.

Chapter III



Integrated Discussion

III.1 Integrated Discussion

The neurotoxicity of “ecstasy” is believed to result from a large range of factors, including hyperthermia, sustained release of 5-HT and dopamine from nerve endings, inhibition of neurotransmitter synthesis, MAO-mediated metabolism of monoamine neurotransmitters, sustained stimulation of receptors and hepatic formation of reactive metabolites, among others (Capela *et al.*, 2009; Carvalho *et al.*, 2012). Such factors may act collectively in a synergetic and/or additive manner in developing neuronal degeneration and neurotoxicity, though their influence, at molecular and cellular level, remains to be fully identified.

There is a general consensus that *in vitro* methods can provide useful information concerning basic biological processes underlying neurotoxicity, and detailed information about specific mechanisms of action. Indeed, *in vitro* models have their higher potential in experiments in which mechanistic hypothesis are tested. Furthermore, *in vitro* approaches may be useful to explore several target sites where there is a significant understanding of basic biological processes. To better understand the mechanisms involved in MDMA-related neurotoxicity, the studies presented in this thesis were performed in different *in vitro* neuronal models in order to explore the involvement of particular targets and pathways on neuronal actions of MDMA.

III.1.1 Studies in mouse brain synaptosomes

Reports on the acute- and long-lasting neurotoxic effects of MDMA are mainly focused on the damage of the serotonergic and dopaminergic systems. Nevertheless, many reports in laboratory animals emphasize that MDMA-induced neuronal injury is observed in different brain areas, such as the parietal CTX, the insular/perirhinal CTX, the ventromedial/ventrolateral thalamus and the *tenia tecta* (Commins *et al.*, 1987; Schmued, 2003; Armstrong and Noguchi, 2004; Tamburini *et al.*, 2006; Warren *et al.*, 2007). Studies in MDMA users analyzing the location of MDMA-induced neuronal degeneration throughout the entire brain have also reported effects on the parietal CTX, HIP, striatum or *raphe nuclei* (Quednow *et al.*, 2006; Capela *et al.*, 2009; Adamaszek *et al.*, 2010; Tai *et al.*, 2011; Carvalho *et al.*, 2012; Parrott, 2012). It is generally believed that the acute effects of MDMA in the brain result from its actions on the monoaminergic system, in which the best characterized effect is the acute and sustained release of 5-HT and dopamine from nerve endings (Green *et al.*, 2003; Alves *et al.*, 2007).

Compelling evidences have also established that metabolites formed by the peripheral metabolism of MDMA may be involved in its neurotoxic effects. This seems the most parsimonious explanation for the observation that MDMA or MDA administration directly

into the brain did not reproduce the neurotoxic effects that are usually observed following their peripheral administration (Paris and Cunningham, 1992; Esteban *et al.*, 2001). Nevertheless, the direct injection of thioether MDMA metabolites into the brain produced prolonged 5-HT depletions and neurobehavioral changes similar to those observed after peripheral administration of MDMA or MDA (Miller *et al.*, 1996; Miller *et al.*, 1997; Bai *et al.*, 1999; Easton *et al.*, 2003). Furthermore, the attenuation in MDMA-mediated serotonergic deficits through inhibition of CYP450 (Gollamudi *et al.*, 1989) supports a substantial role for metabolism in MDMA's neurotoxicity. In accordance, over the last few years these observations have received considerable experimental support *in vitro* (Capela *et al.*, 2006a; Capela *et al.*, 2007b; Ferreira *et al.*, 2013). Using this background as a starting point, our initial studies were performed in a subcellular *in vitro* neuronal system, synaptosomes, and aimed to appraise the toxicity of MDMA and its metabolites α-MeDA, N-Me-α-MeDA and 5-(GSH)-α-MeDA, as well as of monoamine neurotransmitters 5-HT and dopamine, dopamine precursor L-Dopa and dopamine metabolite DOPAC.

Incubation of synaptosomes with these compounds led to a concentration- and time-dependent H_2O_2 formation, an effect partially prevented by the antioxidants NAC, ascorbic acid and melatonin. In association with H_2O_2 generation, the studied compounds induced a stimulation of the synaptosomal Na^+/K^+ ATPase activity, in a concentration-dependent manner, which was partially rescued by NAC. Given the remarkable role of the Na^+/K^+ ATPase in regulating neural excitability, an impairment of the Na^+/K^+ ATPase activity might lead to neuronal dysfunction (Clapcote *et al.*, 2009; Benarroch, 2011). In fact, abnormal Na^+/K^+ ATPase activity has been reported to be involved in several neurological diseases, such as bipolar disorder (Abdollahi and Karami-Mohajeri, 2012) or Alzheimer's disease (Yoon *et al.*, 2012), and neurotoxicological phenomena (Grauer *et al.*, 2008; Vijayaraghavan, 2009; Yuan *et al.*, 2013b). Our studies also found a stimulation of the Na^+/K^+ ATPase activity in synaptosomes exposed to phenazine methosulfate (PMS), a chemical generator of superoxide radicals (which may be easily converted to H_2O_2, spontaneously or enzymatically by superoxide dismutase), suggesting, therefore, the involvement of ROS in this effect. In accordance, H_2O_2 was described to play a role in CD95-induced internalization of the Na^+/K^+ ATPase in human T cells (Yin *et al.*, 2007). Additionally, in MDCK cells, it was also demonstrated that the suppression of ROS activity by NAC blocked low K^+-induced increased activity, protein abundance and cell surface location of the Na^+/K^+ ATPase (Zhou *et al.*, 2003), thus supporting a role for ROS-regulated pathways in the stimulant effect triggered by MDMA metabolites and monoamine neurotransmitters on the Na^+/K^+ ATPase activity. Since Na^+/K^+ ATPase plays a remarkable role in regulating the neuronal Na^+/K^+ equilibrium, an increase in its activity may render neurons more prone to excitability. Indeed, activation of the Na^+/K^+ ATPase

was previously reported in cultured rat cerebellar neurons exposed to GLU (Marcaida *et al.*, 1996) and the MDMA-induced neurotoxicity in cultured rat cortical neurons was partially rescued by the NMDA receptor antagonist MK-801 (Capela *et al.*, 2006b). Therefore, these resuts suggest that abnormalities on the Na^+/K^+ ATPase function triggered by MDMA metabolites and monoamine neurotransmitters may contribute to the stimulant and/or neurotoxic effects of MDMA.

In mouse brain synaptosomes, we also demonstrated that the H_2O_2 generation triggered by MDMA metabolites and monoamine neurotransmitters was independent on the mitochondrial polarization status, and the consequent toxic effects did not alter the number of polarized mitochondria. Though mitochondria, namely complexes I and III of the ETC, are described to be the main site of ROS generation in the cell (Votyakova and Reynolds, 2001; Reale *et al.*, 2012), our results suggest that other mechanisms independent on mitochondrial pathways may be involved in the toxic effects induced by the studied compounds in this experimental model. Indeed, the mechanisms underlying the toxicity of MDMA metabolites is thought to involve the inherent reactivity of their catechol moiety (Carvalho *et al.*, 2004b). MDMA metabolites are redox active, being prone to oxidation to the corresponding *ortho*-quinones (Spencer *et al.*, 1998; Macedo *et al.*, 2007), which may further undergo redox cycling to the corresponding semi-quinone radicals, with consequent ROS formation (Erives *et al.*, 2008), in accordance, therefore, with our results. Additionally, the presence of the catechol group in the chemical structure of dopamine, L-Dopa and DOPAC (Meiser *et al.*, 2013) raises the possibility that a similar mechanism may contribute to the H_2O_2 generated by these compounds in our synaptosome model. Nevertheless, we also demonstrated that DA- and 5-HT-induced H_2O_2 formation was dependent on their metabolism by MAO. In fact, studies using MAO inhibitors constitute one of the most convincing evidences supporting an involvement of monoamine neurotransmitters in MDMA's neurotoxicity. MAO-B inhibition with deprenyl not only attenuated the MDMA-induced mitochondrial toxicity in the brain of an adolescent rat model (Alves *et al.*, 2007), but also protected against MDMA-induced serotonergic neuronal degeneration (Sprague and Nichols, 1995), in a similar extension to those observed in mice knockout for MAO-B enzyme (Fornai *et al.*, 2001).

Our studies in mouse brain synaptosomes also revealed that, in association with increased H_2O_2 generation, the studied compounds also promoted oxidative modifications in synaptosomal macromolecules. MDMA metabolite 5-(GSH)-α-MeDA induced a concentration- and time-dependent increase in lipid peroxidation levels, which was fully prevented by NAC. In accordance, *in vivo*, MDMA was reported to induce lipid peroxidation in whole rat brain mitochondria (Alves *et al.*, 2007; Alves *et al.*, 2009a; Alves *et al.*, 2009b). Furthermore, MDMA-induced neurotoxicity in the mice model was also

associated with increased lipid peroxidation in the striatum (Camarero *et al.*, 2002; Peraile *et al.*, 2013).

In this study, it was also clearly demonstrated an increase in protein carbonylation levels for the MDMA metabolite 5-(GSH)-α-MeDA and for DOPAC. In addition, a concentration-dependent increase in quinoproteins formation was also found for MDMA metabolites, as well as for dopamine, L-Dopa and DOPAC. As already referred, the presence of the catechol group in these compounds confer them a particular reactivity. The catechol group may easily undergo redox cycling to the corresponding *ortho*-quinones (Spencer *et al.*, 1998; Macedo *et al.*, 2007), which, being highly reactive electrophilic intermediates (Capela *et al.*, 2009; Carvalho *et al.*, 2012), may bind to proteins. The absence of the catechol group in MDMA and 5-HT structures may explain the non-significant results obtained for these compounds at this level.

In the same synaptosomal model, we also observed that the studied compounds produced significant modifications on glutathione status. Exposure to the tested compounds resulted in significant increases in intrasynaptosomal glutathione content (more marked after 1h of exposure) and increased intrasynaptosomal GSSG levels (more marked for the concentration of 200 μM). Additionally, we found that the increase in intrasynaptosomal glutathione content elicited by the studied compouds did not result from a *de novo* synthesis of GSH, but rather by an uptake mechanism from the incubation medium. Therefore, these results agree the major role for oxidative stress-related mechanisms that have been attributed to MDMA-induced neurotoxicity (Capela *et al.*, 2009; Carvalho *et al.*, 2012).

These studies also revealed that the dopamine precursor L-Dopa and the dopamine metabolite DOPAC may play a role in MDMA´s neurotoxicity. In fact, L-Dopa was previously reported to potentiate the serotonergic deficits associated with a single administration of MDMA to rats (Schmidt *et al.*, 1991). In addition, DOPAL, the aldehyde precursor of DOPAC, was shown to induce selective loss of dopaminergic neurons when directly injected into the *substantia nigra* and ventral tegmental area of rats (Burke *et al.*, 2003).

Our findings in the synaptosome model suggest that MDMA metabolites, in association with monoamine neurotransmitters, may be major effectors in “ecstasy”-induced neuronal degeneration and neurotoxicity. Additionally, new data supporting a role for Na^+/K^+ ATPase on neuronal effects of MDMA were also provided. Despite this, more than the monoamine neurotransmitters, MDMA metabolites α-MeDA, N-Me-α-MeDA and 5-(GSH)-α-MeDA were powerful stressors in the synaptosome model, in line with previous reports in other neuronal models (Capela *et al.*, 2006a; Capela *et al.*, 2007b; Ferreira *et al.*, 2013), suggesting, thereby, that MDMA-induced neurotoxicity may be largely dependent

on the systemically formed metabolites. Therefore, to better understand the role of metabolism in MDMA's neurotoxicity, our further studies were accomplished in a cellular system, the SH-SY5Y cell line (manuscripts 3 and 4).

III.1.2 Studies in SH-SY5Y differentiated cells

SH-SY5Y cells present most of the intracellular homeostatic mechanisms observed in neurons on their physiological environment, most of which are absent in the synaptosome model. As such, this cell line has been widely used in experimental neurotoxicological studies (Presgraves *et al.*, 2003; Wang and Xu, 2005; Shavali and Sens, 2008; Lopes *et al.*, 2010; Ferreira *et al.*, 2013). In our studies, it was demonstrated that SH-SY5Y cells differentiated with RA followed by TPA presented a functionally mature neuronal phenotype with dopaminergic characteristics, as traduced by increased DAT and TH expression, which is in accordance with previous outcomes (Presgraves *et al.*, 2003). The higher ability of RA/TPA-differentiated SH-SY5Y cells to uptake and retain DA, compared to their undifferentiated state (Presgraves *et al.*, 2003; Ferreira *et al.*, 2013), and the higher susceptibility to the neurotoxic actions of MPP^+ (a classical dopaminergic neurotoxin, whose its toxic effect depends on DAT) (Presgraves *et al.*, 2003) support the notion that SH-SY5Y cell differentiated with RA followed by TPA present a characteristically dopaminergic phenothype. Therefore, considering the evidences showing MDMA-induced long-lasting abnormalities on the dopaminergic system, which has been mostly disclosed in the mice model (Cadet *et al.*, 2001; Escobedo *et al.*, 2005; Granado *et al.*, 2008; Granado *et al.*, 2011), the use of the RA/TPA-differentiated SH-SY5Y cells may provide a significant understanding about the molecular and cellular mechanisms of neuronal degeneration associated with MDMA.

Our initial studies performed in mouse brain synaptosomes ascertained the toxicity of MDMA metabolites α-MeDA, N-Me-α-MeDA and 5-(GSH)-α-MeDA. However, following systemic formation of GSH conjugates of α-MeDA and N-Me-α-MeDA, they can be transported into the brain and further metabolized to NAC conjugates (Monks *et al.*, 2004). In accordance, following s.c. administration of MDMA to rats, both GSH- and NAC-conjugated metabolites were identified and quantified in the striatum (Jones *et al.*, 2005; Erives *et al.*, 2008). Additionally, since thioether MDMA metabolites are more redox active than their catechol precursors (Macedo *et al.*, 2007), conferring them a higher neurotoxic potential (Capela *et al.*, 2006a; Capela *et al.*, 2007b), in our studies performed in the SH-SY5Y cell line we extended the findings observed on the synaptosome model and tested not only the catechol MDMA metabolites, but also their corresponding GSH and NAC adducts.

Our studies in SH-SY5Y differentiated cells clearly showed that, following long exposure periods of 24 or 48h, MDMA did not induce cytotoxicity, as evaluated by the 3-[4,5-dimethylthiazol-2-yl]-2,5-diphenyltetrazolium (MTT) reduction and *L*-lactic dehydrogenase (LDH) release assays. Nevertheless, for the same times of exposure, MDMA metabolites were toxic to SH-SY5Y differentiated cells. Furthermore, the corresponding GSH-monoconjugated metabolites of α-MeDA and N-Me-α-MeDA revealed to be more potent neurotoxins than their catechol precursors. Indeed, a previous study showed that the conjugation of the catechol MDMA metabolites with GSH or NAC at the 5 position reduced the oxidation potential, when compared with the non-conjugated compound (Macedo et al., 2007). Noteworthy, the lower oxidation potential observed for these GSH or NAC adducts correlated with a higher toxicity of these compounds to rat cultured cortical neurons (Capela *et al.*, 2006a; Capela *et al.*, 2007b; Macedo *et al.*, 2007). Therefore, our results confirmed that the GSH conjugation dramatically increases the neurotoxic potential of the catechol MDMA metabolites. However, the half-life of the GSH conjugates in the brain is short, as a result of their conversion to the respective NAC adducts (Esteban *et al.*, 2001), though the latter retain the toxicity of their GSH precursors (Jones *et al.*, 2005). In accordance, our studies also demonstrated that 5-(NAC)-α-MeDA and 5-(NAC)-N-Me-α-MeDA, which are slowly eliminated and, consequently, persistent in the brain (Jones *et al.*, 2005; Erives *et al.*, 2008), were potent neurotoxins to SH-SY5Y differentiated cells, in agreement, therefore, with previous findings observed in cultured rat cortical neurons (Capela *et al.*, 2006a; Capela *et al.*, 2007b).

Our studies also revealed that the toxicity of catechol MDMA metabolites to SH-SY5Y differentiated cells was potentiated by hyperthermia (40ºC). Indeed, many *in vivo* and *in vitro* studies support the notion that hyperthermia plays a major role in MDMA-induced neuronal cell death. MDMA was shown to cause acute dose-dependent hyperthermia in several *in vivo* experimental models (Blessing and Seaman, 2003; Saadat *et al.*, 2004; Alves *et al.*, 2007; Pontes *et al.*, 2008a; Hrometz *et al.*, 2011; Takamatsu *et al.*, 2011; Schütte *et al.*, 2013), including non-human primates (Crean *et al.*, 2006; Taffe *et al.*, 2006; Von Huben *et al.*, 2006; Taffe, 2012). In humans, following some reports of fatalities associated with overheating in MDMA users, with core body temperatures over 40ºC (Henry *et al.*, 1992; Chadwick *et al.*, 2001), many other studies have shown the potential of MDMA to induce acute hyperthermia (McCann *et al.*, 1996; Freedman *et al.*, 2005; Farré *et al.*, 2007). In addition, *in vitro* studies simulating the hyperthermic conditions that are attained *in vivo* confirmed that the hyperthermic response associated with MDMA plays a major role in drug-induced neurotoxicity (Capela *et al.*, 2006a; Capela *et al.*, 2006b; Capela *et al.*, 2007b), corroborating, therefore, our results.

Contrary to the catechol MDMA metabolites α-MeDA and N-Me-α-MeDA, the toxicity elicited by 5-(GSH)-α-MeDA and 5-(glutathion-*S*-yl)-*N*-methyl-α-methyldopamine [5-(GSH)-N-Me-α-MeDA] was independent on the temperature of exposure, whereas their respective NAC conjugates revealed to be more toxic under normothermic conditions. A previous study in cultured rat cortical neurons demonstrated a temperature-dependent toxicity for GSH- and NAC-conjugated metabolites of MDMA, after a short time of exposure of 6h (Capela *et al.*, 2007b). It is possible that variations in receptors and/or transporters or in intracellular regulatory mechanisms between neuronal models, as well as the different times of exposure tested in these studies may explain these differences. However, to confirm this hypothesis, further studies are needed.

In our studies in SH-SY5Y differentiated cells, the stability of MDMA metabolites over time was also assessed by HPLC analysis with electrochemical detection. In cell culture medium, it was observed an over time decrease in the concentration of MDMA metabolites α-MeDA, N-Me-α-MeDA, 5-(GSH)-α-MeDA and 5-(NAC)-α-MeDA, which was faster under hyperthermic conditions. However, the catechol metabolites α-MeDA and N-Me-α-MeDA were more stable than the adducts 5-(GSH)-α-MeDA and 5-(NAC)-α-MeDA. Previous *in vitro* studies demonstrated an over time decrease in N-Me-α-MeDA and α-MeDA concentrations in biological media, which was associated with oxidation to the corresponding aminochromes (Carvalho *et al.*, 2004c). The reactive intermediates produced during the oxidation of these catechol metabolites into reactive *ortho*-quinones and/or aminochromes can be conjugated with GSH, to form the corresponding glutathionyl adducts (Hiramatsu *et al.*, 1990), thus indicating that dynamic processes in the biological medium may influence the toxicity of MDMA metabolites. Additionally, our studies also revealed that MDMA metabolites α-MeDA, N-Me-α-MeDA and 5-(NAC)-α-MeDA were poorly accumulated into the cells, thus suggesting that extracellular mechanisms may contribute to the toxic effects induced by MDMA metabolites in SH-SY5Y differentiated cells.

Corroborating our results obtained in the synaptosome model, in which NAC prevented the H_2O_2 production induced by MDMA metabolites and monoamine neurotransmitters, NAC pre-incubation significantly protected SH-SY5Y differentiated against the toxic insult elicited by MDMA metabolites, as evaluated by the MTT reduction assay. Indeed, many studies have highlighted the importance of the neuronal redox status on the neurotoxic effects mediated by MDMA and its metabolites, as revealed by NAC-conferred protective effect (Capela *et al.*, 2006a; Capela *et al.*, 2007b), thus evidencing a major role for oxidative stress-related mechanisms in the pathogenesis of MDMA.

Our studies also demonstrated that SH-SY5Y differentiated cells exposed to MDMA for 48h, under normothermic conditions, presented a significant reduction in intracellular

glutathione content. MDMA-induced glutathione depletion has already been reported in non-neuronal cells, including isolated rat (Beitia *et al.*, 1999; Carvalho *et al.*, 2004b) and mouse (Carvalho *et al.*, 2001) hepatocytes. However, in our study, MDMA metabolites triggered an increase in intracellular glutathione content, which corroborates our results obtained in the synaptosome model. Many conditions are known to change glutathione homeostasis, namely oxidative stress, which may activate cellular defense systems, resulting in increased GSH levels (Godwin *et al.*, 1992; Shi *et al.*, 1994). In accordance, similar results were demonstrated by previous studies performed in SH-SY5Y cells after exposure to neurotoxic insults mediating oxidative stress (Núñez *et al.*, 2004; Aguirre *et al.*, 2007), including the catechol MDMA metabolites α-MeDA and N-Me-α-MeDA (Ferreira *et al.*, 2013).

It is important to analyze the rational of concentrations of the tested componds in order to support the translation of the data to the animal and human scenario. The concentrations of MDMA used in the present studies (manuscripts 1, 2 and 3) are in accordance with previous *in vitro* studies (Simantov and Tauber, 1997; Chipana *et al.*, 2008b; Rozas *et al.*, 2012; Capela *et al.*, 2013). Similarly to MDMA, several *in vitro* studies have also used MDMA metabolites at the range of concentrations similar to those tested in our studies (Capela *et al.*, 2006a; Capela *et al.*, 2007b; Escubedo *et al.*, 2011; Ferreira *et al.*, 2013). In a human controlled study, following a single 100 mg oral dose of MDMA, N-Me-α-MeDA reached plasma concentrations (154.5 µg/L) similar to those observed for MDMA (181.6 µg/L) (Segura *et al.*, 2001). Furthermore, some reports suggest that MDMA metabolites may accumulate into the brain following a multiple dosage regimen that is often used in animal studies (Jones *et al.*, 2005; Erives *et al.*, 2008) to mimetize the pattern of MDMA abuse by humans. On the other hand, some environmental conditions have also been shown to influence the MDMA's brain levels *in vivo*, as observed in mice, in which restraint, cold stress or co-administration of ethanol raised striatal concentrations of MDMA by 3- to 7-fold (Johnson *et al.*, 2004). Additionally, since the evaluation of mechanistic interactions of MDMA and its metabolites, at molecular and cellular level, is more easily demonstrated by using a high concentration approach, our initial studies were performed according to this background.

Despite this, in addressing the role of metabolism in the context of MDMA-induced neurotoxicity, some studies have demonstrated that MDMA and its metabolites, including catechol precursors and corresponding GSH and NAC conjugates, co-exist in the brain following peripheral administration of MDMA (Chu *et al.*, 1996; Jones *et al.*, 2005; Erives *et al.*, 2008). Therefore, it is expected that the neurotoxic effects of MDMA may result from a combined effect of the parent compound and its metabolites. Accordingly, our next hypothesis tested was that the combined effects of MDMA and its metabolites, at low

micromolar concentrations that may be attained *in vivo*, may induce neurotoxicity *in vitro* (manuscript 4).

In rats, after oral administration of MDMA (20 mg/Kg), high concentrations of the drug were found in the brain (17.17 nmol/g brain) (Mueller *et al.*, 2009). In the same way, following s.c. injection of MDMA to rats (from 5 to 20 mg/Kg), its brain and plasma concentrations ranged from 0.74 to 147.65 nmol/g brain and from 0.00 to 15.78 µM, respectively (Chu *et al.*, 1996), showing, therefore, that brain accumulation of MDMA is clearly favored. Additionally, the combined concentration of 4 thioether metabolites in rat striatal dialysate reached a maximum of 13 µM, which remained relatively unchanged for approximately 4h after exposure to MDMA (20 mg/kg, s.c., four times at 12-h intervals) (Erives *et al.*, 2008). Knowing that the lack of metabolic competence (CYP450-mediated metabolism) constitutes one of the most important limitations of *in vitro* neuronal models (Ferguson and Tyndale, 2011), how can be determined, *in vitro*, whether MDMA and its metabolites act in a combined manner in developing neurotoxic effects? To answer this question, we performed studies with MDMA and 6 of its major metabolites, α-MeDA, N-Me-α-MeDA, 5-(GSH)-α-MeDA, 5-(GSH)-N-Me-α-MeDA, 5-(NAC)-α-MeDA and 5-(NAC)-N-Me-α-MeDA, as a mixture. This approach circumvents the limitation of the use of *in vitro* neuronal models for studies with drugs in which systemic metabolism greatly contributes to their effects at brain level. Thus, the mixture composition was fixed at equal concentrations of 10 or 20 µM for each compound, and its effects, in SH-SY5Y differentiated cells, were assessed after 24 or 48h of exposure.

Incubation of SH-SY5Y differentiated cells with the mixture of MDMA and its metabolites, each compound at 10 or 20 µM, for periods of 24 or 48h, resulted in significant toxicity, as revealed by the MTT reduction and LDH release assays. Furthermore, when tested alone, and at the same concentrations that are present in the mixture, MDMA and its metabolites elicited non-significant or minor effects on cell viability, agreeing, therefore, with the hypothesis that a combined effect among parent compound and metabolites may be involved on MDMA´s neurotoxic actions.

Our experiments also showed that the toxicity of the mixture of MDMA and its metabolites was potentiated by hyperthermia (40ºC) and NAC fully protected SH-SY5Y differentiated cells against the toxic effects, at both normothermic and hyperthermic conditions. In this work, such as initially observed in SH-SY5Y differentiated cells exposed to the catechol MDMA metabolite N-Me-α-MeDA (manuscript 3), the toxicity elicited by the mixture of MDMA and its metabolites was accompanied by caspase 3 activation. Indeed, increased caspase 3 activation was previously reported in cultured rat cortical (Capela *et al.*, 2007a), hippocampal (Capela *et al.*, 2013) and cerebellar granule (Jiménez *et al.*, 2004) neurons exposed to MDMA. Furthermore, increased caspase 3 activity was also

observed in SH-SY5Y undifferentiated cells exposed to N-Me-α-MeDA (Felim *et al.*, 2009) and in cultured rat cortical neurons exposed to NAC-conjugated metabolites of MDMA (Capela *et al.*, 2007b). In addition, a previous study also demonstrated caspase 3 activation in mice amygdala and HIP after MDMA administration *in vivo* (Tamburini *et al.*, 2006).

In our studies in SH-SY5Y differentiated cells, by inhibiting DAT-mediated transport the toxicity of the mixture of MDMA and its metabolites was not significantly modified. This result indicated that the toxicity induced by this mixture relied on DAT-independent mechanisms. Though MDMA is known to modulate DAT function (Itzhak *et al.*, 2003; Verrico *et al.*, 2007), an independence on DAT-uptake system in the toxic effects elicited by high concentrations of catechol MDMA metabolites α-MeDA and N-Meα-MeDA was previously reported (Ferreira *et al.*, 2013). From this, it may be hypothesized that MDMA metabolites may access the cell through other mechanisms or, even, activate extracellular pathways or promote the generation of toxic reactive species outside the cell, which may trigger intracellular injury. These postulated hypotheses are strengthened by the low concentrations of MDMA metabolites that we demonstrated to be attainable inside of the cells following different times of exposure (manuscript 3).

Our studies clearly demonstrated a time-dependent ROS formation in SH-SY5Y differentiated cells exposed to the mixture of MDMA and its metabolites, corroborating, therefore, our previous findings observed in mouse brain synaptosomes exposed to MDMA metabolites. In accordance, other studies showed increased ROS production in cultured rat cortical neurons exposed to the MDMA metabolites 5-(GSH)-N-Me-α-MeDA, 5-(NAC)-α-MeDA and 5-(NAC)-N-Me-α-MeDA (Capela *et al.*, 2007b). Furthermore, MDMA metabolites 5-(GSH)-α-MeDA and 2,5-(GSH)-α-MeDA and, to a lesser extent, MDA and MDMA, induced a concentration- and time-dependent increased ROS formation in both human SERT- and human DAT-transfected SK-N-MC cells (Jones *et al.*, 2004). Therefore, the increased ROS formation in the brain of rats administrated with MDMA reported by several studies (Colado *et al.*, 1997; Colado *et al.*, 1999; Shankaran *et al.*, 1999a) suggests that a combined effect of parent compound and metabolites may contribute to this effect.

Our study also demonstrated that the mixture of MDMA and its metabolites induced significant increases in intracellular total glutathione content in SH-SY5Y differentiated cells. This corroborates our results obtained in the synaptosome model with MDMA metabolites and monoamine neurotransmitters, as well as in SH-SY5Y differentiated cells exposed to each MDMA metabolite alone. In synaptosomes, an uptake mechanism from the incubation medium was associated with the increased intrasynaptosomal total glutathione content. However, in SH-SY5Y differentiated cells, the increase in intracellular

total glutathione levels elicited by the mixture of MDMA and its metabolites resulted from a *de novo* GSH synthesis, as ascertained in our experiments with BSO. Despite this, in non-neuronal cells, it was previously reported that both MDMA and its metabolites induced GSH depletion associated with increased GSSG levels (Carvalho *et al.*, 2004a; Carvalho *et al.*, 2004b). Particularly, SH-SY5Y cells present highly efficient mechanisms for GSSG extrusion, such as the MRP1 transporter (Aguirre *et al.*, 2007). Furthermore, since intracellular GSSG is maintained at extremely low levels, as a result of the MRP1 activity, the intracellular regulation of GSH synthesis may be impaired. Thus, in the absence of normal feedback mechanisms, uncontrolled GSH synthesis may occur. In accordance, impaired regulation of GSH synthesis was previously reported in SH-SY5Y cells exposed to 6-hydroxydopamine (Tirmenstein *et al.*, 2005). Additionally, in our experiments, SH-SY5Y differentiated cells exposed to BSO alone presented lower intracellular levels of GSH than control cells. Since GSH synthesis was inhibited, this reduction may be explained by GSH conversion to GSSG, which is efficiently extruded by MRP1 transporter. Therefore, the increase in intracellular glutathione content that we observed in SH-SY5Y differentiated cells exposed either to each MDMA metabolite alone (manuscript 3) or to the mixture of MDMA and its metabolites (manuscript 4), more than related to the toxic effects of MDMA metabolites, may result from particular characteristics of this experimental model. Corroborating this hypothesis are previous studies demonstrating, in the same expriemental model, an increase in intracellular total glutathione content when other experimental paradigms were used (Núñez *et al.*, 2004; Tirmenstein *et al.*, 2005; Aguirre *et al.*, 2007; Ferreira *et al.*, 2013).

In this study, we also observed an increase in intracellular Ca^{2+} levels in SH-SY5Y differentiated cells exposed to the mixture of MDMA and its metabolites. In line with this result, a sustained increase in intracellular Ca^{2+} levels was also previously reported in PC12 cells exposed to MDMA (Garcia-Ratés *et al.*, 2010). Furthermore, in neurons, a correct Ca^{2+} homeostasis is likely to contribute to the proper neuronal function and survival (Oliveira *et al.*, 2006; Oliveira and Gonçalves, 2009). In addition, since Ca^{2+} acts as a key second messenger in intracellular cascades, sustained intracellular Ca^{2+} accumulation has been implicated as a trigger for neuronal degeneration (Tymianski *et al.*, 1993; Oliveira *et al.*, 2006) and neurotoxicity (Xu *et al.*, 2013). Nevertheless, when we used the selective intracellular Ca^{2+} chelator BAPTA acetoxymethyl ester (BAPTA/AM), the toxicity of the mixture of MDMA and its metabolites in SH-SY5Y differentiated cells was not significantly modified. Therefore, this suggests an independence on Ca^{2+}-regulated intracellular pathways in the toxicity of the mixture of MDMA and its metabolites in SH-SY5Y differentiated cells.

Although our studies in mouse brain synaptosomes and SH-SY5Y differentiated cells helped in clarifying the mechanistic basis involved in MDMA-associated neurotoxicity, to better explore the pathways involved at molecular and cellular level we employed further studies in primary neuronal cultures from mice HIP (manuscripts 5 and 6).

III.1.3 Studies in cultured hippocampal neurons

In the cellular world, neurons are unique, possessing a characteristic morphology with extensive neuritic projections, existing in a postmitotic state, and depending on mitochondrial respiration as their primary source of energy production (90% of the neuronal ATP is generated by mitochondria) (Van Laar and Berman, 2013). Failure to maintain this bioenergetic status is suggested to play a primary role in neuronal death and disease (Lin and Beal, 2006). Preserving health in this existence is dependent upon the proper maintenance of a healthy population and distribution of functional mitochondria. In neurons, mitochondria are highly dynamic organelles that, by undergoing fusion and fission events, are efficiently translocated along the neuronal processes, frequently changing direction, pausing or switching to persistent docking (Kang *et al.*, 2008; MacAskill and Kittler, 2010; López-Doménech *et al.*, 2012; Plucińska *et al.*, 2012; Sheng and Cai, 2012). Additionally, these dynamic processes are tightly regulated by a multiplicity of factors, including cytosolic Ca^{2+} (Cereghetti *et al.*, 2008; Saotome *et al.*, 2008; Macaskill *et al.*, 2009b; Wang and Schwarz, 2009). A schematic representation of mitochondrial fusion, fission and transport in neurons is illustrated in Figure 12.

The neuritic mitochondrial population is tasked to provide energy for synaptic development and function, as well as for all processes that occur out of the cell body (Mironov, 2009). Furthermore, multiple studies have demonstrated that the deregulation of fusion, fission or transport greatly alters synapse formation and function (Li *et al.*, 2004; Verstreken *et al.*, 2005; Li *et al.*, 2008). Therefore, a correct mitochondrial distribution, by allowing the supply of specific energetic needs in all sites of the cell, is critical for proper neuronal morphology and function.

In recent years, a more detailed picture has emerged about the cellular mechanisms ensuring mitochondrial integrity and their relevance for neuronal degeneration. In the field of MDMA's research, there is a general consensus that mitochondrial-dependent pathways can provide a major understanding concerning pathological processes underlying drug's neurotoxicity (Quinton and Yamamoto, 2006; Alves *et al.*, 2007; Alves *et al.*, 2009a; Alves *et al.*, 2009b; Puerta *et al.*, 2010). Administration of a neurotoxic binge dose of MDMA (10 mg/kg, i.p., four times, at 2-h intervals), to an adolescent rat model, induced long-term modifications in brain mitochondria, as evidenced by increased lipid

peroxidation, protein carbonylation (Alves *et al.*, 2007; Alves *et al.*, 2009a; Alves *et al.*, 2009b), deletions on mtDNA and reduced expression of the subunit II of mitochondrial complex I and subunit I of complex IV (Alves *et al.*, 2007; Alves *et al.*, 2009a). Furthermore, in rat striatum, MDMA (10 mg/kg, i.p., 4 times, at 2-h intervals) was also shown to cause an inhibition of mitochondrial complexes I and II (Quinton and Yamamoto, 2006). In addition, MDMA-induced dopamine depletion in mice striatum was associated with decreased activity of the mitochondrial complex I (Puerta *et al.*, 2010). Therefore, these data suggest that MDMA-induced neurotoxicity may involve compromised mitochondrial function, such as it has been suggested in liver (Beitia *et al.*, 1999; Pontes *et al.*, 2008b; Pontes *et al.*, 2008c; Nakagawa *et al.*, 2009; Custódio *et al.*, 2010).

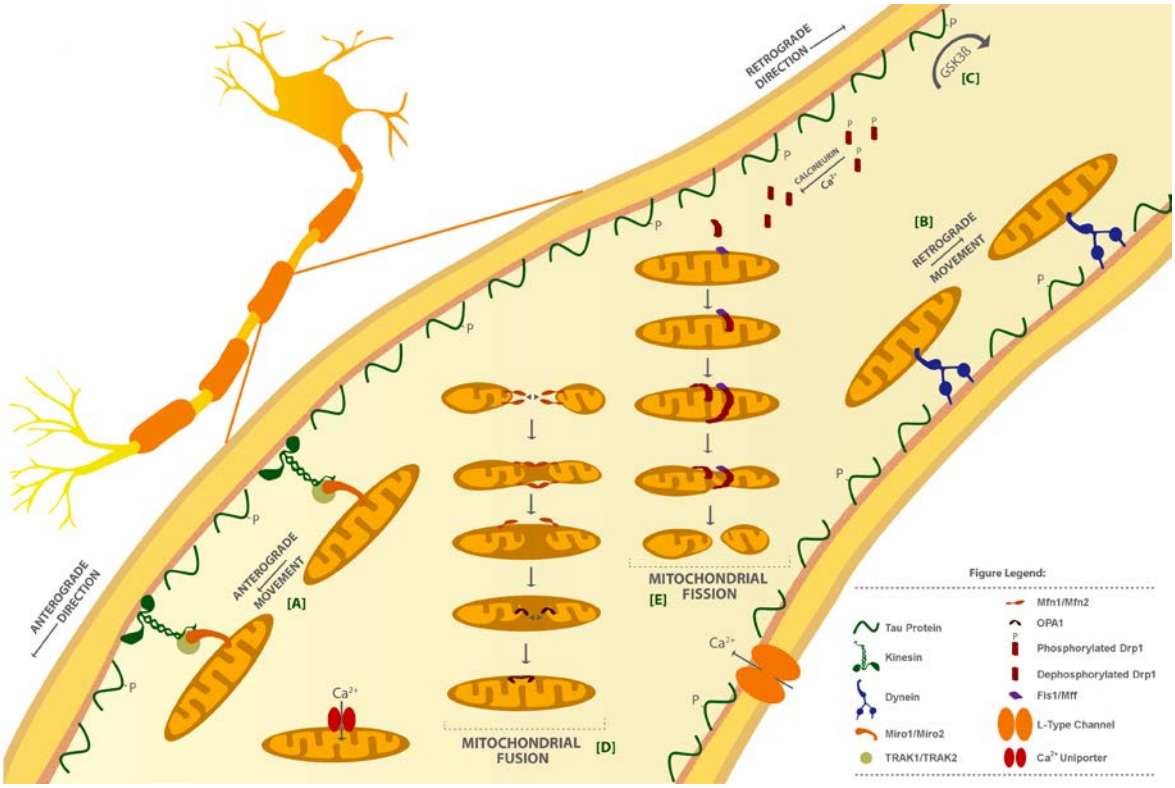


Figure 12. Mitochondrial fusion, fission and transport in neurons.
Mitochondrial are highly dynamic organelles, which must be transported, often to considerable distances, from their sites of synthesis in the neuronal soma, to axons and dendrites. Long-range transport of mitochondria is mainly regulated by motor proteins along the microtubules. In axons, anterograde mitochondrial transport is mediated by kinesin motors, linked to the mitochondrial outer membrane protein Miro through the adaptor proteins TRAK1/TRAK2 [A]. Axonal transport of mitochondria in retrograde direction is mediated by cytoplasmic dynein motors [B]. Microtubule-associated protein Tau, by assembly and maintenance of microtubules, plays a major role on mitochondrial trafficking control. Its phosphorylation status, which is highly dependent on the glycogen synthase 3β (GSK3β) activity, is critical in regulating mitochondrial transport [C]. By controlling organelle size and shape, mitochondrial fusion/fission events play also a major role on mitochondrial trafficking control. Mitochondrial fusion is mediated by mitofusin 1 (Mfn1), mitofusin 2 (Mfn2) and optic atrophy 1 (OPA1) proteins. Mfns are involved in outer mitochondrial membrane fusion, whereas OPA1 mediates fusion of the inner mitochondrial membrane [D]. Mitochondrial fission is mediated by dynamin-related protein 1 (Drp1). When mitochondrial fission is stimulated, Drp1 is dephosphorylated by calcineurin (Ca^{2+}-regulated event), which translocates to mitochondria, thus promoting, via adaptors mitochondrial fission protein 1 (Fis1) and/or mitochondrial fission factor (Mff), mitochondrial fission [E].

Therefore, based on the following outcomes:

(1) MDMA-induced neurotoxic effects involve mitochondrial injury (Alves *et al.*, 2007; Alves *et al.*, 2009a; Alves *et al.*, 2009b; Puerta *et al.*, 2010), in which mitochondrial bioenergetics may be compromised;

(2) Defective mitochondrial bioenergetics is suggested to play a primary role in neuronal death (Lin and Beal, 2006);

(3) Bioenergetic condition, in part, regulates and even drives the fusion/fission balance of mitochondrial dynamics (Rossignol *et al.*, 2004; Twig *et al.*, 2008b);

(4) Alterations in mitochondrial dynamics can also alter the bioenergetic status of both individual mitochondria and of the cell (Barsoum *et al.*, 2006; Palau *et al.*, 2009; Van Bergen *et al.*, 2011);

(5) A correct balance between fusion and fission events are crucial in sustaining the robust mitochondrial structure and function and to a correct transport of mitochondria over long distances (Amiri and Hollenbeck, 2008; Saxton and Hollenbeck, 2012; Itoh *et al.*, 2013);

(6) The maintenance of a healthy population and distribution of functional mitochondria are critical for proper neuronal function and survival (Millecamps and Julien, 2013),

it is likely to assume that neurons and their mitochondria depend on an intricate balance between mitochondrial bioenergetics and dynamics, raising, thereby, the following hypothesis: Is neuronal mitochondrial dynamics affected by MDMA?

To address this hypothesis we studied the putative deleterious effects of MDMA and its metabolites on mitochondrial dynamics, using cultured mice hippocampal neurons as experimental model (manuscripts 5 and 6). MDMA use appears to be associated with cognitive impairments and dysfunction of inhibitory circuits in the HIP (Jacobsen *et al.*, 2004). Accordingly, many human and animal studies emphasize that HIP is particularly vulnerable to MDMA's actions (Ricaurte *et al.*, 1988b; Fornai *et al.*, 2001; Gouzoulis-Mayfrank *et al.*, 2003; Itzhak *et al.*, 2003; Busceti *et al.*, 2008). Therefore, cultured hippocampal neurons constitute a suitable model to betther understand the effects of MDMA on mitochondrial dynamics and their implications in pathological processes underlying neurotoxicity. Primary hippocampal cultures obtained from embryos contain a more homogeneous neuronal population, constituted essentially by pyramidal neurons (low content in dentate granule cells and interneurons) (Herculano-Houzel, 2011), thus allowing to obtain a more homogeneous experimental response. Additionally, this system has been widely used as *in vitro* experimental model to study mitochondrial dynamics *in situ* (MacAskill *et al.*, 2009a; Macaskill *et al.*, 2009b; Clayton *et al.*, 2012; Fang *et al.*, 2012; López-Doménech *et al.*, 2012). Thus, based on our previous studies, the effects

either of MDMA alone or of the mixture of MDMA and its metabolites on neuronal mitochondrial dynamics were studied, following a short (90 min) or a long (24h) period of exposure.

Exposure to a non-cytotoxic concentration of MDMA (1.6 mM), for 90 min, dramatically reduced mitochondrial trafficking along axonal processes of cultured hippocampal neurons, in a time-dependent manner, which was correlated with increased mitochondrial fragmentation. Furthermore, a similar reduction in mitochondrial trafficking and increased mitochondrial fragmentation was also demonstrated in hippocampal neurons exposed to the non-cytotoxic mixture of MDMA and its metabolites, each compound at 10 µM, for 24h (the same time-point used in our studies performed in SH-SY5Y differentiated cells). The 20 µM mixture revealed to be much toxic to the cultures (MTT reduction assay), thus invalidating further studies of mitochondrial transport. Since high energy demands and the requirement to maintain cellular homeostasis at sites distant to the cell body make neurons particularly vulnerable to mitochondrial dysfunction (Itoh *et al.*, 2013), it has been suggested that disrupted mitochondrial translocation may contribute to the pathophysiology of neuronal injury (Deheshi *et al.*, 2013). In addition, other evidences indicate that terminal axons and cell body may be damaged independently and by distinct mechanisms (Lee *et al.*, 2012b). Therefore, considering that the selective loss of nerve terminals is a characteristic marker of the MDMA-associated neurotoxicity (Capela *et al.*, 2009), these findings provide a new possible explanation about the putative mechanisms involved in acute- and long-term effects of MDMA into the brain.

A functional link between mitochondrial neuronal trafficking control and intracellular Ca^{2+} levels has been established (Rintoul *et al.*, 2003; Chang *et al.*, 2006; Macaskill *et al.*, 2009b; Wang and Schwarz, 2009). An elevation on cytosolic Ca^{2+} efficiently inhibited mitochondrial transport along neuronal processes of hippocampal neurons (Macaskill *et al.*, 2009b; Wang and Schwarz, 2009). Additionally, recent studies identified Miro, a Rho GTPase protein anchored in the outer mitochondrial membrane with two EF hand Ca^{2+}-binding domains (Fransson *et al.*, 2006), as a Ca^{2+} sensor in regulating mitochondrial mobility (Saotome *et al.*, 2008; Macaskill *et al.*, 2009b; Wang and Schwarz, 2009).

Similarly to the effect that we observed in SH-SY5Y differentiated cells exposed to the mixture of MDMA and its metabolites, in cultured hippocampal neurons MDMA triggered a time-dependent increase in intracellular Ca^{2+} levels, both in the cell body and neuronal extensions. Thus, by transfecting hippocampal neuronal cultures with wild-type Miro1 protein or a mutant form (Miro1 ΔEF) lacking the EF hand Ca^{2+}-binding domains, the involvement of Ca^{2+}-regulated Miro-dependent mechanisms on the mitochondrial trafficking deficits elicited by MDMA were explored. With this approach, we demonstrated

an independence on Miro1 regulatory functions through cytosolic Ca^{2+} in MDMA-induced mitochondrial trafficking impairment.

Besides cytosolic Ca^{2+}, many other regulators of mitochondrial transport have been described, including Tau protein (Morel *et al.*, 2010; Vossel *et al.*, 2010). In our studies, by using Tau-null hippocampal neurons obtained from Tau knockout embryos, it was demonstrated a partial dependence on Tau protein for the effects of MDMA on mitochondrial trafficking, by a phosphorylation mechanism involving GSK3β. Indeed, MDMA was previously shown to induce a time-dependent increase in Tau phosphorylation in mice HIP, in which a dependence on GSK3β activity was also established (Busceti *et al.*, 2008).

Although many reports have recognized a pivotal role for Tau protein in regulating mitochondrial movement (Mandelkow *et al.*, 2004; Darios *et al.*, 2005; Vossel *et al.*, 2010), involving GSK3β (Morel *et al.*, 2010; Llorens-Martín *et al.*, 2011), different mechanisms have been proposed. Some studies associated increased Tau phosphorylation with improved mitochondrial transport (Mandelkow *et al.*, 2004; Llorens-Martín *et al.*, 2011). Therefore, from these studies it was suggested the existence of a competition mechanism between motor proteins and Tau for interaction with the microtubule surface. On the other hand, other reports established a causal link between increased Tau phosphorylation and impaired mitochondrial movement (Morel *et al.*, 2010; Hongo *et al.*, 2012), which suggested an alternative model in regulating mitochondrial transport by Tau protein, i.e., increased Tau phosphorylation leads to impaired mitochondrial transport by microtubule destabilization. Our results indicate an association between MDMA-induced increased Tau phosphorylation and defective mitochondrial transport, thus corroborating this last mechanism. However, we found a lower dependence on Tau regulatory functions on mitochondrial trafficking deficits elicited by the mixture of MDMA and its metabolites in cultured hippocampal neurons. These results suggest the existence of small mechanistic differences between MDMA alone, at a high concentration, and the mixture of MDMA and its metabolites, at low micromolar concentrations, which constitutes a more real approximation of the *in vivo* scenario. Additionally, these results also suggest that other mechanisms instead of Tau protein may be involved on the reported mitochondrial trafficking deficits.

Our observations linking impaired mitochondrial transport to increased mitochondrial fragmentation suggest that mitochondrial fusion/fission machinery may be involved on the reported mitochondrial trafficking deficits. Indeed, the existence of a correct balance between fusion and fission events appears to be critical in sustaining a correct transport of mitochondria over long distances (Amiri and Hollenbeck, 2008; Saxton and Hollenbeck, 2012; Itoh *et al.*, 2013). We demonstrated that the over-expression of functional Mfn2 in

hippocampal neurons almost completely rescued the mitochondrial trafficking deficits elicited by MDMA, whereas for the mixture of MDMA and its metabolites a complete rescue was observed. Indeed, Mfn2 was previously shown to interact with the components of the mitochondrial transport apparatus (Misko *et al.*, 2010). In agreement, studies in Mfn2-null neurons showed a marked reduction on mitochondrial density in their dendrites (Chen *et al.*, 2007a) and impaired mitochondrial transport along their axonal processes (Misko *et al.*, 2010). Additionally, in hippocampal neurons over-expressing Mfn2 R94Q, a CMT2A mutant protein with impaired fusion and transport properties (Detmer and Chan, 2007; Misko *et al.*, 2010), we demonstrated that the mitochondrial trafficking deficits induced either by MDMA or by the mixture of MDMA and its metabolites were not rescued. In accordance, a previous study showed that the over-expression of Mfn2 R94Q did not recover the mitochondrial transport abnormalities observed in Mfn2-null neurons (Misko *et al.*, 2010; Misko *et al.*, 2012). Therefore, since in our studies functional Mfn2 was required to reverse the effects either of MDMA or of the mixture of MDMA and its metabolites on mitochondrial transport, these data suggest that an alteration in fusion mechanisms may be involved on these effects. To confirm this hypothesis, we performed experiments with cultured hippocampal neurons over-expressing Drp1 K38A, a mutant Drp1 construct that down-regulates mitochondrial fission (Zhao *et al.*, 2011). Using this approach, we demonstrated a partial rescue of the mitochondrial trafficking impairment induced either by MDMA or by the mixture of MDMA and its metabolites. Since Drp1 K38A mutant inhibits endogenous fission without affecting mitochondrial fusion (Zhao *et al.*, 2011), these data also support a role for fission events in MDMA- and mixture-regulated phenotypes. In line with this, previous studies associated impaired synaptic formation and function, resulting from reduced mitochondrial translocation to the synaptic terminals, with Drp1 inhibition (Li *et al.*, 2004; Verstreken *et al.*, 2005). Furthermore, a role for fission events on mitochondrial transport was also reported in Drp1-null neurons, since their large and spherical mitochondria were exclusively localized in the cell body (Kageyama *et al.*, 2012). Therefore, our experiments with hippocampal neurons over-expressing fusion/fission proteins indicated that Mfn2 and Drp1 largely mediated the mitochondrial trafficking deficits induced either by MDMA or by the mixture of MDMA and its metabolites. Additionally, these experiments, in association with the increased mitochondrial fragmentation observed, also suggest that MDMA and the mixture of MDMA and its metabolites may alter the fusion/fission mitochondrial equilibrium. Taking into account the above referred findings, a mechanistic pathway for MDMA-induced deregulation of mitochondrial neuronal trafficking is illustrated in Figure 13. The present findings provide new data supporting a role for mitochondrial dynamics on neuronal effects of MDMA.

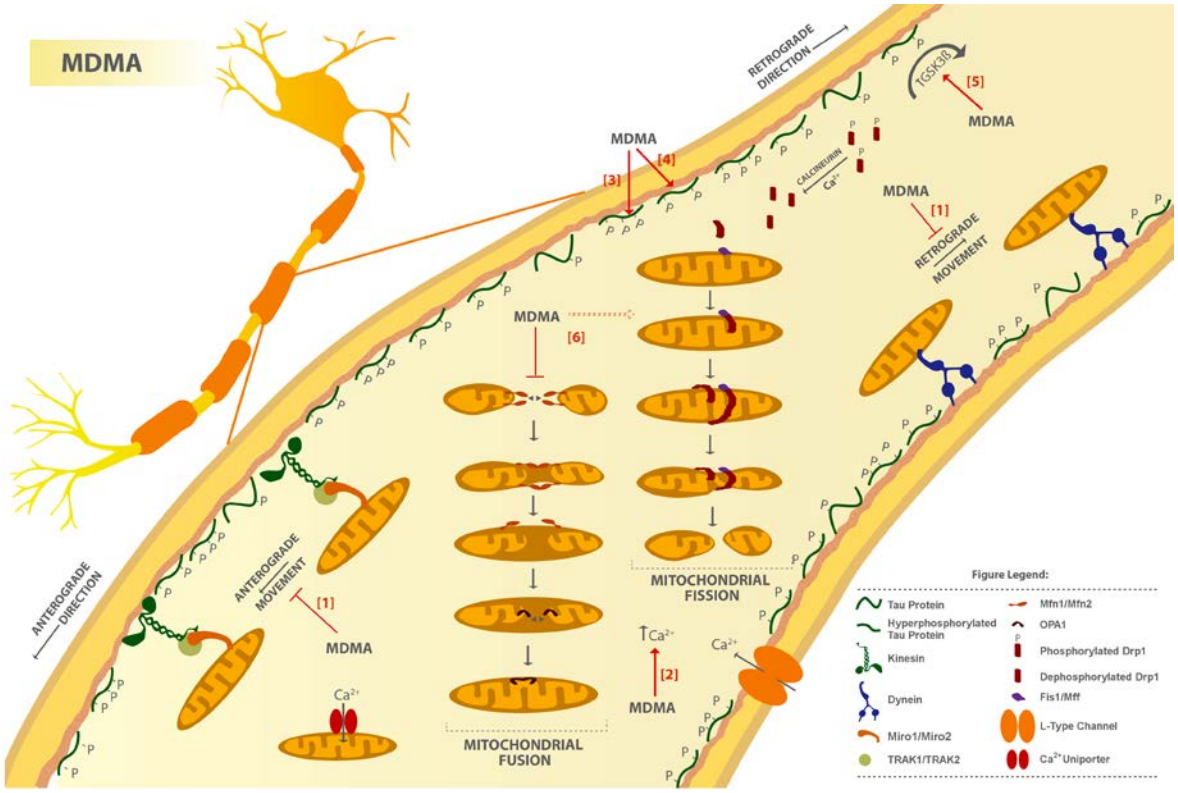


Figure 13. Postulated mechanisms for the mitochondrial trafficking impairment induced by MDMA in hippocampal neurons.
MDMA impairs axonal transport of mitochondria, in both anterograde and retrograde directions [1], though the velocity is only affected in anterograde direction. Intracellular Ca^{2+} raises, both in the cell body and neuronal extensions [2], are associated with the transport deficits induced by MDMA, though these effects most likely rely on Miro1-independent mechanisms [2]. Nevertheless, MDMA increases Tau phosphorylation in residue Threonine181 [3], which contributes partially to its effects on mitochondrial neuronal trafficking, most likely due to microtubules destabilization [4]. This increase in Tau phosphorylation promoted by MDMA appears to be mediated by glycogen synthase 3β (GSK3β) [5]. Furthermore, MDMA increases mitochondrial fragmentation. Over-expression of functional mitofusin 2 (Mfn2) or dynamin-related protein 1 (Drp1) K38A, a Drp1 construct that down-regulates mitochondrial fission, partially rescue the trafficking deficits elicited by MDMA. However over-expression of Mfn2 R94Q, a Charcot-Marie-Tooth neuropathy 2A (CMT2A) mutant protein with impaired fusion and transport properties, does not recover the MDMA´s mitochondrial phenotype, indicating that MDMA may alter mitochondrial fusion/fission mechanisms [6] and, thus, compromise mitochondrial transport.

Neurons, perhaps more than any other cell types, depend on mitochondrial trafficking for their survival. Thus, an incorrect distribution of mitochondria may be a critical problem for the correct neuronal functioning (Schwarz, 2013). By controlling organelle size and shape, mitochondrial fusion and fission also facilitate the efficient microtubule-mediated active transport of mitochondria into the long dendritic and axonal extensions of neurons (Jahani-Asl *et al.*, 2010; Qi *et al.*, 2012). Therefore, impaired mitochondrial transport may result in defective mitochondrial location at synaptic terminals, affecting the proper synaptic functionality and integrity (Li *et al.*, 2004; Verstreken *et al.*, 2005). Notably, the loss of serotonergic terminals in MDMA-administrated rats is by far the most studied neurotoxic event (Rudnick and Wall, 1992; Capela *et al.*, 2009). Nevertheless, long-term degenerative effects were also seen in other species, including non-human primates

(Ricaurte *et al.*, 1988b; Insel *et al.*, 1989). In addition, defective mitochondrial transport has been implicated in the pathogenesis of several neurodegenerative diseases (Calkins *et al.*, 2011; Shirendeb *et al.*, 2011; Exner *et al.*, 2012; Sheng and Cai, 2012; Shirendeb *et al.*, 2012; DuBoff *et al.*, 2013; Itoh *et al.*, 2013), which are also characterized by loss of neuronal tissue.

On the other hand, cell culture studies have demonstrated that excessive mitochondrial fragmentation play an active role in apoptosis (Frank *et al.*, 2001; Estaquier and Arnoult, 2007; Pereira *et al.*, 2010), autophagic cell death (Barsoum *et al.*, 2006; Twig *et al.*, 2008a; Twig *et al.*, 2008b) and necrosis (Wang *et al.*, 2012b; Zhou *et al.*, 2012). Impaired mitochondrial fragmentation triggered by some neurotoxicants, like rotenone or MPP^+, has been associated with cell death in neuronal cultures (Büeler, 2009; Wang *et al.*, 2011a; Qi *et al.*, 2012). Accordingly, a reduction in mitochondrial fission results in longer and more interconnected mitochondrial tubules, thus preventing the cell death (Barsoum *et al.*, 2006; Yuan *et al.*, 2007). Additionally, alterations in mitochondrial morphology affect functional interactions with the endoplasmic reticulum and trigger an altered mitochondrial function. Severe damage or the permanent failure of mitochondrial surveillance mechanisms, as it occurs in several neurodegenerative disorders, may ultimately result in a collapse of the mitochondrial network and neuronal death (Rugarli and Langer, 2012).

Therefore, the results presented in this thesis, indicating defective mitochondrial fusion/fission and trafficking along axonal processes of cultured hippocampal neurons, may add an important understanding about the real mechanisms involved in MDMA-induced degeneration of nerve terminals and neuronal death, though, clearly, much remains to be learned about this cascade of events.

Main Conclusions

III.2 Main Conclusions

The recognition of the mechanisms involved on the neuronal degeneration and death triggered by drugs of abuse are, clearly, of special interest. Despite the emerging number of data over the last years concerning the potential of MDMA to induce neuronal dysfunction, degeneration and loss, the mechanistic basis at molecular and cellular level are still not completely understood. The studies described in this thesis aimed to contribute to a better understanding of the role of metabolism, hyperthermia and monoamine neurotranmitters on MDMA's neurotoxicity, with special emphasis on mitochondrial-dependent pathways. Therefore, from the studies performed in the scope of this thesis, the following main conclusions may be taken:

► MDMA metabolites and monoamine neurotransmitters were more toxic than the parent compound MDMA to mouse brain synaptosomes, after short incubation periods (until 3h). The toxic effects involved H_2O_2 formation, in a concentration- and time-dependent manner, which was independent on mitochondrial pathways and partially rescued by antioxidants. MAO-mediated metabolism contributed to the H_2O_2 formation induced by monoamine neurotransmitters.

► The toxic effects induced by MDMA metabolites and monoamine neurotransmitters in mouse brain synaptosomes involved modifications on synaptosomal GSH turnover and increased lipid peroxidation, protein carbonylation and quinoproteins formation, though did not ensue in modifications on mitochondrial polarization status.

► MDMA metabolites and monoamine neurotransmitters induced an increase on the Na^+/K^+ ATPase activity in mouse brain synaptosomes, which is partially attenuated by NAC, supporting, therefore, a role for ROS-regulated pathways. This is the first report demonstrating a modulation of the Na^+/K^+ ATPase activity by MDMA metabolites.

► MDMA metabolites were more toxic than the parent compound MDMA to SH-SY5Y differentiated cells, after long periods of exposure of 24 or 48h. The catechol metabolites α-MeDA and N-Me-α-MeDA induced cell death in a concentration- and time-dependent manner, which was potentiated by hyperthermia. GSH and NAC monoconjugates of α-MeDA and N-Me-α-MeDA were more toxic than the catechol precursors and their toxicity, though concentration-dependent, was independent on the exposure time and differently modulated by hyperthermia. NAC protected against the toxicity of MDMA metabolites

► The concentration of MDMA metabolites in the cell culture medium decreased over time, an effect accelerated under hyperthermic conditions. In SH-SY5Y differentiated cells, MDMA metabolites were poorly accumulated in the intracellular compartment.

► The mixture of MDMA and its metabolites, at low micromolar concentrations, induced toxicity to SH-SY5Y differentiated cells, in a time- and temperature-dependent manner, an effect fully protected by the antioxidant NAC and accompanied by caspase 3 activation. As a mixture, MDMA and its metabolites present a different toxicity profile, compared to each compound alone, even at equimolar concentrations.

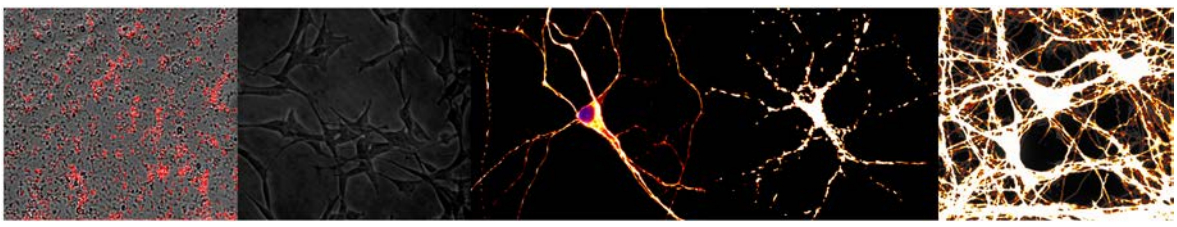
► The toxicity of the mixture of MDMA and its metabolites in SH-SY5Y differentiated cells involved increased ROS formation, *de novo* synthesis of GSH and increased intracellular free Ca^{2+} levels. Nevertheless, a DAT-mediated uptake mechanism did not seem to be involved on the toxic effects elicited by this mixture. This is the first study to demonstrate, *in vitro*, that MDMA and its metabolites, at a range of concentrations with high relevance to the *in vivo* scenario, may act in a combined manner in developing neurotoxicity.

► MDMA, as well as the mixture of MDMA and its metabolites, at non-cytotoxic concentrations, dramatically impaired mitochondrial trafficking along axonal processes of hippocampal neurons.

► MDMA-induced mitochondrial trafficking arrest was linked to an over time increase in intracellular Ca^{2+} levels, both in the cell body and neuronal extensions of hippocampal neurons, though the MDMA's mitochondrial trafficking phenotype relied on Miro1-independent mechanisms.

► MDMA-induced mitochondrial trafficking impairment was dependent on Tau protein, by a phosphorylation-dependent mechanism via GSK3β. The trafficking deficits triggered either by MDMA or by the mixture of MDMA and its metabolites were linked to increased mitochondrial fragmentation and largely depended on Mfn2 and Drp1 functions, thus supporting a role for fusion/fission events in MDMA- and mixture-regulated mitochondrial trafficking phenotype. These are the first studies to demonstrate that MDMA alters mitochondrial fusion/fission and trafficking in neurons, which may have considerable implications in MDMA-induced neuronal dysfunction, degeneration and neurotoxicity.

Chapter IV



References

IV.1 References

Abdollahi M, Karami-Mohajeri S (2012). A comprehensive review on experimental and clinical findings in intermediate syndrome caused by organophosphate poisoning. Toxicol Appl Pharmacol 258:309-314.

Adamaszek M, Khaw AV, Buck U, Andresen B, Thomasius R (2010). Evidence of neurotoxicity of ecstasy: sustained effects on electroencephalographic activity in polydrug users. PLoS ONE 5:e14097.

Adem A, Mattsson ME, Nordberg A, Påhlman S (1987). Muscarinic receptors in human SH-SY5Y neuroblastoma cell line: regulation by phorbol ester and retinoic acid-induced differentiation. Brain Res 430:235-242.

Adikes RC, Unrath WC, Yengo CM, Quintero OA (2013). Biochemical and bioinformatic analysis of the myosin-XIX motor domain. Cytoskeleton 70:281-295.

Agoston D, Hargittai P, Nagy A (1983). Effects of a 4-aminopyridine in calcium movements and changes of membrane potential in pinched-off nerve terminals from rat cerebral cortex. J Neurochem 41:745-751.

Aguirre P, Valdés P, Aracena-Parks P, Tapia V, Núñez MT (2007). Upregulation of γ-glutamate-cysteine ligase as part of the long-term adaptation process to iron accumulation in neuronal SH-SY5Y cells. Am J Physiol Cell Physiol 292:2197-2203.

Alami NH, Jung P, Brown A (2009). Myosin Va increases the efficiency of neurofilament transport by decreasing the duration of long-term pauses. J Neurosci 29:6625-6634.

Ali SF, Newport GD, Scallet AC, Binienda Z, Ferguson SA, Bailey JR, et al. (1993). Oral administration of 3,4-methylenedioxymethamphetamine (MDMA) produces selective serotonergic depletion in the nonhuman primate. Neurotoxicol Teratol 15:91-96.

Alves E, Binienda Z, Carvalho F, Alves CJ, Fernandes E, de Lourdes Bastos M, et al. (2009a). Acetyl-l-carnitine provides effective *in vivo* neuroprotection over 3,4-methylenedioximethamphetamine-induced mitochondrial neurotoxicity in the adolescent rat brain. Neuroscience 158:514-523.

Alves E, Summavielle T, Alves CJ, Custódio JB, Fernandes E, Lourdes Bastos M, et al. (2009b). Ecstasy-induced oxidative stress to adolescent rat brain mitochondria *in vivo*: influence of monoamine oxidase type A. Addict Biol 14:185-193.

Alves E, Summavielle T, Alves CJ, Gomes-da-Silva J, Barata JC, Fernandes E, et al. (2007). Monoamine oxidase-B mediates ecstasy-induced neurotoxic effects to adolescent rat brain mitochondria. J Neurosci 27:10203-10210.

Amacher DE, Schomaker SJ (1994). Effects of hexachlorophene on myelin marker enzymes in rat oligodendrocytes. Toxicol In Vitro 8:1-11.

Amato JL, Bankson MG, Yamamoto BK (2006). Prior exposure to chronic stress and MDMA potentiates mesoaccumbens dopamine release mediated by the 5-HT1B receptor. Neuropsychopharmacology 32:946-954.

Amiri M, Hollenbeck PJ (2008). Mitochondrial biogenesis in the axons of vertebrate peripheral neurons. Dev Neurobiol 68:1348-1361.

Armstrong BD, Noguchi KK (2004). The neurotoxic effects of 3,4-methylenedioxymethamphetamine (MDMA) and methamphetamine on serotonin, dopamine, and GABA-ergic terminals: an *in vitro* autoradiographic study in rats. Neurotoxicology 25:905-914.

Arrue A, Ruiz-Ortega JA, Ugedo L, Giralt MT (2003). Short-term effects of 3,4-methylenedioximethamphetamine on noradrenergic activity in locus coeruleus and hippocampus of the rat. Neurosci Lett 337:123-126.

Ashrafi G, Schwarz TL (2013). The pathways of mitophagy for quality control and clearance of mitochondria. Cell Death Differ 20:31-42.

Astashkina A, Mann B, Grainger DW (2012). A critical evaluation of *in vitro* cell culture models for high-throughput drug screening and toxicity. Pharmacol Ther 134:82-106.

Attwell D, Laughlin SB (2001). An energy budget for signaling in the grey matter of the brain. J Cereb Blood Flow Metab 21:1133-1145.

Bai F, Jones DC, Lau SS, Monks TJ (2001). Serotonergic neurotoxicity of 3,4-(±)-methylenedioxyamphetamine and 3,4-(±)-methylendioxymethamphetamine (ecstasy) is potentiated by inhibition of γ-glutamyl transpeptidase. Chem Res Toxicol 14:863-870.

Bai F, Lau SS, Monks TJ (1999). Glutathione and N-acetylcysteine conjugates of α-methyldopamine produce serotonergic neurotoxicity: possible role in methylenedioxyamphetamine-mediated neurotoxicity. Chem Res Toxicol 12:1150-1157.

Bains R, Moe MC, Vinje ML, Berg-Johnsen J (2009). Sevoflurane and propofol depolarize mitochondria in rat and human cerebrocortical synaptosomes by different mechanisms. Acta Anaesthesiol Scand 53:1354-1360.

Bajpai P, Sangar MC, Singh S, Tang W, Bansal S, Chowdhury G, et al. (2013). Metabolism of 1-methyl-4-phenyl-1,2,3,6-tetrahydropyridine by mitochondrion-targeted cytochrome P450 2D6: implications in Parkinson disease. J Biol Chem 288:4436-4451.

Bal-Price AK, Hogberg HT, Buzanska L, Coecke S (2010). Relevance of *in vitro* neurotoxicity testing for regulatory requirements: challenges to be considered. Neurotoxicol Teratol 32:36-41.

Bal-Price AK, Suñol C, Weiss DG, van Vliet E, Westerink RHS, Costa LG (2008). Application of *in vitro* neurotoxicity testing for regulatory purposes: symposium III summary and research needs. Neurotoxicology 29:520-531.

Ballatori N, Krance SM, Marchan R, Hammond CL (2009). Plasma membrane glutathione transporters and their roles in cell physiology and pathophysiology. Mol Aspects Med 30:13-28.

Baloh RH, Schmidt RE, Pestronk A, Milbrandt J (2007). Altered axonal mitochondrial transport in the pathogenesis of Charcot-Marie-Tooth disease from mitofusin 2 mutations. J Neurosci 27:422-430.

Banker G, Goslin K (1988). Developments in neuronal cell culture. Nature 336:185 - 186.

Banker G, Goslin K (1998). Types of nerve cell cultures: their advantages and limitations. In: Banker G and Goslin K (ed). Culturing Nerve Cells. Massachusetts Institute of Technology: Massachusetts, USA, pp 11-36.

Bankson MG, Yamamoto BK (2004). Serotonin–GABA interactions modulate MDMA-induced mesolimbic dopamine release. J Neurochem 91:852-859.

Baranowska-Bosiacka I, Strużyńska L, Gutowska I, Machalińska A, Kolasa A, Kłos P, et al. (2013). Perinatal exposure to lead induces morphological, ultrastructural and molecular alterations in the hippocampus. Toxicology 303:187-200.

Barsoum MJ, Yuan H, Gerencser AA, Liot G, Kushnareva Y, Gräber S, et al. (2006). Nitric oxide-induced mitochondrial fission is regulated by dynamin-related GTPases in neurons. EMBO J 25:3900-3911.

Baughman JM, Perocchi F, Girgis HS, Plovanich M, Belcher-Timme CA, Sancak Y, et al. (2011). Integrative genomics identifies MCU as an essential component of the mitochondrial calcium uniporter. Nature 476:341-345.

Baumann MH, Clark RD, Budzynski AG, Partilla JS, Blough BE, Rothman RB (2004). N-Substituted Piperazines Abused by Humans Mimic the Molecular Mechanism of 3,4-Methylenedioxymethamphetamine (MDMA, or /`Ecstasy/'). Neuropsychopharmacology 30:550-560.

Beitia G, Cobreros A, Sainz L, Cenarruzabeitia E (1999). 3,4-Methylenedioxymethamphetamine (ecstasy)-induced hepatotoxicity: effect on cytosolic calcium signals in isolated hepatocytes. Liver 19:234-241.

Benarroch EE (2011). Na^+, K^+-ATPase: functions in the nervous system and involvement in neurologic disease. Neurology 76:287-289.

Benda C (1898). Weitere Mitteilungen über die Mitochondria. Verh Dtsch Physiol Ges:376-383.

Bersier MG, Peña C, Rodríguez de Lores Arnaiz G (2011). Changes in Na^+, K^+-ATPase activity and alpha 3 subunit expression in CNS after administration of Na^+, K^+-ATPase inhibitors. Neurochem Res 36:297-303.

Bexis S, Docherty JR (2009). Role of α1- and β3-adrenoceptors in the modulation by SR59230A of the effects of MDMA on body temperature in the mouse. Br J Pharmacol 158:259-266.

Biedler JL, Helson L, Spengler BA (1973). Morphology and growth, tumorigenicity, and cytogenetics of human neuroblastoma cells in continuous culture. Cancer Res 33:2643-2652.

Biedler JL, Roffler-Tarlov S, Schachner M, Freedman LS (1978). Multiple neurotransmitter synthesis by human neuroblastoma cell lines and clones. Cancer Res 38:3751-3757.

Billups B, Forsythe ID (2002). Presynaptic mitochondrial calcium sequestration influences transmission at mammalian central synapses. J Neurosci 22:5840-5847.

Blessing WW, Seaman B (2003). 5-hydroxytryptamine2A receptors regulate sympathetic nerves constricting the cutaneous vascular bed in rabbits and rats. Neuroscience 117:939-948.

Blessing WW, Seaman B, Pedersen NP, Ootsuka Y (2003). Clozapine reverses hyperthermia and sympathetically mediated cutaneous vasoconstriction induced by 3,4-methylenedioxymethamphetamine (ecstasy) in rabbits and rats. J Neurosci 23:6385-6391.

Bolla KI, McCann UD, Ricaurte GA (1998). Memory impairment in abstinent MDMA ("Ecstasy") users. Neurology 51:1532-1537.

Breier JM, Bankson MG, Yamamoto BK (2006). L-Tyrosine contributes to (+)-3,4-methylenedioxymethamphetamine-induced serotonin depletions. J Neurosci 26:290-299.

Breier JM, Gassmann K, Kayser R, Stegeman H, De Groot D, Fritsche E, et al. (2010). Neural progenitor cells as models for high-throughput screens of developmental neurotoxicity: state of the science. Neurotoxicol Teratol 32:4-15.

Brickley K, Pozo K, Stephenson FA (2011). N-acetylglucosamine transferase is an integral component of a kinesin-directed mitochondrial trafficking complex. Biochim Biophys Acta 1813:269-281.

Brickley K, Smith MJ, Beck M, Stephenson FA (2005). GRIF-1 and OIP106, members of a novel gene family of coiled-coil domain proteins: association *in vivo* and *in vitro* with kinesin. J Biol Chem 280:14723-14732.

Brickley K, Stephenson FA (2011). Trafficking kinesin protein (TRAK)-mediated transport of mitochondria in axons of hippocampal neurons. J Biol Chem 286:18079-18092.

Broening HW, Bowyer JF, Slikker WJ (1995). Age-dependent sensitivity of rats to the long-term effects of the serotonergic neurotoxicant (+/-)-3,4-methylenedioxymethamphetamine (MDMA) correlates with the magnitude of the MDMA-induced thermal response. J Pharmacol Exp Ther 275:325-333.

Bruinink A, Reiser P, Müller M, Gähwiler BH, Zbinden G (1992). Neurotoxic effects of bismuth *in vitro*. Toxicol In Vitro 6:285-293.

Büeler H (2009). Impaired mitochondrial dynamics and function in the pathogenesis of Parkinson's disease. Exp Neurol 218:235-246.

Burke WJ, Li SW, Williams EA, Nonneman R, Zahm DS (2003). 3,4-Dihydroxyphenylacetaldehyde is the toxic dopamine metabolite *in vivo*: implications for Parkinson's disease pathogenesis. Brain Res 989:205-213.

Busceti CL, Biagioni F, Riozzi B, Battaglia G, Storto M, Cinque C, et al. (2008). Enhanced tau phosphorylation in the hippocampus of mice treated with 3,4-methylenedioxymethamphetamine ("ecstasy"). J Neurosci 28:3234-3245.

Büttner A (2011). The neuropathology of drug abuse. Neuropathol Appl Neurobiol 37:118-134.

Cadet JL, Thiriet N, Jayanthi S (2001). Involvement of free radicals in MDMA-induced neurotoxicity in mice. Ann Med Interne 152:57-59.

Cadoni C, Solinas M, Pisanu A, Zernig G, Acquas E, Di Chiara G (2005). Effect of 3,4-methylendioxymethamphetamine (MDMA, “ecstasy”) on dopamine transmission in the nucleus accumbens shell and core. Brain Res 1055:143-148.

Cai Q, Gerwin C, Sheng ZH (2005). Syntabulin-mediated anterograde transport of mitochondria along neuronal processes. J Cell Biol 170:959-969.

Cai Q, Lu L, Tian JH, Zhu YB, Qiao H, Sheng ZH (2010). Snapin-regulated late endosomal transport is critical for efficient autophagy-lysosomal function in neurons. Neuron 68:73-86.

Calkins MJ, Manczak M, Mao P, Shirendeb U, Reddy PH (2011). Impaired mitochondrial biogenesis, defective axonal transport of mitochondria, abnormal mitochondrial dynamics and synaptic degeneration in a mouse model of Alzheimer's disease. Hum Mol Genet 20:4515-4529.

Camarasa J, Pubill D, Escubedo E (2006). Association of caffeine to MDMA does not increase antinociception but potentiates adverse effects of this recreational drug. Brain Res 1111:72-82.

Camarero J, Sanchez V, O'Shea E, Green AR, Colado MI (2002). Studies, using *in vivo* microdialysis, on the effect of the dopamine uptake inhibitor GBR 12909 on 3,4-methylenedioxymethamphetamine (‘ecstasy’)-induced dopamine release and free radical formation in the mouse striatum. J Neurochem 81:961-972.

Capela JP, Carmo H, Remião F, Bastos ML, Meisel A, Carvalho F (2009). Molecular and cellular mechanisms of ecstasy-induced neurotoxicity: an overview. Mol Neurobiol 39:210-271.

Capela JP, da Costa Araújo S, Costa VM, Ruscher K, Fernandes E, Bastos ML, et al. (2013). The neurotoxicity of hallucinogenic amphetamines in primary cultures of hippocampal neurons. NeuroToxicology 34:254-263.

Capela JP, Fernandes E, Remiao F, Bastos ML, Meisel A, Carvalho F (2007a). Ecstasy induces apoptosis via 5-HT_{2A}-receptor stimulation in cortical neurons. Neurotoxicology 28:868-875.

Capela JP, Macedo C, Branco PS, Ferreira LM, Lobo AM, Fernandes E, et al. (2007b). Neurotoxicity mechanisms of thioether ecstasy metabolites. Neuroscience 146:1743-1757.

Capela JP, Meisel A, Abreu AR, Branco PS, Ferreira LM, Lobo AM, et al. (2006a). Neurotoxicity of ecstasy metabolites in rat cortical neurons, and influence of hyperthermia. J Pharmacol Exp Ther 316:53-61.

Capela JP, Ruscher K, Lautenschlager M, Freyer D, Dirnagl U, Gaio AR, et al. (2006b). Ecstasy-induced cell death in cortical neuronal cultures is serotonin 2A-receptor-dependent and potentiated under hyperthermia. Neuroscience 139:1069-1081.

Carvalho M, Carmo H, Costa VM, Capela JP, Pontes H, Remião F, et al. (2012). Toxicity of amphetamines: an update. Archives of Toxicology 86:1167-1231.

Carvalho M, Carvalho F, Bastos ML (2001). Is hyperthermia the triggering factor for hepatotoxicity induced by 3,4-methylenedioxymethamphetamine (ecstasy)? An *in vitro* study using freshly isolated mouse hepatocytes. Arch Toxicol 74:789-793.

Carvalho M, Milhazes N, Remiao F, Borges F, Fernandes E, Amado F, et al. (2004a). Hepatotoxicity of 3,4-methylenedioxyamphetamine and alpha-methyldopamine in isolated rat hepatocytes: formation of glutathione conjugates. Arch Toxicol 78:16-24.

Carvalho M, Remiao F, Milhazes N, Borges F, Fernandes E, Carvalho F, et al. (2004b). The toxicity of N-methyl-alpha-methyldopamine to freshly isolated rat hepatocytes is prevented by ascorbic acid and N-acetylcysteine. Toxicology 200:193-203.

Carvalho M, Remião F, Milhazes N, Borges F, Fernandes E, Monteiro MC, et al. (2004c). Metabolism is required for the expression of ecstasy-induced cardiotoxicity *in vitro*. Chem Res Toxicol 17:623-632.

Cassarino DS, Parks JK, Parker Jr WD, Bennett Jr JP (1999). The parkinsonian neurotoxin MPP^+ opens the mitochondrial permeability transition pore and releases cytochrome c in isolated mitochondria via an oxidative mechanism. Biochim Biophys Acta 1453:49-62.

Ceccatelli S, Bose R, Edoff K, Onishchenko N, Spulber S (2013). Long-lasting neurotoxic effects of exposure to methylmercury during development. J Intern Med 273:490-497.

Cecchi C, Pensalfini A, Liguri G, Baglioni S, Fiorillo C, Guadagna S, et al. (2008). Differentiation increases the resistance of neuronal cells to amyloid toxicity. Neurochem Res 33:2516-2531.

Cereghetti GM, Stangherlin A, de Brito OM, Chang CR, Blackstone C, Bernardi P, et al. (2008). Dephosphorylation by calcineurin regulates translocation of Drp1 to mitochondria. Proc Natl Acad Sci U S A 105:15803-15808.

Cernaianu G, Brandmaier P, Scholz G, Ackermann OP, Alt R, Rothe K, et al. (2008). All-trans retinoic acid arrests neuroblastoma cells in a dormant state. Subsequent nerve growth factor/brain-derived neurotrophic factor treatment adds modest benefit. J Pediatr Surg 43:1284-1294.

Chada SR, Hollenbeck PJ (2004). Nerve growth factor signaling regulates motility and docking of axonal mitochondria. Curr Biol 14:1272-1276.

Chadwick IS, Curry PD, Linsley A, Freemont AJ, Doran B (2001). Ecstasy, 3-4 methylenedioxymethamphetamine (MDMA), a fatality associated with coagulopathy and hyperthermia. J R Soc Med 84:371.

Chan DC (2006). Mitochondria: dynamic organelles in disease, aging, and development. Cell 125:1241-1252.

Chan NC, Salazar AM, Pham AH, Sweredoski MJ, Kolawa NJ, Graham RLJ, et al. (2011). Broad activation of the ubiquitin–proteasome system by Parkin is critical for mitophagy. Hum Mol Genet 20:1726-1737.

Chang CR, Blackstone C (2010). Dynamic regulation of mitochondrial fission through modification of the dynamin-related protein Drp1. Ann N Y Acad Sci 1201:34-39.

Chang DTW, Honick AS, Reynolds IJ (2006). Mitochondrial trafficking to synapses in cultured primary cortical neurons. J Neurosci 26:7035-7045.

Chang KT, Niescier RF, Min KT (2011). Mitochondrial matrix Ca^{2+} as an intrinsic signal regulating mitochondrial motility in axons. Proc Natl Acad Sci U S A 108:15456-15461.

Chang Y, Wang S (2010). Hypericin, the active component of St. John's wort, inhibits glutamate release in the rat cerebrocortical synaptosomes via a mitogen-activated protein kinase-dependent pathway. Eur J Pharmacol 634:53-61.

Chen H, Detmer SA, Ewald AJ, Griffin EE, Fraser SE, Chan DC (2003). Mitofusins Mfn1 and Mfn2 coordinately regulate mitochondrial fusion and are essential for embryonic development. J Cell Biol 160:189-200.

Chen H, McCaffery JM, Chan DC (2007a). Mitochondrial fusion protects against neurodegeneration in the cerebellum. Cell 130:548-562.

Chen H, Murray J, Kornberg B, Dethloff L, Rock D, Nikam S, et al. (2006). Metabolism-dependent mutagenicity of a compound containing a piperazinyl indazole motif: role of a novel P450-mediated metabolic reaction involving a putative oxaziridine intermediate. Chem Res Toxicol 19:1341-1350.

Chen JX, Sun YJ, Wang P, Long DX, Li W, Li L, et al. (2013). Induction of autophagy by TOCP in differentiated human neuroblastoma cells lead to degradation of cytoskeletal components and inhibition of neurite outgrowth. Toxicology 310:92-97.

Chen S, Owens GC, Crossin KL, Edelman DB (2007b). Serotonin stimulates mitochondrial transport in hippocampal neurons. Mol Cell Neurosci 36:472-483.

Chen S, Owens GC, Edelman DB (2008). Dopamine inhibits mitochondrial motility in hippocampal neurons. PLoS ONE 3:e2804.

Chen S, Owens GC, Makarenkova H, Edelman DB (2010). HDAC6 regulates mitochondrial transport in hippocampal neurons. PLoS ONE 5:e10848.

Chen T, Yang W, Li Y, Chen X, Xu S (2011). Mono-(2-ethylhexyl) phthalate impairs neurodevelopment: Inhibition of proliferation and promotion of differentiation in PC12 cells. Toxicol Lett 201:34-41.

Cheung Y, Lau WK, Yu M, Lai CS, Yeung S, So K, et al. (2009). Effects of all-trans-retinoic acid on human SH-SY5Y neuroblastoma as in vitro model in neurotoxicity research. Neurotoxicology 30:127-135.

Chinopoulos C, Adam-Vizi V (2001). Mitochondria deficient in complex I activity are depolarized by hydrogen peroxide in nerve terminals: relevance to Parkinson's disease. J Neurochem 76:302-306.

Chipana C, Camarasa J, Pubill D, Escubedo E (2006). Protection against MDMA-induced dopaminergic neurotoxicity in mice by methyllycaconitine: Involvement of nicotinic receptors. Neuropharmacology 51:885-895.

Chipana C, Camarasa J, Pubill D, Escubedo E (2008a). Memantine prevents MDMA-induced neurotoxicity. NeuroToxicology 29:179-183.

Chipana C, García-Ratés S, Camarasa J, Pubill D, Escubedo E (2008b). Different oxidative profile and nicotinic receptor interaction of amphetamine and 3,4-methylenedioxy-methamphetamine. Neurochem Int 52:401-410.

Cho K, Cai Y, Yi H, Yeh A, Aslanukov A, Ferreira PA (2007). Association of the kinesin-binding domain of RanBP2 to KIF5B and KIF5C determines mitochondria localization and function. Traffic 8:1722-1735.

Cho KI, Yi H, Desai R, Hand AR, Haas AL, Ferreira PA (2009). RANBP2 is an allosteric activator of the conventional kinesin-1 motor protein, KIF5B, in a minimal cell-free system. EMBO Rep 10:480-486.

Choi SW, Gerencser AA, Nicholls DG (2009). Bioenergetic analysis of isolated cerebrocortical nerve terminals on a microgram scale: spare respiratory capacity and stochastic mitochondrial failure. J Neurochem 109:1179-1191.

Choi YJ, Park JS, Lee SH (2013). Size-controllable networked neurospheres as a 3D neuronal tissue model for Alzheimer's disease studies. Biomaterials 34:2938-2946.

Chu T, Kumagai Y, DiStefano EW, Cho AK (1996). Disposition of methylenedioxymethamphetamine and three metabolites in the brains of different rat strains and their possible roles in acute serotonin depletion. Biochem Pharmacol 51:789-796.

Ciccarone V, Spengler BA, Meyers MB, Biedler JL, Ross RA (1989). Phenotypic diversification in human neuroblastoma cells: expression of distinct neural crest lineages. Cancer Res 49:219-225.

Cipolat S, Martins de Brito O, Dal Zilio B, Scorrano L (2004). OPA1 requires mitofusin 1 to promote mitochondrial fusion. Proc Natl Acad Sci U S A 101:15927-15932.

Cipolat S, Rudka T, Hartmann D, Costa V, Serneels L, Craessaerts K, et al. (2006). Mitochondrial rhomboid PARL regulates cytochrome c release during apoptosis via OPA1-dependent cristae remodeling. Cell 126:163-175.

Clapcote SJ, Duffy S, Xie G, Kirshenbaum G, Bechard AR, Schack VR, et al. (2009). Mutation I810N in the α3 isoform of Na^+,K^+-ATPase causes impairments in the sodium pump and hyperexcitability in the CNS. Proc Natl Acad Sci U S A 106:14085-14090.

Clayton KB, Podlesniy P, Figueiro-Silva J, López-Doménech G, Benitez L, Enguita M, et al. (2012). NP1 regulates neuronal activity-dependent accumulation of BAX in mitochondria and mitochondrial dynamics. J Neurosci 32:1453-1466.

Coecke S, Eskes C, Gartlon J, Kinsner A, Price A, van Vliet E, et al. (2006). The value of alternative testing for neurotoxicity in the context of regulatory needs. Environ Toxicol Pharmacol 21:153-167.

Colado MI, Camarero J, Mechan AO, Sanchez V, Esteban B, Elliott JM, et al. (2001). A study of the mechanisms involved in the neurotoxic action of 3,4-methylenedioxymethamphetamine (MDMA, 'ecstasy') on dopamine neurones in mouse brain. Br J Pharmacol 134:1711-1723.

Colado MI, Granados R, O'Shea E, Esteban B, Green AR (1998). Role of hyperthermia in the protective action of clomethiazole against MDMA ('ecstasy')-induced neurodegeneration, comparison with the novel NMDA channel blocker AR-R15896AR. Br J Pharmacol 124:479-484.

Colado MI, O'Shea E, Granados R, Murray TK, Green AR (1997). *In vivo* evidence for free radical involvement in the degeneration of rat brain 5-HT following administration of MDMA ("ecstasy") and p-chloroamphetamine but not the degeneration following fenfluramine. Br J Pharmacol 121:889-900.

Colado MI, O'Shea E, Esteban B, Granados R, Green AR (1999). *In vivo* evidence against clomethiazole being neuroprotective against MDMA ('ecstasy')-induced degeneration of rat brain 5-HT nerve terminals by a free radical scavenging mechanism. Neuropharmacology 38:307-314.

Colado MI, T K Murray TK, Green AG (1993). 5-HT loss in rat brain following 3,4 methylenedioxymethamphetamine (MDMA), p-chloroamphetamine and fenfluramine administration and effects of chlormethiazole and dizocilpine. Br J Pharmacol 108:583-589.

Colle D, Santos DB, Hartwig JM, Godoi M, Braga AL, Farina M (2013). Succinobucol versus probucol: higher efficiency of succinobucol in mitigating 3-NP-induced brain mitochondrial dysfunction and oxidative stress *in vitro*. Mitochondrion 13:125-133.

Commins DL, Vosmer G, Virus RM, Woolverton WL, Schuster CR, Seiden LS (1987). Biochemical and histological evidence that methylenedioxymethylamphetamine (MDMA) is toxic to neurons in the rat brain. J Pharmacol Exp Ther 241:338-345.

Cooper MJ, Hutchins GM, Cohen PS, Helman LJ, Mennie RJ, Israel MA (1990). Human neuroblastoma tumor cell lines correspond to the arrested differentiation of chromaffin adrenal medullary neuroblasts. Cell Growth Differ 1:149-159.

Costa LG (1988). Interactions of neurotoxicants with neurotransmitter systems. Toxicology 49:359-366.

Costa LG (1998a). Neurotoxicity testing: a discussion of *in vitro* alternatives. Environ Health Perspect 106 505-510.

Costa LG (1998b). Signal transduction in environmental neurotoxicity. Annu Rev Pharmacol Toxicol 38:21-43.

Costa LG, Fattori V, Giordano G, Vitalone A (2007). An *in vitro* approach to assess the toxicity of certain food contaminants: methylmercury and polychlorinated biphenyls. Toxicology 237:65-76.

Costa LG, Giordano G, Guizetti M (2011a). *In vitro* approaches to developmental neurotoxicity. In: Gupta RC (ed). Reproductive and developmental toxicology. Academic Press: San Diego, CA, USA, pp 159-166.

Costa LG, Giordano G, Guizzetti M (2011b). Predictive models for neurotoxicity assessment. In: Xu JJ and Urban L (ed). Predictive toxicology in drug safety. Cambridge University Press: New York, USA, pp 135-152.

Council NR (2012) *The future of animals, cells, models, and systems in research, development, education, and testing; Proceedings of a symposium*. Washington D C, USA: National Academy of Sciences.

Cowan RL, Lyoo IK, Sung SM, Ahn KH, Kim MJ, Hwang J, et al. (2003). Reduced cortical gray matter density in human MDMA (Ecstasy) users: a voxel-based morphometry study. Drug Alcohol Depend 72:225-235.

Crean RD, Davis SA, Von Huben SN, Lay CC, Katner SN, Taffe MA (2006). Effects of (±)3,4-methylenedioxymethamphetamine, (±)3,4-methylenedioxyamphetamine and methamphetamine on temperature and activity in rhesus macaques. Neuroscience 142:515-525.

Crespi D, Mennini T, Gobbi M (1997). Carrier-dependent and Ca^{2+}-dependent 5-HT and dopamine release induced by (+)-amphetamine, 3,4-methylendioxy-methamphetamine, p-chloroamphetamine and (+)-fenfluramine. Br J Pharmacol 121:1735-1743.

Culbreth ME, Harrill JA, Freudenrich TM, Mundy WR, Shafer TJ (2012). Comparison of chemical-induced changes in proliferation and apoptosis in human and mouse neuroprogenitor cells. Neurotoxicology 33:1499-1510.

Cunha-Oliveira T, Rego AC, Cardoso SM, Borges F, Swerdlow RH, Macedo T, et al. (2006). Mitochondrial dysfunction and caspase activation in rat cortical neurons treated with cocaine or amphetamine. Brain Res 1089:44-54.

Custódio JBA, Santos MS, Gonçalves DIR, Moreno AJM, Fernandes E, Bastos ML, et al. (2010). Comparative effects of 3,4-methylenedioxymethamphetamine and 4-methylthioamphetamine on rat liver mitochondrial function. Toxicology 270:99-105.

d'Ydewalle C, Krishnan J, Chiheb DM, Van Damme P, Irobi J, Kozikowski AP, et al. (2011). HDAC6 inhibitors reverse axonal loss in a mouse model of mutant HSPB1-induced Charcot-Marie-Tooth disease. Nat Med 17:968-974.

Dafters RI, Lynch E (1998). Persistent loss of thermoregulation in the rat induced by 3,4-methylenedioxymethamphetamine (MDMA or "Ecstasy") but not by fenfluramine. Psychopharmacology 138:207-212.

Daneman R (2012). The blood–brain barrier in health and disease. Ann Neurol 72:648-672.

Danial NN, Korsmeyer SJ (2004). Cell death: critical control points. Cell 116:205-219.

Darios F, Muriel MP, Khondiker ME, Brice A, Ruberg M (2005). Neurotoxic calcium transfer from endoplasmic reticulum to mitochondria is regulated by cyclin-dependent kinase 5-dependent phosphorylation of tau. J Neurosci 25:4159-4168.

Datki Z, Juhász A, Gálfi M, Soós K, Papp R, Zádori D, et al. (2003). Method for measuring neurotoxicity of aggregating polypeptides with the MTT assay on differentiated neuroblastoma cells. Brain Res Bull 62:223-229.

de Groot MWGDM, Westerink RHS, Dingemans MML (2013). Don't judge a neuron only by its cover: neuronal function in *in vitro* developmental neurotoxicity testing. Toxicol Sci 132:1-7.

de la Torre R, Farré M (2004). Neurotoxicity of MDMA (ecstasy): the limitations of scaling from animals to humans. Trends Pharmacol Sci 25:505-508.

de la Torre R, Puerta E, Aguirre N (2009). Comment on the letter by Green, Gabrielsson, Marsden, and Fone, MDMA: on the translation from rodent to human dosing. Psychopharmacology 204:379-380.

De Robertis E, Pellegrino de Iraldi A, Rodriguez de Lores Garnaiz G, Salganicoff F (1962). Cholinergic and non-cholinergic nerve endings in rat brain. I. Isolation and subcellular distribution of acetylcholine and acetylcholinesterase. J Neurochem 9:23-35.

De Stefani D, Raffaello A, Teardo E, Szabò I, Rizzuto R (2011). A forty-kilodalton protein of the inner membrane is the mitochondrial calcium uniporter. Nature 476:336-340.

De Vries GH, Boullerne AI (2010). Glial cell lines: an overview. Neurochem Res 35:1978-2000.

Deheshi S, Pasqualotto BA, Rintoul GL (2013). Mitochondrial trafficking in neuropsychiatric diseases. Neurobiol Dis 51:66-71.

del Amo EM, Urtti A, Yliperttula M (2008). Pharmacokinetic role of L-type amino acid transporters LAT1 and LAT2. Eur J Pharm Sci 35:161-174.

Delettre C, Lenaers G, Griffoin JM, Gigarel N, Lorenzo C, Belenguer P, et al. (2000). Nuclear gene OPA1, encoding a mitochondrial dynamin-related protein, is mutated in dominant optic atrophy. Nat Genet 26:207-210.

Detmer SA, Chan DC (2007). Complementation between mouse Mfn1 and Mfn2 protects mitochondrial fusion defects caused by CMT2A disease mutations. J Cell Biol 176:405-414.

Di Iorio CR, Watkins TJ, Dietrich MS, Cao A, Blackford JU, Rogers B, et al. (2012). EVidence for chronically altered serotonin function in the cerebral cortex of female 3,4-methylenedioxymethamphetamine polydrug users. Arch Gen Psychiatry 69:399-409.

Ding H, Dolan PJ, Johnson GVW (2008). Histone deacetylase 6 interacts with the microtubule-associated protein tau. J Neurochem 106:2119-2130.

Dompierre JP, Godin JD, Charrin BC, Cordelières FP, King SJ, Humbert S, et al. (2007). Histone deacetylase 6 inhibition compensates for the transport deficit in Huntington's disease by increasing tubulin acetylation. J Neurosci 27:3571-3583.

Dubey M, Chaudhury P, Kabiru H, Shea TB (2008). Tau inhibits anterograde axonal transport and perturbs stability in growing axonal neurites in part by displacing kinesin cargo: Neurofilaments attenuate tau-mediated neurite instability. Cell Motil Cytoskeleton 65:89-99.

DuBoff B, Feany M, Götz J (2013). Why size matters – balancing mitochondrial dynamics in Alzheimer's disease. Trends Neurosci 36:325-335.

Dunkley PR, Heath JW, Harrison SM, Jarvie PE, Glenfield PJ, Rostas JAP (1988). A rapid Percoll gradient procedure for isolation of synaptosomes directly from an S1 fraction: homogeneity and morphology of subcellular fractions. Brain Res 441:59-71.

Dunkley PR, Jarvie PE, Heath JW, Kidd GJ, Rostas JAP (1986). A rapid method for isolation of synaptosomes on Percoll gradients. Brain Res 372:115-129.

Dunkley PR, Jarvie PE, Robinson PJ (2008). A rapid Percoll gradient procedure for preparation of synaptosomes. Nat Protoc 3:1718-1728.

Easton N, Fry J, O'Shea E, Watkins A, Kingston S, Marsden CA (2003). Synthesis, *in vitro* formation, and behavioural effects of glutathione regioisomers of alpha-methyldopamine with relevance to MDA and MDMA (ecstasy). Brain Res 987:144-154.

Easton N, Marsden CA (2006). Ecstasy: are animal data consistent between species and can they translate to humans? J Psychopharmacol 20:194-210.

Ebneth A, Godemann R, Stamer K, Illenberger S, Trinczek B, Mandelkow E-M, et al. (1998). Overexpression of Tau protein inhibits kinesin-dependent trafficking of vesicles, mitochondria, and endoplasmic reticulum: implications for Alzheimer's disease. J Cell Biol 143:777-794.

Edsjö A, Lavenius E, Nilsson H, Hoehner JC, Simonsson P, Culp LA, et al. (2003). Expression of trkB in human neuroblastoma in relation to MYCN expression and retinoic acid treatment. Lab Invest 83:813-823.

Ehses S, Raschke I, Mancuso G, Bernacchia A, Geimer S, Tondera D, et al. (2009). Regulation of OPA1 processing and mitochondrial fusion by m-AAA protease isoenzymes and OMA1. J Cell Biol 187:1023-1036.

Elinos-Calderón D, Robledo-Arratia Y, Pérez-De La Cruz V, Maldonado PD, Galván-Arzate S, Pedraza-Chaverrí J, et al. (2010). Antioxidant strategy to rescue synaptosomes from oxidative damage and energy failure in neurotoxic models in rats: protective role of S-allylcysteine. J Neural Transm 117:35-44.

Elmariah SB, Hughes EG, Oh EJ, Balice-Gordon RJ (2005). Neurotrophin signaling among neurons and glia during formation of tripartite synapses. Neuron Glia Biol 1:1-11.

Epp JR, Chow C, A. GL (2013). Hippocampus-dependent learning influences hippocampal neurogenesis. Front Neurosci 7:57.

Erecinska M, Nelson D, Silver IA (1996). Metabolic and energetic properties of isolated nerve ending particles (synaptosomes). Biochim Biophys Acta 1277:13-34.

Erives GV, Lau SS, Monks TJ (2008). Accumulation of neurotoxic thioether metabolites of 3,4-(±)-methylenedioxymethamphetamine in rat brain. J Pharmacol Exp Ther 324:284-291.

Erkekoglu P, Baydar T (2013). Acrylamide neurotoxicity. Nutr Neurosci.

Escobedo I, O'Shea E, Orio L, Sanchez V, Segura M, de la Torre R, et al. (2005). A comparative study on the acute and long-term effects of MDMA and 3,4-dihydroxymethamphetamine (HHMA) on brain monoamine levels after i.p. or striatal administration in mice. Br J Pharmacol 144:231-241.

Escubedo E, Abad S, Torres I, Camarasa J, Pubill D (2011). Comparative neurochemical profile of 3,4-methylenedioxymethamphetamine and its metabolite alpha-methyldopamine on key targets of MDMA neurotoxicity. Neurochem Int 58:92-101.

Estaquier J, Arnoult D (2007). Inhibiting Drp1-mediated mitochondrial fission selectively prevents the release of cytochrome c during apoptosis. Cell Death Differ 14:1086-1094.

Esteban B, O'Shea E, Camarero J, Sanchez V, Green AR, Colado MI (2001). 3,4-Methylenedioxymethamphetamine induces monoamine release, but not toxicity, when administered centrally at a concentration occurring following a peripherally injected neurotoxic dose. Psychopharmacology 154:251-260.

Exner N, Lutz AK, Haass C, Winklhofer KF (2012). Mitochondrial dysfunction in Parkinson's disease: molecular mechanisms and pathophysiological consequences. EMBO J 31:3038-3062.

Falk EM, Cook VJ, Nichols DE, Sprague JE (2002). An antisense oligonucleotide targeted at MAO-B attenuates rat striatal serotonergic neurotoxicity induced by MDMA. Pharmacol Biochem Behav 72:617-622.

Fang C, Bourdette D, Banker G (2012). Oxidative stress inhibits axonal transport: implications for neurodegenerative diseases. Mol Neurodegener 7:29.

Farfel GM, Seiden LS (1995). Role of hypothermia in the mechanism of protection against serotonergic toxicity. Experiments using 3,4-methylenedioxymethamphetamine, dizocilpine, CGS 19755 and NBQX. J Pharmacol Exp Ther 272:860-867.

Farfel GM, Vosmer GL, Seiden LS (1992). The N-methyl-d-aspartate antagonist MK-801 protects against serotonin depletions induced by methamphetamine, 3,4-methylenedioxymethamphetamine and p-chloroamphetamine. Brain Res 595:121-127.

Farré M, Abanades S, Roset PN, Peiró AM, Torrens M, O'Mathúna B, et al. (2007). Pharmacological interaction between 3,4-methylenedioxymethamphetamine (ecstasy) and paroxetine: pharmacological effects and pharmacokinetics. J Pharmacol Exp Ther 323:954-962.

Fath T, Ke YD, Gunning P, Götz J, Ittner LM (2009). Primary support cultures of hippocampal and substantia nigra neurons. Nat Protoc 4:78-85.

Feldman RG, White RF, Eriator II (1993). Trimethyltin encephalopathy. Arch Neurol 50:1320-1324.

Felim A, Herrera G, Neudörffer A, Blanco M, O'Connor J, Largeron M (2009). Synthesis and *in vitro* cytotoxicity profile of the R-enantiomer of 3,4-dihydroxymethamphetamine (R-(−)-HHMA): comparison with related catecholamines. Chem Res Toxicol 23:211-219.

Ferguson CS, Tyndale RF (2011). Cytochrome P450 enzymes in the brain: emerging evidence of biological significance. Trends Pharmacol Sci 32:708-714.

Fernàndez-Castillo N, Orejarena MJ, Ribasés M, Blanco E, Casas M, Robledo P, et al. (2012). Active and passive MDMA ('ecstasy') intake induces differential transcriptional changes in the mouse brain. Genes Brain Behav 11:38-51.

Ferreira PS, Nogueira TB, Costa VM, Branco PS, Ferreira LM, Fernandes E, et al. (2013). Neurotoxicity of “ecstasy” and its metabolites in human dopaminergic differentiated SH-SY5Y cells. Toxicol Lett 216:159-170.

Fiege M, Wappler F, Weisshorn R, Gerbershagen MU, Menge M, Schulte Esch J (2003). Induction of malignant hyperthermia in susceptible swine by 3,4-methylenedioxymethamphetamine (“ecstasy”). Anesthesiology 99:1132-1136.

Fischer C, Hatzidimitriou G, Wlos J, Katz J, Ricaurte G (1995). Reorganization of ascending 5-HT axon projections in animals previously exposed to the recreational drug (+/-)3,4-methylenedioxymethamphetamine (MDMA, "ecstasy"). J Neurosci 15:5476-5485.

Flaskos J (2012). The developmental neurotoxicity of organophosphorus insecticides: A direct role for the oxon metabolites. Toxicol Lett 209:86-93.

Fornai F, Giorgi FS, Gesi M, Chen K, Alessrì MG, Shih JC (2001). Biochemical effects of the monoamine neurotoxins DSP-4 and MDMA in specific brain regions of MAO-B-deficient mice. Synapse 39:213-221.

Fornai F, Lenzi P, Frenzilli G, Gesi M, Ferrucci M, Lazzeri G, et al. (2004). DNA damage and ubiquitinated neuronal inclusions in the substantia nigra and striatum of mice following MDMA (ecstasy). Psychopharmacology 173:353-363.

Foth BJ, Goedecke MC, Soldati D (2006). New insights into myosin evolution and classification. Proc Natl Acad Sci U S A 103:3681-3686.

Frank S, Gaume B, Bergmann-Leitner ES, Leitner WW, Robert EG, Catez F, et al. (2001). The role of dynamin-related protein 1, a mediator of mitochondrial fission, in apoptosis. Dev Cell 1:515-525.

Franklin JL (2011). Redox regulation of the intrinsic pathway in neuronal apoptosis. Antioxid Redox Signal 14:1437-1448.

Fransson Å, Ruusala A, Aspenström P (2006). The atypical Rho GTPases Miro-1 and Miro-2 have essential roles in mitochondrial trafficking. Biochem Biophys Res Commun 344:500-510.

Freedman RR, Johanson C, Tancer ME (2005). Thermoregulatory effects of 3,4-methylenedioxymethamphetamine (MDMA) in humans. Psychopharmacology 183:248-256.

Freeman MR (2010). Specification and morphogenesis of astrocytes. Science 330:774-778.

Frega M, Pasquale V, Tedesco M, Marcoli M, Contestabile A, Nanni M, et al. (2012). Cortical cultures coupled to micro-electrode arrays: A novel approach to perform *in vitro* excitotoxicity testing. Neurotoxicol Teratol 34:116-127.

Frezza C, Cipolat S, Martins de Brito O, Micaroni M, Beznoussenko GV, Rudka T, et al. (2006). OPA1 Controls Apoptotic Cristae Remodeling Independently from Mitochondrial Fusion. Cell 126:177-189.

Friedman JR, Lackner LL, West M, Di Benedetto JR, Nunnari J, Voeltz GK (2011). ER tubules mark sites of mitochondrial division. Science 334:358-362.

Fujita T, Maturana AD, Ikuta J, Hamada J, Walchli S, Suzuki T, et al. (2007). Axonal guidance protein FEZ1 associates with tubulin and kinesin motor protein to transport mitochondria in neurites of NGF-stimulated PC12 cells. Biochem Biophys Res Commun 361:605-610.

Fujita Y, Hiroyama M, Sanbe A, Yamauchi J, Murase S, Tanoue A (2008). ETOH inhibits embryonic neural stem/precursor cell proliferation via PLD signaling. Biochem Biophys Res Commun 370:169-173.

Gandre-Babbe S, van der Bliek AM (2008). The novel tail-anchored membrane protein Mff controls mitochondrial and peroxisomal fission in mammalian cells. Mol Biol Cell 19:2402-2412.

Gao HL, Li C, Nabeka H, Shimokawa T, Saito S, Wang ZY, et al. (2013). Attenuation of MPTP/MPP^+ toxicity *in vivo* and *in vitro* by an 18-mer peptide derived from prosaposin. Neuroscience 236:373-393.

Garcia-Ratés S, Camarasa J, Sánchez-García AI, Gandía L, Escubedo E, Pubill D (2010). The effects of 3,4-methylenedioxymethamphetamine (MDMA) on nicotinic receptors: Intracellular calcium increase, calpain/caspase 3 activation, and functional upregulation. Toxicol Appl Pharmacol 244:344-353.

Gegg ME, Cooper JM, Chau KY, Rojo M, Schapira AHV, Taanman JW (2010). Mitofusin 1 and mitofusin 2 are ubiquitinated in a PINK1/parkin-dependent manner upon induction of mitophagy. Hum Mol Genet 19:4861-4870.

Geissler M, Gottschling C, Aguado A, Rauch U, Wetzel CH, Hatt H, et al. (2013). Primary hippocampal neurons, which lack four crucial extracellular matrix molecules, display abnormalities of synaptic structure and function and severe deficits in perineuronal net formation. J Neurosci 33:7742-7755.

Giordano G, Kavanagh TJ, Costa LG (2009). Mouse cerebellar astrocytes protect cerebellar granule neurons against toxicity of the polybrominated diphenyl ether (PBDE) mixture DE-71. Neurotoxicology 30:326-329.

Glater EE, Megeath LJ, Stowers RS, Schwarz TL (2006). Axonal transport of mitochondria requires milton to recruit kinesin heavy chain and is light chain independent. J Cell Biol 173:545-557.

Godoi GL, de Oliveira Porciúncula L, Schulz JF, Kaufmann FN, da Rocha JB, de Souza DO, et al. (2013). Selenium compounds prevent amyloid β-peptide neurotoxicity in rat primary hippocampal neurons. Neurochem Res.

Godwin AK, Meister A, O'Dwyer PJ, Huang CS, Hamilton TC, Anderson ME (1992). High resistance to cisplatin in human ovarian cancer cell lines is associated with marked increase of glutathione synthesis. Proc Natl Acad Sci U S A 89:3070-3074.

Goldoni M, Vettori MV, Alinovi R, Caglieri A, Ceccatelli S, Mutti A (2003). Models of neurotoxicity: extrapolation of benchmark doses *in vitro*. Risk Anal 23:505-514.

Gollamudi R, Ali SF, Lipe G, Newport G, Webb P, Lopez M, et al. (1989). Influence of inducers and inhibitors on the metabolism *in vitro* and neurochemical effects *in vivo* of MDMA. Neurotoxicology 10:455-466.

Gómez-Nicola D, Fransen NL, Suzzi S, Perry VH (2013). Regulation of microglial proliferation during chronic neurodegeneration. J Neurosci 33:2481-2493.

Goni-Allo B, Ó Mathúna B, Segura M, Puerta E, Lasheras B, Torre R, et al. (2008). The relationship between core body temperature and 3,4-methylenedioxymethamphetamine metabolism in rats: implications for neurotoxicity. Psychopharmacology 197:263-278.

Gordon CJ, Fogelson L (1994). Metabolic and thermoregulatory responses of the rat maintained in acrylic or wire-screen cages: Implications for pharmacological studies. Physiol Behav 56:73-79.

Goritz C, Mauch DH, Pfrieger FW (2005). Multiple mechanisms mediate cholesterol-induced synaptogenesis in a CNS neuron. Mol Cell Neurosci 29:190-201.

Gough B, Ali SF, Slikker Jr W, Holson RR (1991). Acute effects of 3,4-methylenedioxymethamphetamine (MDMA) on monoamines in rat caudate. Pharmacol Biochem Behav 39:619-623.

Gouzoulis-Mayfrank E, Thimm B, Rezk M, Hensen G, Daumann J (2003). Memory impairment suggests hippocampal dysfunction in abstinent ecstasy users. Prog Neuropsychopharmacol Biol Psychiatry 27:819-827.

Govindarajan N, Rao P, Burkhardt S, Sananbenesi F, Schlüter OM, Bradke F, et al. (2013). Reducing HDAC6 ameliorates cognitive deficits in a mouse model for Alzheimer's disease. EMBO Mol Med 5:52-63.

Gradinaru D, Minn A, Artur Y, Minn A, Heydel J (2012). Effect of oxidative stress on UDP-glucuronosyltransferases in rat astrocytes. Toxicol Lett 213:316-324.

Graham DG, Amarnath V, Valentine WM, Pyle SJ, Anthony DC (1995). Pathogenetic studies of hexane and carbon disulfide neurotoxicity. Crit Rev Toxicol 25:91-112.

Grahame-Smith DG (1971). Studies *in vivo* on the relationship between brain tryptophan, brain 5-HT synthesis and hyperactivity in rats treated with a monoamine oxidase inhibitor and L-tryptophan. J Neurochem 18:1053-1066.

Granado N, Ares-Santos S, Oliva I, O´Shea E, Martin ED, Colado MI, et al. (2011). Dopamine D2-receptor knockout mice are protected against dopaminergic neurotoxicity induced by methamphetamine or MDMA. Neurobiol Dis 42:391-403.

Granado N, O'Shea E, Bove J, Vila M, Colado MI, Moratalla R (2008). Persistent MDMA-induced dopaminergic neurotoxicity in the striatum and substantia nigra of mice. J Neurochem 107:1102-1112.

Grauer E, Chapman S, Rabinovitz I, Raveh L, Weissman BA, Kadar T, et al. (2008). Single whole-body exposure to sarin vapor in rats: long-term neuronal and behavioral deficits. Toxicol Appl Pharmacol 227:265-274.

Gray EG, Whittaker VP (1962). The isolation of nerve endings from brain: an electron-microscopic study of cell fragments derived by homogenization and centrifugation. J Anat 96:79-88.

Green AR, King MV, Shortall SE, Fone KCF (2012). Lost in translation: preclinical studies on 3,4-methylenedioxymethamphetamine provide information on mechanisms of action, but do not allow accurate prediction of adverse events in humans. Br J Pharmacol 166:1523-1536.

Green AR, Mechan AO, Elliott JM, O'Shea E, Colado MI (2003). The pharmacology and clinical pharmacology of 3,4-methylenedioxymethamphetamine (MDMA, "ecstasy"). Pharmacol Rev 55:463-508.

Grob CS, Poland RE, Chang L, Ernst T (1996). Psychobiologic effects of 3,4-methylenedioxymethamphetamine in humans: methodological considerations and preliminary observations. Behav Brain Res 73:103-107.

Guarnieri S, Pilla R, Morabito C, Sacchetti S, Mancinelli R, Fanò G, et al. (2009). Extracellular guanosine and GTP promote expression of differentiation markers and induce S-phase cell-cycle arrest in human SH-SY5Y neuroblastoma cells. Int J Dev Neurosci 27:135-147.

Gudelsky GA, Nash JF (1996). Carrier-mediated release of serotonin by 3,4-methylenedioxymethamphetamine: implications for serotonin-dopamine interactions. J Neurochem 66:243-249.

Guo X, Macleod GT, Wellington A, Hu F, Panchumarthi S, Schoenfield M, et al. (2005). The GTPase dMiro iIs required for axonal transport of mitochondria to drosophila synapses. Neuron 47:379-393.

Hagiwara H, Yorifuji H, Sato-Yoshitake R, Hirokawa N (1994). Competition between motor molecules (kinesin and cytoplasmic dynein) and fibrous microtubule-associated proteins in binding to microtubules. J Biol Chem 269:3581-3589.

Halassa MM, Fellin T, Haydon PG (2007). The tripartite synapse: roles for gliotransmission in health and disease. Trends Mol Med 13:54-63.

Hamida SB, Tracqui A, de Vasconcelos AP, Szwarc E, Lazarus C, Kelche C, et al. (2009). Ethanol increases the distribution of MDMA to the rat brain: possible implications in the ethanol-induced potentiation of the psychostimulant effects of MDMA. Int J Neuropsychopharmacol 12:749-759.

Harrill JA, Robinette BL, Freudenrich T, Mundy WR (2013). Use of high content image analyses to detect chemical-mediated effects on neurite sub-populations in primary rat cortical neurons. Neurotoxicology 34:61-73.

Harry GJ, Billingsley M, Bruinink A, Campbell IL, Classen W, Dorman DC, et al. (1998). *In vitro* techniques for the assessment of neurotoxicity. Environ Health Perspect 106:131-158.

Hatten ME (1985). Neuronal regulation of astroglial morphology and proliferation *in vitro*. J Cell Biol 100:384-396.

Hatten ME (1987). Neuronal inhibition of astroglial cell proliferation is membrane mediated. J Cell Biol 104:1353-1360.

Hatzidimitriou G, McCann UD, Ricaurte GA (1999). Altered serotonin innervation patterns in the forebrain of monkeys treated with (+/-)3,4-methylenedioxymethamphetamine seven years previously: factors influencing abnormal recovery. J Neurosci 19:5096-5107.

Head B, Griparic L, Amiri M, Gandre-Babbe S, van der Bliek AM (2009). Inducible proteolytic inactivation of OPA1 mediated by the OMA1 protease in mammalian cells. J Cell Biol 187:959-966.

Henry JA, Jeffreys KJ, Dawling S (1992). Toxicity and deaths from 3,4-methylenedioxymethamphetamine ("ecstasy"). Lancet 340:384-387.

Herculano-Houzel S (2011). Not all brains are made the same: new views on brain scaling in evolution. Brain Behav Evol 78:22-36.

Hernandez-Rabaza V, Navarro-Mora G, Velazquez-Sanchez C, Ferragud A, Marin MP, Garcia-Verdugo JM, et al. (2010). Neurotoxicity and persistent cognitive deficits induced by combined MDMA and alcohol exposure in adolescent rats. Addict Biol 15:413-423.

Hettiarachchi NT, Boyle JP, Bauer CC, Dallas ML, Pearson HA, Hara S, et al. (2012). Peroxynitrite mediates disruption of Ca^{2+} homeostasis by carbon monoxide via Ca^{2+} ATPase degradation. Antioxid Redox Signal 17:744-755.

Heupel K, Sargsyan V, Plomp JJ, Rickmann M, Varoqueaux F, Zhang W, et al. (2008). Loss of transforming growth factor-beta 2 leads to impairment of central synapse function. Neural Dev 3:25.

Heusinkveld HJ, Molendijk J, van den Berg M, Westerink RH (2013). Azole fungicides disturb intracellular Ca^{2+} in an additive manner in dopaminergic PC12 cells. Toxicol Sci 134:374-381.

Hewitt KE, Green AR (1994). Chlormethiazole, dizocilpine and haloperidol prevent the degeneration of serotonergic nerve terminals induced by administration of MDMA ('Ecstasy') to rats. Neuropharmacology 33:1589-1595.

Hill EJ, Woehrling EK, Prince M, Coleman MD (2008). Differentiating human NT2/D1 neurospheres as a versatile *in vitro* 3D model system for developmental neurotoxicity testing. Toxicology 249:243-250.

Hill SL, Thomas SHL (2011). Clinical toxicology of newer recreational drugs. Clin Toxicol 49:705-719.

Hiramatsu M, Kumagai Y, Unger SE, Cho AK (1990). Metabolism of methylenedioxymethamphetamine: formation of dihydroxymethamphetamine and a quinone identified as its glutathione adduct. J Pharmacol Exp Ther 254:521-527.

Hirokawa N, Niwa S, Tanaka Y (2010). Molecular motors in neurons: transport mechanisms and roles in brain function, development, and disease. Neuron 68:610-638.

Ho P, Ho J, Liu H, So D, Tse Z, Chan K, et al. (2012). Mitochondrial neuronal uncoupling proteins: a target for potential disease-modification in Parkinson's disease. Transl Neurodegener 1:3.

Ho R, Eggert A, Hishiki T, Minturn JE, Ikegaki N, Foster P, et al. (2002). Resistance to chemotherapy mediated by TrkB in neuroblastomas. Cancer Res 62:6462-6466.

Hogberg HT, Bal-Price AK (2011). Domoic acid-induced neurotoxicity is mainly mediated by the AMPA/KA receptor: comparison between immature and mature primary cultures of neurons and glial cells from rat cerebellum. J Toxicol 2011:543512.

Hogberg HT, Kinsner-Ovaskainen A, Coecke S, Hartung T, Bal-Price AK (2010). mRNA expression is a relevant tool to identify developmental neurotoxicants using an *in vitro* approach. Toxicol Sci 113:95-115.

Hogberg HT, Sobanski T, Novellino A, Whelan M, Weiss DG, Bal-Price AK (2011). Application of micro-electrode arrays (MEAs) as an emerging technology for developmental neurotoxicity: Evaluation of domoic acid-induced effects in primary cultures of rat cortical neurons. Neurotoxicology 32:158-168.

Hondebrink L, Meulenbelt J, Meijer M, van den Berg M, Westerink RHS (2011). High concentrations of MDMA (‘ecstasy’) and its metabolite MDA inhibit calcium influx and depolarization-evoked vesicular dopamine release in PC12 cells. Neuropharmacology 61:202-208.

Hongo H, Kihara T, Kume T, Izumi Y, Niidome T, Sugimoto H, et al. (2012). Glycogen synthase kinase-3β activation mediates rotenone-induced cytotoxicity with the involvement of microtubule destabilization. Biochem Biophys Res Commun 426:94-99.

Horiuchi D, Barkus RV, Pilling AD, Gassman A, Saxton WM (2005). APLIP1, a kinesin binding JIP-1/JNK scaffold protein, influences the axonal transport of both vesicles and mitochondria in Drosophila. Curr Biol 15:2137-2141.

Hrometz SL, Thatcher KE, Ebert JA, Mills EM, Sprague JE (2011). Identification of a possible role for atrial natiuretic peptide in MDMA-induced hyperthermia. Toxicol Lett 206:234-237.

Huang TY, Lin LS, Cho KC, Chen SJ, Kuo YM, Yu L, et al. (2012). Chronic treadmill exercise in rats delicately alters the Purkinje cell structure to improve motor performance and toxin resistance in the cerebellum. J Appl Physiol 113:889-895.

Hyman SE, Malenka RC, Nestler EJ (2006). Neural mechanisms of addiction: The role of reward-related learning and memory. Annu Rev Neurosci 29:565-598.

Hysek CM, Simmler LD, Ineichen M, Grouzmann E, Hoener MC, Brenneisen R, et al. (2011). The norepinephrine transporter inhibitor reboxetine reduces stimulant effects of MDMA ("Ecstasy") in humans. Clin Pharmacol Ther 90:246-255.

Ikeda H, Pastuszko A, Ikegaki N, Kennett RH, Wilson DF (1994). 3,4-dihydroxyphenylalanine (dopa) metabolism and retinoic acid induced differentiation in human neuroblastoma. Neurochem Res 19:1487-1494.

Ikuta J, Maturana A, Fujita T, Okajima T, Tatematsu K, Tanizawa K, et al. (2007). Fasciculation and elongation protein zeta-1 (FEZ1) participates in the polarization of hippocampal neuron by controlling the mitochondrial motility. Biochem Biophys Res Commun 353:127-132.

Im AR, Kim YH, Uddin MR, Chae S, Lee HW, Kim YH, et al. (2013). Betaine protects against rotenone-induced neurotoxicity in PC12 cells. Cellular and Molecular Neurobiology 33:625-635.

Ingerman E, Perkins EM, Marino M, Mears JA, McCaffery JM, Hinshaw JE, et al. (2005). Dnm1 forms spirals that are structurally tailored to fit mitochondria. J Cell Biol 170:1021-1027.

Insel TR, Battaglia G, Johannessen JN, Marra S, De Souza EB (1989). 3,4-Methylenedioxymethamphetamine ("ecstasy") selectively destroys brain serotonin terminals in rhesus monkeys. J Pharmacol Exp Ther 249:713-720.

Ishihara N, Eura Y, Mihara K (2004). Mitofusin 1 and 2 play distinct roles in mitochondrial fusion reactions via GTPase activity. J Cell Sci 117:6535-6546.

Ishihara N, Nomura M, Jofuku A, Kato H, Suzuki SO, Masuda K, et al. (2009). Mitochondrial fission factor Drp1 is essential for embryonic development and synapse formation in mice. Nat Cell Biol 11:958-966.

Itoh K, Nakamura K, Iijima M, Sesaki H (2013). Mitochondrial dynamics in neurodegeneration. Trends Cell Biol 23:64-71.

Itzhak Y, Ali SF, Achat CN, Anderson KL (2003). Relevance of MDMA ("ecstasy")-induced neurotoxicity to long-lasting psychomotor stimulation in mice. Psychopharmacology 166:241-248.

Iyer SPN, Akimoto Y, Hart GW (2003). Identification and cloning of a novel family of coiled-coil domain proteins that interact with O-GlcNAc transferase. J Biol Chem 278:5399-5409.

Izco M, Orio L, O'Shea E, Colado MI (2007). Binge ethanol administration enhances the MDMA-induced long-term 5-HT neurotoxicity in rat brain. Psychopharmacology 189:459-470.

Jacobsen LK, Mencl WE, Pugh KR, Skudlarski P, Krystal JH (2004). Preliminary evidence of hippocampal dysfunction in adolescent MDMA (“ecstasy”) users: possible relationship to neurotoxic effects. Psychopharmacology 173:383-390.

Jaehne EJ, Salem A, Irvine RJ (2008). The effect of long-term repeated exposure to 3,4-methylenedioxymethamphetamine on cardiovascular and thermoregulatory changes. Psychopharmacology 201:161-170.

Jahani-Asl A, Germain M, Slack RS (2010). Mitochondria: joining forces to thwart cell death. Biochim Biophys Acta 1802:162-166.

Jalava A, Akerman K, Heikkilä J (1993). Protein kinase inhibitor, staurosporine, induces a mature neuronal phenotype in SH-SY5Y human neuroblastoma cells through an alpha-, beta-, and zeta-protein kinase C-independent pathway. J Cell Physiol 155:301-312.

Jalava A, Heikkilä J, Lintunen M, Åkerman K, Pahlman S (1992). Staurosporine induces a neuronal phenotype in SH-SY5Y human neuroblastoma cells that resembles that induced by the phorbol ester 12-O-tetradecanoyl phorbol-13 acetate (TPA). FEBS Lett 300:114-118.

James DI, Parone PA, Mattenberger Y, Martinou JC (2003). hFis1, a novel component of the mammalian mitochondrial fission machinery. J Biol Chem 278:36373-36379.

Jankowska-Kulawy A, Bielarczyk H, Pawełczyk T, Wróblewska M, Szutowicz A (2010). Acetyl-CoA and acetylcholine metabolism in nerve terminal compartment of thiamine deficient rat brain. J Neurochem 115:333-342.

Jantas D, Pytel M, Mozrzymas JW, Leskiewicz M, Regulska M, Antkiewicz-Michaluk L, et al. (2008). The attenuating effect of memantine on staurosporine-, salsolinol- and doxorubicin-induced apoptosis in human neuroblastoma SH-SY5Y cells. Neurochem Int 52:864-877.

Jiménez-Mateos EM, González-Billault C, Dawson HN, Vitek MP, Avila J (2006). Role of MAP1B in axonal retrograde transport of mitochondria. Biochem J 397:53-59.

Jiménez A, Jordà EG, Verdaguer E, Pubill D, Sureda FX, Canudas AM, et al. (2004). Neurotoxicity of amphetamine derivatives is mediated by caspase pathway activation in rat cerebellar granule cells. Toxicol Appl Pharmacol 196:223-234.

Johnson EA, O'Callaghan JP, Miller DB (2004). Brain concentrations of d-MDMA are increased after stress. Psychopharmacology 173:278-286.

Johnson M, Bush LG, Hanson GR, Gibb JW (1993). Effects of ritanserin on the 3,4-methylenedioxymethamphetamine-induced decrease in striatal serotonin concentration and on the increase in striatal neurotensin and dynorphin A concentrations. Biochem Pharmacol 46:770-772.

Johnson MP, Hoffman AJ, Nichols DE (1986). Effects of the enantiomers of MDA, MDMA and related analogues on [3H]serotonin and [3H]dopamine release from superfused rat brain slices. Eur J Pharmacol 132:269-276.

Jokanović M, Kosanović M, Brkić D, Vukomanović P (2011). Organophosphate induced delayed polyneuropathy in man: An overview. Clin Neurol Neurosurg 113:7-10.

Jones DC, Duvauchelle C, Ikegami A, Olsen CM, Lau SS, de la Torre R, et al. (2005). Serotonergic neurotoxic metabolites of ecstasy identified in rat brain. J Pharmacol Exp Ther 313:422-431.

Jones DC, Lau SS, Monks TJ (2004). Thioether metabolites of 3,4-methylenedioxyamphetamine and 3,4-methylenedioxymethamphetamine inhibit human serotonin transporter (hSERT) function and simultaneously stimulate dopamine uptake into hSERT-expressing SK-N-MC cells. J Pharmacol Exp Ther 311:298-306.

Jung JE, Moon JY, Ghil SH, Yoo BS (2009). 2,3,7,8-Tetrachlorodibenzo-p-dioxin (TCDD) inhibits neurite outgrowth in differentiating human SH-SY5Y neuroblastoma cells. Toxicol Lett 188:153-156.

Kaech S, Banker G (2006). Culturing hippocampal neurons. Nat Protoc 1:2406-2415.

Kageyama Y, Zhang Z, Roda R, Fukaya M, Wakabayashi J, Wakabayashi N, et al. (2012). Mitochondrial division ensures the survival of postmitotic neurons by suppressing oxidative damage. J Cell Biol 197:535-551.

Kalant H (2001). The pharmacology and toxicology of "ecstasy" (MDMA) and related drugs. CMAJ 165:917-928.

Kang JS, Tian JH, Pan PY, Zald P, Li C, Deng C, et al. (2008). Docking of axonal mitochondria by syntaphilin controls their mobility and affects short-term facilitation. Cell 132:137-148.

Karle KN, Möckel D, Reid E, Schöls Lr (2012). Axonal transport deficit in a KIF5A –/– mouse model. Neurogenetics 13:169-179.

Kauppinen RA, McMahon HT, Nicholls DG (1988). Ca^{2+}-dependent and Ca^{2+}-independent glutamate release, energy status and cytosolic free Ca^{2+} concentration in isolated nerve terminals following metabolic inhibition: possible relevance to hypoglycaemia and anoxia. Neuroscience 27:175-182.

Kehr J, Ichinose F, Yoshitake S, Goiny M, Sievertsson T, Nyberg F, et al. (2011). Mephedrone, compared with MDMA (ecstasy) and amphetamine, rapidly increases both dopamine and 5-HT levels in nucleus accumbens of awake rats. Br J Pharmacol 164:1949-1958.

Kim C, Choi H, Jung ES, Lee W, Oh S, Jeon NL, et al. (2012). HDAC6 inhibitor blocks amyloid beta-induced impairment of mitochondrial transport in hippocampal neurons. PLoS ONE 7:e42983.

Kim JY, S. S, Dietz K, He Y, Howell O, Reynolds R, et al. (2010). HDAC1 nuclear export induced by pathological conditions is essential for the onset of axonal damage. Nat Neurosci 13:180-189.

Kimura K, Ito M, Amano M, Chihara K, Fukata Y, Nakafuku M, et al. (1996). Regulation of myosin phosphatase by Rho and Rho-associated kinase (Rho-kinase). Science 273:245-248.

King SJ, Schroer TA (2000). Dynactin increases the processivity of the cytoplasmic dynein motor. Nat Cell Biol 2:20-24.

Kish SJ, Furukawa Y, Ang L, Vorce SP, Kalasinsky KS (2000). Striatal serotonin is depleted in brain of a human MDMA (Ecstasy) user. Neurology 55:294-296.

Köhling R, Melani R, Koch U, Speckmann EJ, Koudelka-Hep M, Thiébaud P, et al. (2005). Detection of electrophysiological indicators of neurotoxicity in human and rat brain slices by a three-dimensional microelectrode array. Altern Lab Anim 33:579-589.

Kohn J, Durham HD (1993). S9 liver fraction is cytotoxic to neurons in dissociated culture. Neurotoxicology 14:381-386.

Koike T, Ninomiya T (2000). Alteration of veratridine neurotoxicity in sympathetic neurons during developmentn *in vitro*. Neuroreport 11:151-155.

Koob GF, Volkow ND (2009). Neurocircuitry of addiction. Neuropsychopharmacology 35:217-238.

Koshiba T, Detmer SA, Kaiser JT, Chen H, McCaffery JM, Chan DC (2004). Structural basis of mitochondrial tethering by mitofusin complexes. Science 305:858-862.

Koutsopoulos OS, Laine D, Osellame L, Chudakov DM, Parton RG, Frazier AE, et al. (2010). Human Miltons associate with mitochondria and induce microtubule-dependent remodeling of mitochondrial networks. Biochim Biophys Acta 1803:564-574.

Krug AK, Balmer NV, Matt F, Schönenberger F, Merhof D, Leist M (2013). Evaluation of a human neurite growth assay as specific screen for developmental neurotoxicants. Arch Toxicol.

Kühne A, Kaiser R, Schirmer M, Heider U, Muhlke S, Niere W, et al. (2007). Genetic polymorphisms in the amino acid transporters LAT1 and LAT2 in relation to the pharmacokinetics and side effects of melphalan. Pharmacogenet Genomics 17:505-517

Kumaria A, Tolias CM (2008). *In vitro* models of neurotrauma. Br J Neurosurg 22:200-206.

Kume T, Kawato Y, Osakada F, Izumi Y, Katsuki H, Nakagawa T, et al. (2008). Dibutyryl cyclic AMP induces differentiation of human neuroblastoma SH-SY5Y cells into a noradrenergic phenotype. Neurosci Lett 443:199-203.

Kunitz O, Ince A, Kuhlen R, Rossaint R (2003). Hyperpyrexia and rhabdomyolysis after ecstasy (MDMA) intoxication. Anaesthesist 52:511-515.

Lambert JD, Jones RS, Andreasen M, Jensen MS, Heinemann U (1989). The role of excitatory amino acids in synaptic transmission in the hippocampus. Comp Biochem Physiol A Comp Physiol 93:195-201.

Lazarus BD, Love DC, Hanover JA (2009). O-GlcNAc cycling: Implications for neurodegenerative disorders. Int J Biochem Cell Biol 41:2134-2146.

Lee JS, Yoon YG, Yoo SH, Jeong NY, Jeong SH, Lee SY, et al. (2012a). Histone deacetylase inhibitors induce mitochondrial elongation. J Cell Physiol 227:2856-2869.

Lee S, Sterky FH, Mourier A, Terzioglu M, Cullheim S, Olson L, et al. (2012b). Mitofusin 2 is necessary for striatal axonal projections of midbrain dopamine neurons. Hum Mol Genet 21:4827-4835.

LeFew WR, McConnell ER, Crooks JL, Shafer TJ (2013). Evaluation of microelectrode array data using Bayesian modeling as an approach to screening and prioritization for neurotoxicity testing. Neurotoxicology 36:34-41.

Legendre P, Rosenmund C, Westbrook GL (1993). Inactivation of NMDA channels in cultured hippocampal neurons by intracellular calcium. J Neurosci 13:674-684.

Leonardi E, T., Azmitia EC (1994). MDMA (ecstasy) inhibition of MAO type A and type B: comparisons with fenfluramine and fluoxetine (Prozac). Neuropsychopharmacology 10:231-238.

LePage KT, Dickey RW, Gerwick WH, Jester EL, Murray TF (2005). On the use of neuro-2a neuroblastoma cells versus intact neurons in primary culture for neurotoxicity studies. Crit Rev Neurobiol 17:27-50.

Li H, Chen Y, Jones AF, Sanger RH, Collis LP, Flannery R, et al. (2008). Bcl-xL induces Drp1-dependent synapse formation in cultured hippocampal neurons. Proc Natl Acad Sci U S A 105:2169-2174.

Li XX, He GR, Mu X, Xu B, Tian S, Yu X, et al. (2012). Protective effects of baicalein against rotenone-induced neurotoxicity in PC12 cells and isolated rat brain mitochondria. Eur J Pharmacol 674:227-233.

Li Y, Lim S, Hoffman D, Aspenstrom P, Federoff HJ, Rempe DA (2009). HUMMR, a hypoxia- and HIF-1α–inducible protein, alters mitochondrial distribution and transport. J Cell Biol 185:1065-1081.

Li Z, Okamoto KI, Hayashi Y, Sheng M (2004). The importance of dendritic mitochondria in the morphogenesis and plasticity of spines and synapses. Cell 119:873-887.

Liechti ME, Saur MR, Gamma A, Hell D, Vollenweider FX (2000). Psychological and physiological effects of MDMA ('ecstasy') after pretreatment with the 5-HT(2) antagonist ketanserin in healthy humans. Neuropsychopharmacology 23:396-404.

Liechti ME, Vollenweider FX (2000). Acute psychological and physiological effects of MDMA (ecstasy) after haloperidol treatment in healthy humans. Eur Neuropsychopharmacol 10:289-295.

Lin MT, Beal MF (2006). Mitochondrial dysfunction and oxidative stress in neurodegenerative diseases. Nature 443:77-795.

Liu S, Sawada T, Lee S, Yu W, Silverio G, Alapatt P, et al. (2012). Parkinson's disease–associated kinase PINK1 regulates Miro protein level and axonal transport of mitochondria. PLoS Genet 8:e1002537.

Liu X, Weaver D, Shirihai O, Hajnóczky G (2009). Mitochondrial 'kiss-and-run': interplay between mitochondrial motility and fusion-fission dynamics. EMBO J 28:3074-3089.

Liu Y, Lo YC, Qian L, Crews FT, Wilson B, Chen HL, et al. (2011). Verapamil protects dopaminergic neuron damage through a novel anti-inflammatory mechanism by inhibition of microglial activation. Neuropharmacology 60:373-380.

Llorens-Martín M, López-Doménech G, Soriano E, Avila J (2011). GSK3β is involved in the relief of mitochondria pausing in a tau-dependent manner. PLoS ONE 6:e27686.

Lopes FM, Schröder R, Júnior MLC, Zanotto-Filho A, Müller CB, Pires AS, et al. (2010). Comparison between proliferative and neuron-like SH-SY5Y cells as an *in vitro* model for Parkinson´s disease studies. Brain Res 1337:85-94.

López-Arnau R, Martínez-Clemente J, Pubill D, Escubedo E, Camarasa J (2012). Comparative neuropharmacology of three psychostimulant cathinone derivatives: butylone, mephedrone and methylone. Br J Pharmacol 167:407-420.

López-Doménech G, Serrat R, Mirra S, D'Aniello S, Somorjai I, Abad A, et al. (2012). The Eutherian Armcx genes regulate mitochondrial trafficking in neurons and interact with Miro and Trak2. Nat Commun 3:814.

Losón OC, Song Z, Chen H, Chan DC (2013). Fis1, Mff, MiD49, and MiD51 mediate Drp1 recruitment in mitochondrial fission. Mol Biol Cell 24:659-667.

Lu C, Lin T, Wang S (2010). Memantine depresses glutamate release through inhibition of voltage-dependent Ca^{2+} entry and protein kinase C in rat cerebral cortex nerve terminals: an NMDA receptor-independent mechanism. Neurochem Int 57:168-176.

Lv H, Wang L, Li W, Qiao X, Li Y, Wang Z, et al. (2013). Mitofusin 2 gene mutation causing early-onset CMT2A with different progressive courses. Clin Neuropathol 32:16-23.

Ma H, Cai Q, Lu W, Sheng ZH, Mochida S (2009). KIF5B motor adaptor syntabulin maintains synaptic transmission in sympathetic neurons. J Neurosci 29:13019-13029.

MacAskill AF, Brickley K, Stephenson FA, Kittler JT (2009a). GTPase dependent recruitment of Grif-1 by Miro1 regulates mitochondrial trafficking in hippocampal neurons. Mol Cell Neurosci 40:301-312.

MacAskill AF, Kittler JT (2010). Control of mitochondrial transport and localization in neurons. Trends Cell Biol 20:102-112.

Macaskill AF, Rinholm JE, Twelvetrees AE, Arancibia-Carcamo IL, Muir J, Fransson A, et al. (2009b). Miro1 is a calcium sensor for glutamate receptor-dependent localization of mitochondria at synapses. Neuron 61:541-555.

Macedo C, Branco PS, Ferreira LM, Lobo AM, Capela JP, Fernandes E, et al. (2007). Sinthesis and cyclic voltammetry studies of 3,4-methylenedioxymetamphetamine (MDMA) human metabolites. J Health Sci 53:31-42.

Maekawa F, Tsuboi T, Oya M, Aung KH, Tsukahara S, Pellerin L, et al. (2013). Effects of sodium arsenite on neurite outgrowth and glutamate AMPA receptor expression in mouse cortical neurons. Neurotoxicology 37:197-206.

Malberg JE, Sabol KE, Seiden LS (1996). Co-administration of MDMA with drugs that protect against MDMA neurotoxicity produces different effects on body temperature in the rat. J Pharmacol Exp Ther 278:258-267.

Malberg JE, Seiden LS (1998). Small Changes in Ambient Temperature Cause Large Changes in 3,4-Methylenedioxymethamphetamine (MDMA)-Induced Serotonin Neurotoxicity and Core Body Temperature in the Rat. J Neurosci 18:5086-5094.

Mallick A, Bodenham AR (1997). MDMA induced hyperthermia: a survivor with an initial body temperature of 42.9 degrees C. J Accid Emerg Med 14:336-338.

Mandelkow EM, Thies E, Trinczek B, Biernat J, Mandelkow E (2004). MARK/PAR1 kinase is a regulator of microtubule-dependent transport in axons. J Cell Biol 167:99-110.

Mannangatti P, Arapulisamy O, Shippenberg TS, Ramamoorthy S, Jayanthi LD (2011). Cocaine up-regulation of the norepinephrine transporter requires threonine 30 phosphorylation by p38 mitogen-activated protein kinase. J Biol Chem 286:20239-20250.

Marcaida G, Kosenko E, Miñana M, Grisolía S, Felipo V (1996). Glutamate induces a calcineurin-mediated dephosphorylation of Na^+,K^+-ATPase that results in its activation in cerebellar neurons in culture. J Neurochem 66:99-104.

Marchitti SA, Deitrich RA, Vasiliou V (2007). Neurotoxicity and metabolism of the catecholamine-derived 3,4-dihydroxyphenylacetaldehyde and 3,4-dihydroxyphenylglycolaldehyde: the role of aldehyde dehydrogenase. Pharmacol Rev 59:125-150.

Martínez-Clemente J, Escubedo E, Pubill D, Camarasa J (2012). Interaction of mephedrone with dopamine and serotonin targets in rats. Eur Neuropsychopharmacol 22:231-236.

Mastroeni D, Grover A, Leonard B, Joyce JN, Coleman PD, Kozik B, et al. (2009). Microglial responses to dopamine in a cell culture model of Parkinson's disease. Neurobiol Aging 30:1805-1817.

McBain CJ, Freund TF, Mody I (1999). Glutamatergic synapses onto hippocampal interneurons: precision timing without lasting plasticity. Trends Neurosci 22:228-235.

McCann UD, Mertl M, Eligulashvili V, Ricaurte GA (1999). Cognitive performance in (±) 3,4-methylenedioxymethamphetamine (MDMA, “ecstasy”) users: a controlled study. Psychopharmacology 143:417-425.

McCann UD, Ridenour A, Shaham Y, Ricaurte GA (1994). Serotonin neurotoxicity after (+/-)3,4-methylenedioxymethamphetamine (MDMA; "Ecstasy"): a controlled study in humans. Neuropsychopharmacology 10:129-138.

McCann UD, Slate SO, Ricaurte GA (1996). Adverse reactions with 3,4-methylenedioxymethamphetamine (MDMA; "ecstasy"). Drug Saf 15:107-115.

McCann UD, Szabo Z, Vranesic M, Palermo M, Mathews WB, Ravert HT, et al. (2008). Positron emission tomographic studies of brain dopamine and serotonin transporters in abstinent (±)3,4-methylenedioxymethamphetamine (“ecstasy”) users: relationship to cognitive performance. Psychopharmacology 200:439-450.

McConnell ER, McClain MA, Ross J, LeFew WR, Shafer TJ (2012). Evaluation of multi-well microelectrode arrays for neurotoxicity screening using a chemical training set. Neurotoxicology 33:1048-1057.

McManus MF, Chen L, Vallejo I, Vallejo M (1999). Astroglial differentiation of cortical precursor cells triggered by activation of the cAMP-dependent signaling pathway. J Neurosci 19:9004-9015.

McNamara R, Kerans A, O'Neill B, Harkin A (2006). Caffeine promotes hyperthermia and serotonergic loss following co-administration of the substituted amphetamines, MDMA (“Ecstasy”) and MDA (“Love”). Neuropharmacology 50:69-80.

Meacham CA, Freudenrich TM, Anderson WL, Sui L, Lyons-Darden T, Barone Jr S, et al. (2005). Accumulation of methylmercury or polychlorinated biphenyls in *in vitro* models of rat neuronal tissue. Toxicol Appl Pharmacol 205:177-187.

Mechan A, Yuan J, Hatzidimitriou G, Irvine RJ, McCann UD, Ricaurte GA (2005). Pharmacokinetic profile of single and repeated oral doses of MDMA in squirrel monkeys: relationship to lasting effects on brain serotonin neurons. Neuropsychopharmacology 31:339-350.

Mechan AO, Esteban B, O'Shea E, Elliott JM, Colado MI, Green AR (2002). The pharmacology of the acute hyperthermic response that follows administration of 3,4-methylenedioxymethamphetamine (MDMA, ‘ecstasy’) to rats. Br J Pharmacol 135:170-180.

Mechan AO, O'Shea E, Elliott MJ, Colado M, Green AR (2001). A neurotoxic dose of 3,4-methylenedioxymethamphetamine (MDMA; ecstasy) to rats results in a long term defect in thermoregulation. Psychopharmacology 155:413-418.

Meiser J, Weindl D, Hiller K (2013). Complexity of dopamine metabolism. Cell Commun Signal 11:34.

Meyer MR, Peters FT, Maurer HH (2008). The role of human hepatic cytochrome P450 isozymes in the metabolism of racemic 3,4-methylenedioxy-methamphetamine and its enantiomers. Drug Metab Dispos 36:2345-2354.

Michaelsen K, Lohmann C (2010). Calcium dynamics at developing synapses: mechanisms and functions. Eur J Neurosci 32:218-223.

Millecamps S, Julien JP (2013). Axonal transport deficits and neurodegenerative diseases. Nat Rev Neurosci 14:161-176.

Miller RT, Lau SS, Monks TJ (1996). Effects of intracerebroventricular administration of 5-(glutathion-*S*-yl)-α-methyldopamine on brain dopamine, serotonin, and norepinephrine concentrations in male Sprague-Dawley rats. Chem Res Toxicol 9:457-465.

Miller RT, Lau SS, Monks TJ (1997). 2,5-bis-(glutathion-*S*-yl)-[alpha]-methyldopamine, a putative metabolite of (±)-3,4-methylenedioxyamphetamine, decreases brain serotonin concentrations. Eur J Pharmacol 323:173-180.

Minin AA, Kulik AV, Gyoeva FK, Li Y, Goshima G, Gelfand VI (2006). Regulation of mitochondria distribution by RhoA and formins. J Cell Sci 119:659-670.

Mironov SL (2007). ADP regulates movements of mitochondria in neurons. Biophys J 92:2944-2952.

Mironov SL (2009). Complexity of mitochondrial dynamics in neurons and its control by ADP produced during synaptic activity. Int J Biochem Cell Biol 41:2005-2014.

Misiti F, Martorana GE, Nocca G, Di Stasio E, Giardina B, Clementi ME (2004). Methionine 35 oxidation reduces toxic and pro-apoptotic effects of the amyloid β-protein fragment (31–35) on isolated brain mitochondria. Neuroscience 126:297-303.

Misko A, Jiang S, Wegorzewska I, Milbrandt J, Baloh RH (2010). Mitofusin 2 is necessary for transport of axonal mitochondria and interacts with the Miro/Milton complex. J Neurosci 30:4232-4240.

Misko AL, Sasaki Y, Tuck E, Milbrandt J, Baloh RH (2012). Mitofusin2 mutations disrupt axonal mitochondrial positioning and promote axon degeneration. J Neurosci 32:4145-4155.

Mlinar B, Corradetti R (2003). Endogenous 5-HT, released by MDMA through serotonin transporter- and secretory vesicle-dependent mechanisms, reduces hippocampal excitatory synaptic transmission by preferential activation of 5-HT1B receptors located on CA1 pyramidal neurons. Eur J Neurosci 18:1559-1571.

Mollereau C, Zajac J, Roumy M (2007). Staurosporine differentiation of NPFF2 receptor-transfected SH-SY5Y neuroblastoma cells induces selectivity of NPFF activity towards opioid receptors. Peptides 28:1125-1128.

Monks TJ, Jones DC, Fengju B, Lau SS (2004). The role of metabolism in 3,4-Methylenodioxyamphetamine and 3,4-Methylenodioxymethamphetamine (Ecstasy) toxicity. Ther Drug Monit 26:132-136.

Monks TJ, Lau SS (1997). Biological reactivity of polyphenolic-glutathione conjugates. Chem Res Toxicol 10:1296-1313.

Moors M, Rockel TD, Abel J, Cline JE, Gassmann K, Schreiber T, et al. (2009). Human neurospheres as three-dimensional cellular systems for developmental neurotoxicity testing. Environ Health Perspect 117:1131-1138.

Morel M, Authelet M, Dedecker R, Brion JP (2010). Glycogen synthase kinase-3β and the p25 activator of cyclin dependent kinase 5 increase pausing of mitochondria in neurons. Neuroscience 167:1044-1056.

Morfini G, Szebenyi G, Elluru R, Ratner N, Brady ST (2002). Glycogen synthase kinase 3 phosphorylates kinesin light chains and negatively regulates kinesin-based motility. EMBO J 21:281-293.

Morris RL, Hollenbeck PJ (1995). Axonal transport of mitochondria along microtubules and F-actin in living vertebrate neurons. J Cell Biol 131:1315-1326.

Moser VC, Aschner M, Richardson RJ, Philbert MA (2010). Toxic response of the nervous system. In: Klaassen C and Watkins J (ed). Casarett & Doull´s Essentials of Toxicology. The McGray-Hill Companies, Inc.: USA, pp 217-232.

Mozdy AD, McCaffery JM, Shaw JM (2000). Dnm1p GTPase-mediated mitochondrial fission is a multi-step process requiring the novel integral membrane component Fis1p. J Cell Biol 151:367-380.

Mueller M, Maldonado-Adrian C, Yuan J, McCann UD, Ricaurte GA (2013). Studies of (±)-3,4-methylenedioxymethamphetamine (MDMA) metabolism and disposition in rats and mice: relationship to neuroprotection and neurotoxicity profile. J Pharmacol Exp Ther 344:479-488.

Mueller M, Yuan J, Felim A, Neudörffer A, Peters FT, Maurer HH, et al. (2009). Further studies on the role of metabolites in (±)-3,4-methylenedioxymethamphetamine-induced serotonergic neurotoxicity. Drug Metab Dispos 37:2079-2086.

Mueller M, Yuan J, Maldonado Adrian C, McCann UD, Ricaurte GA (2011). Inhibition of 3,4-methylenedioxymethamphetamine metabolism leads to marked decrease in 3,4-dihydroxymethamphetamine formation but no change in serotonin neurotoxicity: Implications for mechanisms of neurotoxicity. Synapse 65:983-990.

Nag S (2011). Morphology and properties of astrocytes. In: Nag S (ed). The blood-brain and other neural barriers. Humana Press: New York, USA, pp 69-100.

Nair SG, Gudelsky GA (2004). Protein kinase C inhibition differentially affects 3,4-methylenedioxymethamphetamine-induced dopamine release in the striatum and prefrontal cortex of the rat. Brain Res 1013:168-173.

Naisbitt S, Valtschanoff J, Allison DW, Sala C, Kim E, Craig AM, et al. (2000). Interaction of the postsynaptic density-95/guanylate kinase domain-associated protein complex with a light chain of myosin-V and dynein. J Neurosci 20:4524-4534.

Nakagawa T, Kaneko S (2008). Neuropsychotoxicity of abused drugs: Molecular and neural mechanisms of neuropsychotoxicity induced by methamphetamine, 3,4-methylenedioxymethamphetamine (ecstasy), and 5-Methoxy-N,N-diisopropyltryptamine (foxy). J Pharmacol Sci 106:2-8.

Nakagawa Y, Suzuki T, Tayama S, Ishii H, Ogata A (2009). Cytotoxic effects of 3,4-methylenedioxy-N-alkylamphetamines, MDMA and its analogues, on isolated rat hepatocytes. Arch Toxicol 83:69-80.

Nalavadi VC, Griffin LE, Picard-Fraser P, Swanson AM, Takumi T, Bassell GJ (2012). Regulation of zipcode binding protein 1 transport dynamics in axons by myosin Va. J Neurosci 32:15133-15141.

Narendra D, Walker JE, Youle R (2012). Mitochondrial quality control mediated by PINK1 and Parkin: links to parkinsonism. Cold Spring Harb Perspect Biol 4:a011338.

Nash JF, Brodkin J (1991). Microdialysis studies on 3,4-methylenedioxymethamphetamine-induced dopamine release: effect of dopamine uptake inhibitors. J Pharmacol Exp Ther 259:820-825.

Nash JF, Meltzer HY, Gudelsky GA (1990). Effect of 3,4-methylenedioxymethamphetamine on 3,4-dihydroxyphenylalanine accumulation in the striatum and nucleus accumbens. J Neurochem 54:1062-1067.

Nedergaard M, Verkhratsky A (2012). Artifact versus reality-How astrocytes contribute to synaptic events. Glia 60:1013-1023.

Nicholls DG (1993). The glutamatergic nerve terminal. Eur J Biochem 212:613-631.

Nisijima K, Kuboshima K, Shioda K, Yoshino T, Iwamura T, Kato S (2012). Memantine attenuates 3,4-methylenedioxymethamphetamine-induced hyperthermia in rats. Neurosci Lett 531:198-203.

Núñez MT, Gallardo V, Muñoz P, Tapia V, Esparza A, Salazar J, et al. (2004). Progressive iron accumulation induces a biphasic change in the glutathione content of neuroblastoma cells. Free Radic Biol Med 37:953-960.

O'Hearn E, Battaglia G, De Souza EB, Kuhar MJ, Molliver ME (1988). Methylenedioxyamphetamine (MDA) and methylenedioxymethamphetamine (MDMA) cause selective ablation of serotonergic axon terminals in forebrain: immunocytochemical evidence for neurotoxicity. J Neurosci 8:2788-2803.

O'Shea E, Esteban B, Camarero J, Green AR, Colado MI (2001). Effect of GBR 12909 and fluoxetine on the acute and long term changes induced by MDMA (‘ecstasy’) on the 5-HT and dopamine concentrations in mouse brain. Neuropharmacology 40:65-74.

O'Shea E, Granados R, Esteban B, Colado MI, Green AR (1998). The relationship between the degree of neurodegeneration of rat brain 5-HT nerve terminals and the dose and frequency of administration of MDMA ("ecstasy"). Neuropharmacology 37:919-926.

O'Shea E, Orio L, Escobedo I, Sanchez V, Camarero J, Green AR, et al. (2006). MDMA-induced neurotoxicity: long-term effects on 5-HT biosynthesis and the influence of ambient temperature. Br J Pharmacol 148:778-785.

Oettinghaus B, Licci M, Scorrano L, Frank S (2012). Less than perfect divorces: dysregulated mitochondrial fission and neurodegeneration. Acta Neuropathol 123:189-203.

Oliveira JMA, Chen S, Almeida S, Riley R, Goncalves J, Oliveira CR, et al. (2006). Mitochondrial-dependent Ca^{2+} handling in Huntington's disease striatal cells: effect of histone deacetylase inhibitors. J Neurosci 26:11174-11186.

Oliveira JMA, Gonçalves J (2009). *In situ* mitochondrial Ca^{2+} buffering differences of intact neurons and astrocytes from cortex and striatum. J Biol Chem 284:5010-5020.

Onoue K, Jofuku A, Ban-Ishihara R, Ishihara T, Maeda M, Koshiba T, et al. (2013). Fis1 acts as a mitochondrial recruitment factor for TBC1D15 that is involved in regulation of mitochondrial morphology. J Cell Sci 126:176-185.

Otera H, Wang C, Cleland MM, Setoguchi K, Yokota S, Youle RJ, et al. (2010). Mff is an essential factor for mitochondrial recruitment of Drp1 during mitochondrial fission in mammalian cells. J Cell Biol 191:1141-1158.

Påhlman S, Mamaeva S, Meyerson G, Mattsson ME, Bjelfman C, Ortoft E, et al. (1990). Human neuroblastoma cells in culture: a model for neuronal cell differentiation and function. Acta Physiol Scand Suppl 592:25-37.

Påhlman S, Ruusala AI, Abrahamsson L, Odelstad L, Nilsson K (1983). Kinetics and concentration effects of TPA-induced differentiation of cultured human neuroblastoma cells. Cell Differ 12:165-170.

Pal S, Ahir M, Sil PC (2012). Doxorubicin-induced neurotoxicity is attenuated by a 43-kD protein from the leaves of Cajanus indicus L. via NF-κB and mitochondria dependent pathways. Free Radic Res 46:785-798.

Palau F, Estela A, Pla-Martín D, Sánchez-Piris M (2009). The role of mitochondrial network dynamics in the pathogenesis of Charcot-Marie-Tooth disease. Adv Exp Med Biol 652:129-137.

Palmer CS, Osellame LD, Laine D, Koutsopoulos OS, Frazier AE, Ryan MT (2011). MiD49 and MiD51, new components of the mitochondrial fission machinery. EMBO Rep 12:565-573.

Pardo-Lozano R, Farré M, Yubero-Lahoz S, O'Mathúna B, Torrens M, Mustata C, et al. (2012). Clinical pharmacology of 3,4-methylenedioxymethamphetamine (MDMA, "ecstasy"): The influence of gender and genetics (CYP2D6, COMT, 5-HTT). PLoS ONE 7:e47599.

Paris JM, Cunningham KA (1992). Lack of serotonin neurotoxicity after intraraphe microinjection of (+)-3,4-methylenedioxymethamphetamine (MDMA). Brain Res Bull 28:115-119.

Parrott AC (2012). MDMA and 5-HT neurotoxicity: the empirical evidence for its adverse effects in humans – no need for translation. Br J Pharmacol 166:1518-1520.

Partilla JS, Dempsey AG, Nagpal AS, Blough BE, Baumann MH, Rothman RB (2006). Interaction of amphetamines and related compounds at the vesicular monoamine transporter. J Pharmacol Exp Ther 319:237-246.

Patel MM, Belson MG, Longwater AB, Olson KR, Miller MA (2005). Methylenedioxymethamphetamine (ecstasy)-related hyperthermia. J Emerg Med 29:451-454.

Patel NJ, Fullone JS, Anders MW (1993). Brain uptake of S-(1,2-dichlorovinyl)glutathione and S-(1,2-dichlorovinyl)-L-cysteine, the glutathione and cysteine S-conjugates of the neurotoxin dichloroacetylene. Brain Res Mol Brain Res 17:53-58.

Pathak D, Sepp KJ, Hollenbeck PJ (2010). Evidence that myosin activity opposes microtubule-based axonal transport of mitochondria. J Neurosci 30:8984-8992.

Patil H, Cho K, Lee J, Yang Y, Orry A, Ferreira PA (2013). Kinesin-1 and mitochondrial motility control by discrimination of structurally equivalent but distinct subdomains in Ran-GTP-binding domains of Ran-binding protein 2. Open Biol 3:120183.

Pedersen NP, Blessing WW (2001). Cutaneous vasoconstriction contributes to hyperthermia induced by 3,4-methylenedioxymethamphetamine (ecstasy) in conscious rabbits. J Neurosci 21:8648-8654.

Pehek EA, Nocjar C, Roth BL, Byrd TA, Mabrouk OS (2005). Evidence for the preferential involvement of 5-HT2A serotonin receptors in stress- and drug-induced dopamine release in the rat medial prefrontal cortex. Neuropsychopharmacology 31:265-277.

Pendyala G, Buescher JL, Fox HS (2012). Methamphetamine and inflammatory cytokines increase neuronal Na^+/K^+-ATPase Isoform 3: relevance for HIV associated neurocognitive disorders. PLoS ONE 7:e37604.

Peraile I, Granado N, Torres E, Gutiérrez-López MD, Moratalla R, Colado MI, et al. (2013). Cocaine potentiates MDMA-induced oxidative stress but not dopaminergic neurotoxicity in mice: implications for the pathogenesis of free radical-induced neurodegenerative disorders. Psychopharmacology 230:125-135.

Pereira C, Chaves S, Alves S, Salin B, Camougrand N, Manon S, et al. (2010). Mitochondrial degradation in acetic acid-induced yeast apoptosis: the role of Pep4 and the ADP/ATP carrier. Mol Microbiol 76:1398-1410.

Pigino G, Morfini G, Pelsman A, Mattson MP, Brady ST, Busciglio J (2003). Alzheimer's presenilin 1 mutations impair kinesin-based axonal transport. J Neurosci 23:4499-4508.

Pilling AD, Horiuchi D, Lively CM, Saxton WM (2006). Kinesin-1 and Dynein are the primary motors for fast transport of mitochondria in Drosophila motor axons. Mol Biol Cell 17:2057-2068.

Pimentel VC, Zanini D, Cardoso AM, Schmatz R, Bagatini MD, Gutierres JM, et al. (2013). Hypoxia–ischemia alters nucleotide and nucleoside catabolism and Na^+,K^+-ATPase activity in the cerebral cortex of newborn rats. Neurochem Res 38:886-894.

Piper BJ, Fraiman JB, Owens CB, Ali SF, Meyer JS (2007). Dissociation of the neurochemical and behavioral toxicology of MDMA ("Ecstasy") by citalopram. Neuropsychopharmacology 33:1192-1205.

Plucińska G, Paquet D, Hruscha A, Godinho L, Haass C, Schmid B, et al. (2012). *In vivo* imaging of disease-related mitochondrial dynamics in a vertebrate model system. J Neurosci 32:16203-16212.

Pontes H, Duarte JA, de Pinho PG, Soares ME, Fernandes E, Dinis-Oliveira RJ, et al. (2008a). Chronic exposure to ethanol exacerbates MDMA-induced hyperthermia and exposes liver to severe MDMA-induced toxicity in CD1 mice. Toxicology 252:64-71.

Pontes H, Santos-Marques MJ, Fernandes E, Duarte JA, Remião F, Carvalho F, et al. (2008b). Effect of chronic ethanol exposure on the hepatotoxicity of ecstasy in mice: an *ex vivo* study. Toxicol In Vitro 22:910-920.

Pontes H, Sousa C, Silva R, Fernandes E, Carmo H, Remião F, et al. (2008c). Synergistic toxicity of ethanol and MDMA towards primary cultured rat hepatocytes. Toxicology 254:42-50.

Poole AC, Thomas RE, Andrews LA, McBride HM, Whitworth AJ, Pallanck LJ (2008). The PINK1/Parkin pathway regulates mitochondrial morphology. Proc Natl Acad Sci U S A 105:1638-1643.

Popov V, Medvedev NI, Davies HA, Stewart MG (2005). Mitochondria form a filamentous reticular network in hippocampal dendrites but are present as discrete bodies in axons: A three-dimensional ultrastructural study. J Comp Neurol 492:50-65.

Potapenko ES, Biancardi VC, Zhou Y, Stern JE (2013). Astrocytes modulate a postsynaptic NMDA–GABAA-receptor crosstalk in hypothalamic neurosecretory neurons. J Neurosci 33:631-640.

Presgraves S, Ahmed T, Borwege S, Joyce J (2003). Terminally differentiated SH-SY5Y cells provide a model system for studying neuroprotective effects of dopamine agonists. Neurotox Res 5:579-598.

Pubill D, Chipana C, Camins A, Pallàs M, Camarasa J, Escubedo E (2005). Free radical production induced by methamphetamine in rat striatal synaptosomes. Toxicol Appl Pharmacol 204:57-68.

Puerta E, Hervias I, Goñi-Allo B, Zhang SF, Jordán J, Starkov AA, et al. (2010). Methylenedioxymethamphetamine inhibits mitochondrial complex I activity in mice: a possible mechanism underlying neurotoxicity. Br J Pharmacol 160:233-245.

Qi X, Qvit N, Su Y, Mochly-Rosen D (2012). Novel Drp1 inhibitor diminishes aberrant mitochondrial fission and neurotoxicity. J Cell Sci 126:789-802.

Quednow BB, Jessen F, Kühn K, Maier W, Daum I, Wagner M (2006). Memory deficits in abstinent MDMA (ecstasy) users: neuropsychological evidence of frontal dysfunction. J Psychopharmacol 20:373-384.

Quintero OA, DiVito MM, Adikes RC, Kortan MB, Case LB, Lier AJ, et al. (2009). Human Myo19 Is a novel myosin that associates with mitochondria. Curr Biol 19:2008-2013.

Quinton MS, Yamamoto BK (2006). Causes and consequences of methamphetamine and MDMA toxicity. AAPS J 8:337-347.

Radio NM, Breier JM, Shafer TJ, Mundy WR (2008). Assessment of chemical effects on neurite outgrowth in PC12 cells using high content screening. Toxicol Sci 105:106-118.

Radio NM, Mundy WR (2008). Developmental neurotoxicity testing *in vitro*: models for assessing chemical effects on neurite outgrowth. Neurotoxicology 29:361-376.

Rahman A, Brew BJ, Guillemin GJ (2011). Lead dysregulates rerine/threonine protein phosphatases in human neurons. Neurochem Res 36:195-204.

Ranieri M, Brajkovic S, Riboldi G, Ronchi D, Rizzo F, Bresolin N, et al. (2013). Mitochondrial fusion proteins and human diseases. Neurol Res Int 2013:293893.

Reale M, Pesce M, Priyadarshini M, Kamal MA, Patruno A (2012). Mitochondria as an easy target to oxidative stress events in Parkinson's disease. CNS Neurol Disord Drug Targets 11:430-438.

Reneman L, Booij J, de Bruin K, Reitsma JB, de Wolff FA, Gunning WB, et al. (2001). Effects of dose, sex, and long-term abstention from use on toxic effects of MDMA (ecstasy) on brain serotonin neurons. Lancet 358:1864-1869.

Reneman L, Endert E, de Bruin K, Lavalaye J, Feenstra MG, de Wolff FA, et al. (2002). The acute and chronic effects of MDMA ("ecstasy") on cortical 5-HT2A receptors in rat and human brain. Neuropsychopharmacology 26:387-396.

Renoir T, Païzanis E, Yacoubi ME, Saurini F, Hanoun N, Melfort M, et al. (2008). Differential long-term effects of MDMA on the serotoninergic system and hippocampal cell proliferation in 5-HTT knock-out vs. wild-type mice. Int J Neuropsychopharmacol 11:1149-1162.

Ricaurte GA, DeLanney LE, Irwin I, Langston JW (1988a). Toxic effects of MDMA on central serotonergic neurons in the primate: importance of route and frequency of drug administration. Brain Res 446:165-168.

Ricaurte GA, Forno LS, Wilson MA, DeLanney LE, Irwin I, Molliver ME, et al. (1988b). ±3,4-methylenedioxymethamphetamine selectively damages central serotonergic neurons in nonhuman primates. JAMA 260:51-55.

Ricaurte GA, McCann UD (1992). Neurotoxic amphetamine analogues: effects in monkeys and implications for humans. Ann N Y Acad Sci 648:371-382.

Ricaurte GA, Yuan J, McCann UD (2000). (+/-)3,4-Methylenedioxymethamphetamine ('Ecstasy')-induced serotonin neurotoxicity: studies in animals. Neuropsychobiology 42:5-10.

Rintoul GL, Bennett VJ, Papaconstandinou NA, Reynolds IJ (2006). Nitric oxide inhibits mitochondrial movement in forebrain neurons associated with disruption of mitochondrial membrane potential. J Neurochem 97:800-806.

Rintoul GL, Filiano AJ, Brocard JB, Kress GJ, Reynolds IJ (2003). Glutamate decreases mitochondrial size and movement in primary forebrain neurons. J Neurosci 23:7881-7888.

Risher WC, Eroglu C (2012). Thrombospondins as key regulators of synaptogenesis in the central nervous system. Matrix Biol 31:170-177.

Roberts GMP, Nestor L, Garavan H (2009). Learning and memory deficits in ecstasy users and their neural correlates during a face-learning task. Brain Res 1292:71-81.

Roberts KM, Fitzpatrick PF (2013). Mechanisms of tryptophan and tyrosine hydroxylase. IUBMB Life 65:350-357.

Rochlin MW, Wickline KM, Bridgman PC (1996). Microtubule stability decreases axon elongation but not axoplasm production. J Neurosci 16:3236-3246.

Rodsiri R, Spicer C, Green AR, Marsden CA, Fone KCF (2011). Acute concomitant effects of MDMA binge dosing on extracellular 5-HT, locomotion and body temperature and the long-term effect on novel object discrimination in rats. Psychopharmacology 213:365-376.

Rojo M, Legros F, Chateau D, Lombès A (2002). Membrane topology and mitochondrial targeting of mitofusins, ubiquitous mammalian homologs of the transmembrane GTPase Fzo. J Cell Sci 115:1663-1674.

Rossato LG, Costa VM, Pinho PG, Arbo MD, Freitas V, Vilain L, et al. (2013). The metabolic profile of mitoxantrone and its relation with mitoxantrone-induced cardiotoxicity. Arch Toxicol 87:1809-1820.

Rossignol R, Gilkerson R, Aggeler R, Yamagata K, Remington SJ, Capaldi RA (2004). Energy substrate modulates mitochondrial structure and oxidative capacity in cancer cells. Cancer Res 64:985-993.

Rothman RB, Baumann MH, Dersch CM, Romero DV, Rice KC, Carroll FI, et al. (2001). Amphetamine-type central nervous system stimulants release norepinephrine more potently than they release dopamine and serotonin. Synapse 39:32-41.

Rozas C, Loyola S, Ugarte G, Zeise ML, Reyes-Parada M, Pancetti F, et al. (2012). Acutely applied MDMA enhances long-term potentiation in rat hippocampus involving D1/D5 and 5-HT2 receptors through a polysynaptic mechanism. Eur Neuropsychopharmacol 22:584-595.

Rudnick G, Wall SC (1992). The molecular mechanism of "ecstasy" [3,4-methylenedioxy-methamphetamine (MDMA)]: serotonin transporters are targets for MDMA-induced serotonin release. Proc Natl Acad Sci U S A 89:1817-1821.

Rugarli EI, Langer T (2012). Mitochondrial quality control: a matter of life and death for neurons. EMBO J 31:1336-1349.

Rump TJ, Muneer PMA, Szlachetka AM, Lamb A, Haorei C, Alikunju S, et al. (2010). Acetyl-l-carnitine protects neuronal function from alcohol-induced oxidative damage in the brain. Free Radic Biol Med 49:1494-1504.

Russo GJ, Louie K, Wellington A, Macleod GT, Hu F, Panchumarthi S, et al. (2009). Drosophila Miro Is Required for Both Anterograde and Retrograde Axonal Mitochondrial Transport. J Neurosci 29:5443-5455.

Saadat KS, Elliott JM, Colado MI, Green AR (2004). Hyperthermic and neurotoxic effect of 3,4-methylenedioxymethamphetamine (MDMA) in guinea pigs. Psychopharmacology 173:452-453.

Sadée W, Yu VC, Richards ML, Preis PN, Schwab MR, Brodsky FM, et al. Expression of neurotransmitter receptors and myc protooncogenes in subclones of a human neuroblastoma cell line. Cancer Res 47:5207-5212.

Sanchez M, Gastaldi L, Remedi M, Cáceres A, Landa C (2008). Rotenone-induced toxicity is mediated by Rho-GTPases in hippocampal neurons. Toxicol Sci 104:352-361.

Sanchez V, O'shea E, Saadat KS, Elliott JM, Colado MI, Green AR (2004). Effect of repeated ('binge') dosing of MDMA to rats housed at normal and high temperature on neurotoxic damage to cerebral 5-HT and dopamine neurones. J Psychopharmacol 18:412-416.

Saotome M, Safiulina D, Szabadkai G, Das S, Fransson Å, Aspenstrom P, et al. (2008). Bidirectional Ca^{2+}-dependent control of mitochondrial dynamics by the Miro GTPase. Proc Natl Acad Sci U S A 105:20728-20733.

Sapir T, Levy T, Sakakibara A, Rabinkov A, Miyata T, Reiner O (2013). Shootin1 acts in concert with KIF20B to promote polarization of migrating neurons. J Neurosci 33:11932-11942.

Sau D, Rusmini P, Crippa V, Onesto E, Bolzoni E, Ratti A, et al. (2011). Dysregulation of axonal transport and motorneuron diseases. Biol Cell 103:87-107.

Saxton WM, Hollenbeck PJ (2012). The axonal transport of mitochondria. J Cell Sci 125:2095-2104.

Schildknecht S, Pöltl D, Nagel DM, Matt F, Scholz D, Lotharius J, et al. (2009). Requirement of a dopaminergic neuronal phenotype for toxicity of low concentrations of 1-methyl-4-phenylpyridinium to human cells. Toxicol Appl Pharmacol 241:23-35.

Schilt T, de Win MM, Koeter M, Jager G, Korf DJ, van den Brink W, et al. (2007). Cognition in novice ecstasy users with minimal exposure to other drugs: A prospective cohort study. Arch Gen Psychiatry 64:728-736.

Schmidt CJ, Abbate GM, Black CK, Taylor VL (1990a). Selective 5-hydroxytryptamine2 receptor antagonists protect against the neurotoxicity of methylenedioxymethamphetamine in rats. J Pharmacol Exp Ther 255:478-483.

Schmidt CJ, Black CK, Abbate GM, Taylor VL (1990b). Methylenedioxymethamphetamine-induced hyperthermia and neurotoxicity are independently mediated by 5-HT2 receptors. Brain Res 529:85-90.

Schmidt CJ, Black CK, Taylor VL (1991). L-DOPA potentiation of the serotonergic deficits due to a single administration of 3,4-methylenedioxymethamphetamine, p-chloroamphetamine or methamphetamine to rats. Eur J Pharmacol 203:41-49.

Schmidt CJ, Levin JA, Lovenberg W (1987). *In vitro* and *in vivo* neurochemical effects of methylenedioxymethamphetamine on striatal monoaminergic systems in the rat brain. Biochem Pharmacol 36:747-755.

Schmidt CJ, Taylor VL (1987). Depression of rat brain tryptophan hydroxylase activity following the acute administration of methylenedioxymethamphetamine. Biochem Pharmacol 36:4095-4102.

Schmidt CJ, Wu L, Lovenberg W (1986). Methylenedioxymethamphetamine: a potentially neurotoxic amphetamine analogue. Eur J Pharmacol 124:175-178.

Schmued LC (2003). Demonstration and localization of neuronal degeneration in the rat forebrain following a single exposure to MDMA. Brain Res 974:127-133.

Schouw MLJ, Gevers S, Caan MWA, Majoie CBLM, Booij J, Nederveen AJ, et al. (2012). Mapping serotonergic dysfunction in MDMA (ecstasy) users using pharmacological MRI. Eur Neuropsychopharmacol 22:537-545.

Schreiber T, Gassmann K, Götz C, Hübenthal U, Moors M, Krause G, et al. (2010). Polybrominated diphenyl ethers induce developmental neurotoxicity in a human *in vitro* model: evidence for endocrine disruption. Environ Health Perspect 118:572-578.

Schütte JK, Schäfer U, Becker S, Oldewurtel C, Starosse A, Singler P, et al. (2013). 3,4-Methylenedioxymethamphetamine induces a hyperthermic and hypermetabolic crisis in pigs with and without a genetic disposition for malignant hyperthermia. Eur J Anaesthesiol 30:29-37

Schwaninger AE, Meyer MR, Barnes AJ, Kolbrich-Spargo EA, Gorelick DA, Goodwin RS, et al. (2012). Stereoselective urinary MDMA (ecstasy) and metabolites excretion kinetics following controlled MDMA administration to humans. Biochem Pharmacol 83:131-138.

Schwarz TL (2013). Mitochondrial trafficking in neurons. Cold Spring Harb Perspect Biol 5:a011304.

Schwarzer C, Barnikol-Watanabe S, Thinnes FP, Hilschmann N (2002). Voltage-dependent anion-selective channel (VDAC) interacts with the dynein light chain Tctex1 and the heat-shock protein PBP74. Int J Biochem Cell Biol 34:1059-1070.

Scorza MC, Carrau C, Silveira R, Zapata-Torres G, Cassels BK, Reyes-Parada M (1997). Monoamine oxidase inhibitory properties of some methoxylated and alkylthio amphetamine derivatives: structure-activity relationships. Biochem Pharmacol 54:1361-1369.

Seeger MA, Rice SE (2010). Microtubule-associated protein-like binding of the kinesin-1 tail to microtubule. J Biol Chem 285:8155-8162.

Segura M, Ortuño J, Farré M, McLure JA, Pujadas M, Pizarro N, et al. (2001). 3,4-Dihydroxymethamphetamine (HHMA). A major *in vivo* 3,4-methylenedioxymethamphetamine (MDMA) metabolite in humans. Chem Res Toxicol 14:1203-1208.

Shahpasand K, Uemura I, Saito T, Asano T, Hata K, Shibata K, et al. (2012). Regulation of mitochondrial transport and inter-microtubule spacing by tau phosphorylation at the sites hyperphosphorylated in alzheimer's disease. J Neurosci 32:2430-2441.

Shankaran M, Gudelsky GA (1998). Effect of 3,4-methylenedioxymethamphetamine (MDMA) on hippocampal dopamine and serotonin. Pharmacol Biochem Behav 61:361-366.

Shankaran M, Gudelsky GA (1999). A neurotoxic regimen of MDMA suppresses behavioral, thermal and neurochemical responses to subsequent MDMA administration. Psychopharmacology 147:66-72.

Shankaran M, Yamamoto BK, Gudelsky GA (1999a). Involvement of the serotonin transporter in the formation of hydroxyl radicals induced by 3,4-methylenedioxymethamphetamine. Eur J Pharmacol 385:103-110.

Shankaran M, Yamamoto BK, Gudelsky GA (1999b). Mazindol attenuates the 3,4-methylenedioxymethamphetamine-induced formation of hydroxyl radicals and long-term depletion of serotonin in the striatum. J Neurochem 72:2516-2522.

Shastry P, Basu A, Rajadhyaksha MS (2001). Neuroblastoma cell lines - a versatile in vitro model in neurobiology. Int J Neurosci 108:109-126.

Shavali S, Sens DA (2008). Synergistic neurotoxic effects of arsenic and dopamine in human dopaminergic neuroblastoma SH-SY5Y cells. Toxicol Sci 102:254-261.

Shemesh OA, Erez H, Ginzburg I, Spira ME (2008). Tau-induced traffic jams reflect organelles accumulation at points of microtubule polar mismatching. Traffic 9:458-471.

Shen EY, Ali SF, Meyer JS (2011). Chronic administration of THC prevents the behavioral effects of intermittent adolescent MDMA administration and attenuates MDMA-induced hyperthermia and neurotoxicity in rats. Neuropharmacology 61:1183-1192.

Sheng Z, Cai Q (2012). Mitochondrial transport in neurons: impact on synaptic homeostasis and neurodegeneration. Nat Rev Neurosci 13:77-93.

Shi MM, Kugelman A, Iwamoto T, Tian L, Forman HJ (1994). Quinone-induced oxidative stress elevates glutathione and induces gamma-glutamylcysteine synthetase activity in rat lung epithelial L2 cells. J Biol Chem 269:26512-26517.

Shioda K, Nisijima K, Yoshino T, Kuboshima K, Iwamura T, Yui K, et al. (2008). Risperidone attenuates and reverses hyperthermia induced by 3,4-methylenedioxymethamphetamine (MDMA) in rats. Neurotoxicology 29:1030-1036.

Shirendeb U, Reddy AP, Manczak M, Calkins MJ, Mao P, Tagle DA, et al. (2011). Abnormal mitochondrial dynamics, mitochondrial loss and mutant huntingtin oligomers in Huntington's disease: implications for selective neuronal damage. Hum Mol Genet 20:1438-1455.

Shirendeb UP, Calkins MJ, Manczak M, Anekonda V, Dufour B, McBride JL, et al. (2012). Mutant huntingtin's interaction with mitochondrial protein Drp1 impairs mitochondrial biogenesis and causes defective axonal transport and synaptic degeneration in Huntington's disease. Hum Mol Genet 21:406-420.

Simantov R, Tauber M (1997). The abused drug MDMA (Ecstasy) induces programmed death of human serotonergic cells. FASEB J 11:141-146.

Slot AJ, Wise DD, Deeley RG, Monks TJ, Cole SPC (2008). Modulation of human multidrug resistance protein (MRP) 1 (ABCC1) and MRP2 (ABCC2) transport activities by endogenous and exogenous glutathione-conjugated catechol metabolites. Drug Metab Dispos 36:552-560.

Smirnova E, Griparic L, Shurland DL, van der Bliek AM (2001). Dynamin-related protein Drp1 is required for mitochondrial division in mammalian cells. Mol Biol Cell 12:2245-2256.

Söderström S, Ebendal T (1995). *In vitro* toxicity of methyl mercury: effects on nerve growth factor (NGF)-responsive neurons and on NGF synthesis in fibroblasts. Toxicol Lett 75:133-144.

Song Z, Ghochani M, McCaffery JM, Frey TG, Chan DC (2009). Mitofusins and OPA1 mediate sequential steps in mitochondrial membrane fusion. Mol Biol Cell 20:3525-3532.

Spencer JPE, Jenner P, Daniel SE, Lees AJ, Marsden DC, Halliwell B (1998). Conjugates of catecholamines with cysteine and GSH in Parkinson's disease: possible mechanisms of formation involving reactive oxygen species. J Neurochem 71:2112-2122.

Sprague JE, Nichols DE (1995). The monoamine oxidase-B inhibitor L-deprenyl protects against 3,4-methylenedioxymethamphetamine-induced lipid peroxidation and long-term serotonergic deficits. J Pharmacol Exp Ther 273:667-673.

Stahnke T, Richter-Landsberg C (2004). Triethyltin-induced stress responses and apoptotic cell death in cultured oligodendrocytes. Glia 46:334-344.

Stamer K, Vogel R, Thies E, Mandelkow E, Mandelkow E-M (2002). Tau blocks traffic of organelles, neurofilaments, and APP vesicles in neurons and enhances oxidative stress. J Cell Biol 156:1051-1063.

Stobart JL, Anderson CM (2013). Multifunctional role of astrocytes as gatekeepers of neuronal energy supply. Front Cell Neurosci 7:38.

Stone DM, Hanson GR, Gibb JW (1987). Differences in the central serotonergic effects of methylenedioxymethamphetamine (MDMA) in mice and rats. Neuropharmacology 26:1657-1661.

Stone DM, Johnson M, Hanson GR, Gibb JW (1988). Role of endogenous dopamine in the central serotonergic deficits induced by 3,4-methylenedioxymethamphetamine. J Pharmacol Exp Ther 247:79-87.

Stone DM, Stahl DC, Hanson GR, Gibb JW (1986). The effects of 3,4-methylenedioxymethamphetamine (MDMA) and 3,4-methylenedioxyamphetamine (MDA) on monoaminergic systems in the rat brain. Eur J Pharmacol 128:41-48.

Stoothoff W, Jones PB, Spires-Jones TL, Joyner D, Chhabra E, Bercury K, et al. (2009). Differential effect of three-repeat and four-repeat tau on mitochondrial axonal transport. J Neurochem 111:417-427.

Stowers RS, Megeath LJ, Górska-Andrzejak J, Meinertzhagen IA, Schwarz TL (2002). Axonal transport of mitochondria to synapses depends on Milton, a novel drosophila protein. Neuron 36:1063-1077.

Sudo H, Baas PW (2010). Acetylation of microtubules influences their sensitivity to severing by katanin in neurons and fibroblasts. J Neurosci 30:7215-7226.

Suñol C, Babot Z, Fonfría E, Galofré M, García D, Herrera N, et al. (2008). Studies with neuronal cells: From basic studies of mechanisms of neurotoxicity to the prediction of chemical toxicity. Toxicol In Vitro 22:1350-1355.

Szabadkai G, Duchen MR (2008). Mitochondria: the hub of cellular Ca^{2+} signaling. Physiology 23:84-94.

Tabakman R, Lecht S, Sephanova S, Arien-Zakay H, Lazarovici P (2004). Interactions between the cells of the immune and nervous system: neurotrophins as neuroprotection mediators in CNS injury. Prog Brain Res 146:387-401.

Taffe MA (2012). Δ9-Tetrahydrocannabinol attenuates MDMA-induced hyperthermia in rhesus monkeys. Neuroscience 201:125-133.

Taffe MA, Lay CC, Von Huben SN, Davis SA, Crean RD, Katner SN (2006). Hyperthermia induced by 3,4-methylenedioxymethamphetamine in unrestrained rhesus monkeys. Drug Alcohol Depend 82:276-281.

Taguchi N, Ishihara N, Jofuku A, Oka T, Mihara K (2007). Mitotic phosphorylation of dynamin-related GTPase Drp1 participates in mitochondrial fission. J Biol Chem 282:11521-11529.

Tai YF, Hoshi R, Brignell CM, Cohen L, Brooks DJ, Curran HV, et al. (2011). Persistent nigrostriatal dopaminergic abnormalities in ex-users of MDMA ("Ecstasy"): an 18F-dopa PET study. Neuropsychopharmacology 36:735-743.

Takamatsu Y, Shiotsuki H, Kasai S, Sato S, Iwamura T, Hattori N, et al. (2011). Enhanced hyperthermia induced by MDMA in parkin knockout mice. Curr Neuropharmacol. 9:96-99.

Takeshita M, Banno Y, Nakamura M, Otsuka M, Teramachi H, Tsuchiya T, et al. (2011). The pivotal role of intracellular calcium in oxaliplatin-induced inhibition of neurite outgrowth but not cell death in differentiated PC12 cells. Chem Res Toxicol 24:1845-1852.

Takeuchi H, Yanagida T, Inden M, Takata K, Kitamura Y, Yamakawa K, et al. (2009). Nicotinic receptor stimulation protects nigral dopaminergic neurons in rotenone-induced Parkinson's disease models. J Neurosci Res 87:576-585.

Tamburini I, Blandini F, Gesi M, Frenzilli G, Nigro M, Giusiani M, et al. (2006). MDMA induces caspase-3 activation in the limbic system but not in striatum. Ann N Y Acad Sci 1074:377-381.

Tanaka A, Cleland MM, Xu S, Narendra DP, Suen DF, Karbowski M, et al. (2010). Proteasome and p97 mediate mitophagy and degradation of mitofusins induced by Parkin. J Cell Biol 191:1367-1380.

Telford JE, Kilbride SM, Davey GP (2010). Decylubiquinone increases mitochondrial function in synaptosomes. J Biol Chem 285:8639-8645.

Thies E, Mandelkow EM (2007). Missorting of tau in neurons causes degeneration of synapses that can bBe rescued by the kinase MARK2/Par-1. J Neurosci 27:2896-2907.

Thomasius R, Zapletalova P, Petersen K, Buchert R, Andresen B, Wartberg L, et al. (2006). Mood, cognition and serotonin transporter availability in current and former ecstasy (MDMA) users: the longitudinal perspective. J Psychopharmacol 20:211-225.

Tieu K, Zuo DM, Yu PH (1999). Differential effects of staurosporine and retinoic acid on the vulnerability of the SH-SY5Y neuroblastoma cells: Involvement of Bcl-2 and p53 proteins. J Neurosci Res 58:426-435.

Tiffany-Castiglioni E (2004). *In vitro* neurotoxicology: introduction to concepts. In: Tiffany-Castiglioni E (ed). *In vitro* neurotoxicology: principales and challenges. Humana Press Inc.: Totowa, New Jersey, USA, pp 1-28.

Tilson HA, Kodavanti PR, Mundy WR, Bushnell PJ (1998). Neurotoxicity of environmental chemicals and their mechanism of action. Toxicol Lett 102-103:631-635.

Tirmenstein MA, Hu CX, Scicchitano MS, Narayanan PK, McFarland DC, Thomas HC, et al. (2005). Effects of 6-hydroxydopamine on mitochondrial function and glutathione status in SH-SY5Y human neuroblastoma cells. Toxicol In Vitro 19:471-479.

Torres-Altoro MI, Mathur BN, Drerup JM, Thomas R, Lovinger DM, O'Callaghan JP, et al. (2011). Organophosphates dysregulate dopamine signaling, glutamatergic neurotransmission, and induce neuronal injury markers in striatum. J Neurochem 119:303-313.

Trinczek B, Ebneth A, Mandelkow EM, Mandelkow E (1999). Tau regulates the attachment/detachment but not the speed of motors in microtubule-dependent transport of single vesicles and organelles. J Cell Sci 112:2355-2367.

Tsushima J, Nishimura K, Tashiro N, Takata K, Ashihara E, Yoshimoto K, et al. (2012). Protective effect of planarian DJ-1 against 6-hydroxydopamine-induced neurotoxicity. Neurosci Res 74:277-283.

Twig G, Elorza A, Molina AJ, Mohamed H, Wikstrom JD, Walzer G, et al. (2008a). Fission and selective fusion govern mitochondrial segregation and elimination by autophagy. EMBO J 27:433-446.

Twig G, Hyde B, Shirihai OS (2008b). Mitochondrial fusion, fission and autophagy as a quality control axis: the bioenergetic view. Biochim Biophys Acta 1777:1092-1097.

Twig G, Liu X, Liesa M, Wikstrom JD, Molina AJA, Las G, et al. (2010). Biophysical properties of mitochondrial fusion events in pancreatic β-cells and cardiac cells unravel potential control mechanisms of its selectivity. Am J Physiol Cell Physiol 299:477-487.

Tymianski M, Charlton MP, Carlen PL, Tator CH (1993). Source specificity of early calcium neurotoxicity in cultured embryonic spinal neurons. J Neurosci 13:2085-2104.

Ullian EM, Sapperstein SK, Christopherson KS, Barres BA (2001). Control of synapse number by glia. Science 291:657-661.

Vaccarino FM, Fagel DM, Ganat Y, Maragnoli ME, Ment LR, Ohkubo Y, et al. (2007). Astroglial cells in development, regeneration, and repair. Neuroscientist 13:173-185.

Vafai SB, Mootha VK (2012). Mitochondrial disorders as windows into an ancient organelle. Nature 491:374-383.

Valente MJ, Carvalho F, Bastos ML, Pinho PG, Carvalho M (2012). Contribution of oxidative metabolism to cocaine-induced liver and kidney damage. Curr Med Chem 19:5601-5606.

Valiathan RR, Weisman LS (2008). Pushing for answers: is myosin V directly involved in moving mitochondria? J Cell Biol 181:15-18.

Van Bergen NJ, Crowston JG, Kearns LS, Staffieri SE, Hewitt AW, Cohn AC, et al. (2011). Mitochondrial oxidative phosphorylation compensation may preserve vision in patients with OPA1-linked autosomal dominant optic atrophy. PLoS ONE 6:e21347.

Van Laar VS, Berman SB (2013). The interplay of neuronal mitochondrial dynamics and bioenergetics: implications for Parkinson's disease. Neurobiol Dis 51:43-55.

van Vliet E, Morath S, Eskes C, Linge J, Rappsilber J, Honegger P, et al. (2008). A novel *in vitro* metabolomics approach for neurotoxicity testing, proof of principle for methyl mercury chloride and caffeine. Neurotoxicology 29:1-12.

van Vliet E, Stoppini L, Balestrino M, Eskes C, Griesinger C, Sobanski T, et al. (2007). Electrophysiological recording of re-aggregating brain cell cultures on multi-electrode arrays to detect acute neurotoxic effects. Neurotoxicology 28:1136-1146.

van Spronsen M, Mikhaylova M, Lipka J, Schlager MA, van den Heuvel DJ, Kuijpers M, et al. (2013). TRAK/milton motor-adaptor proteins steer mitochondrial trafficking to axons and dendrites. Neuron 77:485-502.

Vanattou-Saïfoudine N, Gossen A, Harkin A (2011). A role for adenosine A1 receptor blockade in the ability of caffeine to promote MDMA “Ecstasy”-induced striatal dopamine release. Eur J Pharmacol 650:220-228.

Varadi A, Johnson-Cadwell LI, Cirulli V, Yoon Y, Allan VJ, Rutter GA (2004). Cytoplasmic dynein regulates the subcellular distribution of mitochondria by controlling the recruitment of the fission factor dynamin-related protein-1. J Cell Sci 117:4389-4400.

Verheyden SL, Hadfield J, Calin T, Curran VH (2002). Sub-acute effects of MDMA (±3,4-methylenedioxymethamphetamine, "ecstasy") on mood: evidence of gender differences. Psychopharmacology 161:23-31.

Verrico CD, Miller GM, Madras B (2007). MDMA (Ecstasy) and human dopamine, norepinephrine, and serotonin transporters: implications for MDMA-induced neurotoxicity and treatment. Psychopharmacology 189:489-503.

Verstreken P, Ly CV, Venken KJT, Koh T, Zhou Y, Bellen HJ (2005). Synaptic mitochondria are critical for mobilization of reserve pool vesicles at drosophila neuromuscular junctions. Neuron 47:365-378.

Vijayaraghavan S (2009). Glial-neuronal interactions-implications for plasticity and drug addiction. The AAPS Journal 11:123-132.

Visan A, Hayess K, Sittner D, Pohl EE, Riebeling C, Slawik B, et al. (2012). Neural differentiation of mouse embryonic stem cells as a tool to assess developmental neurotoxicity *in vitro*. Neurotoxicology 33:1135-1146.

Viviani B, Corsini E, Galli CL, Marinovich M (1998). Glia increase degeneration of hippocampal neurons through release of tumor necrosis factor-α. Toxicol Appl Pharmacol 150:271-276.

Von Huben SN, Lay CC, Crean RD, Davis SA, Katner SN, Taffe MA (2006). Impact of ambient temperature on hyperthermia induced by (+/-) 3,4-methylenedioxymethamphetamine in rhesus macaques. Neuropsychopharmacology 32:673-681.

Vossel KA, Zhang K, Brodbeck J, Daub AC, Sharma P, Finkbeiner S, et al. (2010). Tau reduction prevents Aβ-induced defects in axonal transport. Science 330:198.

Votyakova TV, Reynolds IJ (2001). ΔΨm-Dependent and -independent production of reactive oxygen species by rat brain mitochondria. J Neurochem 79:266-277.

Wagner W, McCroskery S, Hammer Iii JA (2011). An efficient method for the long-term and specific expression of exogenous cDNAs in cultured Purkinje neurons. J Neurosci Methods 200:95-105.

Walker QD, Williams CN, Jotwani RP, Waller ST, Francis R, Kuhn CM (2007). Sex differences in the neurochemical and functional effects of MDMA in Sprague–Dawley rats. Psychopharmacology 189:435-445.

Wang F, Zhai H, Huang L, Li H, Xu Y, Qiao X, et al. (2012a). Aspirin protects dopaminergic neurons against lipopolysaccharide-induced neurotoxicity in primary midbrain cultures. J Mol Neurosci 46:153-161.

Wang X, Schwarz TL (2009). The mechanism of Ca^{2+}-dependent regulation of kinesin-mediated mitochondrial motility. Cell 136:163-174.

Wang X, Su B, Liu W, He X, Gao Y, Castellani RJ, et al. (2011a). DLP1-dependent mitochondrial fragmentation mediates 1-methyl-4-phenylpyridinium toxicity in neurons: implications for Parkinson's disease. Aging Cell 10:807-823.

Wang X, Winter D, Ashrafi G, Schlehe J, Wong YL, Selkoe D, et al. (2011b). PINK1 and Parkin target Miro for phosphorylation and degradation to arrest mitochondrial motility. Cell 147:893-906.

Wang X, Xu J (2005). Possible involvement of Ca^{2+} signaling in rotenone-induced apoptosis in human neuroblastoma SH-SY5Y cells. Neurosci Lett 376:127-132.

Wang Z, Jiang H, Chen S, Du F, Wang X (2012b). The mitochondrial phosphatase PGAM5 functions at the convergence point of multiple necrotic death pathways. Cell 148:228-243.

Warburg O (1913). Über Sauerstoffatmende Körnchen aus Leberzellen und über Sauerstoffatmung in Berkefeld-Filtralen Wässriger Leberextrakte. Arch Gesamte Physiol 154:599-617.

Warren MW, Zheng W, Kobeissy FH, Cheng Liu M, Hayes RL, Gold MS, et al. (2007). Calpain- and caspase-mediated alphaII-spectrin and tau proteolysis in rat cerebrocortical neuronal cultures after ecstasy or methamphetamine exposure. Int J Neuropsychopharmacol 10:479-489.

Watanabe N, Madaule P, Reid T, Ishizaki T, Watanabe G, Kakizuka A, et al. (1997). p140mDia, a mammalian homolog of Drosophila diaphanous, is a target protein for Rho small GTPase and is a ligand for profilin. EMBO J 16:3044- 3056.

Weihofen A, Thomas KJ, Ostaszewski BL, Cookson MR, Selkoe DJ (2009). Pink1 forms a multiprotein complex with Miro and Milton, linking Pink1 function to mitochondrial trafficking. Biochemistry 48:2045-2052.

Weiss C, Winkler H, Laslop A (2001). Regulation of chromogranin biosynthesis by neurotrophic growth factors in neuroblastoma cells. Neurochem Int 38:43-52.

Wenker SD, Chamorro ME, Vota DM, Callero MA, Vittori DC, Nesse AB (2010). Differential antiapoptotic effect of erythropoietin on undifferentiated and retinoic acid-differentiated SH-SY5Y cells. J Cell Biochem 110:151-161.

Westerink RHS, Ewing AG (2008). The PC12 cell as model for neurosecretion. Acta Physiol 192:273-285.

Westmark PR, Westmark CJ, Jeevananthan A, Malter JS (2011). Preparation of synaptoneurosomes from mouse cortex using a discontinuous percoll-sucrose density gradient. J Vis Exp:e3196.

Whittaker VP (1993). Thirty years of synaptosome research. J Neurocytol 22:735-742.

Wilson TJ, Slupe AM, Strack S (2013). Cell signaling and mitochondrial dynamics: Implications for neuronal function and neurodegenerative disease. Neurobiol Dis 51:13-26.

Win-Shwe T, Fujimaki H (2010). Neurotoxicity of toluene. Toxicol Lett 198:93-99.

Windisch M, Hutter-Paier B, Jerkovic L, Imbimbo B, Villetti G (2003). The protective effect of ganstigmine against amyloid beta25–35 neurotoxicity on chicken cortical neurons is independent from the cholinesterase inhibition. Neurosci Lett 341:181-184.

Wszelaki N, Melzig MF (2011). Research on an *in vitro* cell system for testing the neurotoxicity of kynurenine pathway metabolites. Pharmazie 66:899-903.

Xu B, Xu Z, Deng Y, Liu W, Yang H, Wei Y (2013). MK-801 protects against intracellular Ca^{2+} overloading and improves N-methyl-D-aspartate receptor expression in cerebral cortex of methylmercury-poisoned rats. J Mol Neurosci 49:162-171.

Xu F, Farkas S, Kortbeek S, Zhang FX, Chen L, Zamponi G, et al. (2012). Mercury-induced toxicity of rat cortical neurons is mediated through N-methyl-D-Aspartate receptors. Mol Brain 5:30.

Yamamoto BK, Spanos LJ (1988). The acute effects of methylenedioxymethamphetamine on dopamine release in the awake-behaving rat. Eur J Pharmacol 148:195-203.

Yamazaki T, Yamamoto M, Ishihara Y, Komatsu S, Munetsuna E, Onizaki M, et al. (2013). De Novo synthesized estradiol protects against methylmercury-induced neurotoxicity in cultured rat hippocampal slices. PLoS ONE 8:e55559.

Yang D, Peng C, Li X, Fan X, Li L, Ming M, et al. (2008). Pitx3-transfected astrocytes secrete brain-derived neurotrophic factor and glial cell line-derived neurotrophic factor and protect dopamine neurons in mesencephalon cultures. J Neurosci Res 86:3393-3400.

Yeh SY, Hsu F (1991). The neurochemical and stimulatory effects of putative metabolites of 3,4-methylenedioxyamphetamine and 3,4-methylenedioxymethamphetamine in rats. Pharmacol Biochem Behav 39:787-790.

Yin W, Cheng W, Shen W, Shu L, Zhao J, Zhang J, et al. (2007). Impairment of Na^+,K^+-ATPase in CD95(APO-1)-induced human T-cell leukemia cell apoptosis mediated by glutathione depletion and generation of hydrogen peroxide. Leukemia 21:1669-1678.

Yoon M, Campbell JL, Andersen ME, Clewell HJ (2012). Quantitative *in vitro* to *in vivo* extrapolation of cell-based toxicity assay results. Crit Rev Toxicol 42:633-652.

Yoon Y, Krueger EW, Oswald BJ, McNiven MA (2003). The mitochondrial protein hFis1 regulates mitochondrial fission in mammalian cells through an interaction with the dynamin-like protein DLP1. Mol Cell Biol 23:5409-5420.

Youle RJ, van der Bliek AM (2012). Mitochondrial fission, fusion, and stress. Science 337:1062-1065.

Yu W, Sun Y, Guo S, Lu B (2011). The PINK1/Parkin pathway regulates mitochondrial dynamics and function in mammalian hippocampal and dopaminergic neurons. Hum Mol Genet 20:3227-3240.

Yuan H, Chen R, Zhu Y, Peng C, Zhu X (2013a). The neuroprotective effect of overexpression of calbindin-D28k in an animal model of Parkinson's disease. Mol Neurobiol 47:117-122.

Yuan H, Gerencser AA, Liot G, Lipton SA, Ellisman M, Perkins GA, et al. (2007). Mitochondrial fission is an upstream and required event for bax foci formation in response to nitric oxide in cortical neurons. Cell Death Differ 14:462-471.

Yuan Y, Jiang CY, Xu H, Sun Y, Hu FF, Bian JC, et al. (2013b). Cadmium-induced apoptosis in primary rat cerebral cortical neurons culture is mediated by a calcium signaling pathway. PLoS ONE 8:e64330.

Zakzanis KK, Young DA, Campbell Z (2003). Prospective memory impairment in abstinent MDMA ("Ecstasy") users. Cogn Neuropsychiatry 8:141-153.

Zanelli SA, Trimmer PA, Solenski NJ (2006). Nitric oxide impairs mitochondrial movement in cortical neurons during hypoxia. J Neurochem 97:724-736.

Zhang F, Shi JS, Zhou H, Wilson B, Hong JS, Gao HM (2010). Resveratrol protects dopamine neurons against lipopolysaccharide-induced neurotoxicity through its anti-inflammatory actions. Mol Pharmacol 78:466-477.

Zhao J, Liu T, Jin S, Wang X, Qu M, Uhlen P, et al. (2011). Human MIEF1 recruits Drp1 to mitochondrial outer membranes and promotes mitochondrial fusion rather than fission. EMBO J 30:2762-2778.

Zhou J, Sun Y, Zhao X, Deng Z, Pu X (2013). 3-O-demethylswertipunicoside inhibits MPP^+-induced oxidative stress and apoptosis in PC12 cells. Brain Res 1508:53-62.

Zhou X, Yin W, Doi SQ, Robinson SW, Takeyasu K, Fan X (2003). Stimulation of Na,K-ATPase by low potassium requires reactive oxygen species. Am J Physiol Cell Physiol 285:319-326.

Zhou Z, Han V, Han J (2012). New components of the necroptotic pathway. Protein & Cell 3:811-817.